

รายงานฉบับสมบูรณ์

โครงการวิจัยเรื่อง

การศึกษาตัวบ่งชี้ลักษณะของพลอยที่ผ่านการปรับปรุงคุณภาพด้วย
ความร้อนหรือรังสี ปีที่ 3

โดย

รศ. ดร. วิสุทธิ	พิศุทธอนันท์	หัวหน้าโครงการ
ผศ. ดร. พรสวาท	วัฒนกุล	ที่ปรึกษาโครงการ
นาง วิลาวัลย์	อติชาติ	ที่ปรึกษาโครงการ
Dr. Tobias	Häger	นักวิจัย
น.ศ. ชนียา	สมบุญ	นักวิจัย
นศ. กฤตยา	ปัทมาลัย	นักวิจัย
นาย ทนง	ฉัตรวัฒนสุข	นักวิจัยและเลขานุการ

ได้รับเงินสนับสนุนจาก

สถาบันวิจัยและพัฒนาอัญมณีและเครื่องประดับแห่งชาติ

ธันวาคม 2547

รายงานฉบับสมบูรณ์

โครงการวิจัยเรื่อง



การศึกษาตัวบ่งชี้ลักษณะของพลอยที่ผ่านการปรับปรุงคุณภาพด้วย ความร้อนหรือรังสี ปีที่ 3

โดย

รศ. ดร. วิสุทธิ์	พิศุทธอนนท์	หัวหน้าโครงการ
ผศ. ดร. พรสวาท	วัฒนกุล	ที่ปรึกษาโครงการ
นาง วิลาวัลย์	อติชาติ	ที่ปรึกษาโครงการ
Dr. Tobias	Häger	นักวิจัย
น.ส. ชนียา	สมบุญ	นักวิจัย
นส. กฤตยา	ปัทมาลัย	นักวิจัย
นาย ทนง	ลีลาวัฒนสุข	นักวิจัยและเลขานุการ

ได้รับเงินสนับสนุนจาก

สถาบันวิจัยและพัฒนาอัญมณีและเครื่องประดับแห่งชาติ

ธันวาคม 2547

สัญญาเลขที่ RM4/2546

โครงการ “การศึกษาตัวบ่งชี้ลักษณะพลอยที่ผ่านการปรับปรุงคุณภาพด้วยความร้อนหรือรังสี”

รายงานการวิจัยฉบับสมบูรณ์ของโครงการครั้งที่ 2 ปีที่ 3

(ประจำปีงบประมาณ 2546)

ตั้งแต่วันที่ 1 มกราคม ถึง 31 ธันวาคม 2547

รายงานในช่วงตั้งแต่วันที่ 1 มกราคม ถึง 31 ธันวาคม 2547

ชื่อหัวหน้าโครงการ: รศ.ดร. วิสุทธิ์ พิสุทธิอนันท์

หน่วยงาน: ภาควิชาธรณีวิทยา คณะวิทยาศาสตร์ จุฬาลงกรณ์มหาวิทยาลัย

วัตถุประสงค์ของโครงการเพื่อ

1. เพื่อศึกษากลไกการเกิดสีของพลอยคอร์ันดัมที่เผาด้วยการรมวิธีใหม่โดยการเติมธาตุเบริลเลียม
2. เพื่อพัฒนาการตรวจสอบการเพิ่มคุณภาพ พลอยคอร์ันดัมด้วยความร้อนอย่างถูกต้องและแม่นยำ

อุปสรรคที่พบในการดำเนินงาน

ไม่พบอุปสรรคที่เป็นสาระสำคัญในการดำเนินงาน

มี (โปรดระบุ)

ได้ขอขยายเวลาการทำวิจัยออกไปอีก 6 เดือน เนื่องจาก

1. ได้ใช้เวลาค่อนข้างมากในช่วงต้นปี สำหรับการเขียนและตรวจแก้ ผลงานวิจัยส่วนแรก ที่ดำเนินการตีพิมพ์เผยแพร่ ในวารสารวิชาการอัญมณีระดับนานาชาติ
2. งานวิจัยบางส่วน เกี่ยวกับการศึกษา ถึงสาเหตุของการเกิดสีในพลอยเผาด้วยการเติมสารเบริลเลียม ยังไม่แล้วเสร็จสมบูรณ์ เพราะได้มีการดำเนินการส่งเคราะห์คอร์ันดัม ที่มีกรใส่เฉพาะธาตุเหล็กเท่านั้น แล้วนำมาเผากับสารเบริลเลียม เพื่อพิสูจน์บทบาทของธาตุเบริลเลียม ว่ามีส่วนในการทำให้เกิดสีให้กระจ่างมากยิ่งขึ้น และเพื่อแก้ข้อสงสัยของนักวิชาการอัญมณีระดับชาติ และนานาชาติ ที่เคยได้ตั้งข้อสังเกต หลังจากที่ผลงานวิจัยในส่วนแรก ได้มีการนำเสนอในที่ประชุมวิชาการหลายครั้ง และได้มีการตีพิมพ์เผยแพร่ในวารสารอัญมณีระดับนานาชาติ ไปเมื่อประมาณกลางปี 2547 นี้

๘
553.8407
๗๒๗๑
2547

เลขที่.....
เลขทะเบียน..... 6545
วันเดือนปี..... ๙ ก.ย. 2548

3. ได้นำผลงานวิจัยที่แก้วเสร็จสมบูรณ์บางส่วน ไปเสนอในการประชุม 27th International Gemmological Congress (27th IGC) ที่เมือง Wuhan ประเทศสาธารณรัฐประชาชนจีน ระหว่างวันที่ 12 – 21 กันยายน 2547
4. ได้นำผลงานวิจัยบางส่วนในเรื่องการปรับปรุงคุณภาพและการตรวจสอบพลอยคอร์นคัม ไปเสนอในการประชุม Gemmological Seminar 47 ณ กรุงปักกิ่ง ประเทศสาธารณรัฐประชาชนจีน เมื่อวันที่ 9 พฤศจิกายน 2547
5. รายงานวิจัยฉบับสมบูรณ์มีเนื้อหามาก โดยต้องประมวลครอบคลุมงานวิจัยทั้ง 3 ปี จึงใช้เวลามากกว่าปกติ

ลงนาม



(วิสุทธิ์ พิสุทธิธานนท์)

หัวหน้าโครงการ

รายงานการวิจัยฉบับสมบูรณ์

โครงการศึกษาตัวบ่งชี้ลักษณะของพลอยที่ผ่านการปรับปรุงคุณภาพด้วยความร้อนหรือรังสี
ครั้งที่ 2 ของปีที่ 2 (ประจำปีงบประมาณ 2546)

มกราคม - ธันวาคม 2547

โครงการวิจัยนี้ได้รับเงินสนับสนุนจากสถาบันวิจัยและพัฒนาอัญมณีและเครื่องประดับแห่งชาติ (สวอ.)

รหัสโครงการ RM4/2546

ธันวาคม 2547

คำนำ

รายงานการวิจัยฉบับสมบูรณ์นี้ เป็นรายงานครั้งที่ 2 ของปีที่ 3 (ประจำปีงบประมาณ 2546) มีเนื้อหาที่ได้ประมวลครอบคลุมงานวิจัยทั้ง 3 ปี ได้แบ่งเนื้อหาออกเป็น 8 บท ในบทที่ 1 ถึง 4 นั้น เป็นการศึกษา สาเหตุและกลไกการเกิดสี ของพลอยคอร์นดัม ที่เผาด้วยการรมวิธีใหม่โดยการเติมสารเบริลเลียม ส่วนในบทที่ 5 ถึง 7 นั้น เป็นศึกษาเรื่องการตรวจสอบ การเพิ่มคุณภาพพลอยคอร์นดัมด้วยความร้อน โดยวิธีการทดลองในห้องปฏิบัติการ และการตรวจสอบพลอยในตลาดพลอย สำหรับบทที่ 8 เป็นบทสรุปย่อ โดยในแต่ละบทได้ประมวลเนื้อหาเป็นภาษาอังกฤษที่สามารถนำไปปรับแต่งตีพิมพ์เผยแพร่ต่อไปได้

ในบทที่ 1 เป็นผลงานวิจัย เกี่ยวกับการเกิดสีเหลืองและสีน้ำตาล ในพลอยแซฟไฟร์ ที่เผาด้วยการเติมสารเบริลเลียม บทนี้ได้เขียนขึ้น จากข้อมูลวิจัยในสองปีแรก และได้ตีพิมพ์เผยแพร่แล้วในวารสาร Journal of Gemmology ฉบับที่ 2 ของปีนี้ (2547, ดู ใน Appendix A)

บทที่ 2 เป็นผลงานวิจัยเกี่ยวกับการเผาพลอยคอร์นดัมสังเคราะห์บริสุทธิ์ และพลอยคอร์นดัมสังเคราะห์ที่มีการใส่เฉพาะธาตุเหล็กเท่านั้น โดยทำการเผาด้วยวิธีปกติโดยใช้ความร้อนเพียงอย่างเดียว และเผาด้วยวิธีเติมสารเบริลเลียม เพื่อพิสูจน์บทบาทของธาตุเบริลเลียม ว่ามีส่วนในการทำให้เกิดสีน้ำตาล และสีเหลืองได้จริง และเพื่อแก้ข้อสงสัยของนักวิชาการอัญมณีระดับชาติ และนานาชาติ ที่เคยได้ตั้งข้อสังเกต หลังจากตีพิมพ์ผลงานวิจัยในส่วนแรก ได้มีการนำเสนอในที่ประชุมวิชาการหลายครั้ง และได้มีการตีพิมพ์เผยแพร่ในวารสารวิชาการอัญมณีระดับนานาชาติดังกล่าว ไปเมื่อประมาณกลางปี 2547 นี้

บทที่ 3 เป็นผลการศึกษาเปรียบเทียบ ทางด้านสี กับปริมาณและปฏิสัมพันธ์ของธาตุร่องรอย ในพลอยไพไรต์ธรรมชาติที่เผาด้วยวิธีปกติ และที่เผาพลอยด้วยวิธีเติมสารเบริลเลียม หรือศึกษาปฏิสัมพันธ์ของระบบ Be+Mg+Fe+Ti ในพลอยธรรมชาติ

บทที่ 4 เป็นผลการศึกษาเปรียบเทียบ ทางด้านสี กับปริมาณและปฏิสัมพันธ์ของธาตุร่องรอย ในพลอยทับทิมและแซฟไฟร์สีชมพู ที่เผาด้วยวิธีปกติ และเผาด้วยวิธีเติมสารเบริลเลียม หรือศึกษาปฏิสัมพันธ์ของระบบ Be+Mg+Fe+Ti+Cr ในพลอยธรรมชาติและพลอยสังเคราะห์ ผลงานบางส่วนในเรื่องนี้ ได้นำเสนอในการประชุมนานาชาติ Geo- and Material-Science on Gem-Minerals of Vietnam (GEO-MAT-GEM 2003) ณ กรุงฮานอย ประเทศเวียดนาม เมื่อวันที่ 1-8 ตุลาคม 2546 และบางส่วน ได้นำเสนอในการประชุม 27th International Gemmological Congress (27th IGC) ที่เมือง Wuhan ประเทศสาธารณรัฐประชาชนจีน ระหว่างวันที่ 12 - 21 กันยายน 2547 (ดู ใน Appendices B และ C)

บทที่ 5 เป็นผลการศึกษา การเปลี่ยนแปลงของพลอยแซปไฟร์ จากแหล่งพลอยอิลากา ประเทศมาดากัสการ์ ซึ่งเป็นพลอยที่มีกำเนิดร่วมกับหินแปร จากการทดลองเผาที่อุณหภูมิต่างๆกัน โดยการเปรียบเทียบพลอยก่อนและหลังเผา ณ อุณหภูมิต่างๆ กัน

บทที่ 6 เป็นผลการศึกษา การเปลี่ยนแปลง ของพลอยแซปไฟร์ จากแหล่งพลอยดิโอโก ประเทศมาดากัสการ์ ซึ่งเป็นพลอยที่มีกำเนิดร่วมกับหินภูเขาไฟบะซอลต์ จากการทดลองเผาที่อุณหภูมิต่างๆกัน โดยการเปรียบเทียบพลอยก่อนและหลังเผา ณ อุณหภูมิต่างๆ กัน

บทที่ 7 เป็นผลการศึกษาเกี่ยวกับ หลักฐานที่สามารถใช้เป็นตัวบ่งชี้ พลอยสดและพลอยเผา ด้วยวิธีปกติ ในพลอยไพฑินจากประเทศมาดากัสการ์ และประเทศเมียนมา ที่ปรากฏอยู่ในตลาดพลอย โดยที่พลอยดังกล่าว ได้มาจากผู้ประกอบการที่เชื่อถือได้ เพื่อเทียบกับผลการทดลองในห้องปฏิบัติการ ที่ได้นำเสนอในบทที่ 5 และ 6

บทที่ 8 เป็นบทสรุปย่อ เกี่ยวกับการปรับปรุงคุณภาพและวิธีการตรวจสอบ พลอยทับทิม และแซปไฟร์ ด้วยกรรมวิธีต่างๆ ตั้งแต่อดีตจนถึงปัจจุบัน โดยจะเน้นกรรมวิธีและวิธีการตรวจสอบ การปรับปรุงคุณภาพพลอยคอร์ันดัมที่พบบ่อยในตลาดพลอย ผลงานในเรื่องนี้ได้นำเสนอในการประชุม Gemmological Seminar 47 ณ กรุงปักกิ่ง ประเทศสาธารณรัฐประชาชนจีน เมื่อวันที่ 9 พฤศจิกายน 2547 (ดู ใน Appendix D)

รศ.ดร. วิสุทธิ์ พิสุทธอนนท์

หัวหน้าโครงการ

ธันวาคม 2547

บทสรุปสำหรับผู้บริหาร

รายงานการวิจัยฉบับสมบูรณ์นี้ ได้แบ่งเนื้อหาออกเป็น 8 บท โดยในแต่ละบทได้สรุปเป็นเนื้อที่สำคัญได้ดังต่อไปนี้

บทที่ 1 เป็นผลงานวิจัย เกี่ยวกับการหาสาเหตุ และกลไก ของการเกิดสีเหลือง และสีน้ำตาล ในพลอยแซฟไฟร์ที่เผาด้วยวิธีเตมสารเบริลเลียม โดยทำการทดลองกับ พลอยสังเคราะห์ และ พลอยธรรมชาติไร้สี ด้วยวิธีการฉายรังสี และวิธีเผาทั้งสารเบริลเลียม ศึกษาเปรียบเทียบสเปกตรัมการดูดกลืนแสงในช่วง UV-Vis ของพลอยดังกล่าวทั้งก่อนและหลังการทดลอง และตรวจวัดปริมาณธาตุร่องรอยในพลอยดังกล่าวด้วยเครื่องมือ LA-ICP-MS ผลการศึกษาสามารถสรุปในเบื้องต้นได้ว่า กระบวนการเผาโดยการเตมสารเบริลเลียม ทำให้เกิดศูนย์กลางสีเหลืองที่เสถียรในพลอยธรรมชาติ ซึ่งมีความสัมพันธ์กับธาตุเหล็กในพลอย บรรยากาศออกซิเดชันในห้องเผา โดยที่ธาตุเบริลเลียมที่แพร่เข้าไปในโครงสร้างผลึกมีหน้าที่ทำให้ศูนย์กลางสีเหลืองดังกล่าวเสถียร สำหรับพลอยสังเคราะห์ไร้สีที่บริสุทธิ์ปราศจากธาตุเหล็ก นั้น พบว่า กระบวนการเผาโดยการเตมสารเบริลเลียม ทำให้เกิดศูนย์กลางสีน้ำตาลที่เสถียร โดยที่สเปกตรัมการดูดกลืนแสงในช่วง UV-Vis ของศูนย์กลางสีน้ำตาลนั้น แตกต่างจากของศูนย์กลางสีเหลืองอย่างชัดเจน ยังสามารถสรุปในเบื้องต้นได้ว่า ธาตุเบริลเลียมน่าจะทำหน้าที่คล้ายกับธาตุแมกนีเซียมที่ได้มีการศึกษามาก่อน

บทที่ 2 เป็นผลงานวิจัยเพื่อพิสูจน์บทบาทของธาตุเบริลเลียม ว่ามีส่วนในการทำให้เกิดศูนย์กลางสีน้ำตาล และศูนย์กลางสีเหลืองที่เสถียร ได้จริง ตามที่ได้สรุปไว้เบื้องต้นในบทที่ 1 โดยในบทที่ 2 นี้เป็นการทดลองกับพลอยสังเคราะห์ 2 แบบ แบบแรกเป็นการทดลองกับพลอยคอร์ันดัมสังเคราะห์ใสบริสุทธิ์ ทั้งนี้เพื่อควบคุม และเข้าใจบทบาทของธาตุเบริลเลียมที่ปราศจากอิทธิพลของธาตุเจือปนอื่นๆ โดยทำการทดลองเปรียบเทียบการเผาพลอยด้วยวิธีปกติโดยใช้ความร้อนเพียงอย่างเดียวกับการเผาด้วยวิธีการเตมสารเบริลเลียม ศึกษาเปรียบเทียบสเปกตรัมการดูดกลืนแสงในช่วง UV-Vis ของพลอยดังกล่าวทั้งก่อนและหลังการทดลอง และตรวจวัดปริมาณธาตุร่องรอยในพลอยดังกล่าวด้วยเครื่องมือ LA-ICP-MS พบว่าธาตุเบริลเลียมมีส่วนในการทำให้เกิดศูนย์กลางสีน้ำตาลที่เสถียร ได้จริง และที่สำคัญมาก คือการทดลองแบบที่ 2 กับพลอยคอร์ันดัมสังเคราะห์ที่ใสเฉพาะธาตุเหล็กเท่านั้น โดยวิธีการฉายรังสี และวิธีเผาทั้งสารเบริลเลียม ศึกษาเปรียบเทียบสเปกตรัมการดูดกลืนแสงในช่วง UV-Vis ของพลอยดังกล่าวทั้งก่อนและหลังการทดลอง และตรวจวัดปริมาณธาตุร่องรอยในพลอยดังกล่าว

ด้วยเครื่องมือ LA-ICP-MS พบว่าธาตุเบริลเลียมและเหล็กในโครงสร้างพลอย (ระบบ Be+Fe) กับสภาวะบรรยากาศออกซิเดชันในห้องเผา ทำให้เกิดศูนย์กลางสี่เหลี่ยมที่เสถียรได้จริง โดยที่ธาตุเบริลเลียมทำหน้าที่เหมือนกับธาตุแมกนีเซียมที่ได้มีการศึกษาในระบบ Mg+Fe มาก่อน

บทที่ 3 เป็นผลการศึกษาปฏิสัมพันธ์ของธาตุในระบบ Be+Mg+Fe+Ti ในพลอยไพลิตินธรรมชาติ โดยเป็นการศึกษาเปรียบเทียบ ทางด้านสี กับปริมาณและปฏิสัมพันธ์ของธาตุร่องรอยดังกล่าว ที่ได้ทำการวิเคราะห์ด้วยเครื่องมือ LA-ICP-MS โดยเผาพลอยไพลิตินธรรมชาติด้วยวิธีปรกติ และด้วยวิธีการเติมสารเบริลเลียม พบว่าพลอยไพลิติน ที่ผ่านการเผาด้วยการเติมสารเบริลเลียม โดยผู้ประกอบการจากจังหวัดจันทบุรี จำนวน 2 ตัวอย่าง มีขอบสีเหลืองปรากฏให้เห็นอย่างชัดเจนหลังเผา พบว่าบริเวณขอบสีเหลือง มีปริมาณธาตุเบริลเลียมสูงขึ้นอย่างเห็นได้ชัด และค่อย ๆ ลดลงบริเวณส่วนกลางเม็ดพลอยที่ยังคงเป็นสีน้ำเงิน แสดงว่าธาตุเบริลเลียมได้แพร่เข้าไปในโครงสร้างพลอย และยังพบอีกว่าบริเวณขอบสีเหลืองมีปริมาณ $(Be+Mg) > Ti$ แต่บริเวณส่วนกลางของเม็ดพลอยที่มีสีน้ำเงินมี $(Be+Mg) < Ti$ ข้อมูลดังกล่าวเป็นหลักฐานที่บ่งชี้ได้อย่างแน่ชัด ว่าสีเหลืองนั้นจะเกิดขึ้นได้ก็ต่อเมื่อมีธาตุเบริลเลียม และธาตุแมกนีเซียมเหลือ หลังจากไปจับเป็นกลุ่มโครงสร้าง $MgTiO_3$ หรือ $BeTiO_3$ โดยที่ Be และ Mg ที่เหลือร่วมกับธาตุเหล็กและการเผาในบรรยากาศออกซิเดชัน ทำให้เกิดศูนย์กลางสี่เหลี่ยมที่บริเวณขอบ ส่วนสีน้ำเงินบริเวณกลางเม็ดนั้น มีสาเหตุมาจากธาตุไทเทเนียมที่เหลือหลังจากเกิดกลุ่มโครงสร้าง $MgTiO_3$ หรือ $BeTiO_3$ มีการแลกเปลี่ยนประจุกับธาตุเหล็ก ($Fe^{2+} - Ti^{4+}$ intervalent charge transfer) เกิดเป็นสีน้ำเงินขึ้น เหตุผลดังกล่าวยังสามารถสนับสนุนได้จากผลวิเคราะห์ธาตุร่องรอยในพลอยสีน้ำเงินที่เผาด้วยวิธีปรกติอีก 2 ตัวอย่าง ที่ปรากฏว่าไม่มีธาตุเบริลเลียมในโครงสร้างพลอย และพลอยสีน้ำเงินดังกล่าว มีปริมาณ $Ti > Mg$ ทั้งสองตัวอย่าง

บทที่ 4 เป็นผลการศึกษาปฏิสัมพันธ์ของธาตุในระบบ Be+Mg+Fe+Ti+Cr ในพลอยทับทิมและแซปไฟร์สีชมพูธรรมชาติและสังเคราะห์ โดยเป็นการศึกษาเปรียบเทียบ ทางด้านสี กับปริมาณและปฏิสัมพันธ์ของธาตุร่องรอยดังกล่าว ที่ได้ทำการวิเคราะห์ด้วยเครื่องมือ LA-ICP-MS โดยเผาพลอยทับทิมและแซปไฟร์สีชมพูดังกล่าวด้วยวิธีปรกติ และด้วยวิธีเติมสารเบริลเลียม โดยแบ่งพลอยออกเป็น 5 กลุ่ม ดังนี้

กลุ่มแรก เป็นการศึกษาสเปกตรัมการดูดกลืนแสงในช่วง UV-Vis ของพลอยแซปไฟร์สีชมพูจากแหล่งพลอยอิตาลีภาค ประเทศมาดากัสการ์ ก่อนและหลังเผาด้วยวิธีเติมสารเบริลเลียม พบว่าพลอย

แซปไฟร์สีชมพูก่อนเผาเปลี่ยนเป็นสีชมพูอมส้มหลังเผา เสปคตรัมการดูดกลืนแสงในช่วง UV-Vis แสดงว่าสีส้มที่เกิดจากการเผาเป็นผลบวกของสีเหลืองกับสีชมพู

กลุ่มที่สองเป็นการศึกษา ทางด้านสี กับปริมาณและปฏิสัมพันธ์ของธาตุร่องรอยในพลอยแซปไฟร์สีชมพู และสีส้ม ที่ไม่ได้ผ่านการเผาด้วยวิธีเดิมสารเบริลเลียม พบว่า ไม่มีธาตุเบริลเลียมในพลอยดังกล่าว และพบว่าจะต้องมี $Mg > Ti$ ประมาณ 30 atom mole ppm จึงสามารถเกิดสีส้มได้

กลุ่มที่สาม เป็นการศึกษา ทางด้านสี กับปริมาณและปฏิสัมพันธ์ของธาตุร่องรอยในพลอยทับทิม และแซปไฟร์สีชมพู ที่มี $Ti > Mg$ และเผาด้วยวิธีปกติ และด้วยวิธีเดิมสารเบริลเลียม พบว่า สีส้มเกิด ได้ยากมาก ถึงแม้ว่าจะเผาด้วยวิธีเดิมสารเบริลเลียมเป็นเวลานาน และ พบว่ามี $Ti > (Be+Mg)$ ในเม็ดพลอย แสดงว่า Mg และ Be ใน โครงสร้างพลอยส่วนใหญ่ไปรวมเป็นกลุ่ม $BeTiO_3$ และ $MgTiO_3$ จนหมด ไม่มี Mg และ Be เหลือพอที่จะไปก่อให้เกิดศูนย์กลางสีเหลืองได้ ยกเว้นบางเม็ดที่มีขอบสีส้ม พบว่าที่ขอบสีส้มมี $(Be+Mg) > Ti$ ดังนั้น พลอยที่มีปริมาณธาตุไทเทเนียมสูง เช่น พลอยทับทิมจากแหล่งมอญ ประเทศเมียนมาร์ และทับทิมจากประเทศเวียดนาม ซึ่งเป็นทับทิมที่เกิดในหินอ่อน โดยกระบวนการแปรสภาพ ซึ่งมักมีธาตุเหล็กต่ำและธาตุไทเทเนียมสูง จึงไม่เหมาะที่จะนำมาเผาด้วยวิธีเดิมสารเบริลเลียม เพราะไม่สามารถเปลี่ยนเป็นสีส้มได้ง่าย

กลุ่มที่สี่ เป็นการศึกษา ทางด้านสี กับปริมาณและปฏิสัมพันธ์ของธาตุร่องรอยในพลอยแซปไฟร์สีน้ำตาลแดง และชมพู ที่มี $Ti \sim$ หรือ $< Mg$ เพียงเล็กน้อย และเผาด้วยวิธีปกติและวิธีเดิมสารเบริลเลียม พลอยกลุ่มนี้ได้แก่ พลอยแซปไฟร์สีน้ำตาลแดง จากแหล่งชองเกีย ประเทศทาจิกิสถาน และพลอยแซปไฟร์กลุ่ม โทนสีชมพู ชมพูอมม่วง จากแหล่งพลอยอิลากา ประเทศมาดากัสการ์ พบว่า เมื่อเผาด้วยวิธีปกติสีพลอยยังเหมือนเดิม เพียงแต่สีชมพูเด่นขึ้นเนื่องจากสีอมม่วงลดลง แต่เมื่อเผาด้วยวิธีเดิมสารเบริลเลียม พบว่าพลอยเปลี่ยนเป็นสีชมพูอมส้ม หรือสีส้มได้ง่าย และมีปริมาณ $(Be+Mg) > Ti$ โดยเฉพาะบริเวณขอบสีส้ม

กลุ่มที่ห้า เป็นการศึกษา ทางด้านสี กับปริมาณและปฏิสัมพันธ์ของธาตุร่องรอยในพลอยทับทิมสังเคราะห์ที่มีโครเมียมเป็นธาตุร่องรอยที่สำคัญเพียงธาตุเดียว หลังเผาด้วยวิธีเดิมธาตุเบริลเลียมแล้ว พบว่าพลอยเปลี่ยนเป็นสีแดงอมส้ม โดยมีธาตุเบริลเลียมแพร่เข้าไปใน โครงสร้าง แสดงว่าการเกิดสีส้มอาจเกิดจากผลรวมของธาตุ Cr และ Be โดยไม่จำเป็นต้องมีธาตุเหล็กก็ได้ แต่เมื่อเผาด้วยวิธีปกติ สีแดงยังคงเหมือนเดิม

บทที่ 5 เป็นการศึกษา การเปลี่ยนแปลงจากการทดลองเผาพลอยแซปไฟร์กลุ่มสีชมพู ม่วงแดง และม่วง จากแหล่งพลอยอิลากา ประเทศมาดากัสการ์ ซึ่งเป็นพลอยที่มีกำเนิดร่วมกับหินแปร โดย

นำมาทดลองเผาที่อุณหภูมิสูงสุดที่ 800°C , 1000°C , 1200°C , 1400°C และ 1600°C และคงอุณหภูมิสูงสุดเป็นเวลานาน 1 ชั่วโมง ในบรรยากาศการเผาแบบออกซิเดชัน และทำการการเปรียบเทียบพลอยก่อนและหลังเผา ณ อุณหภูมิต่างๆ กัน พบว่าช่วงอุณหภูมิที่เหมาะสมในการลดหรือกำจัดสีอมม่วงหรือแกมม่าน้ำเงินในกลุ่มพลอยสีชมพู คือ 1000°C ถึง 1200°C นอกจากนี้ยังพบว่า แร่เซอร์คอน ซึ่งเป็นมลทินภายในพลอยมีลักษณะใสก่อนเผา เปลี่ยนเป็นขุ่นขาวหลังเผาที่ 1600°C มลทินเส้นเข็มรุโกล์ที่เป็นเส้นยาวสมบูรณ์ตัดกันด้วยมุม $60/120$ องศา ก่อนเผา เปลี่ยนเป็นลักษณะขาดเป็นจุด ๆ หลังเผาที่ 1600°C ลักษณะดังกล่าวสามารถใช้เป็นตัวบ่งชี้การเผาได้

บทที่ 6 เป็นการศึกษา การเปลี่ยนแปลงจากการทดลองเผาพลอยแซปไฟร์ จากแหล่งพลอยดีโอโก ประเทศมาดากัสการ์ ซึ่งเป็นพลอยที่มีกำเนิดร่วมกับหินภูเขาไฟบะซอลต์ โดยทำการเผาที่อุณหภูมิ 1350° และ 1650° เซลเซียสเป็นเวลา 3 ชั่วโมง ในบรรยากาศแบบรีดักชัน และทำการเปรียบเทียบพลอยก่อนและหลังเผา ณ อุณหภูมิต่างๆ กัน พบว่า มีการเปลี่ยนแปลงลักษณะภายในที่สำคัญคือ ลักษณะหม่า น้านมขุ่นๆ มีปริมาณลดลง พร้อมกับ ลักษณะแถบสีน้ำเงินปรากฏเด่นชัดขึ้นและสีน้ำเงินเข้มขึ้น เมื่อเผาไปที่อุณหภูมิสูง ลักษณะการแตกเป็นรูปร่างรอบๆ มลทินผลึกแรมบางแรมปรากฏให้เห็นชัดที่อุณหภูมิสูง สามารถใช้เป็นตัวบ่งชี้การเผาได้

บทที่ 7 เป็นผลการศึกษาเกี่ยวกับ หลักฐานที่สามารถใช้เป็นตัวบ่งชี้ พลอยสดและพลอยเผาด้วยวิธีปกติ โดยศึกษาจากพลอยไพลินของประเทศมาดากัสการ์ จำนวน 31 ตัวอย่าง และ ของประเทศเมียนมา จำนวน 6 ตัวอย่าง ที่ ได้มาจากผู้ประกอบการที่เชื่อถือได้ เพื่อเทียบกับผลการทดลองในห้องปฏิบัติการที่ได้นำเสนอในบทที่ 5 และ 6 โดยทั้งหมดเป็นพลอยไพลินที่มีกำเนิดร่วมกับหินแปร พบว่าลักษณะสำคัญที่สามารถใช้เป็นตัวบ่งชี้ว่าเป็นพลอยสด ซึ่งมีลักษณะคล้าย ๆ กันทั้ง 2 แหล่ง คือ มลทินเส้นเข็มรุโกล์ที่เป็นเส้นยาวสมบูรณ์ตัดกันด้วยมุม $60/120$ องศา ลักษณะมลทินอื่น ๆ เช่น มลทินผลึกแรมและมลทินของไหลที่มีรูปร่างสมบูรณ์ และลักษณะการดูกลืนรังสีอินฟราเรดที่ไม่ปรากฏที่ตำแหน่ง 3309 cm^{-1} สำหรับหลักฐานที่ใช้เป็นตัวบ่งชี้ว่าเป็นพลอยเผาจากทั้ง 2 แหล่ง ได้แก่ ลักษณะมลทินเส้นเข็มรุโกล์ที่มีขนาดเป็นจุด ๆ ลักษณะรอยแตกรูปร่างล้อมรอบมลทินผลึกแรม และในบางครั้งมลทินผลึกแรมปรากฏลักษณะขุ่นขาวที่เกิดจากความร้อน รอยแตกสมานที่มีการเปลี่ยนแปลง และลักษณะการดูกลืนรังสีอินฟราเรดที่ปรากฏชัดเจนที่ตำแหน่ง 3309 cm^{-1} ที่เกิดจาก O-H stretching เป็นต้น ซึ่งผลที่ได้นี้สอดคล้องกับข้อมูลที่ได้จากการทดลองเผาในห้องปฏิบัติการมาก่อนเช่นกัน

บทที่ 8 เป็นบทสรุปย่อ เกี่ยวกับการปรับปรุงคุณภาพและวิธีการตรวจสอบ พลอยทับทิม และ แซปไฟร์ ด้วยกรรมวิธีต่างๆ ตั้งแต่อดีตจนถึงปัจจุบัน โดยจะเน้นกรรมวิธีและวิธีการตรวจสอบ การปรับปรุงคุณภาพพลอยคอรัันดัม ที่พบบ่อยในตลาดพลอย ซึ่งก็คือการเผาพลอยด้วยวิธีต่างๆกันเป็นส่วนใหญ่ ได้แก่ 1) การเผาพลอยด้วยวิธีปรกติโดยใช้ความร้อนอย่างเฉียว สามารถตรวจสอบได้จาก ลักษณะมลทินเส้นเข็มรุ ไทล์ที่มักขาดเป็นจุด ๆ ลักษณะมลทินแร่ที่เปลี่ยนไป ลักษณะรอยแตกรูปงาน ล้อมรอบมลทินผลึกแร่ ลักษณะขอบสีน้ำเงินล้อมมลทินที่มีธาตุไทเทเนียมเป็นองค์ประกอบ 2) การเผาพลอยด้วยการใส่สารฟลัก เพื่อประสานและบดบังรอยแตก สามารถตรวจสอบได้จากลักษณะมลทิน ฟลักที่สมานรอยแตก และในหลุมบนผิว 3) การเผาพลอยด้วยวิธีการแพร่ธาตุจากภายนอกเข้าไปในเม็ดพลอยในระดับต้น สามารถตรวจสอบได้จากความเข้มของสีบางๆที่แตกต่างกันในแต่ละหน้าเจียรในเมื่อจุ่มพลอยในน้ำยาความหนาแน่นสูง และตรวจปริมาณธาตุที่แพร่เข้าไปที่มีปริมาณสูงผิดปกติด้วยเครื่องมือ EDXRF 4) การเผาพลอยด้วยวิธีการแพร่ธาตุจากภายนอกเข้าไปในเม็ดพลอยในระดับลึก หรือ การเผาด้วยวิธีเติมธาตุเบริลเลียม สามารถตรวจสอบได้จาก ลักษณะขอบสีเหลืองหรือส้ม หรือ ลักษณะแถบน้ำเงินล้อมด้วยขอบขาวที่ยังหลงเหลืออยู่ เมื่อจุ่มพลอยในน้ำยาความหนาแน่นสูง ลักษณะอื่นๆที่อาจช่วยประกอบ ได้แก่ ลักษณะมลทินแร่ที่ถูกทำลายอย่างรุนแรงด้วยความร้อนที่ค่อนข้างสูงและการเผาที่ยาวนาน ลักษณะการตกผลึกใหม่ของพลอยบริเวณผิว ลักษณะสีเหลืองอมเขียวที่ค่อนข้างประหลาด ลักษณะการเรืองแสงที่เป็นสีเหลืองขุ่นผิดปกติ เป็นต้น สำหรับพลอยที่ไม่แสดงลักษณะที่กล่าวมาแล้วอาจใช้เครื่องมือ LIBS หรือ LA-ICP-MS หรือ SIMS ตรวจวัดหาธาตุที่แพร่เข้าไปบริเวณผิวก็ได้ และวิธีสุดท้ายที่พบเมื่อกลางปี 2547 นี้ ได้แก่ 5) การอุดแก้วตะกั่วในรอยแตก สามารถตรวจสอบได้จาก ลักษณะการสะท้อนแสงสีฟ้าจากรอยแตก ฟองอากาศแบนๆในรอยแตก และตรวจหาธาตุตะกั่วด้วยเครื่องมือ EDXRF หรือ ในภาพเอ็กซ์เรย์ เป็นต้น

CONTENTS

	Pages
Chapter 1 Yellow and Brown coloration in Beryllium-Treated Sapphires References	1 - 39
Chapter 2 Beryllium-Diffusion Experiments on Pure Synthetic and Fe-Doped Synthetic Sapphires References	40 - 54
Chapter 3 'Classical' versus 'Beryllium' Heat-Treated Blue Sapphires References	55 - 74
Chapter 4 'Classical' versus 'Beryllium' Heat-Treated Ruby and Pink Sapphires References	75 - 134
Chapter 5 Characteristics of Ilakaka Pink sapphires before and after Heat-Treatment Experiment References	135 - 161
Chapter 6 Characteristics of Diego Blue Sapphires before and after Heat Treatment Experiment References	162 - 178
Chapter 7 'Some Characteristics of Un-Heated and Heated Natural Sapphires from the Trades References	197 - 215

CONTENTS

	Pages
Chapter 8 Ruby and Sapphire Treatments and Their Identification: A Summary of This Study and Other Recent Advancements References	216 - 263

Appendix A, B, C and D



CONTENTS (Figures)

		Page
Figure 1.1	Pink-orange, orange, yellow sapphires and ruby treated with the new heating technique. Treatment conditions are unknown (Photos by Somboon, GIT).	21
Figure 1.2	Surface-related colour zones in a yellow sapphire. Size of the stone is 10.06 x 11.57 mm. (Immersion, Photo by Leelawatanasuk, GIT).	21
Figure 1.3	Surface-related colour zones in a pink-orange sapphire. Size of the stone is 5.2 x 6.63 mm. (Immersion, Photo by Somboon, GIT).	21
Figure 1.4	An example showing a slice of a classical external Ti diffusion treated sapphire causing the blue coloured rim. Sample size is 4x7 mm (Immersion, Photo by Häger).	21
Figure 1.5	Internal diffusion of Ti from rutile inclusions into the corundum lattice showing the blue haloes (Photo by Häger).	21
Figure 1.6	UV-Vis Spectra of an un-treated yellow sapphire from Thailand (Khao Phloi Wean, Chanthaburi) with E perpendicular to c-axis (o-ray, black) and E parallel to c-axis (e-ray, red). The colour is due mainly to Fe^{3+} forbidden transition.	22
Figure 1.7	UV-Vis-spectra of a heat-treated natural yellow sapphire from Sri Lanka with E perpendicular to c-axis (o-ray, black) and E parallel to c-axis (e-ray, red). The colour is due to stable defect centres.	22
Figure 1.8	Photos of the 2.44 ct flame-fusion-grown colourless sapphire (PKSCS02) before treatment (a), pale brown after X-ray irradiation treatment (b), and almost colourless after a fading test (c). Afterward the sample was cut in half and six-points on a traverse (d) were analyzed across the cut surface using LA-ICP-MS (see also Table 1.1 and Figure 1.9). (Photos by Somboon, GIT and Lomthong, KU)	24
Figure 1.9	UV-Vis spectra of the 2.44 ct cube of flame-fusion-grown colourless sapphire (PKSCS02) before treatment (c), pale brown after X-ray	24

CONTENTS (Figures)

		Page
Figure 1.10	Photos of the 0.73 ct natural colourless sapphire (POMCS04) before treatment (a), yellow after X-ray irradiation treatment (b), and almost colourless after a fading test (c). A five-point-profile (d) was analyzed across the cut surface afterward using LA-ICP-M (see also Table 1.2 and Figure 11). (Photos by Somboon, GIT and Lomthong, KU)	25
Figure 1.11	UV-Vis spectra of the 0.73 ct natural colourless sapphire(POMCS04) before treatment (a), after X-ray irradiation treatment (b), and after a fading test (c).	25
Figure 1.12	UV-Vis spectra of an Irradiated natural sapphire heated up at a rate of 2oC/min: spectra were recorded every 10oC (Spectrum at 110oC was missing because of technical problems and wave-like pattern in the spectra about 600 to 800 nm are due to experimental inconsistencies). The irradiated yellow colour was gradually faded towards the high temperatures.	26
Figure 1.13	Photos of a 3.85 ct flame-fusion-grown colourless sapphire (PKSCS01) before treatment (a), and pale brown after Be-treatment under unknown condition (b). The pale brown rim and colourless core are better seen under immersion (c). After the treatment the sample was cut in half and a five-point profile (d) was analyzed across the cut surface using LA-ICP-MS (see also Table 1.3, Figures 1.14 and 1.15). The other half was then cut into three pieces; one piece was kept as the reference and the other two were heated in a pure nitrogen atmosphere at 1,650oC for 3 hours which turns the stone colourless (e). One of the colorless pieces was then re-heated in air (i.e. oxidation conditions) at 1,650oC for 1 hour, which turned the sample back to pale brownish (f). (Photos by Somboon, GIT and Lomthong, KU)	27

CONTENTS (Figures)

		Page
Figure 1.14	UV-Vis Spectra of the flame-fusion-grown sapphire (PKSCS01) before treatment (a) and after Be-heat treatment (b) under unknown condition. Spectrum c was recorded from a “watch glass” sapphire (WG02), which had been turned pale brown from originally colourless material by our own heating experiment at 1750oC in an oxidising atmospheres with chrysoberyl in the crucible.	28
Figure 1.15	Plots of trace element content variation across the cut surface of the pale brown Be- treated flame-fusion-grown sapphire (PKSCS01), see Figure 1.13d and text for discussion.	29
Figure 1.16	Photos of a 13.51 ct disc of colourless “watch glass” sapphire (WG01) before treatment (a), and pale brown throughout the entire disc after Be-treatment under unknown condition (b). After the treatment, a five-point profile (c) was analyzed across the 1.25-mm-thick cut surface using LA-ICP-MS (see also Table 1.4 and Figure 1.17). The other half of the sample was then cut into 3 pieces, one piece was kept as the reference whereas the other two pieces were heated in a pure nitrogen atmosphere at 1650oC for 3 hours which turned the stone colorless (d). One of the resulting colourless pieces was re-heated in air (in oxidation conditions) at 1650oC for 1 hour which turned the sample back into pale brown again (e). (Photos by Somboon, GIT and Lomthong, KU).	30
Figure 1.17	Plots of trace element content variation across the 1.25-mm-thick cut surface of the pale brown Be-treated “watch glass” sapphire disc (WG01). The contents of Be are dominant over those of Mg and Ti in almost all the points analysed, and (Be+Mg) > Ti in all analyzed points (cf. Figure 1.16c).	31

CONTENTS (Figures)

		Page
Figure 1.18	Photos of a 0.80 ct natural colourless sapphire (POMCS03) before treatment (a), yellow after Be-heat treatment (b), and in the immersion liquid (c). A five-point profile (d) was analyzed across the cut surface after the treatment using LA-ICP-MS (see also Table V and Figure 1.20). The other half was heated in a reducing atmosphere at 1650oC for 3 hours, which turned the stone colourless (e). (Photos by Somboon, GIT and Lomthong, KU)	32
Figure 1.19	UV-Vis Spectra of the natural colourless sample (POMCS03) before treatment (a) and after the Be-heat treatment (b) (see also Figure 1.18a, b).	33
Figure 1.20	Plots of trace element content variation across the cut surface of the Be-treated natural colourless sapphire (POMCS03), which became yellow after the treatment, cf. Figure 1.18d and see text for discussion.	34
Figure 1.21	Photo of a yellow sapphire (PPYS1) reportedly heat-treated with Be under unknown condition by a Thai heater. The sample appears yellow throughout the entire stone and lacks a surface-related colour zone. A five- point profile was analyzed across its cut surface (see also Table 1.6 and Figure1. 22), (Photo by Somboon, GIT and Lomthong, KU).	35
Figure 1.22	Plots of trace element content variation across the cut surface of the yellow Be-treated sapphire (PPYS1). No significant variation of Be, Mg and Ti content (also other trace elements, see Table 1.6) across the profile. All the points analysed (Figure 1.21) however, show (Be+Mg) > Ti.	36

CONTENTS (Figures)

		Page
Figure 1.23	Photos of a 2.44 ct Madagascan orangey yellow rough sapphire (MadaRough01) reportedly heat-treated with Be under unknown condition in Thailand (a). The sample appears orangey yellow throughout the entire stone and lacks a surface-related colour zone. A five-point profile was analyzed across the cut surface (b) on one half (see also Table 1.7 and Figure 1.24). The other half was heated in a reducing atmosphere at 1650oC for 3 hours, which turned the stone colourless (c). (Photos by Somboon, GIT and Lomthong, KU)	37
Figure 1.24	Plots of trace element content variation across the cut surface of the orangey yellow Be-treated rough sapphire (MadaRough01, Figure 1.23b). The analyses show higher Be content at the rims and gradually decreasing toward the core. The contents of Mg and Ti and other trace elements (see Table 1.7) however, show no consistent variation across the profile. At all the points analyzed $(Be+Mg) > Ti$.	38
Figure 1.25	Comparison of the UV-Vis spectra of synthetic samples: irradiated with X-rays (turned brown after treatment, a), diffusion treated with Be (turned brown after treatment, b), and doped with Mg (brown to violet specimen was obtained, c).	39
Figure 1.26	Comparison of the UV-Vis spectra of yellow sapphires: a natural sample irradiated with X-rays (b), natural samples with Be-treatment (c and f), a natural sample from Sri Lanka (d), the difference of absorption spectra between an orange Be-treated sapphire and its original pink sample (a), a synthetic sample double-doped with Mg and Fe (e).	39
Figure 2.1	Photos of the LA-ICP-MS unit used for trace element analysis in this study, located at the Macquaries University, Sydney, Australia.	45

CONTENTS (Figures)

		Page
Figure 2.2	A colorless sapphire disc (THSCS01) was cut in half, one half was heat-treated with ground chrysoberyl in a crucible (a, brown) while the other half was heat-treated in another crucible without chrysoberyl (b, colourless). After the treatment five-points on a traverse were analyzed on the polished surface of each half. (Photo by Somboon, GIT)	46
Figure 2.3	Plots of trace element contents analyzed on the surface of the sapphire disc (THSCS01), see text for discussion.	47
Figure 2.4	UV-Vis spectra of the flame-fusion-grown sapphire (PKSCS01) before treatment (a) and after Be- treatment under unknown condition by a Thai heater (b). Spectrum c was recorded from the brown half (THSCS01) treated with Be by our own experiment.	48
Figure 2.5	Photos of a Fe-doped flame-fusion-grown colourless sapphire before treatment (a), yellow after X-ray irradiation treatment (b), colourless after a fading test (c), yellow again after Be-treatment (d) and the colour was stable under the fading test. (Photo by Häger)	49
Figure 2.6	Photos of the Fe-doped sapphire treated with Be and cut in half (a), showing abundant gas bubbles (b and c). Two traverses (X1 and X2) were analyzed across the cut surface (d) using LA-ICP-MS (see also Table 2.2 and Figure 2.9).(Photo by Somboon, GIT)	50
Figure 2.7	UV-Vis spectra of the Fe-doped flame-fusion-grown sapphire before treatment (a), after X-ray irradiation treatment (b), after a fading test (c), and after Be-treatment (d). The spectrum produced by Be-treatment is exactly the same as that of the irradiation treatment and similar to those of the Mg+Fe doped flame-fusion-grown sapphire and a natural Sri Lankan yellow sapphire coloured by stable defect centres (see Figure 2.8).All spectra were measured with E perpendicular to c-axis (o-ray).	51

CONTENTS (Figures)

		Page
Figure 2.8	UV-Vis Spectra of a natural Sri Lankan yellow sapphire coloured by stable defect centres in comparison to a synthetic flame fusion grown sapphire doped with 50 ppm Mg and 50 ppm Fe (Hager, 2001).	52
Figure 2.9	Plots of the trace element content along the traverse X1 of the Fe-doped synthetic sapphire treated with Be. The Fe and Be contents are constantly high across the cut surface while the other elements are extremely low.	54
Figure 3.1	A natural blue sapphire (DIF1) reportedly underwent a 'classical' heat-treatment was cut in half. A five-point-profile was analyzed across the cut surface using LA-ICP-MS. (Photo by Lomthong, KU)	60
Figure 3.2	Plots of the trace element content variation across the cut surface of the blue sapphire (DIF1) treated with a 'classical' heating. The analyses show negligible contents of Be and Ti >> Mg in all points analyzed.	61
Figure 3.3	An Australian blue sapphire (AUS1) reportedly underwent a 'classical' heat-treatment was cut in half. A five-point-profile was analyzed across the cut surface using LA-ICP-MS (Photo by Lomthong, KU)	32
Figure 3.4	Plots of the trace element content variation across the cut surface of the Australian blue sapphire (AUS1) treated with a 'classical' heating. The analyses show negligible contents of Be and Ti > Mg in all point analyzed.	63

CONTENTS (Figures)

		Page
Figure 3.5	A natural blue sapphire (PPBS1) reportedly heat-treated with Be under unknown condition by a Thai heater and cut in half. The sample shows a thin surface-related yellow rim surrounding the blue core. High magnification reveals that the blue core contains oriented blue dots probably resulting from partial dissolution of rutile needles. A five-point profile was analyzed across the cut surface with two points in the surface-related yellow zone (rims) and three points in the blue core. (Photo by Lomthong, KU)	64
Figure 3.6	Plots of the trace element content variation across the cut surface of the Be-treated blue sapphire (PPBS1). The Be content are obviously high at the yellow rims and are negligible in the blue core. The content of Mg and Ti (also other trace elements) however show no consistent variation across the profile. The analyses also show $(\text{Be}+\text{Mg}) > \text{Ti}$ at the yellow rims in contrast to $\text{Ti} > (\text{Be}+\text{Mg})$ in the blue core.	66
Figure 3.7	A rectangular block of a natural blue-green sapphire (BG1) heat-treated with Be by a Thai heater showing a thin surface-related yellow rim surrounding the complex-zoned blue core (a, in immersion liquid). After the treatment the sample was cut in half (b, in immersion; c, in air) and a five-point profile was analyzed across the cut surface using LA-ICP-MS. Two points on both rims are very close to the yellow zone (rim) while three points in the middle are definitely in the blue core. (Photo by Somboon, GIT)	66
Figure 3.8	Plots of the trace element content variation across the cut surface of the Be-treated blue-green sapphire (BG1). The Be contents are obviously high at the rims and decrease toward the core. The analyses show $\text{Ti} > (\text{Be}+\text{Mg})$ in all the analyzed points which are still	68

CONTENTS (Figures)

		Page
Figure 3.9	(a) The rectangular block of the Be-treated natural blue-green sapphire (BG1) in immersion liquid. (b) The photo of the right face of (a), which are definitely in the yellow rim, showing seven analyzed points. (Photo by Somboon, GIT)	69
Figure 3.10	Plots of the trace element contents analyzed on the outer surface of the Be-treated blue-green sapphire (BG1). The analyses show obviously high Be contents and $Ti > Mg$ in contrast to $(Be+Mg) > Ti$ at all the analyzed points which are definitely in the yellow rim.	71
Figure 3.11	A natural blue sapphire was cut in half; the left half was heat-treated with ground chrysoberyl in a crucible while the right half was heated in another crucibles without chrysoberyl. The heating condition for both crucibles was 1,750oC for 30 hours in air. After heat treatment the left half shows obviously surface-related yellow rim whereas the right half is blue throughout the stone. (Photo by Häger)	72
Figure 3.12	Approximate compositions of the stones plotted in the (oxidizing atmosphere) triangular diagram model proposed by Häger (1996).	73
Figure 3.13	Approximate compositions of the stones plotted in the (reducing atmosphere) triangular diagram model proposed by (Häger, 1996).	74
Figure 4.1	Colours of eleven Ilakaka (Madagascar) sapphires before treatment (above, pink) and after Be-treatment under unknown condition by a Thai heater (below, orangey pink and orange). (Photo by Somboon, GIT)	86
Figure 4.2	Surface related orange zone can be seen when the stones are immersed in methylene iodide solution. (Photo by Somboon, GIT)	88
Figure 4.3	UV-Vis spectra of a pale pink Madagascan sapphire before treatment and the pink-orange sapphire after treatment with Be (a). Residual spectrum after the subtraction of the one before treatment from the other after Be-treatment (b).	89

CONTENTS (Figures)

		Page
Figure 4.4	An un-treated pink Madagascan sapphire (GITMDP18) was cut in half and a six-point profile was analyzed across the cut surface using LA-ICP-MS. (Photo by Lomthong, KU)	91
Figure 4.5	Plot of trace element content variation across the cut surface of the un-treated pink Madagascan sapphire (GITMDP18, Figure 4.4) showing Mg > Ti (< ~ 30 atom mole ppm which is not enough to create orange coloration) and negligible Be contents in all points analyzed.	92
Figure 4.6	A 'classically' heat-treated orange sapphire (KN1) was cut in half and a five-point profile was analyzed across the cut surface using LA-ICP-MS. (Photo by Lomthong, KU)	93
Figure 4.7	Plot of trace element content variation across the cut surface of the 'classically' heat-treated orange sapphire (KN1, Figure 4.6) showing Mg > Ti (> 30 atom mole ppm which is enough to create orange coloration) and negligible Be contents in all points analyzed.	94
Figure 4.8	Mong Hsu (Myanmar) and Vietnamese rubies of metamorphic origin reportedly treated unsuccessfully by a Be-heating technique (Themelis, 2003).	96
Figure 4.9	Three Mong Hsu rubies still appear red, purplish red or pink after a Be-treatment by a Thai heater. (Photo by Somboon, GIT)	97
Figure 4.1	Five Vietnamese rubies still appear red, purplish or bluish red or pink after the same Be-treatment as in Figure 4.9. (Photo by Somboon, GIT)	98
Figure 4.11	Three orange Songea (Tanzania) sapphires were treated from originally brownish red stones under the same Be-heating run as in Figures 4.9 and 4.10. Note the surface-related colour zones are clearly seen in immersion	99

CONTENTS (Figures)

		Page
Figure 4.12	Close examination of a Be-treated Mong Hsu Ruby (CR0054) shows very thin surface-related yellow or orange rim in immersion liquid. Top photo, before cutting; Bottom photo, after cutting in half. Close-space points on a traverse were analyzed across the cut surface using LA-ICP-MS. (Photo by Somboon, GIT)	100
Figure 4.13	Another Be-treated Mong Hsu Ruby (CR119) shows very thin surface-related yellow or orange rim in immersion liquid. Top photo before cutting; Bottom photo, after cutting in half. Close-space points on a traverse were analyzed across the cut surface using LA-ICP-MS. (Photo by Somboon, GIT)	101
Figure 4.14	A Be-treated Vietnamese Ruby (CRVN02) shows thin patchy surface-related yellow or orange rim in immersion liquid. Top photo, before cutting; Bottom photo, after cutting in half. Close-space points on a traverse were analyzed across the cut surface using LA-ICP-MS. (Photo by Somboon, GIT)	102
Figure 4.15a	Plots of trace element content variation across the cut surface of the Be-treated Mong Hsu ruby (CR0054). The lower diagram is an enlargement of the upper diagram. Note the extremely high contents of Be and Fe at the rims	104
Figure 4.15b	Plots of trace element content variation across the cut surface of the Be-treated Mong Hsu ruby (CR0054). The lower diagram is an enlargement of the upper diagram. The analyses show $(Be+Mg) \gg Ti$ which corresponds fairly well with very thin yellow or orange rims in contrast to $(Be+Mg) < Ti$ in the red core area.	105

CONTENTS (Figures)

		Page
Figure 4.16a	Plots of trace element content variation across the cut surface of the Be-treated Mong Hsu ruby (CR119). The lower diagram is an enlargement of the upper diagram. Note the extremely high contents of Be and Fe at the rims.	107
Figure 4.16b	Plots of trace element content variation across the cut surface of the Be-treated Mong Hsu ruby (CR119). The lower diagram is an enlargement of the upper diagram. The analyses show $(\text{Be}+\text{Mg}) \gg \text{Ti}$ which corresponds fairly well with very thin yellow or orange rims in contrast to $(\text{Be}+\text{Mg}) < \text{Ti}$ in the red core area.	108
Figure 4.17a	Plots of trace element content variation across the cut surface of the Be-treated Vietnamese ruby (CRV N02). The lower diagram is an enlargement of the upper diagram. Note the extremely high contents of Be and Fe at the rim.	110
Figure 4.17b	Plots of trace element content variation across the cut surface of the Be-treated Vietnamese ruby (CR0054). The lower diagram is an enlargement of the upper diagram. The analyses show $(\text{Be}+\text{Mg}) \gg \text{Ti}$ which corresponds fairly well with very thin yellow or orange rims in contrast to $(\text{Be}+\text{Mg}) < \text{Ti}$ in the red core area.	111
Figure 4.18	An Andila ruby (AR02) reportedly heat-treated with Be. Top, before cutting in immersion liquid showing obviously a surface related yellow or orange rim and a blue core; Bottom, a half-cut piece showing a five-point across the cut surface using LA-ICP-MS. Three points in the middle are within the blue zone while the other two points are at the yellow or orange rim. The blue zone is caused by internal diffusion of Ti-bearing inclusions. (Photo by Somboon, GIT and Lomthong, KU)	112

CONTENTS (Figures)

		Page
Figure 4.19	Plot of trace element content variation across the cut surface of the Be-treated Andila Ruby (AR02, Figure 4.15) showing Ti > or ~Mg contents in all points analyzed. The Be contents are obviously high at the orange rims and are negligible in the blue zone. Two points at both rims show Be+Mg > Ti whereas three points in the blue zone show Ti > Be+Mg.	114
Figure 4.20	A rough Ilakaka violet sapphire (THMPS04) was cut into three pieces. One piece was kept as the reference (a, violet) while the second piece was heat-treated with ground chrysoberyl in a crucible (b, darker violet) and piece was heat-treated in another crucible without chrysoberyl (c, still violet). The heating condition for both crucibles was 1750oC for 30 hours in air. After the treatment the sample b and c were lightly polished and five-points on a traverse were analyzed on the polished surface of each piece using LA-ICP-MS. (Photo by Somboon, GIT)	115
Figure 4.21	Plot of trace element content variation across lightly polished surfaces of the rough Ilakaka violet sapphire (THMPS04, Figure 4.20). The analyses on the 'classically' heat-treated piece (c) show no detectable Be and Ti > Mg in all points analyzed . The analyses on the Be-treated piece (b) show a diffusion of Be into the corundum lattice but Ti contents are still in excess or slightly less than Be+Mg in all points analyzed.	116
Figure 4.22	An orange Songea sapphire (SGDH09) reportedly underwent a Be-treatment was cut in half and a five-point profile was analyzed across the cut surface using LA-ICP-MS. (Photo by Lomthong, KU)	118

CONTENTS (Figures)

		Page
Figure 4.23	Plot of trace element content variation across the cut surface of the Be-treated orange Songea sapphire (SGDH09, Figure 4.22) showing slight $Mg > Ti$ contents in all analyzed points. The Be contents are obviously high at the rims and are negligible in the core. The Be+Mg contents therefore exceed Ti contents especially at the rims.	119
Figure 4.24	A rough Songea sapphire (THSR01) was cut into two pieces, one piece was heat-treated with ground chrysoberyl in a crucible (a, orange) while the other piece was heat-treated in another crucible without chrysoberyl (b, brownish red). The heating condition for both crucibles was 1750oC for 30 hours in air. After the treatment both samples were lightly polished and five-points on a traverse were analyzed on the polished surface of each piece using LA-ICP-MS. (Photo by Somboon, GIT)	120
Figure 4.25	Plot of trace element content variation across lightly polished surfaces of the rough Songea sapphire (THSR01, Figure 4.24). The analyses on the ‘classically’ heat-treated piece (b) show no detectable Be and about equal proportion of Ti and Mg in all points analyzed. The analyses on the Be-treated piece (a) also show $Ti \sim Mg$ and significant amount of Be diffused into the corundum lattice by which $Be+Mg > Ti$ in all points analyzed.	121
Figure 4.26	An orangey pink Madagascan sapphire (WSMDIF7) reportedly underwent a Be-treatment was cut in half and a five-point profile was analyzed across the cut surface using LA-ICP-MS. (Photo by Lomthong, KU)	122

CONTENTS (Figures)

		Page
Figure 4.27	<p>Plot of trace element content variation across the cut surface of orangey pink Madagascan sapphire (WSMDIF7, Figure 4.26) showing Be diffusion into the corundum lattice from an external source and slight excess of Mg over Ti contents in all the analyzed points. The Be+Mg contents therefore exceed Ti content especially at rims.</p>	123
Figure 4.28	<p>A rough Ilakaka (Madagascar) pink sapphire (THMPS05) was cut into three pieces. One piece was kept as the reference (a, violetish pink) while the second piece was heat-treated with ground chrysoberyl in a crucible (b, orange) and the third piece was heat-treated in another crucible without chrysoberyl (c, pink). The heating condition for both crucibles was 1750°C for 30 hours in air. After the treatment the sample b and c were lightly polished and five-points on a traverse were analyzed on the polished surface of each piece using LA-ICP-MS. (Photo by Somboon, GIT)</p>	124
Figure 4.29	<p>Plot of trace element content variation across lightly polished surfaces of the rough Ilakaka pink sapphire (THMPS05, Figure 4.28). The analyses on the ‘classically’ heat-treated piece (c) show no detectable Be and slight Mg > Ti in all points analyzed. The analyses on the Be-treated piece (b) also show slight Ti > Mg and significant amount of Be diffused into the corundum lattice by which Be+Mg >> Ti in all points analyzed.</p>	125

CONTENTS (Figures)

	Page
Figure 4.30	126
<p>A rough Ilakaka (Madagascar) pink sapphire (THMPS01) was cut into three pieces. One piece was kept as the reference (a, violetish pink) while the second piece was heat-treated with ground chrysoberyl in a crucible (b, orange) and the third piece was heat-treated in another crucible without chrysoberyl (c, pink). The heating condition for both crucibles was 1750oC for 30 hours in air. After the treatment the sample b and c were lightly polished and five-points on a traverse were analyzed on the polished surface of each piece using LA-ICP-MS. (Photo by Somboon, GIT)</p>	
Figure 4.31	127
<p>Plot of trace element content variation across lightly polished surfaces of the rough Ilakaka pink sapphire (THMPS01, Figure 4.30). The analyses on the 'classically' heat-treated piece (c) show no detectable Be and slight $Mg > Ti$ in all points analyzed. The analyses on the Be-treated piece (b) also show slight $Ti > Mg$ and significant amount of Be diffused into the corundum lattice by which $Be+Mg \gg Ti$ in all points analyzed.</p>	
Figure 4.32	128
<p>A rough Ilakaka (Madagascar) pink sapphire (THMPS02) was cut into three pieces. One piece was kept as the reference (a, pink) while the second piece was heat-treated with ground chrysoberyl in a crucible (b, orange) and the third piece was heat-treated in another crucible without chrysoberyl (c, pink). The heating condition for both crucibles was 1750oC for 30 hours the treatment the sample b and c were lightly polished and five-points on a traverse were analyzed on the polished surface of each piece using LA-ICP-MS. (Photo by Somboon, GIT)</p>	

CONTENTS (Figures)

		Page
Figure 4.33	Plot of trace element content variation across lightly polished surfaces of the rough Ilakaka pink sapphire (THMPS02, Figure 4.32). The analyses on the ‘classically’ heat-treated piece (c) show no detectable Be and slight $Mg > Ti$ in all points analyzed. The analyses on the Be-treated piece (b) also show slight $Ti > Mg$ and significant amount of Be diffused into the corundum lattice by which $Be+Mg \gg Ti$ in all points analyzed.	129
Figure 4.34	A synthetic ruby (PPSR1) reportedly treated with Be shows orangey red color. The stone was cut in half and a five-point profile was analyzed across the cut surface using LA-ICP-MS. (Photo by Lomthong, KU)	131
Figure 4.35	Plot of trace element content variation across the cut surface of the Be-treated synthetic ruby (PPSR1), Figure 4.34). The Be contents are obviously high at the rims and decrease toward the core indicating Be diffusion into the corundum lattice from an external source.	132
Figure 4.36	A synthetic ruby was cut in half; the left half was heat-treated with ground chrysoberyl in a crucible while the right half was heated in another crucible without chrysoberyl. The heating condition for both crucibles was 1,750°C for 30 hours in air. After the treatment the left half shows surface-related orange rim while the right half is still red. (Photo by Somboon, GIT)	133
Figure 4.37	Approximate compositions of the stones plotted in the triangular diagram model proposed by Häger (1996).	134
Figure 5.1	Lindberg electric furnace (Model 59256-E6) and accessory.	136
Figure 5.2	Most zircon inclusions in these two sapphire samples were clear and appear unchanged after a step-heating from 800°C to 1600°C.	140

CONTENTS (Figures)

		Page
Figure 5.4	A cluster of zircon inclusions was still unchanged after the step-heating from 800°C to 1600°C (sample no. PP6, 140X).	141
Figure 5.5	Another cluster of zircon inclusions with minor tension disc(incircle) was still unchanged after the step-heating from 800°C to 1600°C (sample no. PK3, 70X).	142
Figure 5.6	Many zircon clusters with tension cracks (in circle) were still unchanged after the step-heating from 800°C to 1600°C.	143
Figure 5.7	Most of individual zircon inclusions were still unchanged after the step-heating from 800°C-1600°C whereas the zircon cluster (in circle) showed minor tension crack at 1000°C. At 1400°C and 1600°C, this tension crack became more obvious (sample no. P6, 70X).	144
Figure 5.8	A zircon inclusion with slight tension crack was still unchanged at 800°C. At 1000°C-1600°C, this tension crack was obviously expanded (sample no. P5, 140X).	144
Figure 5.9	A relatively large and clear zircon inclusion (in circle) was still unchanged at 800°C. However, at 1000°C, the crystal began to alter into whitish, cloudy appearance (turbid) with minor tension crack. The tension crack became more obvious at 1400°C. The crystal was partially decomposed at 1600°C (sample no. P6, 70X).	145
Figure 5.10	Zircon inclusions (in circle) showed tension crack at 1200°C. At 1600°C, they began to decompose into whitish, cloudy appearance (turbid) with obvious tension crack (sample no. P6, 70X).	146
Figure 5.11	Most zircon inclusions were still unchanged after the step-heating from 800° to 1600°C except the crystal in circle began to alter with minor tension crack at 1400°C. At 1600°C, it was obviously altered into whitish, cloudy appearance (turbid) with well developed tension crack (sample no. LP9, 140X).	146
Figure 5.12	Most of the zircon inclusions were still unchanged after the step-heating from 800°C to 1600°C except some crystals in circle became turbid at 1600°C (sample no. PP6, 140X).	147

CONTENTS (Figures)

		Page
Figure 5.13	Most of the zircon inclusions were still unchanged after the step-heating from 800°C to 1600°C except some crystals in circle became turbid at 1600°C (sample no. LP3, 140X).	147
Figure 5.14	Most of the zircon inclusions were still unchanged after the step heating from 800°C to 1600°C except some crystals in circle became turbid at 1600°C.	148
Figure 5.15	Most zircon inclusions were still unchanged after the step-heating from 800°C to 1600°C except some crystals in circle became turbid at 1600°C.	149
Figure 5.16	Zircon clusters with minor tension discs before heating. The tension discs were noticeably expanded at 800°C and became more obvious at higher temperatures. It should also be noted that some crystals in zircon clusters appear turbid at 1200°C. The decomposition of those zircon crystals became more pronounced at higher temperatures (sample no. PK8, 70X).	150
Figure 5.17	A zircon clusters was still unchanged at 800°C. The tension discs began to develop at 1000°C. At 1400°C to 1600°C, these tension discs became more obvious (sample no. PP4, 140X).	151
Figure 5.18	A zircon cluster was still unchanged at 800°C but showed an obvious development of tension discs at 1000°C to 1600°C. Furthermore, most crystals in the cluster became turbid at 1400°C while a monazite inclusion was altered at 1600°C (sample no. PP4, 140X).	151
Figure 5.19	Showing zircon clusters with slight tension crack before heating. They were still unchanged at 800°C to 1200°C (sample no. PP6, 140X). (A) At 1400°C, some zircon crystals in the clusters began to decompose into whitish cloudy appearance and were obviously decomposed at 1600°C (B) At 1400°C, tension crack was expanded and some zircon crystals in the clusters began to decompose. These crystals were obviously decomposed at 1600°C.	152

CONTENTS (Figures)

		Page
Figure 5.20	Showing zircon clusters with minor tension crack before heating. They were still unchanged at 800 ^o to 1200 ^o C,. At 1400 ^o C, some zircon crystals in the clusters began to decompose into whitish cloudy appearance and the tension crack was expanded. At 1600 ^o C, the crack expanded more and the crystals clearly became turbid (sample no. LP3, 70X).	153
Figure 5.21	A monazite inclusion was still unchanged after a step-heating from 800 ^o C to 1600 ^o C (sample no. PK3, 70X).	154
Figure 5.22	A mica inclusion was still the same at 800 ^o C. At 1000 ^o C, the crystal began to alter and was altered more at higher temperatures. The tension crack start to form around the inclusion at 1200 ^o C and it became more and more obvious at 1400 ^o and 1600 ^o C (sample no. P6, 70X).	155
Figure 5.23	Another mica inclusion was still unchanged at 800 ^o C. At 1000 ^o C, the inclusion was partially altered or appeared slightly turbid with minor tension crack. The alteration and tension crack became more and more obvious at 1200 ^o , 1400 ^o and 1600 ^o C (sample no. LP3, 70X).	156
Figure 5.24	Colour of some rutile inclusions was changed from dark brown-black to red with minor tension crack at 800 ^o C. At higher temperatures (1400 ^o C -1600 ^o C) red colour was more intense and the tension crack became more obvious (sample no. PP3).	157
Figure 5.25	obvious and the inclusions showed melted boundary at higher temperatures (sample no. PP3, 70X).	158
Figure 5.26	Rutile needles intersecting each other at 60 ^o /120 ^o angles were still unchanged at 800-1400 ^o C but partially dissolved into the host sapphire creating a dot-like pattern at 1600 ^o C (sample no. MV2).	158
Figure 5.27	Rutile silks were still unchanged when heated at lower	159

CONTENTS (Figures)

		Page
Figure 5.28	Milky and dust zones became clearer at 1600°C.	160
Figure 5.29	A sapphire showed a faint fingerprint at 800°C and it was more and more obvious at 1000°C and 1600°C (sample no. P6, 70X).	161
Figure 5.30	Fingerprints in an unheated sapphire were expanded at 1200°C and 1600°C (sample no. PP6, 50X).	161
Figure 6.1	Growth pattern of a Diego sapphire before treatment (A). At 1,350°C (B) and 1,650°C (C) the colour zones became more and more intense and the milky characteristic was progressively disappeared.	164
Figure 6.2	A similar feature to Figure 6.1	165
Figure 6.3	Ditto.	166
Figure 6.4	Ditto.	167
Figure 6.5	Ditto.	168
Figure 6.6	Ditto.	169
Figure 6.7	Milky appearance of a sapphire before treatment (A). At 1,350°C (B) and 1,650°C (C), the milky appearance was progressively reduced.	170
Figure 6.8	Ditto.	171
Figure 6.9	Fracture-filled yellow materials in a sapphire before treatment (A). At 1,350°C (B) and 1,650°C (C), the materials were progressively clear.	172
Figure 6.10	Fracture-filled orange materials in a sapphire before treatment (A). At 1,350°C (B) and 1,650°C (C), the materials were progressively clear.	172
Figure 6.11	Ditto.	174
Figure 6.12	Solid inclusions before treatment (A), the formation of tension cracks or discoids surrounding the inclusions at 1,350°C (B) and 1,650°C (C).	175
Figure 6.13	Small tension disc was already formed around a ferrocolumbite inclusion before treatment. It was obviously expanded at 1,350°C (B)	176

CONTENTS (Figures)

		Page
Figure 6.14	A cluster of zircon inclusions before treatment (A). The inclusions became turbid with tension discs at 1,350°C (B) and 1,650°C (C).	177
Figure 6.15	Changes of Raman spectra of a zircon inclusion in a violet sapphire after heat treatment.	178
Figure 7.1	Series of un-heated Ilakaka blue sapphires (13 samples) varying from pale to very dark blue (with the courtesy of World Sapphires Co. Ltd.)	184
Figure 7.2	The 4.18 ct un-heated Ilakaka blue sapphires with hazy appearance.	184
Figure 7.3	Fine long rutile silks associated with very fine particles which make the stone appear hazy typical of un-heated sample.	185
Figure 7.4	Rather sharp edge dark fingerprint.	185
Figure 7.5	This 1.83 ct un-heated Ilakaka blue sapphires commonly shows hazy appearance.	186
Figure 7.6	The hazy appearance with well-formed fingerprints or healed fractures of the un-heated stone.	186
Figure 7.7	This 3.25 ct un-heated Ilakaka blue sapphires with hazy appearance.	187
Figure 7.8	The well-formed continuous long and sharp rutile silks and zones of dust particles of the un-heated stone.	187
Figure 7.9	Well-formed fingerprints or healed fractures with sharp boundary in un-heated 3.43 ct blue sapphire.	188
Figure 7.10	Close-up of parallel long fluid inclusion fingerprint with sharp boundary.	188
Figure 7.11	Sharp boundary and well formed negative (CO ₂) inclusions in un-heated stone.	189
Figure 7.12	Yellowish orange colour impurity in healed fractures is also suggesting un-heated feature.	189
Figure 7.13	Series of 16 un-heated blue sapphires ranging from pale to dark blue	190

CONTENTS (Figures)

	Page
Figure 7.14 This 0.55 ct un-heated Mada sapphire showing bands of rutile dusts.	191
Figure 7.15 Within the bands of fine dust there are rutile needles cross-cutting in three directions at 60/120 angles.	191
Figure 7.16 An orangey brown inclusion (probably radiocative mineral) with tension cracks also found in un-heated sample.	192
Figure 7.17 Another view of dark brown inclusions (rutile?) with negative crystal inclusions.	192
Figure 7.18 Another un-heated 0.74 ct Mada blue sapphire loaded with inclusions.	193
Figure 7.19 The colourless sillimanite inclusions (confirmed Raman) still well intacted.	193
Figure 7.20 Another view of clusters of sillimanite inclusions .	194
Figure 7.21 The dark red inclusions of unknown mineral (cannot be confirmed by Raman) still well intacted.	194
Figure 7.22 Silky appearance in the 0.38 ct un-heated Mada blue sapphire.	195
Figure 7.23 Long and continuous silks is a good indication of un-heated stone.	195
Figure 7.24 The 0.39 ct Mada blue sapphire showing long and short but continuous needles.	196
Figure 7.25 Close-up of continuous needles (more than three parallel sets) indicating of un-heating condition.	196
Figure 7.26 This 0.46 ct Mada blue sapphire contains many negative crystal inclusions or fluid inclusions in overall hazy or cloudy body.	197
Figure 7.27 Negative crystal inclusions containing CO ₂ (confirmed by Raman) with naturally healed discoids still well intacted in un-heated sample.	197
Figure 7.28 Another 1.06 ct Mada blue sapphire contains many long hollow tubes filled with impurity and well intacted rutile silks.	198
Figure 7.29 The hollow tube filled with dark red impurity is a good indication of	198

CONTENTS (Figures)

		Page
Figure 7.30	Overview of two heated Mada blue sapphires (4.84 ct left, 4.69 ct right).	199
Figure 7.31	Magnification of the one on the right (4.69 ct) showing rather clear stone.	199
Figure 7.32	The stone shows obvious thin-film tension disc due to heating.	200
Figure 7.33	The shiny thin-film discoids surrounding altered turbid inclusions.	200
Figure 7.34	This heated Mada blue sapphires (4.84 ct) showing alternating milky and clear zones indicating that the strong milky zone still remain after heating.	201
Figure 7.35	Showing altered fingerprints.	201
Figure 7.36	FTIR spectra of 4.18 ct un-heated (above) and 4.69 ct heated (below) blue sapphires from Madagascar. The un-heated one shows vary weak OH-streaching peak at 3309 cm ⁻¹ whereas the heated one shows very strong OH-streaching peak at 3309 cm ⁻¹ and other side peaks.	202
Figure 7.37	Series of un-heated and heated Myanmar blue sapphires ranging from medium to dark blue (with the courtesy of World Sapphires Co. Ltd.).	203
Figure 7.38	This 4.32 ct Myanmar blue sapphires showing long and sharp rutile silks with hazy appearance characteristic of natural un-heated stone.	203
Figure 7.39	The rutile silks or needles are long, well-formed and sharp with clear fingerprints.	204
Figure 7.40	Fingerprints or healed fractures are not uncommon in un-heated sample.	204
Figure 7.41	Patchy long and sharp rutile silks are typical of un-heated Burmese 2.77 ct stone.	205
Figure 7.42	The rutile silks are long and sharp with arrow or knife-shape typical of un-heated stone.	205

CONTENTS (Figures)

		Page
Figure 7.43	This 21.89 ct Myanmar heated blue sapphire showing hazy appearance which might be mistaken as natural un-heating stone.	206
Figure 7.44	However when look closer the very fine rutile silks appear as dotted lines which would suggest the heated stone. The very fine milky growth bands may still remain after heat treatment.	206
Figure 7.45	The inclusion also show shiny tension disc indicating the heated stone.	207
Figure 7.46	Another inclusion with thin-film tension disc indicating the heated stone.	207
Figure 7.47	This 5.99 ct Myanmar heated blue sapphires showing slight hazy appearance.	208
Figure 7.48	strong thin-film discoids surrounding inclusion is a good indication of heating.	208
Figure 7.49	Altered fingerprints due to heating.	209
Figure 7.50	Shiny tension disc and dotted needles are obvious of heating.	209
Figure 7.51	This 2.74 ct Myanmar blue sapphires showing strong tension disc due to heating.	210
Figure 7.52	Thin-film tension disc is obvious of heating.	210
Figure 7.53	Shiny thin-film tension disc is obvious indication of heating.	211
Figure 7.54	Obviously altered fingerprints due to heating.	211
Figure 7.55	FTIR spectra of 4.32 ct (above) and 2.77 ct (below) un-heated blue sapphires from Myanmar showing vary small OH-streaching peak at 3309 cm ⁻¹ .	212
Figure 7.56	FTIR spectra of 21.89 ct (above) and 2.74 ct (below) heated blue sapphires from Myanmar showing vary strong OH-streaching peak at 3309 cm ⁻¹ and other side peaks.	213
Figure 8.1a	Heat treatment of Madagascan sapphires to improve their color and	221

CONTENTS (Figures)

		Page
Figure 8.1b	Continued (Photos by Somboon, GIT).	222
Figure 8.2	Different types of high temperature (up to $\sim 1850^{\circ}\text{C}$) furnaces commonly used by Thai heaters. (Photos by Singbamroong, GIT)	223
Figure 8.3	A clear zircon inclusion before treatment (in circle) became turbid with well developed tension crack after a stone was heated at 1600°C . (Sample no. LP9, 140X, Photos by Pattamalai, DMR)	224
Figure 8.4	A mica inclusion was obviously altered with tension cracks at 1600°C . (Photos by Pattamalai, DMR)	225
Figure 8.5	Needle inclusions were partially dissolved in the host sapphire creating dot-like pattern after a stone was heated at 1600°C . (Photos by Pattamalai, DMR)	226
Figure 8.6	Partially dissolved rutile-needles with color bleeding. (Photos by Somboon, GIT)	227
Figure 8.7	Milky and dust zones became clearer when a stone was heated at 1600°C . (Photos by Pattamalai, DMR)	228
Figure 8.8	This 5.99 ct Myanmar heated blue sapphires showing slightly hazy appearance (a), strong thin-film discoid surrounding an inclusion is a good indication of heating (b), altered fingerprints are due to heating (c), a shiny tension disc and dotted needles are obvious indication of heating (d). (Photos by Somboon, GIT)	223
Figure 8.9	A 4.69 ct Mada sapphire showing rather clear stone. The stone shows obvious thin-film tension disc due to heating. (Photos by Somboon, GIT)	230
Figure 8.10	Internal diffusion of Ti from rutile inclusions into the corundum lattice showing the blue haloes (~ 0.06 mm) is a good indication of heating. (Photo by Häger).	231
Figure 8.11	Patchy long and sharp rutile silks in un-heated Burmese 2.77 ct stone. The rutile silks are long and sharp with arrow or knife-shape typical of un-heated stone. (Photos by Somboon, GIT)	232

CONTENTS (Figures)

		Page
Figure 8.12	This 3.25 ct un-heated Ilakaka sapphire shows bazy appearance. The well-formed continuous long and sharp rutile silks and zones of dust particles are typical of the un-heated stone. (Photos by Somboon, GIT)	233
Figure 8.13	This 0.46 ct Madagascan blue sapphire contains negative crystal inclusions filled with CO ₂ (confirmed by Raman spectroscopy). The undisturbed fluid inclusions are a good indication of un-heated stone. (Photos by Somboon, GIT)	234
Figure 8.14	A 0.39 ct. Madagascan blue sapphire showing long and short but continuous needles. Continuous needles (more than three parallel sets) indicates an un-heating condition. (Photos by Somboon, GIT)	235
Figure 8.15	An un-heated 0.74 ct Madagascan blue Sapphire contains numerous inclusions (a). The colourless sillimanite inclusions (confirmed Raman spectroscopy) still well intacted (b). The dark red inclusions of unknown mineral (cannot be confirmed by Raman spectroscopy) still well intacted (c). (Photos by Somboon, GIT)	236
Figure 8.16	The presence of flux residues in healed fissures is a good indication of a flux-enhanced heating. (Photos by Leelawathanasuk, GIT)	237
Figure 8.17	Cavity-filling flux-residues appear lower luster reflection on polished surface.	238
Figure 8.18a	A quantification of the amount of flux materials in a stone	239
Figure 8.18b	Continued	240
Figure 8.19	Blue-diffused sapphires showing slices of colourless interior with blue rim (~ 0.09 mm) caused by external diffusion of Ti into the stones.	241
Figure 8.20	A parcel of blue-diffused sapphires (a). The presence of uneven shallow color concentration at different facets and faceted junctions of a blue-diffused sapphire in immersion. (Photos by Somboon, GIT)	242

CONTENTS (Figures)

		Page
Figure 8.21	An elevated concentration of diffused Ti can be detected using EDXRF	243
Figure 8.22	A parcel of diffused rubies showing uneven shallow color concentration at different facets . (immersion; Hughes, 1997)	244
Figure 8.23	Multitude of colours in Be diffusion-treated sapphires such as pink-orange, orange, yellow and orangey red. (Photos by Somboon, GIT)	245
Figure 8.24	Stones before treatment and after treatment with Be	246
Figure 8.25	Surface-related colour zone is a diagnostic features of yellow Be-diffusion treated sapphires. (Immersion; Photos by Leelawatanasuk, GIT).	247
Figure 8.26	Surface-related colour zones in pink-orange sapphires. (Immersion; Photos by Somboon, GIT)	248
Figure 8.27	Blue-green patch surrounding by a white zone is a good indication of yellow Be-diffusion treated sapphires. (Photos by Puttharat,DMR)	249
Figure 8.28	Recrystallization on surface before repolishing is an indicative feature of Be-diffusion treated sapphire. (a) transmitted light, (b) reflected light (Photos by Somboon,GIT)	250
Figure 8.28	Recrystallization on surface after repolishing is an indicative feature of Be-diffusion treated sapphire. (Photos by Somboon,GIT)	251
Figure 8.29	Highly altered inclusions are commonly found in Be diffusion-treated sapphires (Photos by Somboon,GIT)	252
Figure 8.30	Highly altered zircon inclusions in Be diffusion-treated sapphires probably due to rather extreme heating condition. (Photos by Singbamroong, GIT)	253
Figure 8.31	The GemLIBS system at the SSEF (courtesy of Prof. Dr. H.A. Hänni and Dr. M.S. Krzemnicki from SSEF)	254

CONTENTS (Figures)

		Page
Figure 8.32	The Laser beam produces a tiny pit which does not affect the colour, purity and brilliance of a stone. In transmitted light laser pit is difficult to see (healing fissure was present before analysis) in reflected light (a), laser pit is detectable with 80-100µm in diameter, picture width 2.9 mm (b). (Courtesy of Prof. Dr. H.A. Hänni and Dr. M.S. Krzemnicki from SSEF)	255
Figure 8.33	SEEF GemLIBS capable of detecting Be qualitatively down to ~ 3 ppm. It is less expensive and good for routine gem identification. A small Be peak is detected (5 ppm detected with LA-ICP-MS). (Courtesy of Prof. Dr. H.A. Hänni & Dr. M.S. Krzemnicki of SSEF)	256
Figure 8.34	LIBS Analysis of a 'classical' heat treated yellow sapphire. No Be peak is detected.	257
Figure 8.35	LA-ICP-MS produces similar pits (100 µm) as does the SSEF GemLIBS™ (Photos by Somboon, GIT).	258
Figure 8.36	LA-ICP-MS capable of obtaining quantitative analysis for trace elements in ppm levels. It is more expensive and good for research.	259
Figure 8.37	Pb-glass filled fractures in a ruby show hazy appearance (a) and often contain flattened gas bubbles (arrows in b and c). (Photos by Leelawathanasuk, GIT)	260
Figure 8.38	The light reflected from Pb-glass-filled fissures shows blue-flash effect (Photos by Leelawathanasuk, GIT)	261
Figure 8.39	The cavity-filled Pb-glass (arrow) displays high luster but is poorly polished on the surface. (Photos by Leelawathanasuk, GIT)	262
Figure 8.40	The presence of infilling Pb is readily detected by EDXRF	263
Figure 8.41	The presence of infilling Pb also appears in X-ray images (Photos by Leelawathanasuk, GIT)	

CONTENTS (Tables)

		หน้า
Table 1.1	Trace element contents of a flame-fusion-grown colourless sapphire (PKSCS02) untreated with Be, obtained by LA-ICP-MS.	23
Table 1.2	Trace element contents of a natural colourless sapphire (POMCS04) untreated with Be, obtained by LA-ICP-MS.	23
Table 1.3	Trace element contents of the pale brown Be-treated flame-fusion-grown sapphire (PKSCS01) obtained by LA-ICP-MS.	29
Table 1.4	Trace element contents of the pale brown Be-treated “watch glass” sapphire (WG01) obtained by LA-ICP-MS.	31
Table 1.5	Trace element contents of the 0.80 ct Be-treated natural colourless sapphire (POMCS03) which became yellow after the treatment, obtained by LA-ICP-MS.	34
Table 1.6	Trace element contents of the yellow Be-treated sapphire (PPYS1) showing rather high content of Be, Mg, Ti and Fe but low Cr content across the profile. Results obtained from LA-ICP-MS. It appears that the amount of Cr in this sample is insufficient to create pink hue to the stone.	36
Table 1.7	Trace element contents the orangey yellow Be-treated rough sapphire (MadaRough01) showing moderate to high content of Be, Mg, Ti, Fe and Cr across the profile. It appears that the amount of Cr in this sample is sufficient to create pink hue, which turns the stone orangey.	38
Table 2.1	Trace element contents of the colourless sapphire disc (THSCS01) obtained from LA-ICP-MS.. CH’s are points analyzed on the colourless half (b) and BeH’s are those on the brown half (a).	46
Table 2.2	Trace element contents along the traverse X1 of the Fe-doped sapphire treated with Be, obtained by LA-ICP-MS.	53

CONTENTS (Tables)

		หน้า
Table 3.1	Trace element contents of the blue sapphire (DIF1) showing high contents of Ti and Fe but negligible content of Be, obtained by LA-ICP-MS.	60
Table 3.2	Trace element contents of the Australian sapphire (AUS1) showing high contents of Ti and Fe but negligible contents of Be, obtained by LA-ICP-MS.	62
Table 3.3	Trace element content of the Be-treated blue sapphire (PPBS1) showing rather high Fe contents, obtained by LA-ICP-MS.	64
Table 3.4	Trace element content of the Be-treated blue-green sapphire (BG1) analyzed across the cut surface showing rather high Fe contents, obtained by LA-ICP-MS.	67
Table 3.5	Trace element content of the Be-treated blue-green sapphire (BG1) analyzed on the outer surface showing rather high contents of Be and Fe, obtained by LA-ICP-MS.	70
Table 4.1	Trace element content of the un-treated pink Madagascan sapphire (GITMDP18) showing negligible Be but high Cr and Fe contents, obtained by LA-ICP-MS.	91
Table 4.2	Trace element content of the 'classically' heat-treated orange sapphire (KN1) showing negligible Be but high Cr and Fe contents, obtained by LA-ICP-MS.	93
Table 4.3	Trace element contents of a Be-treated Mong Hsu ruby (CR0054) showing rather high contents of Cr and Ti but low Mg, Fe and Be across the profile except at the rims where there are extremely high contents of Be and Fe suggesting a contamination from chrysoberyl. Results obtained from LA-ICP-MS.	103

CONTENTS (Tables)

		หน้า
Table 4.4	Trace element contents of a Be-treated Mong Hsu ruby (CR119) showing rather high contents of Cr and Ti but low Mg, Fe and Be across the profile except at the rims where there are extremely high contents of Be and Fe suggesting a contamination from chrysoberyl. Results obtained from LA-ICP-MS.	106
Table 4.5	Trace element contents of a Be-treated Vietnamese ruby (CRVN02) showing rather high contents of Cr and Ti but low Mg, Fe and Be across the profile except at the rims where there are extremely high contents of Be and Fe suggesting a contamination from chrysoberyl. Results obtained from LA-ICP-MS.	109
Table 4.6	Trace element content of a Be-treated Andila ruby (AR02) showing rather high contents of Cr and Fe, obtained by LA-ICP-MS	113
Table 4.7	Trace element contents of the rough Ilakaka violet sapphire (THMPS04) obtained by LA-ICP-MS. CH's are points analyzed on the 'classically' heat-treated piece and BeH's are those on the Be-treated piece.	115
Table 4.8	Trace element content of the orange Songea sapphire (SGDH09) showing high Cr and Fe contents, obtained by LA-ICP-MS.	118
Table 4.9	Trace element contents of the rough Songea sapphire (THSR01) obtained by LA-ICP-MS. CH's are points analyzed on the 'classically' heat-treated piece (b) and BeH's are those on the Be-treated piece (a).	120
Table 4.10	Trace element content of the orangey pink Madagascan sapphire (WSMDIF7) showing high Cr and Fe contents, obtained by LA-ICP-MS.	122

CONTENTS (Tables)

		หน้า
Table 4.11	Trace element contents of the rough Ilakaka pink sapphire (THMPS05) obtained by LA-ICP-MS. CH's are points analyzed on the 'classically' heat-treated piece and BeH's are those on the Be-treated piece.	124
Table 4.12	Trace element contents of the rough Ilakaka pink sapphire (THMPS01) obtained by LA-ICP-MS. CH's are points analyzed on the 'classically' heat-treated piece (c) and BeH's are those on the Be-treated piece (b).	126
Table 4.13	Trace element contents of the rough Ilakaka pink sapphire (THMPS02) obtained by LA-ICP-MS. CH's are points analyzed on the 'classically' heat-treated piece (c) and BeH's are those on the Be-treated piece (b).	128
Table 4.14	Trace element contents of the Be-treated synthetic ruby (PPSR1) showing high content of Cr but low contents of other elements, obtained by LA-ICP-MS.	131
Table 7.1	Extinction edge of un-heated Madagascar (Ilakaka) blue sapphires	214
Table 7.2	Extinction edge of heated Madagascar (Ilakaka) blue sapphires	215
Table 7.3	Extinction edge of un-heated Myanmar (Mokok) blue sapphires	215
Table 7.4	Extinction edge of heated Myanmar (Mokok) blue sapphires	215

Chapter 1

Yellow and Brown coloration in Beryllium-Treated Sapphires

Preamble

Majority of content in this chapter has been extracted, rewritten and published in *Journal of Gemmology*, V.2, No.2, p.77-103, 2004 (see Appendix A). However, this chapter still contains more detailed discussion on the mechanism of yellow and brown coloration than what appears in the *Journal*.

Introduction

Gemstone enhancement is traditional in the human history. Since several hundred years rubies have been heated in fire of coal to reduce the blue hue (Nassau, 1984 and 1994; Hughes, 1997). The “classical” high temperature heat treatment of corundum is known since thirty years (Tombs, 1980; Harder, 1980; Crowningshield and Nassau, 1981; Nassau, 1982). Today we understand the mechanisms and the causes of colour much better than in the past. Nevertheless the gemstone industry of Thailand has surprised us once again with a “new” corundum enhancement technique which shows new and unexpected colour distribution and reactions. Examples have been presented on a number of websites (AGTA, GRS) and from Hughes (2002) and McClure et al. (2002). Typical examples of the product of this “new” heating process can be seen in Figure 1.1. Many of those samples show surface-related yellow zones or if the stone contains chromium an orange colour rim was observed (Figures 1.2 and 1.3). To get a better inside view the stones were put into an immersion liquid (methylene iodide) and to improve the contrast a blue glass filter was put between the light source and the stones. The thickness of the surface-related colour zone is about 2.5 mm in Figure 1.2

and about 1.2 mm in Figure 1.3. However, colour rims up to 4 mm were also observed in the lab.

The above presented surface-related colour zones suggest diffusion of a foreign element or combination of elements into the stone. Nevertheless diffusion of a colour producing element into the gem lattice in the millimetre region has not been observed before. The penetration depth of the “classical external”¹ diffusion treatment shown in Figure 1.4 is about 0.09 mm deep². Similar diffusion thickness (0.06 mm in Figure 1.5) can be observed in the case of internal diffusion³, where titanium diffuses from natural rutile inclusions into the corundum lattice.

To understand this new enhancement technique and its mechanism in general, it is necessary to understand the causes of colour of natural yellow sapphires in detail. Two groups of natural yellow sapphires exist. The first group due its colour to spin forbidden transitions of Fe^{3+} (Lehmann and Harder, 1969; Krebs and Maisch, 1971; Ferguson and Fielding, 1971, 1972; Nassau and Valente, 1987). However, the probability of this transition is very low, therefore about approximately 1 weight % Fe^{3+} is needed to create an intense yellow with this mechanism. Sapphires of these groups originate for example from the metamorphic occurrence (Schwarz, 2000 ;per. com.) in Umba, Tanzania or from the basaltic type occurrences in Thailand, Australia and North of Madagascar. Typical spectra of this kind of mechanism are shown in Figure 1.6 with E parallel to c-axis (e-ray) and E perpendicular to c-axis (o-ray).

The second group is coloured by so-called colour centres. The UV-Vis-spectra of this second group are characterized by an increase of the absorption to the UV-part of the

¹External diffusion means the diffusion of a foreign element/s into the stone.

²The penetration depth may vary and depend on temperature and duration of the treatment.

³Internal diffusion means the diffusion of an element/s from natural inclusions into/within the host mineral.

spectrum (Figure 1.7). Sapphires of this group are for example originated from Sri Lanka. The spectrum E parallel to c-axis is very similar to the spectrum E perpendicular to c-axis. Those sapphires therefore show a weak pleochroism.

Regarding the stability of the defect centres, it is possible to differentiate this group into two sub-groups. The first sub-group is due to irradiation of natural sapphires (Lehmann and Harder, 1970; Nikolskaya et al., 1978; Nassau and Valente, 1987). The colour centres of this group are not stable to light and heat. The defect centres of the second sub-group are stable to UV-light and heat up to about 500 or 600°C. It is not possible to differentiate between these two sub-groups on the basis of UV-Vis-spectroscopy. It is only possible on the basis of the fading test (Nassau and Valente 1987).

The defect centres of the second sub-group are stable with respect to light and heat in oxidizing atmosphere. Schmetzer et al. (1982, 1983) mentioned that the colour centres may be stabilized by divalent cations like Fe^{2+} or Mg^{2+} , by trivalent cations like Cr^{3+} or Fe^{3+} or by several di- and tri-valent cations. Häger (1993) and Emmett and Douthit (1993) pointed out the importance of Mg as a stabiliser of the colour centres in natural sapphires and strongly indicated that Mg has to be in excess to intrinsic Ti. In addition Häger (1996, 2001) has shown that Mg, Fe and oxidizing atmosphere are necessary to develop the stable yellow colour centres. Interactions of trace elements in corundum are briefly summarised here in the Box 1.

With the “new” heating technique, pink-orange or orange sapphires can be produced out of original pink or reddish brown corundum and yellow out of colourless or white sapphires by addition of yellow hue to the stones. Even some yellow sapphires can be heat-treated from originally green or blue sapphires by the “new” technique (Coldham, 2002). Hence understanding the cause of added yellow hue by this technique is very

important. Following the press release by Chanthaburi Gem and Jewelry Association (CGA) on February 20, 2003, they disclosed the “new” heating technique as “Be-treatment or Be-heating” technique.

Materials and Methods

In these study two flame-fusion-grown colourless sapphires, a disc of synthetic colourless corundum or “watch glass”, and three natural colourless sapphires were heat-treated under unknown conditions by a heater in Thailand. Five additional orangey yellow, yellow and blue sapphires reportedly heat-treated by the Be-technique in Thailand were also studied. A similar set of sample (two flame-fusion-grown colourless and nine natural colorless sapphires) were also irradiated by soft X-rays (4 mA, 80 kV)

The heat treatment experiments were also carried out by one of the author (TH) to confirm the result. A synthetic colorless (“watch glass”) and two natural colourless and many natural pink sapphires mixed with ground chrysoberyl in the crucibles were heated in a resistance furnace with Super Kanthal 1900 heating elements at 1,750°C in air (oxidizing conditions) for 30 hours.

The samples were photographed and their UV-Vis spectra were recorded before and after the heating and irradiation. Only if the spectrum was not recorded with E-ray perpendicular to c-axis (o-ray), it is remarked. The Hitachi UV-VIS-NIR Spectrophotometer (model U4001) was used for most measurement with additional measurement by a Leica/Leitz UV-Vis microscope attached with Perkin-Elmer Lamda 9 UV-Vis-NIR spectrometer.

The heat-treated and irradiated samples were subjected to a fading test. The samples were put under a 100 light bulb with a distance of 4 cm to fade the unstable colour centres. The samples were then photographed and UV-Vis spectra were recorded again. An irradiated natural sample was put on a heating stage. The heating stage was combined with a Leica microscope coupled with a spectrometer with a resolution of 1 nm. The sample was heated up to 300°C and simultaneously every 10°C a UV-Vis-spectrum was recorded.

After UV-Vis measurement a set of representative samples were cut in half and lightly polished the cut surface and subsequently analyzed for trace elements content by a Laser Ablation Inductively-Coupled-Plasma Mass Spectrometry (LA-ICP-MS). This set of samples includes three synthetic colourless sapphires (one Be-treated flame-fusion-grown, one original flame-fusion-grown cut from the same boule and one disc of synthetic corundum or “watch glass”), two natural colourless sapphires (one Be-treated, one original sample obtained from the same gemstone dealer), two orangey yellow Be-treated natural sapphires and one yellow Be-treated natural sapphire obtained from different heaters. The 5-points profile analysis (Rim1, Mid-Point1, Core, Mid-Point2, Rim2) and 3-points profile analysis (Rim1, Core, Rim2) were performed across the cut surface by this technique.

Detailed descriptions of LA-ICP-MS instrumentation, analytical and calibration procedures are similar to those given by Norman et al. (1996). The UV laser ablation microprobe (a New Wave Research 266 nm Nd: YAG) is coupled to an Agilent 7500 ICP-MS. All analyses were done with a pulse rate of 5 Hz and a beam energy of approximately 0.5 mJ per pulse, producing a spatial resolution of 30-50 micrometers in diameter on the samples. Quantitative results for 9 trace elements (Be, Na, Mg, Ti, V, Cr, Mn, Fe and Ga) were obtained through calibration of relative element sensitivities using the NIST-610 multi-element glass standard and pure Al₂O₃ as internal standards.

The BCR2G basaltic glass standard was also used as an external standard. The detection limits vary from analysis to analysis and are typically less than 1 ppm for Be, V, Ga; less than 4 ppm for Mg, Ti, Mn; less than 13 ppm for Cr; less than 40 ppm for Na and less than 80 ppm for Fe.

Result of the experiment

Irradiation

In the first series of test, the irradiation experiment was carried out on a flame-fusion-grown colourless sapphire and a natural colourless sapphire. The synthetic sample is relatively pure Al_2O_3 in which most of the trace elements including Be are below the detection limits (Table 1.1). The natural sample contains relatively higher trace element content, in particular Mg, Ti and Fe, while the Be content is below the detection limit (Table 1.2). After the irradiation the synthetic one turned pale brown (Figure 1.8) whereas the natural one became intense yellow (Figure 1.10). The UV-Vis spectra of the synthetic sample (Figure 1.9) turned from a flat line before irradiation to a broad absorption band at approximately 400 nm with only a weak absorption to the UV-part of the spectrum after irradiation (similar spectra were reported by Kvapil et al., 1972 and 1973; Govinda, 1976; Lee et al., 1977; Lee and Crawford, 1977; also cited in Schmetzer and Schwarz, 2004). The UV-Vis spectra of the natural sapphire (Figure 1.11) turned from a flat line before irradiation to a pronounced increase of the absorption to the UV-part of the spectrum with a distinct shoulder at approximately 470 nm after irradiation (a resemble result has previously been reported by Schmetzer et al., 1982 and 1983). Colors of all the irradiated samples were not stable during the fading test and they have returned to their original "colourless" ones which can be seen as a flat line on the UV-Vis spectra after fading test (Figures 1.8 and 1.10). The same results were also obtained from several repeated

runs on different flame fusion grown sapphires and natural colourless samples. For example after irradiation of a natural sample in Figure 1.12 the spectra showed the increase of the absorption to the UV-part of the spectrum. The sample was faded during heating process especially in the temperature range between 50°C and 150°C and has turned to its original colour.

Beryllium Heat-Treatment

In the second series of test, the Be-heat-treatment was carried out under unknown condition by a heater in Bangkok on both synthetic and natural colourless sapphires. Similar set of sample was also performed by our own heating experiment.

Be-treated synthetic colourless sapphires

A 3.85 ct cubic sample of colourless flame-fusion grown sapphire after heating under unknown condition by a heater in Bangkok, has turned pale brown at the rim and the brown gradually decreases toward the colourless core (Figure 1.13). The pale brown rim and colourless core are better seen in the immersion liquid (Figure 1.13). This sample turned colourless after heating in reducing condition and returned to pale brown again after re-heating in an oxidizing condition (Figure 1.13). Another 11.03 ct square-cabochon replicate sample cut from the same boule and heat-treated under the same condition also gave exactly the same result (not shown here). Similar brown color was also observed by our own experiment on a colourless, “watch glass”, sample mixed with ground chrysoberyl and heated at 1750°C in an oxidizing condition for 30 hours. Moreover, the same brownish coloration was also reported from the experiments by Emmett and Douthit (2002), Emmett et al. (2003) and Themelis (2003) on colorless flame-fusion-grown, Chzochralski-grown (high purity) and heat-exchanger-grown (ultra-high purity) sapphires.

The UV-Vis spectra of the flame-fusion one turned from a flat line before heating to a broad absorption band at approximately 420 nm with only weak absorption in the UV-part of the spectrum after heating (Figure 1.14). The same UV-Vis spectrum was also obtained from our own run on the “watch glass” sample (Figure 1.14). A resemble result was also found by Emmett et al. (2003). Brown color of all the samples produced by the heater in Bangkok and our Be-treated sample was stable during the fading test. Furthermore both colour and UV-Vis spectra produced by the Be-treatment are almost the same as those produced by irradiation, except that the ones produced by the Be-treatment are stable while those produced by irradiation are faded under normal heat and light.

The LA-ICP-MS results of the five-point-profile analysis on the cut surface of the 3.85 ct cubic sample are listed in Table 1.3. In order to compare among the trace element content and understand their interaction, all cations are calculated as atom mole ppm (or abbreviated as amp) and normalized into 40 atoms of cation which correspond to 60 atoms of oxygen in Al_2O_3 structure. As shown in Table 1.3 and plotted in Figure 1.15, slightly elevated Be content appear at the rim as compared to those at the core and correspond well with the brownish rim. The extremely low Be content at the colourless core are also similar to those analyzed in the un-heated sample cut from the same boule (Table 1.1). Other important trace elements, such as Mg, Ti, V, Cr, Fe and Ga are extremely low in their content without noticeable variation from the core to the rim. Their content are comparable to those in the un-heated sample (mostly below the detection limits) suggesting rather pure Al_2O_3 originally. Similar result is also obtained from the three-point-profile analysis across the cut surface (not shown here).

As shown in Figure 1.15 and Table 1.3, the pale brown rims are dominated essentially by Be. This data therefore suggest that the divalent Be (without Mg) should play an important role in the creation of the brown coloration in this sample. This is because it

is unlikely to create colour in a pure Al_2O_3 system by simple heating without the introduction of element from external source.

We were informed by the heater that the run was intentionally heated without addition of any Be-containing substance, e.g., chrysoberyl. Nonetheless the LA-ICP-MS results has proved without doubt that there are a few ppm of Be diffused into the sample from external source. The Be might have come from the crucible and/or furnace that previously had been heat-treated with Be-containing substance. This could explain why there are such low Be content in this batch of samples (see also the next two samples) as compared with ten of ppm in the other samples obtained from other heaters (see later section). It is also surprised to realize that only a few ppm of Be are enough to create brownish colour in this relatively pure Al_2O_3 sample.

Another 13.51 ct disc of “watch glass” colourless sapphire heat-treated under the same unknown condition as that of the flame-fusion grown ones also gave a similar result (Figures 1.16 and 1. 17, Table 1.4).

Be-treated natural colourless sapphires

A 0.80 ct oval cut of natural colourless sapphire was heat-treated under the same unknown condition as that of the flame-fusion grown and the “watch glass” ones. The whole sample has turned completely intense yellow without surface-related colour after the treatment (Figure 1.18). Other two replicated natural samples (obtained from the same gemstone dealer) from the same run, however, have turned slightly yellow to almost no colour change (not shown here). Similar yellow colour was also observed in our own heating experiment on two natural colourless samples mixed with ground chrysoberyl and heated at 1,750 °C in an oxidizing atmosphere (in air) for 30 hours (not shown here). The UV-Vis spectra of the intense yellow one turned from a flat line before heating to a pronounced increase of the absorption to the UV-part of the

spectrum with a shoulder at 470 nm after heating (Figure 1.19). The yellow colour was stable under fading test.

The LA-ICP-MS results of the 5-point (also 3-point) profiles across the cut surface (Table 1.5 and Figure 1.20) reveal a few ppm of Be (all values are above the detection limits) without noticeable variation from the rim to the core. These Be values are definitely higher than those of the un-heated one (all Be values are below the detection limits; Table 1.2) obtained from the same gemstone dealer. These data therefore suggest that small amount of Be has been diffused into the stone from external source similar to what was found in the flame-fusion grown and the “watch glass” ones, again probably from the contaminated crucible and/or furnace.

All the points analyzed show rather high Mg content (Table 1.5, Figure 1.20) as compared with Ti and Be content. No variation in the Mg and all other trace element content are observed from the core to the rim. The Cr content are extremely low (below detection limit). The sample has strong excess of Mg after calculation of MgTiO_3 clusters (Mg-Ti content vary from 32 to 88 amp). Hence the excess Mg or Mg+Be could lead to the formation of stable yellow coloration in this particular sample.

Yellow and orangey-yellow Be-treated sapphires

All three yellow and orangey yellow sapphires reportedly heat-treated with Be by heaters in Thailand also gave similar results. The LA-ICP-MS results reveal rather high Be content in the samples and the excess of Be+Mg to Ti content in all the points analyzed (only two samples are shown here in Figures 1.21-24 and Tables 1.6-7).

Discussion

Based on the above presented result, the samples can be divided into two groups on the basis of their trace element contents. The first group is pure synthetic colourless sapphires and the second group is dominated by trace contents of iron.

First group: 'pure' colourless sapphires

The first group is synthetic sapphires with extremely low trace element content originally. A few ppm of Be have been found to diffuse into the stones from external source after the Be-treatment as confirmed by LA-ICP-MS analyses and our own Be-heating experiment. Be is the most dominant trace element in the Be-treated samples and directly related to the brown coloration. No variation in the Mg and all other trace element content are observed from the core to the rim. The samples commonly show similar brown colour after irradiation and after the Be-heating process and also similar UV-Vis spectra. Both spectra are dominated by broad absorption bands between approximately 400-420 nm and a weak absorption in the UV-part of the spectra (Figure 1.25). Somewhat similar brownish violet and spectral pattern, in which the broad absorption band is clearly shift to approximately 500 nm (Figure 1.25), could be observed in Mg-doped synthetic sapphires (Häger, 2001 and Wang et al., 1983).

The above experimental results lead us to believe that the unstable brown colour could relate to a defect centre created by irradiation whereas the stable brown colour might have been created by a combination of divalent Be and a defect centre formed during the oxidized Be-heating. One probable lattice defect causing by irradiation of a pure Al_2O_3 system was suggested to be trapped hole centres at oxygen site or O^- adjacent to aluminum vacancy (Kvapil et al., 1972 and 1973; Govinda, 1976; Lee et al., 1977; Lee and Crawford 1977; cited in Schmetzer and Schwarz, 2004). Hence, the irradiation

result reveals that O^{\cdot} without charge compensation from divalent Be or Be^{2+} can cause unstable brown colour absorption broad band maximum at about 400 nm which is easily eliminated and decolored by the return of free electrons when it is exposed to normal light and heat. Similarly the O^{\cdot} could also occur during Be-heating process and was probably stabilized by charge compensation from Be^{2+} which makes the brown colour stable at normal light and heat condition. This stable brown colour absorption band maximum however appears at 420 nm which might have been influenced by diffused Be and could be called Be-related colour centres (or Be- trapped hole centres). This Be-related colour centres is created and stable only in oxidizing heating and is easily eliminated in reducing heat. Similar phenomenon has previously been documented in the Mg-doped synthetic corundum in which its stable brownish violet colour after annealing at high temperature in an oxidizing atmosphere was due to O^{\cdot} compensated by divalent Mg or Mg^{2+} (Wang et al., 1983; Häger, 1992, 1996 and 2001; Emmett and Douthit, 1993). The stable brownish violet absorption band maximum appears at 500 nm which again might have been influenced by larger divalent magnesium and could be called Mg-related color centres (or Mg- trapped hole centres). The Mg-related color centres is also created and stable only in oxidizing heating and easily eliminated by reducing heat. Hence, based on this comparative reasoning we believe that the Be^{2+} is able to act in a similar way as it was found earlier for Mg^{2+} , that is as a charge compensator or stabilizer of the stable brown (Be-related) or brownish violet (Mg-related) colour centres in these synthetic sapphires. It appears from our study that yellow coloration can not be produced by irradiation or Be-heat treatment in pure Al_2O_3 system. It seems that combination with other trace element(s) is required to produce yellow colour centres.

Second group: sapphires with significant Fe content

The natural sapphires belong to the second group. They contain higher trace element content. The elevated Be content have been found in all the analyzed stones undergone Be-treatment process by a number of heaters in Thailand. This again indicate the diffusion of Be into the stones from external source as also confirmed by our own Be-heating experiment (see also Swarovski, 2002; Emmett and Douthit, 2002; Emmett et al. (2003); McClure et al., 2002; Peretti and Günther, 2002; Hänni, H.A., 2002; Hänni and Pettke, 2002; Fritsch et al., 2003; Wang and Green, 2002). No variation in the Mg and all other trace element content are observed from the core to the rim. This is however in contrast to the observation of Peretti and Günther (2002). They found a decrease in those trace elements towards the rim. This discrepancy might be due to different kinds of flux material being used in those runs. The Be-treated samples analyzed generally give intense yellow colour and show excess of Be+Mg content after calculation of MgTiO₃ and/or BeTiO₃ clusters. Some samples however show very pale yellow to almost no colour change which may be due to the complete formation of MgTiO₃ and/or BeTiO₃ clusters. The irradiated ones also give intense yellow after treatment. Both types of treatment have led to the same UV-Vis pattern, a pronounced increase of the absorption to the UV-part of the spectra and a shoulder at about 470 nm (Figure 1.26). Similar colour and spectra can be observed in natural unheated Sri Lankan yellow sapphires and in a synthetic sapphire double-doping with Mg and Fe (Figure 1.26). The colours of the Be-treated sapphires, the Mg + Fe doped synthetic and the natural unheated ones are stable to normal light and heat, while the irradiated colour is not.

The above presented results lead us to believe similarly that the unstable yellow colour produced by irradiation is probably caused by a combination of iron and a defect centre whereas the stable yellow colour centre produced by the oxidized Be-heating is

probably caused by a complex combination of excess Be + Mg, Fe and a defect centre. The presence of Fe and Mg seems to have a certain influence to produce the strong absorption in the UV part of spectrum and 470 nm absorption shoulders in natural unheated Sri Lankan yellow sapphire and in natural irradiated sapphire. This has previously been explained by the Mg + Fe doped synthetic sapphire in which the stable yellow (or brown) colour centre after annealing at high temperature in an oxidizing atmosphere can produce exactly the same type of absorption spectrum. This was suggested to be due to a complex combination of Mg and Fe in which Mg^{2+} can charge-compensate and hence stabilize the trapped hole centres (Wang et al., 1983; Häger, 1996 and 2001). In the irradiated sample however the trapped hole centres might have not been compensated and hence are unstable. This type of absorption spectrum could be called Fe-Mg-related color centres (or Fe-Mg trapped hole centres). In the Be-treated orange sapphire samples, beside the typical chromium and iron related absorption bands and lines, the production of the 470 nm absorption band was found after subtraction by Hänni and Pettke (2002), and with additional UV absorption at 380 nm by Fritsch et al. (2003) and Emmett et al. (2003) and was attributed to (Mg-Fe-Cr) trapped hole centres (Schmetzer and Schwarz, 2004). Those absorption spectra are somewhat different from our Fe-Mg-related spectrum which may be due to the influence of Cr.

The fact that the Be-treated sample can produce exactly the same spectral pattern as the irradiated, the natural Sri Lankan, the synthetic Fe+Mg doped ones and that Be^{2+} is able to charge-compensate and hence stabilize the trapped hole centers as shown in the synthetic samples. This has led us to believe that the Be^{2+} could also act the same way as it was found earlier for the Mg^{2+} (Häger, 2001) that is a stabilizer of yellow colour centre. The exact nature of how the Be, Mg, Fe and Ti interact is however still not clear at the present moment and need further study. The Be^{2+} itself could stabilize trapped hole centres (Fe-Be related colour centres or Fe-Be trapped hole centres) or

form BeTiO_3 clusters which then liberate Mg to stabilize trapped hole centres (Fe-Mg trapped hole centres), (see more discussion in Schmetzer and Schwarz, 2004). We nevertheless can say that the combination of excess Be + Mg, Fe and oxidation condition are necessary to create stable yellow colour centres and Be has a possibility to charge-compensate the trapped hole centres and hence stabilize the yellow colour centres in the Be-treated natural sapphires.

Conclusion

Based on the above experimental and analytical results the roles of the different components which are necessary to create similar stable yellow colour centres as it has been observed in natural yellow sapphires from Sri Lanka are better understood if not yet all clear. It is likely that the combination of excess divalent Be and Mg, after calculation of MgTiO_3 and/or BeTiO_3 clusters, with iron after annealing at high temperature in oxidizing atmosphere could produce stable yellow colour centres of similar UV-Vis pattern as that observed in the natural yellow sapphires from Sri Lanka. In the synthetic samples without iron, however, the brownish colour centres could be created instead. The divalent Be could act in the same way as it was found earlier for Mg (Wang et al., 1983; Häger, 1992, 1993, 1996 and 2001, Emmett and Douthit, 1993), i.e., as a stabilizer of the yellow or brown colour centres.

References

- American Gem Trade Association (AGTA). Orange-pink sapphire alert ofr Jan 8, 2002, www.agta.org
- Chanthaburi Gem and Jewelry Association (CGA). Chanthaburi gem traders and heaters agree to disclose Beryllium treatment. Press Release by CGA, February 20, 2003 <http://www.cga.or.th>
- Coldham, T., 2002. Orange sapphires or Just lemons?. *Australian Gemmologist*, **22**, 288-293
- Crowningshield, R. and Nassau, K., 1981. The Heat and Diffusion Treatment of Natural and Synthetic Sapphires. *Journal of Gemmology*, **17**, 528-541
- Emmett, J. L. and Douthit, T. R., 2002. Beryllium diffusion coloration of sapphire - A summary of ongoing experiments, <http://www.agta.org/consumer/gtclab/treatedsapps04.htm>
- Emmett J.L., Scarratt K., McClure S.F., Moses T., Douthit T.R., Hughes R., Novak S., Shigley J.E., Wang W., Bordelon O., Kane R.E. (2003) Beryllium diffusion of ruby and sapphire. *Gems & Gemology*, **39**(2), 84-135
- Ferguson, J. and Fielding, P. E., 1972. The origins of the colours of natural yellow, green, and blue sapphires. *Aust. J. Chem*, **25**, 1372-1385
- Fritsch, E., Chalain, J.-P., Hänni, H., Devouard, B., Chazot, G., Giuliani, G., Schwarz, D., Rollion-Bard, C., Gamier, V., Barda, S., Ohnenstetter, D., Notari, F., Maitrallet, P., 2003. Le nouveau traitement produisant des couleurs orange à jaune dans les saphirs. *Revue de Gemmologie A.F.G.*, **147**, 11-23
- Gemresearch (GRS). Reports on new treatment from Thailand. Padparadscha Research, Nov.2001, <http://www.gemresearch.ch/news/PadPress/padpress.htm>

- Govinda, S., 1976. Coloration and luminescence in pure chromium-doped Al_2O_3 single crystals irradiated with X-rays at room temperature. *Physica Status Solidi (a)*, 37, 109-117
- Häger, T., 2001. High temperature treatment of natural corundum. In Proceedings of the International Workshop on Material Characterization by Solid State Spectroscopy: The Minerals of Vietnam, Hanoi, Vietnam. April 4-10, 2001
- Häger, T., 1996. Farbrelevante Wechselwirkungen von Spurenelementen in Korund: Ph.D. Thesis, University of Mainz
- Häger, T., 1993. Stabilisierung der Farbzentren von gelben natürlichen Saphiren. *Berichte der Deutschen Mineralogischen Gesellschaft - Beihefte zum European Journal of Mineralogy* . 5, 188
- Häger, T., 1992. Farbgebende und "farbhemmende" Spurenelemente in blauen Saphiren. *Berichte der Deutschen Mineralogischen Gesellschaft - Beihefte zum European Journal of Mineralogy*, 4, 109
- Häoü, H.A., 2002. Orange Treated Sapphire – Towards Finding a Name for a New Product. *Journal of the Gemmological Association of Hong Kong*, 23, 23-29
- Häoü H.A., Pettke, T. (2002) Eine neue Diffusionsbehandlung liefert orangefarbene und gelbe Saphire. *Gemmologie. Zeitschrift der Deutschen Gemmologischen Gesellschaft*, 51(4), 137-152
- Hughes, R.W., 2002. Treated orange sapphires raise concern, Jan. 9, 2002- updated Feb. 1, 2002, http://www.palagems.com/treated_orange_sapphire.htm
- Hughes, R. W., 1997. *Ruby and Sapphire*, RWH Publishing, Boulder
- Harder, H., 1980. Edelsteine durch Brennen von Korunden. *Fortschr. Miner*, 58 Bh. 1, 45-46
- Kvapil, J., Perner, B., Súlóvský, J., Kvapil, J., 1973. Colour centre formation in corundum doped with divalent ions. *Kristall und Technik*, 8(1-3), 247-251
- Kvapil, J., Súlóvský, J., Kvapil, J., Perner, B., 1972. The influence of dopants and annealing on the colour stability of ruby. *Physica Status Solidi (a)*, 9, 665-672

- Lee, K.H., Crawford, J.H. Jr., 1977. Electron centers in single-crystal Al_2O_3 . *Physical Review B*, 15(8), 4065-4070
- Lee, K.H., Holmberg, G.E., Crawford, J.H. Jr., 1977. Optical and ESR studies of hole centers in γ -irradiated Al_2O_3 . *Physica Status Solidi (a)*, 39, 669-674
- Lehmann, G. and Harder, H., 1970. Optical spectra of di- and trivalent iron in corundum. *American Mineralogist*, 55, 98-105
- Nassau, K., 1982. Comment on "Heat treating corundum". - in Editorial forum, *Gems & Gemology*, 18, 109
- McClure, S., Moses, T., Wang, W., Hall, M. and Koivula, J.I., 2002. A new corundum treatment from Thailand. *Gems & Gemology*, 38, 86-90
- Nassau, K. (1984). *Gemstone Enhancement*, Butterworths, London
- Nassau, K. (1994). *Gemstone Enhancement*, Butterworths, London
- Nassau, K. & Valente, K., 1987. The seven types of yellow sapphire and their stability to light. - *Gems and Gemology*, 23, 222-231
- Nikolskaya, L.V., Terekhova, V.M. & Samoilovich, M.I., 1978. On the Origin of Sapphire Color. *Phys. Chem. Minerals*, 3, 213-224
- Norman, M. D., Pearson, N. J., Sharma, A. and Griffin, W. L., 1996. Quantitative analysis of trace element in geological materials by laser ablation ICPMS: instrumental operating conditions and calibration values of NIST glasses. *Geostandards Newsletter*, 20, 247-261
- Peretti, A. and Günther, D., 2002. Colour enhancement of natural fancy sapphires with a new heat-treatment technique. *Contribution to Gemology*, 1, 1-48
- Pisutha-Arnon, V., Häger, T., Wathanakul, P., Atichat, W., 2002. A brief summary on a cause of colour in pink-orange, orange and yellow sapphires produced by the "new" heating technique. *Journal of Gem and Jewelry*, Gem and Jewelry Institute of Thailand (GIT), 3(18), 11-12.

- Pisutha-Amund, V., Häger, T., Wathanakul, P., Atichat, W., 2004. Yellow and brown coloration in beryllium treated sapphires. *Journal of Gemmology*, 29(2), 77-103
- Schmetzer, K. Bosshard, G. & Hänni, H.A. (1982): Naturfarbene und behandelte gelbe und orange-braune Saphire. *Zeitschrift der Deutschen Gemmologischen Gesellschaft*, 31, 265-279
- Schmetzer, K., Bosshard, G. and Hänni, H. A., 1983. Naturally coloured and treated yellow and orange-brown sapphires. *Journal of Gemmology*, 18, 607-622
- Schmetzer, K. and Schwarz, D., 2004. The causes of colour in untreated, heat treated and diffusion treated orange and pinkish-orange sapphires- a review, *Journal of Gemmology*, 29, 149-182.
- Swarovski, 2002. Swarovski scientists identify possible source of beryllium in new treated sapphires. Cited in GIA Publication: *GIA Insider*, 4, 10, May 2002, <http://www.gia.edu/news/ViewIssue.cfm?volume=4&issue=10#3>
- Themelis, T., 2003. *Beryllium-treated rubies and sapphires*, 48p.
- Tombs, G.A. (1980). Further thoughts and questions on Australian sapphires, their composition and treatment. *Zeitschrift der Deutschen Gemmologischen Gesellschaft*, 29, 79-81
- Townsend, M. G., 1968. *Solid State Communication*, 6, 81
- Wang, H. A., Lee, C. H., Kroger, F. A. and Cox, R. T., 1983. Point defects in Alpha-Al₂O₃: Mg studied by electrical conductivity, optical absorption and ESR. *Physical Review B*, 27, 6, 3821-3841
- Wang, W., Green B., 2002. An update on Be-diffused corundum. *Gems & Gemology*, 38(4), 363-365.

BOX 1**Interaction of trace elements in corundum at high temperatures.**

Based on several quantitative experiments it has been shown that not only the classical trace elements like Fe and Ti influences the colour of blue sapphire. One element which is even more important in this scenario is Mg. This element is able to form colourless MgTiO_3 -clusters. If Ti exceeds the Mg- content, the excess of Ti leads in combination with Fe to colour active FeTiO_3 -clusters (Häger 1992). In the case of yellow sapphire, which is coloured by stable defect centres, Mg is in excess after the calculation of the colourless MgTiO_3 -clusters (Häger 1993). This result was supported later by Emmett and Douthit (1993). But in contrast to Emmett and Douthit, it was shown that the excess of Mg in combination with low Fe due to the stable colour centres identical to those of natural yellow sapphires from Sri Lanka, while Mg by itself stabilises another kind of colour centres (Häger 1996). If Ti-content exceeds the sum of Mg + Fe, the excess of Ti will precipitate during heat treatment at 1850°C and oxidizing atmospheres. To summarize the above presented results the following diagrams were developed (Häger 1996, 2001).

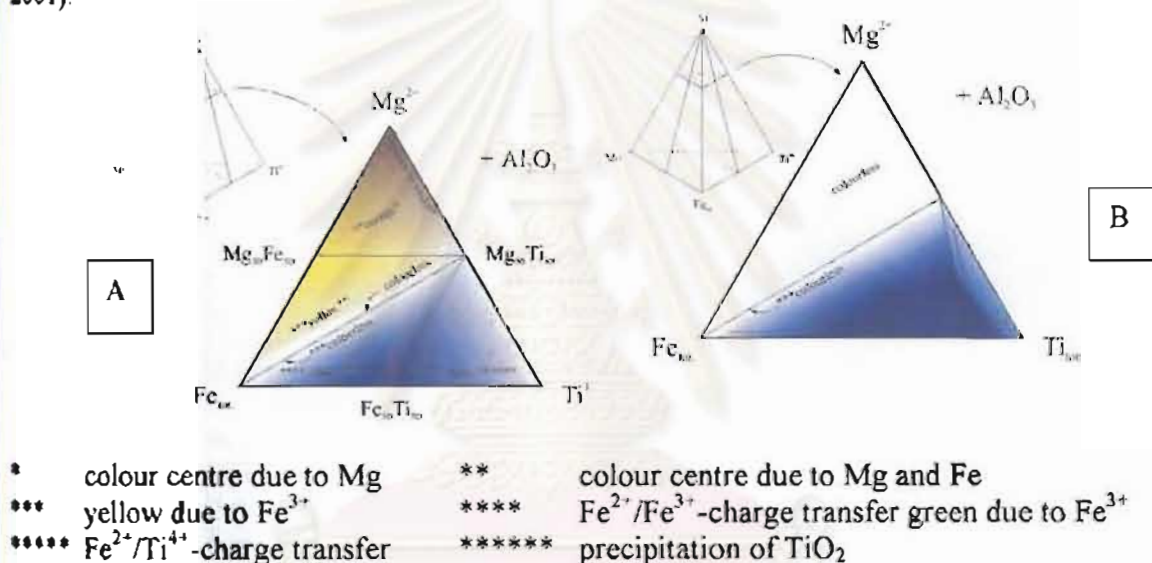


Figure 1: Model representing the interaction of trace elements in the system Mg, Fe, Al and Ti for samples which were heat treated in oxidising (A) and reducing atmospheres (B) at high temperatures.

The diagram in Figure 1 represents the system Al-Mg-Fe-Ti (tetrahedron). Out of this tetrahedron a slice is cut. This slice represents sapphires with total trace element content in the ppm region. The resulting diagram is a triangle. Sapphires of this composition were heat treated at 1850°C and oxidising atmospheres (Figure IA) and at 1750°C and reducing atmospheres (Figure IB)). On the left triangle (Figure IA), the most important line in this large triangle is the connecting line between the Fe corner and $\text{Mg}_{50}\text{-Ti}_{50}$ where the Mg to Ti ratio is always 1:1 and therefore the samples do not show any kind of colour centres or $\text{Fe}^{2+}/\text{Ti}^{4+}$ charge transfer band. Above this line we observe the same stable yellow colour centres as the natural one from Sri Lanka. In the Mg corner we also observe stable defect centres, but not with the same UV-Vis spectral pattern as the samples containing both Fe and Mg. Below the line, where the Ti:Mg ratio is more than 1:1, we observe $\text{Fe}^{2+}/\text{Ti}^{4+}$ -charge transfer bands. If the titanium content exceeds the sum of Mg + Fe we observe the precipitation of a titanium containing phase. Those samples represent in the lower triangle on the right side. If we change now to reducing conditions, the colour centres are destroyed completely and we dissolve more titanium precipitates (Figure IB). The amount of additionally dissolved precipitates depends now on the kind of the reducing gases and the triangle with precipitates gets smaller.



Figure 1.1: Pink-orange, orange, yellow sapphires and ruby treated with the new heating technique. Treatment conditions are unknown (Photos by Somboon, GIT).



Figure 1.2: Surface-related colour zones in a yellow sapphire. Size of the stone is 10.06 x 11.57 mm. (Immersion, Photo by Leelawatanasuk, GIT).

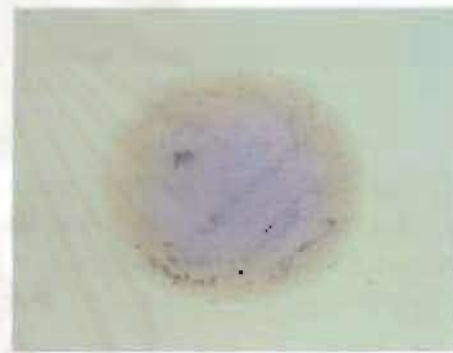


Figure 1.3: Surface-related colour zones in a pink-orange sapphire. Size of the stone is 5.2 x 6.63 mm. (Immersion, Photo by Somboon, GIT).



Figure 1.4: An example showing a slice of a classical external Ti diffusion treated sapphire causing the blue coloured rim. Sample size is 4x7 mm (Immersion, Photo by Häger).



Figure 1.5: Internal diffusion of Ti from rutile inclusions into the corundum lattice showing the blue haloes (Photo by Häger).

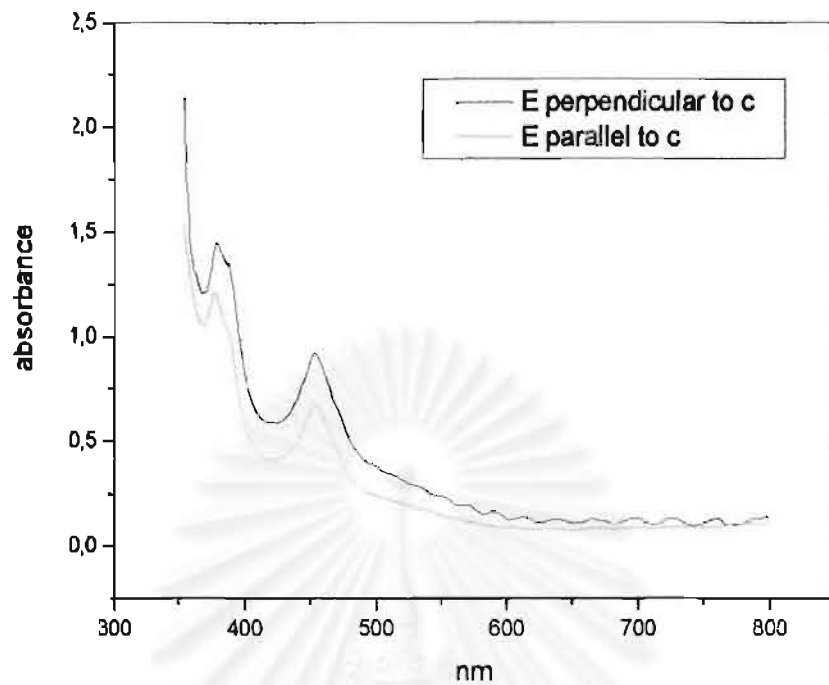


Figure 1.6: UV-Vis Spectra of an un-treated yellow sapphire from Thailand (Khao Phloi Wean, Chanthaburi) with E perpendicular to c-axis (o-ray, black) and E parallel to c-axis (e-ray, red). The colour is due mainly to Fe^{3+} forbidden transition.

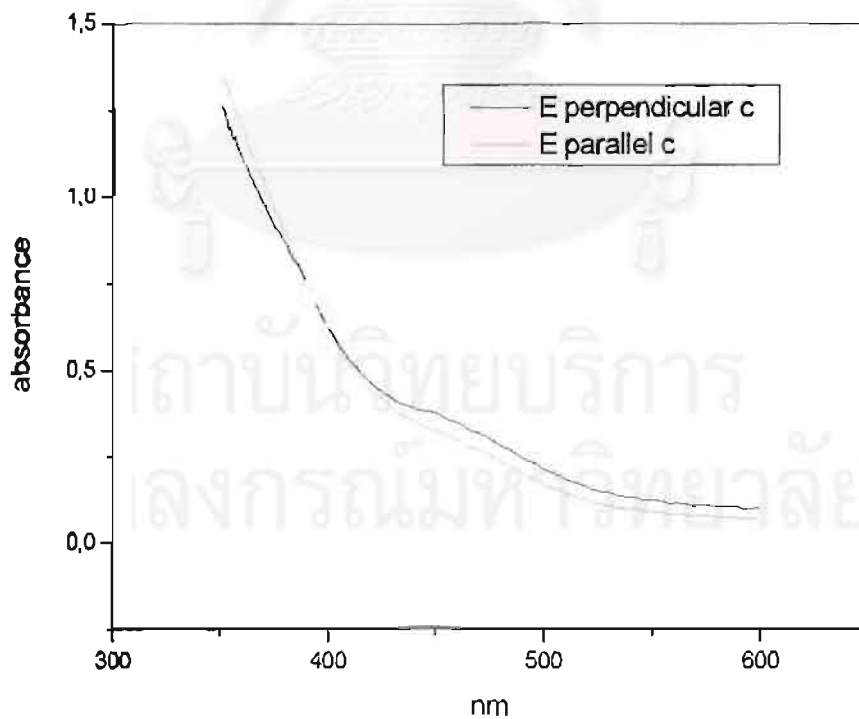


Figure 1.7: UV-Vis-spectra of a heat-treated natural yellow sapphire from Sri Lanka with E perpendicular to c-axis (o-ray, black) and E parallel to c-axis (e-ray, red). The colour is due to stable defect centres.

Table 1.1: Trace element contents of a flame-fusion-grown colourless sapphire (PKSCS02) untreated with Be, obtained by LA-ICP-MS.

	Rim1	Mid-Point1	Core1	Core2	Mid-Point2	Rim2
RAW DATA (ppm by weight)						
Be9	<0.44	<1.63	<0.95	<0.90	<1.47	<0.55
Na23	<20.36	<45.39	<40.97	<44.58	<47.36	<29.61
Mg24	<0.64	<1.39	5.50	1.97	<1.4	4.22
Al27	529250.40	529250.40	529250.40	529250.40	529250.40	529250.40
Ti47	<2.10	<4.79	<3.74	<4.01	<4.83	3.04
V51	<0.30	<0.66	<0.59	<0.59	<0.69	<0.38
Cr53	<8.28	<13.46	<12.58	<13.03	<14.13	<8.77
Mn55	<1.43	<3.19	<2.85	<3.12	<3.23	<2.04
Fe57	<38.79	<87.17	<77.93	<84.32	<90.44	<55.53
Ga71	0.32	<0.56	<0.55	<0.62	<0.65	<0.33
Total %	52.93	52.93	52.93	52.93	52.93	52.93

< = below the detection limit

Table 1.2: Trace element contents of a natural colourless sapphire (POMCS04) untreated with Be, obtained by LA-ICP-MS.

	Rim1	Mid-Point1	Core	Mid-Point2	Rim2
RAW DATA (ppm by weight)					
Be9	<0.4	<0.74	<0.75	<0.95	<0.42
Na23	<16.47	69.54	57.55	<38.04	<15.86
Mg24	76.32	76.08	81.01	90.02	95.57
Al27	529250.40	529250.40	529250.40	529250.40	529250.40
Ti47	101.81	125.65	129.98	141.29	148.59
V51	16.07	16.25	17.44	18.99	17.29
Cr53	25.24	18.87	15.40	16.31	11.39
Mn55	<1.16	<2.63	<2.26	<2.63	<1.11
Fe57	613.78	662.68	719.27	528.96	682.80
Ga71	92.53	85.22	89.82	85.77	99.80
Total %	53.02	53.03	53.04	53.01	53.03

< = below the detection limit

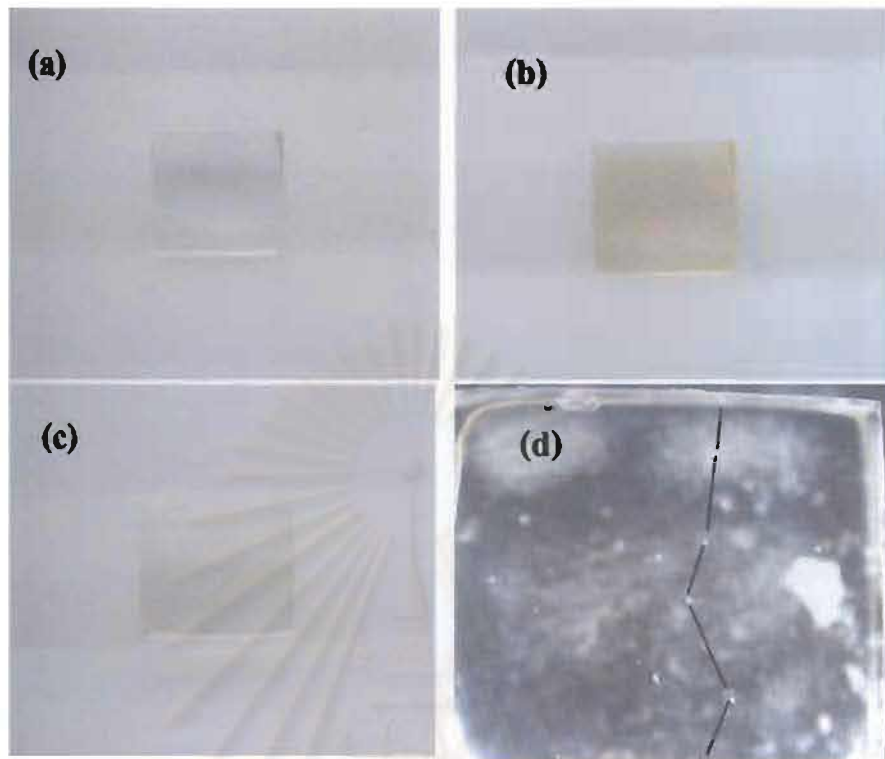


Figure 1.8: Photos of the 2.44 ct flame-fusion-grown colourless sapphire (PKSCS02) before treatment (a), pale brown after X-ray irradiation treatment (b), and almost colourless after a fading test (c). Afterward the sample was cut in half and six-points on a traverse (d) were analyzed across the cut surface using LA-ICP-MS (see also Table 1.1 and Figure 1.9). (Photos by Somboon, GIT and Lomthong, KU)

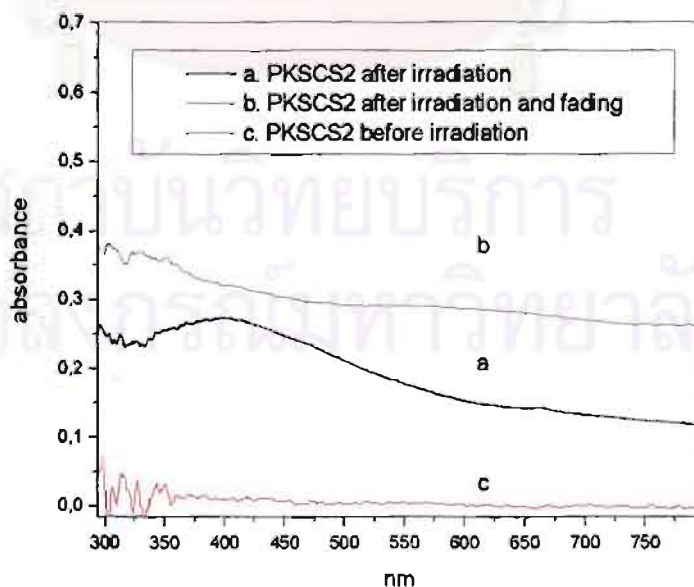


Figure 1.9: UV-Vis spectra of the 2.44 ct cube of flame-fusion-grown colourless sapphire (PKSCS02) before treatment (c), pale brown after X-ray irradiation treatment (a), and after a fading test (b).

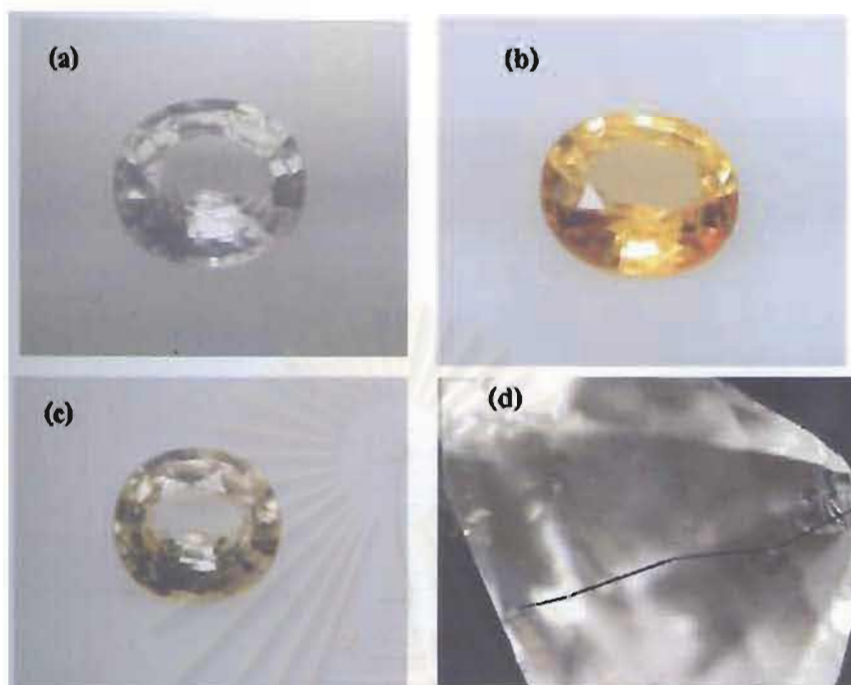


Figure 1.10: Photos of the 0.73 ct natural colourless sapphire (POMCS04) before treatment (a), yellow after X-ray irradiation treatment (b), and almost colourless after a fading test (c). A five-point-profile (d) was analyzed across the cut surface afterward using LA-ICP-MS (see also Table 1.2 and Figure 11). (Photos by Somboon, GIT and Lomthong, KU)

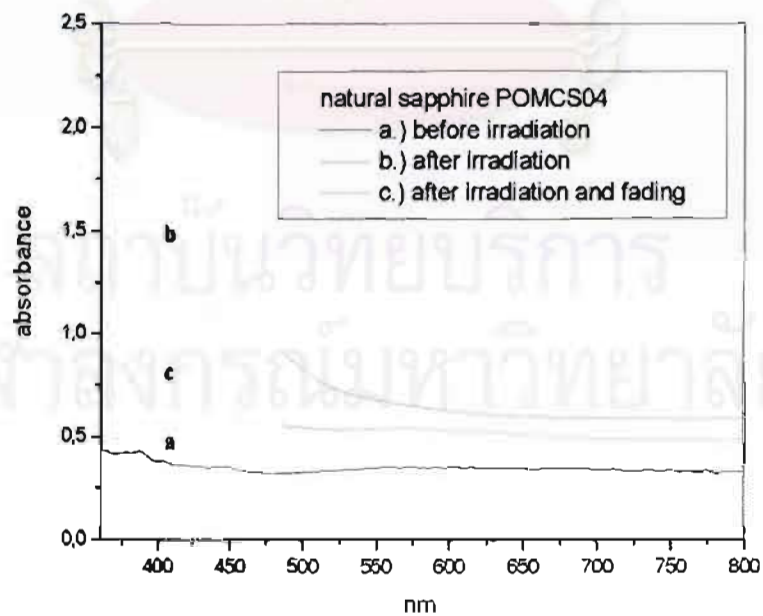


Figure 1.11: UV-Vis spectra of the 0.73 ct natural colourless sapphire (POMCS04) before treatment (a), after X-ray irradiation treatment (b), and after a fading test (c).

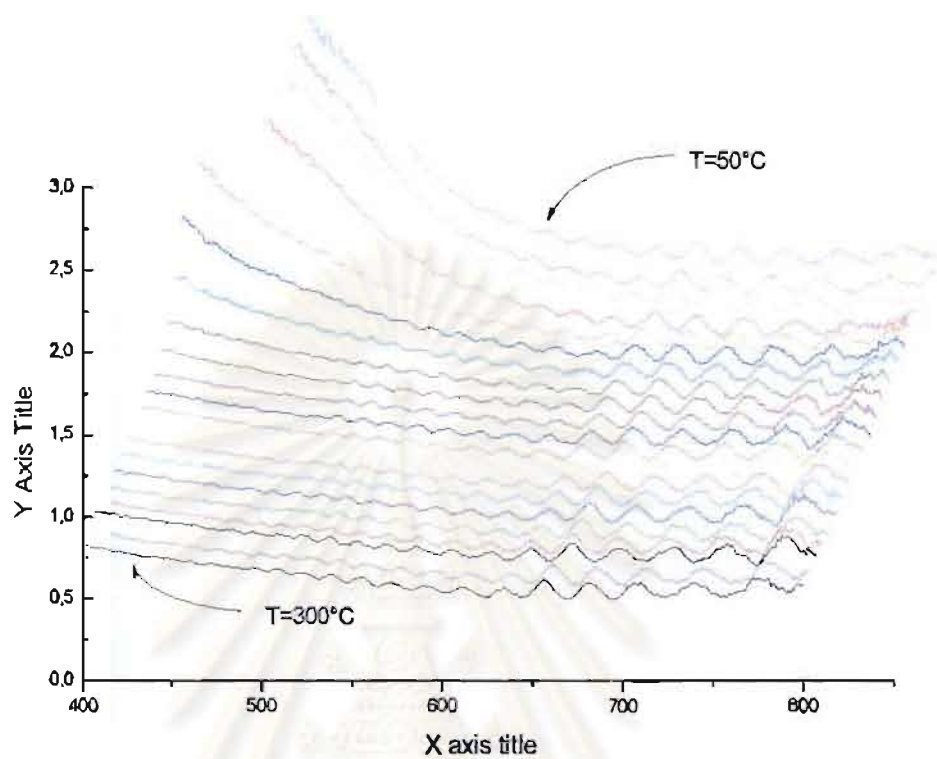


Figure 1.12: UV-Vis spectra of an Irradiated natural sapphire heated up at a rate of 2°C/min; spectra were recorded every 10°C (Spectrum at 110°C was missing because of technical problems and wave-like pattern in the spectra about 600 to 800 nm are due to experimental inconsistencies). The irradiated yellow colour was gradually faded towards the high temperatures.

สถาบันวิทยบริการ
จุฬาลงกรณ์มหาวิทยาลัย

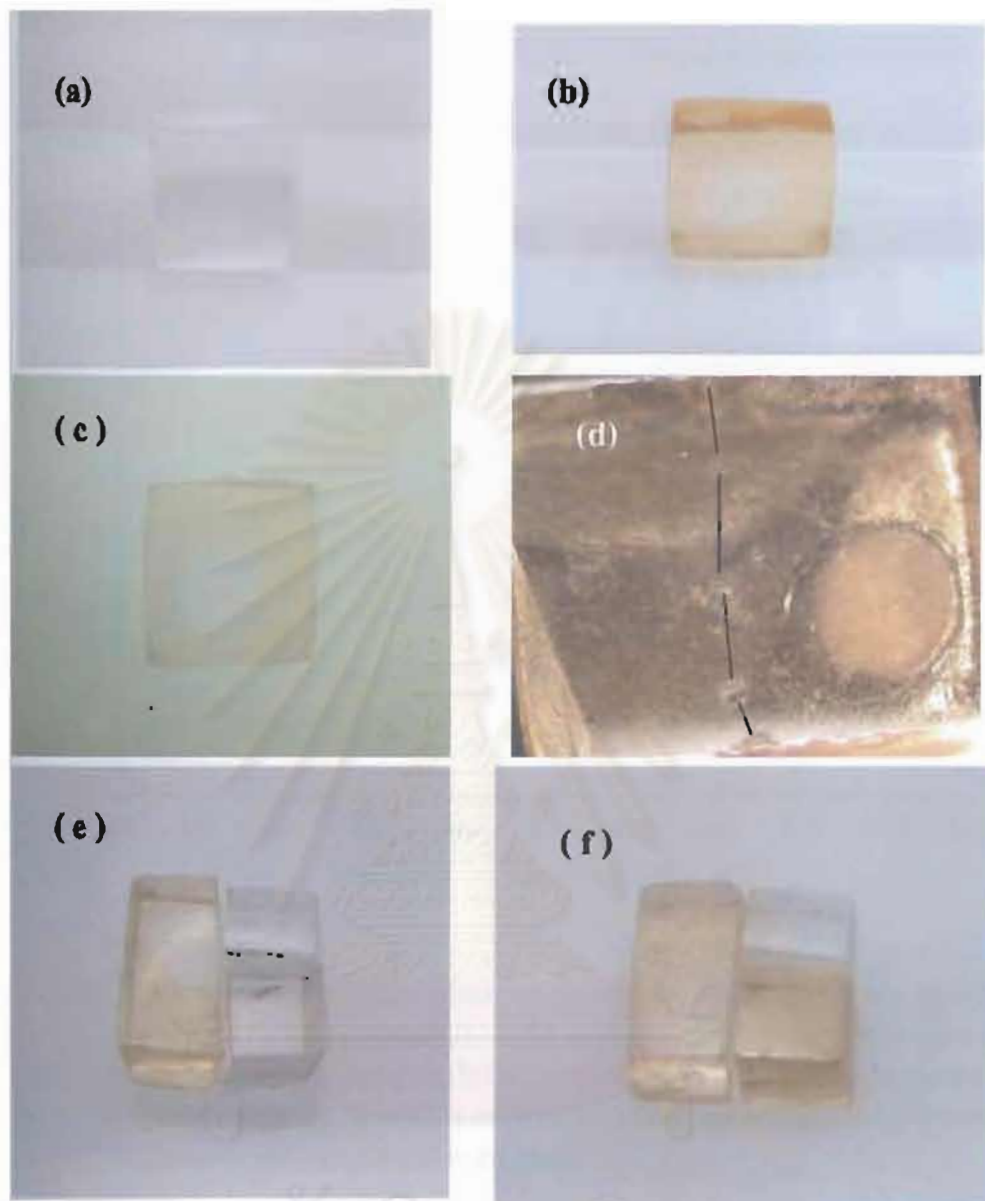


Figure 1.13: Photos of a 3.85 ct flame-fusion-grown colourless sapphire (PKSCS01) before treatment (a), and pale brown after Be-treatment under unknown condition (b). The pale brown rim and colourless core are better seen under immersion (c). After the treatment the sample was cut in half and a five-point profile (d) was analyzed across the cut surface using LA-ICP-MS (see also Table 1.3, Figures 1.14 and 1.15). The other half was then cut into three pieces; one piece was kept as the reference and the other two were heated in a pure nitrogen atmosphere at 1,650°C for 3 hours which turns the stone colourless (e). One of the colorless pieces was then re-heated in air (i.e. oxidation conditions) at 1,650°C for 1 hour, which turned the sample back to pale brownish (f). (Photos by Somboon, JIT and Lomthong, KU)

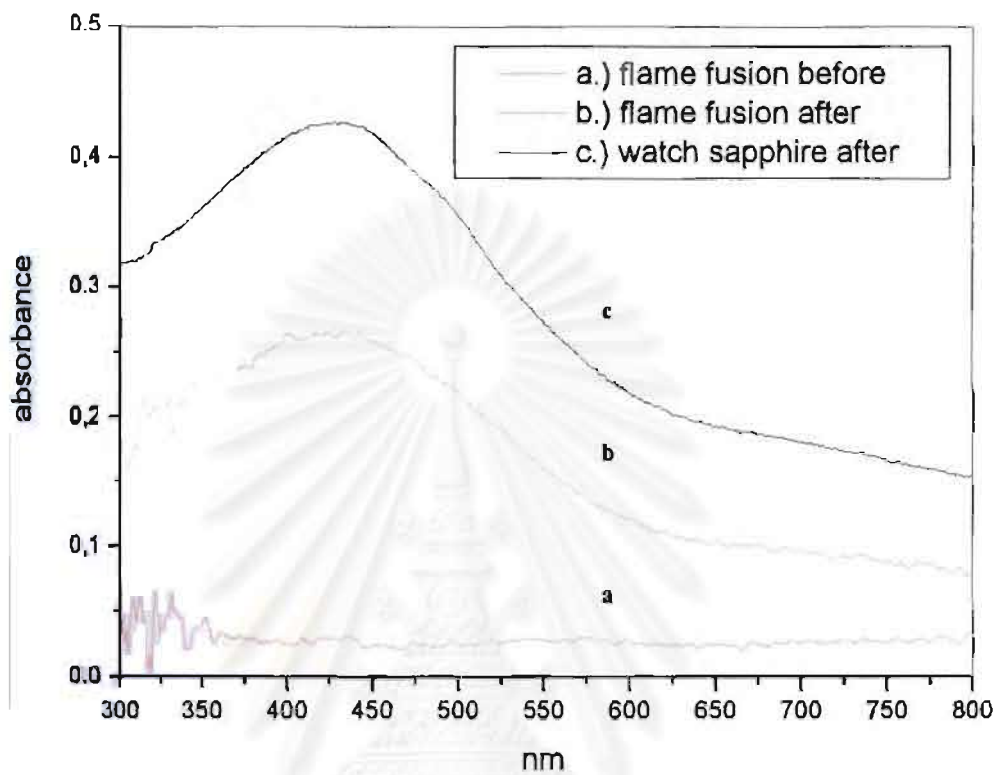


Figure 1.14: UV-Vis Spectra of the flame-fusion-grown sapphire (PKSCS01) before treatment (a) and after Be-heat treatment (b) under unknown condition. Spectrum c was recorded from a "watch glass" sapphire (WG02), which had been turned pale brown from originally colourless material by our own heating experiment at 1750°C in an oxidising atmospheres with chrysoberyl in the crucible.

Table 1.3: Trace element contents of the pale brown Be-treated flame-fusion-grown sapphire (PKSCS01) obtained by LA-ICP-MS.

	Rim1	Mid-Point1	Core	Mid-Point2	Rim2
RAW DATA (ppm by weight)					
Be9	1.60	<1.02	<0.99	3.65	2.15
Na23	<17.83	<39.36	<38.43	<38.41	<16.54
Mg24	0.73	<1.23	<1.26	1.31	<0.51
Al27	529250.40	529250.40	529250.40	529250.40	529250.40
Ti47	<2.04	<4.42	<4.14	<3.99	<1.5
V51	<0.26	<0.56	<0.57	<0.53	<0.25
Cr53	<5.79	<12.7	<12.01	<12.11	<5.25
Mn55	<1.26	<2.78	<2.7	3.20	<1.17
Fe57	<35.74	<78.59	<77.61	<76.8	<33.21
Ga71	0.38	<0.53	<0.51	<0.47	0.29
Total %	52.93	52.93	52.93	52.93	52.93
Cations (Atom Mole ppm)					
Be9	3.62	0.00	0.00	8.26	4.86
Na23	0.00	0.00	0.00	0.00	0.00
Mg24	0.61	0.00	0.00	1.10	0.00
Al27	399995.66	400000.00	400000.00	399989.45	399995.05
Ti47	0.00	0.00	0.00	0.00	0.00
V51	0.00	0.00	0.00	0.00	0.00
Cr53	0.00	0.00	0.00	0.00	0.00
Mn55	0.00	0.00	0.00	1.19	0.00
Fe57	0.00	0.00	0.00	0.00	0.00
Ga71	0.11	0.00	0.00	0.00	0.08
Total (Atom Mole)	40.00	40.00	40.00	40.00	40.00
Mg-Ti	0.61	0.00	0.00	1.10	0.00
Be-Ti	3.62	0.00	0.00	8.26	4.86
(Be+Mg)-Ti	4.23	0.00	0.00	9.36	4.86

≤ = below the detection limit of which 0.00 value is used for calculation of atom mole ppm.

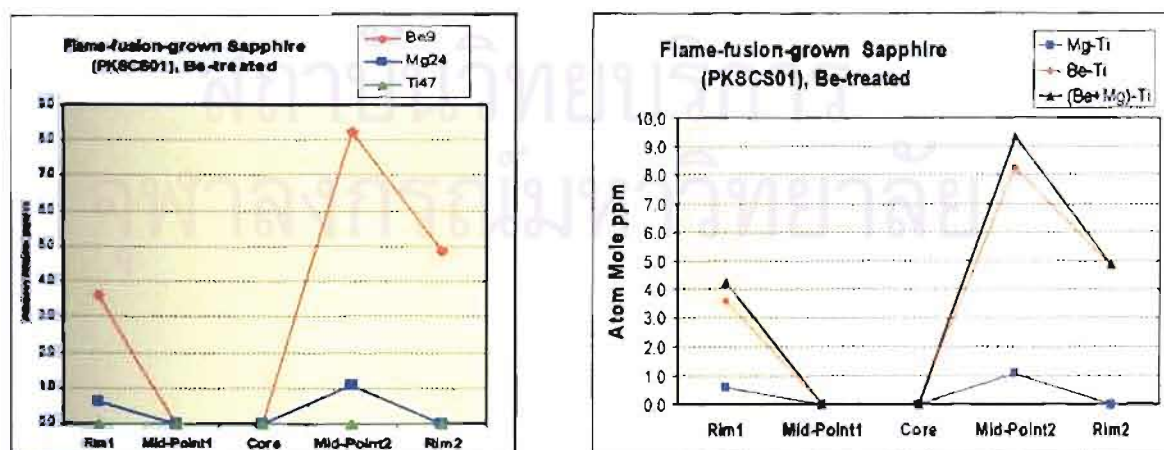


Figure 1.15: Plots of trace element content variation across the cut surface of the pale brown Be-treated flame-fusion-grown sapphire (PKSCS01), see Figure 1.13d and text for discussion.

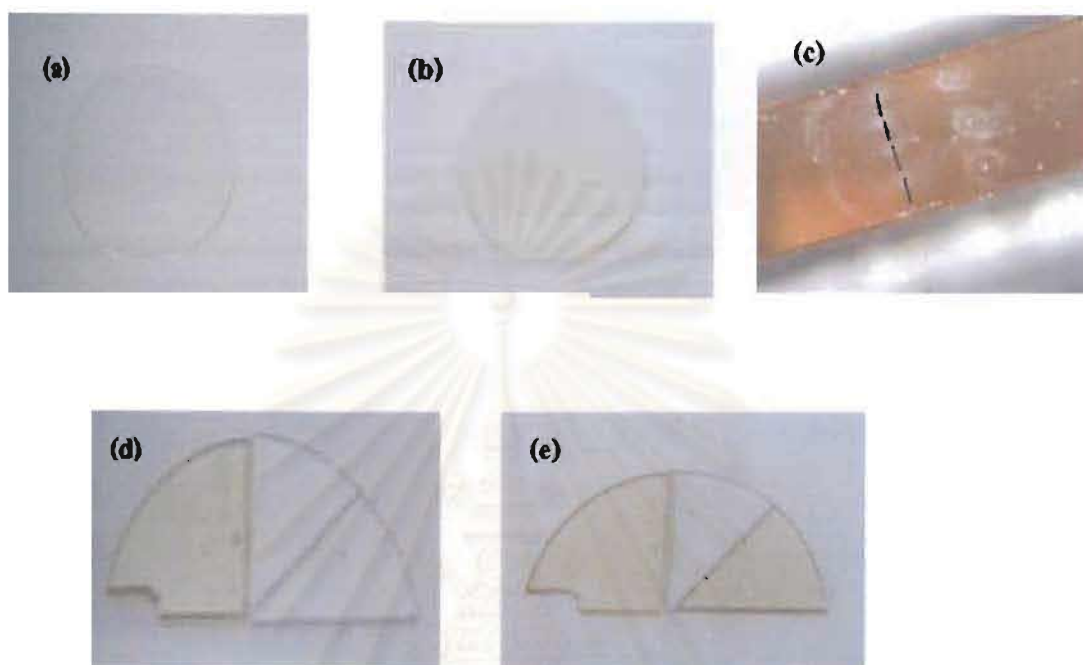


Figure 1.16: Photos of a 13.51 ct disc of colourless “watch glass” sapphire (WG01) before treatment (a), and pale brown throughout the entire disc after Be-treatment under unknown condition (b). After the treatment, a five-point profile (c) was analyzed across the 1.25-mm-thick cut surface using LA-ICP-MS (see also Table 1.4 and Figure 1.17). The other half of the sample was then cut into 3 pieces, one piece was kept as the reference whereas the other two pieces were heated in a pure nitrogen atmosphere at 1650°C for 3 hours which turned the stone colorless (d). One of the resulting colourless pieces was re-heated in air (in oxidation conditions) at 1650°C for 1 hour which turned the sample back into pale brown again (e). (Photos by Somboon, GIT and Lomthong, KU).

Table 1.4: Trace element contents of the pale brown Be-treated “watch glass” sapphire (WG01) obtained by LA-ICP-MS.

	Rim1	Mid-Point1	Core	Mid-Point2	Rim2
RAW DATA (ppm by weight)					
Be9	1.53	3.02	1.29	1.33	1.65
Na23	<26.41	<32.24	<22.57	<23.15	<17.25
Mg24	5.20	3.23	2.40	1.64	<0.58
Al27	529250.40	529250.40	529250.40	529250.40	529250.40
Ti47	4.06	4.06	7.02	<2.52	5.11
V51	<0.38	<0.45	<0.31	<0.33	<0.25
Cr53	<7.97	<9.67	<6.69	<6.86	<5.16
Mn55	<1.84	<2.26	<1.56	<1.61	<1.20
Fe57	<51.43	64.50	<44.45	<43.98	<33.48
Ga71	0.62	0.90	1.03	0.89	1.08
Total %	52.93	52.94	52.93	52.93	52.93
Cations (Atom Mole ppm)					
Be9	3.46	6.83	2.92	3.01	3.73
Na23	0.00	0.00	0.00	0.00	0.00
Mg24	4.36	2.71	2.01	1.38	0.00
Al27	399990.27	399964.92	399991.78	399995.35	399993.78
Ti47	1.73	1.73	2.99	0.00	2.18
V51	0.00	0.00	0.00	0.00	0.00
Cr53	0.00	0.00	0.00	0.00	0.00
Mn55	0.00	0.00	0.00	0.00	0.00
Fe57	0.00	23.55	0.00	0.00	0.00
Ga71	0.18	0.26	0.30	0.26	0.32
Total (Atom Mole)	40.00	40.00	40.00	40.00	40.00
Mg-Ti	2.63	0.98	-0.97	1.38	-2.18
Be-Ti	1.73	5.10	-0.07	3.01	1.56
(Be+Mg)-Ti	6.10	7.81	1.94	4.39	1.56

< = below the detection limit of which 0.00 value is used for calculation of atom mole ppm

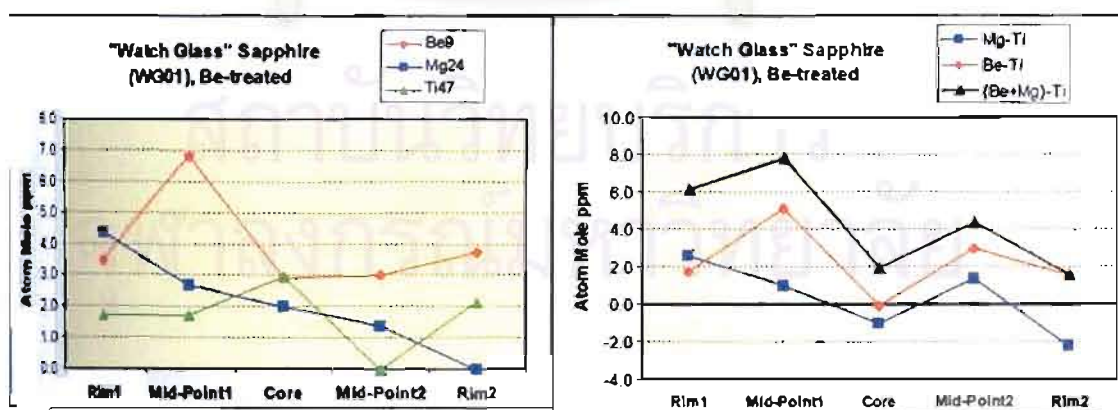


Figure 1.17: Plots of trace element content variation across the 1.25-mm-thick cut surface of the pale brown Be-treated “watch glass” sapphire disc (WG01). The contents of Be are dominant over those of Mg and Ti in almost all the points analysed, and $(\text{Be}+\text{Mg}) > \text{Ti}$ in all analyzed points (cf. Figure 1.16c).

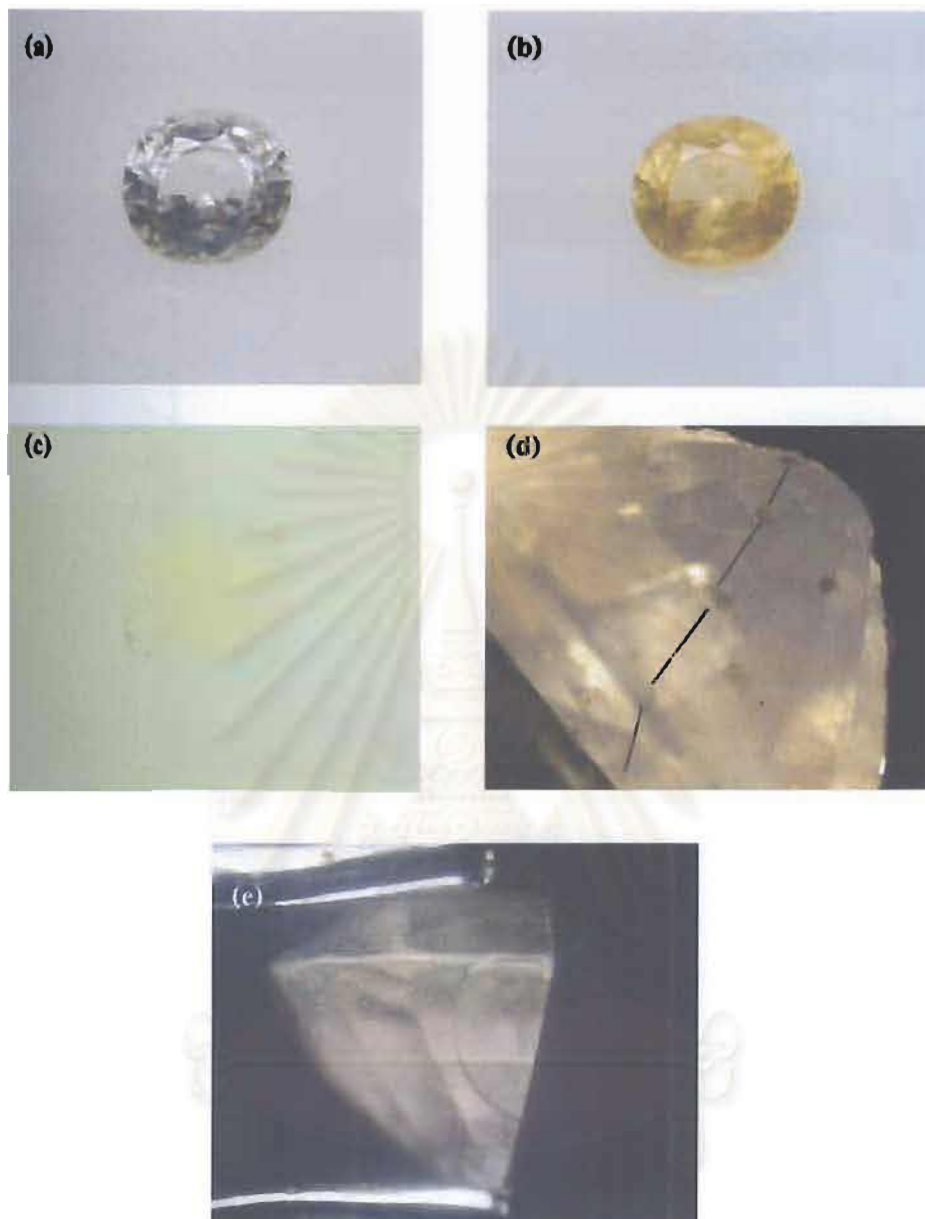


Figure 1.18: Photos of a 0.80 ct natural colourless sapphire (POMCS03) before treatment (a), yellow after Be-heat treatment (b), and in the immersion liquid (c). A five-point profile (d) was analyzed across the cut surface after the treatment using LA-ICP-MS (see also Table V and Figure 1.20). The other half was heated in a reducing atmosphere at 1650°C for 3 hours, which turned the stone colourless (c). (Photos by Somboon, GIT and Lomthong, KU)

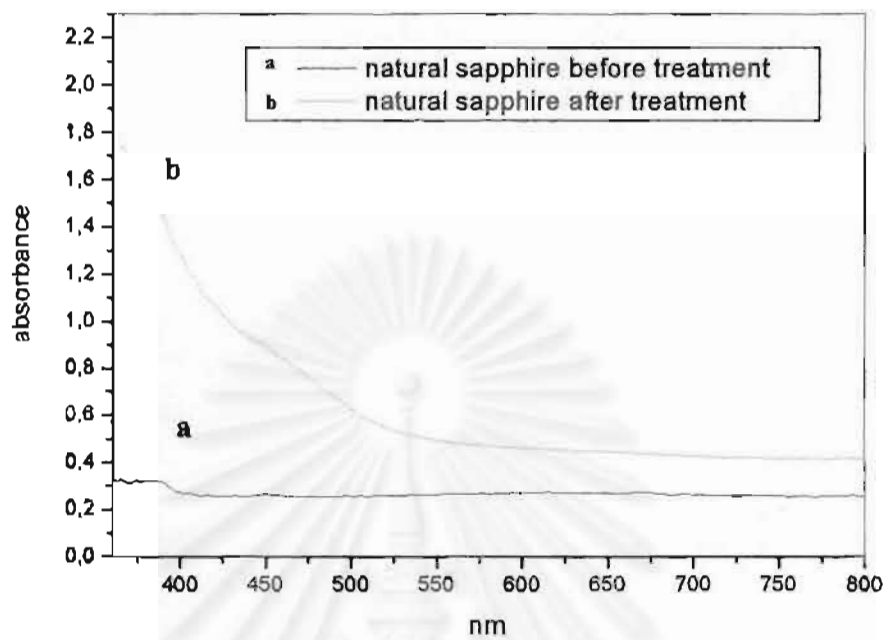


Figure 1.19: UV-Vis Spectra of the natural colourless sample (POMCS03) before treatment (a) and after the Be-heat treatment (b) (see also Figure 1.18a, b).

สถาบันวิทยบริการ
จุฬาลงกรณ์มหาวิทยาลัย

Table 1.5: Trace element contents of the 0.80 ct Be-treated natural colourless sapphire (POMCS03) which became yellow after the treatment, obtained by LA-ICP-MS.

RAW DATA (ppm by weight)					
Be9	1.23	4.68	2.52	2.79	2.90
Na23	<18.10	<33.67	<29.32	<29.56	<18.11
Mg24	95.38	144.81	71.52	67.48	80.15
Al27	529250.40	529250.40	529250.40	529250.40	529250.40
Ti47	74.48	78.19	65.95	58.30	51.33
V51	2.44	2.82	2.47	2.33	1.98
Cr53	<5.28	<9.51	<8.30	<8.73	<5.37
Mn55	<1.25	<2.32	<2.01	<2.05	<1.27
Fe57	347.76	402.65	348.55	325.47	342.53
Ga71	68.88	61.42	58.20	61.22	64.24
Total %	52.98	52.99	52.98	52.98	52.98
Cations (Atom Mole ppm)					
Be9	2.78	10.58	5.7	6.31	6.56
Na23	0	0	0	0	0
Mg24	79.97	121.39	59.97	56.58	67.20
Al27	399737.57	399668.81	399761.10	399774.71	399759.85
Ti47	31.69	33.26	28.06	24.80	21.84
V51	0.98	1.13	0.99	0.93	0.79
Cr53	0.00	0.00	0.00	0.00	0.00
Mn55	0.00	0.00	0.00	0.00	0.00
Fe57	126.89	146.89	127.18	118.76	124.98
Ga71	20.13	17.95	17.01	17.90	18.78
Total (Atom Mole)	40.000	40.000	40.000	40.000	40.000
Mg-Ti	48.283	88.132	31.909	31.777	45.365
Be-Ti	-28.904	-22.678	-22.360	-18.495	-15.280
(Be+Mg)-Ti	51.064	98.713	37.607	38.086	51.923

< = below the detection limit of which 0.00 value is used for calculation of atom mole ppm

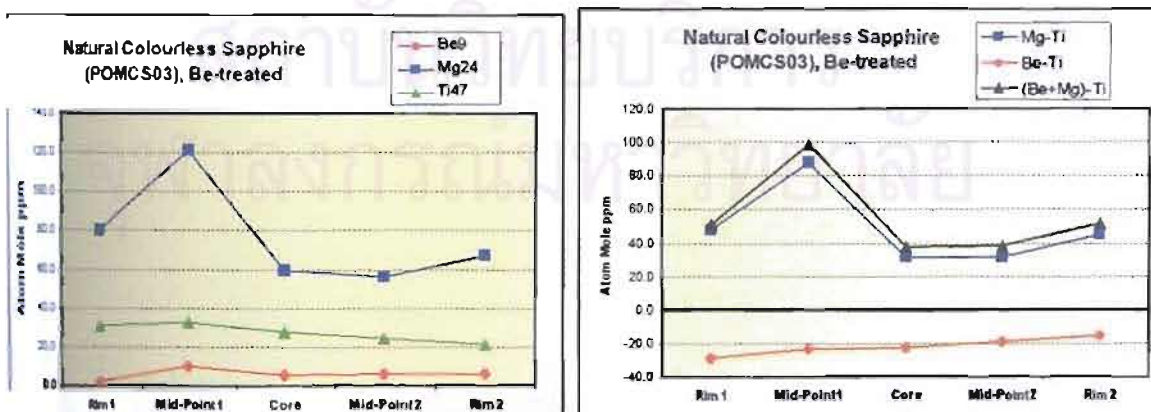


Figure 1.20: Plots of trace element content variation across the cut surface of the Be-treated natural colourless sapphire (POMCS03), which became yellow after the treatment, cf. Figure 1.18d and see text for discussion.

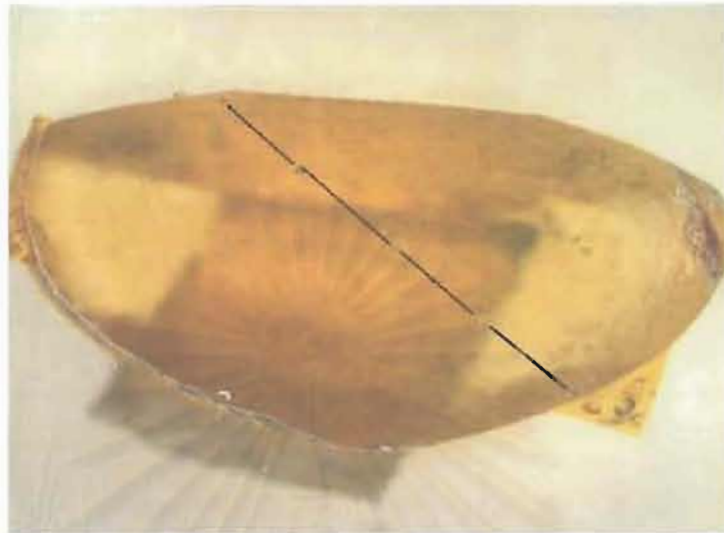


Figure 1.21: Photo of a yellow sapphire (PPYS1) reportedly heat-treated with Be under unknown condition by a Thai heater. The sample appears yellow throughout the entire stone and lacks a surface-related colour zone. A five-point profile was analyzed across its cut surface (see also Table 1.6 and Figure 1.22), (Photo by Somboon, GIT and Lomthong, KU).

สถาบันวิทยบริการ
จุฬาลงกรณ์มหาวิทยาลัย

Table 1.6: Trace element contents of the yellow Be-treated sapphire (PPYS1) showing rather high content of Be, Mg, Ti and Fe but low Cr content across the profile. Results obtained from LA-ICP-MS. It appears that the amount of Cr in this sample is insufficient to create pink hue to the stone.

	Rim1	Mid-Point1	Core	Mid-Point2	Rim2
RAW DATA (ppm by weight)					
Be9	9.14	10.02	10.29	11.27	8.86
Na23	<13.54	<11.63	<13.89	<11.89	<11.30
Mg24	48.01	43.39	42.03	43.44	39.61
Al27	529250.40	529250.40	529250.40	529250.40	529250.40
Ti47	75.47	65.06	71.09	68.82	58.36
V51	20.11	19.62	18.88	19.76	21.50
Cr53	32.58	35.65	35.68	32.94	34.43
Mn55	<0.67	<0.58	<0.72	<0.58	<0.55
Fe57	2237.19	2210.06	2119.11	2375.70	2424.42
Ga71	73.94	74.56	73.07	76.35	81.14
Total %	53.17	53.17	53.16	53.19	53.19
Cations (Atom Mole ppm)					
Be9	20.63	22.62	23.23	25.44	20.00
Na23	0.00	0.00	0.00	0.00	0.00
Mg24	40.18	36.32	35.18	36.35	33.15
Al27	399049.91	399064.88	399096.62	399000.72	398993.41
Ti47	32.05	27.63	30.19	29.22	24.78
V51	8.03	7.84	7.54	7.89	8.58
Cr53	12.75	13.95	13.96	12.89	13.47
Mn55	0.00	0.00	0.00	0.00	0.00
Fe57	814.87	805.02	771.95	865.21	882.94
Ga71	21.57	21.76	21.32	22.27	23.67
Total (Atom Mole)	40.00	40.00	40.00	40.00	40.00
Mg-Ti	8.13	8.69	4.99	7.13	8.37
Be-Ti	-11.42	-5.01	-6.96	-3.79	-4.78
(Be+Mg)-Ti	28.76	31.31	28.22	32.57	28.36

< = below the detection limit of which 0.00 value is used for calculation of atom mole ppm

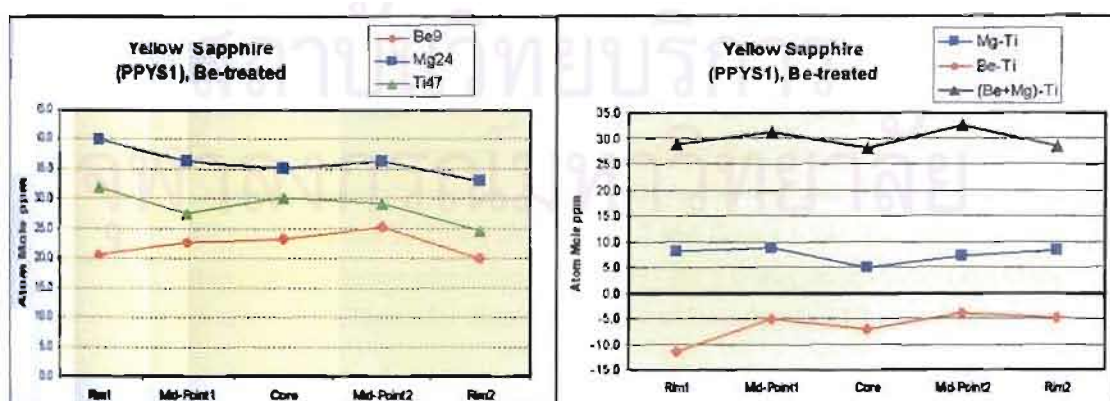


Figure 1.22: Plots of trace element content variation across the cut surface of the yellow Be-treated sapphire (PPYS1). No significant variation of Be, Mg and Ti content (also other trace elements, see Table 1.6) across the profile. All the points analysed (Figure 1.21) however, show (Be+Mg) > Ti.

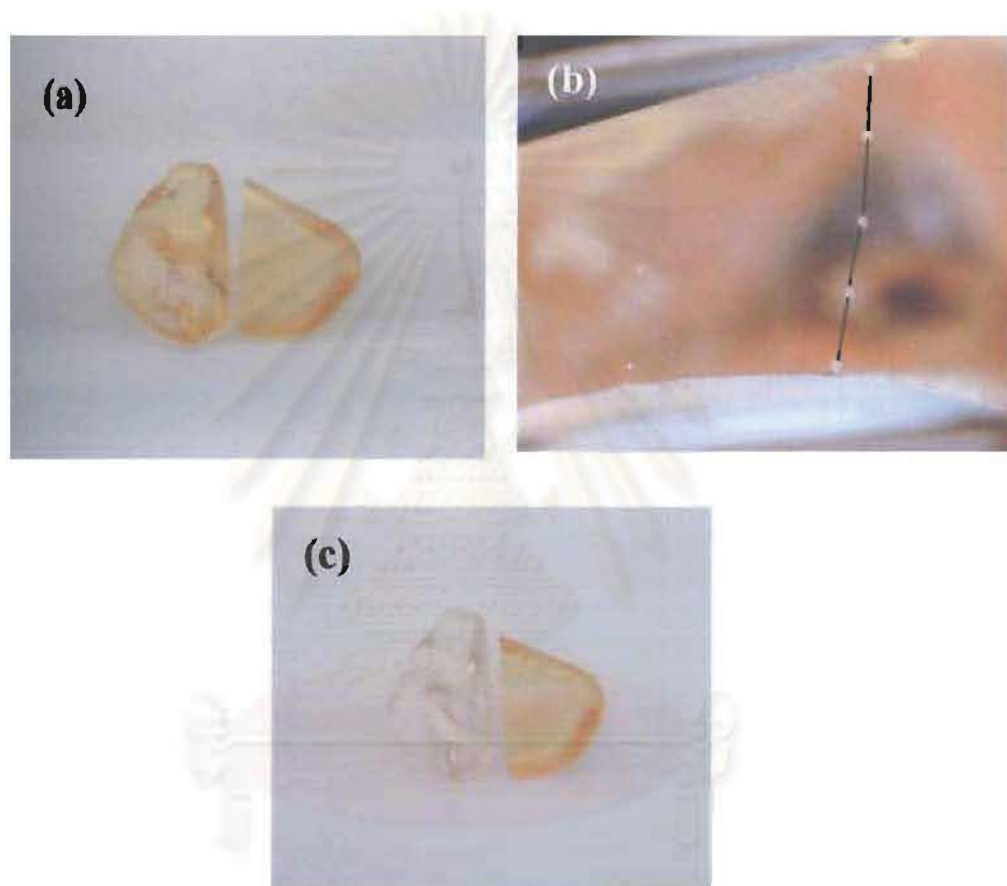


Figure 1.23: Photos of a 2.44 ct Madagascan orangey yellow rough sapphire (MadaRough01) reportedly heat-treated with Be under unknown condition in Thailand (a). The sample appears orangey yellow throughout the entire stone and lacks a surface-related colour zone. A five-point profile was analyzed across the cut surface (b) on one half (see also Table 1.7 and Figure 1.24). The other half was heated in a reducing atmosphere at 1650°C for 3 hours, which turned the stone colourless (c). (Photos by Somboon, GIT and Lomthong, KU)

Table 1.7: Trace element contents the orangey yellow Be-treated rough sapphire (MadaRough01) showing moderate to high content of Be, Mg, Ti, Fe and Cr across the profile. It appears that the amount of Cr in this sample is sufficient to create pink hue, which turns the stone orangey.

	Rim1	Mid-Point1	Core	Mid-Point2	Rim2
RAW DATA (ppm by weight)					
Be9	6.87	4.52	0.82	3.54	5.88
Na23	45.25	96.93	<11.99	15.76	17.37
Mg24	71.34	95.96	85.65	110.10	85.21
Al27	529250.50	529250.50	529250.50	529250.50	529250.50
Ti47	113.57	125.74	131.06	122.41	126.47
V51	7.42	8.94	9.43	10.72	9.07
Cr53	74.00	90.48	90.78	100.04	92.79
Mn55	<0.39	<0.67	<0.60	<0.69	<0.23
Fe57	3575.26	4099.17	4355.35	4697.28	3939.04
Ga71	100.22	116.12	122.64	142.13	124.44
Total %	53.32	53.39	53.40	53.45	53.37
Cations (Atom Mole ppm)					
Be9	15.49	10.18	1.85	7.97	13.25
Na23	39.98	85.59	0.00	13.91	15.34
Mg24	59.62	80.15	71.54	91.92	71.19
Al27	398475.31	398208.18	398213.11	398043.06	398338.32
Ti47	48.16	53.29	55.54	51.86	53.61
V51	2.96	3.56	3.76	4.27	3.62
Cr53	28.91	35.32	35.44	39.04	36.24
Mn55	0.00	0.00	0.00	0.00	0.00
Fe57	1300.37	1489.92	1583.06	1706.61	1432.19
Ga71	29.20	33.81	35.71	41.37	36.24
Total (Atom Mole)	40.00	40.00	40.00	40.00	40.00
Mg-Ti	11.46	26.86	15.99	40.06	17.58
Be-Ti	-32.68	-43.11	-53.70	-43.88	-40.37
(Be+Mg)-Ti	26.95	37.04	17.84	48.03	30.83

< = below the detection limit of which 0.00 value is used for calculation of atom mole ppm

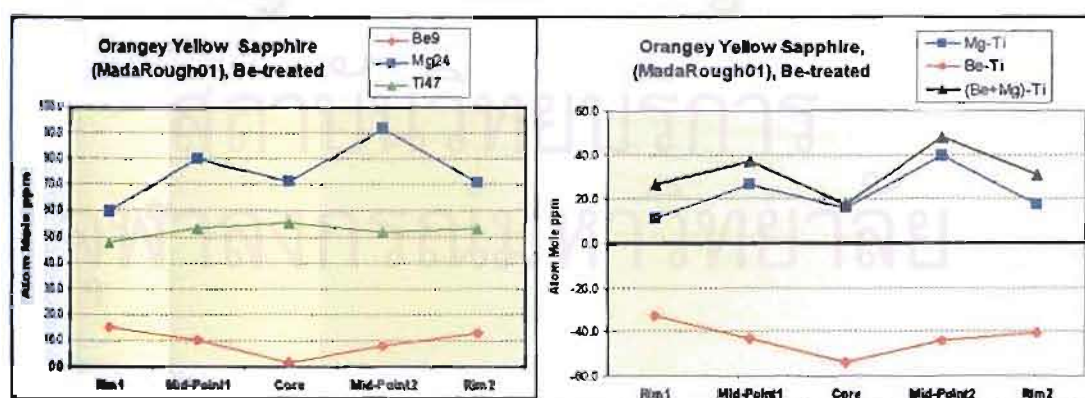


Figure 1.24: Plots of trace element content variation across the cut surface of the orangey yellow Be-treated rough sapphire (MadaRough01, Figure 1.23b). The analyses show higher Be content at the rims and gradually decreasing toward the core. The contents of Mg and Ti and other trace elements (see Table 1.7) however, show no consistent variation across the profile. At all the points analyzed (Be+Mg) > Ti.

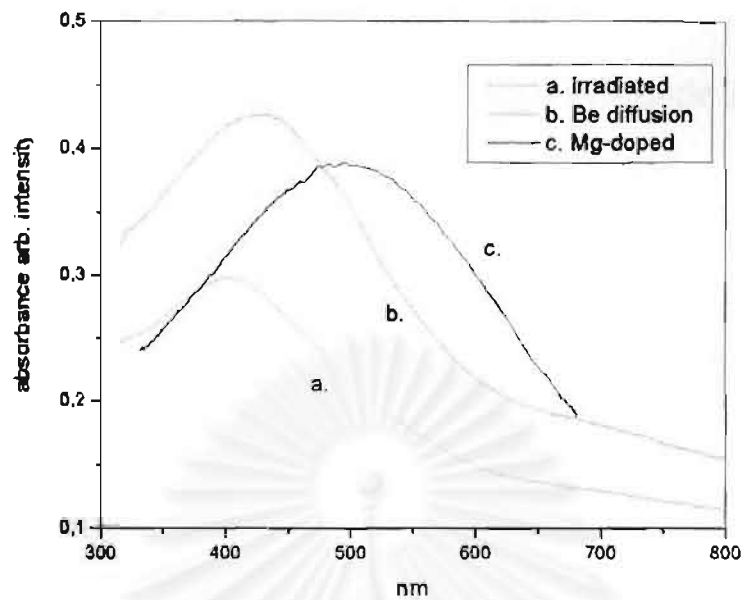


Figure 1.25: Comparison of the UV-Vis spectra of synthetic samples: irradiated with X-rays (turned brown after treatment, a), diffusion treated with Be (turned brown after treatment, b), and doped with Mg (brown to violet specimen was obtained, c).

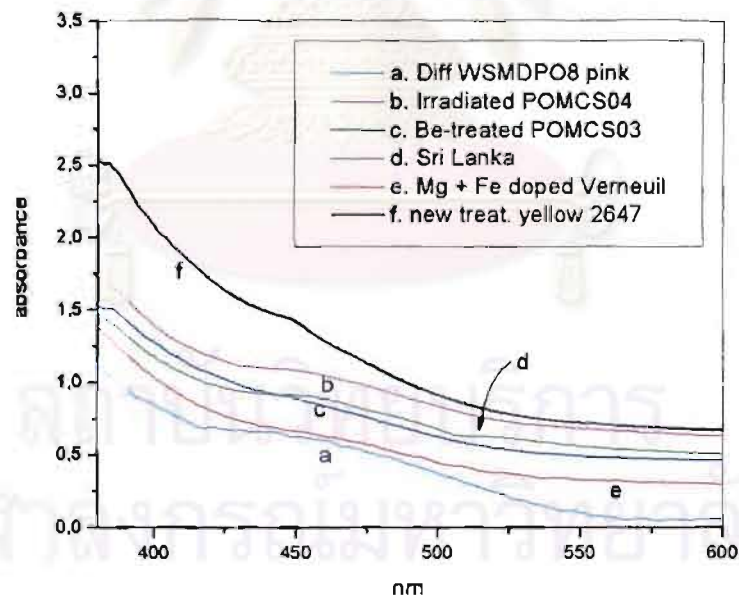


Figure 1.26: Comparison of the UV-Vis spectra of yellow sapphires: a natural sample irradiated with X-rays (b), natural samples with Be-treatment (c and f), a natural sample from Sri Lanka (d), the difference of absorption spectra between an orange Be-treated sapphire and its original pink sample (a), a synthetic sample double-doped with Mg and Fe (e).

Chapter 2

Beryllium-Diffusion Experiments on Pure Synthetic and Fe-Doped Synthetic Sapphires

Introduction

In the first chapter we have presented the UV-Vis-spectroscopic study and the Laser Ablation Inductively-coupled-Plasma Mass Spectrometry (LA-ICP-MS) results of irradiated and Be-treated synthetic and natural colourless sapphires, yellow and orangey yellow Be-treated natural sapphires. We have found that majority of Be-treated sapphires show indications of Be diffusion into the corundum lattice from an external source. We always found that there were the excesses of (Be+Mg) over Ti contents in most of the yellow sapphires. We also found from our own oxidation and reduction heating experiments that oxidizing condition was an important factor in the formation of stable colour centres.

Hence up to the present knowledge we believe that the excess of the divalent elements (Be+Mg), after calculation of colourless MgTiO_3 and/or BeTiO_3 clusters, in combination with iron and the heat treatment in oxidising atmosphere can produce the stable yellow colour centres in the yellow Be-treated natural sapphires. In the synthetic colourless sapphires (without iron), however, the situation is somewhat different. The divalent Be and the heat treatment in oxidising atmosphere could produce stable brown colour centres in the same way as it was found earlier for Mg, i.e. able to produce stable brownish violet colour centres. The result has been presented in several meetings and published both in the national and international Journals (Pisutha-Armond et al., 2002 and 2004; see Appendices).

In the previous study we have made an assumption that the divalent Be acts in the same way as that of Mg, i.e. as a stabiliser of brown or yellow colour centres.

However to prove such an assumption we need to do more Be-diffusion experiments with pure synthetic and Fe-doped synthetic corundum.

'Classical' and Beryllium-Treated colourless Synthetic Sapphires

To prove that Be has indeed involved in brown coloration in pure synthetic sapphire, a comparison experiment was performed on a piece pure synthetic colourless 'watch glass' sapphire that was cut in half. One half was heat-treated with ground chrysoberyl in a crucible while the other half was heated in another crucible without chrysoberyl. The heating condition for both crucibles was 1750°C for 30 hours in an oxidizing atmosphere. After the treatment, the samples were lightly polished and the trace element contents were analyzed using LA-ICP-MS at the GEMOC Key Centre, Department of Earth and Planetary Sciences, the Macquarie University, Sydney, Australia (Figure 2.1). The analytical condition was the same as that in the first chapter.

Result

The sapphire (THSCS01) was still colourless after 'classical' heating but it turned brown after Be-treatment (Figure 2.2). Trace element analyses of the colourless half show that the material is rather pure originally and only traces of Ti and Na are present (Table 2.1). The analyses of the brown half reveal that about 10 ppm by weight or 20 atom mole ppm of Be has diffused into the corundum lattice while the other trace elements are negligible (Figure 2.3 and Table 2.1). The UV-Vis spectrum of the Be-treated brown half shows exactly the same pattern as that of the flame-fusion grown sapphire (PKSCS01) treated under unknown condition by a Thai heater (Figure 2.4). The spectra show the broad absorption band centred at around 420 nm. This experiment has therefore proved that Be did take part in the brown coloration.

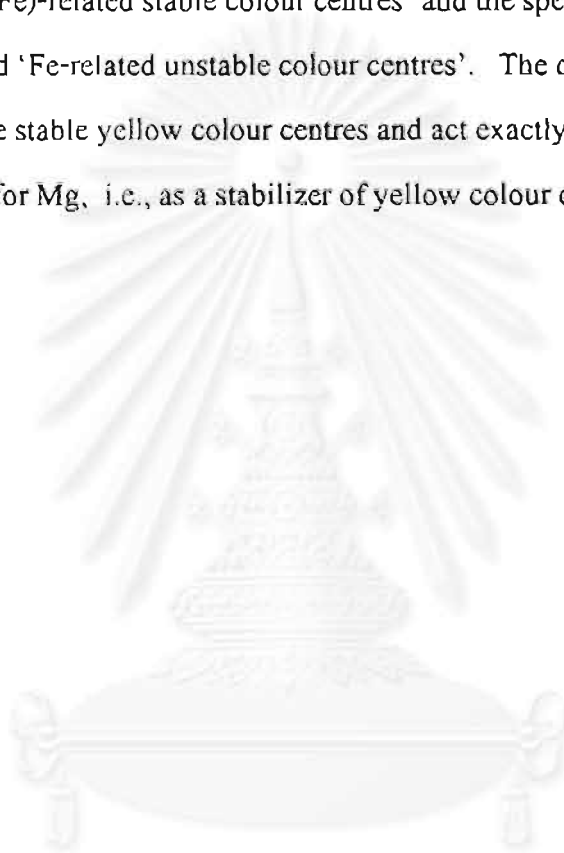
Fe-doped synthetic sapphire treated with Be

In order to definitely prove that Fe was indeed involved in yellow coloration in a Be-treated sapphire with significant Fe, an Fe-doped sapphire was synthesized by a flame-fusion technique. The sample was then irradiated with X-rays and shortly after the irradiation treatment sample was subjected to a fading test. The fading was carried out for one hour at 3 cm distance from a 100W light bulb. The sample was subsequently heated in a crucible with ground chrysoberyl. The heating condition was at 1780°C for 50 hours in an oxidizing atmosphere. The Be-treated sample was then subjected to the fading test again. The sample was photographed and the UV-Vis spectrum was recorded in each step of experiments. The above experiments were carried out by Dr. T. Häger. The sample was then cut in half, lightly polished and analysed for trace element contents across the cut surface using LA-ICP-MS.

Result

The Fe-doped synthetic sapphire was colourless before treatment (Figure 2.5a). The sample contains abundant gas bubbles typical of a flame-fusion grown material (Figure 2.6b and c). The sample became yellow after irradiation treatment (Figure 2.5b) and the absorption spectrum shows a continuous increase toward the UV region and a shoulder at about 460 nm (Figure 2.7). The sample irradiated with X-rays became colourless shortly after a fading test (Figure 2.5c). The sample turned yellow again after treatment with Be and the yellow colour was stable after a fading test (Figure 2.5d). The UV-Vis spectrum of the sample treated with Be shows exactly the same pattern as that of the sample irradiated with X-rays (Figure 2.7). These spectra are also similar to those of a Sri Lankan yellow sapphire coloured by stable defect centres, an Fe+Mg doped synthetic sapphire (Figure 2.8) and a natural sapphire irradiated with X-rays (see figure 1.11). The trace element analyses confirm that significant contents of Be and Fe (about 25-30 atom mole ppm of Be and 50-60 atom mole ppm of Fe) are

present in this synthetic sapphire after Be-treatment while the other trace element contents are negligible. Hence we are certain that it is a system dominated only by Be+Fe without the influence of other trace elements. These experiments have proved without doubt that the Be+Fe system act exactly in the same way as the Mg+Fe system. The spectrum produced by the Be+Fe or Mg+Fe might therefore be called '(Be+Fe) or (Mg+Fe)-related stable colour centres' and the spectrum produced by irradiation is called 'Fe-related unstable colour centres'. The divalent Be is therefore able to produce the stable yellow colour centres and act exactly in the same way as it was found earlier for Mg, i.e., as a stabilizer of yellow colour centres.



References

- Pisutha-Amond, V., Häger, T., Wathanakul, P., Atichat, W., 2002.** A brief summary on a cause of colour in pink-orange, orange and yellow sapphires produced by the “new” heating technique. *Journal of Gem and Jewelry*, Gem and Jewelry Institute of Thailand (GIT), 3(18), 11-12.
- Pisutha-Amond, V., Häger, T., Wathanakul, P., Atichat, W., 2004.** Yellow and brown colouration in beryllium treated sapphires. *Journal of Gemmology*, 29(2), 77-103
- Pisutha-Amond, V., Wathanakul, P., Atichat, W., Haeger, T., Win, T.T., Leelawatanasuk, T., and Sombeon, C., 2003.** Beryllium-treated Vietnamese and Mong Hsu rubies. In: Hofmeister W., Quang V.X., Doa N.Q., and Nghi T. (eds) *Proceedings of the 2nd International Workshop on Geo- and Material-Science on Gem-Minerals of Vietnam, Hanoi, October 1-8, 2003*, 171-5

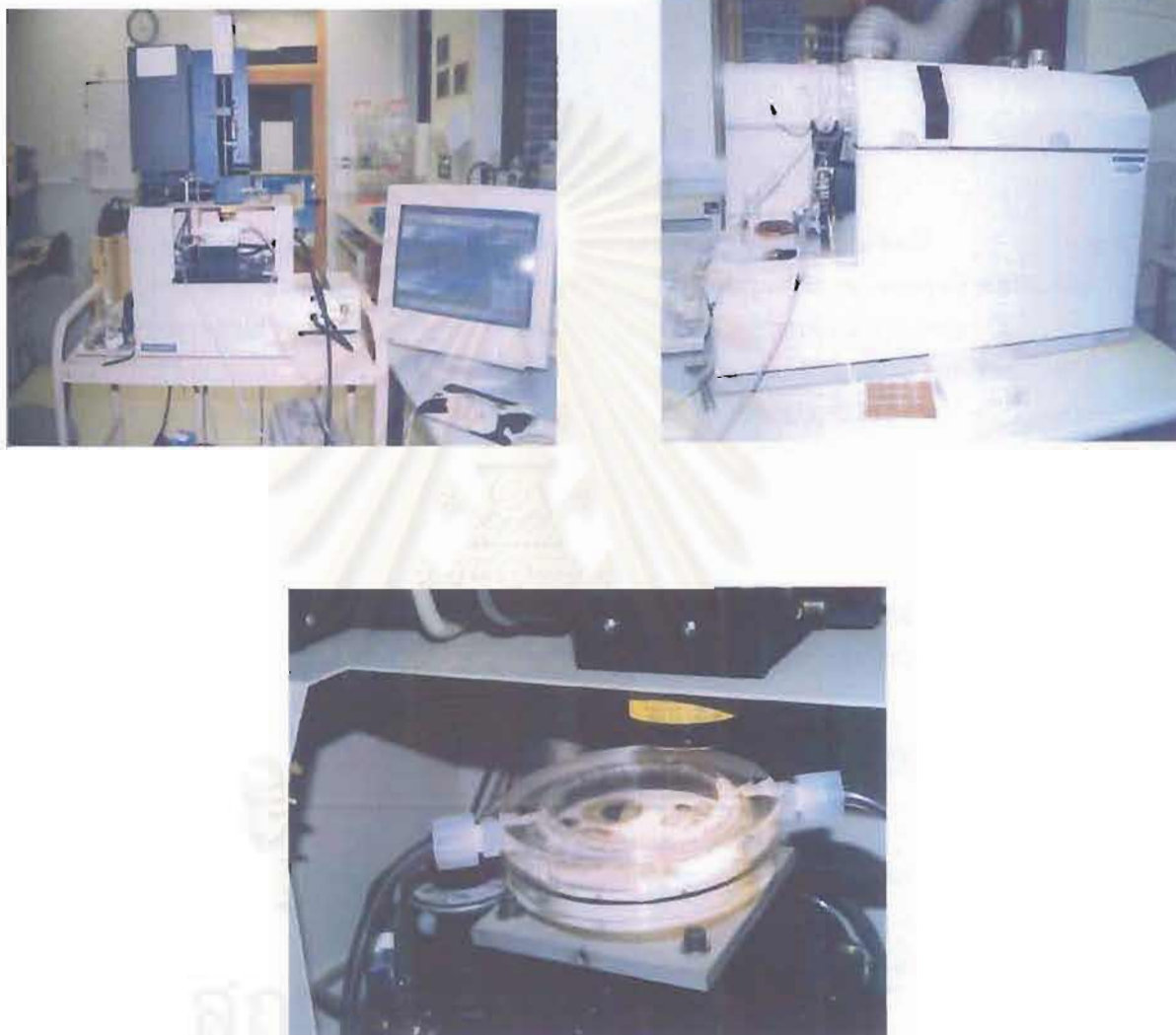


Figure 2.1: Photos of the LA-ICP-MS unit used for trace element analysis in this study, located at the Macquaries University, Sydney, Australia.

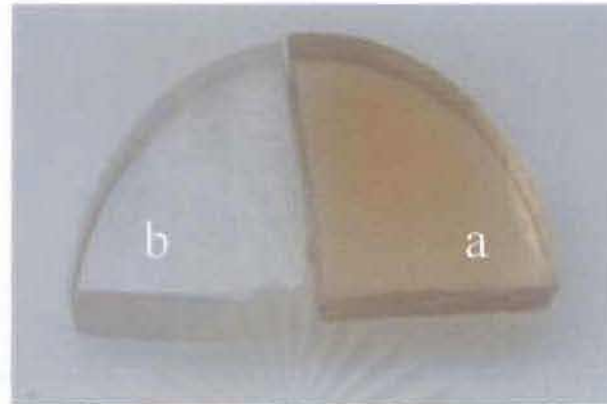


Figure 2.2: A colorless sapphire disc (THSCS01) was cut in half, one half was heat-treated with ground chrysoberyl in a crucible (a, brown) while the other half was heat-treated in another crucible without chrysoberyl (b, colourless). After the treatment five-points on a traverse were analyzed on the polished surface of each half. (Photo by Somboon, GIT)

Table 2.1: Trace element contents of the colourless sapphire disc (THSCS01) obtained from LA-ICP-MS.. CH's are points analyzed on the colourless half (b) and BeH's are those on the brown half (a).

	CH1	CH2	CH3	CH4	CH5	BeH1	BeH2	BeH3	BeH4	BeH5
Cations (ppm by weight)										
Be9	<1.78	<2.37	<1.59	<1.25	<0.79	8.16	8.05	10.21	11.10	10.23
Na23	143.46	133.48	177.53	126.79	91.66	<37.49	113.94	122.62	124.76	161.72
Mg24	<2.73	<4.19	<3.41	<2.50	<1.94	<2.32	<3.44	<3.57	<3.37	<2.40
Al27	529250.40	529250.40	529250.40	529250.40	529250.40	529250.40	529250.40	529250.40	529250.40	529250.40
Ti47	3.31	2.22	2.51	2.78	3.28	3.28	1.43	1.91	2.01	1.36
V51	<0.07	<0.10	<0.08	<0.07	0.06	<0.06	<0.09	<0.09	<0.08	<0.06
Cr53	<1.80	<2.74	<2.16	<1.57	<1.24	<1.56	2.49	<2.37	<2.11	<1.59
Mn55	<0.16	<0.24	<0.20	<0.14	<0.12	<0.14	<0.19	<0.20	<0.19	<0.13
Fe57	<8.82	<14.01	<11.49	<8.13	<6.60	13.49	<10.70	<11.37	<10.54	<7.62
Ga71	<0.03	0.07	0.13	0.14	0.16	0.10	0.14	0.22	0.31	0.38
Total %	52.94	52.94	52.94	52.94	52.93	52.93	52.94	52.94	52.94	52.94
Cations (Atom Mole ppm)										
Be9	0.00	0.00	0.00	0.00	0.00	18.46	18.21	23.09	25.11	23.14
Na23	127.20	118.36	157.40	112.43	81.30	0.00	101.03	108.72	110.62	143.36
Mg24	0.00	0.00	0.00	0.00	0.00	0.00	0.00	0.00	0.00	0.00
Al27	399871.39	399830.66	399841.49	399866.35	399917.23	399975.19	399879.14	399867.31	399863.33	399832.80
Ti47	1.41	0.94	1.07	1.18	1.40	1.40	0.61	0.81	0.86	0.57
V51	0.00	0.00	0.00	0.00	0.02	0.00	0.00	0.00	0.00	0.00
Cr53	0.00	0.00	0.00	0.00	0.00	0.00	0.98	0.00	0.00	0.00
Mn55	0.00	0.00	0.00	0.00	0.00	0.00	0.00	0.00	0.00	0.00
Fe57	0.00	0.00	0.00	0.00	0.00	4.92	0.00	0.00	0.00	0.00
Ga71	0.00	0.02	0.04	0.04	0.05	0.03	0.04	0.06	0.09	0.11
Total (Atom Mole %)	40.00	40.00	40.00	40.00	40.00	40.00	40.00	40.00	40.00	40.00
Be-TI	-1.41	-0.94	-1.07	-1.18	-1.40	-1.40	-0.61	-0.81	-0.86	-0.57
Na-TI	-1.41	-0.94	-1.07	-1.18	-1.40	17.07	17.60	22.28	24.25	22.56
Al-Mg-TI	-1.41	-0.94	-1.07	-1.18	-1.40	17.07	17.60	22.28	24.25	22.56
Be-Mg %	0.00	0.00	0.00	0.00	0.00	74.49	96.77	96.60	96.71	97.58
Ti %	100.00	100.00	100.00	100.00	100.00	5.63	3.23	3.40	3.29	2.42
Fe %	0.00	0.00	0.00	0.00	0.00	19.87	0.00	0.00	0.00	0.00

< = below the detection limit of which 0.00 value is used for calculation of atom mole ppm

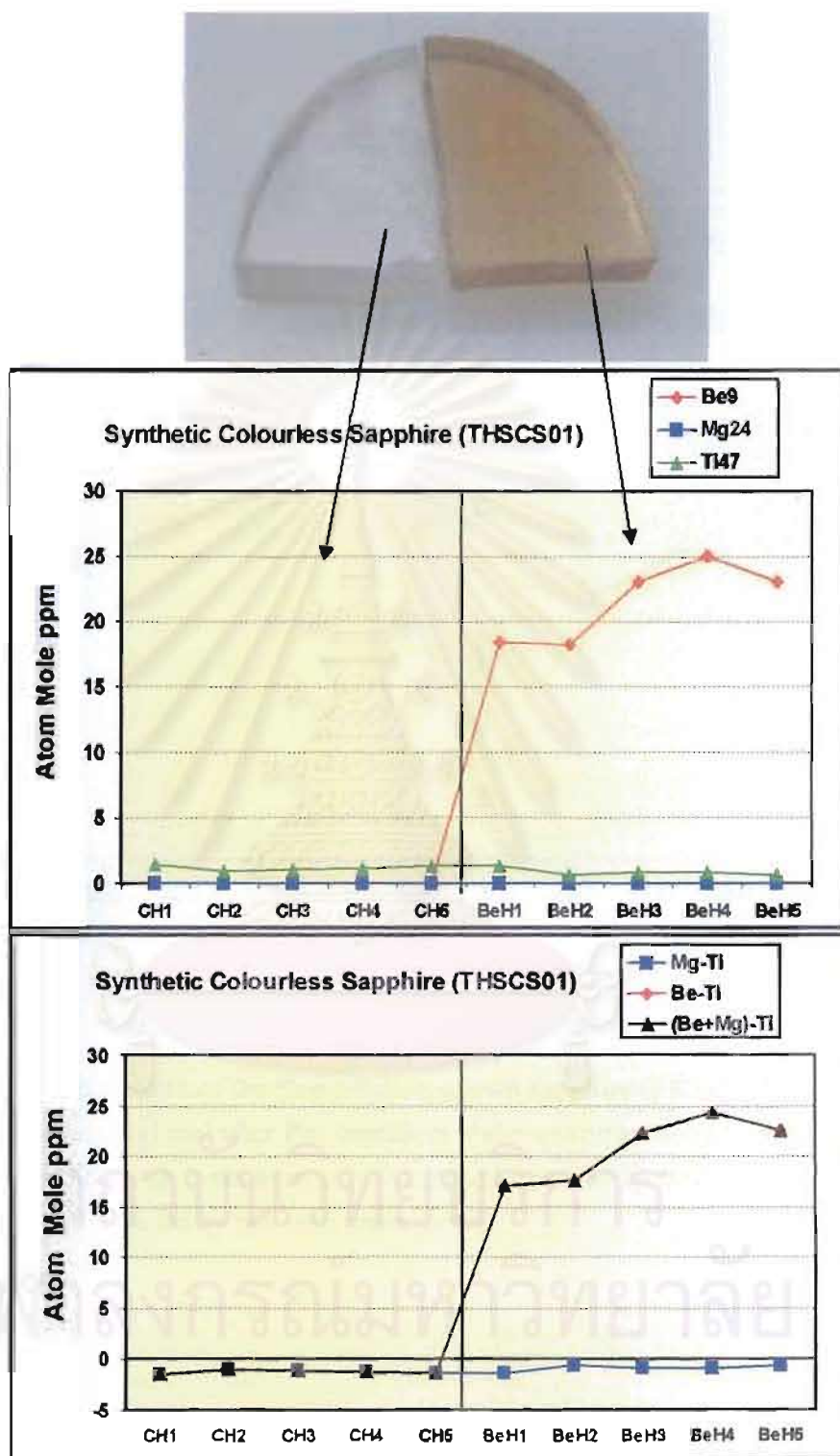


Figure 2.3: Plots of trace element contents analyzed on the surface of the sapphire disc (THSCS01), see text for discussion.

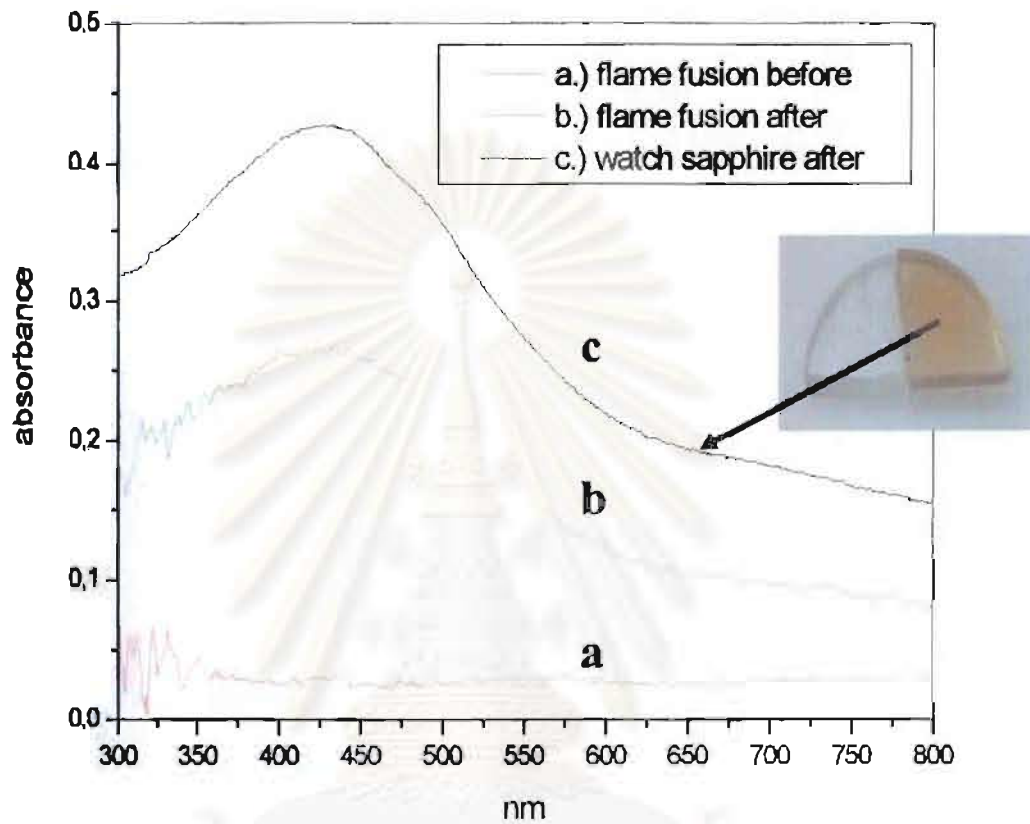


Figure 2.4: UV-Vis spectra of the flame-fusion-grown sapphire (PKSCS01) before treatment (a) and after Be- treatment under unknown condition by a Thai heater (b) Spectrum c was recorded from the brown half (THSCS01) treated with Be by our own experiment.

จุฬาลงกรณ์มหาวิทยาลัย

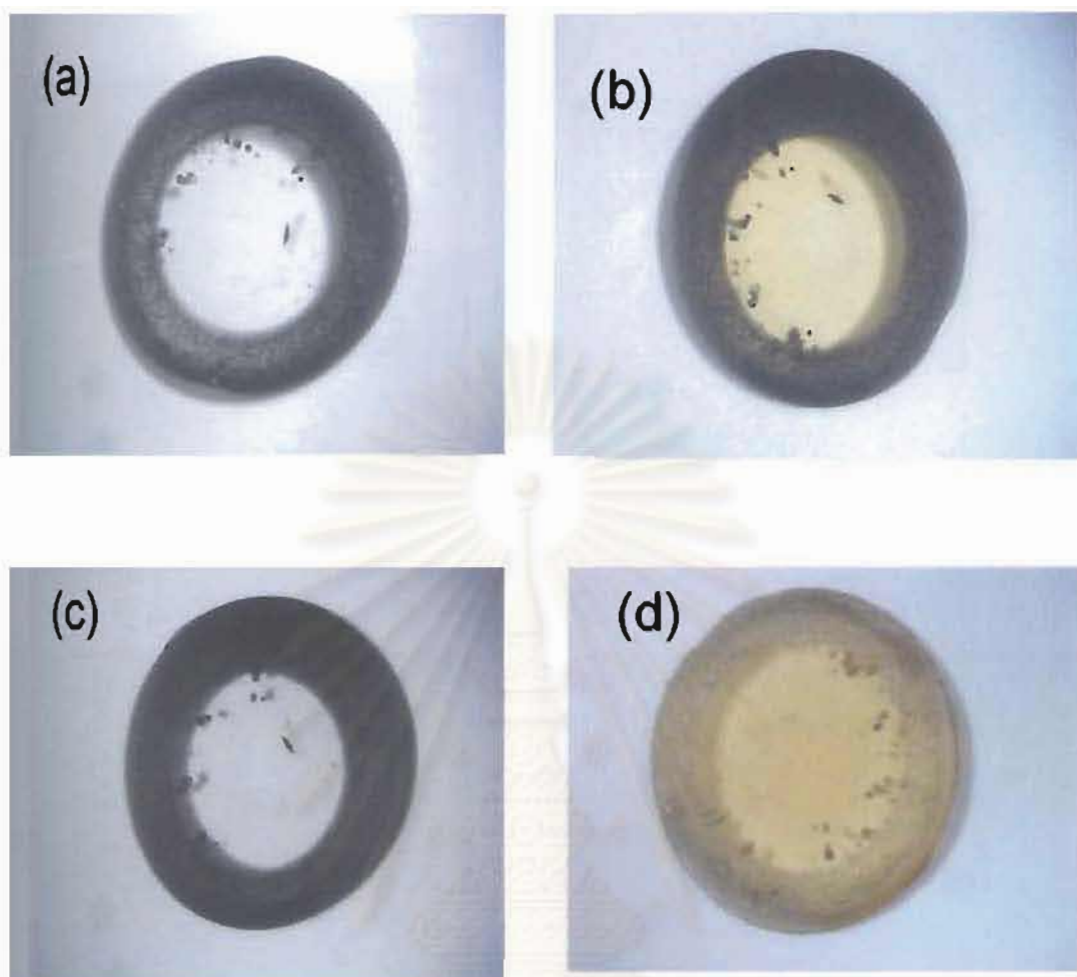


Figure 2.5: Photos of a Fe-doped flame-fusion-grown colourless sapphire before treatment (a), yellow after X-ray irradiation treatment (b), colourless after a fading test (c), yellow again after Be-treatment (d) and the colour was stable under the fading test. (Photo by Häger)

จุฬาลงกรณ์มหาวิทยาลัย

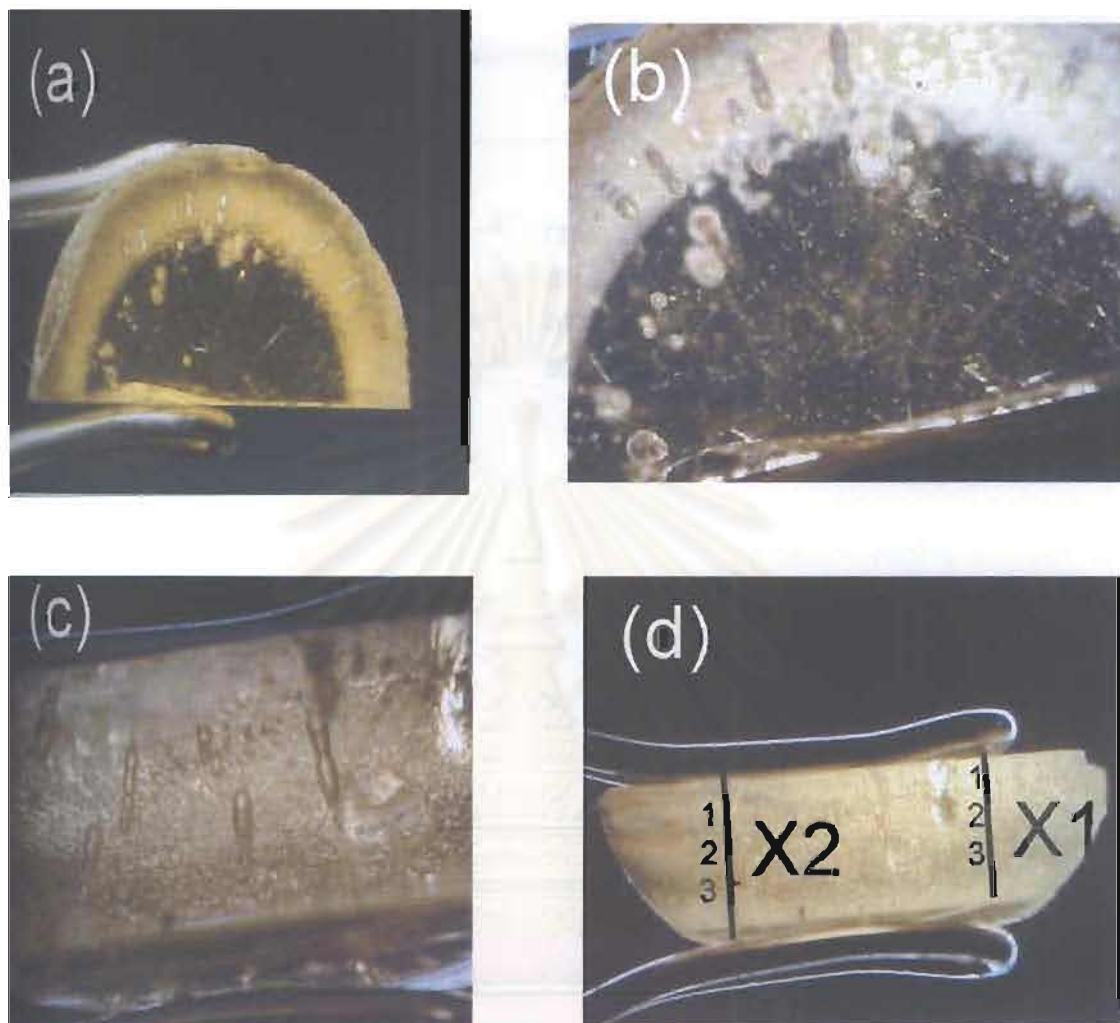


Figure 2.6: Photos of the Fe-doped sapphire treated with Be and cut in half (a), showing abundant gas bubbles (b and c). Two traverses (X1 and X2) were analyzed across the cut surface (d) using LA-ICP-MS (see also Table 2.2 and Figure 2.9).
(Photo by Somboon, GIT)

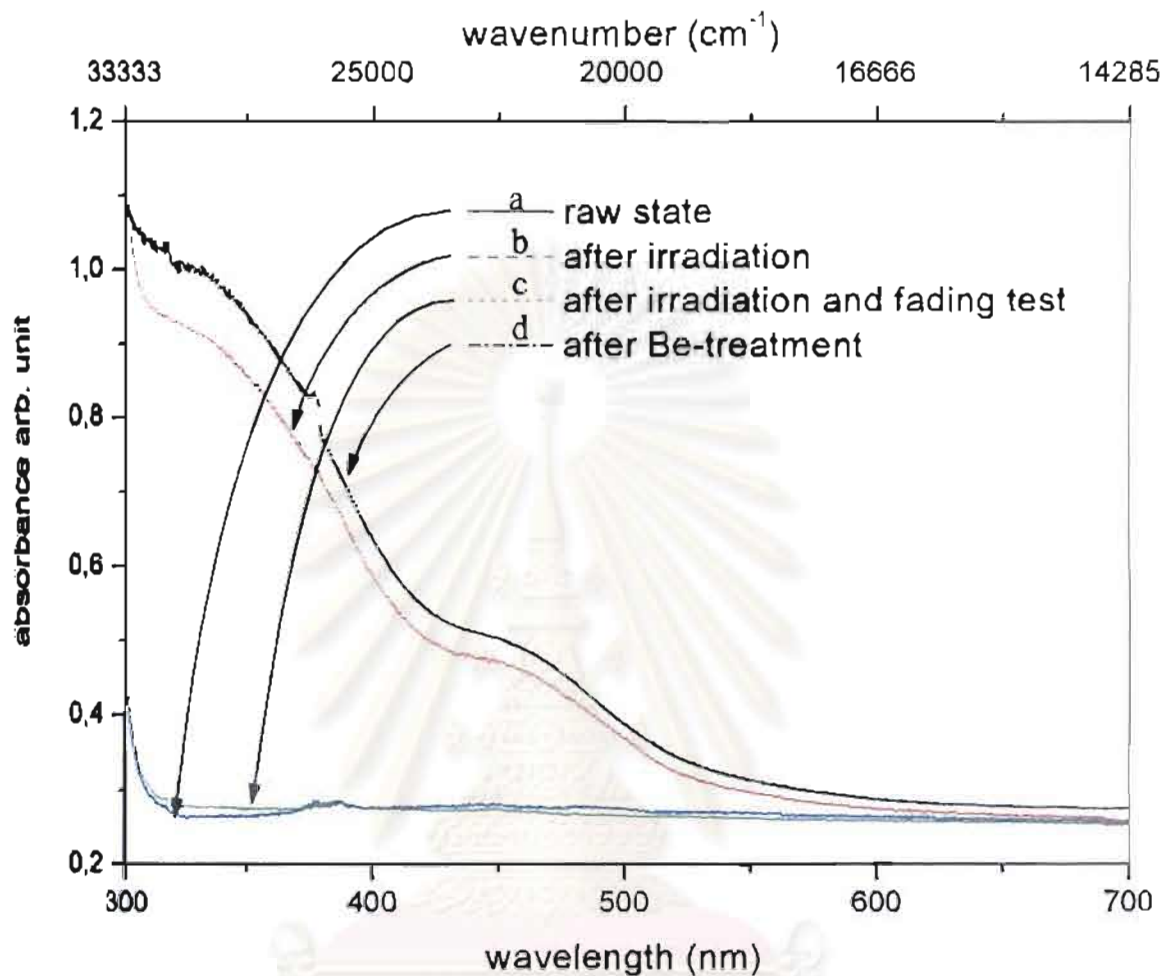


Figure 2.7: UV-Vis spectra of the Fe-doped flame-fusion-grown sapphire before treatment (a), after X-ray irradiation treatment (b), after a fading test (c), and after Be-treatment (d). The spectrum produced by Be-treatment is exactly the same as that of the irradiation treatment and similar to those of the Mg+Fe doped flame-fusion-grown sapphire and a natural Sri Lankan yellow sapphire coloured by stable defect centres (see Figure 2.8). All spectra were measured with E perpendicular to c-axis (o-ray).

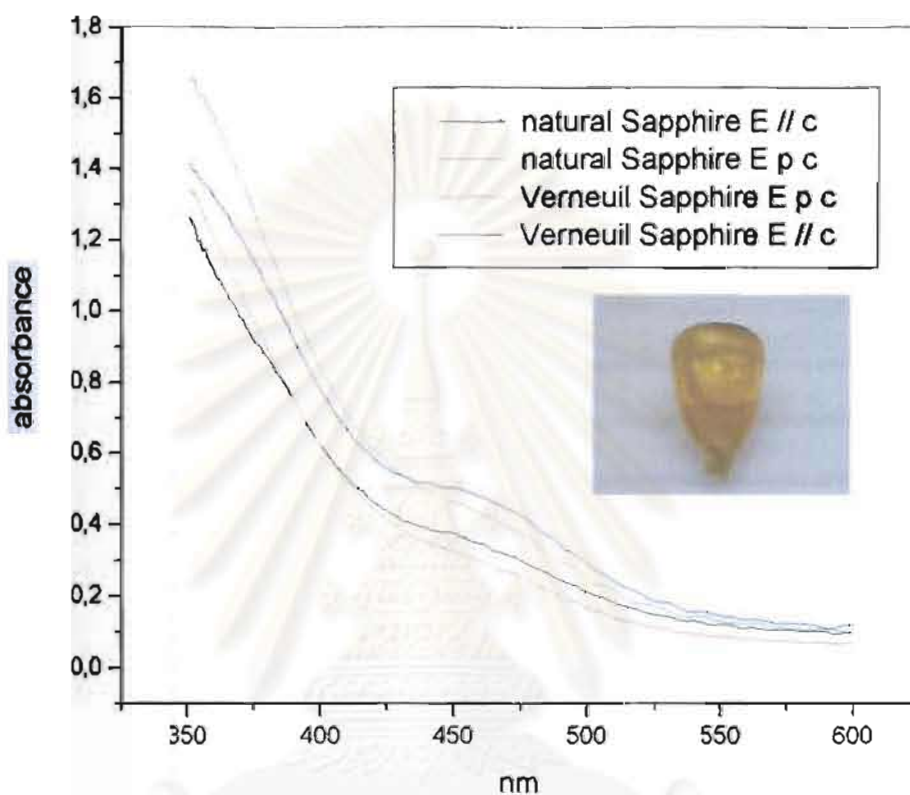


Figure 2.8: UV-Vis Spectra of a natural Sri Lankan yellow sapphire coloured by stable defect centres in comparison to a synthetic flame fusion grown sapphire doped with 50 ppm Mg and 50 ppm Fe (Hager, 2001).

จุฬาลงกรณ์มหาวิทยาลัย

Table 2.2: Trace element contents along the traverse X1 of the Fe-doped sapphire treated with Be, obtained by LA-ICP-MS.

	X1-1	X1-2	X1-3	X1-4	X1-5	X1-6	X1-7	X1-8	X1-9
Cations (ppm by weight)									
Be9	12.91	13.99	13.05	12.74	12.74	11.57	11.41	13.01	13.14
Na23	4.96	13.56	14.10	6.37	7.38	3.93	2.30	2.50	1.87
Mg24	<0.21	0.35	<0.20	<0.20	<0.21	<0.20	<0.19	<0.17	0.35
Al27	529250.40	529250.40	529250.40	529250.40	529250.40	529250.40	529250.40	529250.40	529250.40
Ti47	<0.59	<0.49	<0.59	<0.52	<0.60	<0.54	0.54	<0.47	0.95
V51	<0.05	<0.05	<0.05	<0.05	<0.05	<0.05	<0.05	<0.04	<0.04
Cr53	<0.63	<0.55	<0.64	0.59	<0.60	<0.58	0.81	<0.48	<0.49
Mn55	<0.07	<0.06	<0.07	<0.07	<0.07	<0.06	<0.06	<0.05	0.06
Fe57	159.07	170.66	157.46	151.28	148.81	141.22	151.57	150.39	157.70
Ga71	<0.04	<0.03	<0.04	<0.04	0.04	<0.04	<0.04	<0.03	<0.03
Total %	52.94	52.94	52.94	52.94	52.94	52.94	52.94	52.94	52.94
Cations (Atom Mole ppm)									
Be9	29.20	31.65	29.52	28.82	28.82	26.17	25.81	29.43	29.72
Na23	4.40	12.02	12.50	5.65	6.54	3.49	2.04	2.22	1.66
Mg24	0.00	0.29	0.00	0.00	0.00	0.00	0.00	0.00	0.30
Al27	399908.33	399893.74	399900.50	399910.08	399910.31	399918.79	399916.59	399913.46	399910.32
Ti47	0.00	0.00	0.00	0.00	0.00	0.00	0.23	0.00	0.41
V51	0.00	0.00	0.00	0.00	0.00	0.00	0.00	0.00	0.00
Cr53	0.00	0.00	0.00	0.23	0.00	0.00	0.00	0.00	0.00
Mn55	0.00	0.00	0.00	0.00	0.00	0.00	0.00	0.00	0.02
Fe57	58.06	62.29	57.48	55.22	54.32	51.55	55.33	54.90	57.56
Ga71	0.00	0.00	0.00	0.00	0.01	0.00	0.00	0.00	0.00
Total (Atom Mole %)	40.00	40.00	40.00	40.00	40.00	40.00	40.00	40.00	40.00
Mg-Ti	0.00	0.29	0.00	0.00	0.00	0.00	-0.23	0.00	-0.11
Be-Ti	29.20	31.65	29.52	28.82	28.82	26.17	25.58	29.43	29.32
(Be+Mg)-Ti	29.20	31.94	29.52	28.82	28.82	26.17	25.58	29.43	29.62
(Be+Mg) %	33.46	33.90	33.93	34.28	34.86	33.68	31.72	34.90	34.12
Ti %	0.00	0.00	0.00	0.00	0.00	0.00	0.28	0.00	0.46
Fe%	66.64	68.10	66.07	65.71	66.34	66.32	68.00	65.10	65.42

< = below the detection limit of which 0.00 value is used for calculation of atom mole ppm

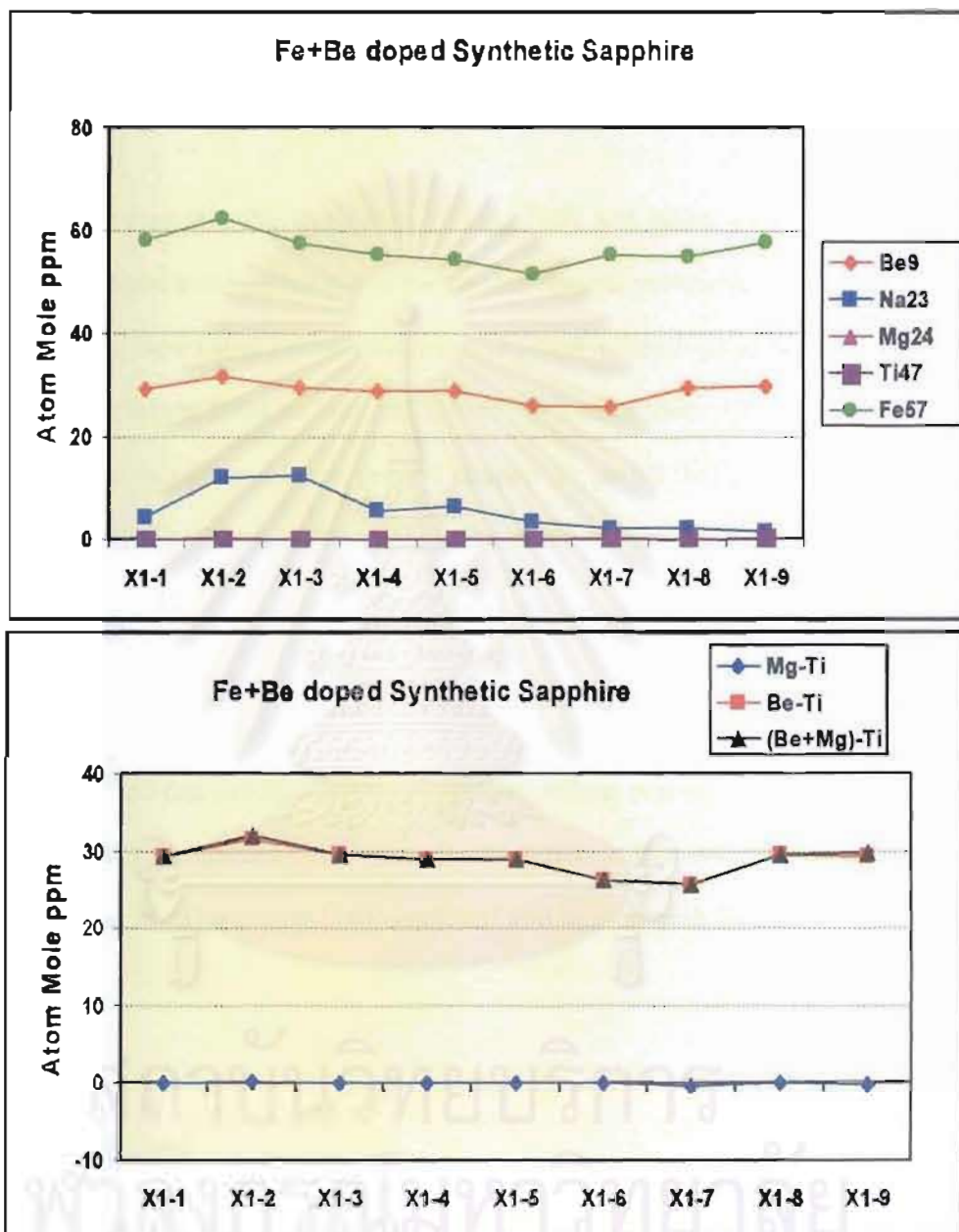


Figure 2.9 Plots of the trace element content along the traverse X1 of the Fe-doped synthetic sapphire treated with Be. The Fe and Be contents are constantly high across the cut surface while the other elements are extremely low.

Chapter 3

'Classical' versus 'Beryllium' Heat-Treated Blue Sapphires

Introduction

In the first chapter (see also Pisutha-Armond et al., 2002 and 2004) we have presented trace element contents and interaction of Be-treated natural yellow sapphires. We discovered that the Be-treated yellow sapphires showed indications of Be diffusion into the corundum lattice from an external source. We have found $(\text{Be}+\text{Mg}) > \text{Ti}$ in most of the yellow sapphires. In the second chapter we prove that the interaction of trace element in Be+Fe system acts exactly in the same way as that in the Mg+Fe system. Hence up to the present knowledge we believe that in the Be+Mg+Ti+Fe system the excess of the divalent elements, Be+Mg, after calculation of colourless MgTiO_3 and/or BeTiO_3 clusters, in combination with iron and the heat treatment in oxidising atmosphere can produce the stable yellow colour centres. To further prove this assumption and understand trace element interaction in this system, additional analyses on natural blue sapphires both untreated and treated with Be need to be carried out.

Samples and method

Two 'classically' heat-treated blue sapphires and two Be-treated blue sapphires obtained from Thai burners were cut in half and lightly polished on the cut surfaces. Five-point profiles were analyzed across the cut surfaces by LA-ICP-MS at the GEMOC Key Centre, Department of Earth and Planetary Sciences, the Macquarie University Sydney, Australia. The analytical condition was the same as that in the previous chapters.

Our own heating experiment was also carried out on a blue sapphire sample cut in half. One half was mixed with ground chrysoberyl in double-crucibles packed with alumina-powders whereas the other half was put in another crucible without chrysoberyl. Both crucibles were heated in a resistance furnace with Super Kanthal 1900 heating elements at 1,750°C in air (oxidizing conditions) for 30 hours to confirm the result. The heating experiment was done with the courtesy of Dr. T. Häger.

Result

'Classically' heat-treated blue sapphires

The analyses of the two 'classically' heat-treated blue sapphires, one from Australia and the other from unknown source, show no detectable Be (below 1 ppm detection limit) across the profiles (Tables 3.2 and 3.2; Figures 3.1 to 3.4). The stones are dominated by Fe and Ti with trace amounts of Mg. All the analyzed points show $Ti > Mg + Be$. The excess Ti after calculation of $MgTiO_3$ and $BeTiO_3$ clusters could form colour active $FeTiO_3$ clusters or Fe-Ti intervalent charge transfer mechanism causing blue coloration of the stones.

Be-treated natural blue sapphires

An oval cut blue sapphire (PPBS1) from an unknown source reportedly heat-treated with Be under unknown conditions by a heater in Chanthaburi show a thin surface-related yellow zone surrounding a blue core (Figures 3.5). High magnification shows that the blue core contains oriented blue dots probably resulting from partially dissolution of rutile needles. The LA-ICP-MS data (Table 3.3; Figures 3.6) reveal the elevated Be content (9 to 27 ppm) of the yellow rims and its absence at the blue core

(below 1 ppm), again indicating Be diffusion into the corundum lattice from an external source. All the analyzed points in the cores show an excess of Ti content after calculation of colourless MgTiO_3 or BeTiO_3 clusters (i.e. Mg-Ti and Be-Ti content show negative values). In the yellow rim there is an excess of Be+Mg over Ti while in the blue core Be+Mg is lower than Ti. This data strongly suggest that a yellow hue can only be formed if there is an excess of Be+Mg over Ti content in the corundum lattice.

Another 2.28 ct rectangular cut of blue-green sapphire (BG1) reportedly from Bang Kacha was also heat-treated with Be under unknown condition by a heater in Chanthaburi. After treatment the sample shows obviously thin surface-related yellow rim surrounding complex-zoned blue core (Figure 3.7). The LA-ICP-MS profile analysis across the cut surface reveals the elevated Be content at the rim (Table 3.4 and Figure 3.8) especially for all the points analyzed at the outer surface of the stone (Table 3.5; Figures 3.9 and 3.10). The blue core shows extremely low Be content (below 1 ppm). All the analyzed points in the blue core show an excess of Ti over Mg+Be content (i.e. after calculation of MgTiO_3 and BeTiO_3 clusters). At the points on both rims, which show the elevated Be contents and are at the boundary of the blue core and the yellow rim, the Ti contents still exceed the sum of Be+Ti (Table 3.4 and Figure 3.8). The excess Ti could therefore form colour active FeTiO_3 clusters which cause blue coloration in the core area. On the contrary, all the points analyzed at the outer surface of the stone which are definitely on the yellow rim (Figure 3.9) show an excess of Be+Mg over Ti (Figure 3.10). It should be noted further that the blue sapphires (PPBS1 and BG1) shown in Figures 3.5 to 3.10 are the stones in which Ti exceeds the Mg content in all analyzed points. This data hence suggest that with the 'classical' heat-treatment it is unlikely to change these stones yellow. With diffusion of Be into the corundum lattice it is now possible to change the balance of the Ti/(Be+Mg) ratio. In the yellow rim the sum of Be+Mg exceeds the Ti content. Hence

the yellow hue can only be formed if there is an excess of Be+Mg over Ti contents in the lattice. This can be confirmed by our own heating experiment of a blue stone in Figure 3.11.

Conclusion

In conclusion for the Be-treated natural blue sapphires, we continued to discover that the sapphires show an indication of Be diffusion into the corundum lattice from an external source. We always found that there is an excess of Be+Mg over Ti contents in the yellow rim in contrast to $Ti > Mg+Be$ in the blue core. These data in combination of the result from the first and second chapters strongly suggest that the excess of Be+Mg in combination with Fe and oxidizing atmosphere have led to the formation of stable yellow colour centres.

It is now possible to change the triangular diagram model proposed by Häger (1996) presented in BOX1 in Chapter 1 in such a way that we can add Be into the Mg corner. In so doing we can plot the approximate compositions of some treated stones into both diagrams as shown in Figures 3.12 and 3.13. The colours of those stones fit such the model nicely.

References

- Häger, T., 2001. High temperature treatment of natural corundum. In Proceedings of the International Workshop on Material Characterization by Solid State Spectroscopy: The Minerals of Vietnam, Hanoi, Vietnam. April 4-10, 2001
- Häger, T., 1996. Farbrelevante Wechselwirkungen von Spurenelementen in Korund: Ph.D. Thesis, University of Mainz
- Peretti, A., Guenther, D., and Graber, A.-L., 2003. The beryllium treatment of fancy sapphires with a new heat-treatment technique (part B). *Contributions to Gemology*, 2, 21-33
- Pisutha-Armond, V., Häger, T., Wathanakul, P., Atichat, W., 2002. A brief summary on a cause of colour in pink-orange, orange and yellow sapphires produced by the “new” heating technique. *Journal of Gem and Jewelry*, Gem and Jewelry Institute of Thailand (GIT), 3(18), 11-12.
- Pisutha-Armond, V., Häger, T., Wathanakul, P., Atichat, W., 2004. Yellow and brown colouration in beryllium treated sapphires. *Journal of Gemmology*, 29(2), 77-103
- Pisutha-Armond, V., Wathanakul, P., Atichat, W., Häger, T., Win, T.T., Leelawatanasuk, T., and Somboon, C., 2003. Beryllium-treated Vietnamese and Mong Hsu rubies. In: Hofmeister W., Quang V.X., Doa N.Q., and Nghi T. (eds) *Proceedings of the 2nd International Workshop on Geo- and Material-Science on Gem-Minerals of Vietnam, Hanoi. October 1-8, 2003*, 171-5
- Schmetzer, K. and Schwarz, D., 2004. The causes of colour in untreated, heat treated and diffusion treated orange and pinkish-orange sapphires- a review, *Journal of Gemmology*, 29, 149-182.



Figure 3.1: A natural blue sapphire (DIF1) reportedly underwent a ‘classical’ heat-treatment was cut in half. A five-point-profile was analyzed across the cut surface using LA-ICP-MS. (Photo by Lomthong, KU)

Table 3.1: Trace element contents of the blue sapphire (DIF1) showing high contents of Ti and Fe but negligible content of Be, obtained by LA-ICP-MS.

	Rim1	Mid-Point1	Core	Mid-Point2	Rim2
Cations (ppm by weight)					
Be9	0.28	<0.52	0.94	0.51	0.27
Na23	10.21	18.02	40.92	<15.36	<9.19
Mg24	5.85	7.03	7.03	4.67	5.94
Al27	529250.40	529250.40	529250.40	529250.40	529250.40
Ti47	869.91	1064.63	1046.40	679.24	778.00
V51	1.12	1.06	1.12	1.60	1.67
Cr53	<1.84	<4.36	<6.13	<3.58	<2.18
Mn55	1.45	1.18	<1.20	<0.72	1.15
Fe57	7645.68	7836.33	7578.34	7416.66	8918.51
Ga71	362.14	368.10	328.05	352.87	425.15
Total %	53.81	53.86	53.83	53.77	53.94
Cations (Atom Mole ppm)					
Be9	0.62	<1.17	2.11	1.15	0.61
Na23	8.98	15.85	35.99	<13.52	<8.07
Mg24	4.87	5.85	5.85	3.89	4.94
Al27	396742.73	396581.88	396672.02	396902.94	396307.82
Ti47	367.31	449.34	441.75	286.91	327.30
V51	0.44	0.42	0.44	0.64	0.66
Cr53	<0.71	<1.70	<2.38	<1.39	<0.85
Mn55	0.53	0.43	<0.44	<0.26	0.42
Fe57	2768.74	2836.63	2743.87	2686.89	3226.13
Ga71	105.05	106.74	95.15	102.41	123.20
Total (Atom Mole %)	40.00	40.00	40.00	40.00	40.00
Mg-Ti	-362.44	-443.49	-435.90	-283.03	-322.36
Be-Ti	-366.68	-448.18	-439.64	-285.77	-326.69
(Be+Mg)-Ti	-361.82	-442.33	-433.79	-281.88	-321.75
(Be+Mg) %	0.17	0.21	0.25	0.17	0.16
Ti %	11.69	13.65	13.83	9.63	9.20
Fe %	88.13	86.14	85.92	90.20	90.65

< = below the detection limit of which the value is used for calculation of atom mole ppm

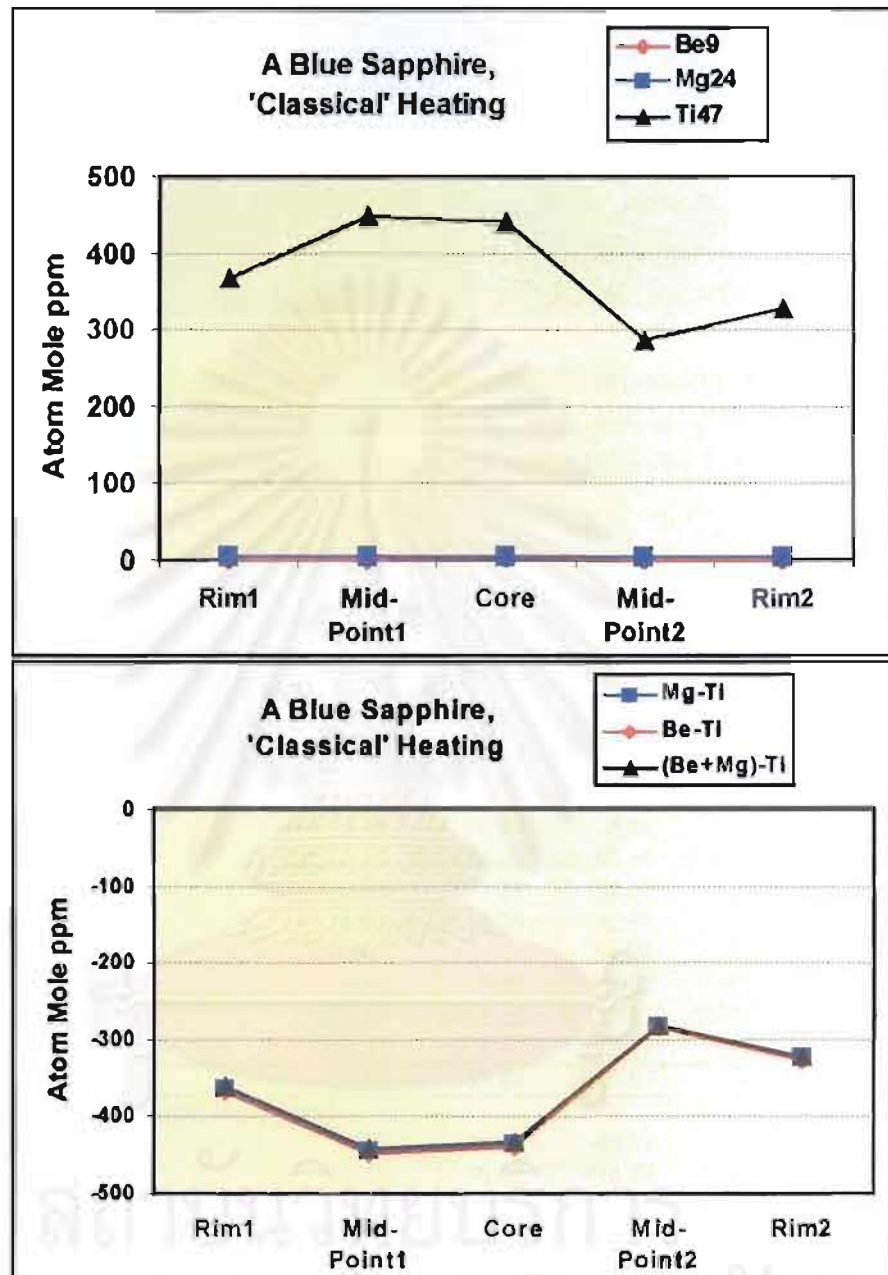


Figure 3.2: Plots of the trace element content variation across the cut surface of the blue sapphire (DIF1) treated with a 'classical' heating. The analyses show negligible contents of Be and Ti \gg Mg in all points analyzed.

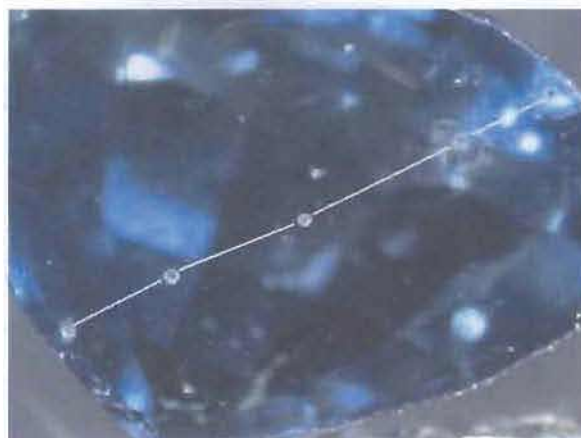


Figure 3.3: An Australian blue sapphire (AUS1) reportedly underwent a ‘classical’ heat-treatment was cut in half. A five-point-profile was analyzed across the cut surface using LA-ICP-MS. (Photo by Lomthong, KU)

Table 3.2: Trace element contents of the Australian sapphire (AUS1) showing high contents of Ti and Fe but negligible contents of Be, obtained by LA-ICP-MS.

	Rim1	Mid-Point1	Core	Mid-Point2	Rim2
RAW DATA (ppm by weight)					
Be9	0.22	<0.46	<0.35	<0.56	<0.21
Na23	<8.18	17.38	<16.81	<27.32	<9.35
Mg24	8.46	9.44	6.68	8.65	8.40
Al27	529250.40	529250.40	529250.40	529250.40	529250.40
Ti47	79.93	71.91	58.88	60.15	66.24
V51	12.22	12.21	12.01	11.45	12.29
Cr53	<1.94	<3.78	<4.09	<6.63	2.28
Mn55	0.81	0.89	<0.80	<1.33	0.85
Fe57	11663.83	9814.32	10158.12	10856.02	11517.28
Ga71	250.81	206.43	207.17	210.10	251.23
Total %	54.13	53.94	53.97	54.04	54.11
Cations (Atom Mole ppm)					
Be9	0.49	<1.03	<0.78	<1.25	<0.47
Na23	<7.18	15.27	<14.77	<23.99	<8.20
Mg24	7.02	7.85	5.55	7.18	6.97
Al27	395660.88	396328.69	396213.73	395950.35	395717.71
Ti47	33.66	30.33	24.83	25.35	27.90
V51	4.84	4.84	4.76	4.54	4.87
Cr53	<0.75	<1.47	<1.59	<2.57	0.88
Mn55	0.30	0.33	<0.29	<0.49	0.31
Fe57	4212.32	3550.37	3673.67	3923.46	4160.00
Ga71	72.56	59.82	60.02	60.83	72.69
Total (Atom Mole%)	40.00	40.00	40.00	40.00	40.00
Mg-Ti	-26.64	-22.48	-19.28	-18.16	-20.92
Be-Ti	-33.16	-29.30	-24.04	-24.09	-27.43
(Be+Mg)-Ti	-26.14	-21.45	-18.49	-16.91	-20.45
(Be+Mg) %	0.18	0.25	0.17	0.21	0.18
Ti %	0.79	0.84	0.67	0.64	0.66
Fe%	99.03	98.91	99.16	99.15	99.16

< = below the detection limit of which the value is used for calculation of atom mole ppm

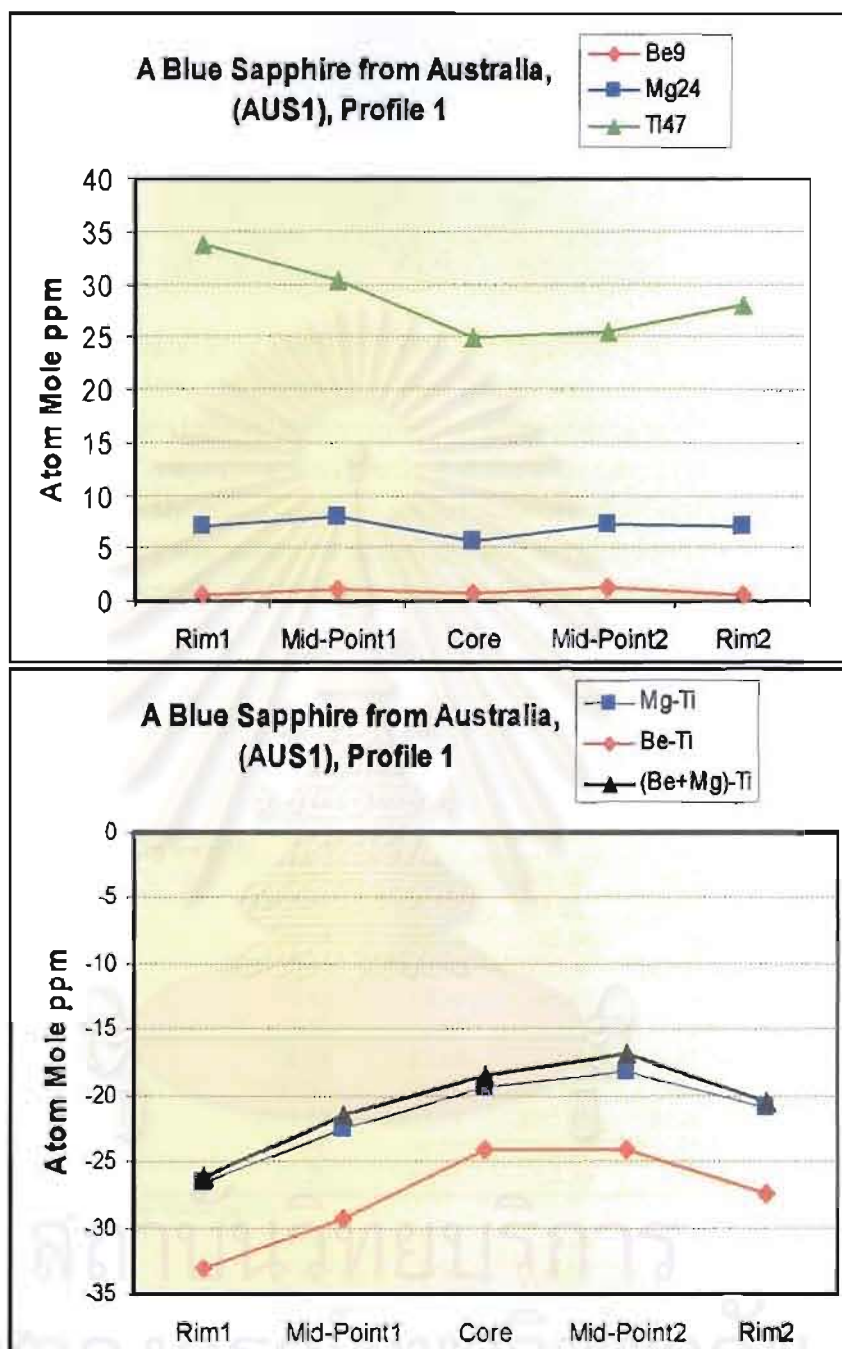


Figure 3.4: Plots of the trace element content variation across the cut surface of the Australian blue sapphire (AUS1) treated with a 'classical' heating. The analyses show negligible contents of Be and Ti > Mg in all points analyzed.



Figure 3.5: A natural blue sapphire (PPBS1) reportedly heat-treated with Be under unknown condition by a Thai heater and cut in half. The sample shows a thi surface-related yellow rim surrounding the blue core. High magnification reveals that the blue core contains oriented blue dots probably resulting from partial dissolution of rutile needles. A five-point profile was analyzed across the cut surface with two points in the surface-related yellow zone (rims) and three points in the blue core. (Photo by Lomthong, KU)

Table 3.3: Trace element content of the Be-treated blue sapphire (PPBS1) showing rather high Fe contents, obtained by LA-ICP-MS.

	Rim1	Mid-Point1	Core	Mid-Point2	Rim2
Cations (ppm by weight)					
Be9	9.15	0.26	<0.17	<0.22	8.71
Na23	<10.82	<9.77	<10.63	<14.53	<12.40
Mg24	24.54	27.14	25.86	25.66	26.55
Al27	529250.40	529250.40	529250.40	529250.40	529250.40
Ti47	60.45	83.16	65.99	79.49	51.58
V51	12.83	12.87	12.47	12.53	12.23
Cr53	36.34	37.86	32.32	31.33	38.61
Mn55	<0.53	<0.48	<0.53	<0.73	<0.62
Fe57	3013.78	4303.34	3015.91	3139.35	3182.56
Ga71	51.66	56.00	53.22	53.84	54.13
Total %	53.25	53.38	53.25	53.26	53.26
Cations (Atom Mole ppm)					
Be9	20.64	0.58	0.00	0.00	19.65
Na23	0.00	0.00	0.00	0.00	0.00
Mg24	20.53	22.68	21.63	21.46	22.20
Al27	398801.73	398340.61	398819.35	398769.19	398742.19
Ti47	25.66	35.25	28.01	33.73	21.89
V51	5.12	5.13	4.98	5.00	4.88
Cr53	14.21	14.79	12.64	12.25	15.09
Mn55	0.00	0.00	0.00	0.00	0.00
Fe57	1097.05	1564.65	1097.87	1142.66	1158.31
Ga71	15.06	16.31	15.52	15.70	15.78
Total (Atom Mole%)	40.00	40.00	40.00	40.00	40.00
Mg-Ti	-5.13	-12.58	-6.38	-12.27	0.32
Be-Ti	-5.02	-34.67	-28.01	-33.73	-2.24
(Be+Mg)-Ti	15.51	-12.00	-6.38	-12.27	19.96
(Be+Mg) %	3.54	1.43	1.89	1.79	3.42
Ti %	2.20	2.17	2.44	2.82	1.79
Fe%	94.26	96.40	95.87	95.39	94.78

the detection limit of which 0.00 value is used for calculation of atom mole ppm

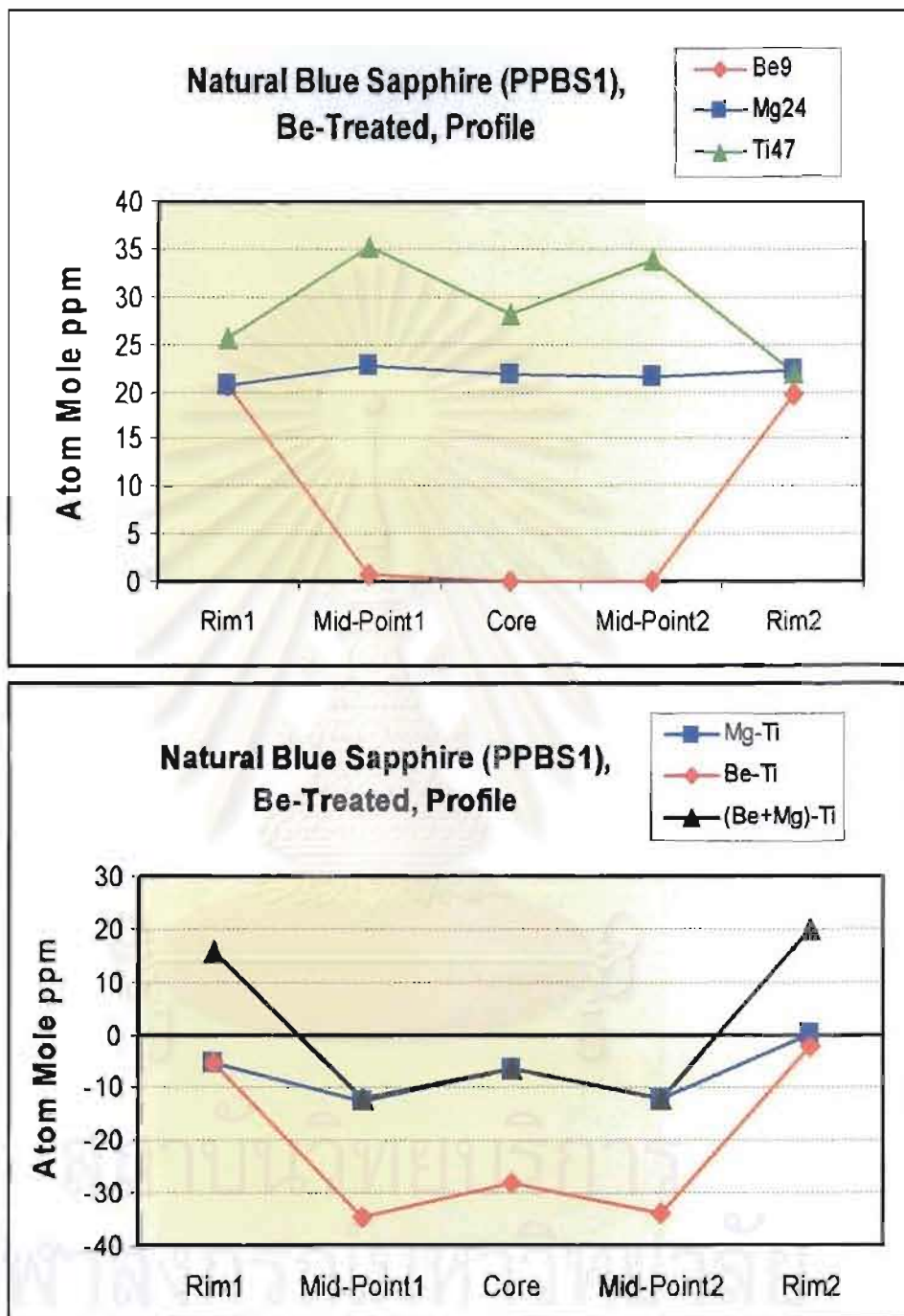


Figure 3.6: Plots of the trace element content variation across the cut surface of the Be-treated blue sapphire (PPBS1). The Be content are obviously high at the yellow rims and are negligible in the blue core. The content of Mg and Ti (also other trace elements) however show no consistent variation across the profile. The analyses also show $(\text{Be}+\text{Mg}) > \text{Ti}$ at the yellow rims in contrast to $\text{Ti} > (\text{Be}+\text{Mg})$ in the blue core.

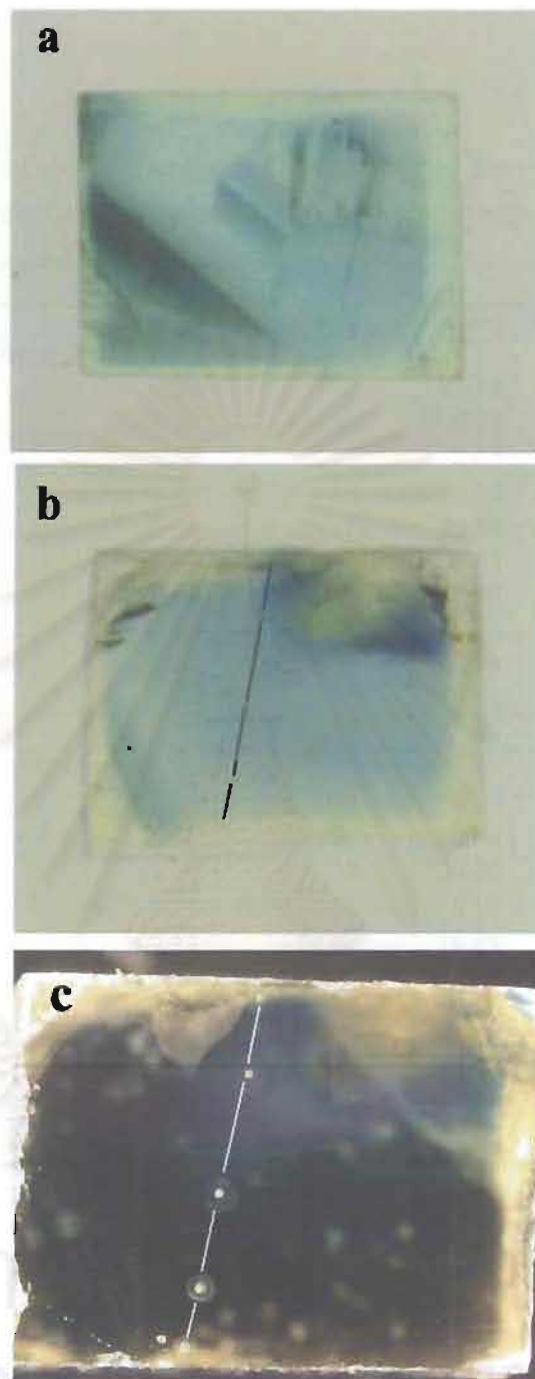


Figure 3.7: A rectangular block of a natural blue-green sapphire (BG1) heat-treated with Be by a Thai heater showing a thin surface-related yellow rim surrounding the complex-zoned blue core (a, in immersion liquid). After the treatment the sample was cut in half (b, in immersion; c, in air) and a five-point profile was analyzed across the cut surface using LA-ICP-MS. Two points on both rims are very close to the yellow zone (rim) while three points in the middle are definitely in the blue core. (Photo by Somboon, GIT)

Table 3.4: Trace element content of the Be-treated blue-green sapphire (BG1) analyzed across the cut surface showing rather high Fe contents, obtained by LA-ICP-MS.

	Rim1	Mid-Point1	Core	Mid-Point2	Rim2
Cations (ppm by weight)					
Be9	5.50	0.77	<0.55	0.66	11.75
Na23	<4.86	<13.20	<18.07	<20.98	31.78
Mg24	5.23	4.93	3.98	2.28	7.08
Al27	529250.50	529250.50	529250.50	529250.50	529250.50
Ti47	48.35	25.17	25.85	33.72	131.51
V51	14.14	14.87	10.49	11.00	15.02
Cr53	<1.08	<3.06	<4.13	<4.83	<1.77
Mn55	0.44	<0.62	<0.85	<1.00	1.02
Fe57	7907.39	9578.26	6644.71	6963.39	8971.28
Ga71	212.79	269.98	179.11	177.18	212.49
Total %	53.75	53.92	53.61	53.65	53.86
Cations (Atom Mole ppm)					
Be9	12.35	1.73	0.00	1.48	26.36
Na23	0.00	0.00	0.00	0.00	27.95
Mg24	4.36	4.10	3.32	1.90	5.89
Al27	397029.72	396433.51	397518.55	397400.65	396568.99
Ti47	20.43	10.62	10.94	14.26	55.50
V51	5.62	5.90	4.17	4.37	5.96
Cr53	0.00	0.00	0.00	0.00	0.00
Mn55	0.16	0.00	0.00	0.00	0.38
Fe57	2865.59	3465.89	2410.97	2525.85	3247.36
Ga71	61.77	78.26	52.06	51.48	61.61
Total (Atom Mole%)	40.00	40.00	40.00	40.00	40.00
Mg-Ti	-16.07	-6.52	-7.62	-12.36	-49.61
Be-Ti	-8.08	-8.89	-10.94	-12.78	-29.15
(Be+Mg)-Ti	-3.72	-4.79	-7.62	-10.88	-23.26
(Be+Mg) %	0.58	0.17	0.14	0.13	0.97
Ti %	0.70	0.30	0.45	0.56	1.66
Fe%	98.72	99.53	99.41	99.31	97.37

< = below the detection limit of which the 0.00 value is used for calculation of atom mole ppm

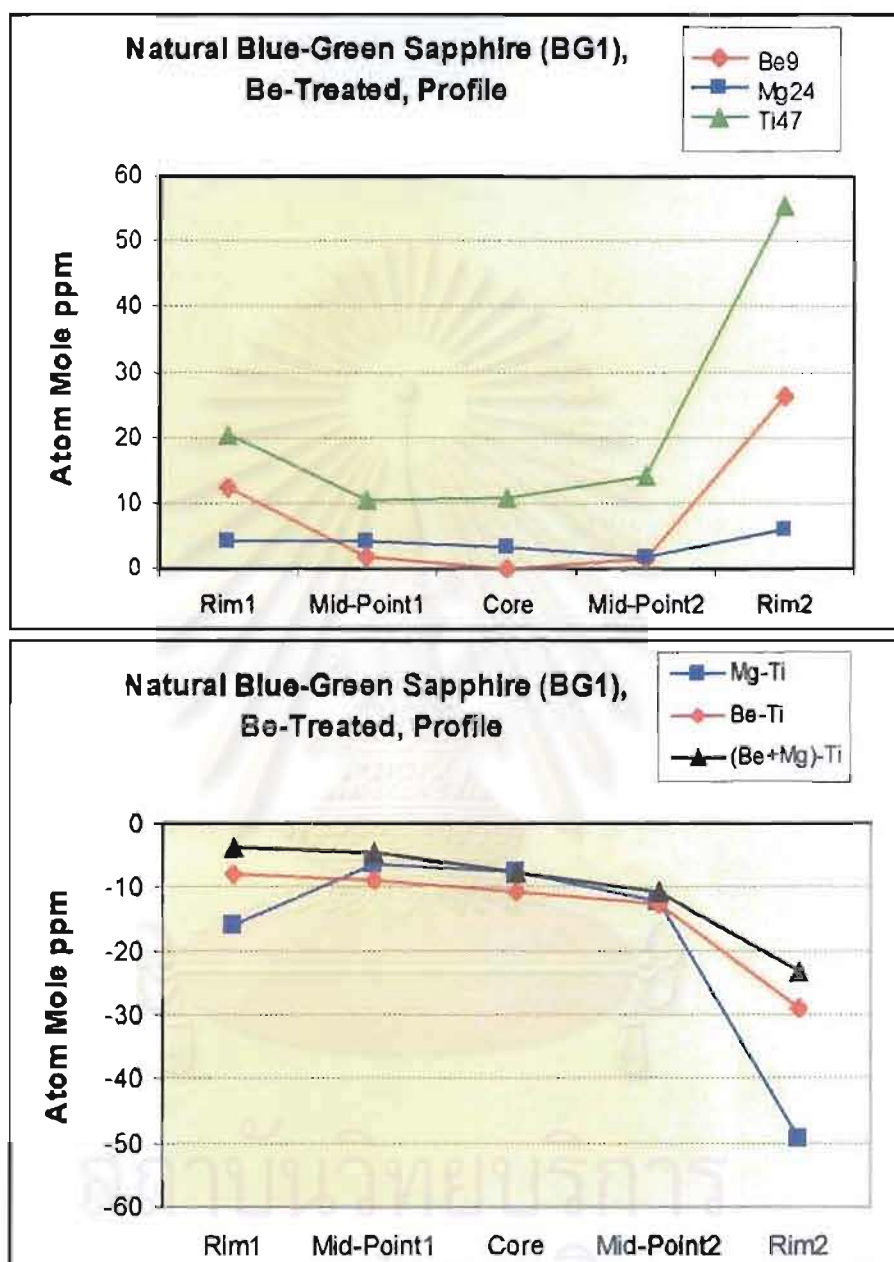


Figure 3.8: Plots of the trace element content variation across the cut surface of the Be-treated blue-green sapphire (BG1). The Be contents are obviously high at the rims and decrease toward the core. The analyses show $Ti > (Be+Mg)$ in all the analyzed points which are still within the blue area.

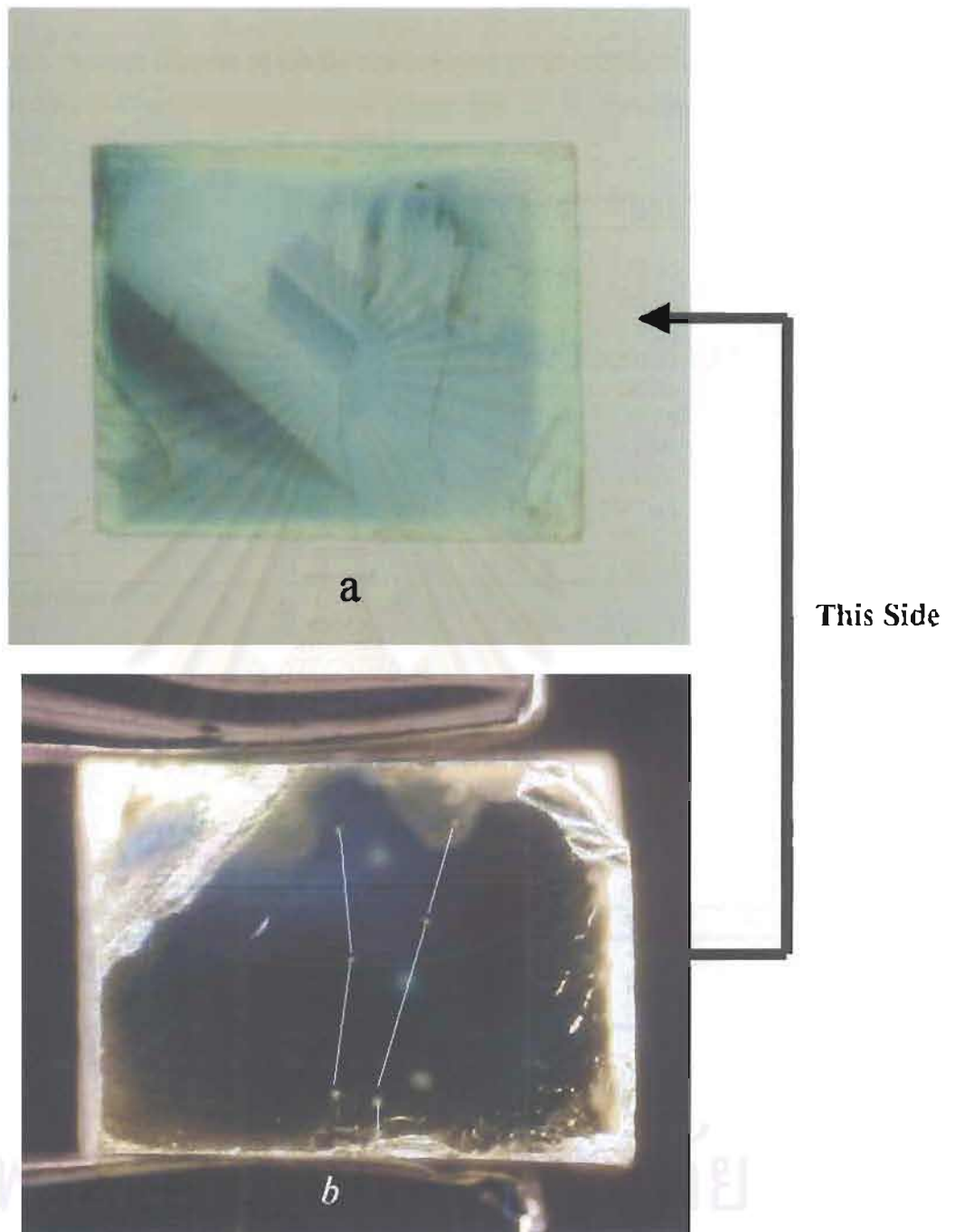


Figure 3.9: (a) The rectangular block of the Be-treated natural blue-green sapphire (BG1) in immersion liquid. (b) The photo of the right face of (a), which are definitely in the yellow rim, showing seven analyzed points. (Photo by Somboon, GIT)

Table 3.5: Trace element content of the Be-treated blue-green sapphire (BG1) analyzed on the outer surface showing rather high contents of Be and Fe, obtained by LA-ICP-MS.

	BG1	BG2	BG3	BG4	BG5	BG6	BG7
Cations (ppm by weight)							
Be9	36.63	18.77	18.60	9.29	9.80	11.34	20.68
Na23	<18.7	<42.08	<41.64	<15.93	<3.85	<4.02	5.95
Mg24	1.93	3.12	3.27	2.57	1.84	1.97	6.40
Al27	529250.50	529250.50	529250.50	529250.50	529250.50	529250.50	529250.50
Ti47	22.77	53.33	58.61	21.82	25.53	26.80	84.51
V51	12.94	12.31	14.04	12.88	10.65	10.74	13.73
Cr53	<5.96	<13.21	<12.95	<6.22	<4.78	<4.98	<4.75
Mn55	<1.29	6.36	<2.91	<1.14	<1.23	<1.29	<1.14
Fe57	8637.73	8144.60	8566.90	8999.09	7047.46	7033.16	8884.90
Ga71	250.66	215.87	229.86	259.11	193.92	191.06	224.38
Total %	53.82	53.78	53.82	53.86	53.65	53.65	53.85
Cations (Atom Mole ppm)							
Be9	82.20	42.14	41.74	20.84	22.03	25.49	46.40
Na23	0.00	0.00	0.00	0.00	0.00	0.00	5.23
Mg24	1.61	2.60	2.72	2.14	1.53	1.64	5.32
Al27	396701.07	396912.18	396756.08	396629.63	397349.06	397350.92	396620.34
Ti47	9.61	22.53	24.75	9.21	10.80	11.33	35.67
V51	5.14	4.89	5.57	5.11	4.23	4.27	5.45
Cr53	0.00	0.00	0.00	0.00	0.00	0.00	0.00
Mn55	0.00	2.34	0.00	0.00	0.00	0.00	0.00
Fe57	3127.67	2950.68	3102.45	3257.93	2556.01	2550.83	3216.51
Ga71	72.71	62.65	66.68	75.14	56.34	55.51	65.07
Total (Atom Mole%)	40.00	40.00	40.00	40.00	40.00	40.00	40.00
Mg-Ti	-8.01	-19.93	-22.02	-7.07	-9.26	-9.69	-30.35
Be-Ti	72.58	19.61	16.99	11.63	11.23	14.16	10.72
(Be+Mg)-Ti	74.19	22.21	19.72	13.77	12.76	16.80	16.05
(Be+Mg) %	2.60	1.48	1.40	0.70	0.91	1.06	1.67
Ti %	0.30	0.76	0.78	0.28	0.42	0.44	1.08
Fe%	97.10	97.77	97.82	99.02	98.67	98.51	97.35

< = below the detection limit of which the 0.00 value is used for calculation of atom mole ppm

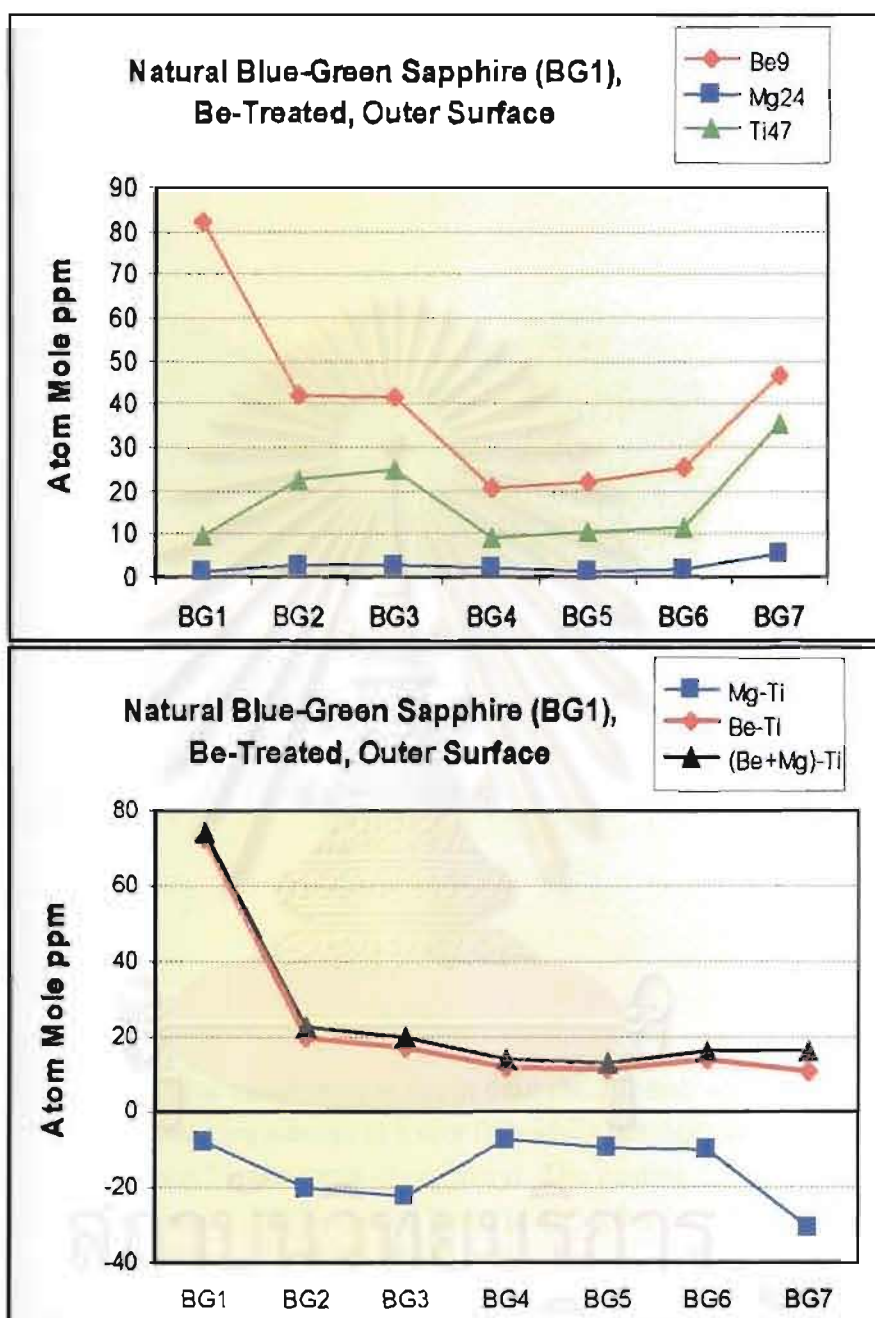


Figure 3.10: Plots of the trace element contents analyzed on the outer surface of the Be-treated blue-green sapphire (BG1). The analyses show obviously high Be contents and $Ti > Mg$ in contrast to $(Be+Mg) > Ti$ at all the analyzed points which are definitely in the yellow rim.



Figure 3.11: A natural blue sapphire was cut in half; the left half was heat-treated with ground chrysoberyl in a crucible while the right half was heated in another crucibles without chrysoberyl. The heating condition for both crucibles was $1,750^{\circ}\text{C}$ for 30 hours in air. After heat treatment the left half shows obviously surface-related yellow rim whereas the right half is blue throughout the stone. (Photo by Häger)

1850°C in an oxidizing atmosphere

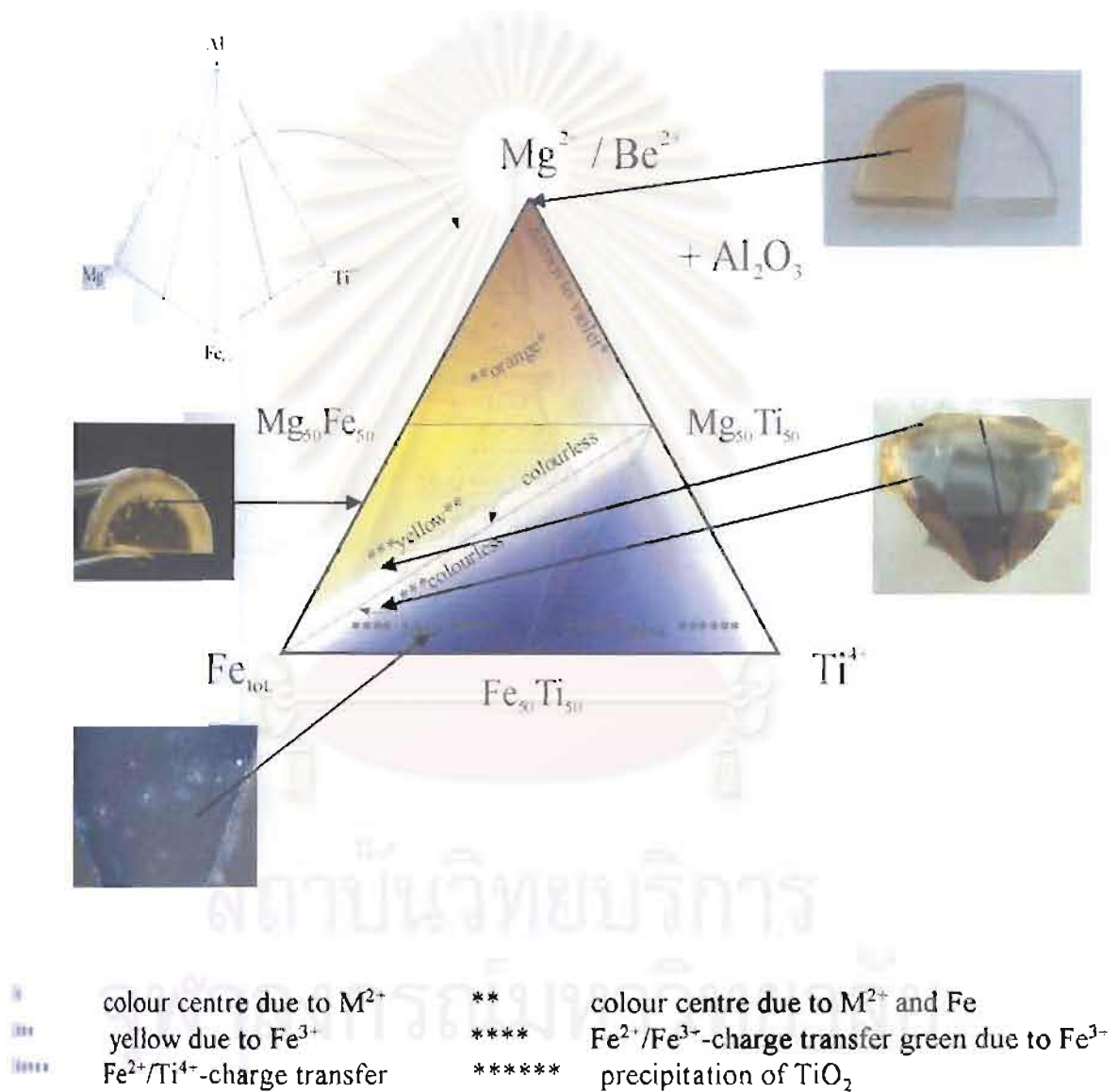


Figure 3.12: Approximate compositions of the stones plotted in the (oxidizing atmosphere) triangular diagram model proposed by Häger (1996).

1750°C in a reducing atmosphere

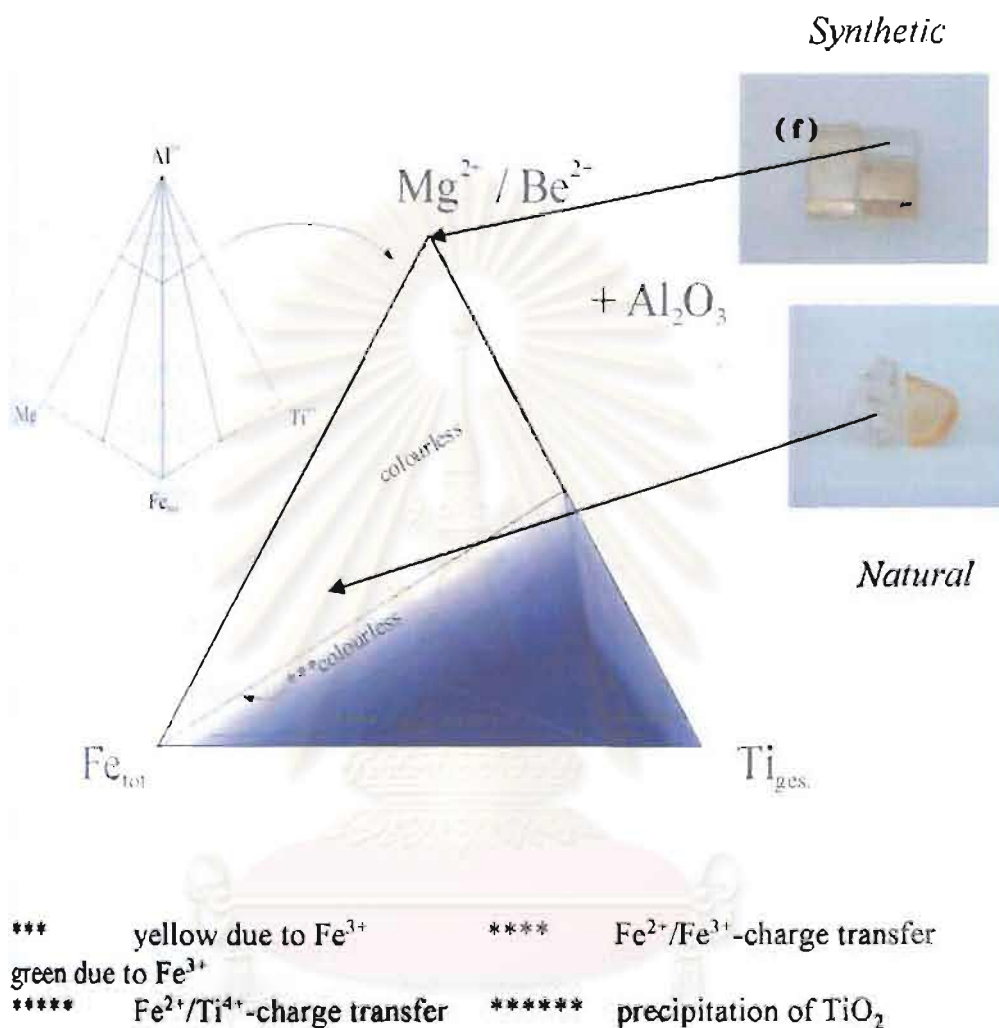


Figure 3.13: Approximate compositions of the stones plotted in the (reducing atmosphere) triangular diagram model proposed by (Häger, 1996).

Chapter 4

'Classical' versus 'Beryllium' Heat-Treated Ruby and Pink Sapphires

Introduction

In the previous chapters we have presented the system dominated by Be+Mg+Fe+Ti. In this chapter we will study the system dominated by Be+Mg+Fe+Ti+Cr. An addition of Cr into the system creates pink or red hue to a stone. As a result the stone can be pink or red, pink-orange, orange, violet or purple depending upon trace element interaction and atmospheric condition at high temperature. In order to give a better understanding of trace element interaction and the cause of colour, additional LA-ICP-MS analyses were carried out on non-Be-treated and Be-treated natural and synthetic ruby and pink sapphires from various sources.

Samples and Method

In the first group of samples, a series (11 faceted stones) of pink Madagascan sapphires was experimentally heat-treated with Be by a Thai heater to preliminarily verify the technique and understand the coloration. The samples were photographed and analyzed for trace element contents by EDXRF and UV-Vis spectra were recorded both before and after the heating experiment.

In the second group of samples, seven pink and orange sapphires and rubies (mostly from Madagascar and some from Tanzania) that have not been heat-treated with Be were analyzed by LA-ICP-MS. The purpose is to find out the background trace element contents of natural corundum.

The third group of samples are natural rubies and sapphire having $Ti > Mg$ contents. These samples are three Mong Hsu (Myanmar), five Vietnamese, one Adila

(Madagascar) rubies and one rough violet Ilakaka (Madagascar) sapphire. Mong Hsu and Vietnamese rubies of metamorphic origin were reportedly treated unsuccessfully by the Be-heating technique (Figure 4.8). The reason for such observation is still unknown and has been speculated to be due their intrinsic chemical elements. However no chemical data on those samples has yet to verify such speculation. In order to understand such observation, nine rubies from Mong Hsu (3), Vietnamese (5) and Adila (1) were heat-treated with Be by a Thai heater under unknown condition. After the treatment some selected stones were cut in half, lightly polished, photographed and performed a profile analysis across the cut surface using LA-ICP-MS. For the violet Ilakaka sapphire, the sample was cut into three pieces by which one piece was kept as the reference. The other two pieces were heat-treated by Dr. T. Häger. One of the two pieces was heat-treated with ground chrysoberyl in a crucible while the other piece was heat-treated in another crucible without chrysoberyl. The heating conditions for both crucibles were at 1,750°C for 30 hours in air. After heat treatment, the samples were photographed, lightly polished and performed a profile analysis using LA-ICP-MS.

The fourth group of samples were natural ruby and pink sapphires having $Ti \sim$ or $<Mg$. These samples are two Songea (Tanzania) sapphire (one is faceted and the other is rough stone) and four Ilakaka pink sapphires (one is faceted and the other three are rough stones). The faceted samples were Be-treated stones obtained from Thai heater or trader. The samples were cut in half, lightly polished, photographed and analyzed for trace element contents across the cut surface using LA-ICP-MS. The rough samples were cut into three pieces (or two pieces) of which two pieces were heat-treated by Dr. T. Häger under the same procedure and condition as the violet sapphire. The samples were then photographed, lightly polished and performed a profile analysis using LA-ICP-MS.

The fifth group of samples are two synthetic rubies heat-treated with Be. The first sample was Be-treated by a Thai heater. The sample was cut in half, lightly polished, photographed and analyzed for trace element contents across the cut surface using LA-ICP-MS. The second sample was cut into two pieces and heat-treated by Dr. T. Häger under the same procedure and condition as the violet sapphire.

First group of samples: Before and After Be-heating experiment

After the Be-treatment the eleven pink Madagascan sapphires turned orangey pink and orange (Figure 4.1). Immersion of the stones in methylene iodide solution reveals surface-related colour zone (Figure 4.2). The residual spectrum obtained by the subtraction of a pale pink sapphire before treatment from that of the pink-orange sapphire after Be-treatment (Figure 4.3) show an increase toward the UV region and a shoulder centred at around 460 nm. This spectral pattern is similar to that found in Sri Lankan yellow sapphire coloured by defect centres (see Figure 1.7). This experiment has proved that an orange sapphire is formed by addition of yellow hue to a pink stone and the yellow coloration is likely related to defect centres.

Second group of samples: Non-Be-treated pink and orange sapphires

Trace element contents of seven pink and orange sapphires (mostly from Madagascar and some from Tanzania) that have not been heat-treated with Be are shown in Tables 4.1 and 4.2, Figures 4.4 to 4.7 (see also Tables 4.7, 4.9, 4.11, 4.12, 4.13, Figures 4.20, 4.21, 4.24, 4.25, 4.28, 4.29, 4.30, 4.31, 4.32 and 4.33). It was found that Be has not been detected in those stones. We found that slight excess of Mg over Ti contents (below about 30 atom mole ppm) is not enough to create orange coloration in 'classical' heat-treatment (Figures 4.4, 4.5, 4.20, 4.21, 4.24, 4.25, 4.28, 4.29, 4.30, 4.31, 4.32 and 4.33). The excess of Mg over Ti contents has to be more than

approximately 30 atom mole ppm before orange coloration can be developed in a stone underwent normal heat treatment (Figures 4.6 and 4.7).

Third group of samples: Be-treated rubies and sapphire with $Ti > Mg$

Beryllium-Treated Mong Hsu (Myanmar) and Vietnamese ruby rubies

After the Be-treatment three Mong Hsu rubies and five Vietnamese rubies grossly remain red, purplish red or pink (Figures 4.9 and 4.10, as compared with strong orange of the Songea samples under the same run Figure 4.11). Close examination of the stones under immersion liquid reveals very thin sometime patchy surface-related yellow or orange rims (Figures 4.12, 4.13 and 4.14). Close space analyses started from the very rim of one side of the cut surface to the other side (Figures 4.15, 4.16 and 4.17, Tables 4.3, 4.4 and 4.5) reveal extremely high content of Be and Fe at the very rims of the samples in which $(Be+Mg) \gg Ti$ and correspond fairly well with very thin yellow or orange rim. The analyzed points within the stone except those closer to the rims show relatively high content of Ti and Cr, and moderate to strong excess of Ti over Mg content ($Ti > Mg$), but rather low concentration of Fe. Minor amount of Be was found to diffuse into the stones from an external source at very shallow depth. Majority of the analyzed points within the stones still have $Ti > (Be+Mg)$.

In these high Ti-containing Mong Hsu and Vietnamese stones in which $Ti > (Mg+Be)$, most of the intrinsic Mg and the diffused Be might have been tied up with the formation of colourless $MgTiO_3$ and $BeTiO_3$ clusters. As a result there is no excess Be and/or Mg to stabilize the yellow or orange colour centers or trapped hole centers (see also Kvapil *et al.*, 1972, 1973; Andreev *et al.*, 1976; Wang *et al.*, 1983; Häger, 1992, 1993, 1996 and 2001; Emmett and Douthit, 1993; Emmett *et al.*, 2003; Pisutha-Armond

et al., 2002 and 2004; Schmetzer and Schwarz, 2004). Hence no substantial yellow hue was added to these red or pink stones that could turn them orange. More heating time and/or higher temperature are required to increase the Be diffusion into the stones in order to achieve a desired colour. It might therefore not be economically feasible to treat this type of stone by the Be-heating technique.

A Beryllium-Treated Adila Ruby

After the Be-treatment the Adila ruby shows obviously a surface-related yellow or orange rim and a blue core or zone under immersion liquid (Figure 4.18). The blue zone originates from blue halo causing by internal diffusion of Ti from Ti-bearing inclusions. A five point profile analysis across the cut surface shows three middle points located within the blue zone and other two points at the orange rim (Figure 4.18). The analyses show Ti > or \sim Mg contents in all points analyzed (Table 4.6, Figure 4.19). Two points on the rims (Figure 4.19) show excess of Be+Mg over Ti contents which correspond quite well with the orange rim. Three points in the middle show the excess of Ti over Be+Mg contents which correspond well with the blue zone (Figure 4.19). This data strongly suggest that an orange hue can only be formed where Be+Mg > Ti occurs in the lattice. With the "classical" heat treatment, it was not possible to turn such the stone orange. With the diffusion of Be into the lattice it is now possible to change the balance of the Ti/(Be+Mg) ratios.

A 'Classical' and Be-Treated violet Ilakaka sapphire

After the treatment, the samples still remain violet and no significant colour change under both 'classical' and Be heat-treatments (Figure 4.20). A profile analysis on the 'classically' heat-treated piece shows no detectable Be and excess of Ti over Mg contents in all the analyzed points (Table 4.7, Figure 4.21). However in the Be-treated piece small amount of Be was found to diffuse into the corundum lattice. Nonetheless,

Ti contents are still in excess or slightly less than Be+Mg contents in all the analyzed points (Table 4.7, Figure 4.21). This could explain why this sample still remains violet under both 'classical' and Be-treatments.

The Fourth group of samples: Be-treated rubies and pink Sapphires with Ti ~ or <Mg

'Classical' and Be-Treated Songea sapphires

The Songea sapphires are obviously orange after the Be-treatment (Figures 4.22 and 4.24) but are brownish red after the 'classical' heat-treatment (Figure 4.24). In the 'classically' heat-treated piece, the analyses show no detectable Be and equal proportion of Ti and Mg in all the analyzed points (Figure 4.25, Table 4.9). This data hence explains why orange coloration can not be formed in this 'classically' heat-treated sample. In the Be-treated samples the analyses shows approximately 1:1 of Mg:Ti ratios or slightly excess of Mg over Ti contents (Figures 4.23 and 4.25, Tables 4.8 and 4.9). Furthermore significant amount of Be was found to diffuse into the corundum lattice, especially near the rim of the stones, by which Be+Mg always exceed Ti in all the analyzed points (Figures 4.20 and 4.21). This data therefore can explain why orange coloration can easily be developed in these Be-treated samples.

'Classical' and Be-Treated pink Ilakaka (Madagascar) sapphires

Similarly the Ilakaka sapphires are obviously orange after the Be treatment but are purer pink (from originally violetish pink) after the 'classical' heat-treatment (Figures 4.26, 4.28, 4.30 and 4.32). In the 'classically' heat-treated samples, the analyses show no detectable Be and slight excess of Mg over Ti contents in all the points analyzed (Figures 4.29, 4.31 and 4.33, Tables 4.11, 4.12 and 4.13). This data suggest that orange coloration still can not be formed in this 'classically' heat-treated samples if there are

less than about 30 atom mole ppm of excess Mg over Ti contents in the corundum lattice. In the Be-treated samples the analyses also show slightly excess of Mg over Ti contents and significant amount of Be diffused into the corundum lattice, especially near rim of the stones, by which Be+Mg always exceed Ti contents in all the analyzed points (Figures 4.27, 4.29, 4.31 and 4.33, Tables 4.19, 4.11, 4.12 and 4.13). This data again can explain why orange coloration can be easily developed in these Be-treated samples.

The Fifth group of samples: Be-Treated Synthetic Rubies

Beryllium-Treated Synthetic Rubies

A synthetic ruby (PPSR1) reportedly heat-treated with Be by a Thai heater appears orangey red (Figure 4.34). The five-point profile analyses (Table 4.14) show high Cr contents while other trace elements are extremely low, in particular Ga, confirming that it is a synthetic ruby. The analyses also show Be diffusion into the corundum lattice from an external source (Figure 4.35). This synthetic ruby contains negligible Fe content and turns orange by the diffusion of Be. This data therefore suggest that combination of Cr and Be (without Fe) could also produce orange coloration. Similar result has also been found by Peretti et al. (2003). With a “classical” heat-treatment (without additional of Be) it is likely that this sample is still red as it contains only Cr without other important trace elements such as Mg, Ti and Fe. This statement can be clearly confirmed by our own heating experiment on a synthetic ruby (Figure 4.36).

Conclusion

The approximate compositions of some treated stones can be plotted in the triangular diagram model proposed by Häger (1996) as shown in Figure 4.37. The colours of those stones fit such the model nicely.

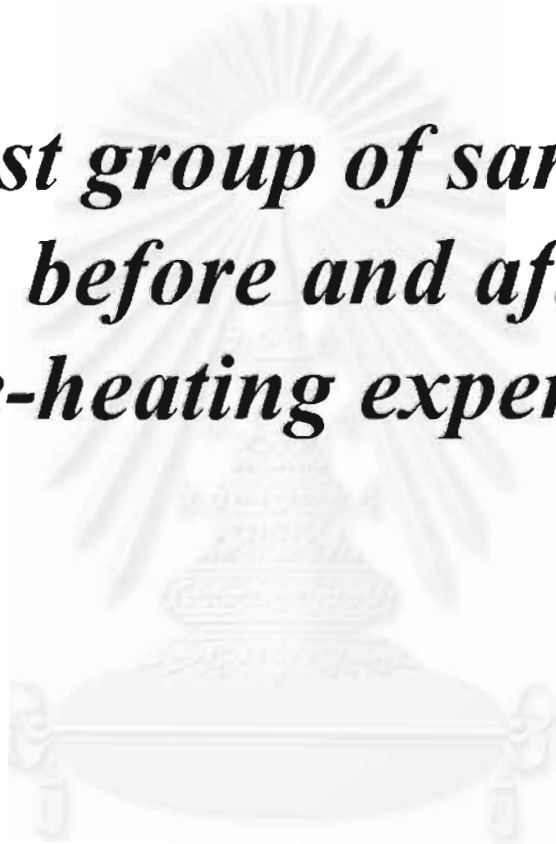


References

- Andreev, D.V., Antonov, V.A., Arsenev, P.A. and Farshtendiker V.L., 1976. Dye centres in magnesium doped corundum monocrystal. *Kristall und Technik*, **11**, 103-108
- Emmett, J.L. and Douthit, T.R., 1993. Heat treating the sapphires of Rock Creek, Montana. *Gems & Gemology*, **29**, 250-272
- Emmett, J.L., Scarratt, K., McClure, S.F., Moses, T., Douthit, T.R., Hughes, R.W., Novak, S., Shigley, J.E., Wang, W., Bordelon, O. and Kane, R.E., 2003. Beryllium diffusion of ruby and sapphire. *Gems & Gemology*, **39**(2), 84-135
- Häger, T., 2001. High temperature treatment of natural corundum. In: Proceedings of the International Workshop on Material Characterization by Solid State Spectroscopy: *The Minerals of Vietnam*, Hanoi, Vietnam. April 4-10, 2001
- Häger, T., 1996. *Farbrelevante Wechselwirkungen von Spurenelementen in Korund*. Ph.D. Thesis. University of Mainz
- Häger, T., 1992. Farbgebende und "farbhemmende" Spurenelemente in blauen Saphiren. *Berichte der Deutschen Mineralogischen Gesellschaft - Beihefte zum European Journal of Mineralogy*, **4**, 109
- Häger, T., 1993. Stabilisierung der Farbzentren von gelben natürlichen Saphiren. *Berichte der Deutschen Mineralogischen Gesellschaft - Beihefte zum European Journal of Mineralogy*. **5**, 188
- Kvapil, J., Perner, B., Súlovský, J., Kvapil, J., 1973. Colour centre formation in corundum doped with divalent ions. *Kristall und Technik*, **8**(1-3), 247-251
- Kvapil, J., Súlovský, J., Kvapil, J., Perner, B., 1972. The influence of dopants and annealing on the colour stability of ruby. *Physica Status Solidi (a)*, **9**, 665-672

- Peretti, A., Guenther, D., and Graber, A.-L., 2003. The beryllium treatment of fancy sapphires with a new heat-treatment technique (part B). *Contributions to Gemology*, 2, 21-33
- Pisutha-Armond, V., Häger, T., Wathanakul, P., Atichat, W., 2002. A brief summary on a cause of colour in pink-orange, orange and yellow sapphires produced by the “new” heating technique. *Journal of Gem and Jewelry*, Gem and Jewelry Institute of Thailand (GIT), 3(18), 11-12.
- Pisutha-Armond, V., Häger, T., Wathanakul, P., Atichat, W., 2004. Yellow and brown colouration in beryllium treated sapphires. *Journal of Gemmology*, 29(2), 77-103
- Pisutha-Armond, V., Wathanakul, P., Atichat, W., Haeger, T., Win, T.T., Leelawatanasuk, T., and Somboon, C., 2003. Beryllium-treated Vietnamese and Mong Hsu rubies. In: Hofmeister W., Quang V.X., Doa N.Q., and Nghi T. (eds) *Proceedings of the 2nd International Workshop on Geo- and Material-Science on Gem-Minerals of Vietnam, Hanoi, October 1-8, 2003*, 171-5
- Schmetzer, K. and Schwarz, D., 2004. The causes of colour in untreated, heat treated and diffusion treated orange and pinkish-orange sapphires- a review, *Journal of Gemmology*, 29, 149-182.
- Themelis, T., 2003. *Beryllium-treated rubies and sapphires*. p. 48
- Wang, H.A., Lcc, C.H., Kroger, F.A. and Cox, R.T., 1983. Point defects in Alpha-Al₂O₃: Mg studied by electrical conductivity, optical absorption and ESR. *Physical Review B*, 27, 6, 3821-3841

***First group of samples:
before and after
Be-heating experiment***



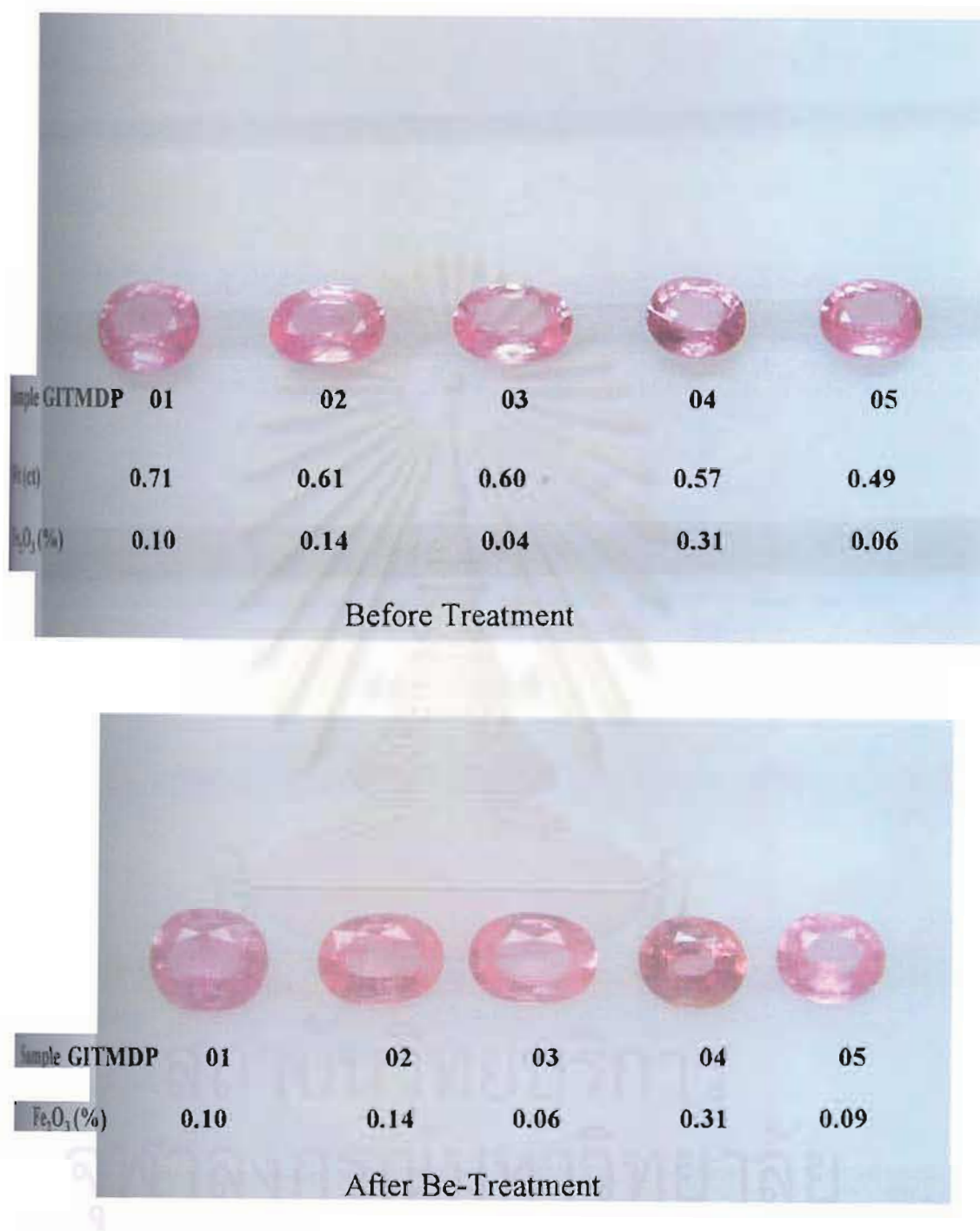


Figure 4.1: Colours of eleven Ilakaka (Madagascar) sapphires before treatment (above, pink) and after Be-treatment under unknown condition by a Thai heater (below orange-pink and orange). (Photo by Somboon, GIT)

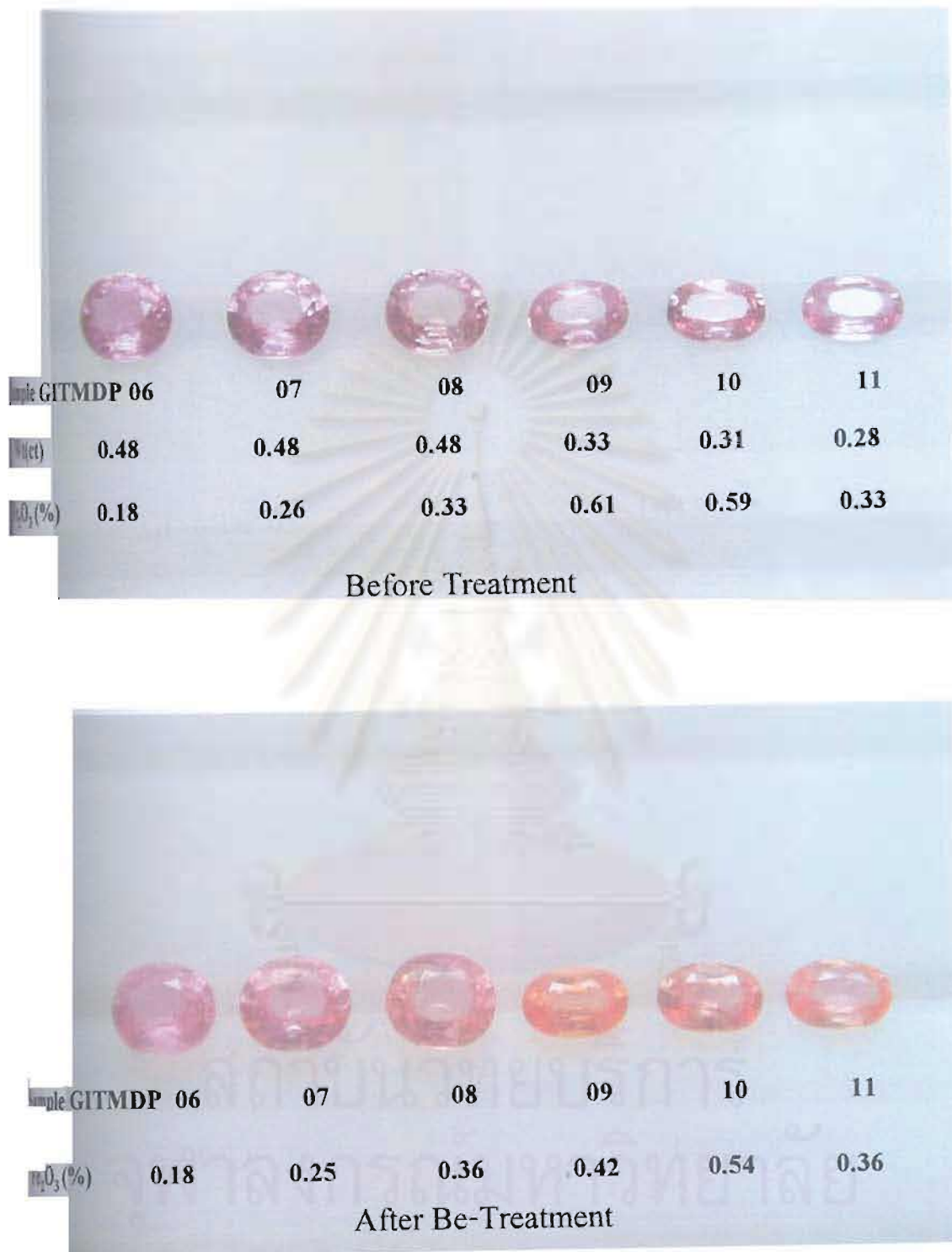


Figure 4.1: (continued)

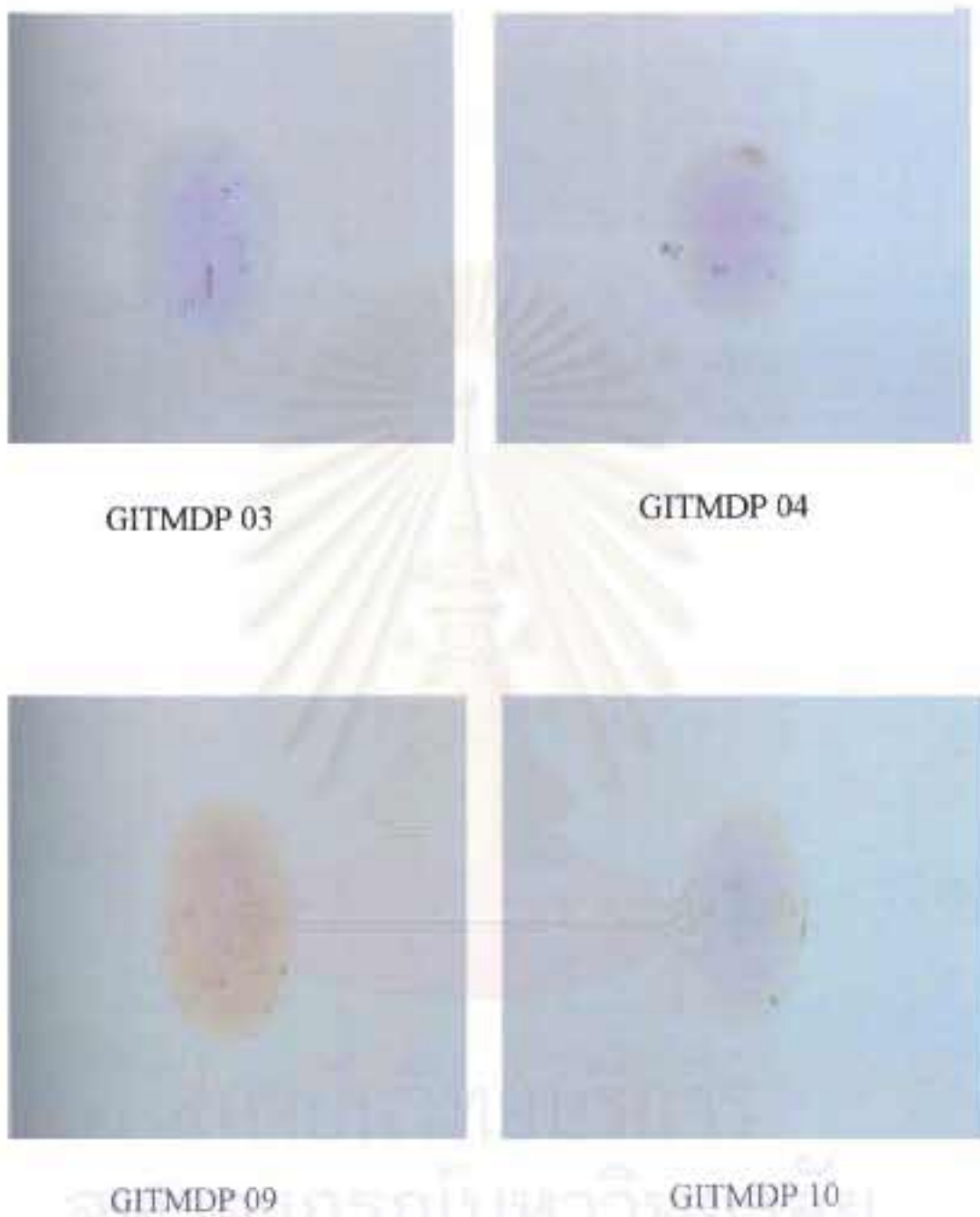
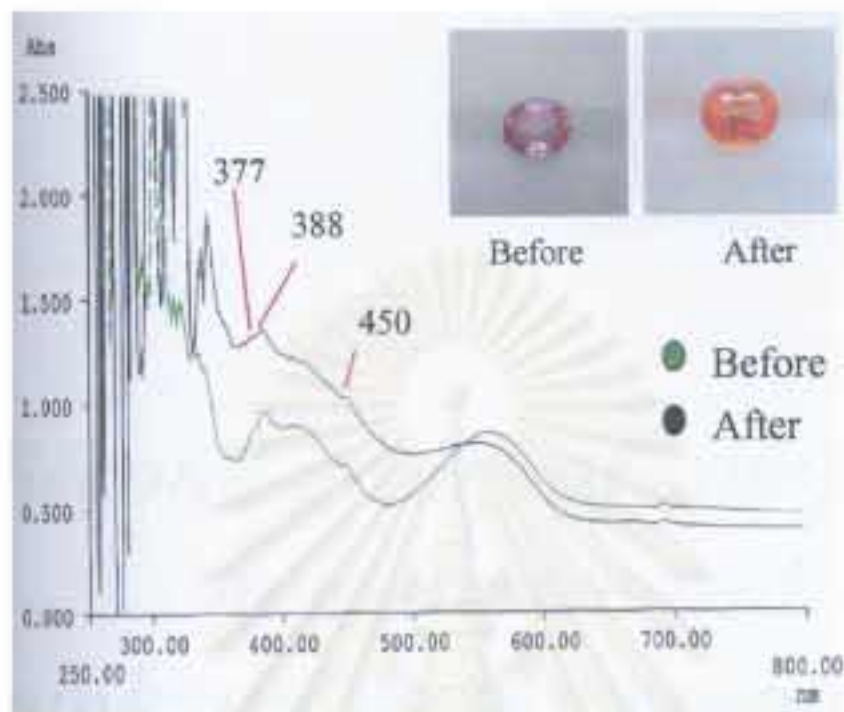


Figure 4.2: Surface related orange zone can be seen when the stones are immersed in methylene iodide solution. (Photo by Somboon, GIT)



(a)



(b)

Figure 4.3: UV-Vis spectra of a pale pink Madagascan sapphire before treatment and the pink-orange sapphire after treatment with Be (a). Residual spectrum after the subtraction of the one before treatment from the other after Be-treatment (b).

*Second group of samples:
non-Be-treated
pink and orange sapphires*



Figure 4.4: An un-treated pink Madagascan sapphire (GITMDP18) was cut in half and a six-point profile was analyzed across the cut surface using LA-ICP-MS. (Photo by Lomthong, KU)

Table 4.1: Trace element content of the un-treated pink Madagascan sapphire (GITMDP1) showing negligible Be but high Cr and Fe contents, obtained by LA-ICP-MS.

	Rim1	Mid-Point1	Core1	Core2	Mid-Point2	Rim2
Cations (ppm by weight)						
Be9	<0.24	<0.18	<0.21	<0.18	<0.16	<0.13
Na23	<11.87	<9.84	<10.34	<9.86	<7.62	<7.95
Mg24	35.69	42.13	41.94	47.08	72.32	51.11
Al27	529250.40	529250.40	529250.40	529250.40	529250.40	529250.40
Ti47	52.07	58.07	56.95	60.66	68.44	67.62
V51	32.09	38.91	36.80	38.77	53.76	46.51
Cr53	428.38	506.57	535.17	516.73	756.63	672.80
Mn55	<0.58	<0.49	<0.51	<0.50	<0.38	<0.40
Fe57	1594.84	1864.87	1949.27	2062.30	3002.53	2415.83
Ga71	74.53	107.78	104.38	101.42	166.27	136.43
Total %	53.15	53.19	53.20	53.21	53.34	53.26
Cations (Atom Mole ppm)						
Be9	0.54	0.41	0.47	0.41	0.36	0.29
Na23	10.51	8.71	9.15	8.72	6.73	7.03
Mg24	29.88	35.26	35.10	39.39	60.44	42.74
Al27	399153.48	399006.46	398966.59	398927.44	398445.88	398720.55
Ti47	22.12	24.66	24.18	25.75	29.02	28.69
V51	12.82	15.54	14.69	15.48	21.44	18.56
Cr53	167.64	198.17	209.33	202.10	295.57	263.01
Mn55	0.21	0.18	0.19	0.19	0.14	0.15
Fe57	581.05	679.18	709.85	750.94	1091.98	879.21
Ga71	21.75	31.44	30.45	29.58	48.44	39.77
Total (Atom Mole%)	40.00	40.00	40.00	40.00	40.00	40.00
Mg-Ti	7.76	10.60	10.91	13.64	31.42	14.05
Be-Ti	-21.58	-24.25	-23.71	-25.35	-28.66	-28.40
(Be+Mg)-Ti	8.30	11.01	11.39	14.05	31.78	14.34
(Be+Mg) %	4.80	4.82	4.62	4.87	5.14	4.53
Ti %	3.49	3.33	3.14	3.15	2.46	3.02
Fe%	91.71	91.84	92.24	91.97	92.40	92.46

< = below the detection limit of which the value is used for calculation of atom mole ppm

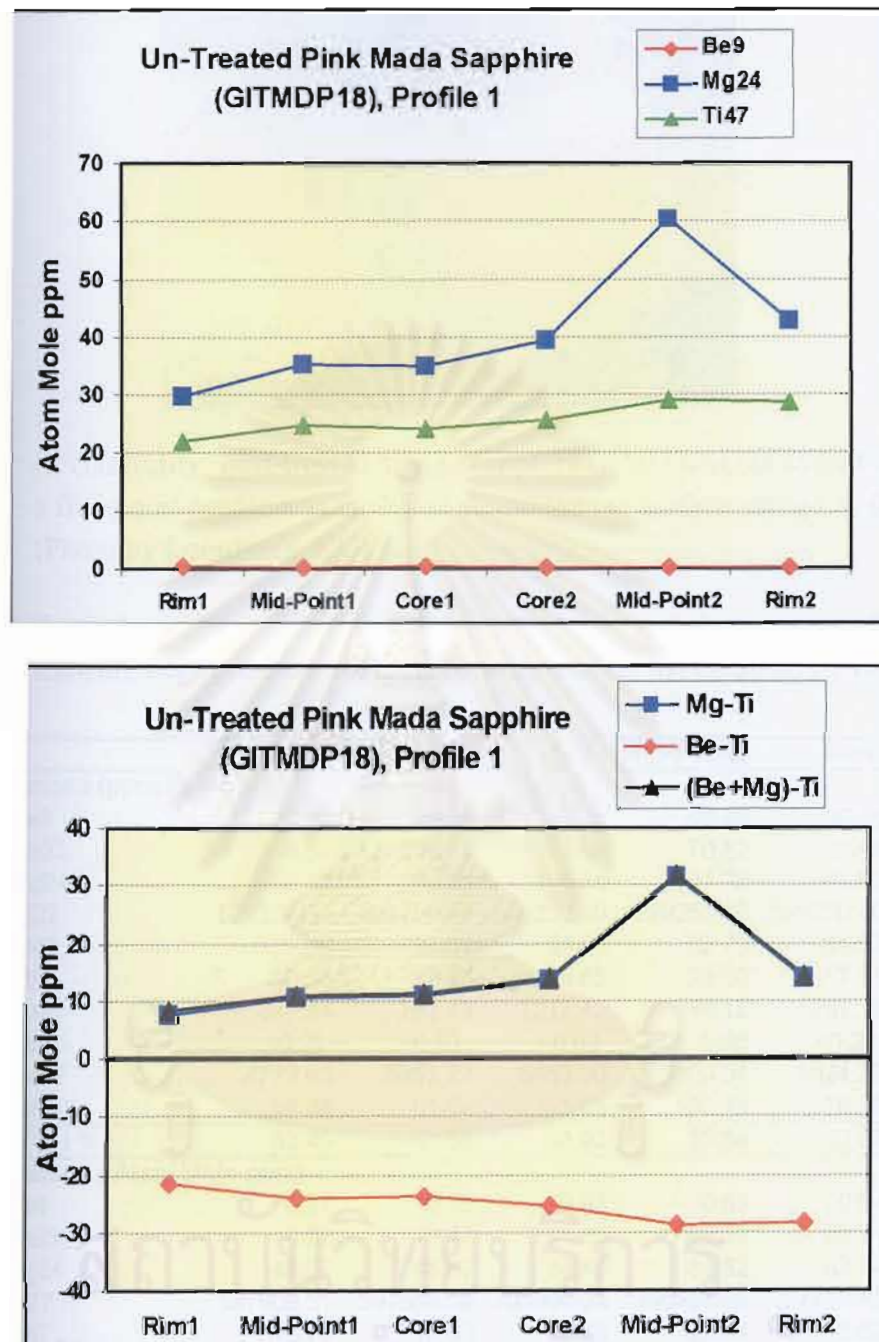


Figure 4.5: Plot of trace element content variation across the cut surface of the un-treated pink Madagascan sapphire (GITMDP18, Figure 4.4) showing Mg > Ti (< ~ 30 atom mole ppm which is not enough to create orange coloration) and negligible Be contents in all points analyzed.



Figure 4.6. A 'classically' heat-treated orange sapphire (KNI) was cut in half and a five-point profile was analyzed across the cut surface using LA-ICP-MS. (Photo by Lomthong, KU)

Table 4.2: Trace element content of the 'classically' heat-treated orange sapphire (KNI) showing negligible Be but high Cr and Fe contents, obtained by LA-ICP-MS

	Rim1	Mid-Point1	Core	Mid-Point2	Rim2
Cations (ppm by weight)					
Be9	<0.12	<0.26	<0.28	<0.28	<0.24
Na23	<5.54	<10.74	<12.89	70.82	23.54
Mg24	58.32	58.35	101.54	101.73	75.63
Al27	529250.40	529250.40	529250.40	529250.40	529250.40
Ti47	37.26	38.01	53.58	52.70	44.03
V51	15.36	15.40	26.85	25.50	17.51
Cr53	677.44	763.43	1212.42	949.12	767.10
Mn55	<0.25	<0.50	<0.62	0.96	<0.36
Fe57	4772.63	5357.72	8453.30	7809.04	5924.22
Ga71	58.38	61.84	121.55	100.73	76.96
Total %	53.49	53.56	53.92	53.84	53.62
Cations (Atom Mole ppm)					
Be9	0.27	0.58	0.63	0.63	0.54
Na23	4.89	9.47	11.33	62.28	20.74
Mg24	48.67	48.67	84.40	84.62	63.04
Al27	397909.51	397658.58	396306.03	396594.65	397419.69
Ti47	15.78	16.09	22.60	22.24	18.62
V51	6.12	6.13	10.65	10.12	6.96
Cr53	264.28	297.64	471.08	369.04	298.89
Mn55	0.09	0.18	0.23	0.35	0.13
Fe57	1733.40	1944.68	3057.84	2826.85	2149.01
Ga71	16.99	17.98	35.22	29.21	22.36
Total (Atom Mole)	40.00	40.00	40.00	40.00	40.00
Mg-Ti	32.89	32.58	61.80	62.38	44.42
Be-Ti	-15.51	-15.50	-21.97	-21.62	-18.08
(Be+Mg)-Ti	33.16	33.17	62.43	63.01	44.96
(Be+Mg) %	2.72	2.45	2.69	2.91	2.85
Ti %	0.88	0.80	0.71	0.76	0.83
Fe%	96.40	96.75	96.60	96.34	96.32

☞ below the detection limit of which the value is used for calculation of atom mole ppm

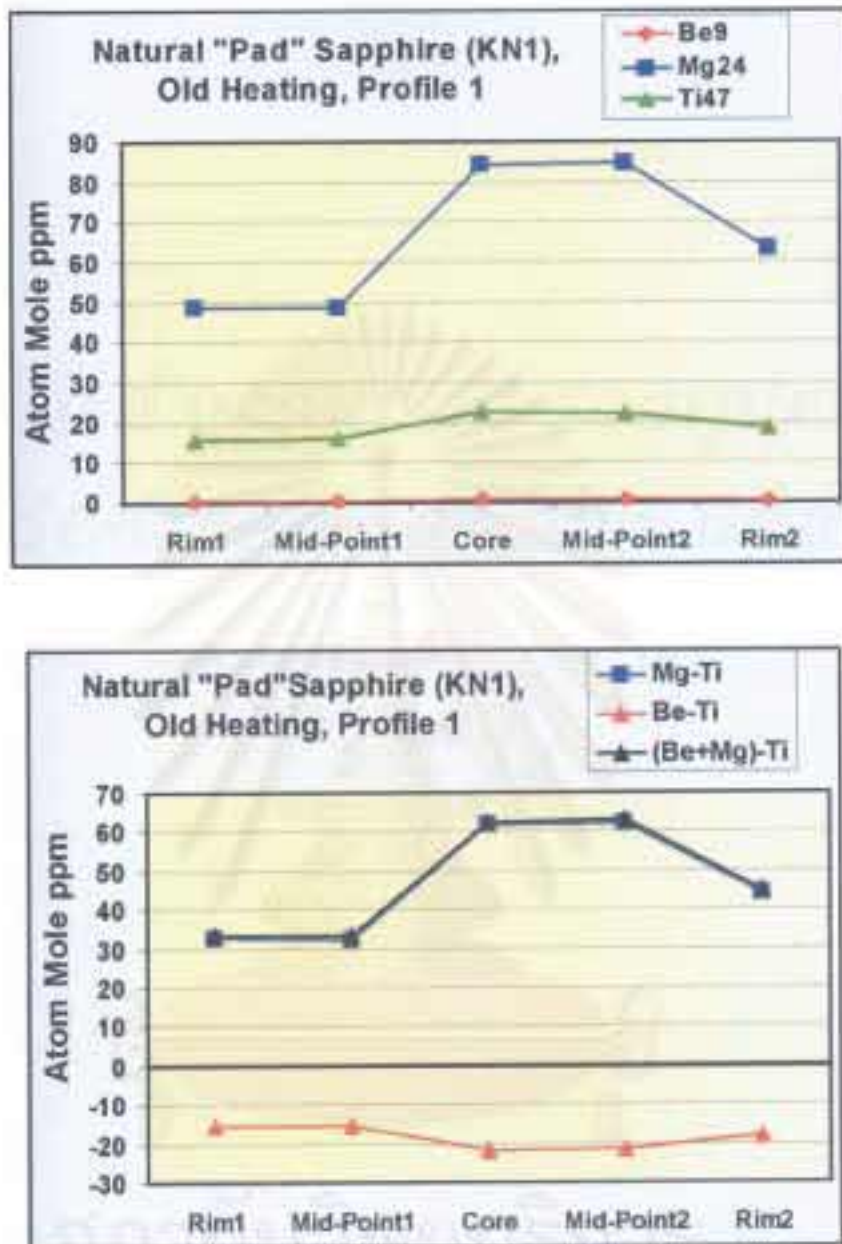
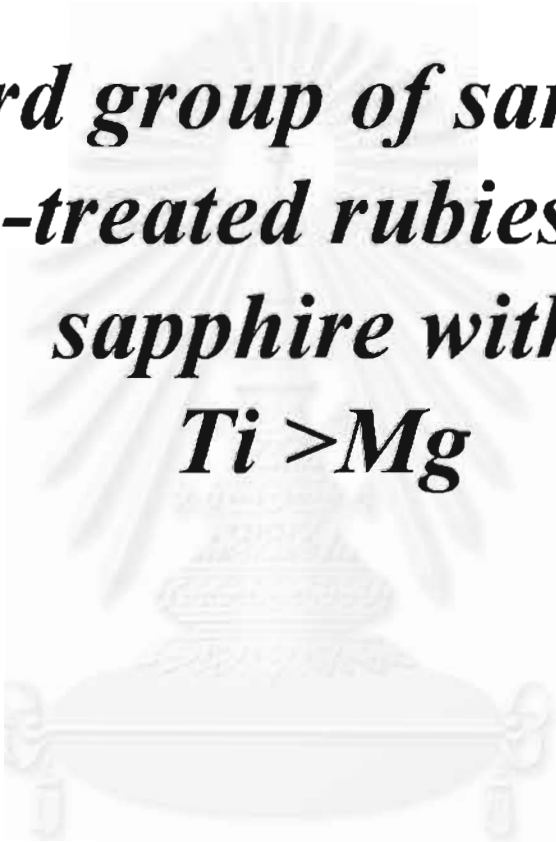


Figure 4.7: Plot of trace element content variation across the cut surface of the 'classically' heat-treated orange sapphire (KN1, Figure 4.6) showing Mg > Ti (> 30 atom mole ppm which is enough to create orange coloration) and negligible Be contents in all points analyzed.

*Third group of samples:
Be-treated rubies and
sapphire with
 $Ti > Mg$*



Mong Hsu (Myanmar) rubies



Before

After

Vietnamese Rubies



Before

After

Figure 4.8: Mong Hsu (Myanmar) and Vietnamese rubies of metamorphic origin reportedly treated unsuccessfully by a Be-heating technique (Themelis, 2003).



Figure 4.9: Three Mong Hsu rubies still appear red, purplish red or pink after a Be-treatment by a Thai heater. (Photo by Somboon, GIT)



Immersion

Figure 4.10: Five Vietnamese rubies still appear red, purplish or bluish red or pink after the same Be-treatment as in Figure 4.9. (Photo by Somboon, GIT)

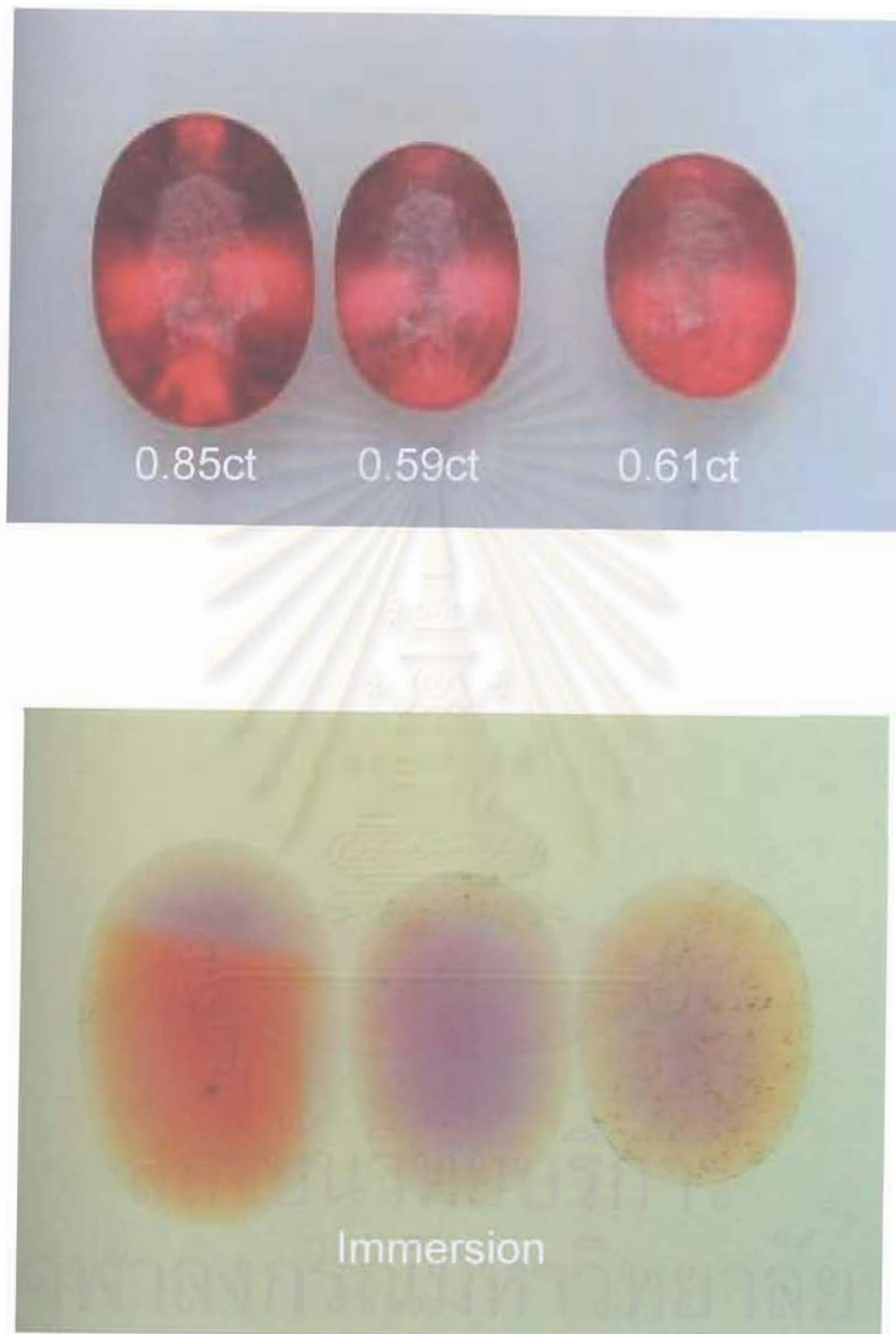
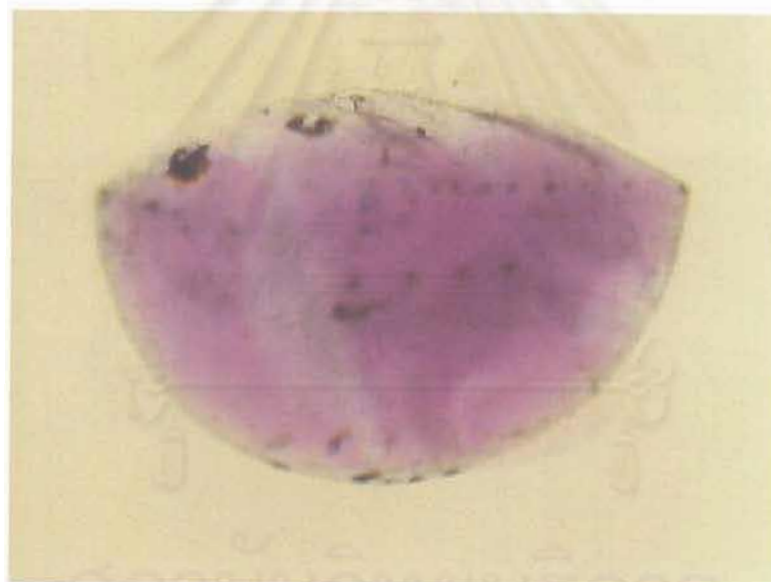


Figure 4.11: Three orange Songea (Tanzania) sapphires were treated from originally brownish red stones under the same Be-heating run as in Figures 4.9 and 4.10. Note the surface-related colour zones are clearly seen in immersion (Photo by Somboon, GIT)



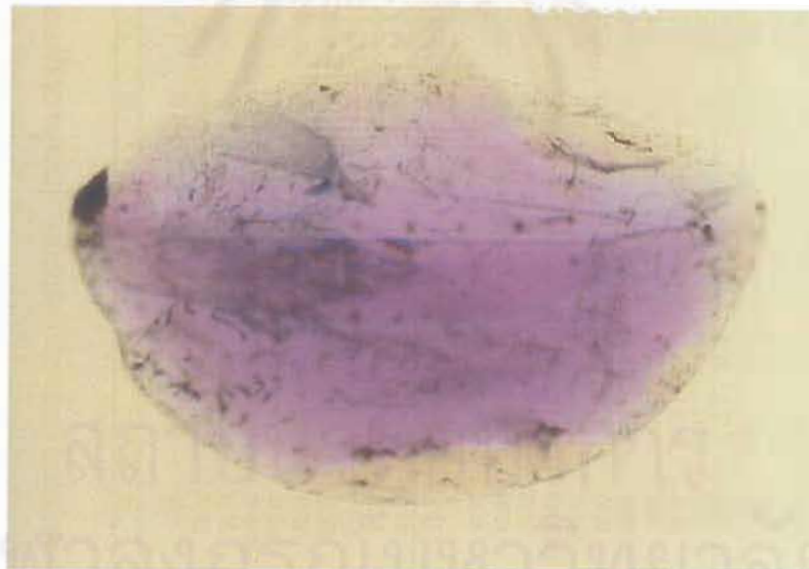
Immersion

Figure 4.12: Close examination of a Be-treated Mong Hsu Ruby (CR0054) shows very thin surface-related yellow or orange rim in immersion liquid. Top photo, before cutting; Bottom photo, after cutting in half. Close-space points on a traverse were analyzed across the cut surface using LA-ICP-MS. (Photo by Somboon, GIT)



Immersion

Figure 4.13: Another Be-treated Mong Hsu Ruby (CR119) shows very thin surface-related yellow or orange rim in immersion liquid. Top photo before cutting; Bottom photo, after cutting in half. Close-space points on a traverse were analyzed across the cut surface using LA-ICP-MS. (Photo by Somboon, GIT)



Immersion

Figure 4.14: A Be-treated Vietnamese Ruby (CRVN02) shows thin patchy surface-related yellow or orange rim in immersion liquid. Top photo, before cutting; Bottom photo, after cutting in half. Close-space points on a traverse were analyzed across the cut surface using LA-ICP-MS. (Photo by Somboon, GIT)

Table 4.3: Trace element contents of a Be-treated Mong Hsu ruby (CR0054) showing rather high contents of Cr and Ti but low Mg, Fe and Be across the profile except at the rims where there are extremely high contents of Be and Fe suggesting a contamination from chrysoberyl. Results obtained from LA-ICP-MS.

	Rim1	S2	S3	S4	S5	S6	S7	S8	S9	S10	S11	S12	S13	S14	S16	S16	S17	S18	S19	Rim2
Cations (ppm by weight)																				
Be9	1328.38	67.17	7.02	4.69	5.87	3.16	4.63	1.95	1.63	1.14	<0.97	0.84	<1.15	<1.27	<0.94	<1.23	<0.75	<0.77	<0.91	8956.48
Na23	181.20	101.88	88.17	72.22	81.85	78.54	108.48	97.51	105.38	136.57	122.35	114.88	120.89	126.55	112.57	125.05	112.03	104.83	99.56	124.94
Mg24	102.59	29.43	27.94	36.34	37.35	24.28	22.47	20.72	22.66	19.69	20.25	16.92	14.45	24.39	20.13	10.91	24.21	24.28	24.26	121.87
Al27	529250.40	529250.40	529250.40	529250.40	529250.40	529250.40	529250.40	529250.40	529250.40	529250.40	529250.40	529250.40	529250.40	529250.40	529250.40	529250.40	529250.40	529250.40	529250.40	529250.40
Ti47	544.95	681.62	691.19	553.49	446.72	238.96	104.12	60.77	67.06	72.71	167.09	375.65	766.63	1297.48	1284.97	1047.01	1398.37	1700.95	1512.57	944.51
V51	103.33	111.35	112.08	152.48	162.55	147.35	147.98	103.44	119.04	101.38	95.90	55.10	54.30	78.58	76.00	70.15	69.78	69.62	68.44	45.85
Cr53	797.92	874.05	841.66	826.60	882.24	1018.43	712.01	1786.56	2660.16	3704.46	4263.37	2212.90	1820.82	2102.21	2012.37	1839.81	1792.93	1755.75	1650.75	1478.02
Mn55	1.88	0.41	<0.10	<0.10	<0.11	<0.12	<0.12	<0.11	0.12	<0.11	<0.11	0.11	<0.12	<0.14	<0.12	<0.13	<0.13	<0.12	<0.11	7.57
Fe57	362.55	57.68	41.76	41.00	43.24	40.47	43.55	37.99	38.73	40.48	39.05	30.62	24.84	42.67	42.76	45.36	38.65	43.00	41.48	1709.18
Ga71	67.11	62.18	60.76	63.48	63.11	68.69	72.80	61.88	63.99	58.58	54.59	42.98	44.26	52.55	52.80	56.71	53.39	53.96	49.01	102.19
Total %	53.27	53.12	53.11	53.10	53.10	53.09	53.05	53.14	53.23	53.34	53.40	53.21	53.21	53.30	53.29	53.24	53.27	53.30	53.27	54.27
Cations (Atom Mole ppm)																				
Be9	2975.98	151.61	15.85	10.59	13.26	7.14	10.46	4.40	3.66	2.57	2.18	1.89	2.59	2.86	2.12	2.77	1.69	1.74	2.05	19202.83
Na23	159.13	90.14	78.04	63.94	72.46	69.54	96.09	86.29	93.17	120.62	108.00	101.59	106.90	111.81	99.47	110.54	99.00	92.61	87.99	105.01
Mg24	85.22	24.63	23.39	30.43	31.28	20.33	18.83	17.34	18.95	16.45	16.91	14.15	12.09	20.38	16.82	9.12	20.24	20.29	20.28	96.88
Al27	396048.01	399018.47	399181.92	399241.89	399248.69	399309.00	399456.18	399093.86	398735.52	398310.68	398069.92	398811.96	398797.46	398431.38	398489.15	398653.20	398527.94	398419.14	398546.39	379025.37
Ti47	229.69	289.45	293.64	235.17	189.81	101.55	44.26	25.81	28.46	30.82	70.79	159.44	325.37	550.17	544.95	444.21	593.10	721.24	641.56	381.00
V51	40.95	44.46	44.77	60.92	64.95	58.88	59.16	41.31	47.50	40.41	38.20	21.99	21.67	31.33	30.31	27.99	27.83	27.76	27.30	17.39
Cr53	309.83	341.93	329.40	323.55	345.34	398.70	278.85	699.04	1039.93	1446.63	1663.88	865.25	711.92	821.18	786.20	719.08	700.54	685.83	645.02	549.24
Mn55	0.89	0.15	0.04	0.04	0.04	0.04	0.04	0.04	0.04	0.04	0.04	0.04	0.04	0.05	0.04	0.05	0.05	0.05	0.04	2.66
Fe57	131.06	21.01	15.22	14.94	15.76	14.75	15.88	13.84	14.10	14.72	14.19	11.15	9.04	15.52	15.55	16.51	14.06	15.64	15.09	591.31
Ga71	19.43	18.14	17.73	18.53	18.42	20.06	21.26	18.06	18.66	17.06	15.89	12.53	12.91	15.31	15.38	16.53	15.56	15.72	14.28	28.32
Total (Atom Mole%)	40.00	40.00	40.00	40.00	40.00	40.00	40.00	40.00	40.00	40.00	40.00	40.00	40.00	40.00	40.00	40.00	40.00	40.00	40.00	40.00
Mg-Ti	-144.47	-264.82	-270.25	-204.74	-158.54	-81.21	-25.44	-8.47	-9.51	-14.37	-53.88	-145.29	-313.29	-529.79	-528.12	-435.09	-572.66	-700.95	-621.28	-284.11
Be-Ti	2746.28	-137.94	-277.79	-224.58	-176.56	-94.41	-33.80	-21.41	-24.78	-28.25	-68.60	-167.54	-322.78	-547.31	-542.83	-441.44	-591.41	-718.50	-639.51	18821.83
(Be+Mg)-Ti	2831.60	-113.21	-254.39	-194.16	-145.28	-74.08	-14.98	-4.07	-5.83	-11.80	-61.70	-143.39	-310.69	-526.93	-526.00	-432.32	-571.17	-699.21	-619.23	18918.72
(Be+Mg) %	89.46	36.21	11.27	14.09	17.81	19.11	32.75	35.42	34.71	29.46	18.35	8.60	4.21	3.95	3.27	2.52	3.49	2.90	3.29	95.20
Ti %	8.71	59.47	84.36	80.78	75.89	70.63	49.50	42.04	43.66	47.74	68.02	85.43	93.20	93.42	94.05	83.99	94.28	95.04	94.49	1.88
Fe%	3.83	4.32	4.37	6.13	6.30	10.26	17.76	22.54	21.63	22.80	13.63	5.97	2.59	2.63	2.68	3.49	2.23	2.06	2.22	2.92

< = below the detection limit of which the value is used for calculation of atom mole ppm

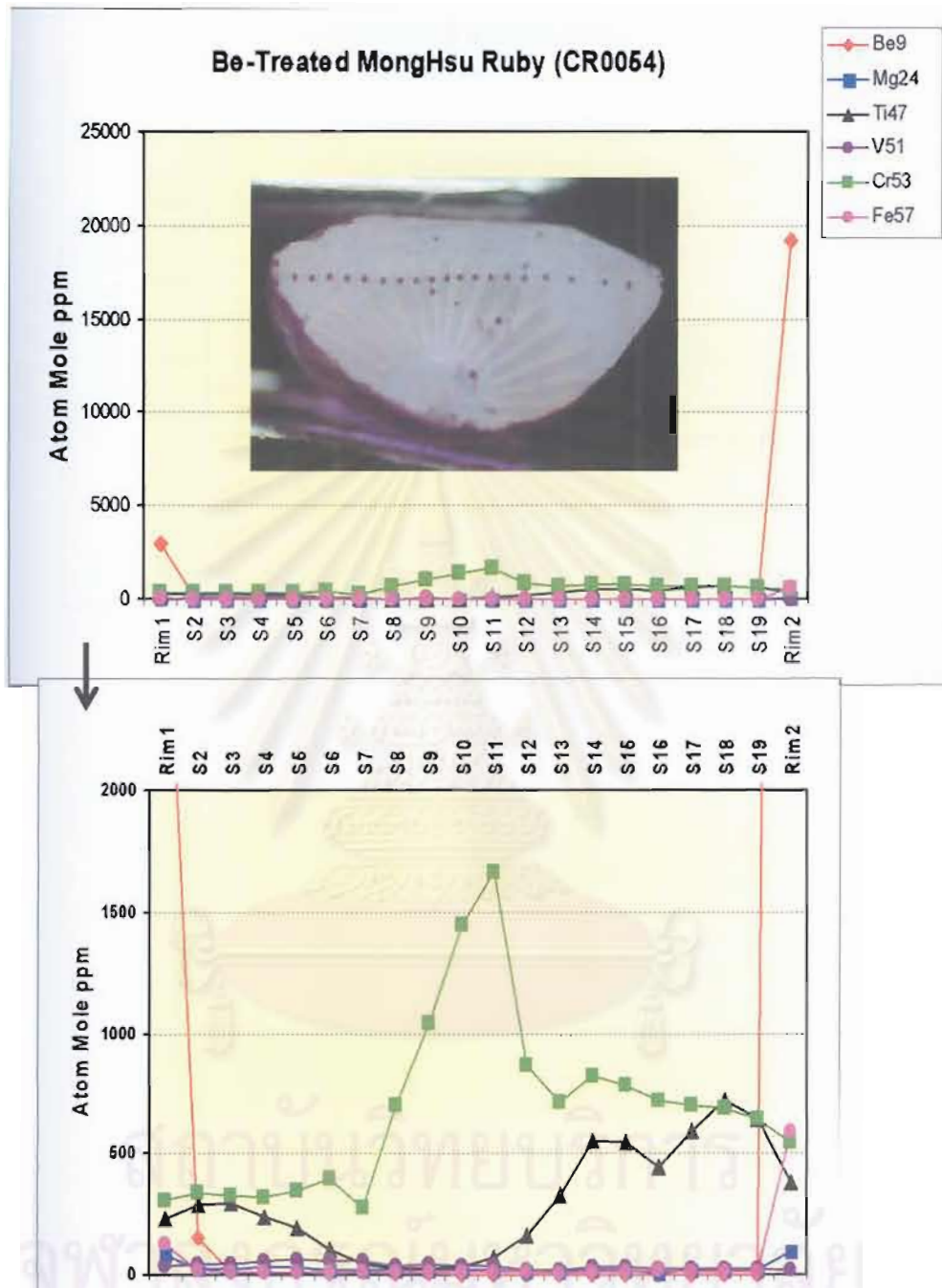


Figure 4.15a: Plots of trace element content variation across the cut surface of the Be-treated Mong Hsu ruby (CR0054). The lower diagram is an enlargement of the upper diagram. Note the extremely high contents of Be and Fe at the rims.

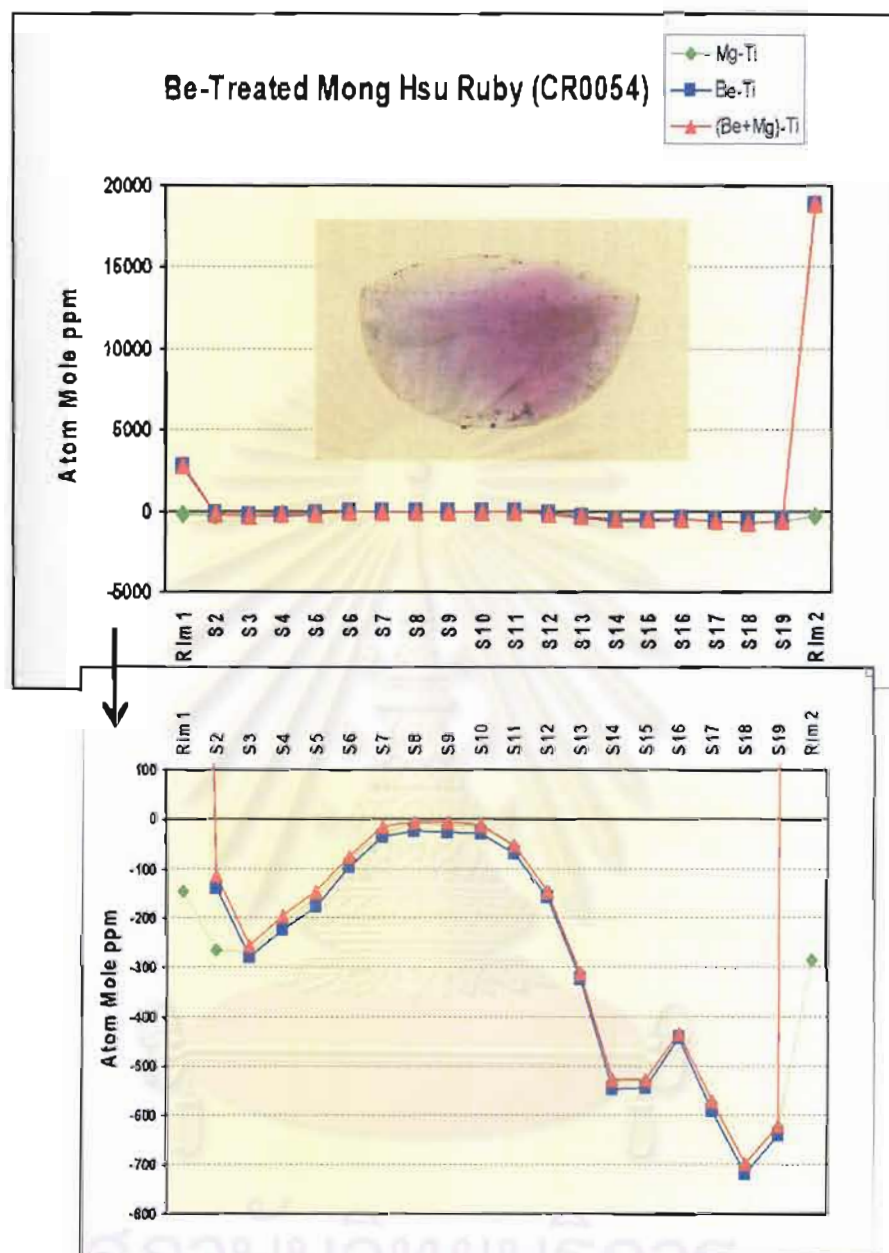


Figure 4.15b: Plots of trace element content variation across the cut surface of the Be-treated Mong Hsu ruby (CR0054). The lower diagram is an enlargement of the upper diagram. The analyses show $(\text{Be}+\text{Mg}) \gg \text{Ti}$ which corresponds fairly well with very thin yellow or orange rims in contrast to $(\text{Be}+\text{Mg}) < \text{Ti}$ in the red core area.

Table 4.4: Trace element contents of a Be-treated Mong Hsu ruby (CR119) showing rather high contents of Cr and Ti but low Mg, Fe and Be across the profile except at the rims where there are extremely high contents of Be and Fe suggesting a contamination from chrysoberyl. Results obtained from LA-ICP-MS.

	Rim1	S2	S3	S4	S5	S6	S7	S8	S9	S10	S11	S12	S13	S14	S15	Rim2
Cations (ppm by weight)																
Be9	7981.35	46.55	3.26	1.85	1.09	0.90	<0.58	<0.62	<0.74	<0.69	<0.68	<0.76	<0.67	<0.88	<0.85	6864.75
Na23	<26.45	55.67	85.82	79.33	75.07	52.45	90.02	89.37	<24.59	77.56	123.46	109.31	120.40	111.19	108.88	99.01
Mg24	167.53	39.22	24.04	19.81	19.32	11.28	10.75	13.69	9.70	9.13	13.81	15.12	25.70	26.84	22.56	132.20
Al27	529250.40	529250.40	529250.40	529250.40	529250.40	529250.40	529250.40	529250.40	529250.40	529250.40	529250.40	529250.40	529250.40	529250.40	529250.40	529250.40
Ti47	254.23	143.10	86.85	292.56	412.45	123.25	61.31	65.45	65.57	69.02	72.39	99.87	580.24	969.73	1028.32	465.12
V51	105.09	180.92	185.30	231.55	226.60	144.10	120.36	123.26	114.98	119.58	121.70	121.58	186.48	210.87	204.81	159.71
Cr53	2001.44	1153.74	814.56	999.33	957.02	657.04	2165.61	2338.83	2129.16	2155.92	2266.01	1981.75	2499.22	2590.58	2504.19	2468.82
Mn55	24.71	0.41	<0.08	<0.06	<0.06	<0.07	<0.07	<0.09	<0.11	<0.09	<0.10	<0.11	<0.11	<0.11	<0.11	7.39
Fe57	1630.71	41.28	19.08	12.93	15.22	16.26	14.77	15.80	21.39	19.51	25.19	17.67	17.81	15.60	13.17	1517.75
Ga71	153.73	105.75	104.53	107.00	105.64	103.97	104.30	108.86	104.85	107.22	115.30	112.45	114.23	115.11	112.11	153.40
Total %	54.16	53.10	53.06	53.10	53.11	53.04	53.18	53.20	53.17	53.18	53.20	53.17	53.28	53.33	53.32	54.11
Cations (Atom Mole ppm)																
Be9	17207.01	105.11	7.37	4.18	2.46	2.03	1.31	1.40	1.67	1.56	1.53	1.72	1.51	1.98	1.92	14879.28
Na23	22.35	49.28	76.01	70.23	66.46	46.47	79.64	79.05	21.76	68.61	109.19	96.71	106.40	98.21	96.17	84.12
Mg24	133.92	32.84	20.14	16.59	18.18	9.45	9.00	11.45	8.12	7.64	11.55	12.65	21.48	22.42	18.85	106.25
Al27	381126.78	399182.12	399428.99	399265.01	399238.12	399538.32	398953.09	398878.94	399023.33	398963.43	398869.43	398983.49	398533.81	398331.29	398349.97	383175.53
Ti47	103.12	60.79	36.92	124.31	175.25	52.41	26.03	27.78	27.85	29.31	30.73	42.41	246.10	411.09	435.95	189.67
V51	40.08	72.27	74.07	92.52	90.53	57.62	48.05	49.20	45.91	47.74	48.58	48.54	74.37	84.06	81.65	61.24
Cr53	747.86	451.53	318.99	391.18	374.60	257.37	847.06	914.64	832.95	843.29	886.14	775.20	976.52	1011.70	978.01	927.47
Mn55	8.74	0.15	0.03	0.02	0.02	0.03	0.03	0.03	0.04	0.03	0.04	0.04	0.04	0.04	0.04	2.63
Fe57	567.29	15.04	6.96	4.71	5.55	5.93	5.38	5.75	7.79	7.10	9.17	6.44	6.48	5.67	4.79	530.83
Ga71	42.84	30.87	30.53	31.24	30.84	30.37	30.42	31.75	30.59	31.28	33.63	32.80	33.29	33.53	32.65	42.98
Total (Atom Mole)	40.00	40.00	40.00	40.00	40.00	40.00	40.00	40.00	40.00	40.00	40.00	40.00	40.00	40.00	40.00	40.00
Mg-Ti	30.80	-27.96	-16.78	-107.72	-159.07	-42.95	-17.04	-16.33	-19.73	-21.67	-19.18	-29.75	-224.62	-388.67	-417.10	-83.43
Be-Ti	17103.89	44.32	-29.55	-120.14	-172.78	-50.37	-24.72	-26.39	-26.17	-27.75	-29.20	-40.69	-244.59	-409.11	-434.04	14689.61
(Be+Mg)-Ti	17237.81	77.16	-9.41	-103.55	-156.61	-40.92	-15.73	-14.93	-18.06	-20.11	-17.64	-28.04	-223.11	-388.69	-415.19	14795.86
(Be+Mg) %	96.28	64.53	38.53	13.86	9.35	16.45	24.70	27.71	21.55	20.17	24.70	22.73	8.34	5.53	4.50	95.41
Ti %	0.57	28.44	51.72	82.99	87.87	75.06	62.40	59.89	61.30	64.26	57.99	67.09	89.31	93.18	94.46	1.21
Fe%	3.15	7.04	9.75	3.15	2.78	8.49	12.89	12.40	17.15	15.58	17.31	10.18	2.35	1.29	1.04	3.38

< = below the detection limit of which the value is used for calculation of atom mole ppm

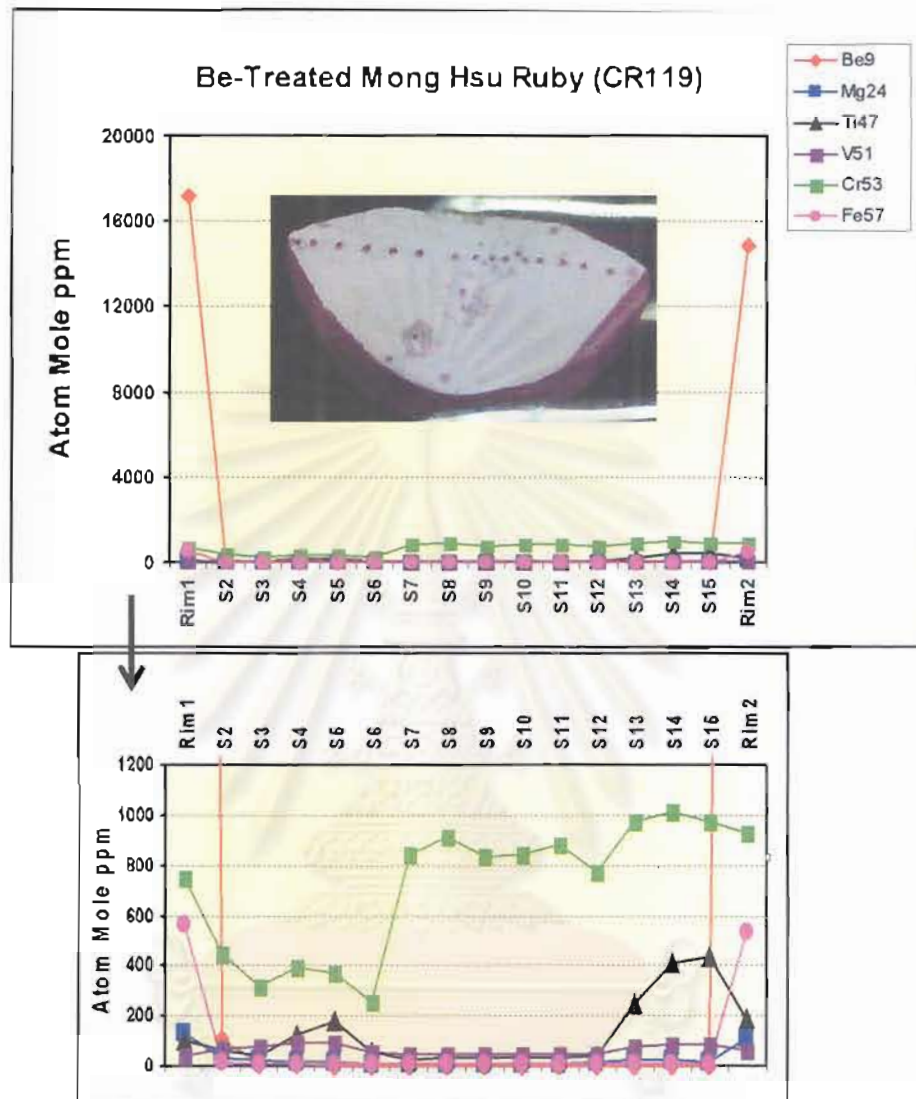


Figure 4.16a: Plots of trace element content variation across the cut surface of the Be-treated Mong Hsu ruby (CR119). The lower diagram is an enlargement of the upper diagram. Note the extremely high contents of Be and Fe at the rims.

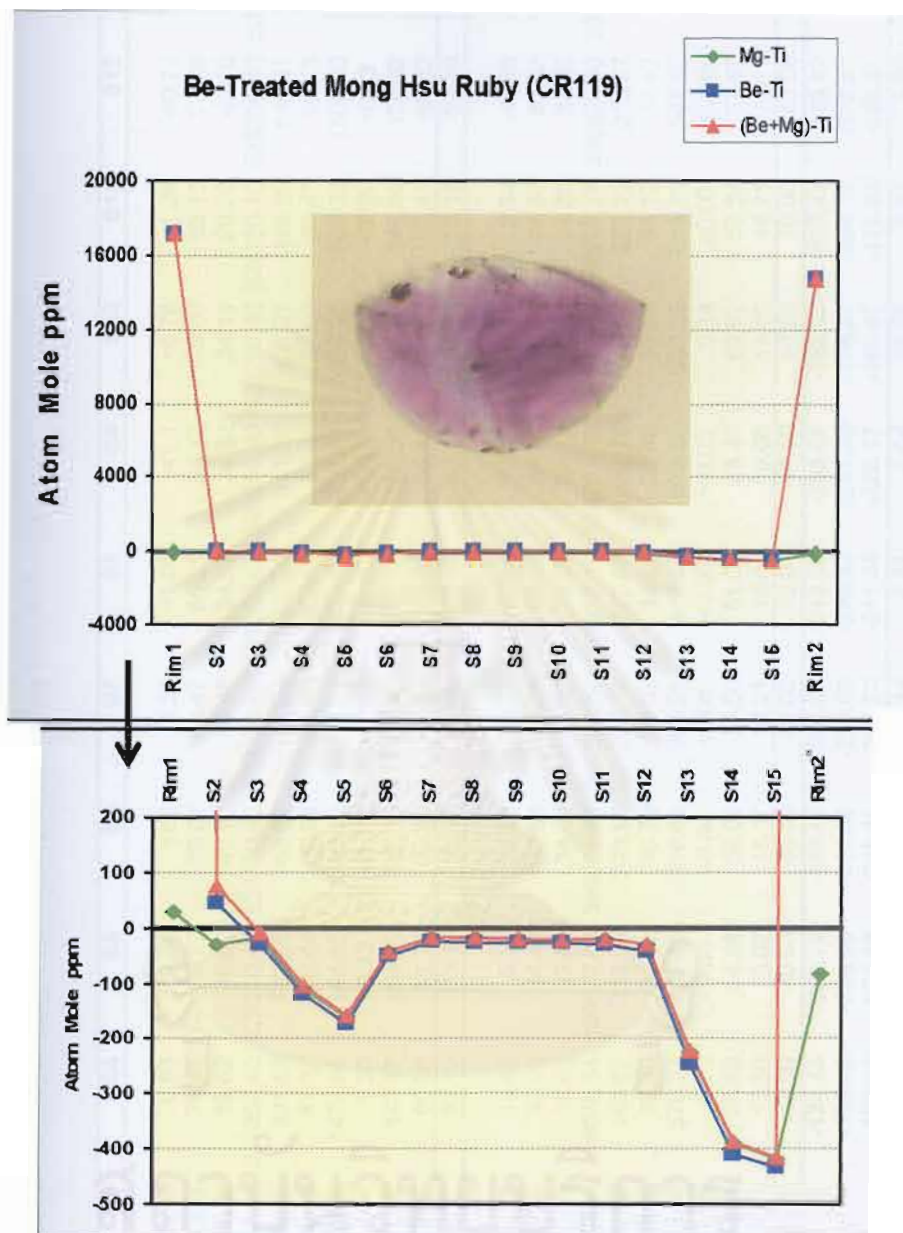


Figure 4.16b: Plots of trace element content variation across the cut surface of the Be-treated Mong Hsu ruby (CR119). The lower diagram is an enlargement of the upper diagram. The analyses show $(\text{Be}+\text{Mg}) \gg \text{Ti}$ which corresponds fairly well with very thin yellow or orange rims in contrast to $(\text{Be}+\text{Mg}) < \text{Ti}$ in the red core area.

Table 4.5: Trace element contents of a Be-treated Vietnamese ruby (CRVN02) showing rather high contents of Cr and Ti but low Mg, Fe and Be across the profile except at the rims where there are extremely high contents of Be and Fe suggesting a contamination from chrysoberyl. Results obtained from LA-ICP-MS.

	Rim1	S2	S3	S4	S5	S6	S7	S8	S9	S10	S11	S12	Rim2
Cations (ppm by weight)													
Be9	13441.18	52.15	84.89	6.83	2.74	1.87	4.50	<1.08	<1.1	<0.78	1.26	<0.71	6.53
Na23	77.52	62.67	43.37	75.81	50.27	38.07	102.47	66.21	64.12	105.06	89.15	74.08	52.84
Mg24	314.12	36.79	36.39	19.62	40.02	40.66	40.48	34.53	34.82	34.11	29.70	40.70	13.78
Al27	529250.40	529250.40	529250.40	529250.40	529250.40	529250.40	529250.40	529250.40	529250.40	529250.40	529250.40	529250.40	529250.40
Ti47	233.53	217.80	240.65	331.68	782.36	762.82	696.64	642.74	611.98	426.27	488.09	645.31	24.18
V51	18.54	75.02	88.27	81.37	89.44	92.04	87.72	87.54	91.41	81.90	85.47	93.73	5.36
Cr53	1283.70	2172.18	2602.05	1477.96	1144.85	1326.00	1453.11	1581.76	1721.91	1676.25	1684.20	1502.90	310.83
Mn55	41.80	4.97	1.95	0.30	<0.12	<0.11	<0.14	<0.17	<0.13	0.37	<0.15	<0.13	<0.10
Fe57	2637.53	182.62	231.86	147.37	150.69	162.18	152.44	141.58	160.51	192.03	146.50	158.92	128.85
Ga71	142.83	65.23	75.21	59.98	61.76	62.30	62.42	64.65	65.42	63.53	62.42	65.52	33.78
Total %	54.74	53.21	53.27	53.15	53.16	53.17	53.19	53.19	53.20	53.18	53.18	53.18	52.98
Cations (Atom Mole ppm)													
Be9	28135.57	117.63	191.35	15.42	6.18	4.22	10.15	<2.44	<2.48	<1.76	2.84	<1.60	14.77
Na23	63.61	55.41	38.32	67.09	44.48	33.68	90.64	58.57	56.71	92.93	78.86	65.53	46.84
Mg24	243.80	30.77	30.41	16.42	33.49	34.02	33.87	28.89	29.13	28.54	24.85	34.05	11.55
Al27	370048.59	398737.35	398479.14	399078.14	399027.06	398971.48	398892.54	398913.19	398864.49	398918.92	398921.79	398922.60	399735.67
Ti47	91.97	92.43	102.06	140.87	332.24	323.90	295.74	272.87	259.78	180.97	207.22	273.97	10.29
V51	6.87	29.94	35.20	32.50	35.72	36.75	35.02	34.95	36.49	32.70	34.12	37.42	2.14
Cr53	465.73	849.17	1016.56	578.27	447.88	518.68	568.28	618.63	673.36	655.59	658.71	587.80	121.82
Mn55	14.35	1.84	0.72	0.11	<0.05	<0.04	<0.05	<0.06	<0.05	0.14	<0.06	<0.05	<0.04
Fe57	890.87	66.46	84.33	53.68	54.88	59.06	55.50	51.55	58.44	69.92	53.34	57.87	47.01
Ga71	38.65	19.02	21.91	17.50	18.02	18.17	18.21	18.86	19.08	18.53	18.21	19.11	9.87
Total (Atom Mole%)	40.00	40.00	40.00	40.00	40.00	40.00	40.00	40.00	40.00	40.00	40.00	40.00	40.00
Mg-Ti	151.83	-61.66	-71.64	-124.46	-298.75	-289.87	-261.87	-243.98	-230.65	-152.43	-182.37	-239.92	1.27
Be-Ti	28043.60	25.20	89.29	-125.46	-326.06	-319.68	-285.69	-270.43	-257.30	-179.21	-204.38	-272.37	4.48
(Be+Mg)-Ti	28287.40	55.97	119.71	-109.03	-292.56	-285.65	-251.72	-241.54	-228.17	-150.67	-179.53	-238.31	16.03
(Be+Mg) %	96.65	48.29	54.33	14.06	9.30	9.08	11.14	8.81	9.04	10.78	9.61	9.70	31.47
Ti %	0.31	30.08	25.00	62.22	77.84	76.90	74.82	76.70	74.26	64.36	71.89	74.55	12.30
Fe%	3.03	21.63	20.66	23.71	12.86	14.02	14.04	14.49	16.70	24.87	18.51	15.75	56.22

< = below the detection limit of which the value is used for calculation of atom mole ppm

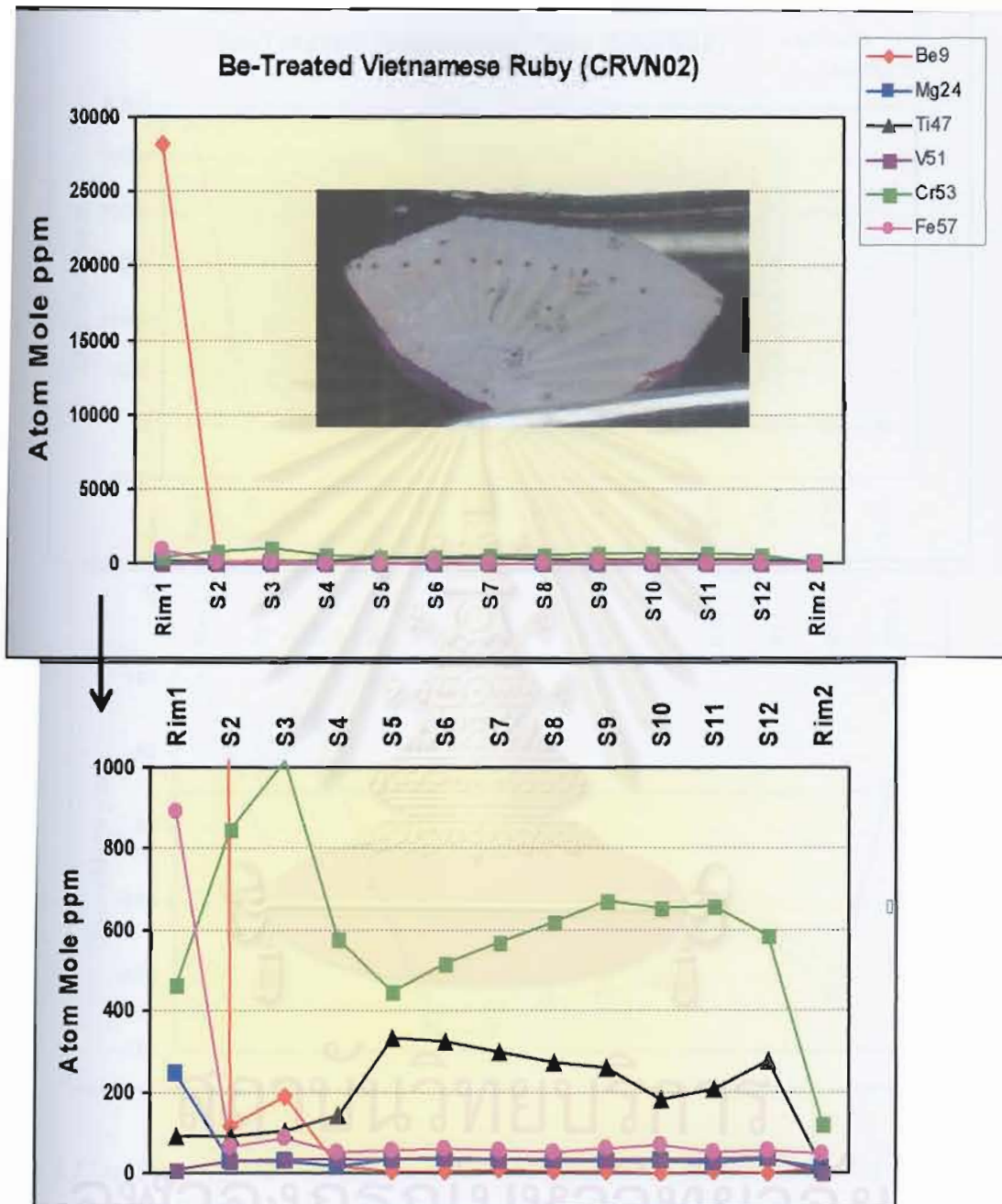


Figure 4.17a: Plots of trace element content variation across the cut surface of the Be-treated Vietnamese ruby (CRV N02). The lower diagram is an enlargement of the upper diagram. Note the extremely high contents of Be and Fe at the rim.

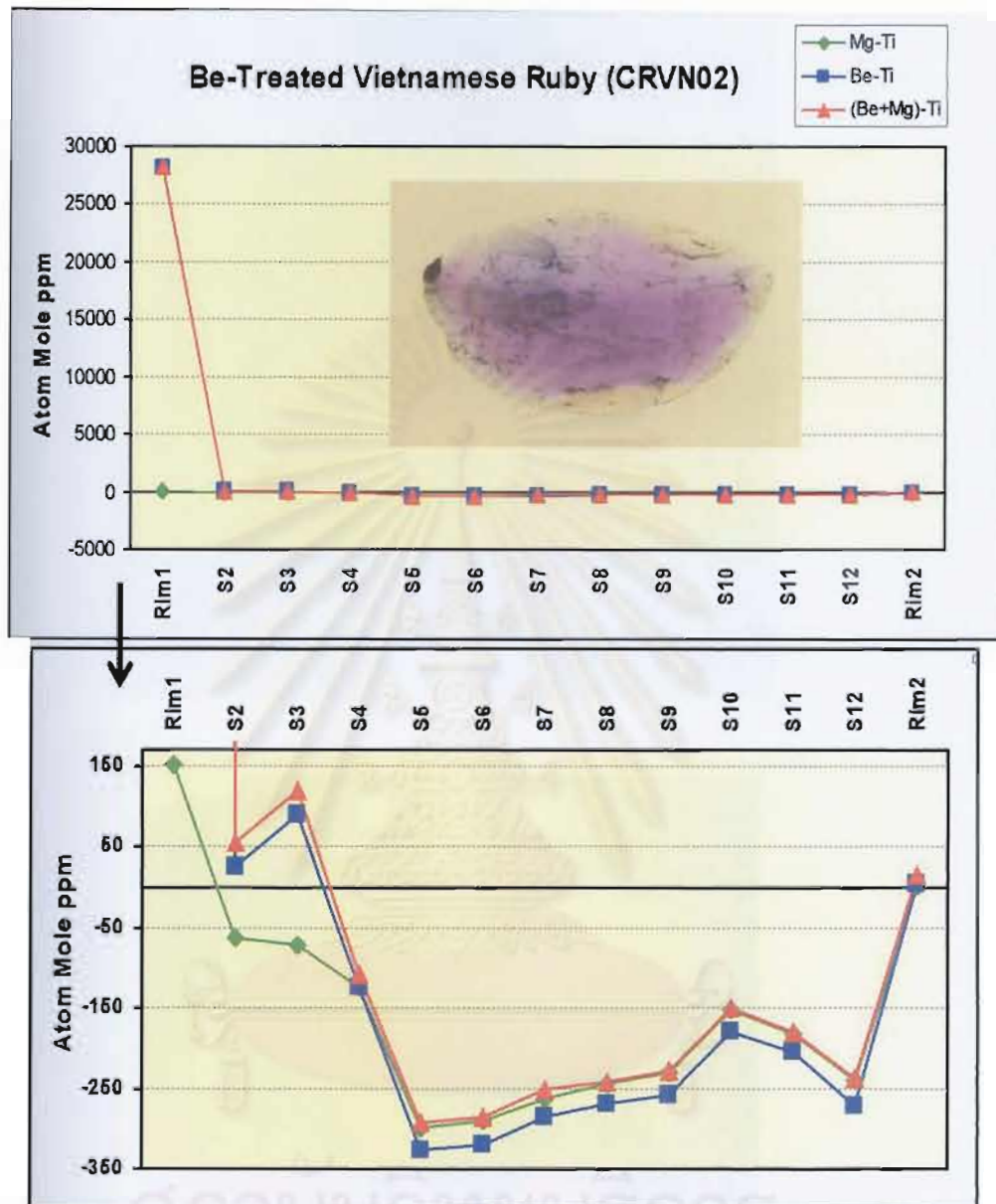


Figure 4.17b: Plots of trace element content variation across the cut surface of the Be-treated Vietnamese ruby (CR0054). The lower diagram is an enlargement of the upper diagram. The analyses show $(\text{Be}+\text{Mg}) \gg \text{Ti}$ which corresponds fairly well with very thin yellow or orange rims in contrast to $(\text{Be}+\text{Mg}) < \text{Ti}$ in the red core area.

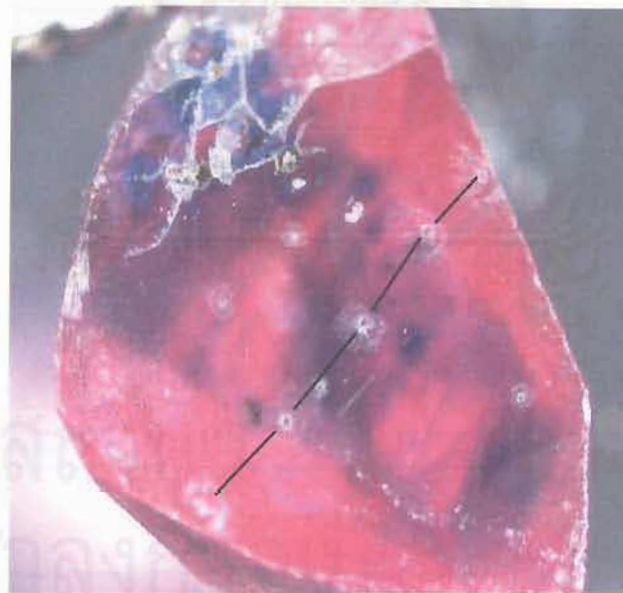
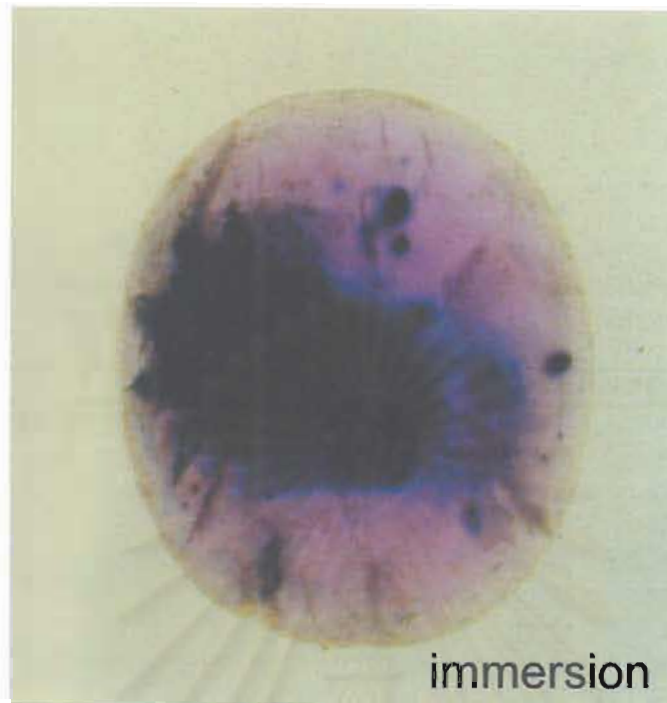


Figure 4.18: An Andila ruby (AR02) reportedly heat-treated with Be. Top, before cutting in immersion liquid showing obviously a surface related yellow or orange rim and a blue core; Bottom, a half-cut piece showing a five-point across the cut surface using LA-ICP-MS. Three points in the middle are within the blue zone while the other two points are at the yellow or orange rim. The blue zone is caused by internal diffusion of Ti-bearing inclusions. (Photo by Somboon, GIT and Lomthong, KU)

Table 4.6: Trace element content of a Be-treated Andila ruby (AR02) showing rather high contents of Cr and Fe, obtained by LA-ICP-MS.

	Rim1	Mid-Point1	Core	Mid-Point2	Rim2
Cations (ppm by weight)					
Be9	25.11	<0.73	<0.68	<0.84	8.25
Na23	56.50	68.59	25.40	<26.32	7.95
Mg24	80.64	88.80	151.96	101.14	64.49
Al27	529250.40	529250.40	529250.40	529250.40	529250.40
Ti47	155.98	199.53	342.25	282.97	124.00
V51	74.03	69.20	82.21	76.78	65.04
Cr53	2157.38	2295.94	3443.06	1991.24	1860.46
Mn55	0.64	<1.19	<1.21	<1.29	<0.28
Fe57	4473.79	3558.40	4219.37	3663.90	3223.15
Ga71	85.38	76.57	84.95	72.85	75.53
Total %	53.64	53.56	53.76	53.55	53.47
Cations (Atom Mole ppm)					
Be9	56.42	<1.64	<1.53	<1.89	18.57
Na23	49.77	60.46	22.35	<23.21	7.01
Mg24	67.19	74.04	126.46	84.35	53.82
Al27	397243.84	397543.14	396779.91	397612.65	397923.60
Ti47	65.94	84.42	144.52	119.74	52.51
V51	29.43	27.53	32.64	30.55	25.90
Cr53	840.22	894.86	1339.38	776.24	725.82
Mn55	0.24	<0.44	<0.45	<0.48	<0.10
Fe57	1622.15	1291.21	1528.11	1329.72	1170.68
Ga71	24.80	22.26	24.65	21.18	21.98
Total (Atom Mole%)	40.00	40.00	40.00	40.00	40.00
Mg-Ti	1.24	-10.38	-18.06	-35.40	1.31
Be-Ti	-9.52	-82.78	-143.00	-117.85	-33.94
(Be+Mg)-Ti	57.67	-8.73	-16.53	-33.51	19.88
(Be+Mg) %	6.82	5.21	7.11	5.62	5.59
Ti %	3.64	5.82	8.03	7.80	4.05
Fe%	89.54	88.97	84.87	86.59	90.36

< = below the detection limit of which the value is used for calculation of atom mole ppm

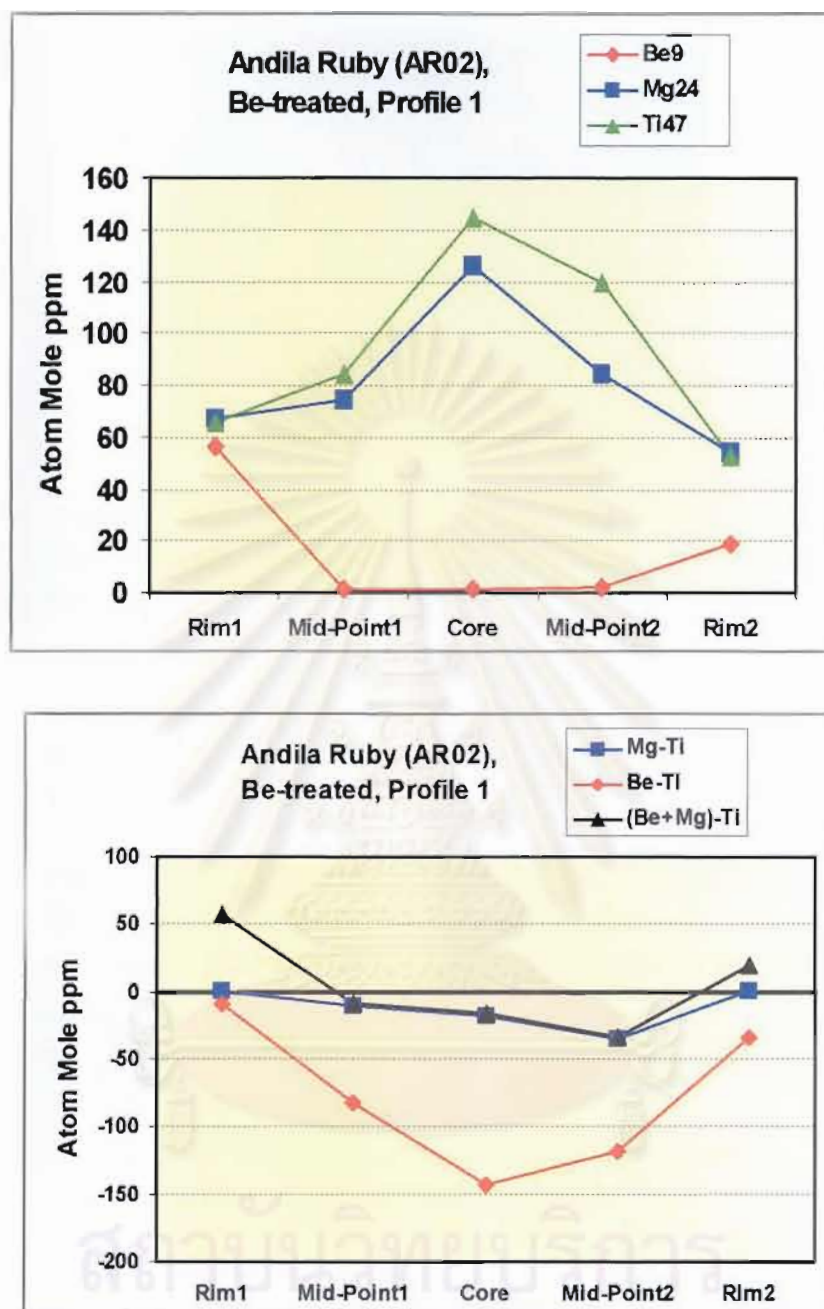


Figure 4.19: Plot of trace element content variation across the cut surface of the Be-treated Andila Ruby (AR02, Figure 4.15) showing Ti > or \sim Mg contents in all points analyzed. The Be contents are obviously high at the orange rims and are negligible in the blue zone. Two points at both rims show Be+Mg > Ti whereas three points in the blue zone show Ti > Be+Mg.

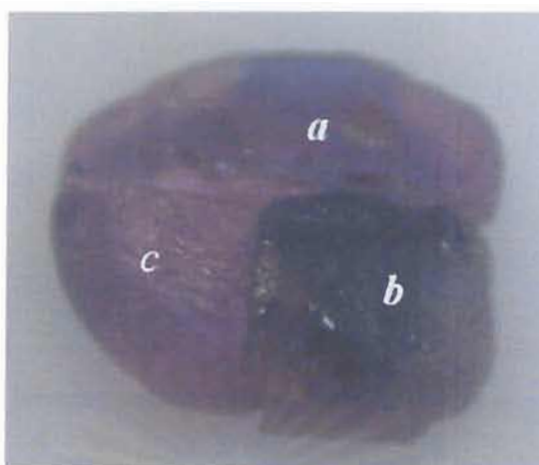


Figure 4.20: A rough Ilakaka violet sapphire (THMPS04) was cut into three pieces. One piece was kept as the reference (a, violet) while the second piece was heat-treated with ground chrysoberyl in a crucible (b, darker violet) and piece was heat-treated in another crucible without chrysoberyl (c, still violet). The heating condition for both crucibles was 1750°C for 30 hours in air. After the treatment the sample b and c were lightly polished and five-points on a traverse were analyzed on the polished surface of each piece using LA-ICP-MS. (Photo by Somboon, GIT)

Table 4.7: Trace element contents of the rough Ilakaka violet sapphire (THMPS04) obtained by LA-ICP-MS. CH's are points analyzed on the 'classically' heat-treated piece and BeH's are those on the Be-treated piece.

	CH1	CH2	CH3	CH4	CH5	BeH2	BeH3	BeH4	BeH5
Cations (ppm by weight)									
Be9	<1.55	<2.29	<1.97	<1.24	<1.44	<1.40	18.83	1.93	40.31
Na23	173.27	135.52	180.69	113.17	132.78	123.23	89.91	110.70	101.01
Mg24	50.45	39.98	43.92	54.93	55.49	56.66	53.29	67.10	72.01
Al27	529250.40	529250.40	529250.40	529250.40	529250.40	529250.40	529250.40	529250.40	529250.40
Ti47	145.87	121.17	103.02	179.40	195.89	212.19	186.05	307.59	298.51
V51	55.18	53.10	56.57	59.34	55.82	54.25	61.10	63.38	62.10
Cr53	619.63	514.90	554.29	643.96	629.64	568.56	625.45	615.46	493.23
Mn55	<0.13	<0.25	<0.27	0.22	0.25	<0.17	<0.14	<0.15	<0.16
Fe57	1213.47	1133.70	1253.00	1378.31	1322.62	1215.63	1354.69	1342.50	1345.67
Ga71	132.80	136.19	142.59	147.89	140.77	130.62	153.50	144.05	144.39
Total %	53.16	53.14	53.16	53.18	53.18	53.16	53.18	53.19	53.18
Cations (Atom Mole ppm)									
Be9	0.00	0.00	0.00	0.00	0.00	0.00	42.49	4.36	90.95
Na23	153.30	119.94	159.87	100.12	117.47	109.03	79.54	97.92	89.34
Mg24	42.22	33.47	36.76	45.96	46.43	47.42	44.59	56.14	60.25
Al27	398997.58	399119.68	399022.23	398957.04	398961.56	399028.48	398947.28	398914.15	398883.01
Ti47	61.88	51.47	43.75	76.17	83.17	90.11	78.99	130.59	126.72
V51	22.03	21.21	22.59	23.69	22.29	21.66	24.39	25.30	24.79
Cr53	242.39	201.48	216.84	251.88	246.28	222.43	244.64	240.71	192.89
Mn55	0.00	0.00	0.00	0.08	0.09	0.00	0.00	0.00	0.00
Fe57	441.93	413.01	456.36	501.92	481.64	442.75	493.30	488.82	489.94
Ga71	38.68	39.74	41.60	43.14	41.06	38.11	44.78	42.02	42.11
Total (Atom Mole%)	40.00	40.00	40.00	40.00	40.00	40.00	40.00	40.00	40.00
Mg-Ti	-19.64	-18.00	-6.99	-30.21	-36.74	-42.69	-34.40	-74.44	-66.48
Be-Ti	-61.86	-51.47	-43.75	-76.17	-83.17	-90.11	-36.50	-126.23	-35.77
(Be+Mg)-Ti	-19.64	-18.00	-6.99	-30.21	-36.74	-42.69	8.09	-70.09	24.48
(Be+Mg) %	7.73	6.72	6.85	7.37	7.60	8.17	13.21	8.90	19.69
Ti %	11.33	10.34	8.15	12.21	13.61	15.53	11.98	19.21	16.50
Fe %	80.94	82.94	85.00	80.43	78.80	76.30	74.81	71.90	63.81

< = below the detection limit of which 0.00 value is used for calculation of atom mole ppm

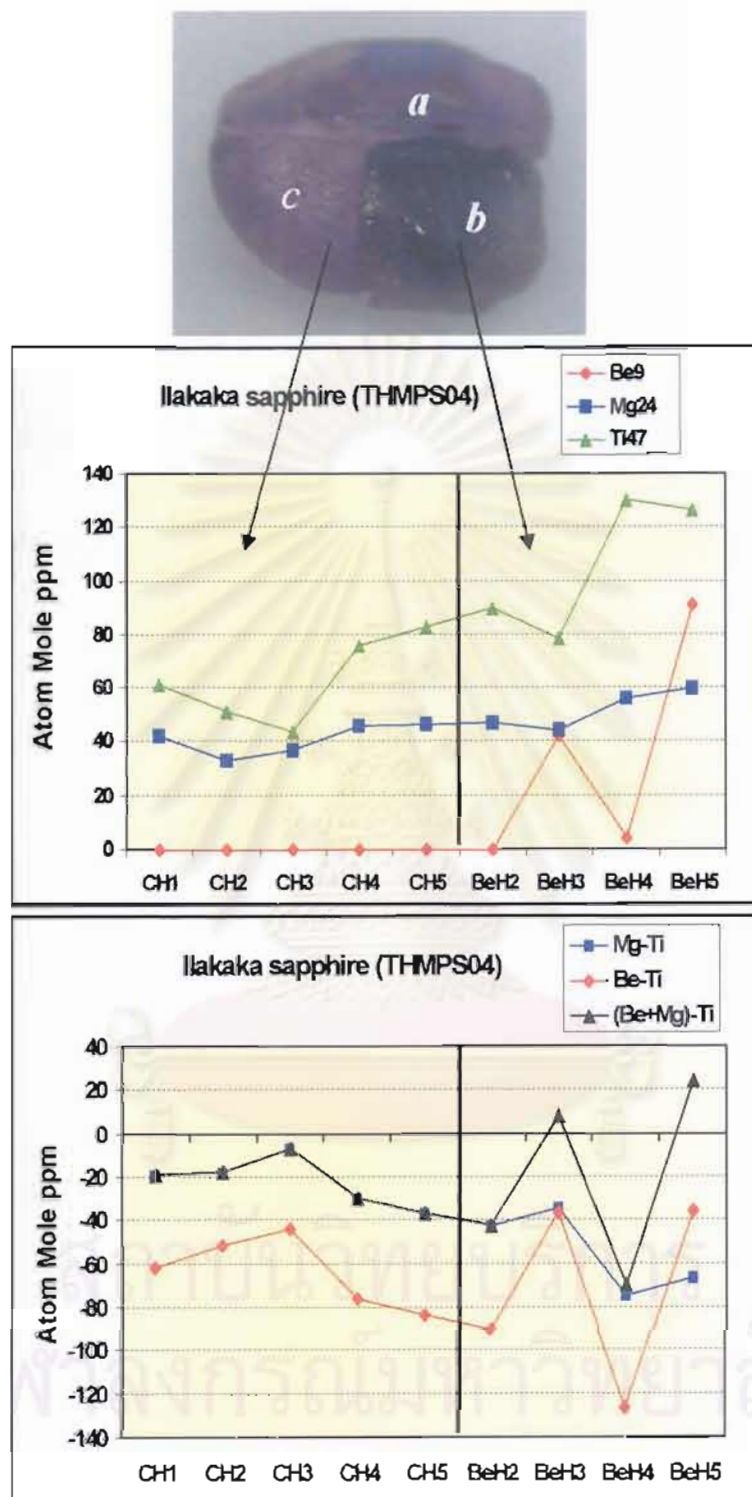


Figure 4.21: Plot of trace element content variation across lightly polished surfaces of the rough Ilakaka violet sapphire (THMPS04, Figure 4.20). The analyses on the 'classically' heat-treated piece (c) show no detectable Be and $Ti > Mg$ in all points analyzed. The analyses on the Be-treated piece (b) show a diffusion of Be into the corundum lattice but Ti contents are still in excess or slightly less than Be+Mg in all points analyzed.

*Fourth group of samples:
Be-treated rubies and pink
sapphires with
Ti ~ or <Mg*

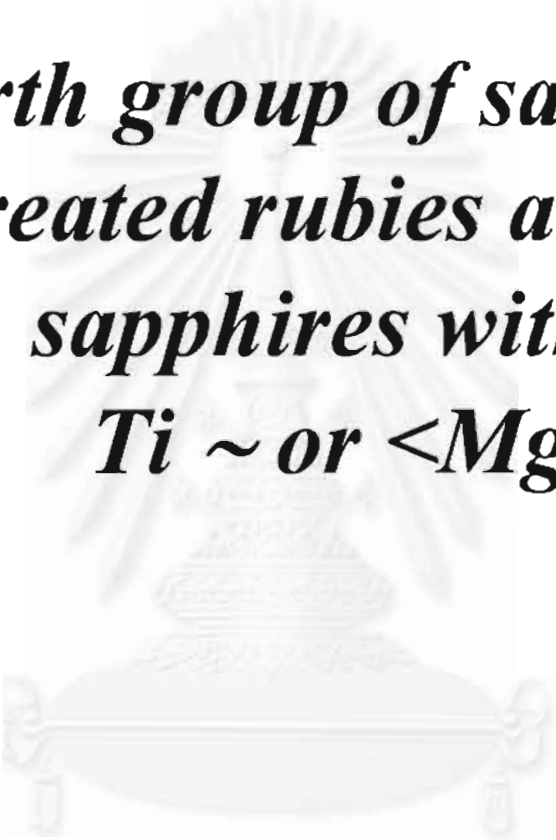




Figure 4.22: An orange Songea sapphire (SGDH09) reportedly underwent a Be-treatment was cut in half and a five-point profile was analyzed across the cut surface using LA-ICP-MS. (Photo by Lomthong, KU)

Table 4.8: Trace element content of the orange Songea sapphire (SGDH09) showing high Cr and Fe contents, obtained by LA-ICP-MS.

	Rim1	Mid-Point1	Core	Mid-Point2	Rim2
Cations (ppm by weight)					
Be9	17.83	<0.22	<0.22	<0.23	12.89
Na23	<10.54	<11.51	<12.32	<10.39	<9.04
Mg24	39.23	44.57	33.52	37.36	41.31
Al27	529250.31	529250.31	529250.31	529250.31	529250.31
Ti47	66.51	64.09	53.24	60.48	65.44
V51	20.22	19.19	19.53	20.03	19.27
Cr53	425.09	424.96	393.95	404.49	412.94
Mn55	<0.51	<0.55	<0.59	<0.50	<0.43
Fe57	2204.61	2218.11	2283.63	2234.70	2356.86
Ga71	76.34	77.72	74.42	75.66	85.88
Total %	53.21	53.21	53.21	53.21	53.23
Cations (Atom Mole ppm)					
Be9	40.23	<0.49	<0.49	<0.52	29.08
Na23	<9.32	<10.18	<10.89	<9.19	<7.99
Mg24	32.82	37.29	28.05	31.26	34.56
Al27	398889.94	398920.42	398922.64	398931.18	398848.19
Ti47	28.23	27.21	22.60	25.68	27.78
V51	8.07	7.66	7.80	8.00	7.69
Cr53	166.24	166.21	154.08	158.20	161.48
Mn55	<0.18	<0.20	<0.22	<0.18	<0.16
Fe57	802.68	807.66	831.52	813.72	858.02
Ga71	22.27	22.67	21.71	22.07	25.05
Total (Atom Mole%)	40.00	40.00	40.00	40.00	40.00
Mg-Ti	4.59	10.08	5.44	5.58	6.78
Be-Ti	12.00	-26.71	-22.11	-25.16	1.30
(Be+Mg)-Ti	44.82	10.58	5.94	6.10	35.86
(Be+Mg) %	8.08	4.33	3.23	3.65	6.70
Ti %	3.12	3.12	2.56	2.95	2.93
Fe%	88.80	92.55	94.21	93.40	90.37

< = below the detection limit of which the value is used for calculation of atom mole ppm

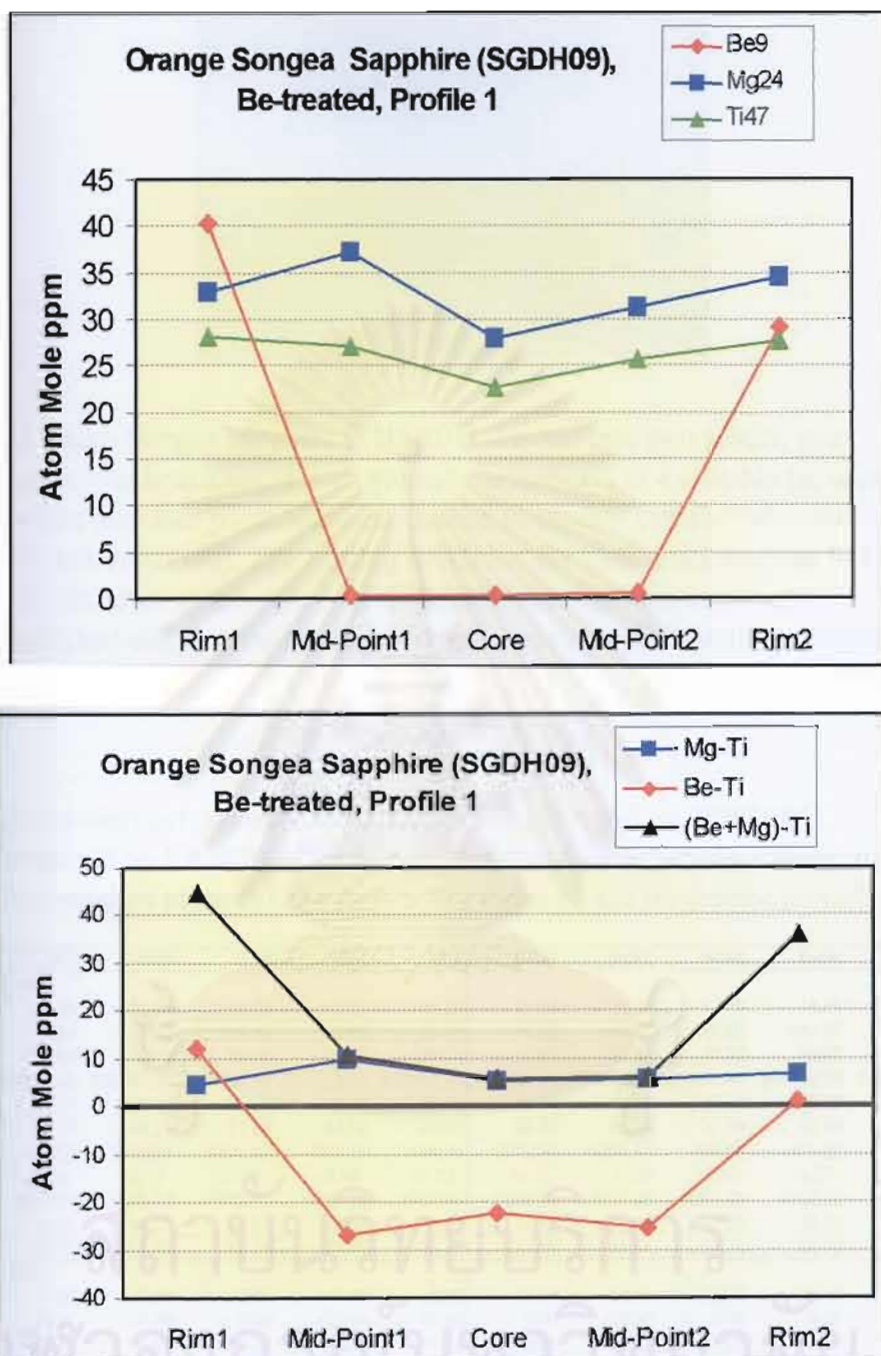


Figure 4.23: Plot of trace element content variation across the cut surface of the Be-treated orange Songea sapphire (SGDH09, Figure 4.22) showing slight $Mg > Ti$ contents in all analyzed points. The Be contents are obviously high at the rims and are negligible in the core. The Be+Mg contents therefore exceed Ti contents especially at the rims.

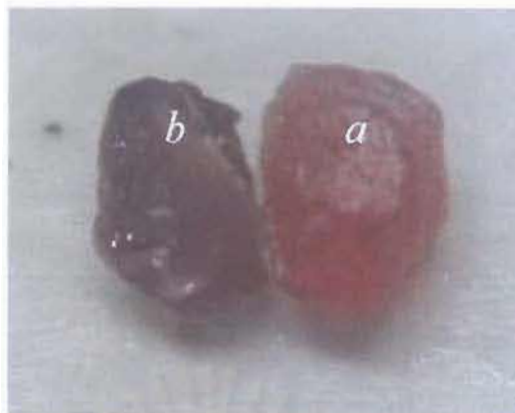


Figure 4.24: A rough Songea sapphire (THSR01) was cut into two pieces, one piece was heat-treated with ground chrysoberyl in a crucible (a, orange) while the other piece was heat-treated in another crucible without chrysoberyl (b, brownish red). The heating condition for both crucibles was 1750°C for 30 hours in air. After the treatment both samples were lightly polished and five-points on a traverse were analyzed on the polished surface of each piece using LA-ICP-MS. (Photo by Somboon, GIT)

Table 4.9: Trace element contents of the rough Songea sapphire (THSR01) obtained by LA-ICP-MS. CH's are points analyzed on the 'classically' heat-treated piece (b) and BeH's are those on the Be-treated piece (a).

	CH1	CH2	CH3	CH4	CH5	BeH1	BeH2	BeH3	BeH4	BeH5	BeH6
Cations (ppm by weight)											
Be9	<1.39	<1.53	<1.28	<1.29	<1.29	23.66	10.06	12.75	14.15	11.43	16.47
Na23	60.64	49.76	<38.49	56.86	47.56	<35.25	<65.38	<48.95	<54.65	<48.11	44.72
Mg24	24.04	22.56	26.09	22.27	25.38	17.85	17.44	25.32	19.40	21.70	27.84
Al27	529250.40	529250.40	529250.40	529250.40	529250.40	529250.40	529250.40	529250.40	529250.40	529250.40	529250.40
Ti47	45.41	58.23	56.24	43.55	48.14	40.72	40.76	46.52	41.89	39.89	51.70
V51	49.31	53.27	51.16	44.73	44.80	32.93	34.14	32.24	32.03	29.50	31.21
Cr53	1422.22	1672.98	1370.92	807.68	834.04	2272.90	1268.17	790.96	821.58	1265.97	2106.82
Mn55	<0.14	<0.15	<0.16	<0.16	<0.13	<0.15	0.28	<0.20	<0.22	<0.19	<0.08
Fe57	6557.04	7255.88	7040.93	6586.28	6751.93	7419.92	7392.25	6901.66	6762.32	6873.54	6729.75
Zn71	48.05	54.75	53.51	49.61	49.22	54.29	51.85	47.55	46.93	46.14	56.84
Total %	53.75	53.84	53.78	53.69	53.71	53.91	53.81	53.71	53.70	53.75	53.83
Cations (Atom Mole ppm)											
Be9	0.00	0.00	0.00	0.00	0.00	53.04	22.58	28.64	31.79	25.66	36.95
Na23	53.37	43.76	0.00	50.08	41.88	0.00	0.00	0.00	0.00	0.00	39.33
Mg24	20.01	18.77	21.72	18.55	21.14	14.84	14.51	21.09	16.16	18.07	23.16
Al27	396944.69	396598.74	396834.98	397178.54	397112.45	396318.88	396746.72	397094.53	397136.83	396931.34	396594.54
Ti47	19.18	24.58	23.75	18.41	20.35	17.18	17.21	19.66	17.70	16.85	21.82
V51	19.59	21.14	20.32	17.78	17.80	13.06	13.55	12.81	12.73	11.72	12.39
Cr53	553.49	650.51	533.38	314.51	324.72	883.15	493.29	307.94	319.88	492.66	819.19
Mn55	0.00	0.00	0.00	0.00	0.00	0.00	0.10	0.00	0.00	0.00	0.00
Fe57	2375.72	2626.63	2550.34	2387.72	2447.37	2684.12	2676.99	2501.53	2451.28	2490.31	2436.15
Zn71	13.95	15.88	15.53	14.41	14.29	15.73	15.04	13.81	13.63	13.39	16.48
Total (Atom Mole%)	40.00	40.00	40.00	40.00	40.00	40.00	40.00	40.00	40.00	40.00	40.00
Mg-Ti	0.83	-5.81	-2.04	0.14	0.79	-2.34	-2.70	1.43	-1.55	1.21	1.34
Be-Ti	-19.18	-24.68	-23.75	-18.41	-20.35	35.87	5.37	8.98	14.08	8.81	15.13
Be+Mg-Ti	0.83	-5.81	-2.04	0.14	0.79	50.70	19.88	30.07	30.24	26.88	38.29
Be+Mg) %	0.83	0.70	0.84	0.77	0.85	2.45	1.36	1.93	1.90	1.71	2.39
Ti %	0.79	0.92	0.92	0.76	0.82	0.62	0.63	0.76	0.70	0.66	0.87
Fe%	98.38	98.38	98.26	98.48	98.33	96.93	98.01	97.30	97.39	97.63	96.76

< = below the detection limit of which 0.00 value is used for calculation of atom mole ppm

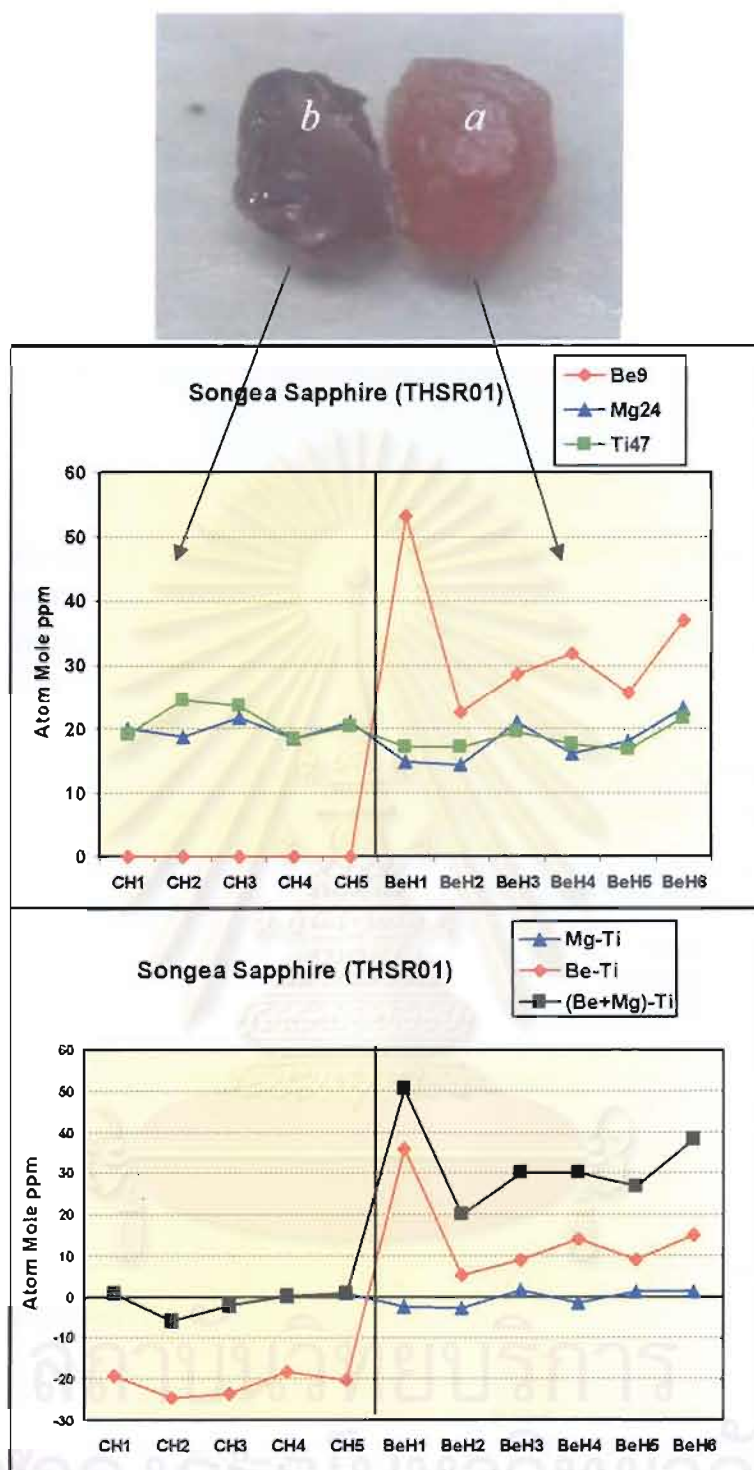


Figure 4.25: Plot of trace element content variation across lightly polished surfaces of the rough Songea sapphire (THSR01, Figure 4.24). The analyses on the 'classically' heat-treated piece (b) show no detectable Be and about equal proportion of Ti and Mg in all points analyzed. The analyses on the Be-treated piece (a) also show $Ti \sim Mg$ and significant amount of Be diffused into the corundum lattice by which $Be+Mg > Ti$ in all points analyzed.



Figure 4.26: An orangey pink Madagascan sapphire (WSMDIF7) reportedly underwent a Be-treatment was cut in half and a five-point profile was analyzed across the cut surface using LA-ICP-MS. (Photo by Lomthong, KU)

Table 4.10: Trace element content of the orangey pink Madagascan sapphire (WSMDIF7) showing high Cr and Fe contents, obtained by LA-ICP-MS.

	Rim1	Mid-Point1	Core	Mid-Point2	Rim2
Cations (ppm by weight)					
Be9	20.54	8.41	0.90	<0.23	15.60
Na23	<9.65	<9.10	<10.79	<10.62	<9.76
Mg24	64.50	75.97	75.64	68.66	69.14
Al27	529250.31	529250.31	529250.31	529250.31	529250.31
Ti47	97.90	93.72	98.80	95.78	94.69
V51	35.54	42.71	41.96	38.94	41.41
Cr53	421.29	526.82	540.55	478.91	477.82
Mn55	<0.47	<0.44	<0.53	<0.52	<0.48
Fe57	1549.04	1972.74	2119.26	1751.86	1962.37
Ga71	83.00	108.23	117.36	102.37	107.12
Total %	53.15	53.21	53.23	53.18	53.20
Cations (Atom Mole ppm)					
Be9	46.37	18.98	2.03	<0.52	35.20
Na23	<8.54	<8.05	<9.54	<9.39	<8.63
Mg24	53.99	63.56	63.28	57.46	57.85
Al27	399081.83	398896.55	398849.14	399020.94	398908.77
Ti47	41.58	39.79	41.94	40.67	40.20
V51	14.19	17.05	16.75	15.55	16.53
Cr53	164.84	206.03	211.38	187.35	186.87
Mn55	<0.17	<0.16	<0.20	<0.19	<0.18
Fe57	564.26	718.27	771.53	638.05	714.52
Ga71	24.22	31.57	34.23	29.87	31.24
Total (Atom Mole%)	40.00	40.00	40.00	40.00	40.00
Mg-Ti	12.41	23.77	21.34	16.79	17.65
Be-Ti	4.79	-20.81	-39.91	-40.15	-5.00
(Be+Mg)-Ti	58.78	42.75	23.37	17.31	52.85
(Be+Mg) %	14.21	9.82	7.43	7.87	10.98
Ti %	5.89	4.73	4.77	5.52	4.74
Fe%	79.90	85.45	87.80	86.61	84.28

<= below the detection limit of which the value is used for calculation of atom mole ppm

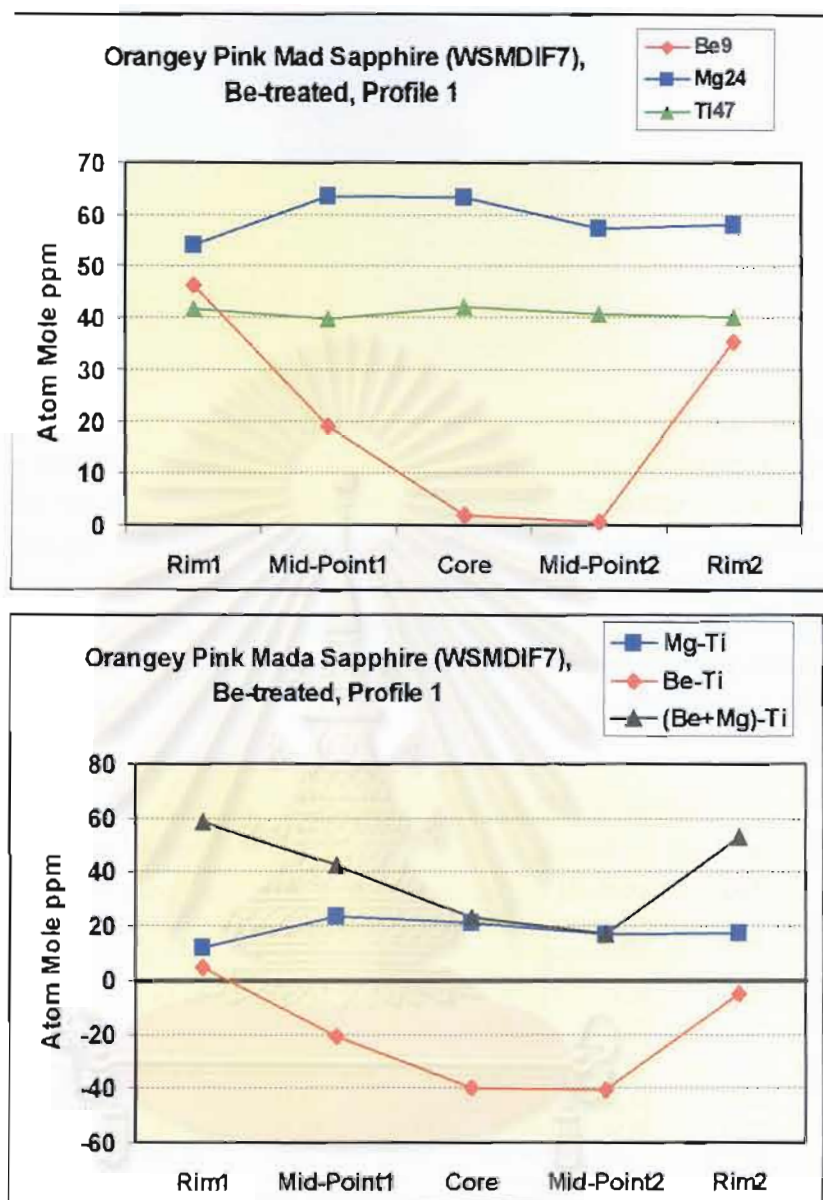


Figure 4.27: Plot of trace element content variation across the cut surface of the orangey pink Madagascan sapphire (WSMDIF7, Figure 4.26) showing Be diffusion into the corundum lattice from an external source and slight excess of Mg over Ti contents in all the analyzed points. The Be+Mg contents therefore exceed Ti content especially at the rims.

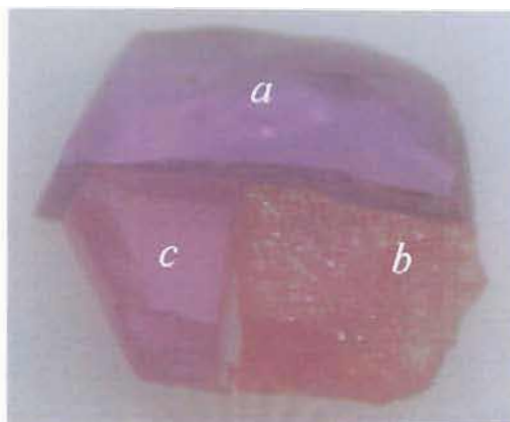


Figure 4.28: A rough Ilakaka (Madagascar) pink sapphire (THMPS05) was cut into three pieces. One piece was kept as the reference (a, violetish pink) while the second piece was heat-treated with ground chrysoberyl in a crucible (b, orange) and the third piece was heat-treated in another crucible without chrysoberyl (c, pink). The heating condition for both crucibles was 1750°C for 30 hours in air. After the treatment the sample b and c were lightly polished and five-points on a traverse were analyzed on the polished surface of each piece using LA-ICP-MS. (Photo by Somboon, GIT)

Table 4.11: Trace element contents of the rough Ilakaka pink sapphire (THMPS05) obtained by LA-ICP-MS. CH's are points analyzed on the 'classically' heat-treated piece and BeH's are those on the Be-treated piece.

	CH1	CH2	CH3	CH4	CH6	BeH2	BeH3	BeH4	BeH6
Cations (ppm by weight)									
Be9	<2.00	<1.23	<1.77	<2.18	<1.21	18.36	14.55	11.77	14.50
Na23	<51.24	<38.62	<50.55	<49.29	101.72	93.76	55.64	98.55	97.61
Mg24	64.62	76.25	69.01	81.77	74.22	76.19	72.46	76.91	72.80
Al27	529250.40	529250.40	529250.40	529250.40	529250.40	529250.40	529250.40	529250.40	529250.40
Ti47	115.00	122.08	123.59	130.46	127.42	123.62	121.80	117.25	119.81
V51	41.79	44.80	41.84	44.18	41.98	42.86	41.29	42.34	41.62
Cr53	524.59	554.65	523.98	546.24	521.98	525.01	517.14	518.34	508.49
Mn55	<0.20	<0.14	<0.19	0.19	0.16	<0.21	<0.21	<0.24	0.39
Fe57	977.92	1054.28	942.96	962.99	964.95	938.29	909.13	934.64	949.00
Ga71	91.15	91.37	84.61	86.78	82.67	88.13	83.35	84.83	81.25
Total %	53.11	53.12	53.10	53.11	53.12	53.12	53.11	53.11	53.11
Cations (Atom Mole ppm)									
Be9	0.00	0.00	0.00	0.00	0.00	41.46	32.86	26.58	32.74
Na23	0.00	0.00	0.00	0.00	90.04	82.99	49.26	87.23	86.40
Mg24	54.12	63.85	57.80	68.48	62.14	63.79	60.67	64.39	60.95
Al27	399291.93	399238.42	399299.46	399268.25	399196.83	399169.08	399230.93	399186.90	399183.74
Ti47	48.87	51.87	52.52	55.44	54.13	52.52	51.75	49.81	50.90
V51	16.70	17.90	16.72	17.65	16.77	17.12	16.50	16.91	16.63
Cr53	205.36	217.10	205.13	213.83	204.29	205.46	202.42	202.86	199.01
Mn55	0.00	0.00	0.00	0.07	0.06	0.00	0.00	0.00	0.14
Fe57	356.41	384.19	343.68	350.95	351.60	341.86	331.29	340.55	345.78
Ga71	26.61	26.67	24.70	25.33	24.13	25.72	24.33	24.76	23.71
Total (Atom Mole %)	40.00	40.00	40.00	40.00	40.00	40.00	40.00	40.00	40.00
Mg-Ti	6.26	11.98	6.28	13.04	8.01	11.27	8.92	14.58	10.06
Be-Ti	-48.87	-61.87	-52.62	-56.44	-54.13	-11.06	-18.89	-23.23	-18.16
(Be+Mg)-Ti	6.26	11.98	6.28	13.04	8.01	62.73	41.78	41.16	42.79
(Be+Mg) %	11.78	12.77	12.73	14.42	13.28	21.06	19.63	18.90	19.11
Ti %	10.64	10.38	11.67	11.67	11.67	10.61	10.86	10.35	10.38
Fe %	77.68	76.86	76.70	73.91	76.15	68.42	69.61	70.76	70.61

< = below the detection limit of which 0.00 value is used for calculation of atom mole ppm

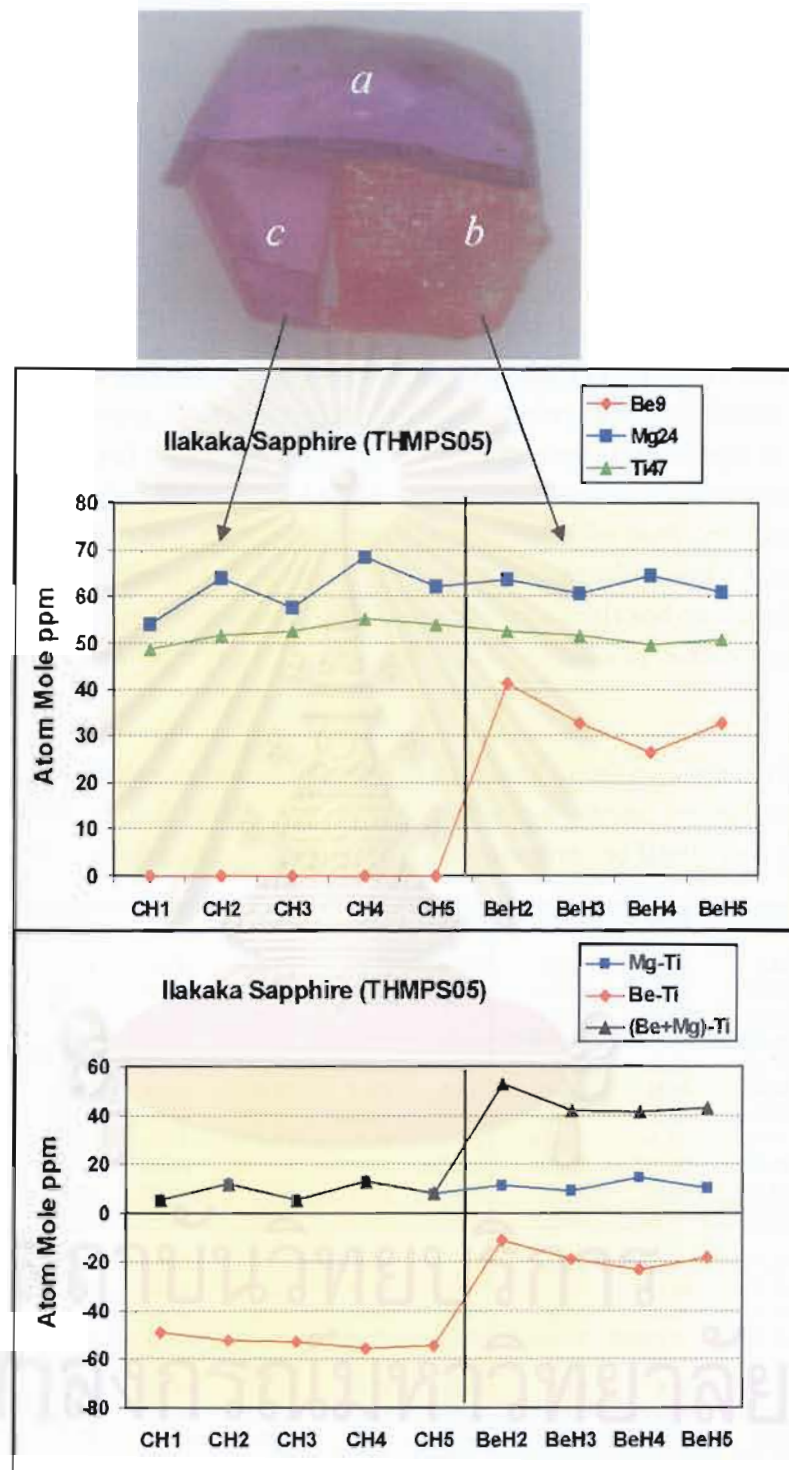


Figure 4.29: Plot of trace element content variation across lightly polished surfaces or the rough Ilakaka pink sapphire (THMPS05, Figure 4.28). The analyses on the 'classically' heat-treated piece (c) show no detectable Be and slight $Mg > Ti$ in all points analyzed. The analyses on the Be-treated piece (b) also show slight $Ti > Mg$ and significant amount of Be diffused into the corundum lattice by which $Be+Mg \gg Ti$ in all points analyzed.

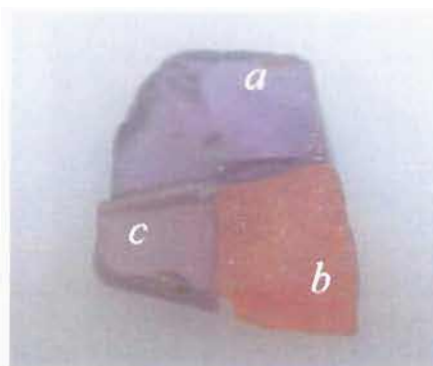


Figure 4.30: A rough Ilakaka (Madagascar) pink sapphire (THMPS01) was cut into three pieces. One piece was kept as the reference (a, violetish pink) while the second piece was heat-treated with ground chrysoberyl in a crucible (b, orange) and the third piece was heat-treated in another crucible without chrysoberyl (c, pink). The heating condition for both crucibles was 1750°C for 30 hours in air. After the treatment the sample b and c were lightly polished and five-points on a traverse were analyzed on the polished surface of each piece using LA-ICP-MS. (Photo by Somboon, GIT)

Table 4.12: Trace element contents of the rough Ilakaka pink sapphire (THMPS01) obtained by LA-ICP-MS. CH's are points analyzed on the 'classically' heat-treated piece (c) and BeH's are those on the Be-treated piece (b).

	CH1	CH2	CH3	CH4	CH5	BeH1	BeH2	BeH3	BeH4	BeH5
Cations (ppm by weight)										
Be9	1.59	<1.41	<1.50	<0.84	<1.02	11.67	8.76	9.66	9.41	13.10
Na23	93.59	134.80	124.18	110.03	71.98	<35.64	128.11	151.25	159.76	94.96
Mg24	60.22	71.28	60.29	65.21	67.37	43.01	36.59	33.63	28.53	32.02
Al27	529250.40	529250.40	529250.40	529250.40	529250.40	529250.40	529250.40	529250.40	529250.40	529250.40
Ti47	102.83	101.84	99.12	100.97	109.79	65.63	56.31	56.79	50.90	54.90
V51	32.45	38.01	35.62	34.55	34.73	23.76	23.25	24.38	24.51	24.47
Cr53	495.56	551.49	537.17	545.81	537.02	305.01	332.84	403.62	392.70	409.10
Mn55	<0.10	<0.15	0.21	0.12	<0.10	<0.13	<0.21	<0.17	<0.18	<0.11
Fe57	2850.94	3160.50	3037.18	2924.80	2932.17	996.75	774.05	748.41	714.16	707.40
Ga71	105.60	115.44	120.50	112.82	112.76	74.28	73.83	71.92	70.82	69.50
Total %	53.30	53.34	53.33	53.31	53.31	53.08	53.07	53.08	53.07	53.07
Cations (Atom Mole ppm)										
Be9	3.58	0.00	0.00	0.00	0.00	26.37	19.79	21.82	21.26	29.60
Na23	82.71	119.07	109.71	97.22	63.61	0.00	113.45	133.93	141.47	84.10
Mg24	50.34	59.56	50.38	54.50	56.31	36.03	30.65	28.17	23.90	26.82
Al27	398545.30	398364.83	398434.11	398481.72	398510.43	399395.72	399368.84	399330.39	399347.20	399388.00
Ti47	43.62	43.18	42.03	42.82	46.56	27.90	23.93	24.14	21.63	23.34
V51	12.94	15.15	14.20	13.78	13.85	9.50	9.29	9.74	9.80	9.78
Cr53	193.64	215.39	209.84	213.24	209.82	119.43	130.32	158.02	153.75	160.19
Mn55	0.00	0.00	0.08	0.04	0.00	0.00	0.00	0.00	0.00	0.00
Fe57	1037.11	1149.20	1104.55	1063.81	1066.56	363.37	282.16	272.79	260.32	257.88
Ga71	30.77	33.62	35.10	32.87	32.86	21.69	21.56	21.00	20.68	20.30
Total (Atom Mole%)	40.00	40.00	40.00	40.00	40.00	40.00	40.00	40.00	40.00	40.00
Mg-Ti	6.72	16.38	8.35	11.68	9.75	8.13	6.72	4.03	2.26	3.49
Be-Ti	-40.03	-43.18	-42.03	-42.82	-46.56	-1.53	-4.14	-2.31	-0.38	6.26
(Be+Mg)-Ti	10.31	16.38	8.35	11.68	9.75	34.60	26.51	25.85	23.52	33.08
(Be+Mg) %	4.75	4.76	4.21	4.69	4.82	13.75	14.15	14.41	13.80	16.71
Ti %	3.84	3.45	3.51	3.69	3.98	6.15	6.71	6.96	6.61	6.91
Fe%	91.40	91.79	92.28	91.62	91.20	80.10	79.14	78.63	79.58	76.38

< = below the detection limit of which 0.00 value is used for calculation of atom mole ppm

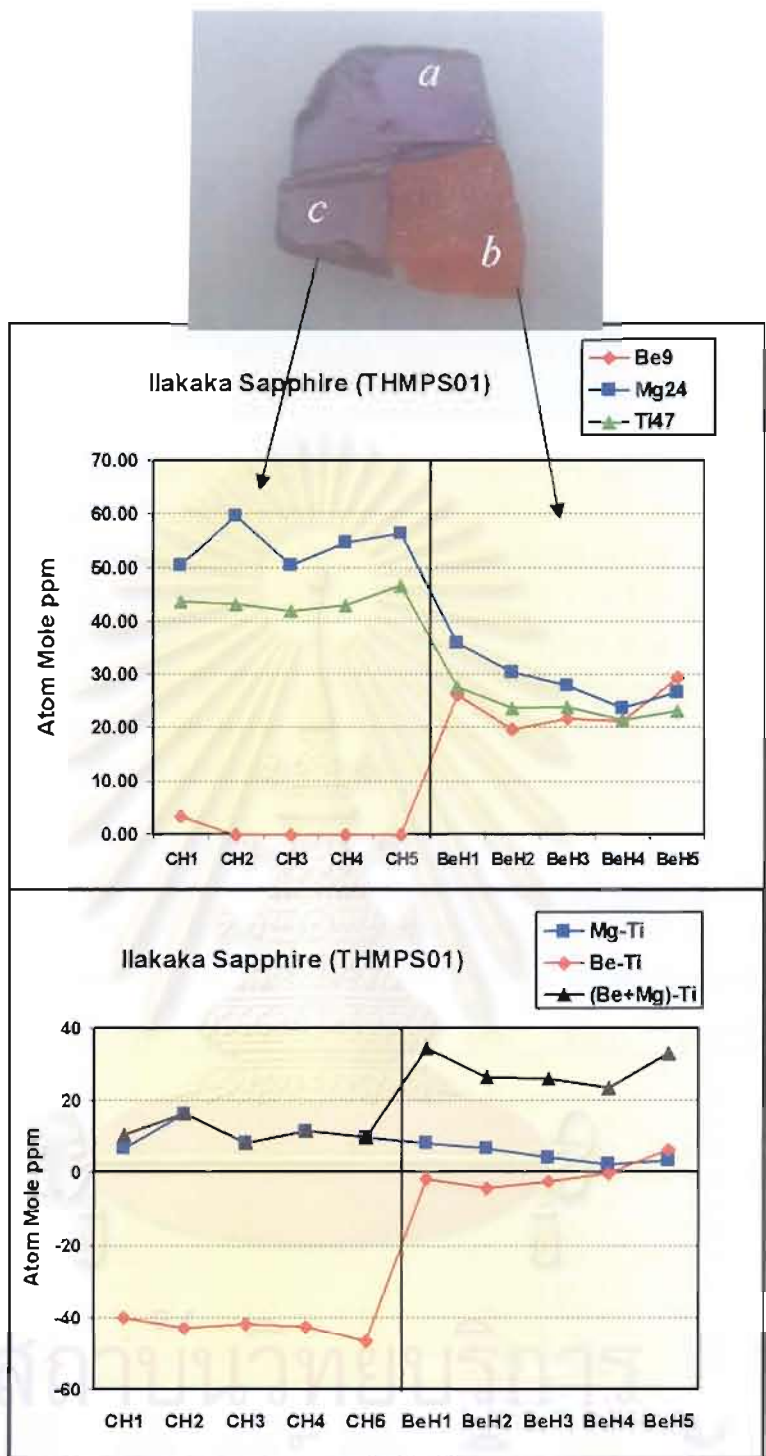


Figure 4.31: Plot of trace element content variation across lightly polished surfaces or the rough Ilakaka pink sapphire (THMPS01, Figure 4.30). The analyses on the ‘classically’ heat-treated piece (c) show no detectable Be and slight Mg > Ti in all points analyzed. The analyses on the Be-treated piece (b) also show slight Ti > Mg and significant amount of Be diffused into the corundum lattice by which Be+Mg >> Ti in all points analyzed.

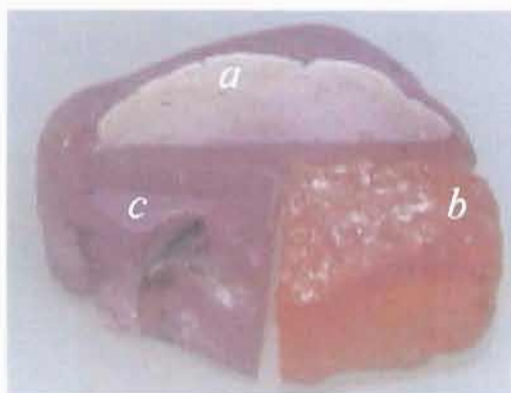


Figure 4.32: A rough Ilakaka (Madagascar) pink sapphire (THMPS02) was cut into three pieces. One piece was kept as the reference (a, pink) while the second piece was heat-treated with ground chrysoberyl in a crucible (b, orange) and the third piece was heat-treated in another crucible without chrysoberyl (c, pink). The heating condition for both crucibles was 1750°C for 30 hours. After the treatment the sample b and c were lightly polished and five-points on a traverse were analyzed on the polished surface of each piece using LA-ICP-MS. (Photo by Somboon, GIT)

Table 4.13: Trace element contents of the rough Ilakaka pink sapphire (THMPS02) obtained by LA-ICP-MS. CH's are points analyzed on the 'classically' heat-treated piece (c) and BeH's are those on the Be-treated piece (b).

	CH1	CH2	CH3	CH4	CH5	BeH1	BeH2	BeH3	BeH4
Cations (ppm by weight)									
Be9	<1.42	<1.56	<1.60	<1.62	<0.81	14.07	12.35	12.15	10.43
Na23	151.45	164.58	138.56	110.05	77.04	73.29	87.25	100.85	95.32
Mg24	32.04	30.01	40.11	45.70	51.18	51.36	48.93	43.79	29.80
Al27	529250.40	529250.40	529250.40	529250.40	529250.40	529250.40	529250.40	529250.40	529250.40
Ti47	54.12	47.79	53.66	76.68	75.74	78.30	85.01	70.75	52.00
V51	28.56	26.46	26.29	25.07	25.52	24.93	25.78	25.09	25.71
Cr53	371.39	364.25	332.84	321.06	338.48	350.39	313.17	316.68	336.87
Mn55	0.17	<0.19	<0.18	0.19	0.12	<0.12	<0.20	<0.18	<0.19
Fe57	456.45	436.52	422.53	433.44	458.99	449.94	441.78	406.91	415.75
Ga71	65.40	62.74	60.98	61.20	59.49	58.74	59.97	57.38	60.61
Total %	53.25	53.25	53.25	53.25	53.25	53.25	53.25	53.25	53.25
Cations (Atom Mole ppm)									
Be9	0.00	0.00	0.00	0.00	0.00	31.80	27.91	27.46	23.57
Na23	134.15	145.79	122.75	97.49	68.25	64.92	77.29	89.34	84.45
Mg24	26.85	25.14	33.61	38.29	42.89	43.04	41.00	36.69	24.97
Al27	399473.52	399478.02	399507.98	399519.82	399529.06	399498.52	399506.07	399517.20	399533.34
Ti47	23.01	20.32	22.82	32.60	32.20	33.29	36.14	30.08	22.11
V51	11.42	10.58	10.51	10.02	10.20	9.97	10.31	10.03	10.28
Cr53	145.46	142.66	130.37	125.76	132.58	137.24	122.66	124.04	131.96
Mn55	0.06	0.00	0.08	0.07	0.05	0.00	0.00	0.00	0.00
Fe57	166.43	159.17	154.08	158.06	167.38	164.07	161.10	148.39	151.62
Ga71	19.10	18.33	17.81	17.88	17.38	17.16	17.52	16.76	17.71
Total (Atom Mole%)	40.00	40.00	40.00	40.00	40.00	40.00	40.00	40.00	40.00
Mg-Ti	3.84	4.83	10.79	5.69	10.68	9.74	4.86	6.61	2.86
Be-Ti	-23.01	-20.32	-22.82	-32.60	-32.20	-1.48	-8.23	-2.62	1.46
(Be+Mg)-Ti	3.84	4.83	10.79	6.69	10.68	41.54	32.77	34.07	26.43
(Be+Mg) %	12.41	12.29	16.97	16.73	17.69	27.49	25.89	26.44	21.84
Ti %	10.64	9.93	10.84	14.24	13.28	12.23	13.58	12.40	9.96
Fe %	76.96	77.78	73.20	69.03	69.03	60.28	60.53	61.16	68.21

< = below the detection limit of which 0.00 value is used for calculation of atom mole ppm

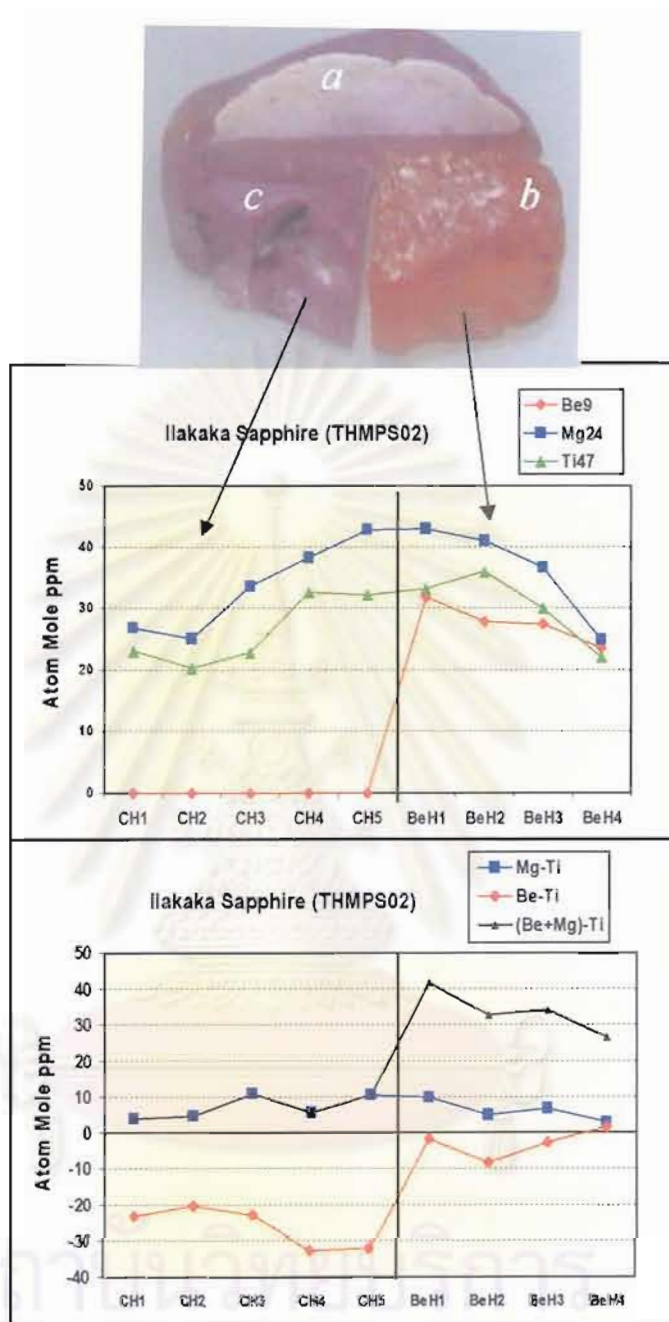
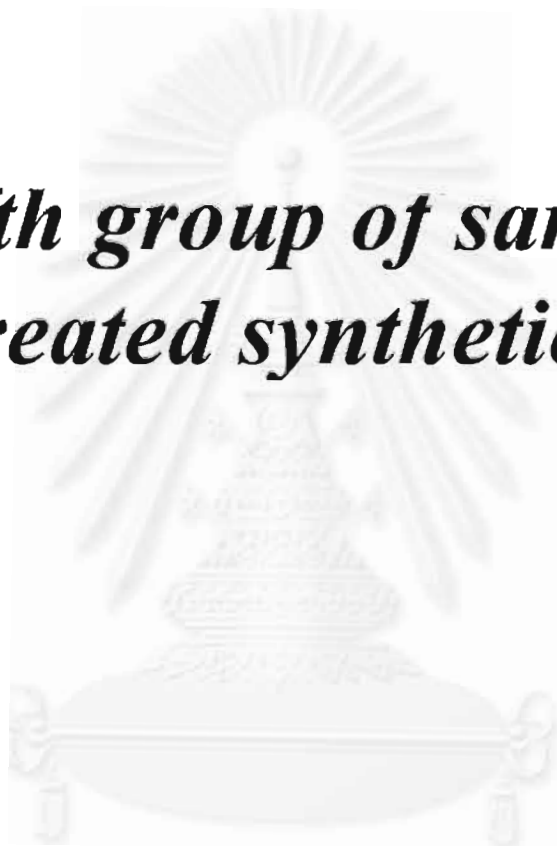


Figure 4.33: Plot of trace element content variation across lightly polished surfaces of the rough Ilakaka pink sapphire (THMPS02, Figure 4.32). The analyses on the 'classically' heat-treated piece (c) show no detectable Be and slight $Mg > Ti$ in all points analyzed. The analyses on the Be-treated piece (b) also show slight $Ti > Mg$ and significant amount of Be diffused into the corundum lattice by which $Be+Mg \gg Ti$ in all points analyzed.

***Fifth group of samples:
Be-treated synthetic Rubies***



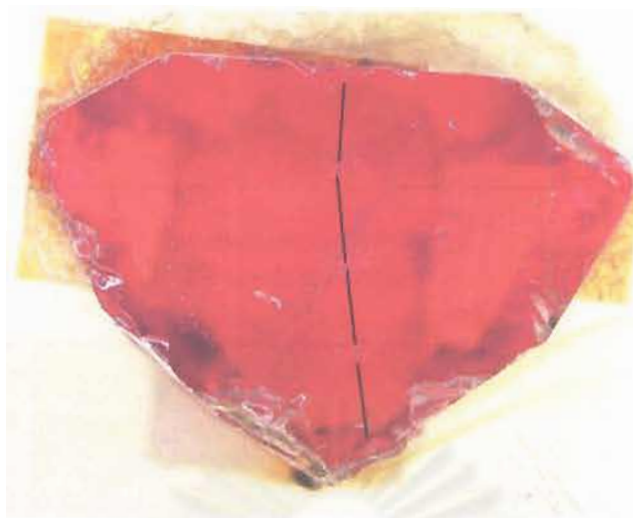


Figure 4.34: A synthetic ruby (PPSR1) reportedly treated with Be shows orangey red color. The stone was cut in half and a five-point profile was analyzed across the cut surface using LA-ICP-MS. (Photo by Lomthong, KU)

Table 4.14: Trace element contents of the Be-treated synthetic ruby (PPSR1) showing high content of Cr but low contents of other elements, obtained by LA-ICP-MS.

	Rim1	Mid-Point1	Core	Mid-Point2	Rim2
Cations (ppm by weight)					
Be9	5.48	2.98	0.18	<0.17	7.08
Na23	<10.97	<12.30	<10.51	<12.24	<8.81
Mg24	<0.65	<0.74	<0.63	<0.77	1.54
Al27	529250.31	529250.31	529250.31	529250.31	529250.31
Ti47	<0.81	<2.69	<0.84	0.83	4.37
V51	0.18	<0.12	<0.10	0.12	0.24
Cr53	2722.37	2685.94	3054.39	2752.87	3241.84
Mn55	<0.55	<0.61	<0.53	<0.60	<0.44
Fe57	<18.50	<21.32	<18.31	<21.40	<15.15
Ga71	0.18	0.13	0.16	0.12	0.17
Total %	53.20	53.20	53.23	53.20	53.25
Cations (Atom Mole ppm)					
Be9	12.37	6.72	0.41	<0.38	15.97
Na23	<9.70	<10.88	<9.29	<10.83	<7.79
Mg24	<0.54	<0.62	<0.53	<0.64	1.29
Al27	398905.28	398922.06	398788.27	398903.08	398700.07
Ti47	<0.34	<1.14	<0.36	0.35	1.85
V51	0.07	<0.05	<0.04	0.05	0.10
Cr53	1064.70	1050.50	1194.20	1076.62	1267.21
Mn55	<0.20	<0.23	<0.20	<0.22	<0.16
Fe57	<6.74	<7.76	<6.66	<7.79	<5.51
Ga71	0.05	0.04	0.05	0.03	0.05
Total (Atom Mole%)	40.00	40.00	40.00	40.00	40.00
Mg-Ti	0.20	-0.52	0.17	0.29	-0.57
Be-Ti	12.02	5.58	0.05	0.03	14.11
(Be+Mg)-Ti	12.57	6.20	0.58	0.68	15.40
(Be+Mg) %	64.58	45.20	11.73	11.21	70.08
Ti %	1.72	7.03	4.48	3.84	7.53
Fe%	33.70	47.78	83.79	84.95	22.39

< below the detection limit of which the value is used for calculation of atom mole ppm

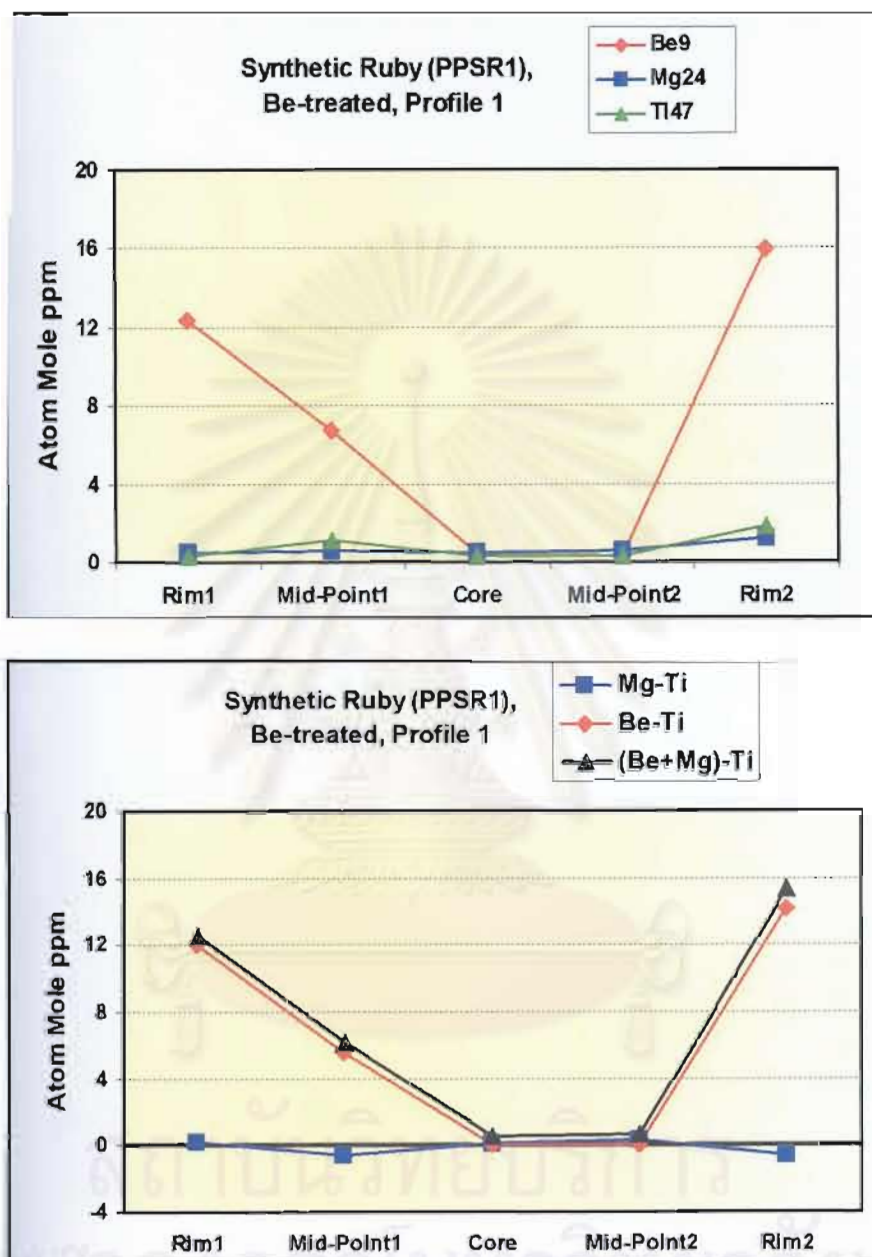


Figure 4.35: Plot of trace element content variation across the cut surface of the Be-treated synthetic ruby (PPSR1), Figure 4.34). The Be contents are obviously high at the rims and decrease toward the core indicating Be diffusion into the corundum lattice from an external source.

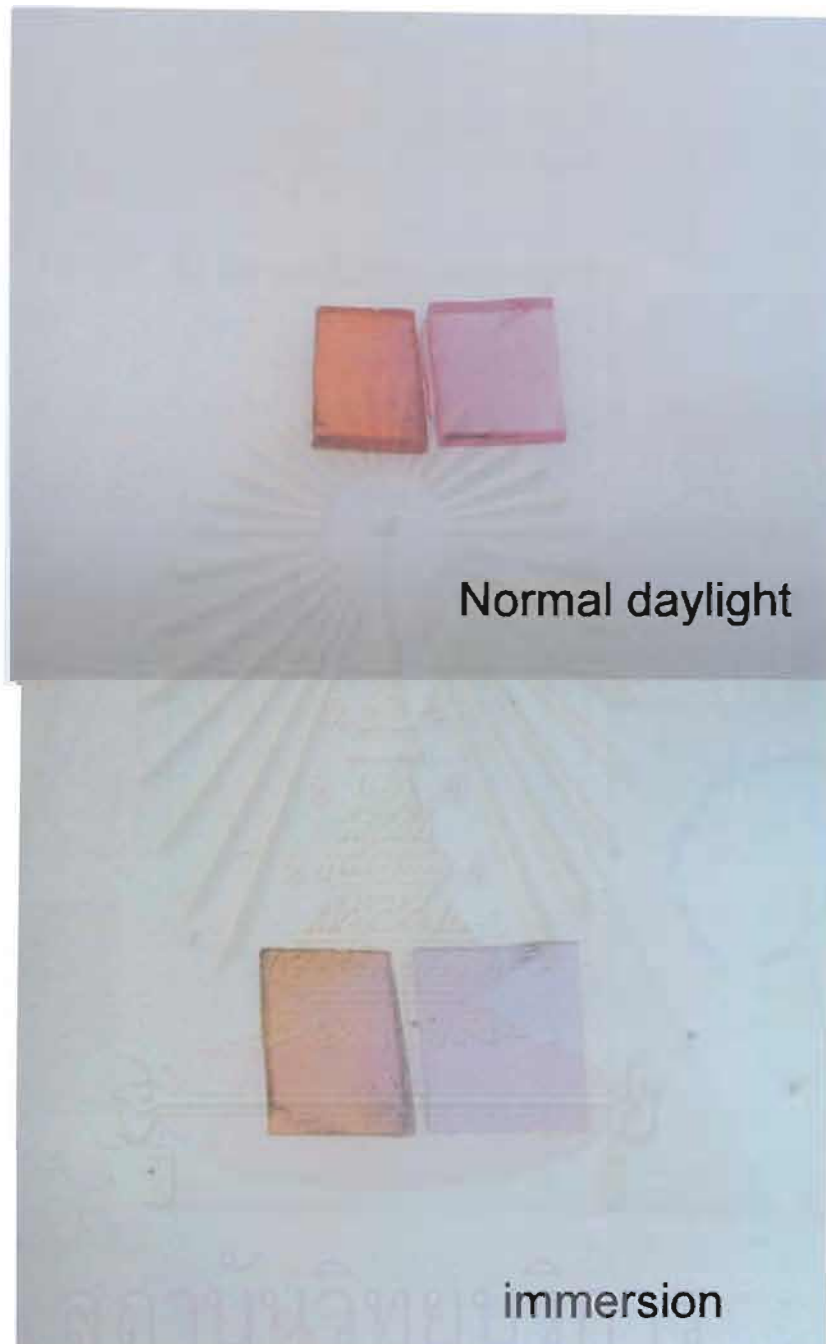


Figure 4.36: A synthetic ruby was cut in half; the left half was heat-treated with ground chrysoberyl in a crucible while the right half was heated in another crucible without chrysoberyl. The heating condition for both crucibles was 1750°C for 30 hours in air. After the treatment the left half shows surface-related orange rim while the right half is still red. (Photo by Somboon, GIT)

1850°C in an oxidizing atmosphere

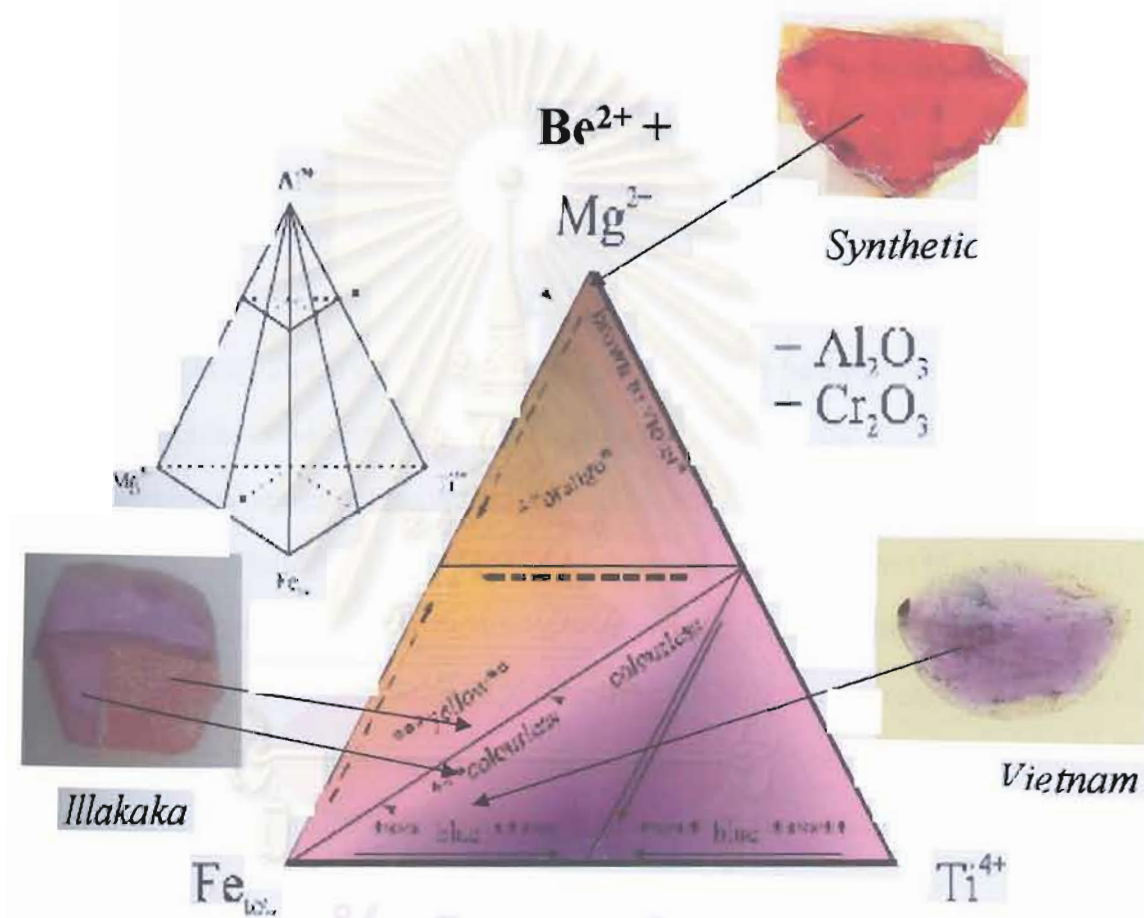


Figure 4.37: Approximate compositions of the stones plotted in the trian diagram model proposed by Häger (1996).

Chapter 5

Characteristics of Ilakaka Pink sapphires before and after Heat-Treatment Experiment

Introduction

Some selected samples of pink, purple and violet sapphires (16 samples) from Ilakaka-Sakaraha area were used for heat-treatment experiment. These stones represent sapphires from metamorphic origin. The samples were heated each time at 5 different maximum temperatures (800°C , 1000°C , 1200°C , 1400°C and 1600°C) for a period of one hour soaking time in an oxidizing atmosphere. These heating conditions were selected because in our earlier heating experiments, we found out that 1000°C for 3 hours soaking time was the heating condition that could cause some change in the internal characteristics and color, such as development of tension disc (discoïd), slight alteration of fingerprints and reduction of blue overcast color in pink sapphire. Hence in order to find out a lowest possible heating effect, 800°C heating condition was also selected for the minimum temperature used for this study. Previous heating experiments also revealed that three hours soaking time was sufficient to observe the difference in color transparency and internal characteristics. So in order to examine a shortest possible heating time, one hour soaking time was chosen for this study. In order to avoid contamination, for example iron stains or secondary silicate minerals which may have coated the sample surface or stuck within the cracks, the samples were soaked in hydrofluoric acid (HF) for one day and then washed thoroughly with water. The samples after cleaning were placed in an alumina crucible for heating in the determined conditions. The furnace and heating cycle used for heating experiment are outlined in the following paragraphs.

Furnace

The furnace used in this experiment was a Lindberg electric furnace Model 59256-E6 (Figure 5.1). This electric furnace could produce an oxidizing atmosphere at temperatures up to 1700°C . The furnace consists of a heating chamber and a control section. The heating chamber is heated using U-shaped molybdenum disilicides (MoSi_2) elements suspended from the roof freely along the side walls. The chamber is insulated with a special high temperature refractory fiber board. The samples were put in a small size (4 centimeters in diameter) alumina crucible which was placed in heating chamber

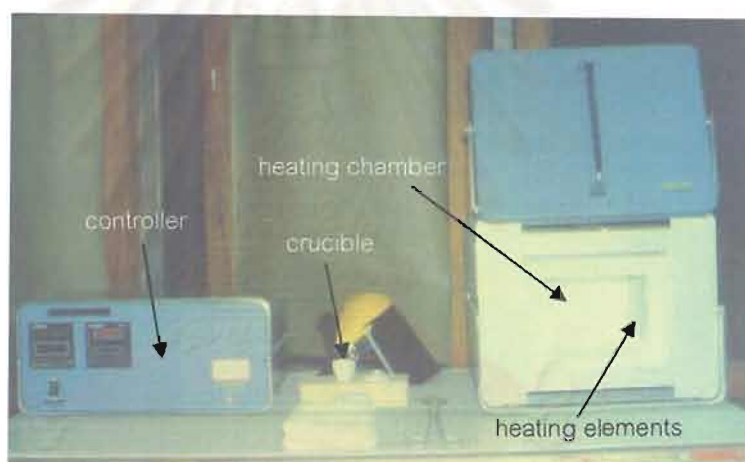


Figure 5.1 Lindberg electric furnace (Model 59256-E6) and accessory.

Heating Cycle

Every heating process is characterized by successive segments: heat-up, processing (soaking), and cool-down. The temperature in an electric furnace was controlled in all segments of the heating process, using the temperature controller. The heat-up is a heating segment from 75°C (beginning controllable temperature) to the maximum temperature. The rate of temperature increase was controlled at about $4^{\circ}\text{C}/\text{minute}$ for all heating conditions.

The processing or soaking segment means the period which the maximum temperature is sustained. In each condition, the soaking time was one hour. The cool-down segment is initiated from the temperature starting to decrease from the processing segment until it eventually reaches a determined temperature, normally at about 600°C before taking sapphires out the furnace. The cool-down rate depends on the conductivity of the furnace. In this study, the cool-down rate was selected at 15°C/minute.

The effect of heat treatment on the internal characteristics

The result of this study revealed that when the sapphires were heated at 800°C for one hour, most of the internal features were still unchanged. However, a few characteristics can be observed at this temperature. When the same sapphires were reheated at 1000°C, 1200°C, 1400°C and 1600°C for a period of one hour soaking time, many internal characteristics were obviously changed. The changes of the internal characteristics can be described as follows:

1. Zircon inclusions usually occur both as clear individual crystal and crystal clusters. Some single crystals and crystal clusters show minor tension cracks or discoids even before heating. After step-heating from 800°C to 1600°C, many zircon crystals were still unchanged (Figures 5.2 to 5.7). Generally, the single crystal has a tendency to change at higher temperature than those of the zircon clusters. Some crystals showed slight development of tension cracks after heated at 1000°C. At higher temperatures some crystals were altered and became turbid due to thermal decomposition and the tension cracks were expanded due to the different degree of thermal expansion of the zircon and the host sapphire (Figures 5.8 to 5.11). Some crystals became turbid without tension crack when heated at 1600°C (Figures 5.12 to 5.15). In the zircon clusters with minor tension cracks before heating, these tension

cracks were obviously expanded after heated at higher temperatures. Some crystals in the cluster were decomposed when re-heated at 1200°C (Figures 5.16 to 5.20).

Rnkin and Edwards (2003) reported the mottled (turbid) appearance and darkening of zircon inclusion in heat-treated corundum from Chimwadzulu Hill, Malawi. They believed that such feature was due to melting and interaction of zircon with host corundum at high temperatures. They have documented that an originally clear zircon at high temperatures was partially or completely replaced by an intergrowth of monoclinic m-ZrO₂ (baddeleyite) and a glass-like phase which was interpreted as quench melt texture in the Al₂O₃-ZrO₂-SiO₂ system. Such system was inferred to have occurred above the eutectic temperature of approximately 1750°C. However, we have observed the alteration of some zircon inclusions at much lower temperature in this study. It is possible that such alteration may occur in an intermediate or low (metamict) zircon grain which was more susceptible to a thermal breakdown than a high zircon. This could explain why many zircon grains were still unchanged while the others became turbid when heated at 1600°C. It should also be noted that the recognition of the phase change (turbid appearance) in a zircon inclusion can provide a useful criterion for detecting heat-treatment of a host sapphire as most zircon crystals are usually clear in an unheated stone. The tension disc around a zircon inclusion is however not a good criterion of heat-treatment as it can also be observed in an unheated stone.

2. A monazite inclusion was slightly decomposed after a step-heating up to 1600°C (Figure 5.18). Another crystal, however, was still unchanged after the step-heating from 800°C to 1600°C (Figure 5.21).

3. Mica inclusions were partially altered or appeared slightly turbid with minor development of tension crack after the stones were heated at 1000°C. The decomposition and tension disc became distinct when re-heated at 1400°C and 1600°C (Figures 5.22 and 5.23).

4. Rutile inclusions occur as black to dark brown crystals and as thin and long needles, known as rutile silks or needles. The black to dark brown crystals were changed to red with minor development of tension crack after the stones were heated at 800°C. When re-heated at higher temperatures they became obviously red with pronounced development of tension cracks and also with melted crystal boundary (Figures 5.24 and 5.25).

Rutile silks or needles are long and short tubes which oriented in 3 directions approximately 60°/120° angles. The needles can fully dissolved in a host corundum, when heated at about its melting point (1825°C) and cooled rapidly (Themelis, 1992). Before the dissolution is complete, it passes through several transformation stage, starting at about 1600°C (lowest dissociation point of the rutile). In this study when the stones were heated at 800°C to 1400°C, the needles were still unchanged. After heated at 1600°C an incomplete or partial dissolution of the needles can be observed in the host corundum creating a dot-like pattern, known as resorbed rutile silks (Figures 5.26). However the needles in some sapphires were dissolved completely in the host sapphires at 1600°C (Figure 5.27).

5. Milky or dust zone became clearer when heated at 1600°C (Figure 5.28).

6. Fingerprints are healed fractures or cracks. In some samples, fingerprints were expanded at higher temperatures (Figures 5.29 and 5.30).

References

- Rankin, A.H., and Edwards, W., 2003. Some effects of extreme heat treatment on zircon inclusions in corundum. *Journal of Gemmology*, 28. 5: 257-264.
- Themelis, T., 1992. *The Heat Treatment of Ruby and Sapphire*: Gemlab Inc. 236p.

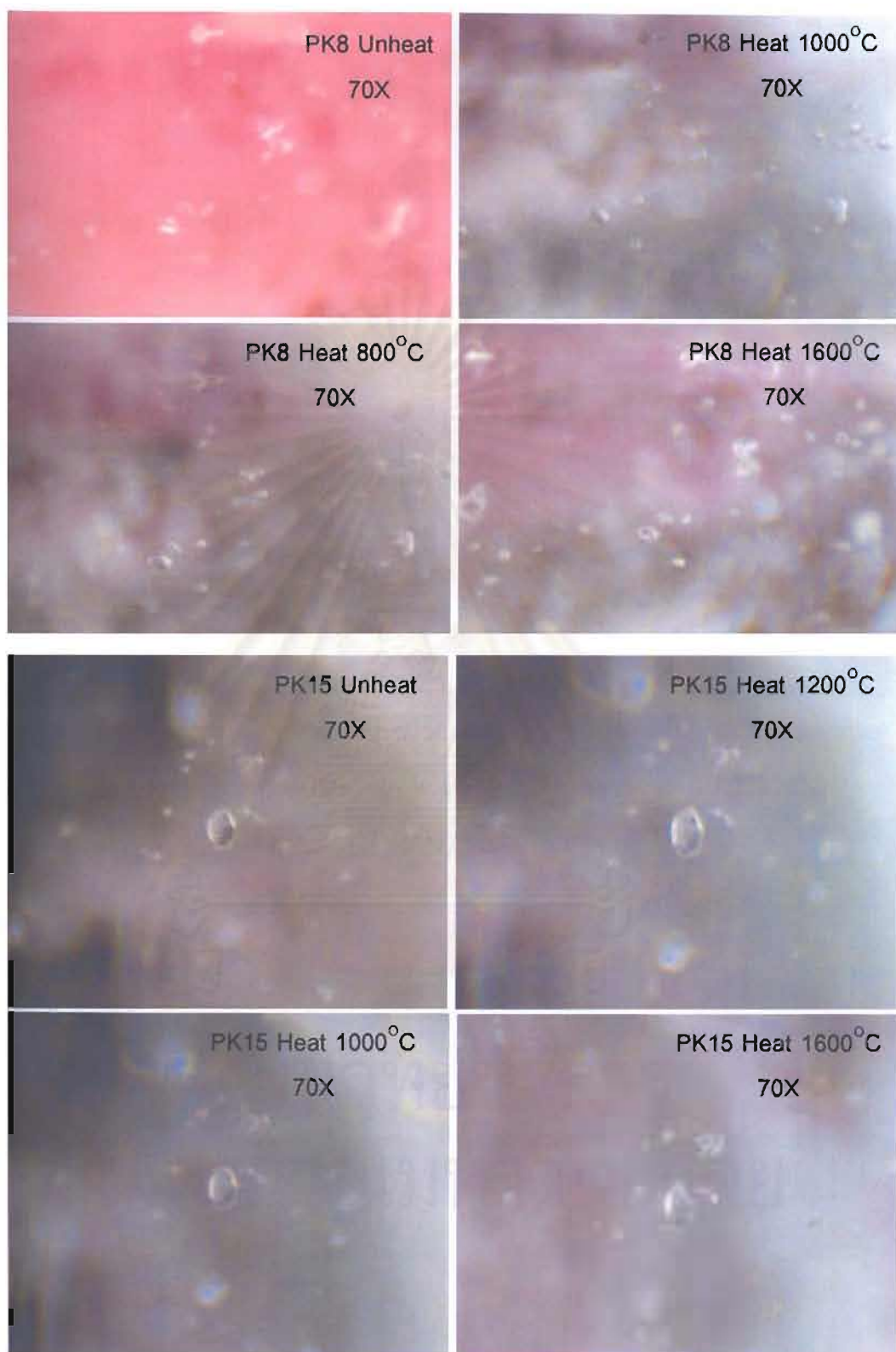


Figure 5.2: Most zircon inclusions in these two sapphire samples were clear and appear unchanged after a step-heating from 800°C to 1600°C.

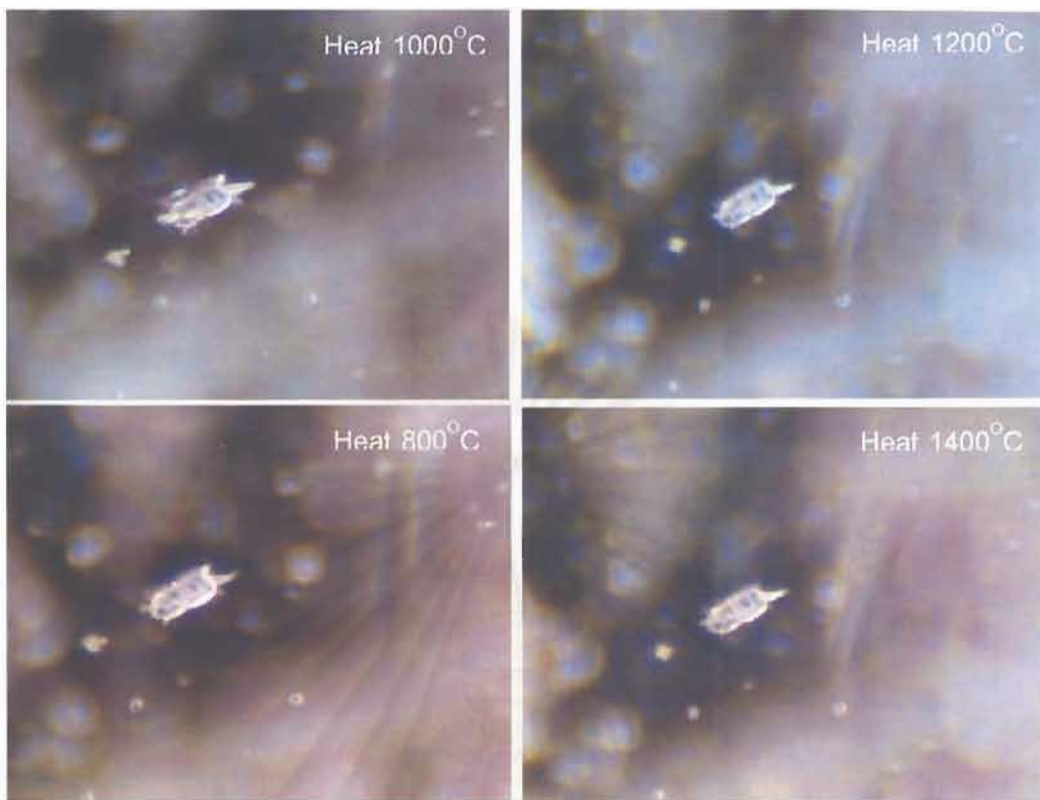


Figure 5.3: A zircon inclusion with minor tension crack was still unchanged after the step-heating from 800°C to 1600°C (sample no. PK15, 70X).

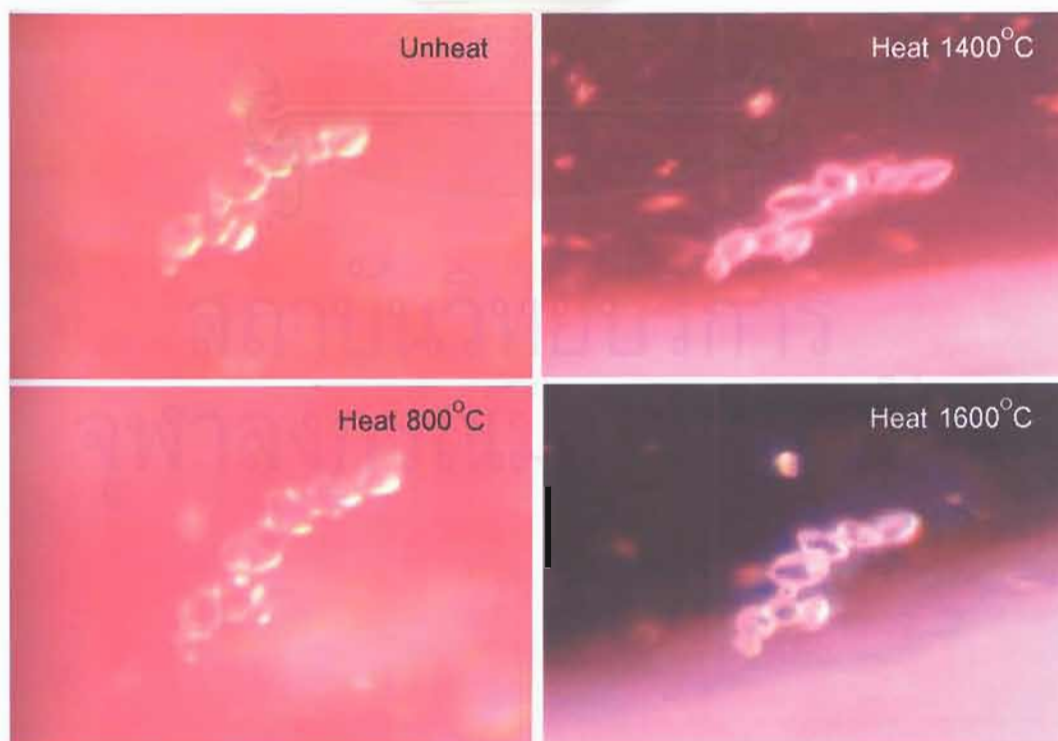


Figure 5.4: A cluster of zircon inclusions was still unchanged after the step-heating from 800°C to 1600°C (sample no. PP6, 140X).

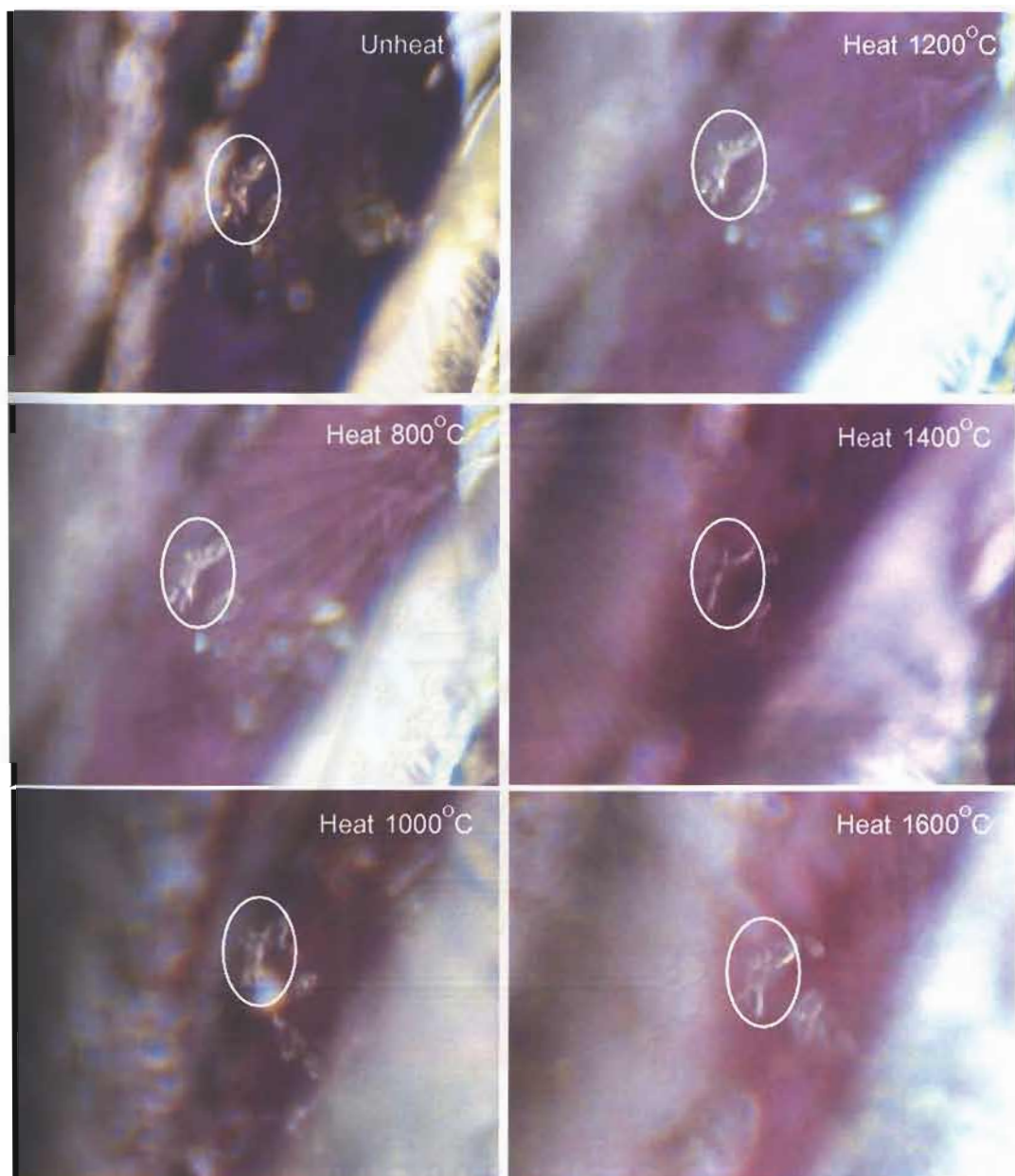


Figure 5.5: Another cluster of zircon inclusions with minor tension disc (in circle) was still unchanged after the step-heating from 800°C to 1600°C (sample no. PK3, 70X).

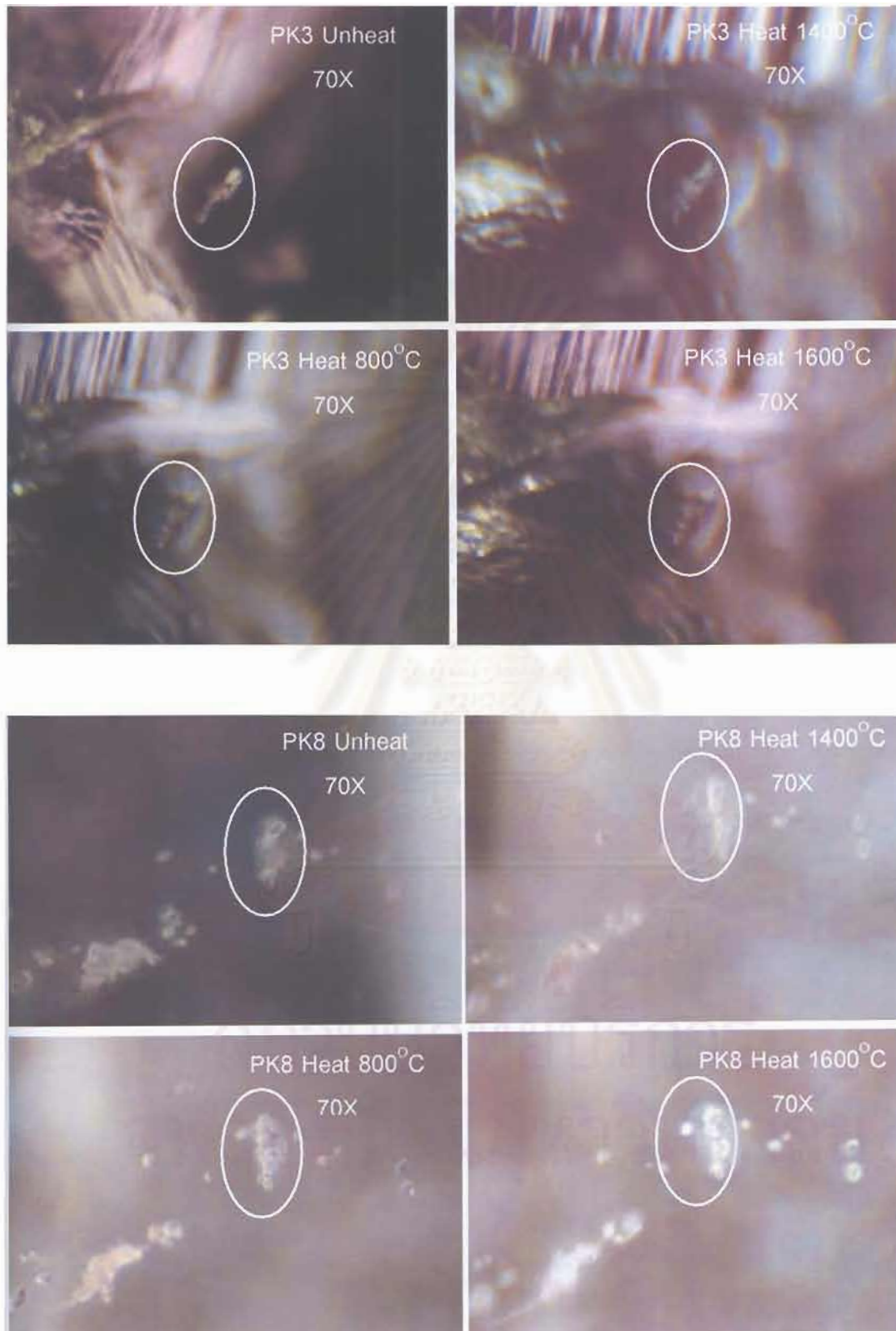


Figure 5.6: Many zircon clusters with tension cracks (in circle) were still unchanged after the step-heating from 800°C to 1600°C.

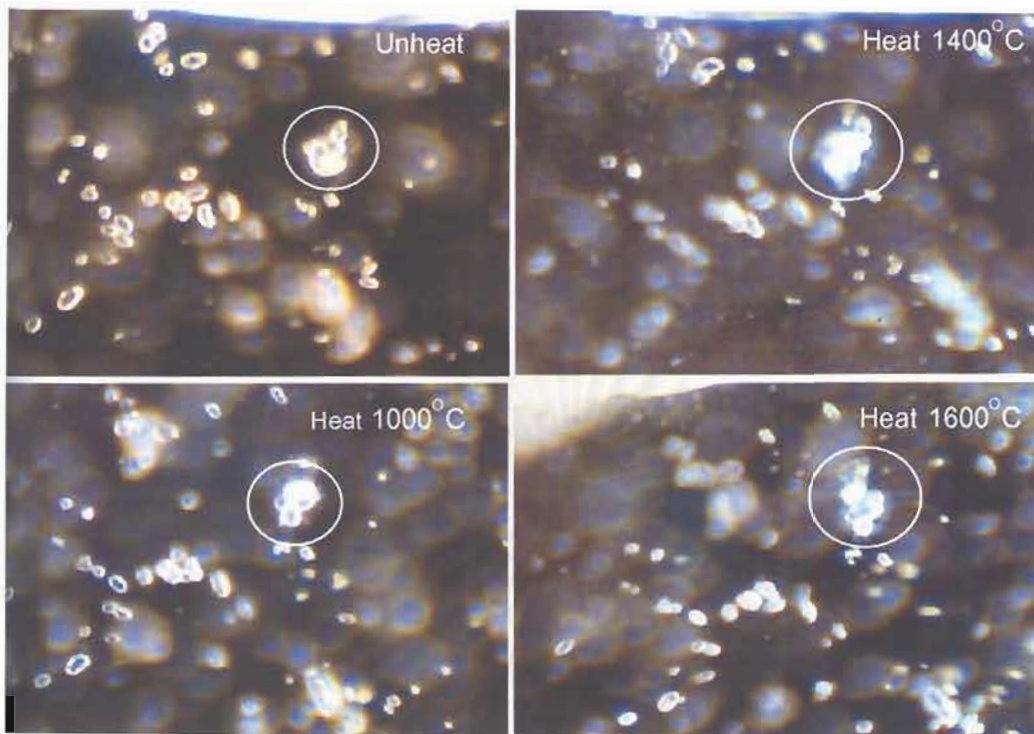


Figure 5.7: Most of individual zircon inclusions were still unchanged after the step-heating from 800°C-1600°C whereas the zircon cluster (in circle) showed minor tension crack at 1000°C. At 1400°C and 1600°C, this tension crack became more obvious (sample no. P6, 70X).

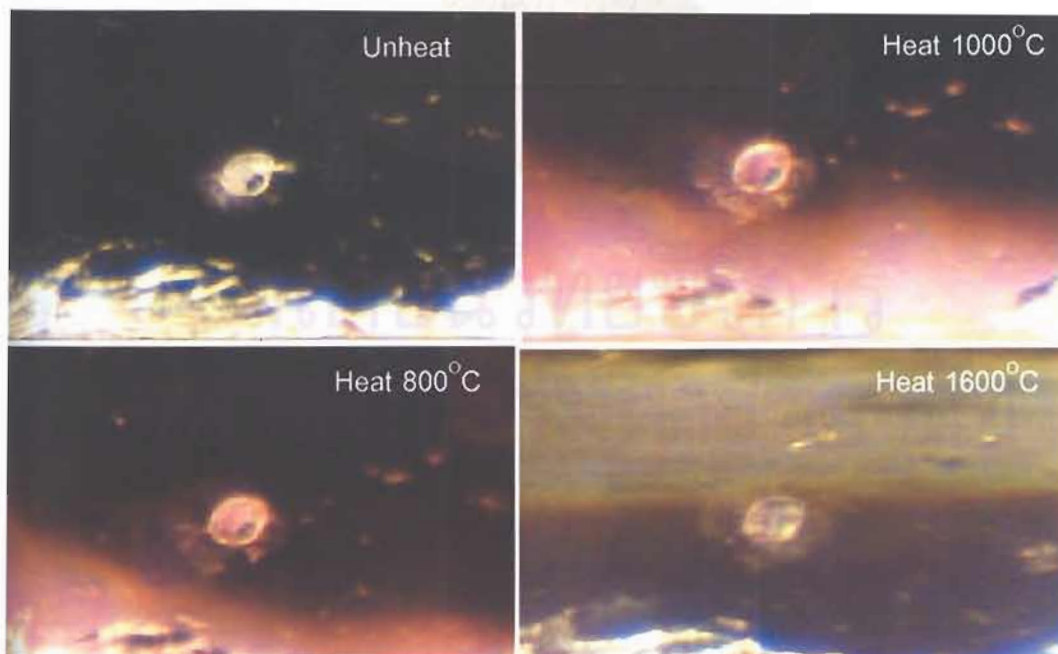


Figure 5.8: A zircon inclusion with slight tension crack was still unchanged at 800°C. At 1000°C-1600°C, this tension crack was obviously expanded (sample no. P5, 140X).

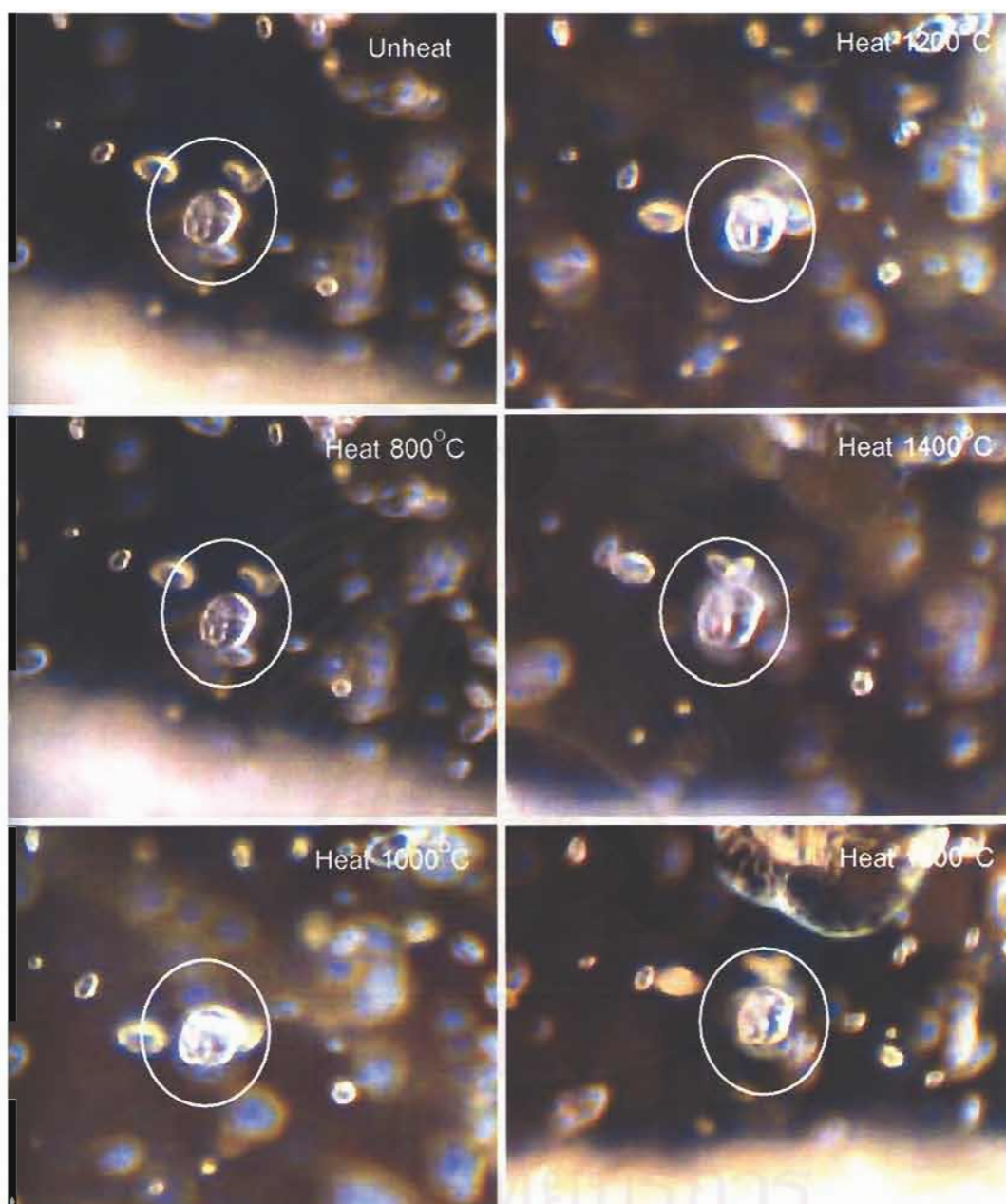


Figure 5.9: A relatively large and clear zircon inclusion (in circle) was still unchanged at 800°C . However, at 1000°C , the crystal began to alter into whitish, cloudy appearance (turbid) with minor tension crack. The tension crack became more obvious at 1400°C . The crystal was partially decomposed at 1600°C (sample no. P6, 70X).

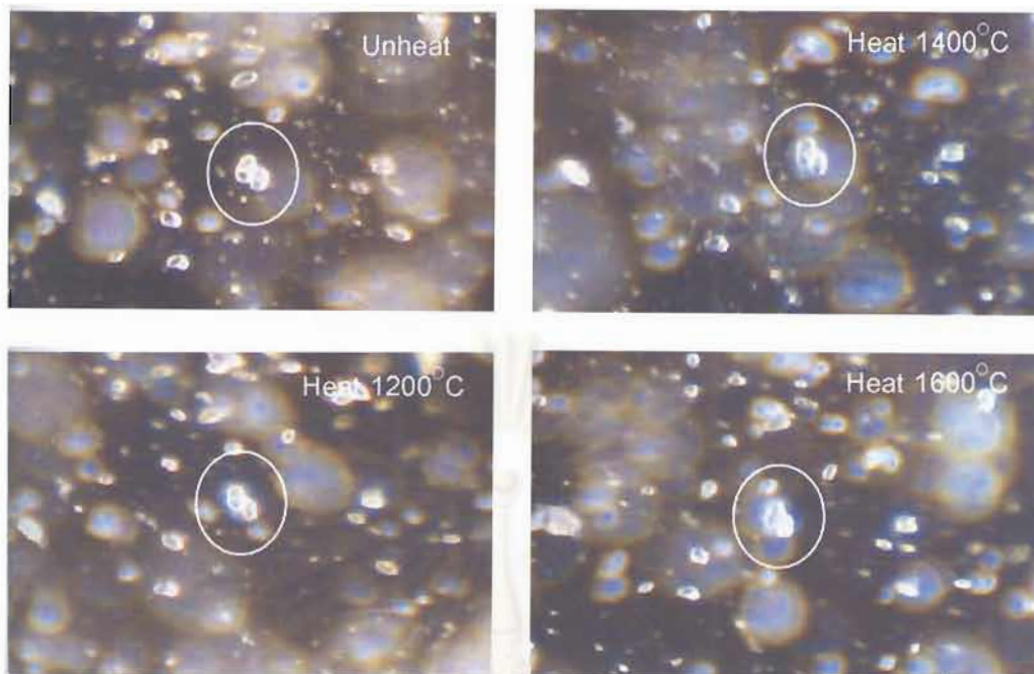


Figure 5.10: Zircon inclusions (in circle) showed tension crack at 1200°C . At 1600°C , they began to decompose into whitish, cloudy appearance (turbid) with obvious tension crack (sample no. P6, 70X).

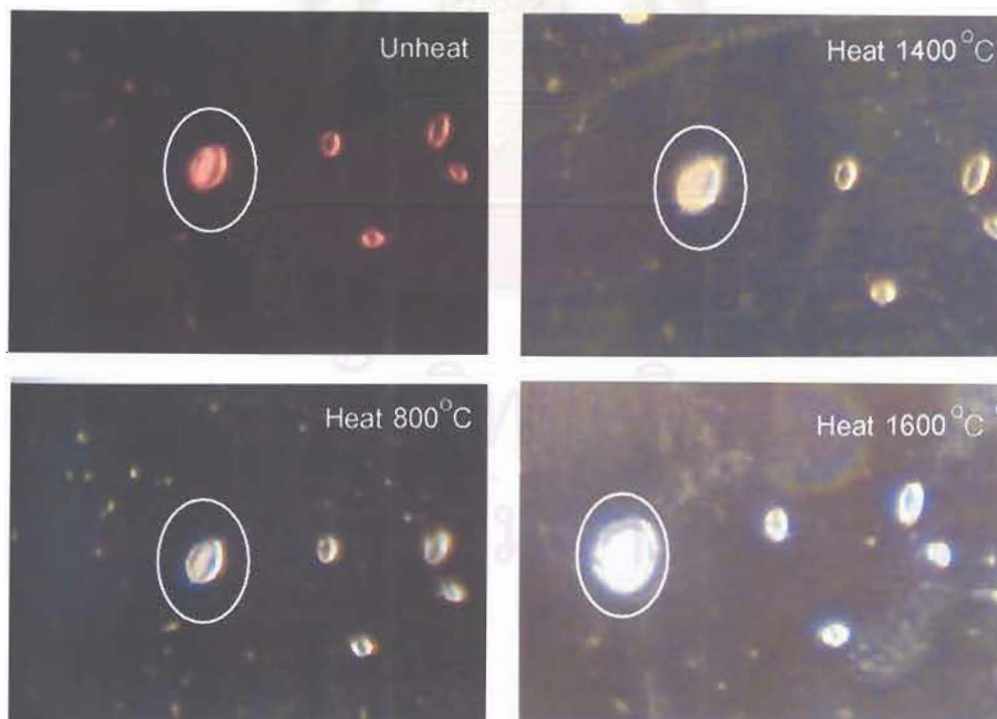


Figure 5.11: Most zircon inclusions were still unchanged after the step-heating from 800° to 1600°C except the crystal in circle began to alter with minor tension crack at 1400°C . At 1600°C , it was obviously altered into whitish, cloudy appearance (turbid) with well developed tension crack (sample no. LP9, 140X).

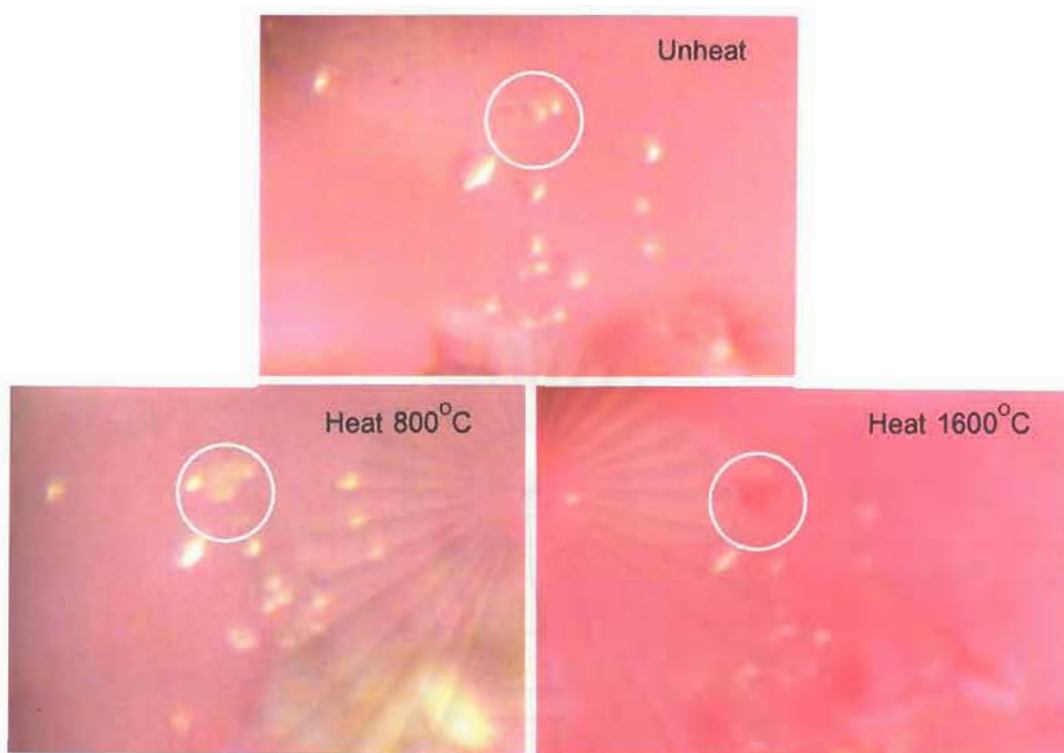


Figure 5.12: Most of the zircon inclusions were still unchanged after the step-heating from 800°C to 1600°C except some crystals in circle became turbid at 1600°C (sample no. PP6, 140X).

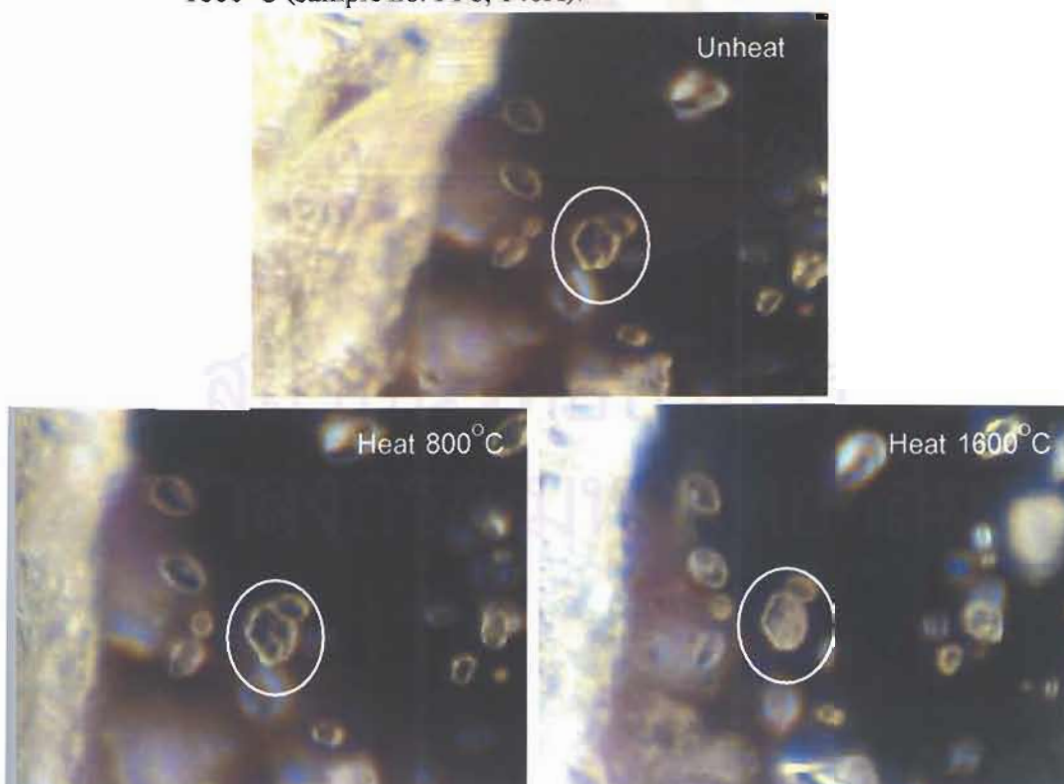


Figure 5.13: Most of the zircon inclusions were still unchanged after the step-heating from 800°C to 1600°C except some crystals in circle became turbid at 1600°C (sample no. LP3, 140X).

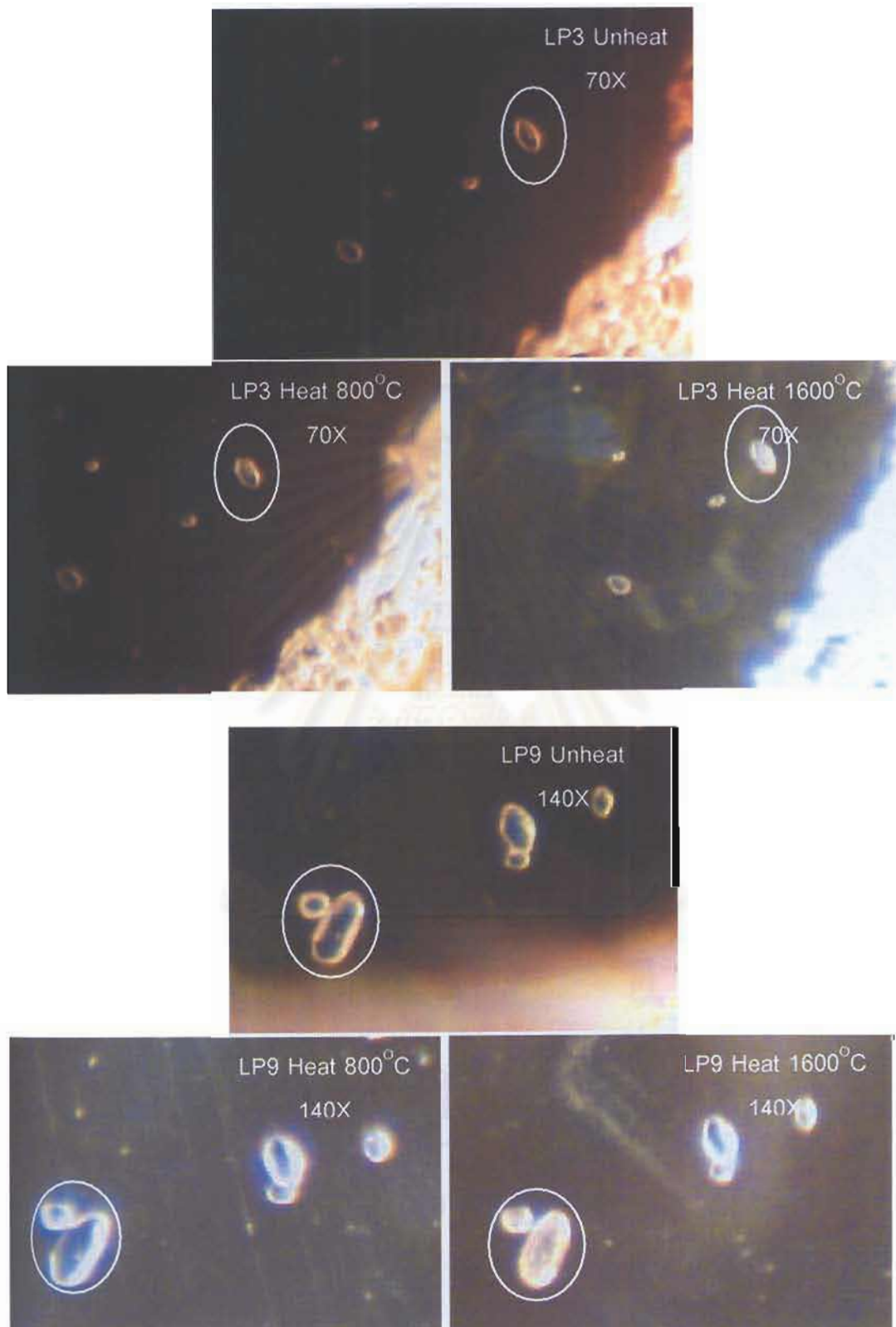


Figure 5.14: Most of the zircon inclusions were still unchanged after the step-heating from 800^o to 1600^oC except some crystals in circle became turbid at 1600^oC.

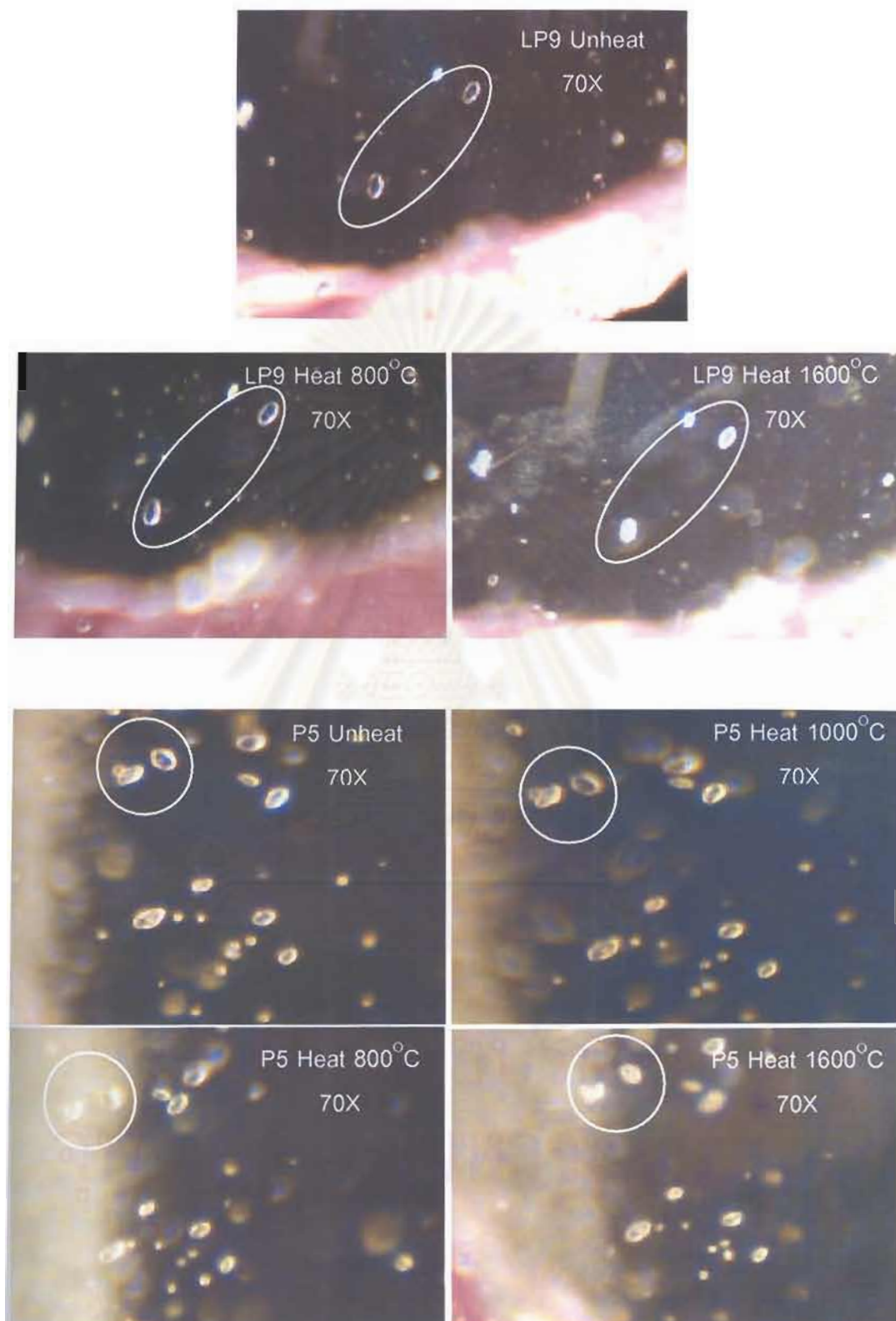


Figure 5.15: Most zircon inclusions were still unchanged after the step-heating from 800° to 1600°C except some crystals in circle became turbid at 1600°C.

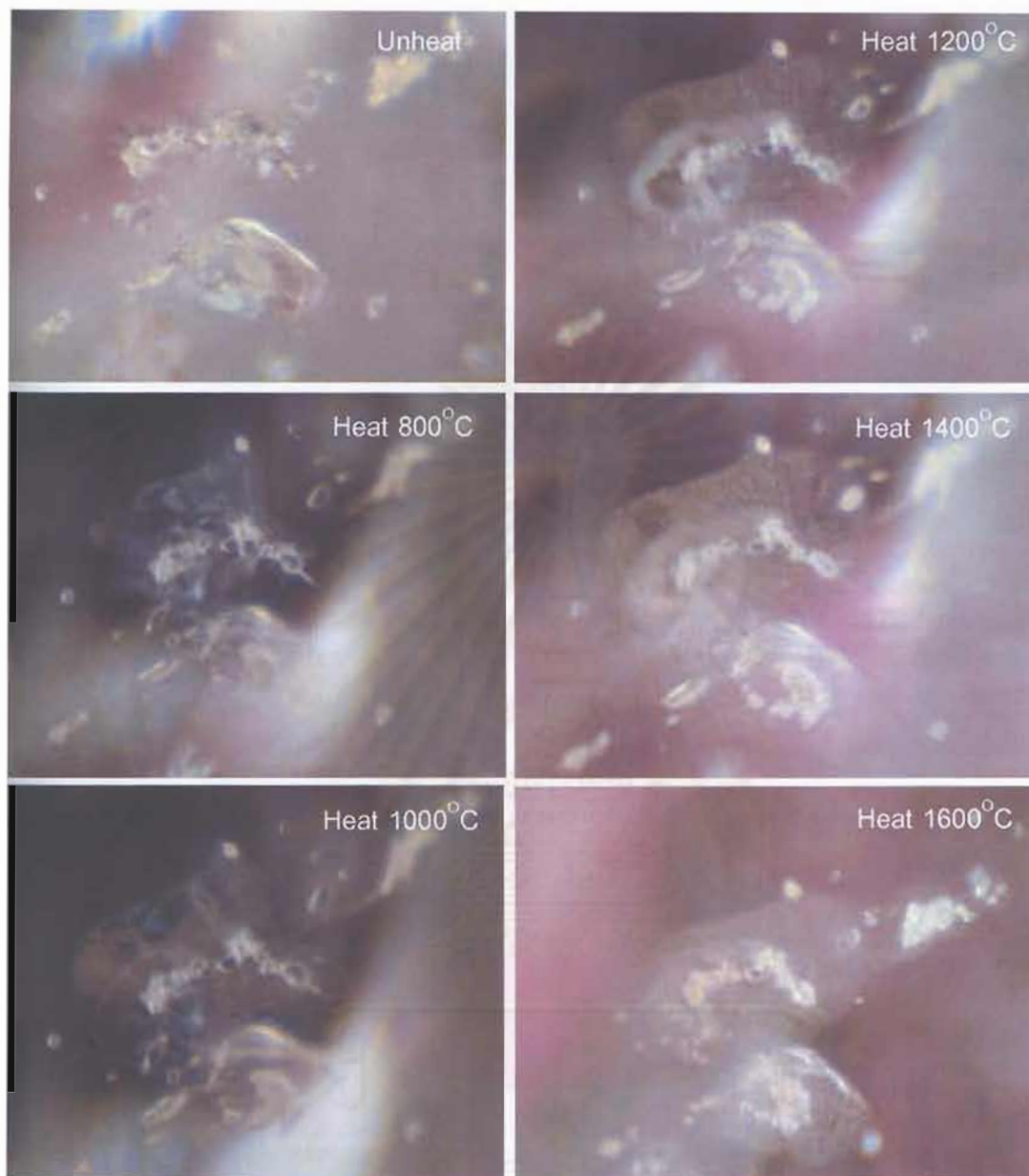


Figure 5.16: Zircon clusters with minor tension discs before heating. The tension discs were noticeably expanded at 800°C and became more obvious at higher temperatures. It should also be noted that some crystals in zircon clusters appear turbid at 1200°C. The decomposition of those zircon crystals became more pronounced at higher temperatures (sample no. PK8, 70X).

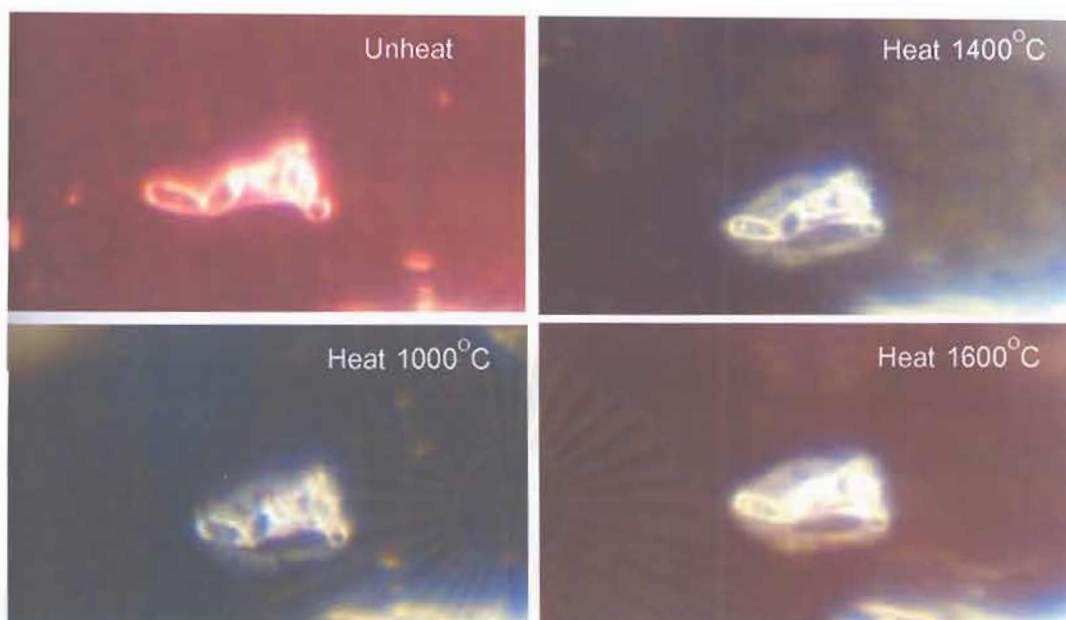


Figure 5.17: A zircon clusters was still unchanged at 800°C. The tension discs began to develop at 1000°C. At 1400°C to 1600°C, these tension discs became more obvious (sample no. PP4, 140X).

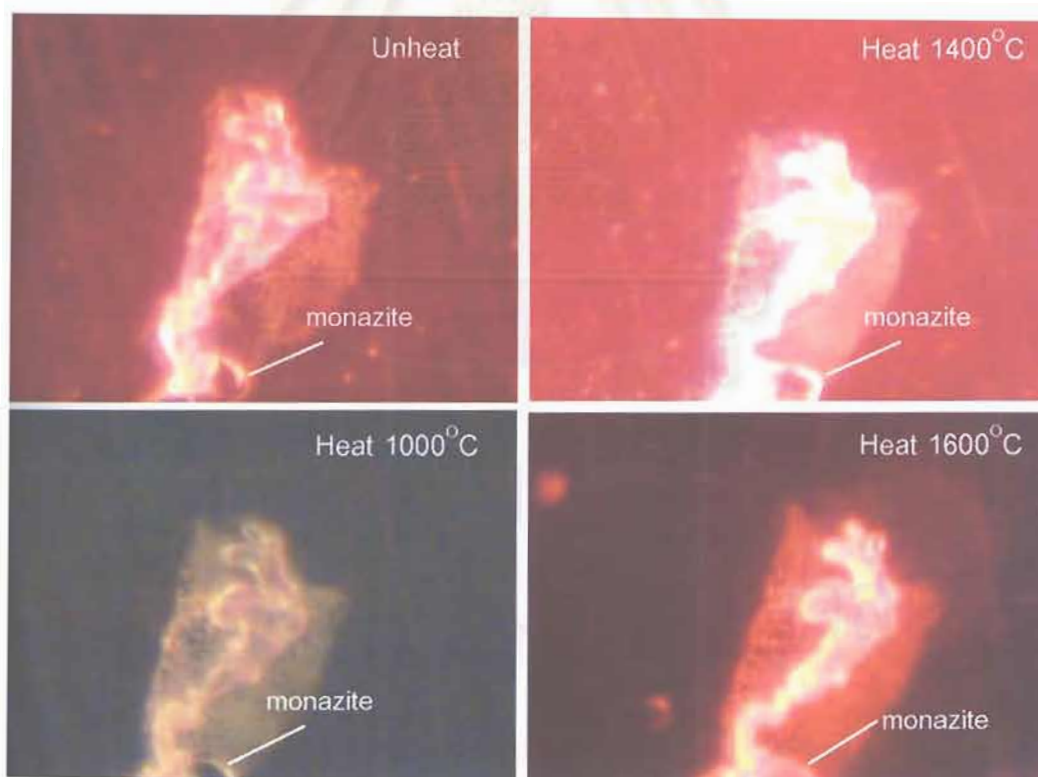


Figure 5.18: A zircon cluster was still unchanged at 800°C but showed an obvious development of tension discs at 1000°C to 1600°C. Furthermore, most crystals in the cluster became turbid at 1400°C while a monazite inclusion was altered at 1600°C (sample no. PP4, 140X).

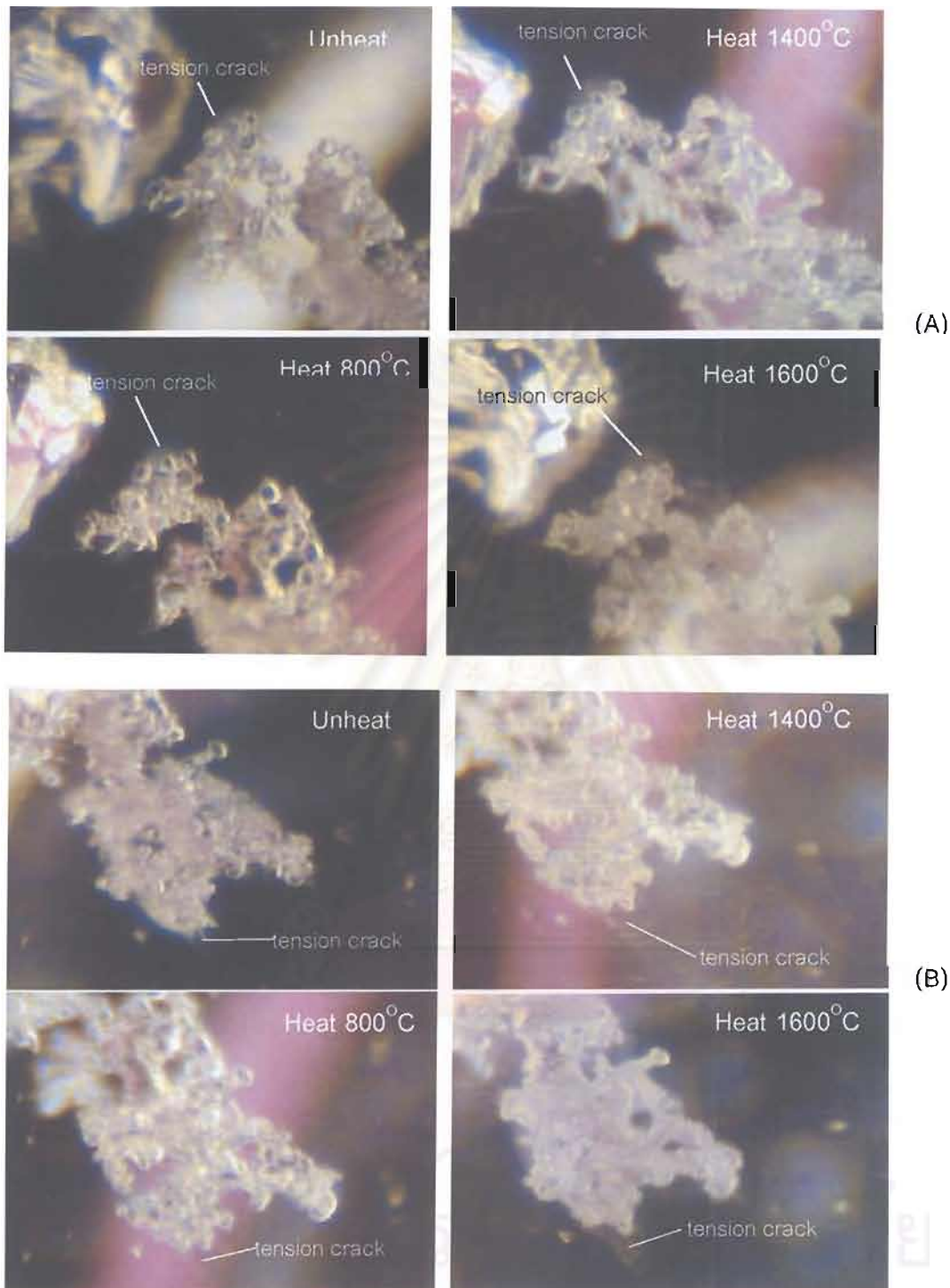


Figure 5.19: Showing zircon clusters with slight tension crack before heating. They were still unchanged at 800^o to 1200^oC (sample no. PP6, 140X). (A) At 1400^oC, some zircon crystals in the clusters began to decompose into whitish cloudy appearance and were obviously decomposed at 1600^oC. (B) At 1400^oC, tension crack was expanded and some zircon crystals in the clusters began to decompose. These crystals were obviously decomposed at 1600^oC.

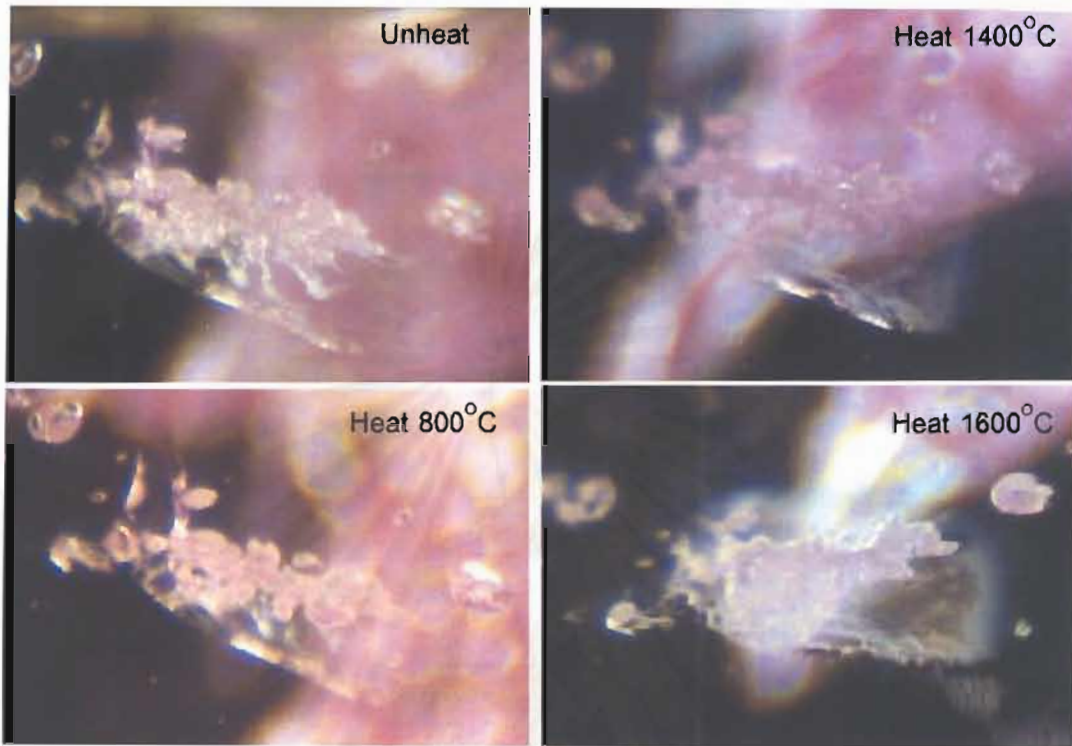


Figure 5.20: Showing zircon clusters with minor tension crack before heating. They were still unchanged at 800^o to 1200^oC,. At 1400^oC, some zircon crystals in the clusters began to decompose into whitish cloudy appearance and the tension crack was expanded. At 1600^oC, the crack expanded more and the crystals clearly became turbid (sample no. LP3, 70X).

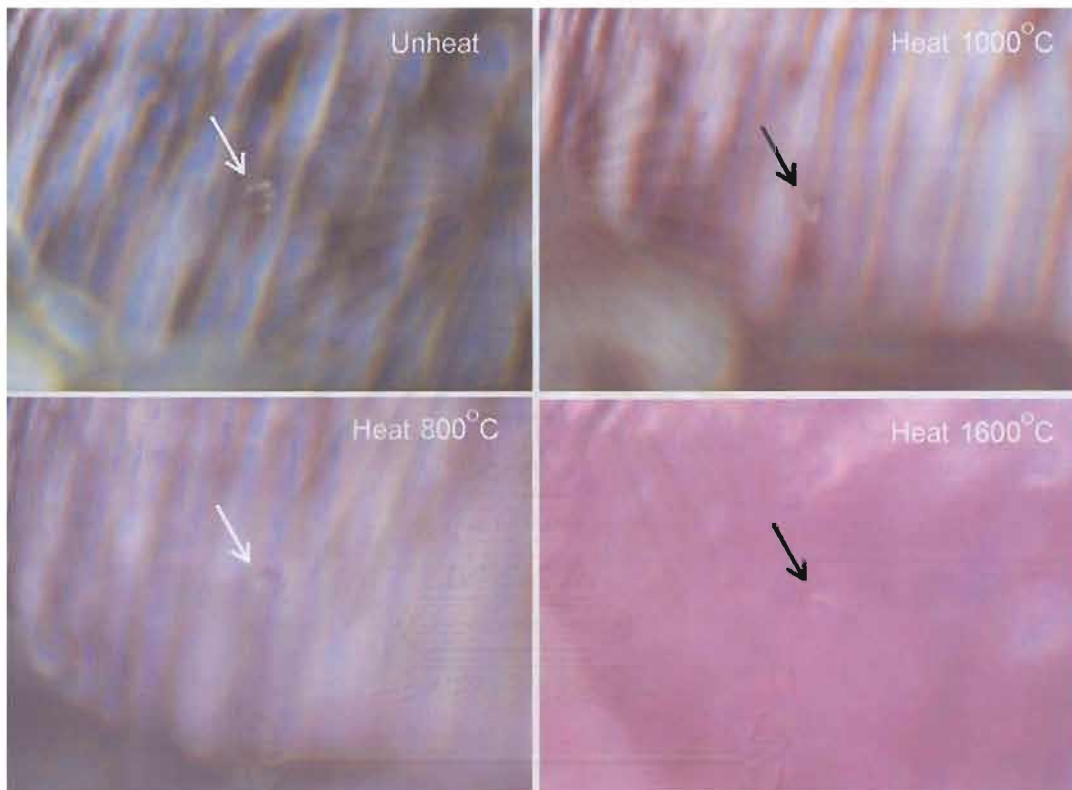


Figure 5.21: A monazite inclusion was still unchanged after a step-heating from 800°C to 1600°C (sample no. PK3, 70X).

จุฬาลงกรณ์มหาวิทยาลัย

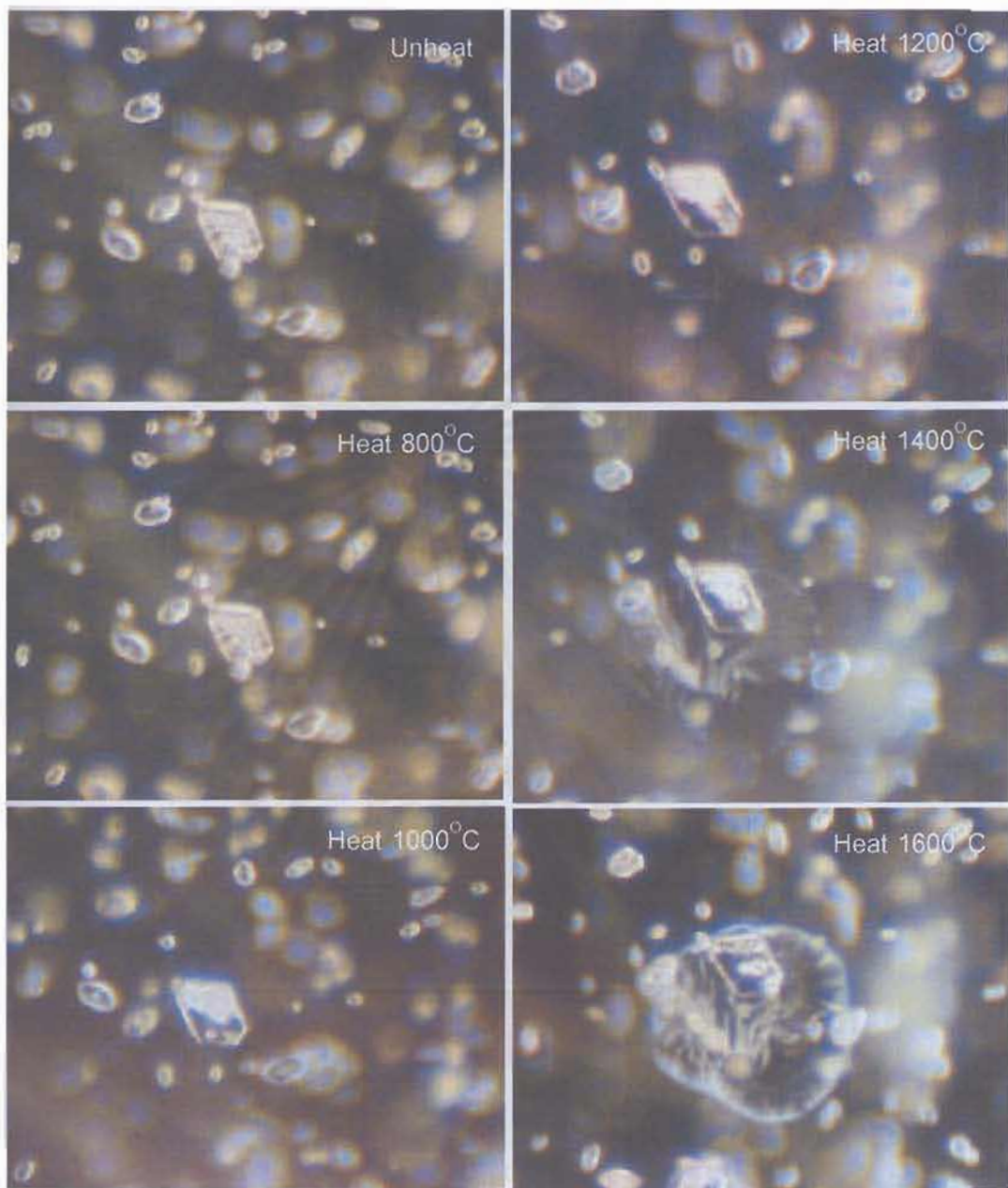


Figure 5.22: A mica inclusion was still the same at 800°C. At 1000°C, the crystal began to alter and was altered more at higher temperatures. The tension crack start to form around the inclusion at 1200°C and it became more and more obvious at 1400°C and 1600°C (sample no. P6, 70X).

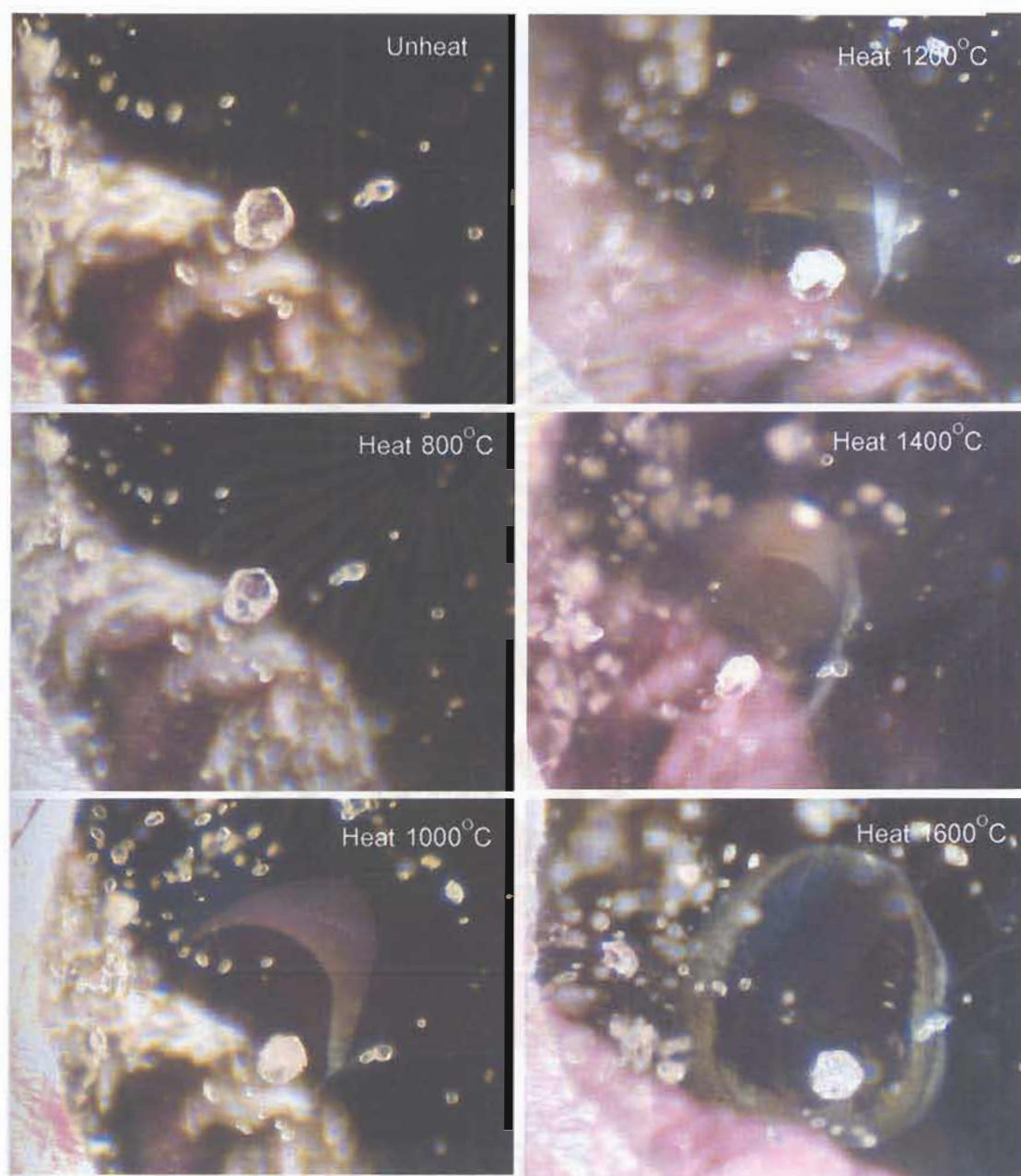


Figure 5.23: Another mica inclusion was still unchanged at 800°C. At 1000°C, the inclusion was partially altered or appeared slightly turbid with minor tension crack. The alteration and tension crack became more and more obvious at 1200°, 1400° and 1600°C (sample no. LP3, 70X).

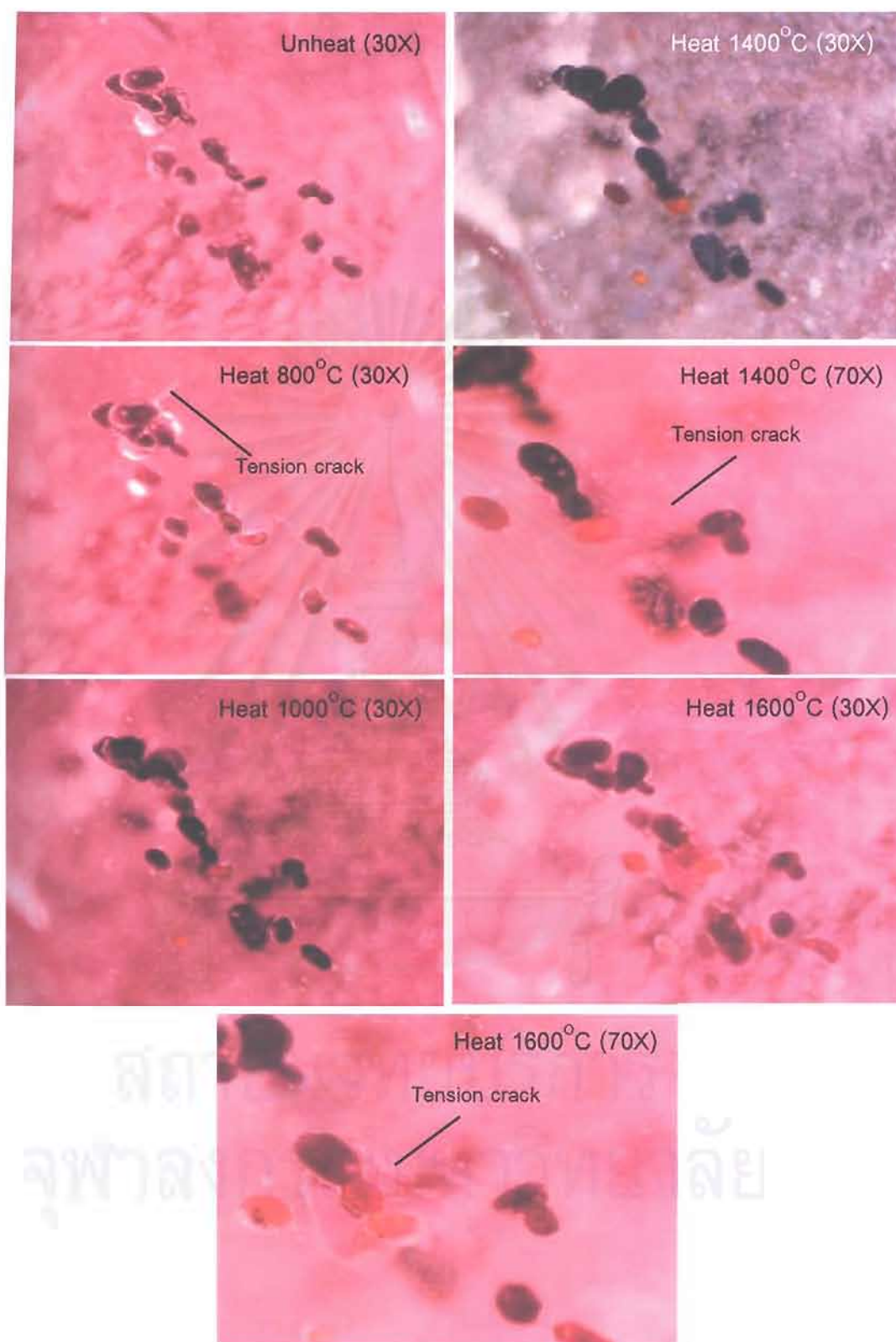


Figure 5.24: Colour of some rutile inclusions was changed from dark brown-black to red with minor tension crack at 800°C . At higher temperatures (1400°C - 1600°C) red colour was more intense and the tension crack became more obvious (sample no. PP3).

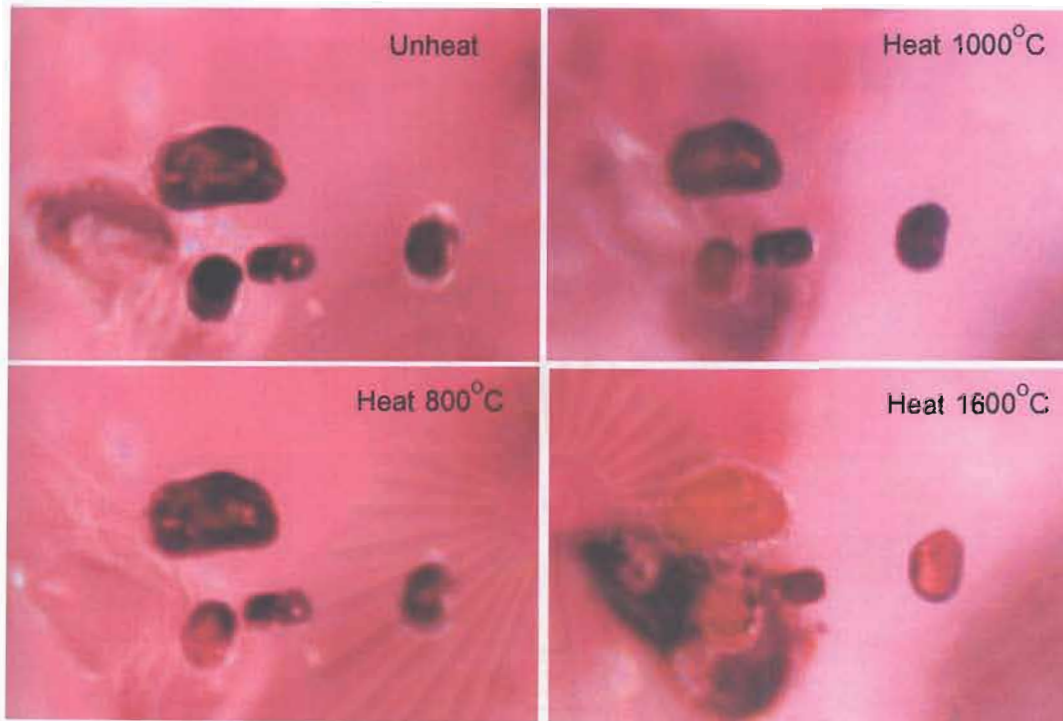


Figure 5.25: Black rutile inclusions were slightly red at 800°C. The red colour was more obvious and the inclusions showed melted boundaries at higher temperatures (sample no. PP3, 70X).

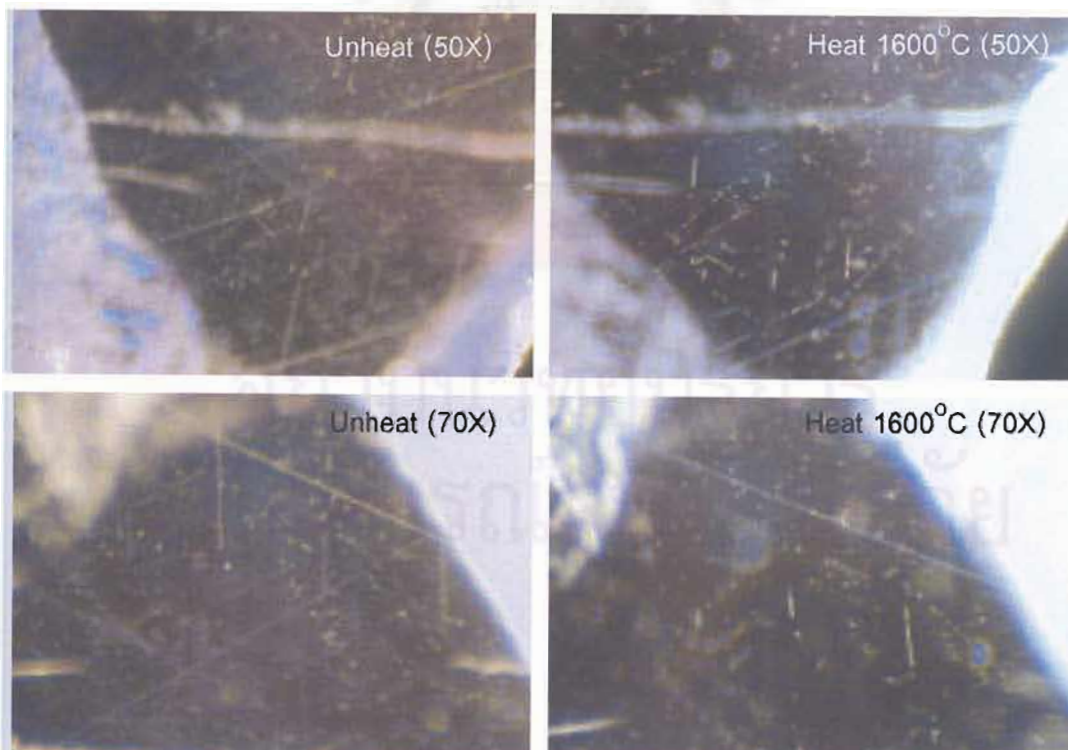


Figure 5.26: Rutile needles intersecting each other at 60°/120° angles were still unchanged at 800-1400°C but partially dissolved into the host sapphire creating a dot-like pattern at 1600°C (sample no. MV2).

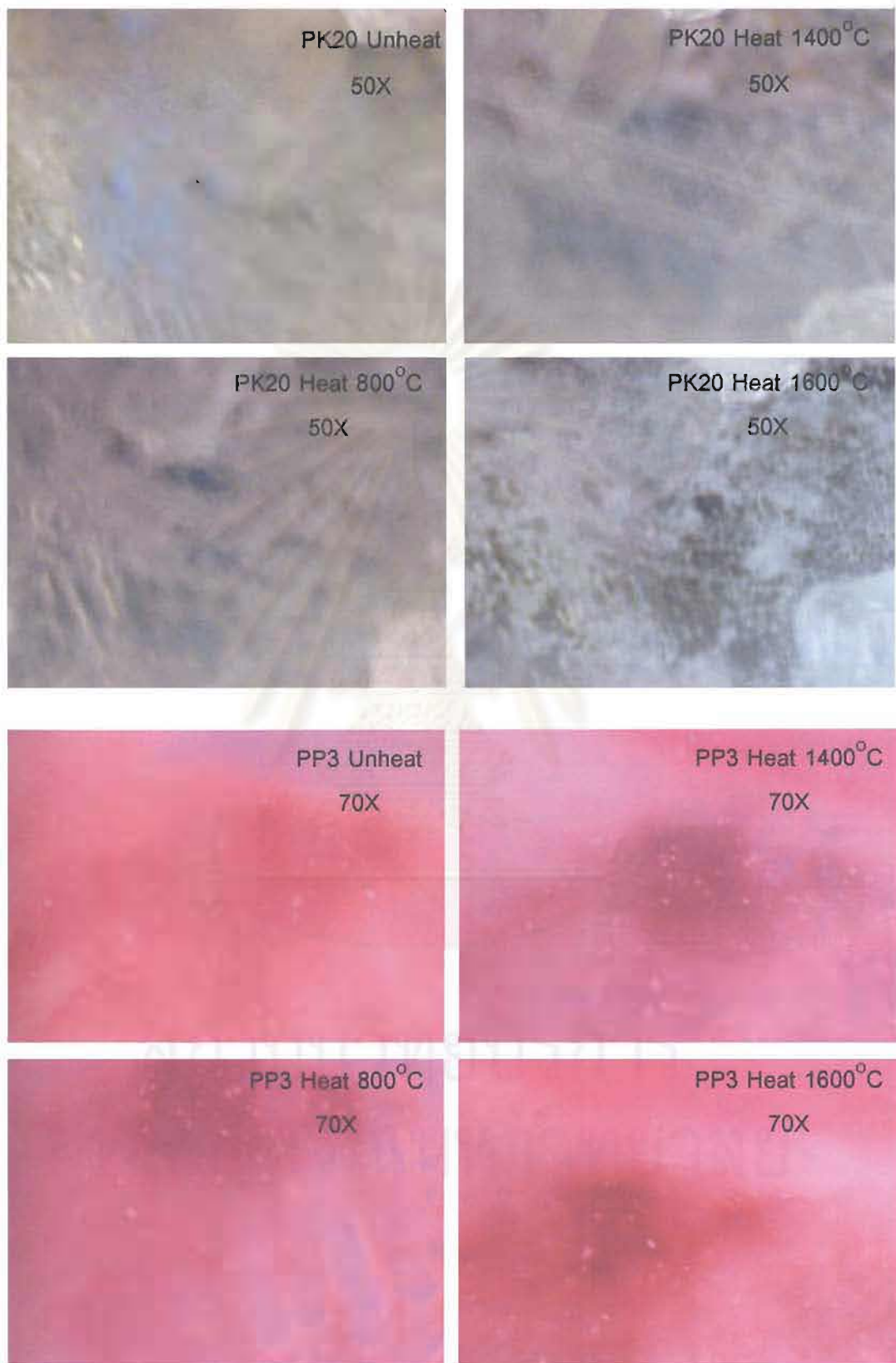


Figure 5.27: Rutile silks were still unchanged when heated at lower temperatures but completely dissolved in the host sapphire at 1600°C

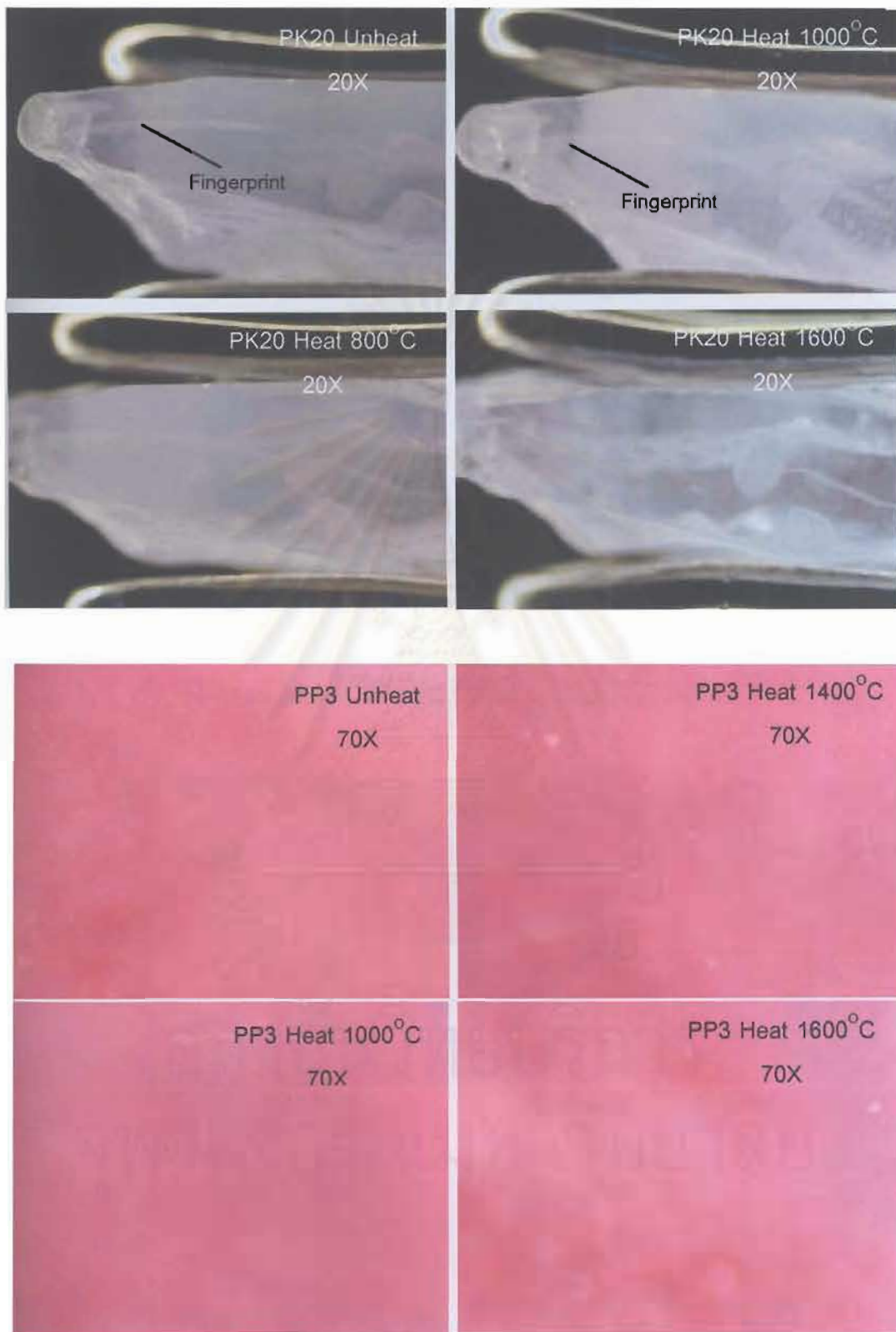


Figure 5.28: Milky and dust zones became clearer at 1600°C.

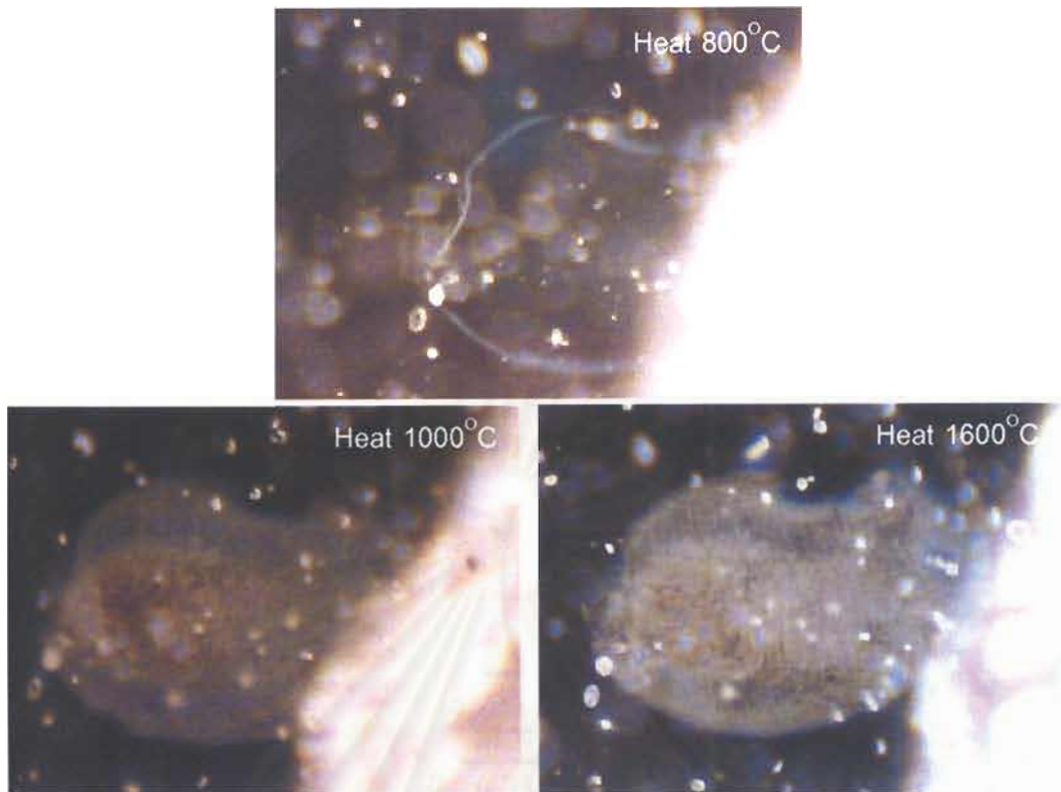


Figure 5.29: A sapphire showed a faint fingerprint at 800°C and it was more and more obvious at 1000° and 1600°C (sample no. P6, 70X).

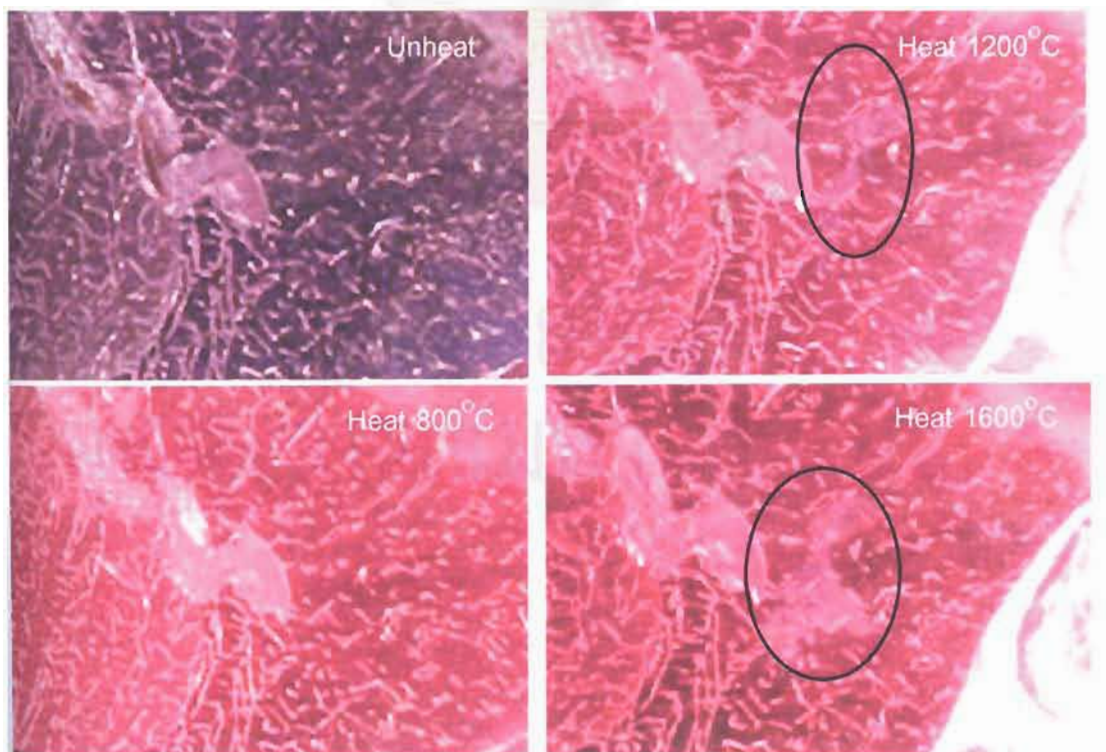


Figure 5.30: Fingerprints in an unheated sapphire were expanded at 1200° and 1600°C (sample no. PP6, 50X).

Chapter 6

Characteristics of Diego Blue Sapphires before and after Heat Treatment Experiment

Thermal enhancement process

Some selected samples of sapphire from Diego Suarez area, northern Madagascar were used for heating experiment. These stones represent sapphires from basaltic origin. The samples were heated at two different conditions, 1,350 and 1,650°C, each for 3 hour soaking time in an electric furnace (Model Linn High Therm HT-1800-PLUS) under pure nitrogen atmosphere which commonly produced neutral to slightly reducing condition. Neutral to reducing condition is usually selected for increase blue hue of sapphire. The heating experiment was carried out at the Department of Geology, Faculty of Science, Chulalongkorn University.

These conditions were selected because from the previous study the heat treatments at 800° and 1,000°C were normally not effect much of the internal characteristics. Hence heating at 1,350° and 1,650°C was chosen in this study. Previous works revealed that three hours soaking time was suitable to observe the difference in colour transparency and internal characteristics. The heating rate was controlled at about 4.5°C/minute and 2°C/minute for heating at 1350 and 1,650°C, respectively. The cool-down rate was approximately 3.5°C/minute.

The effect of heat treatment on internal characteristics

When sapphire samples were heated at 1,350°C for 3 hours and re-heated up to 1,650°C for another 3 hours, some changes did occur and can be documented as follows:

- 1) Growth pattern commonly presents in Diego sapphires and often associates with milky colour zones (Figures 6.1A to 6.6A). At 1,350°C the milky characteristic was partially disappeared and colour zones become more obvious (Figures 6.1B to 6.6B). At 1,650°C colour zones were even more intense (Figures 6.1C to 6.6C).
- 2) Milky or cloudy appearance became less pronounced after heating at 1,350°C for 3 hours (Figures 6.7B and 6.8B) and almost disappeared after heating at 1,650°C for 3 hours (Figures 6.7C and 6.8C). The stones become clear and color is more intense.
- 3) Reddish brown to pale yellowish brown materials filling in fractures were disappeared after reduction heating at 1350° (Figures 6.9B to 6.11B) and 1,650°C (Figures 6.9C to 6.11C). Healed fractures show somewhat altered.
- 4) Tension cracks or discoids surrounding solid inclusions were progressively developed at 1,350°C (Figures 6.12B to 6.14B) and 1,650°C (Figure 6.12C to 6.14C).
- 5) Clear zircon inclusions (Figure 6.14A) were slightly decomposed and became somewhat turbid at 1,350°C (Figure 6.14B). They were even more decomposed and turbid at 1,650°C (Figure 6.14C). The decomposition of zircon can also be detected by a change in Raman spectra shown in Figure 6.15.

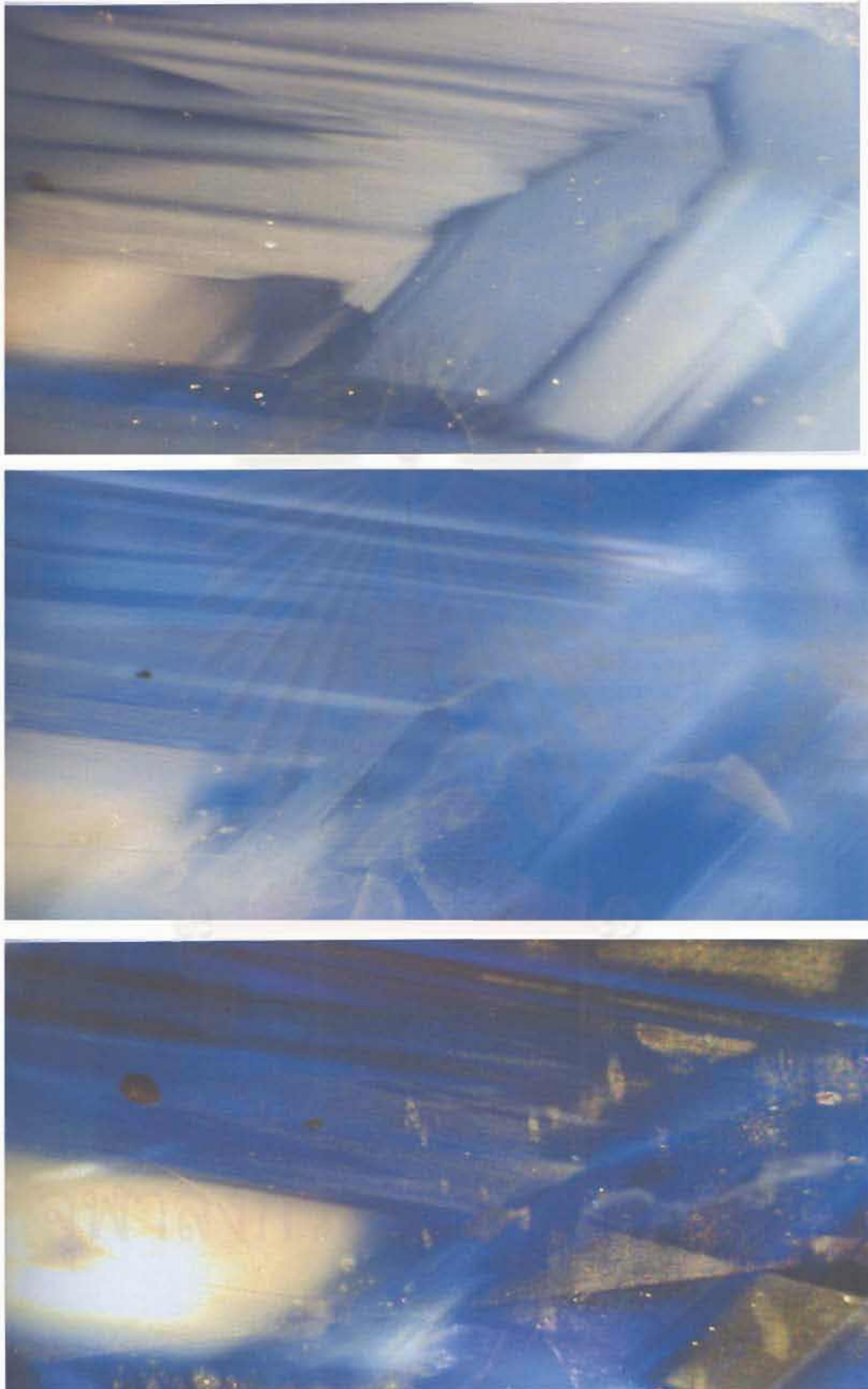


Figure 6.1: Growth pattern of a Diego sapphire before treatment (A). At $1,350^{\circ}\text{C}$ (B) and $1,650^{\circ}\text{C}$ (C) the colour zones became more and more intense and the milky characteristic was progressively disappeared.

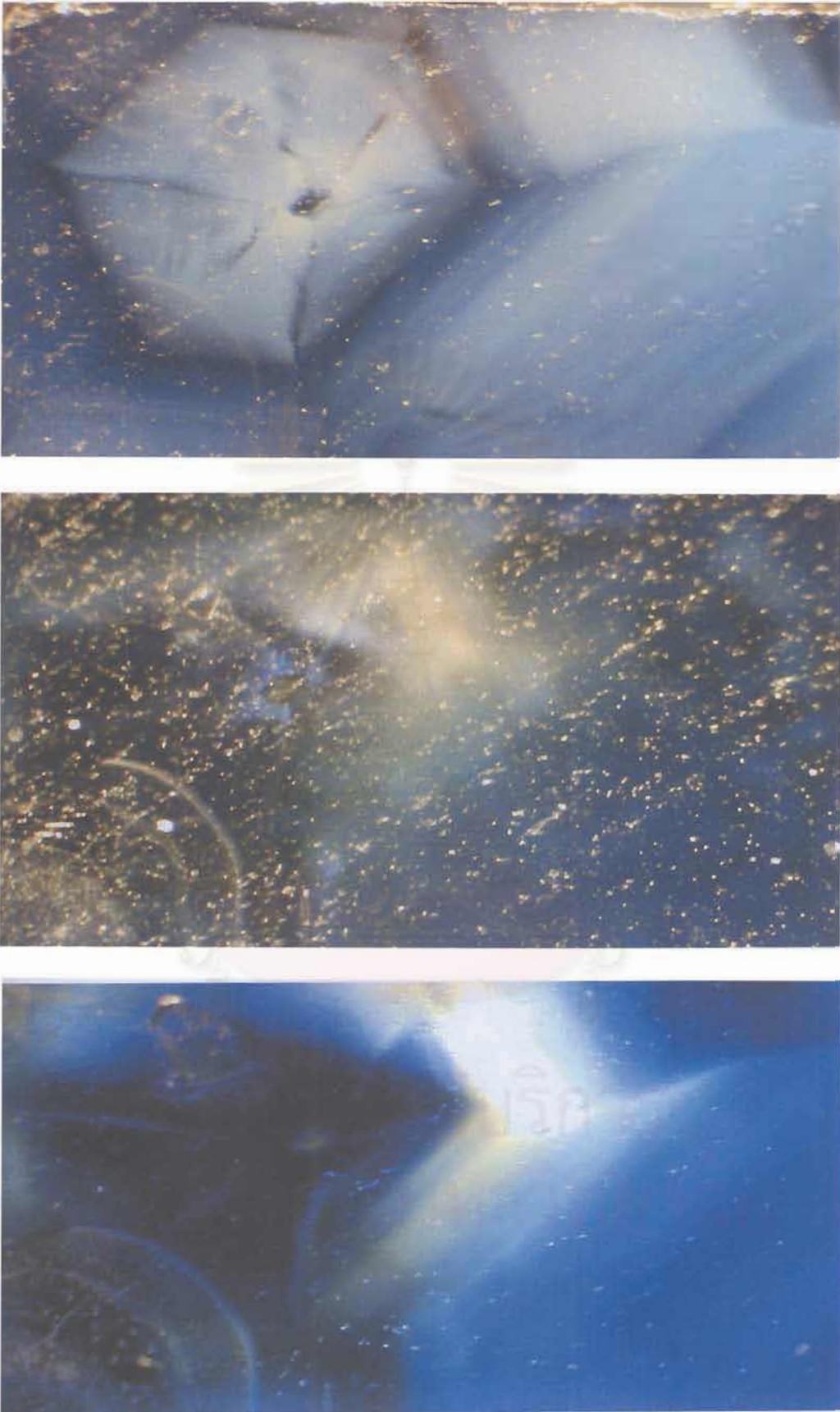


Figure 6.2: A similar feature to Figure 6.1

A



B



C



Figure 6.3: Ditto.

A



B



C



Figure 6.4: Ditto.

A



B

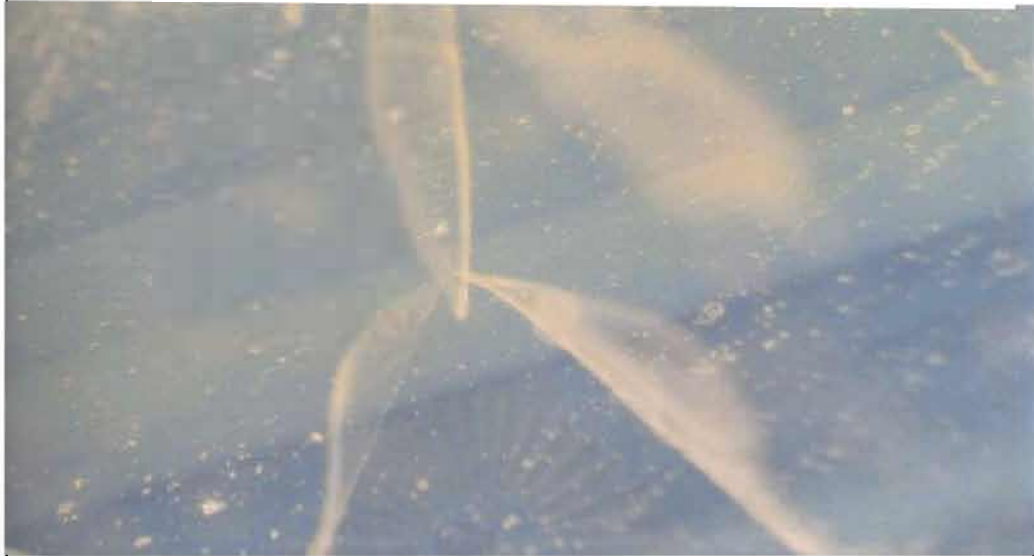


C

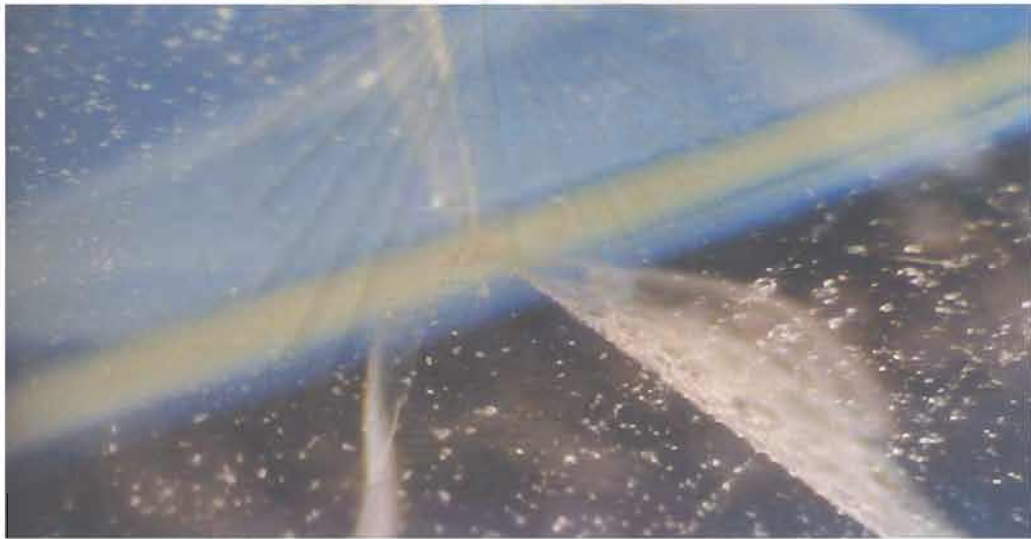


Figure 6.5: Ditto.

A



B



C



Figure 6.6: Ditto

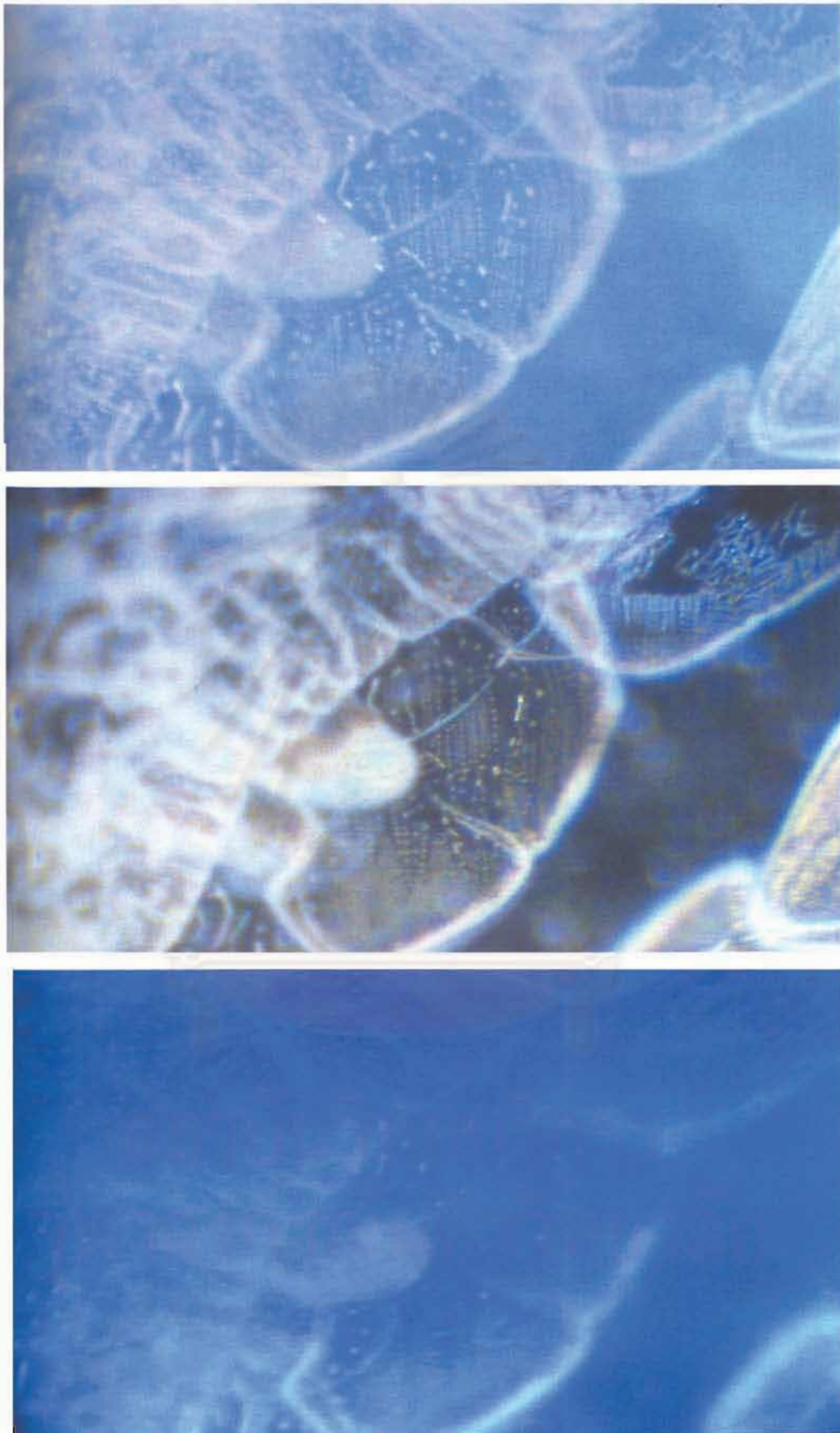


Figure 6.7: Milky appearance of a sapphire before treatment (A). At 1,350°C (B) and 1,650°C (C), the milky appearance was progressively reduced.

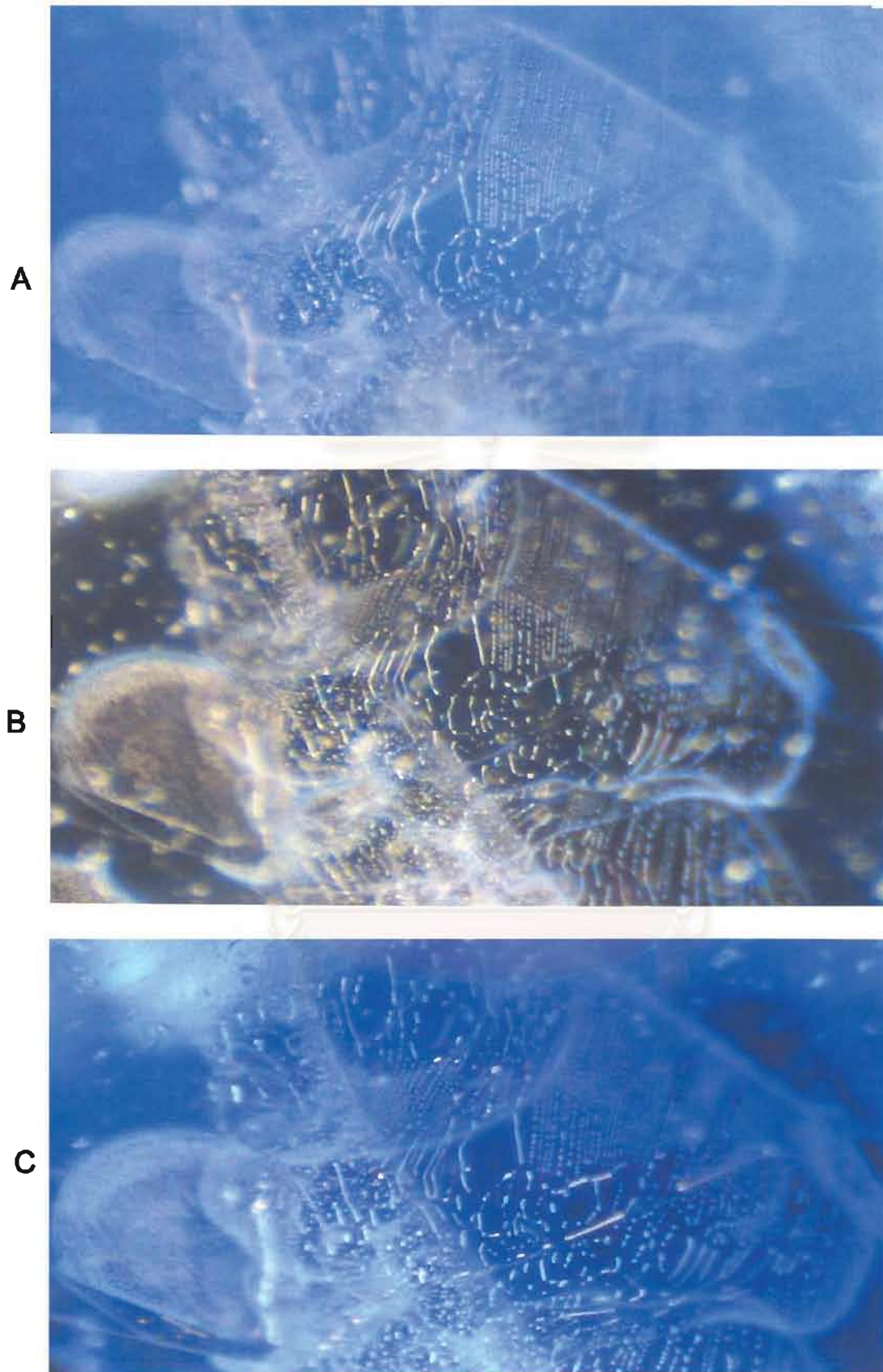


Figure 6.8: Ditto

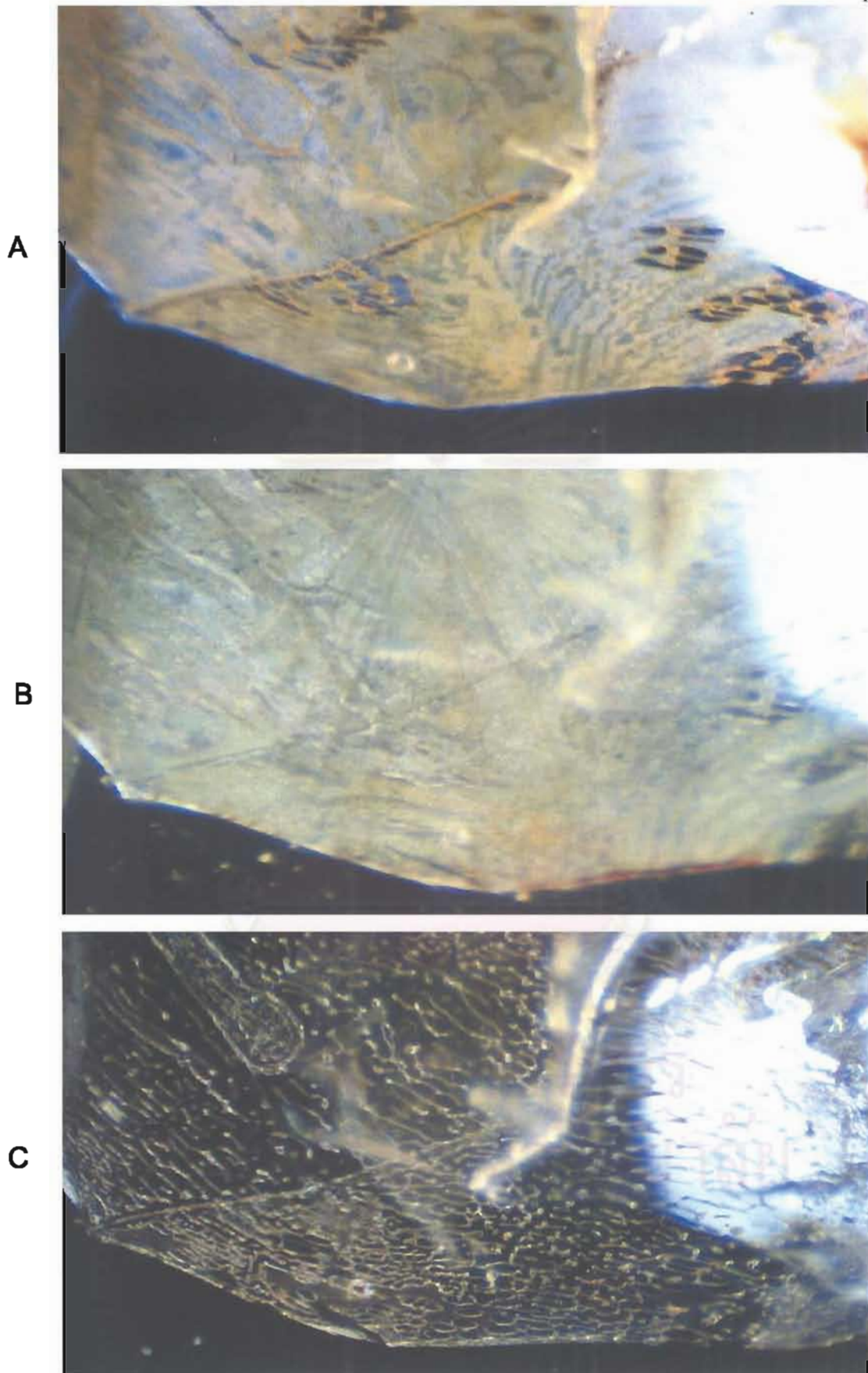


Figure 6.9: Fracture-filled yellow materials in a sapphire before treatment (A). At 1,350° (B) and 1,650°C (C), the materials were progressively clear.

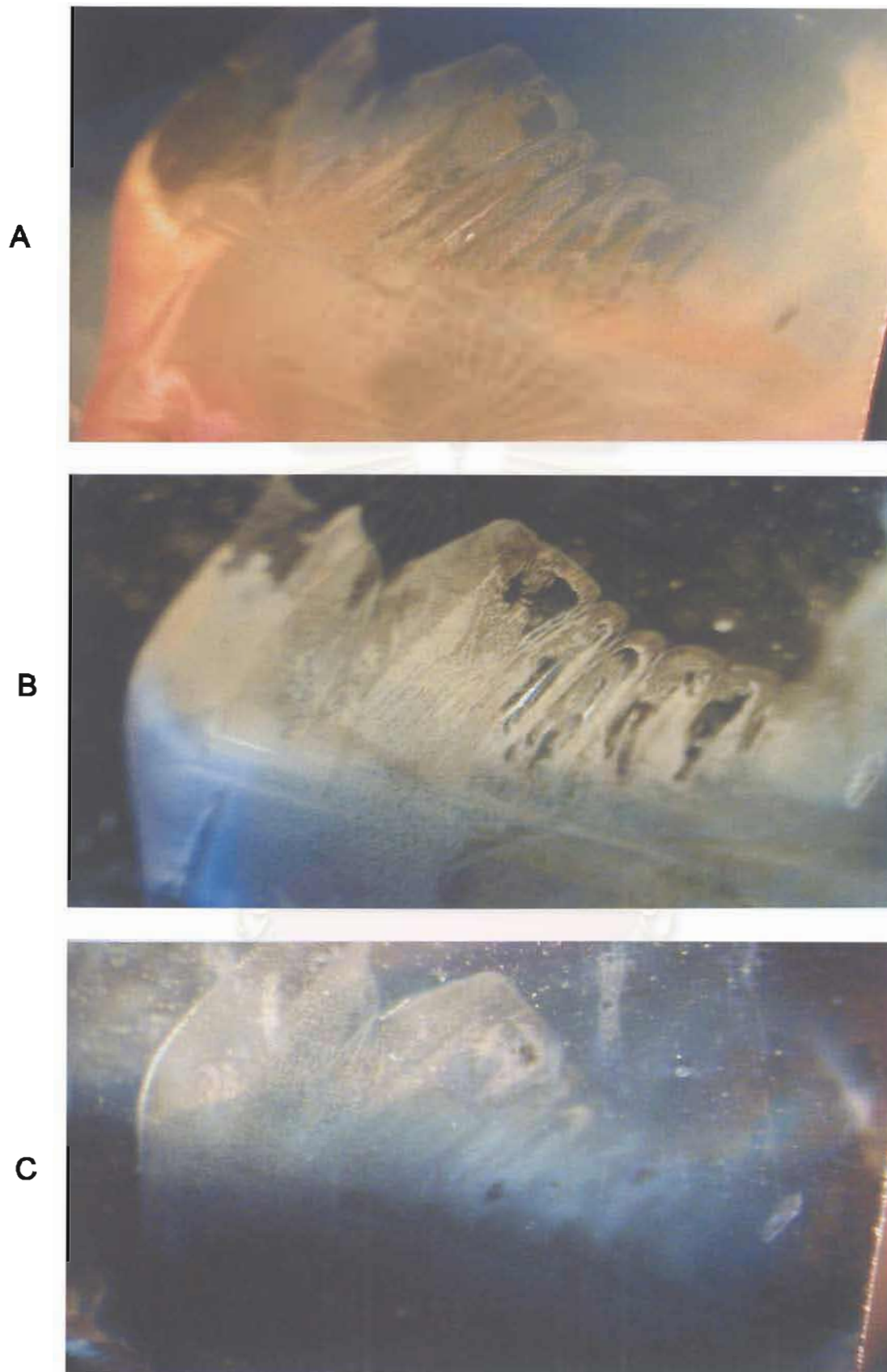
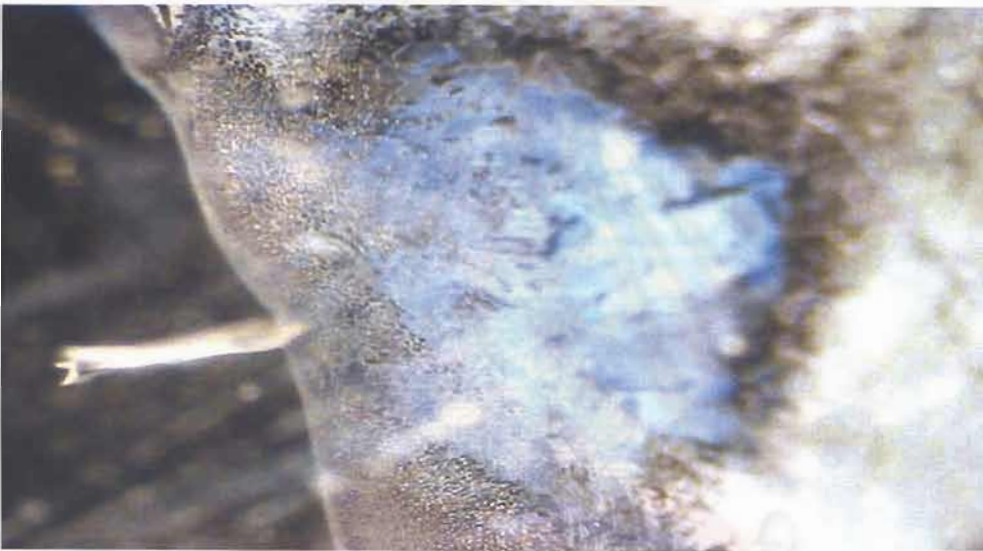


Figure 6.10: Fracture-filled orange materials in a sapphire before treatment (A). At 1.350° (B) and 1.650°C (C), the materials were progressively clear.

A



B



C



Figure 6.11: Ditto.

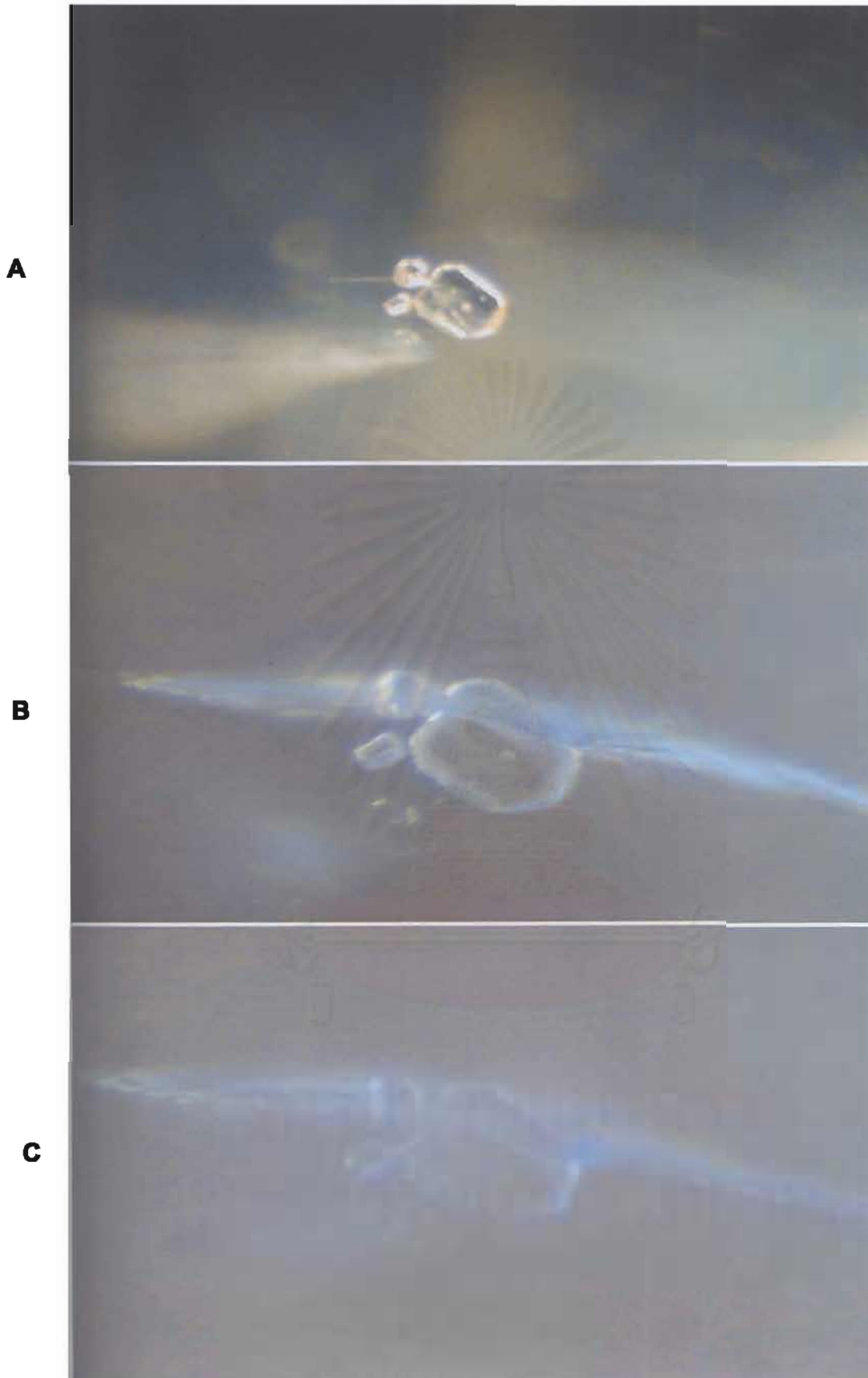


Figure 6.12: Solid inclusions before treatment (A) , the formation of tension cracks or discoids surrounding the inclusions at 1,350°C (B) and 1,650°C (C).

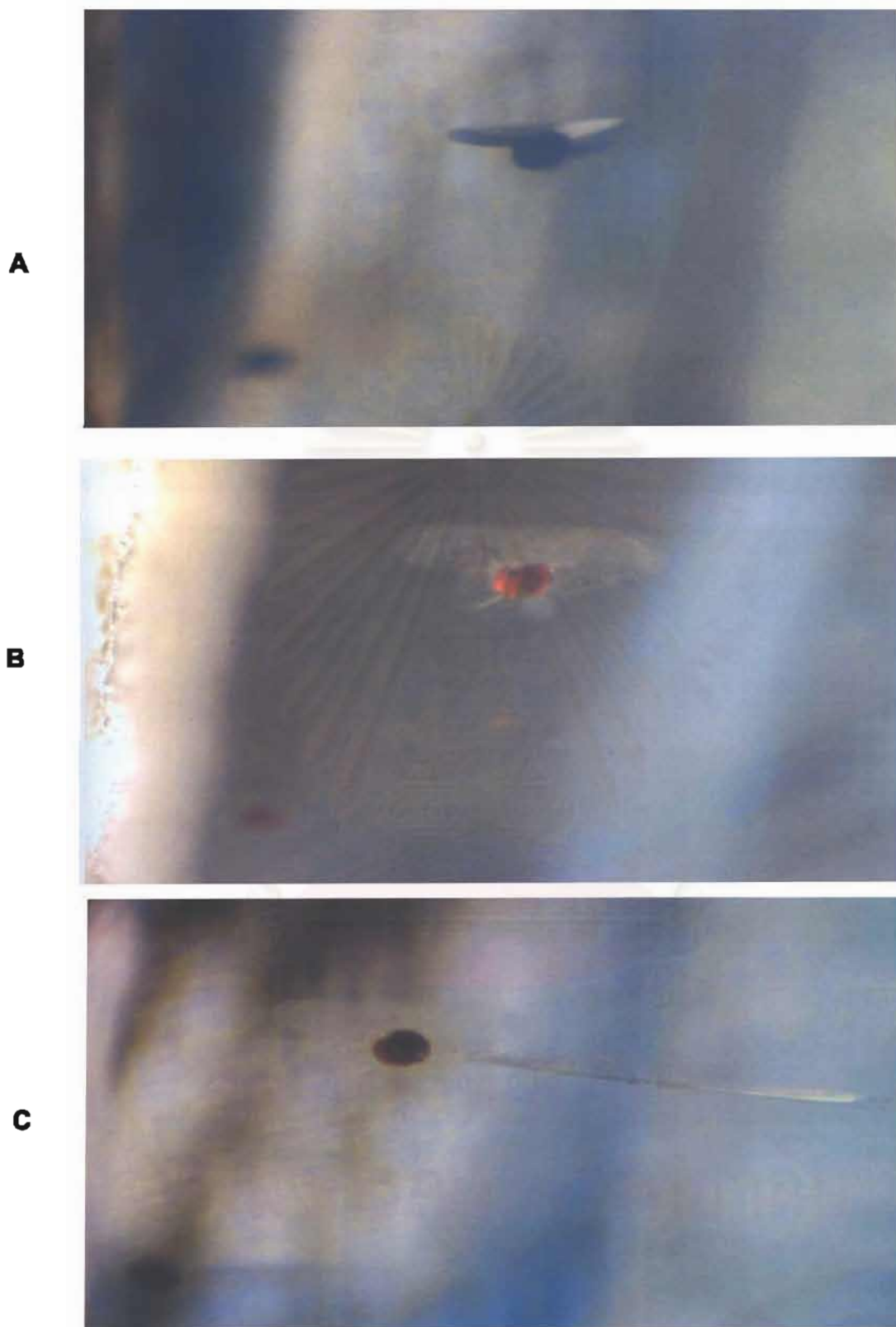


Figure 6.13: Small tension disc was already formed around a ferrocolumbite inclusion before treatment. It was obviously expanded at 1,350°C (B) and 1,650°C (C).

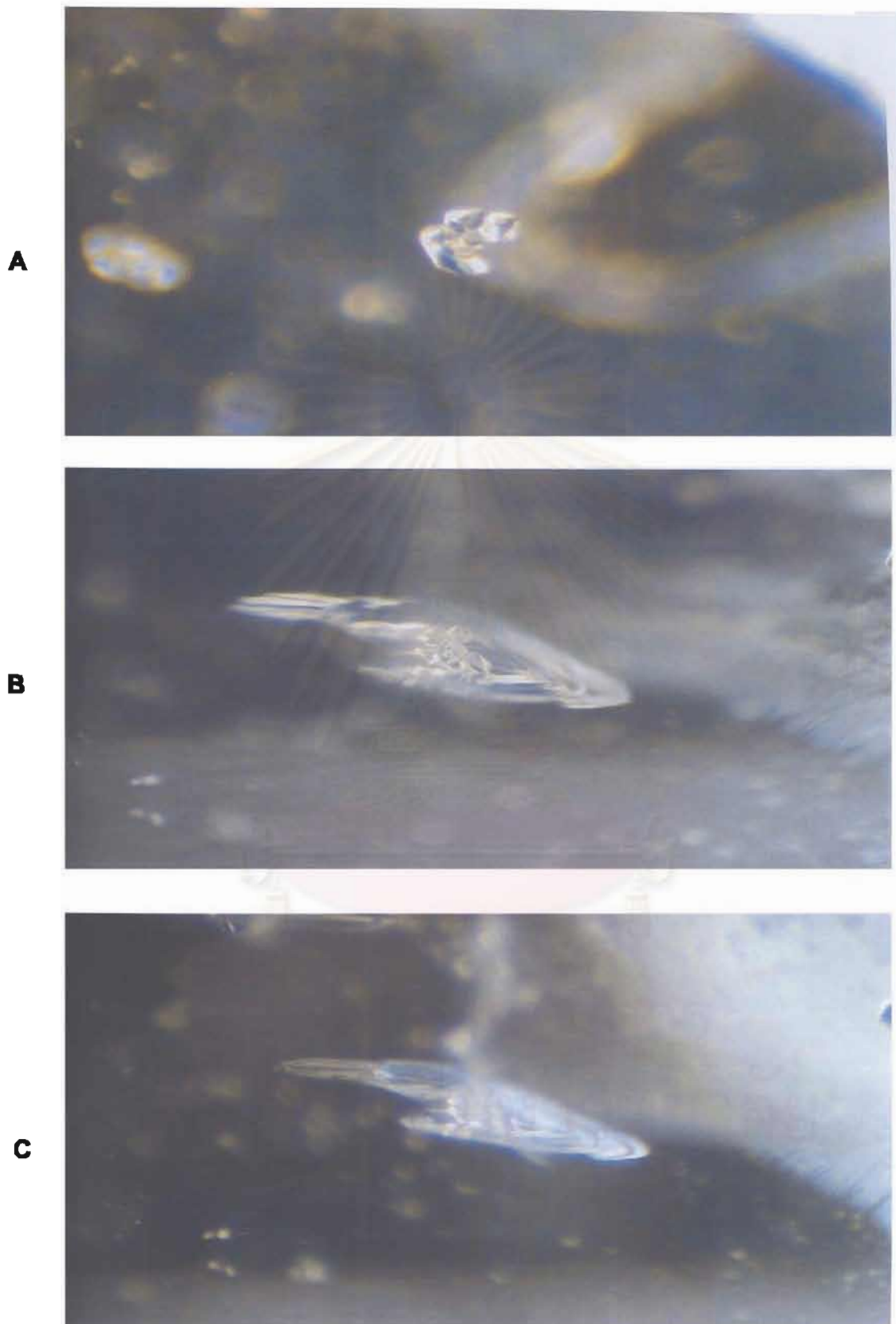


Figure 6.14: A cluster of zircon inclusions before treatment (A). The inclusions became turbid with tension discs at 1,350°C (B) and 1,650°C (C).

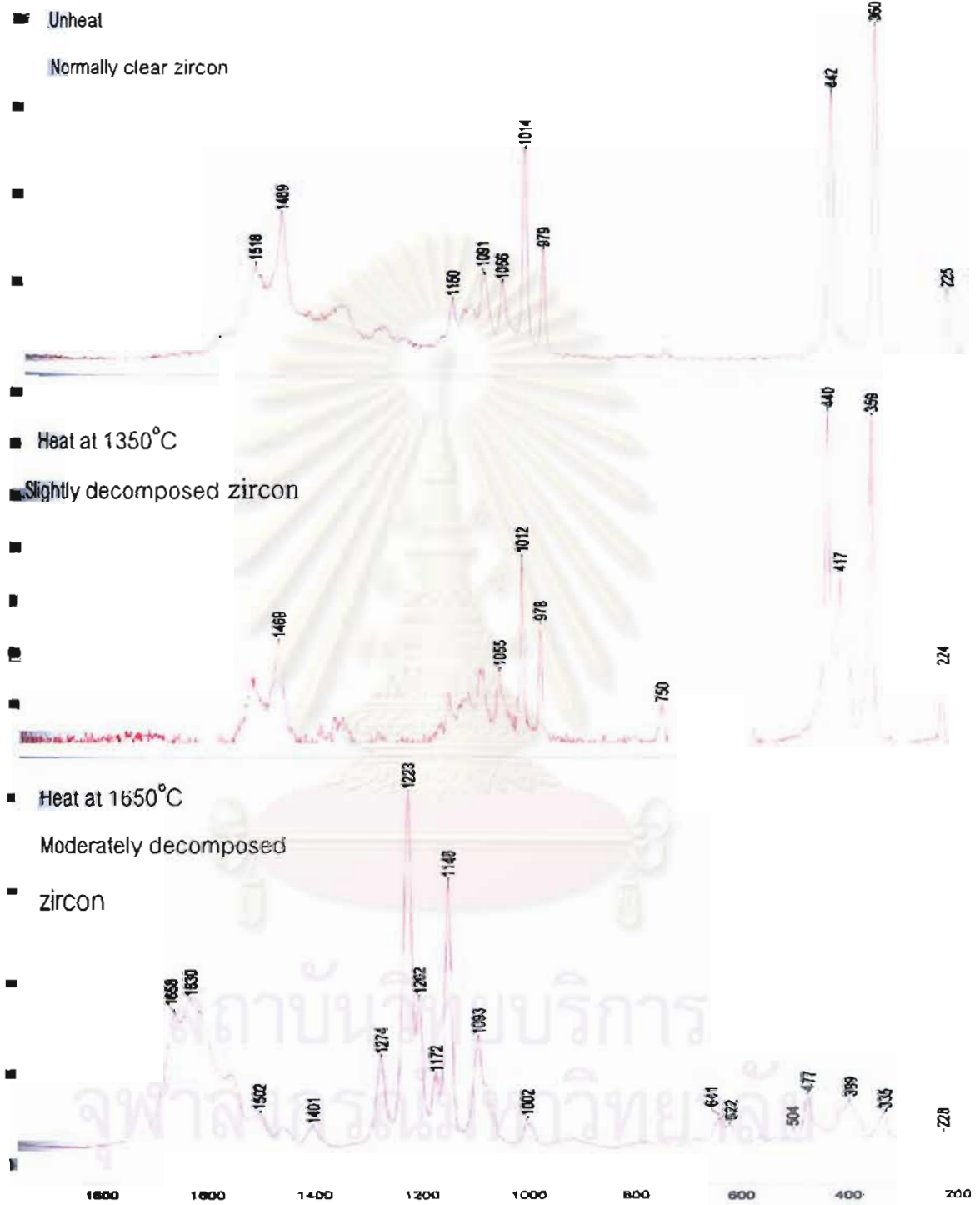


Figure 6.15: Changes of Raman spectra of a zircon inclusion in a violet sapphire after heat treatment.

Chapter 7

Some Characteristics of Un-Heated and Heated Natural Sapphires from the Trades

Introduction

In this chapter some internal characteristics as well as FTIR and UV-Vis-NIR results of naturally un-heated and heated blue sapphires from reliable trades will be given representing the real stones in the gem market. The purpose of this study is to cross-check the result and conclusion of our earlier heat treatment experiment with those of the stones available in the gem market.

Samples and Procedure

Altogether 37 stones were borrowed with the courtesy of World Sapphires Co., Ltd. and Beauty Gems Co., Ltd. They are essentially blue sapphires from Ilakaka, Madagascar (15 samples from World Sapphires Co., Ltd. and 16 samples from Beauty Gems Co., Ltd.) and Mokok, Myanmar (6 samples from World Sapphires Co., Ltd.). The samples were examined and photographed under a gemmological microscope. The FTIR and UV-Vis-NIR spectra were also measured by Nicolet FTIR spectrophotometer (Model Nexus 670) and Hitachi UV-Vis-NIR spectrophotometer (Model U4001) at the Gem and Jewelry Institute of Thailand (GIT).

Result

Un-heated Madagascar blue sapphire

The following internal characteristics and spectra are observed in the 29 un-heated samples, some of which are indicative of natural un-heated features whereas the others are not.

- 1.1 The un-heated stones usually show overall hazy or cloudy appearance resulting from the presence of very fine dust particles along the growth zones and occasionally in combination with rutile silks or needles intersecting in three directions at $60/120^\circ$ (Figures 7.1 to 7.29).
- 1.2 The rutile silks or needles are very fine, long, continuous and sharp indicating of naturally slow cooling condition without subsequent thermal treatment (Figures 7.3, 7.8, 7.15, 7.22, 7.23, 7.24, 7.25). This feature is a good indication of un-heating condition.
- 1.3 Most healed fractures or fingerprints show well-formed, fine and sharp boundary pattern suggesting of naturally slow healing without evidence of subsequent heat treatment (Figures 7.4, 7.6, 7.9, 7.10, 7.11, 7.12).
- 1.4 Most of mineral inclusions as well as negative (fluid) inclusions are clear, well intacted with sharp crystal boundary contact and without tension disc suggesting of naturally occurring condition without evidence of subsequent heat treatment (7.11, 7.18, 7.19, 7.20, 7.21, 7.26, 7.27).
- 1.5 Some tension disc may develop in some mineral inclusions (most likely radioactive minerals) as shown in Figure 7.16.
- 1.6 Yellowish orange or red impurity materials of probably iron-bearing substances in healed fractures or hollow tubes may suggest an un-heat condition (Figures 7.12 and 7.29).
- 1.7 All the 29 un-heated Madagascar blue samples show the absence or a very weak OH-stretching peak at 3309 cm^{-1} which is consistent with our previous

heating experiment (see an example in Figure 7.36). Hence the absence or weakly presence of the OH-stretching peak at 3309 cm^{-1} may be used as another suggestive evidence to indicate the un-heated blue Madagascar (Ilakaka) sapphire.

- 1.8 About half (14) out of the 29 un-heated Madagascar blue sapphires give the extinction edges between 330-350 nm on the UV-Vis-NIR spectra whereas the remaining 15 stones show the extinction edges below that range (Table 7.1). These data suggest that extinction edge can not be used as a positive indication of un-heat condition.

Heated Madagascar blue sapphires

Two heated Madagascar (Ilakaka) blue sapphires from the trade show the following results:

- 2.1 The two heated stones usually show overall clear appearance (Figures 7.30 to 7.33). However, some stones may show milky or cloudy zones alternating with clear zones which suggest that the stone might be heavily loaded with fine dust particles originally (Figures 7.34 and 7.35). Hence the milky zones still remain after heating which might be mistaken as an un-heated stone.
- 2.2 The most obvious indication of heating is shiny thin-film tension discs or discoids surrounding an inclusion (Figures 7.32 and 7.33). Sometimes, the inclusion itself may show turbid appearance (Figure 7.33).
- 2.3 Fingerprints may show somewhat altered (Figure 7.35).
- 2.4 These two heated stones show very strong OH-stretching peak at 3309 cm^{-1} and other side peaks which are consistent with our previous heating experiment (see an example in Figure 7.36). Hence the presence of strong OH-stretching peak at 3309 cm^{-1} may be used as another suggestive evidence to indicate the heated blue Madagascar (Ilakaka) sapphire.

2.5 These two heated Madagascar blue sapphires give the extinction edges between 275-310 nm range on the UV-Vis-NIR spectra which are consistent with our previous heating experiment (Table 7.2). These data however still can not be used as an indication of heating because those of the un-heated stones can also fall in this range (see Table 7.1).

Un-heated Myanmar (Mokok) blue sapphires

Two un-heated Myanmar blue sapphires show the following results:

- 3.1 The un-heated stones usually show overall hazy or cloudy appearance resulting from the presence of very fine dust particles along the growth zones and occasionally in combination with rutile silks or needles intersecting in three directions at $60/120^\circ$ (Figures 7.37 to 7.42).
- 3.2 The rutile silks or needles are patchy (Figures 7.38, 7.41). The silks are very fine, long, continuous and sharp with arrow or knife shape indicating of naturally slow cooling condition without subsequent thermal treatment (Figures 7.38 to 7.42). This feature is a good indication of un-heating condition.
- 3.3 Healed fractures or fingerprints show well-formed, fine and sharp boundary pattern suggesting of naturally slow healing without evidence of subsequent heat treatment (Figures 7.39 and 7.40).
- 3.4 These two un-heated Myanmar blue samples show a very small OH-stretching peak at 3309 cm^{-1} (Figure 7.55). Hence the absence or weakly presence of the OH-stretching peak at 3309 cm^{-1} may be used as another suggestive evidence to indicate the un-heated blue Myanmar (Mokok) sapphire similar to those found in the Madagascar (Ilakaka) blue sapphire.
- 3.5 These two un-heated Myanmar blue sapphires, however, give the extinction edges below the 330-350 nm range on the UV-Vis-NIR spectra (Table 7.3). These data seem to suggest that extinction edge can not be used as a positive indication of un-heating condition.

Heated Myanmar (Mokok) blue sapphires

Four heated Myanmar blue sapphires reveal the following results:

- 4.1 The four heated stones show overall slightly hazy to clear appearance ((Figures 7.43 to 7.54).
- 4.2 One of the important indication of heating is the resorbed rutile silks in the form of oriented dotted pattern intersecting in three directions at $60/120^\circ$ (Figures 7.44).
- 4.3 The most obvious indication of heating is shiny thin-film tension discs or discoids surrounding an inclusion (Figures 7.45, 7.46, 7.48, 7.49, 7.50, 7.51, 7.52 and 7.53).
- 4.4 Healed fractures or fingerprints may show somewhat altered (Figure 7.54).
- 4.5 These four heated stones show very strong OH-stretching peak at 3309 cm^{-1} and other side peaks (see some examples in Figure 7.56). Hence the presence of strong OH-stretching peak at 3309 cm^{-1} may be used as another suggestive evidence to indicate the heated blue Myanmar (Mokok) sapphire similar to those found in the Madagascar (Ilakaka) blue sapphire.
- 4.6 These four blue sapphires give the extinction edges between 275-310 nm range on the UV-Vis-NIR spectra (Table 7.4). These data however still can not be used as an indication of heating because those of the un-heated stones can also fall within this range (see Table 7.3).

จุฬาลงกรณ์มหาวิทยาลัย



Figure 7.1: Series of un-heated Ilakaka blue sapphires (13 samples) varying from pale to very dark blue (with the courtesy of World Sapphires Co. Ltd.)



Figure 7.2: The 4.18 ct un-heated Ilakaka blue sapphires with hazy appearance.



Figure 7.3: Fine long rutile silks associated with very fine particles which make the stone appear bazy typical of un-heated sample.

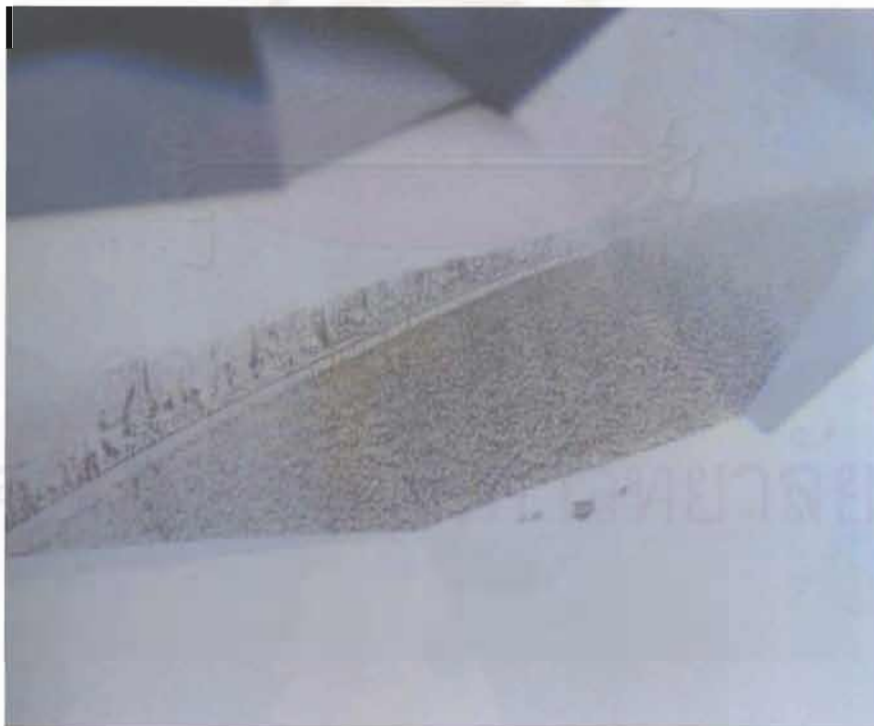


Figure 7.4: Rather sharp edge dark fingerprint.



Figure 7.5: This 1.83 ct un-heated Ilakaka blue sapphires commonly shows hazy appearance.



Figure 7.6: The hazy appearance with well-formed fingerprints or healed fractures of the un-heated stone.

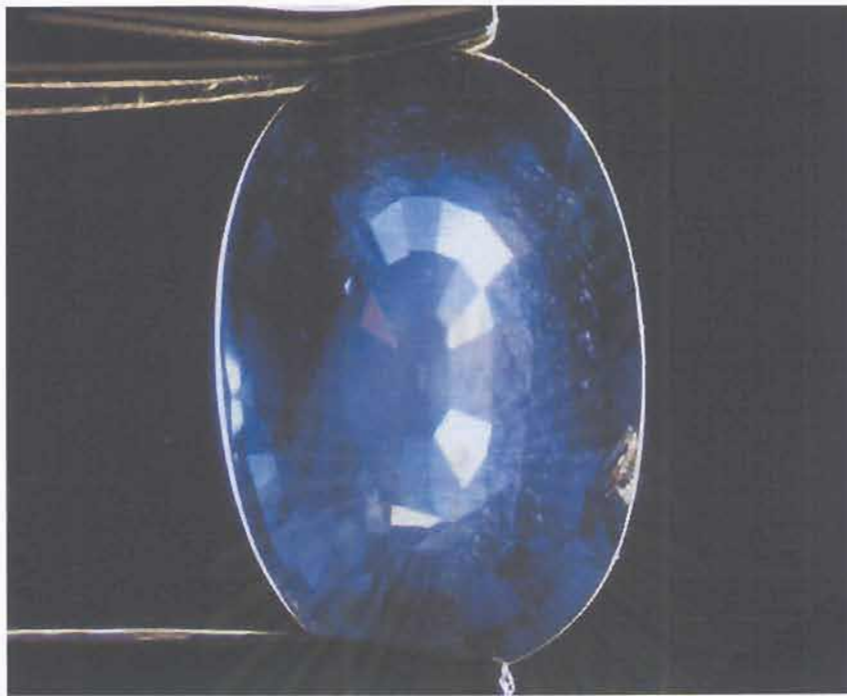


figure 7.7: This 3.25 ct un-heated Ilakaka blue sapphires with hazy appearance.



figure 7.8 The well-formed continuous long and sharp rutile silks and zones of dust particles of the un-heated stone.

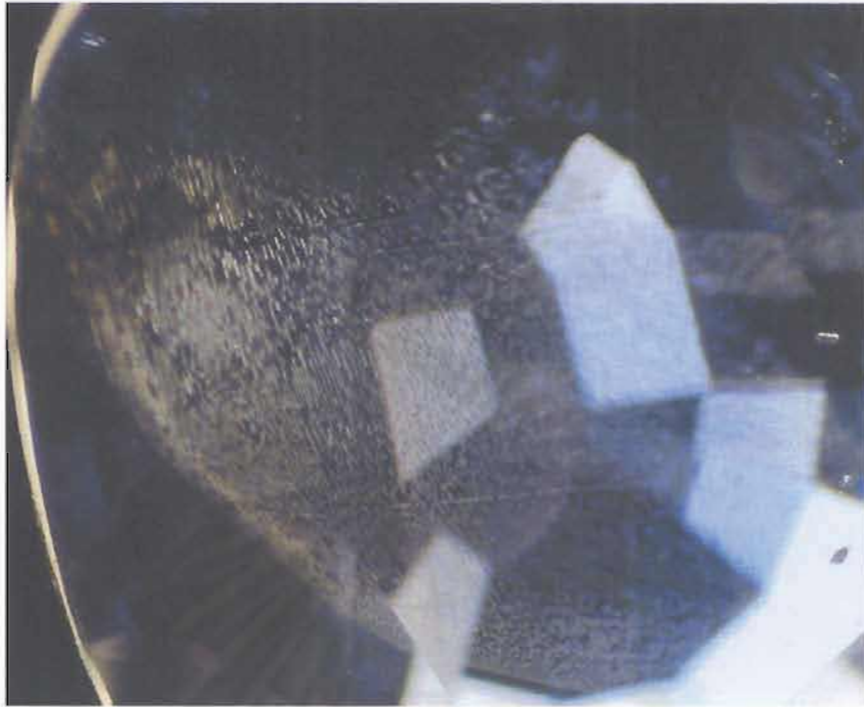


Figure 7.9: Well-formed fingerprints or healed fractures with sharp boundary in un-heated 3.43 ct blue sapphire.



Figure 7.10: Close-up of parallel long fluid inclusion fingerprint with sharp boundary.

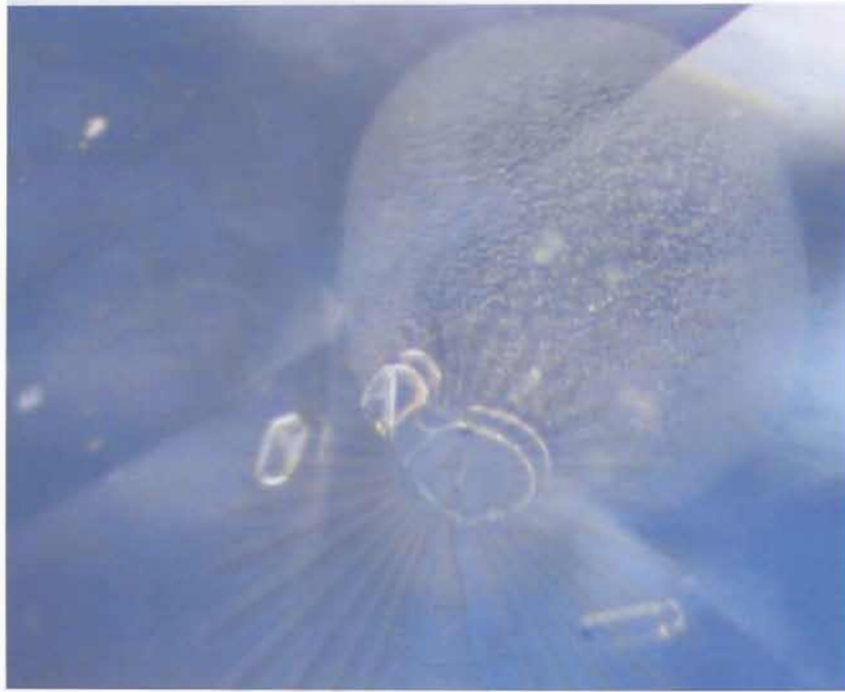


Figure 7.11: Sharp boundary and well formed negative (CO₂) inclusions in un-heated stone.



Figure 7.12: Yellowish orange colour impurity in healed fractures is also suggesting un-heated feature



Figure 7.13: Series of 16 un-heated blue sapphires ranging from pale to dark blue from Madagascar (with the courtesy from the Beauty Gems Co. Ltd.).



Figure 7.14: This 0.55 ct un-heated Mada sapphire showing bands of rutile dusts.



Figure 7.15: Within the bands of fine dust there are rutile needles cross-cutting in three directions at 60/120 angles.



Figure 7.16: An orangey brown inclusion (probably radioactive mineral) with tension cracks also found in un-heated sample.

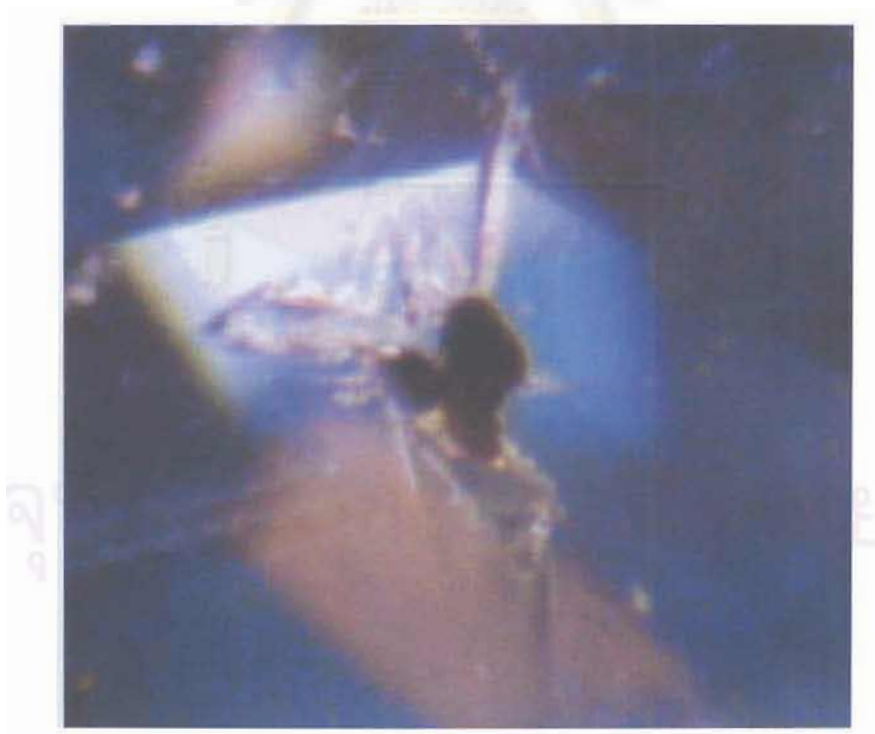


Figure 7.17: Another view of dark brown inclusions (rutile?) with negative crystal inclusions.

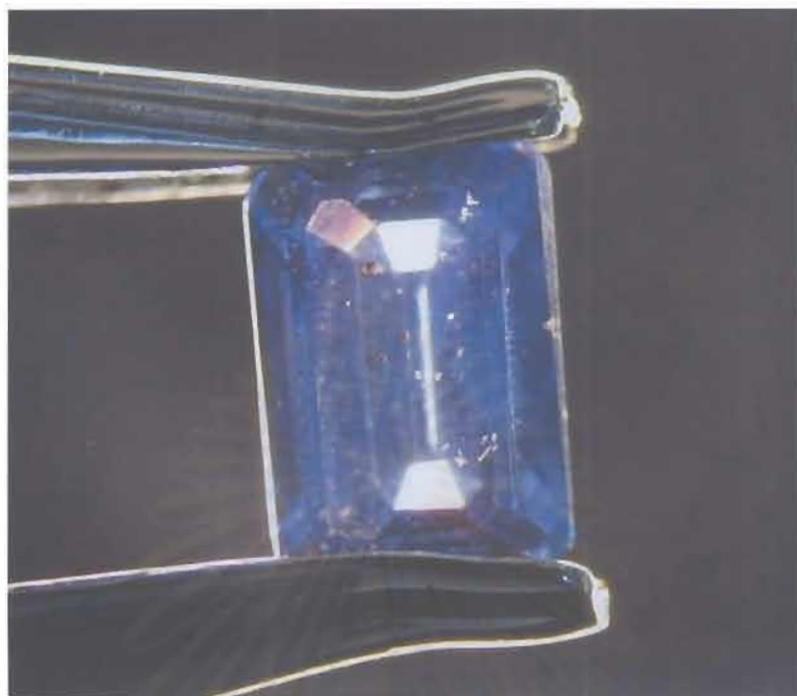


Figure 7.18: Another un-heated 0.74 ct Mada blue sapphire loaded with inclusions.



Figure 7.19: The colourless sillimanite inclusions (confirmed Raman) still well intact.

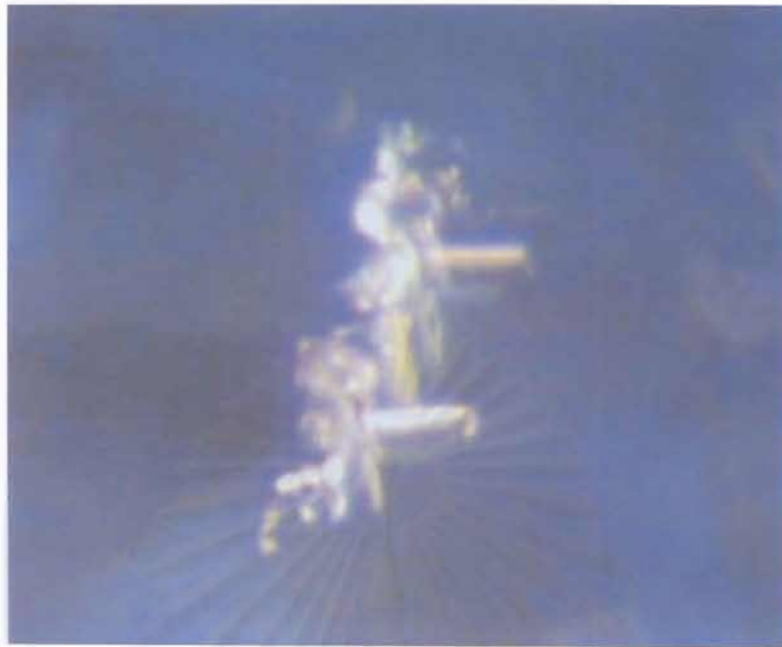


Figure 7.20: Another view of clusters of sillimanite inclusions .



Figure 7.21: The dark red inclusions of unknown mineral (cannot be confirmed by Raman) still well intact.



Figure 7.22: Silky appearance in the 0.38 ct un-heated Mada blue sapphire.

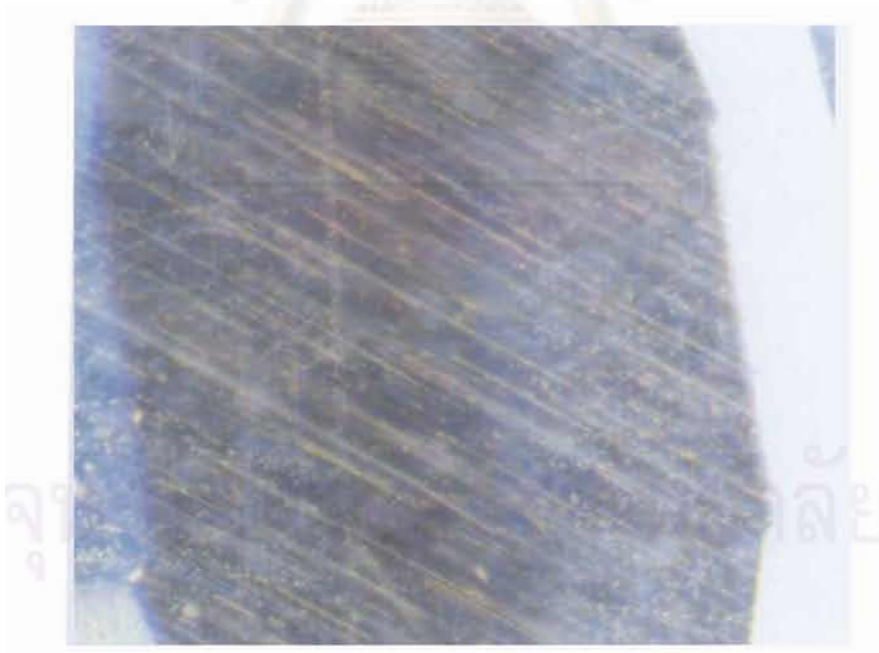


Figure 7.23: Long and continuous silks is a good indication of un-heated stone.

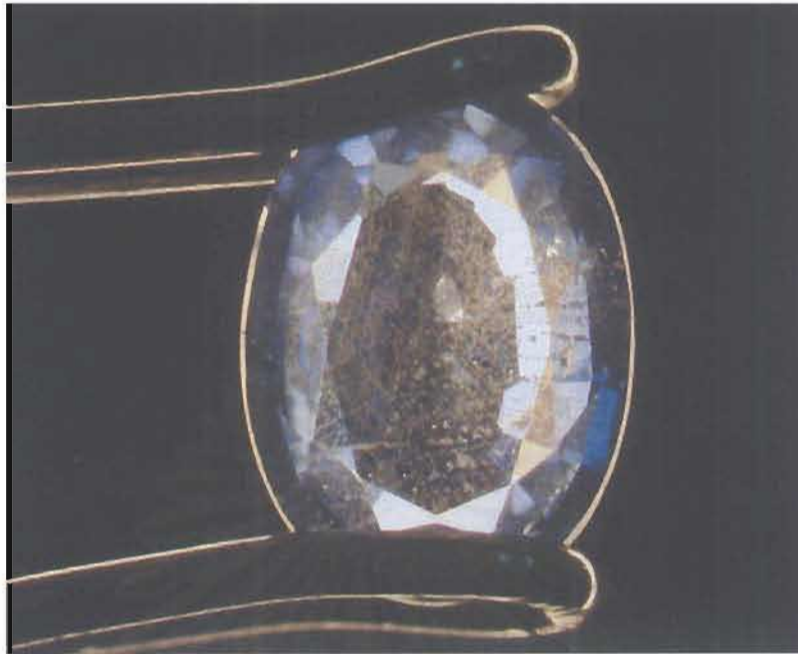


Figure 7.24: The 0.39 ct Mada blue sapphire showing long and short but continuous needles.

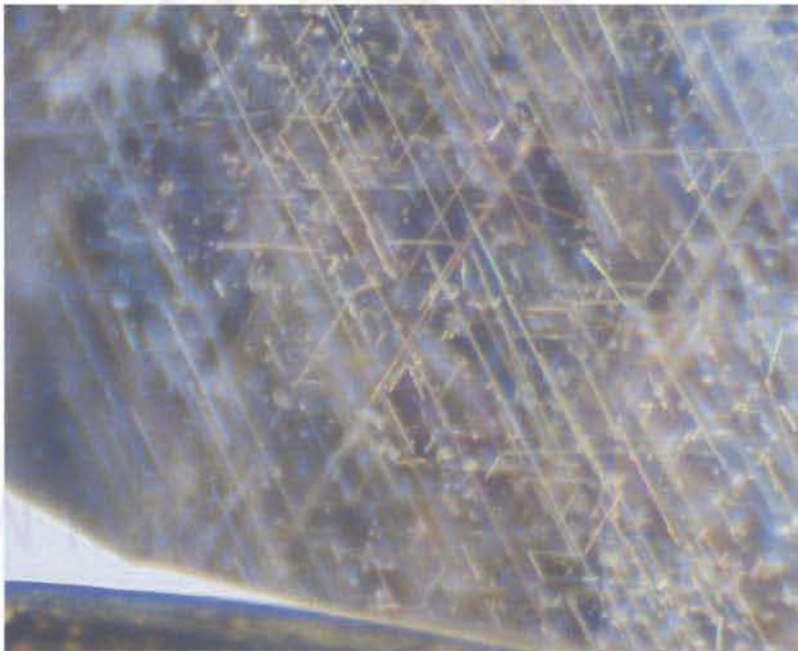


Figure 7.25: Close-up of continuous needles (more than three parallel sets) indicating of un-heating condition.



Figure 7.26: This 0.46 ct Mada blue sapphire contains many negative crystal inclusions or fluid inclusions in overall hazy or cloudy body.



Figure 7.27: Negative crystal inclusions containing CO₂, (confirmed by Raman) with naturally healed discoids still well intact in un-heated sample.



Figure 7.28: Another 1.06 ct Mada blue sapphire contains many long hollow tubes filled with impurity and well intact rutile silks.



Figure 7.29: The hollow tube filled with dark red impurity is a good indication of un-heated stone .



Figure 7.30: Overview of two heated Mada blue sapphires (4.84 ct left, 4.69 ct right).

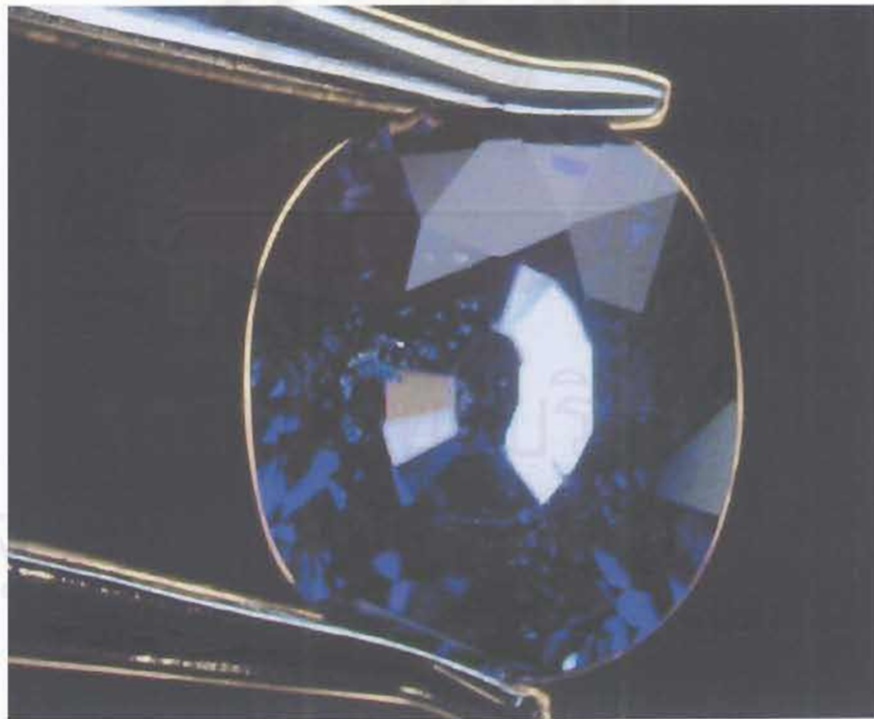


Figure 7.31: Magnification of the one on the right (4.69 ct) showing rather clear stone.



Figure 7.32: The stone shows obvious thin-film tension disc due to heating.



Figure 7.33: The shiny thin-film discoids surrounding altered turbid inclusions.

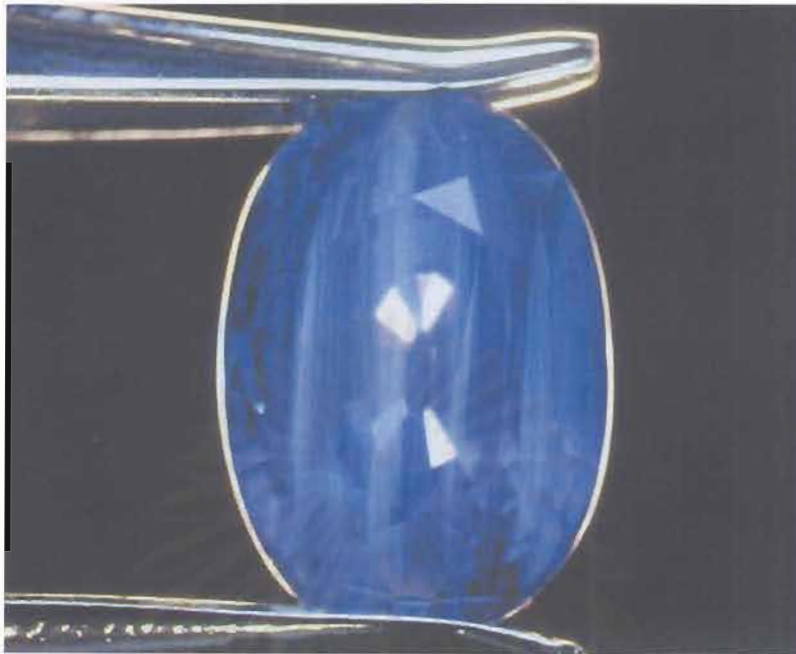


Figure 7.34: This heated Mada blue sapphires (4.84 ct) showing alternating milky and clear zones indicating that the strong milky zone still remain after heating.



Figure 7.35: Showing altered fingerprints.

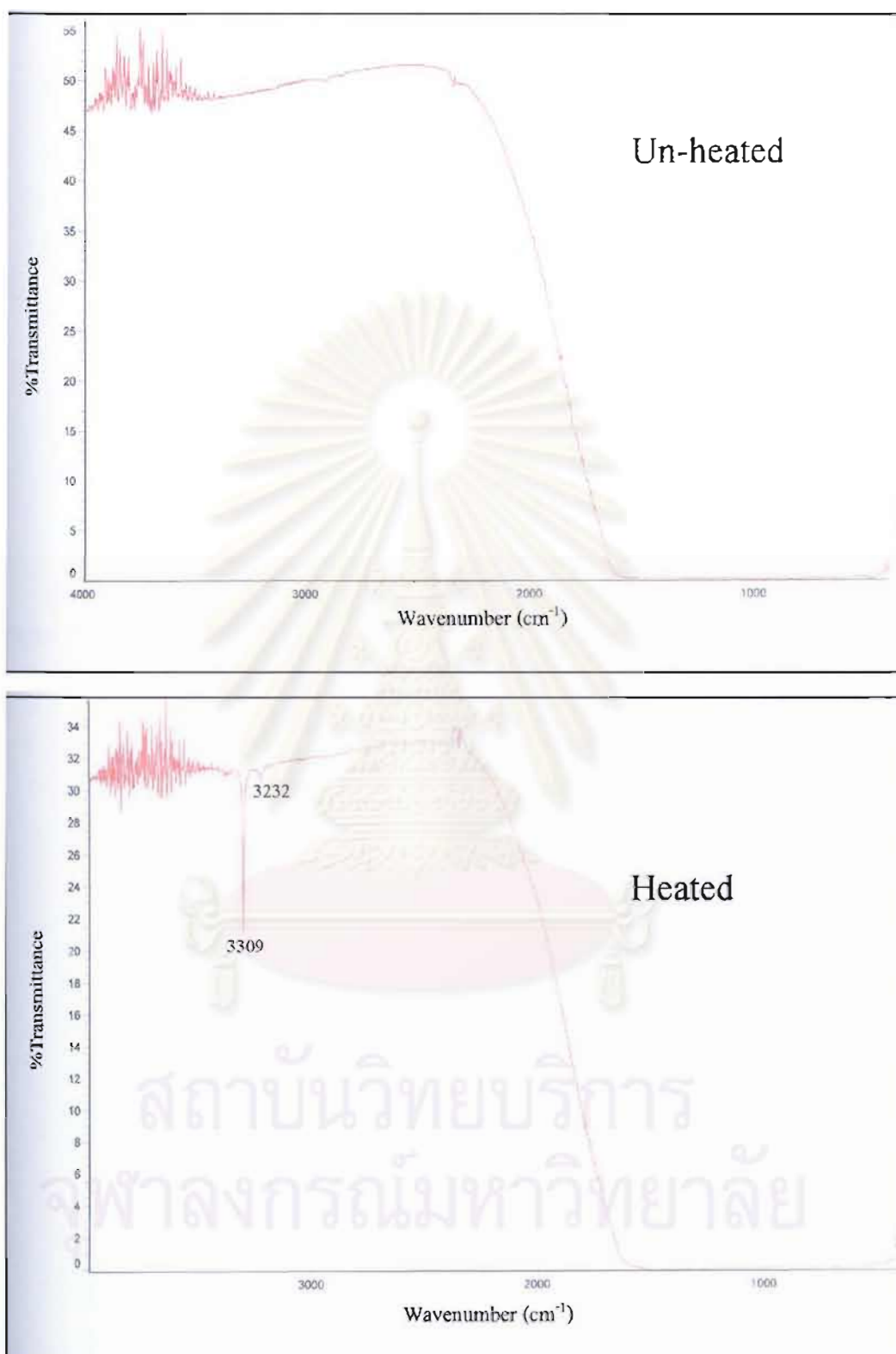


Figure 7.36: FTIR spectra of 4.18 ct un-heated (above) and 4.69 ct heated (below) blue sapphires from Madagascar. The un-heated one shows very weak OH-stretching peak at 3309 cm⁻¹ whereas the heated one shows very strong OH-stretching peak at 3309 cm⁻¹ and other side peaks.



Figure 7.37: Series of un-heated and heated Myanmar blue sapphires ranging from medium to dark blue (with the courtesy of World Sapphires Co. Ltd.).

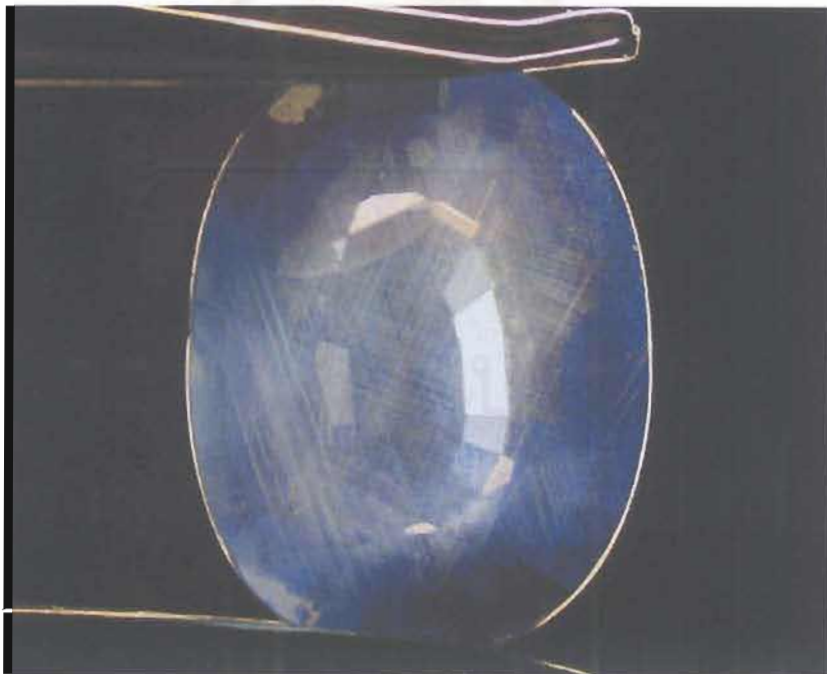


Figure 7.38: This 4.32 ct Myanmar blue sapphires showing long and sharp rutile silks with hazy appearance characteristic of natural un-heated stone.



Figure 7.39: The rutile silks or needles are long, well-formed and sharp with clear fingerprints.



Figure 7.40: Fingerprints or healed fractures are not uncommon in un-heated sample



Figure 7.41: Patchy long and sharp rutile silks are typical of un-heated Burmese 2.77 ct stone.



Figure 7.42: The rutile silks are long and sharp with arrow or knife-shape typical of un-beated stone.



Figure 7.43: This 21.89 ct Myanmar heated blue sapphire showing hazy appearance which might be mistaken as natural un-heating stone.



Figure 7.44: However when look closer the very fine rutile silks appear as dotted lines which would suggest the heated stone. The very fine milky growth bands may still remain after heat treatment.



Figure 7.45: The inclusion also show shiny tension disc indicating the heated stone.



Figure 7.46: Another inclusion with thin-film tension disc indicating the heated stone.

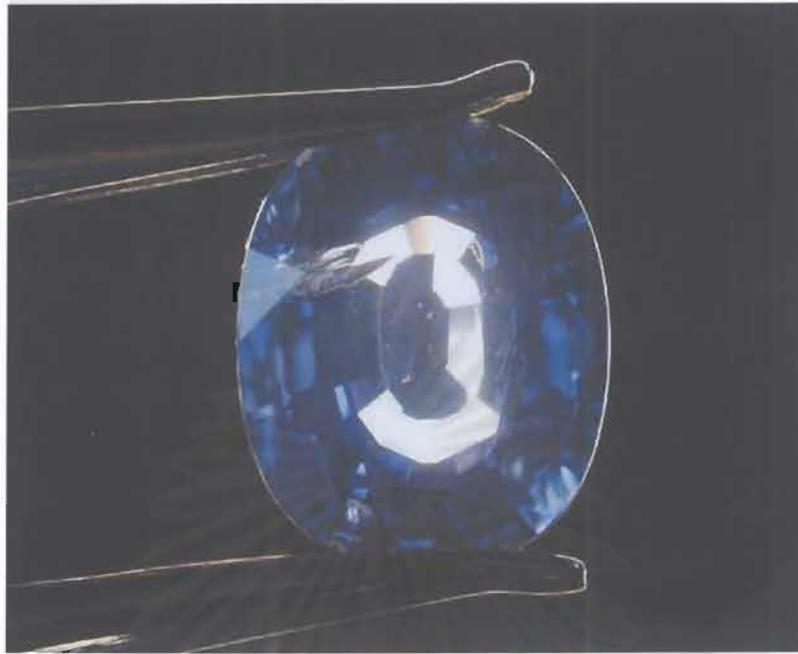


Figure 7.47: This 5.99 ct Myanmar heated blue sapphires showing slight hazy appearance.



Figure 7.48: strong thin-film discoids surrounding inclusion is a good indication of heating.



Figure 7.49: Altered fingerprints due to heating.



Figure 7.50: Shiny tension disc and dotted needles are obvious of heating.



Figure 7.51: This 2.74 ct Myanmar blue sapphires showing strong tension disc due to heating.

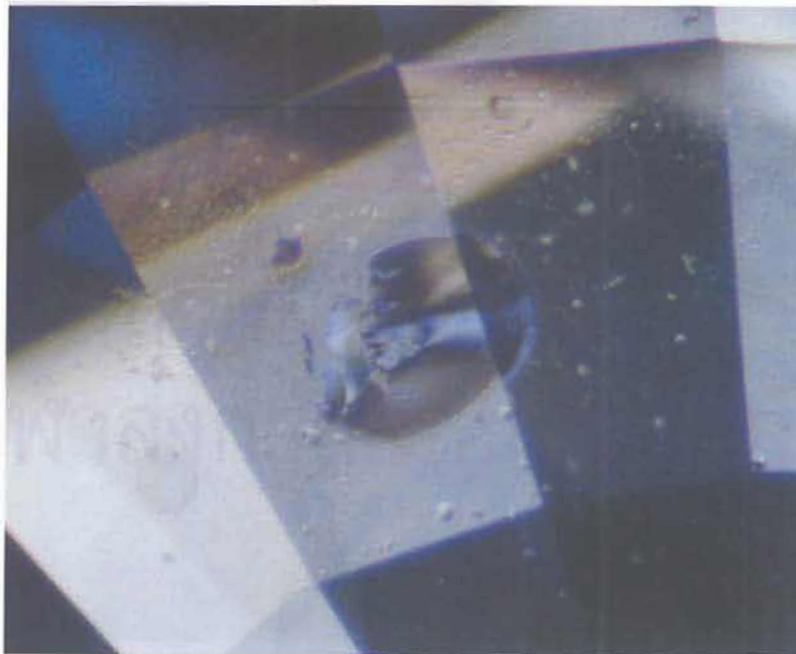


Figure 7.52: Thin-film tension disc is obvious of heating.



Figure 7.53: Shiny thin-film tension disc is obvious indication of heating.

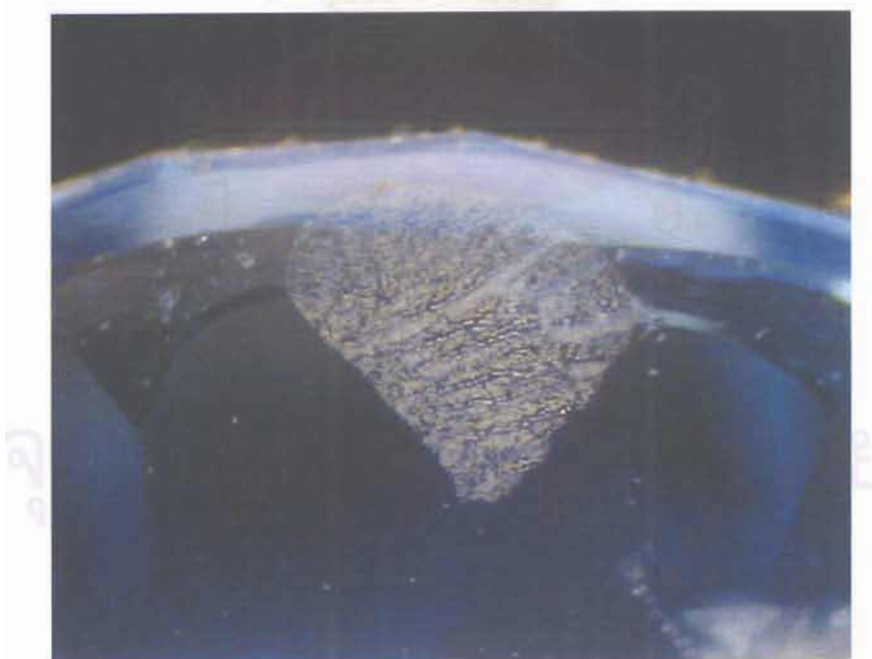


Figure 7.54: Obviously altered fingerprints due to heating

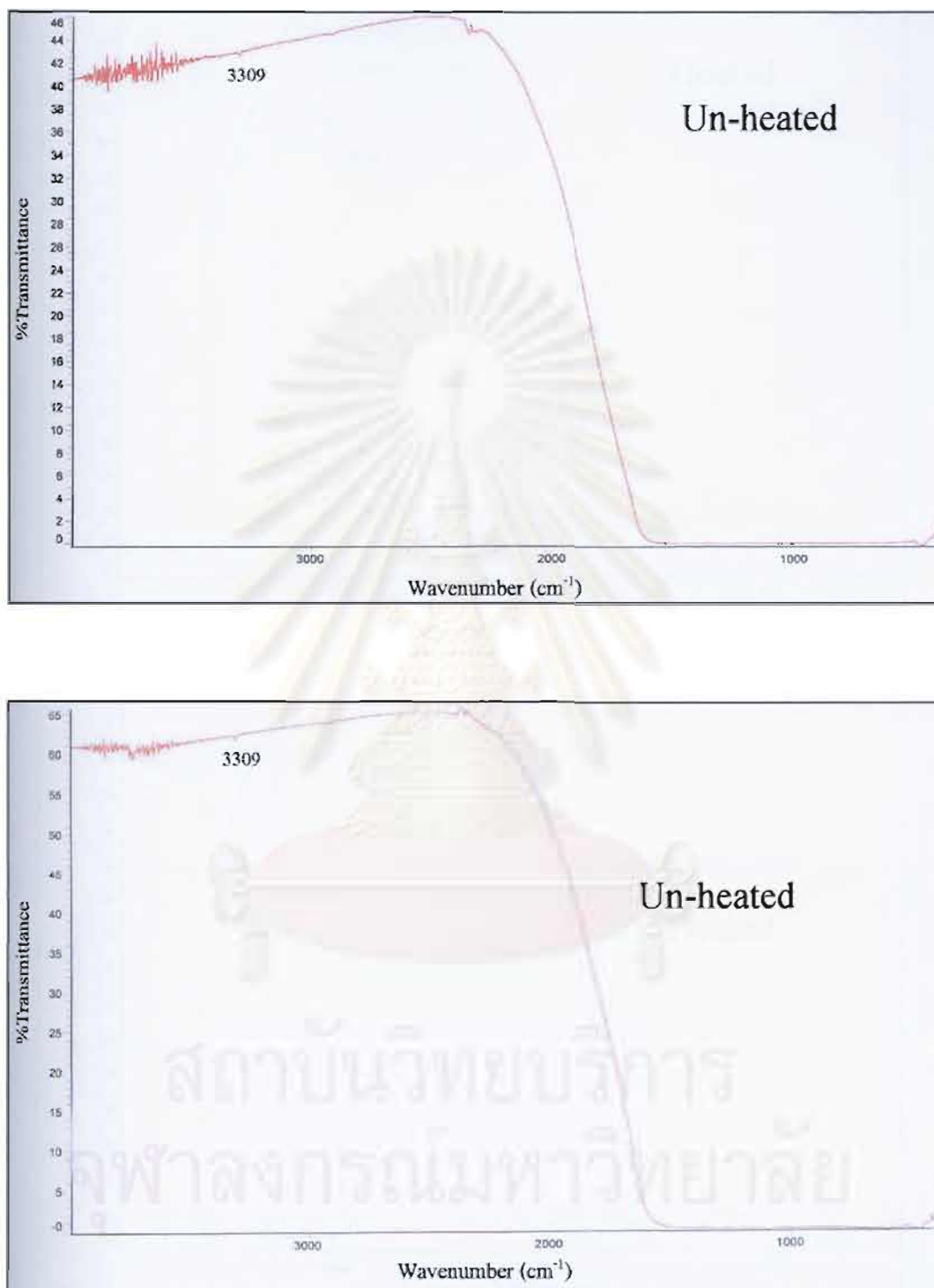


Figure 7.55: FTIR spectra of 4.32 ct (above) and 2.77 ct (below) un-beated blue sapphires from Myanmar showing vary small OH-streaching peak at 3309 cm⁻¹.

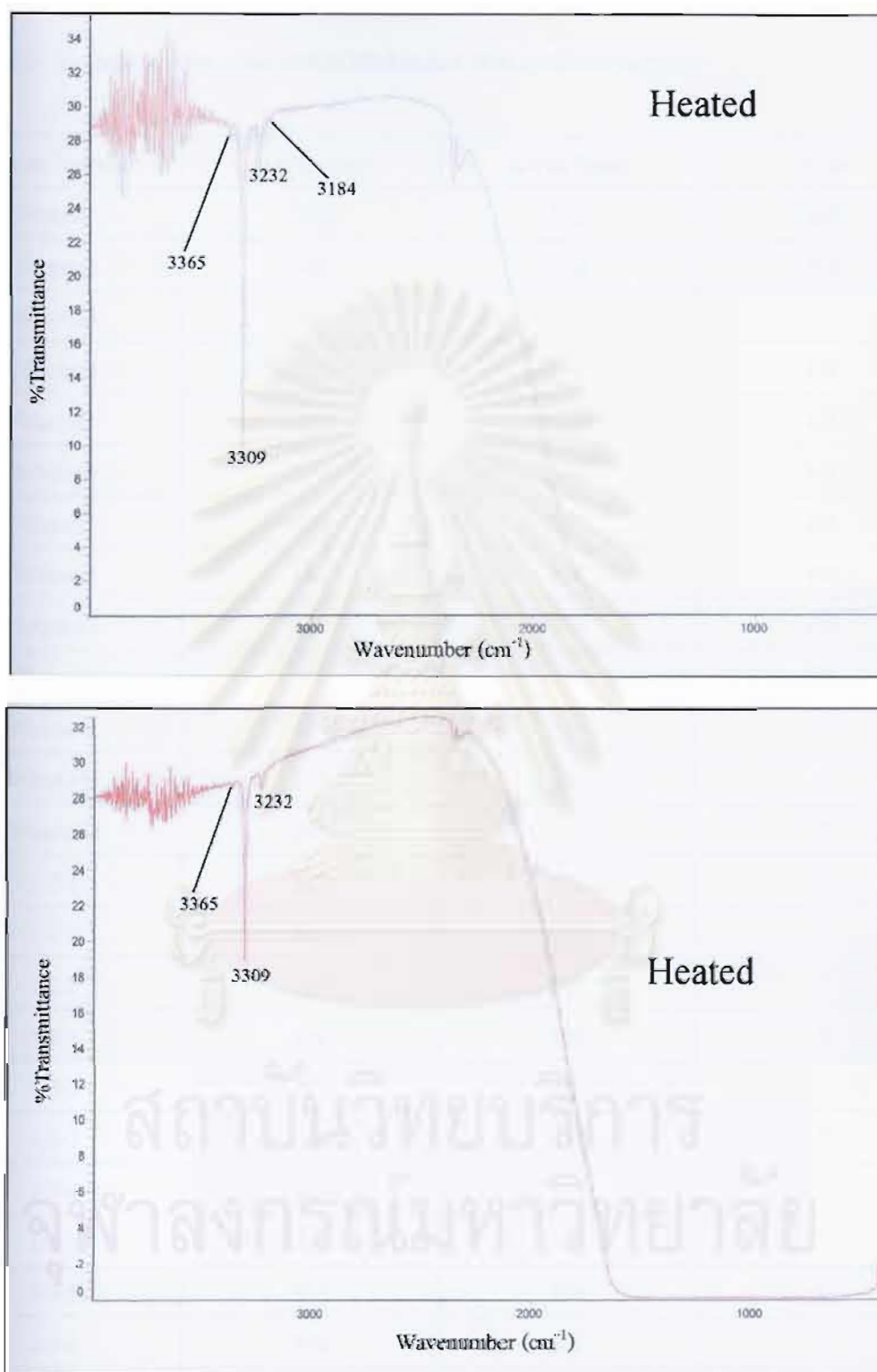


Figure 7.56: FTIR spectra of 21.89 ct (above) and 2.74 ct (below) heated blue sapphires from Myanmar showing very strong OH-stretching peak at 3309 cm⁻¹ and other side peaks.

Table 7.1: Extinction edge of un-heated Madagascar (Ilakaka) blue sapphires

Sample Number	O-ray (nm)	E-ray (nm)	Note
Wbsma1	328	333	OK
Wbsma2	345	336	OK
Wbsma3	312	312	?
Wbsma4	354	346	OK
Wbsma5	337	338	OK
Wbsma6	327	327	OK
Wbsma7	321	330	OK
Wbsma8	340	340	OK
Wbsma9	339	333	OK
Wbsma10	333	339	OK
Wbsma11	327	310	?
Wbsma12	310	324	?
Wbsma13	315	315	?
1-2-1	312	312	?
1-2-2	309	319	?
1-2-3	319	321	?
1-3-1	298	300	?
1-3-2	312	303	?
1-3-3	303	303	?
1-3-4	312	-	?
1-3-5	307	307	?
2-1-1	333	334	OK
2-1-2	306	306	?
2-1-3	340	340	OK
2-2-1	336	339	OK
2-2-2	318	322	?

Sample Number	O-ray (nm)	E-ray (nm)	Note
2-2-3	330	324	OK
2-3-1	313	312	?
2-3-2	331	334	OK

Table 7.2: Extinction edge of heated Madagascar (Ilakaka) blue sapphires

Sample Number	O-ray (nm)	E-ray (nm)	Note
Wbsma14	294	289	OK
Wbsma15	312	294	OK

Table 7.3: Extinction edge of un-heated Myanmar (Mokok) blue sapphires

Sample Number	O-ray (nm)	E-ray (nm)	Note
Wsbmg4	283	298	?
Wsbmg5	286	298	?

Table 7.4: Extinction edge of heated Myanmar (Mokok) blue sapphires

Sample Number	O-ray (nm)	E-ray (nm)	Note
Wsbmg1	303	297	OK
Wsbmg2	300	300	OK
Wsbmg3	300	297	OK
Wsbmg6	292	300	OK

Chapter 8

Ruby and Sapphire Treatments and Their Identification: A Summary of This Study and Other Recent Advancements

Introduction

Because of the scarcity of natural gem-quality ruby and sapphire, many treatment techniques have been practiced to improve inferior quality corundum for many centuries (Hughes, 1997). Among those treatments, 'classical' heating, flux-enhanced heating, shallow diffusion heating, deep diffusion heating and the most recent one Pb-glass filling are more common in the gem market whereas irradiation, dyeing, surface coating and composites are rarely encountered. Emphasis therefore will be given to the first categories.

'Classical' heating

The 'classical' heating has been widely used for enhancement of corundum to improve its color and clarity for some times (Figures 8.1a and b). The stones were heated in different types of high temperature (up to $\sim 1850^{\circ}\text{C}$) furnaces to control the atmosphere without addition of any chemical element. Various types of home-made furnace such as coke furnace, oil furnace, gas furnace and electric furnace, were invented and constantly modified, by trial and error, for treatment of corundum from many sources (Figure 8.2). Such furnaces are eventually proved to be practically low cost and economically suitable for heat treatment of corundum from various sources. This has been an appropriate proprietary among Thai heaters. The detection of heating in corundum is routinely accomplished with magnification by the presence of thermally altered inclusions, such as partially dissolved rutile-needles often with color bleeding, melted crystals, tension-discs surrounding inclusions, blue-halos surrounding Ti-bearing inclusions (Figures 8.3 to 8.10; see also Hughes, 1997; Themelis, 1992; Smith and McClure, 2002). These features are clearly different from those of un-heated stones (Figures 8.11 to 8.15).

Flux-enhanced heating

The flux-enhanced heating is a modification of the classical heating with addition of flux materials such as borax and/or silica to heal fissures or to fill open fractures or cavities. The purpose of the addition of the flux is to prevent a stone from fracturing during high temperature heating and to disguise fissures or fractures by infilling with higher refractive substances, thereby enhancing its clarity. This technique was firstly applied to Mong Hsu ruby which by its nature contained many fractures. Later this technique has also been used for stones from other sources. The treatment is routinely detected with magnification by the presence of flux materials in healed fissures and cavities as well as the presence of thermally altered inclusions as previously outlined (Figures 8.16 and 8.17; see also Hughes, 1997; Themelis, 1992; Themelis, 2004; Smith and McClure, 2002). Attempt has been made to quantify the amount of flux materials in a stone and notify in a gem identification report (see LMHC Information Sheet No.1, 2004: Figure 8.18).

Shallow diffusion heating

The shallow diffusion heating is also a modification of the 'classical' heat-treatment by heating an untreatable (by normal heating) colourless sapphire with color-causing compounds in a crucible. Titanium and iron compounds are commonly used for producing blue sapphires whereas chromium compound is for ruby. These transition elements can only diffuse into the stone and produce colors at very shallow depth (Figure 8.19). Hence the treatment is readily detected with immersion and magnification, by the presence of shallow color concentration at faceted junction, as well as with EDXRF, by the elevated content of those elements (Figures 8.20 to 8.22).

Deep diffusion heating

The deep diffusion heating involves a diffusion of light element, such as beryllium (Be), into a corundum lattice from an external source and is able to produce multitude of colours as shown in Figure 8.23. Be has been proved to take part in the color-causing mechanism in the treated stone, i.e., as a stabilizer of yellow color center (Pisutha-Armond et al., 2002, 2003, 2004a, 2004b) (Figures 8.24). Because of its small size, Be is able to permeate into the corundum lattice much deeper than Ti and Cr do.

As a result, deeper color penetration or even throughout the entire stone has been noticed. Therefore the detection of Be-treated corundum is readily done, with immersion and magnification, by the presence of surface-related color or relict blue zone surrounding by a white rim, occasionally with severely altered inclusions (Figures 8.25 to 8.30; see also Emmett et al., 2003; Peretti and Günther, 2002; Peretti et al., 2003; Themelis, 2003; Schmetzer and Schwartz, 2004, Atichat et al., 2004). However in a stone in which no diagnostic features are present, the treatment can be proved with the detection of elevated Be concentration in the level of ppm value in the stone by using laser induced breakdown spectroscopy (LIBS) –which becomes available in gemological laboratory recently (Figures 8.31 to 8.34; see Hanni et al., 2004)– or by using more sophisticate equipment such as laser ablation-inductively coupled plasma-mass spectrometry (LA-ICP-MS; Figures 8.35 and 8.36) or secondary ion mass spectrometry (SIMS).

Lead-glass filling

Lead-glass filling in ruby –the latest treatment for improvement of its clarity– appears in the gem market in the mid-2004 (Figure 8.37). This technique is similar to previously known fracture-filled treatment in diamond. The treatment involves filling fissures or open fractures with highly refractive glass, known as lead glass. The stones show minor effect from heating suggested very low temperature treatment. The light reflected from Pb-glass-healed fissures show blue-colored reflection, called flash effect (Figure 8.38). The presence of lead in the infilling glass is readily seen on surface or detected by EDXRF or seen in X-ray images (Figures 8.39 to 8.41; see also Kitawaki, 2004; Rockwell and Breeding, 2004, GIT Lab Notes, 2004).

References

- Atichat, W., Sriprasert, B., Wathanakul, P., Pisutha-Armond, V., Sun, T.T., Puttarat, T., Leelawatanasuk, T., 2004. Characteristics of “Beryllium” Heat-treated Yellow Sapphires. *Proceedings of the 29th IGC*, p. 207-214, Wuhan, China
- Emmett, J.L., Scarratt, K., McClure, S.F., Moses, T., Douthit, T.R., Hughes, R.W., Novak, S., Shigley, J.E., Wang, W., Bordelon, O. and Kane, R.E., 2003. Beryllium diffusion of ruby and sapphire. *Gems & Gemology*, **39**(2), 84-135
- Hanni, H.A., Krzemnicki, M.S., Kiefert, L. and Chalain, J.P., 2004. A new tool in analytical gemmology: LIBS. *Proceedings of the 29th IGC*, 63, Wuhan, China
- Hughes, R.W., 1997. *Ruby and Sapphire*. RWH Publishing, Boulder., 511p
- GIT Lab Notes, 2004. New treatment on ruby: lead glass filling <http://www.git.or.th>
- Kitawaki, H., 2004. Lead-glass impregnated ruby. *Gemmology*, Laboratory report of the month of May 2004, GAAJ, **35** (416), (in Japanese with English translation)
- LMHC. 2004. Laboratory Manual Harmonization Committee (LMHC) Information Sheet no. 1, <http://www.git.or.th>
- Peretti, A. and Günther, D., 2002. Colour enhancement of natural fancy sapphires with a new heat-treatment technique (part A). *Contribution to Gemology*, **1**, 1- 48
- Peretti, A., Günther, D., and Graber, A.-L., 2003. The beryllium treatment of fancy sapphires with a new heat-treatment technique (part B). *Contributions to Gemology*, **2**, 21-33
- Pisutha-Armond, V., Häger, T., Wathanakul, P., Atichat, W., 2002. A brief summary on a cause of colour in pink-orange, orange and yellow sapphires produced by the “new” heating technique. *Journal of Gem and Jewelry*, Gem and Jewelry Institute of Thailand (GIT), **3**(18), 11-12.
- Pisutha-Armond, V., Häger, T., Wathanakul, P., Atichat, W., 2004a. Yellow and brown colouration in beryllium treated sapphires. *Journal of Gemmology*, **29**(2), 77-103
- Pisutha-Armond, V., Haeger, T., Wathanakul, P., Atichat, W., Win, T.T., Leelawatanasuk, T., Somboon, C., Sutthirat, C., 2004b. Chemical Characteristic of “Classical” versus “Beryllium” Heat-Treated Ruby and Sapphire. *Proceedings of the 29th IGC*, 92-94, Wuhan, China
- Pisutha-Armond, V., Wathanakul, P., Atichat, W., Haeger, T., Win, T.T., Leelawatanasuk, T., and Somboon, C., 2003. Beryllium-treated Vietnamese and

- Mong Hsu rubies. In: Hofmeister W., Quang V.X., Doa N.Q., and Nghi T. (eds) *Proceedings of the 2nd International Workshop on Geo- and Material-Science on Gem-Minerals of Vietnam. Hanoi. October 1-8, 2003.* 171-5
- Rockwell, K. M. and Breeding, C. M., 2004. Rubies, clarity enhanced with a lead glass filler. *Gems & Gemology*, **40**(3), 247-249
- Schmetzer, K. and Schwarz, D., 2004. The causes of colour in untreated, heat treated and diffusion treated orange and pinkish orange sapphires – a review. *Journal of Gemmology*, **29**(3), 129-162
- Smith, C.P. and McClure, S.F., 2002. Chart of commercially available gem treatments. *Gems & Gemology*. **38**(4). 294-300
- Themelis, T., 1992. *The heat treatment of ruby and sapphire*. GemLab Inc., 244 p., RWFL Publishing
- Themelis, T., 2003. *Beryllium-treated rubies and sapphires*. 48 p., printed in Thailand
- Themelis, T., 2004. *Flux-enhanced rubies and sapphires*. 48 p., printed in Thailand



Figure 8.1a: Heat treatment of Madagascan sapphires to improve their color and clarity. (Photos by Somboon, GIT)



Figure 8.1b: Continued (Photos by Somboon, GIT).



Electric Furnace



Gas Furnace



Oil Furnace



Coke Furnace

Figure 8.2: Different types of high temperature (up to $\sim 1850^{\circ}\text{C}$) furnaces commonly used by Thai heaters. (Photos by Singbamroong, GIT)

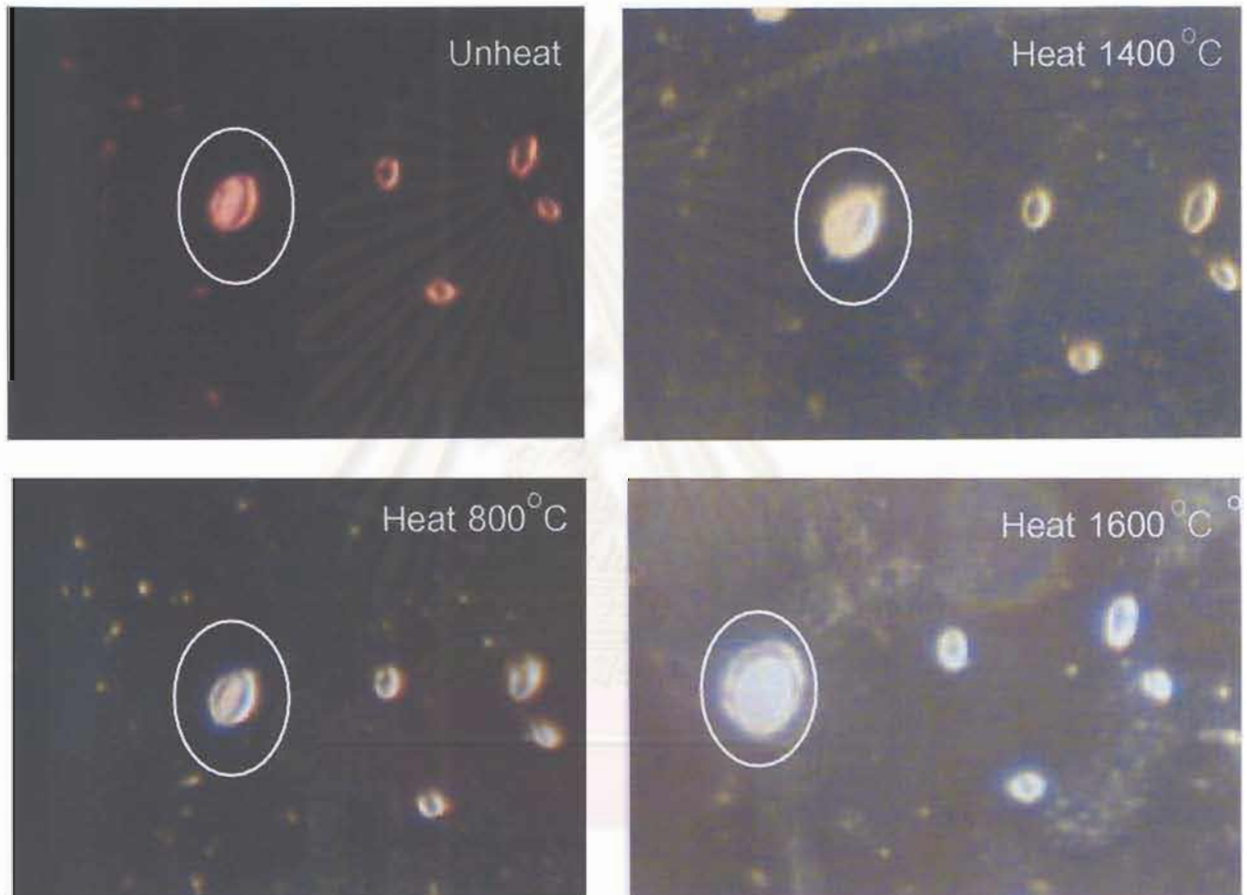


Figure 8.3: A clear zircon inclusion before treatment (in circle) became turbid with well developed tension crack after a stone was heated at 1600°C.
 (Sample no. LP9, 140X, Photos by Pattamalai, DMR)

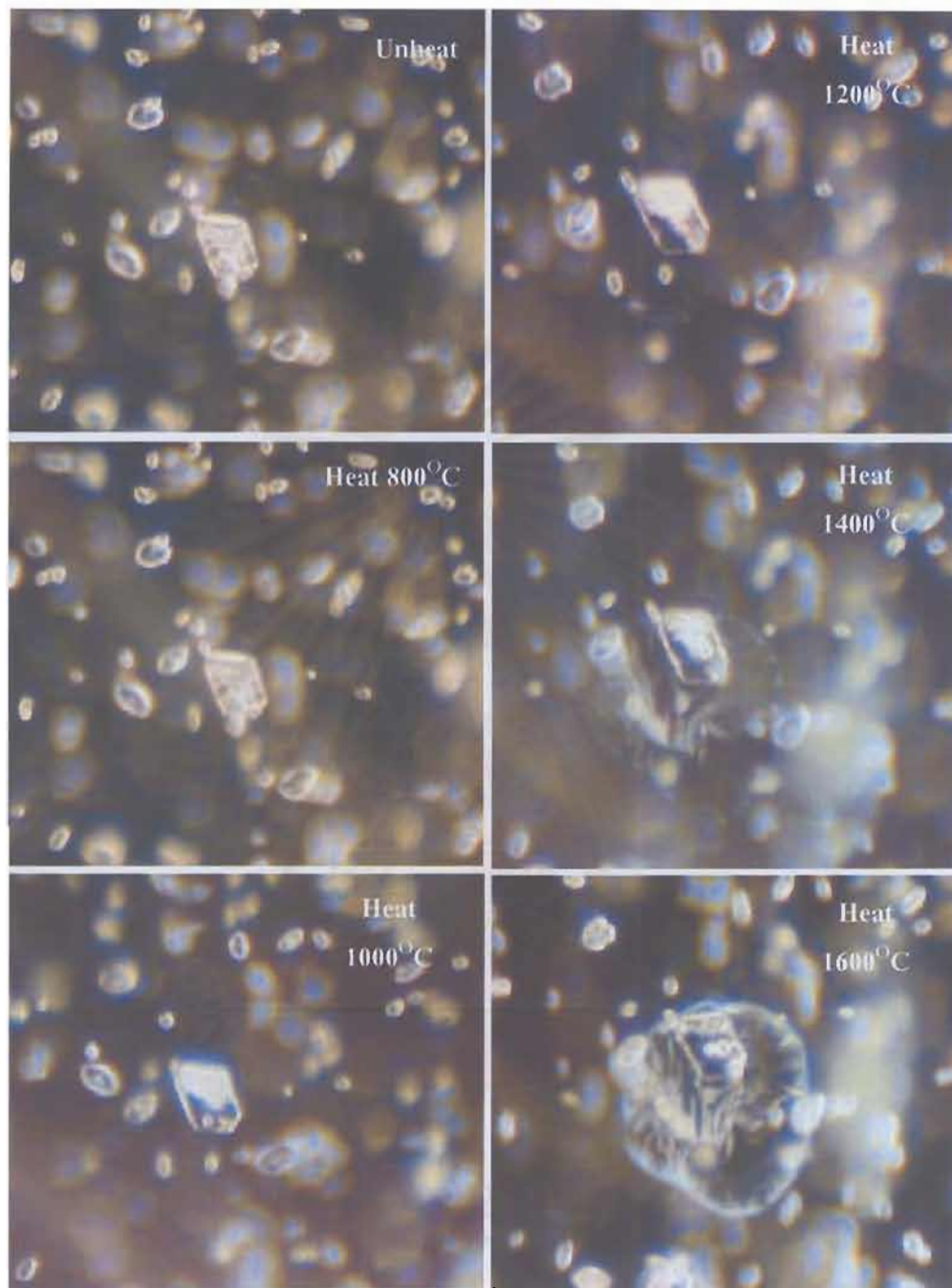


Figure 8.4: A mica inclusion was obviously altered with tension cracks at 1600°C (Photos by Pattamalai, DMR)

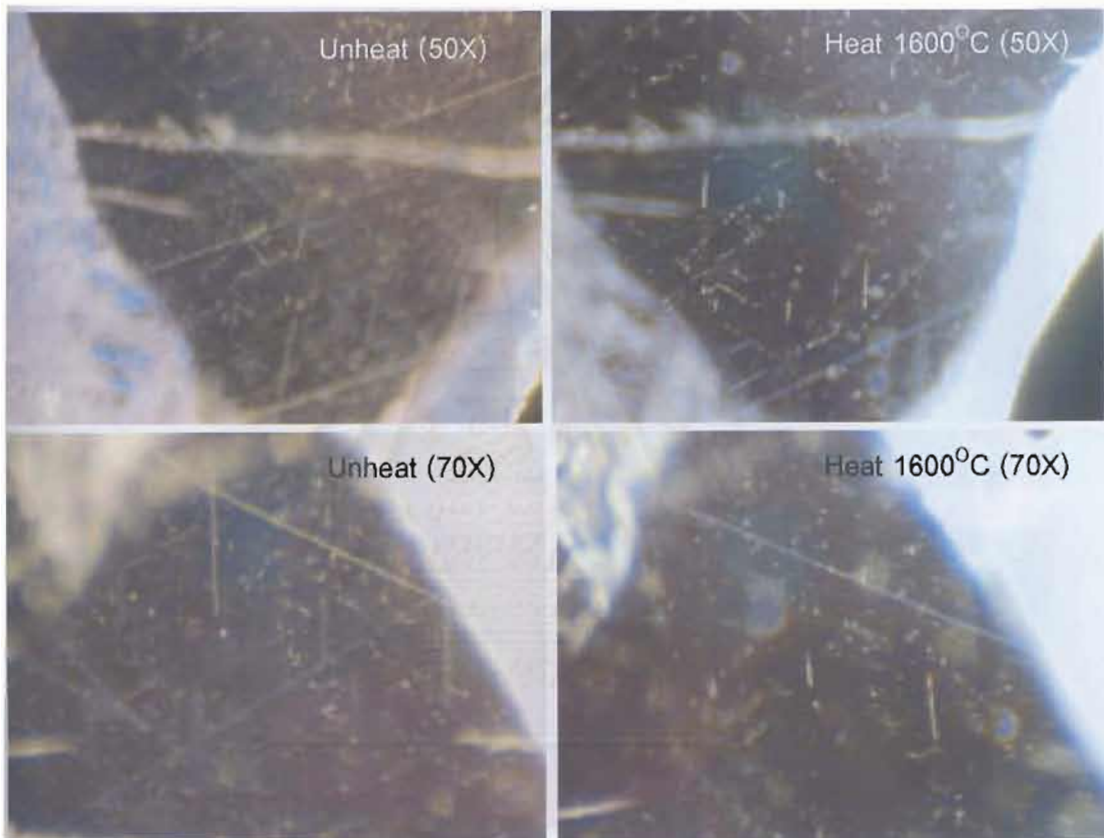


Figure 8.5: Needle inclusions were partially dissolved in the host sapphire creating dot-like pattern after a stone was heated at 1600°C.
(Photos by Pattamalai, DMR)

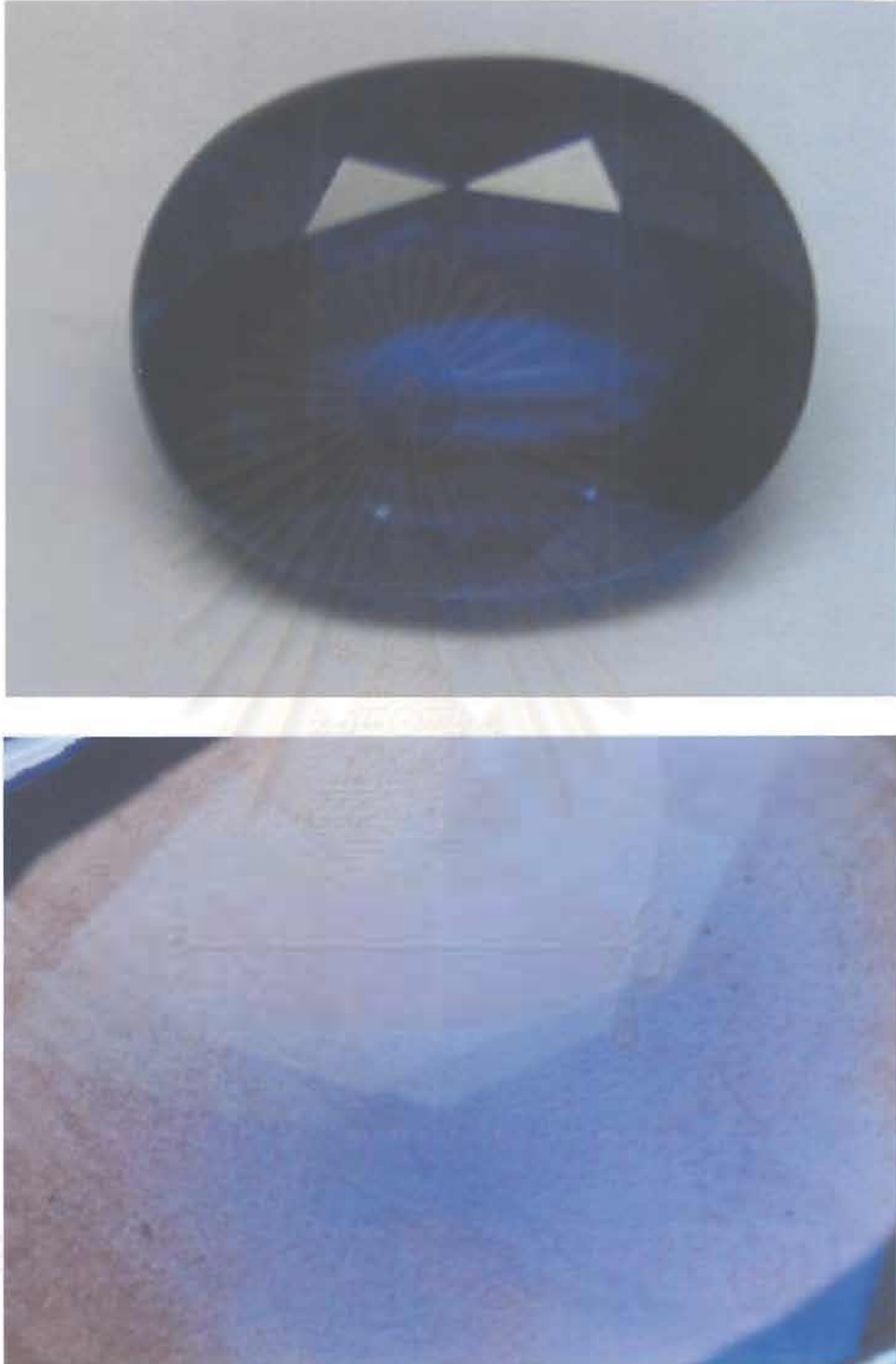


Figure 8.6: Partially dissolved rutile-needles with color bleeding.
(Photos by Somboon, GIT)

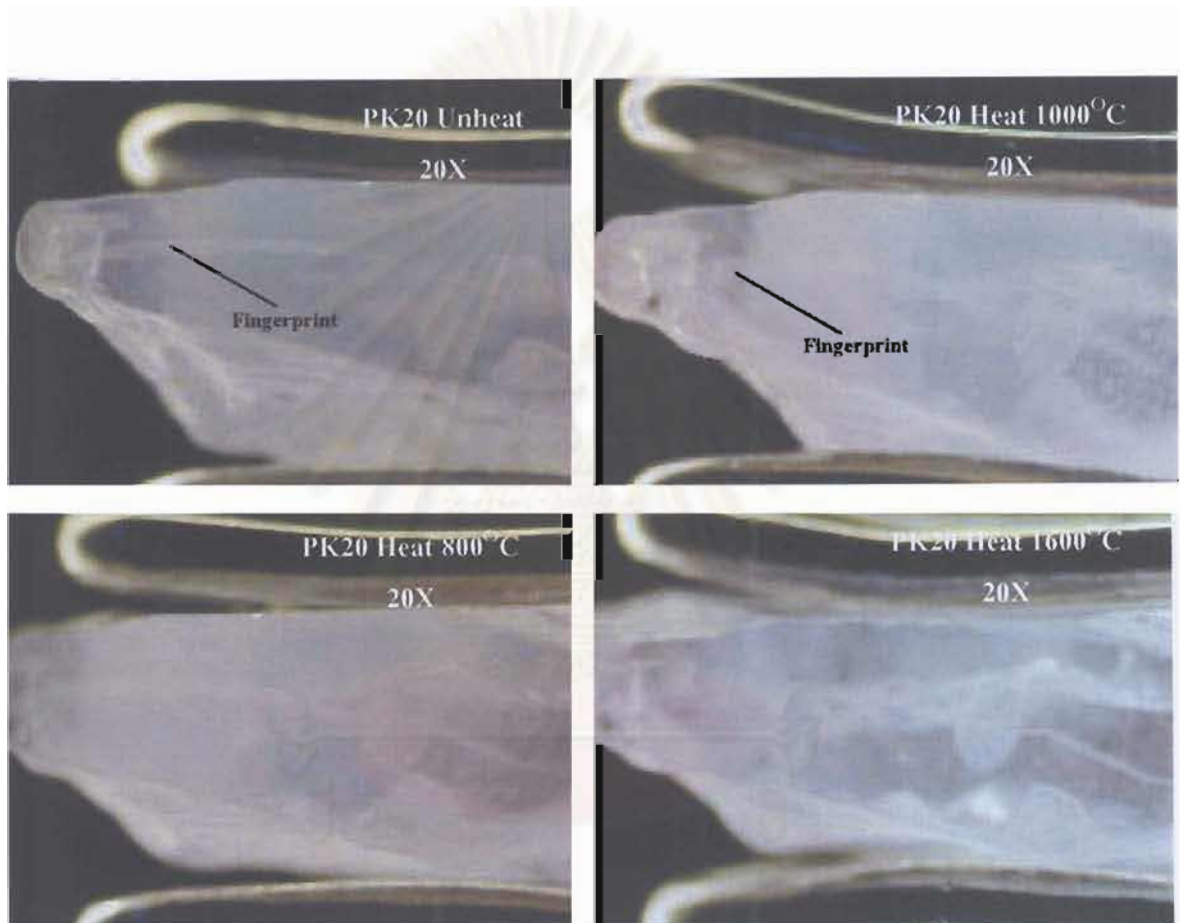


Figure 8.7: Milky and dust zones became clearer when a stone was heated at 1600°C.
(Photos by Pattamalai, DMR)

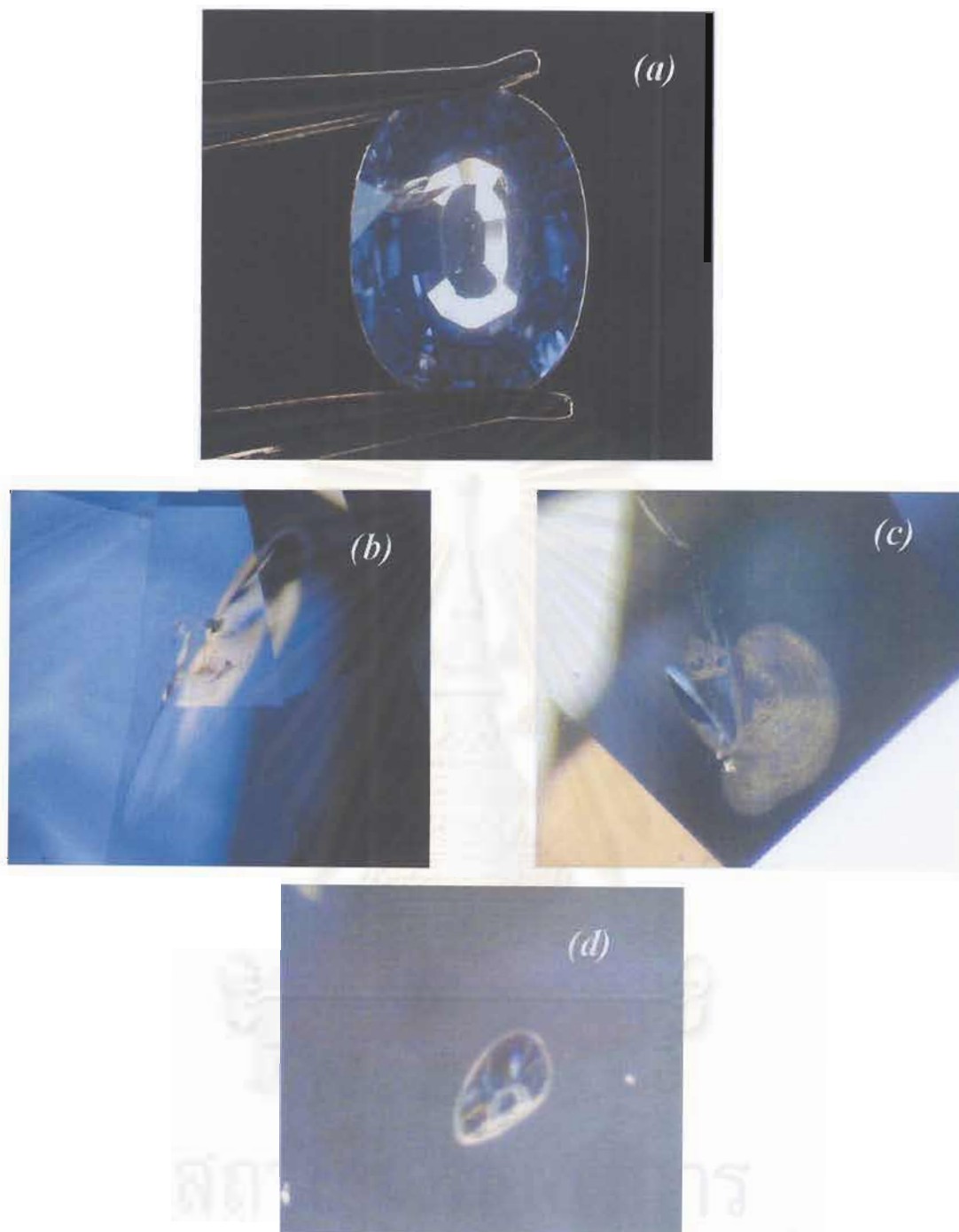


Figure 8.8: This 5.99 ct Myanmar heated blue sapphires showing slightly hazy appearance (a), strong thin-film discoid surrounding an inclusion is a good indication of heating (b), altered fingerprints are due to heating (c), a shiny tension disc and dotted needles are obvious indication of heating (d). (Photos by Somboon, GIT)



Figure 8.9: A 4.69 ct Mada sapphire showing rather clear stone. The stone shows obvious thin-film tension disc due to heating. (Photos by Somboon, GIT)

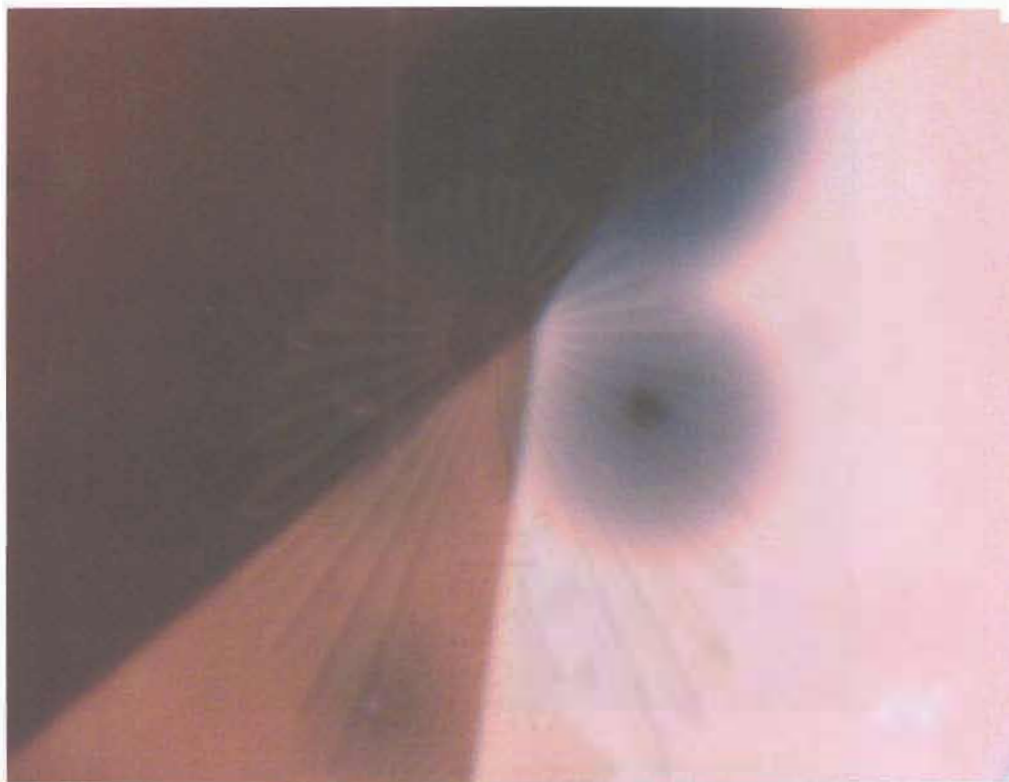


Figure 8.10: Internal diffusion of Ti from rutile inclusions into the corundum lattice showing the blue haloes (~ 0.06 mm) is a good indication of heating. (Photo by Häger).

สถาบันวิทยบริการ
จุฬาลงกรณ์มหาวิทยาลัย

Un-heated stones



Figure 8.11: Patchy long and sharp rutile silks in un-heated Burmese 2.77 ct stone. The rutile silks are long and sharp with arrow or knife-shape typical of un-heated stone. (Photos by Somboon, GIT)

Un-heated stones



Figure 8.12: This 3.25 ct un-heated Ilakaka sapphire shows hazy appearance. The well-formed continuous long and sharp rutile silks and zones of dust particles are typical of the un-heated stone. (Photos by Somboon, GIT)

Un-heated stones



Figure 8.13: This 0.46 ct Madagascan blue sapphire contains negative crystal inclusions filled with CO₂ (confirmed by Raman spectroscopy). The undisturbed fluid inclusions are a good indication of un-heated stone. (Photos by Sornboon, GIT)

Un-heated stones

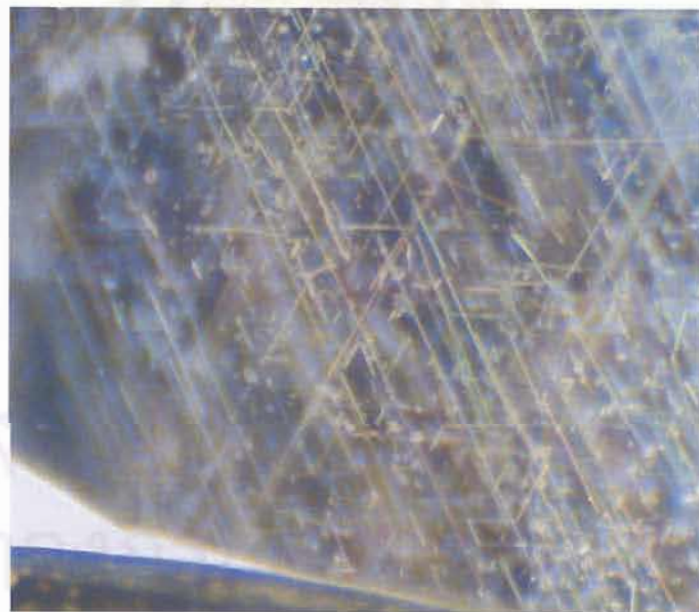
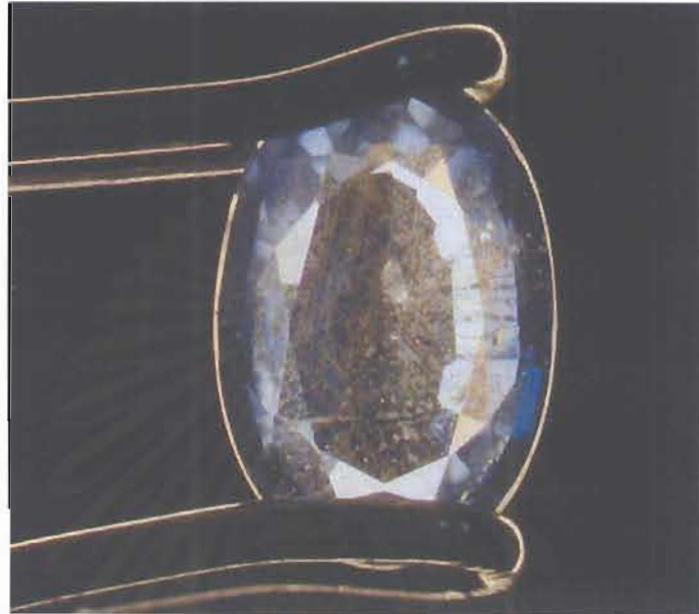


Figure 8.14: A 0.39 ct. Madagascan blue sapphire showing long and short but continuous needles. Continuous needles (more than three parallel sets) indicates an un-heating condition. (Photos by Somboon, GIT)

Un-heated stones

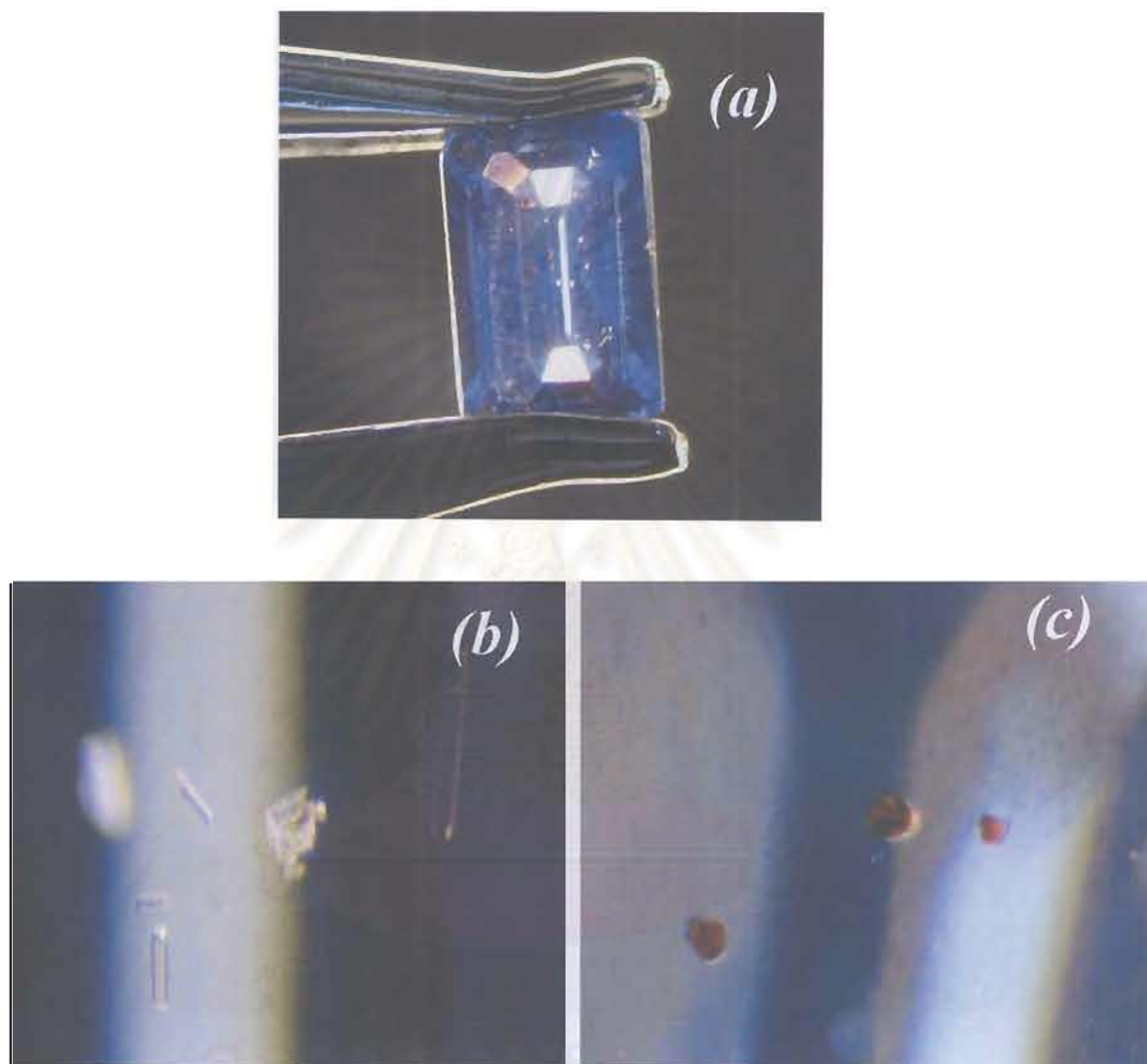


Figure 8.15: An un-heated 0.74 ct Madagascan blue Sapphire contains numerous inclusions (a). The colourless sillimanite inclusions (confirmed Raman spectroscopy) still well intact (b). The dark red inclusions of unknown mineral (cannot be confirmed by Raman spectroscopy) still well intact (c). (Photos by Somboon, GIT)

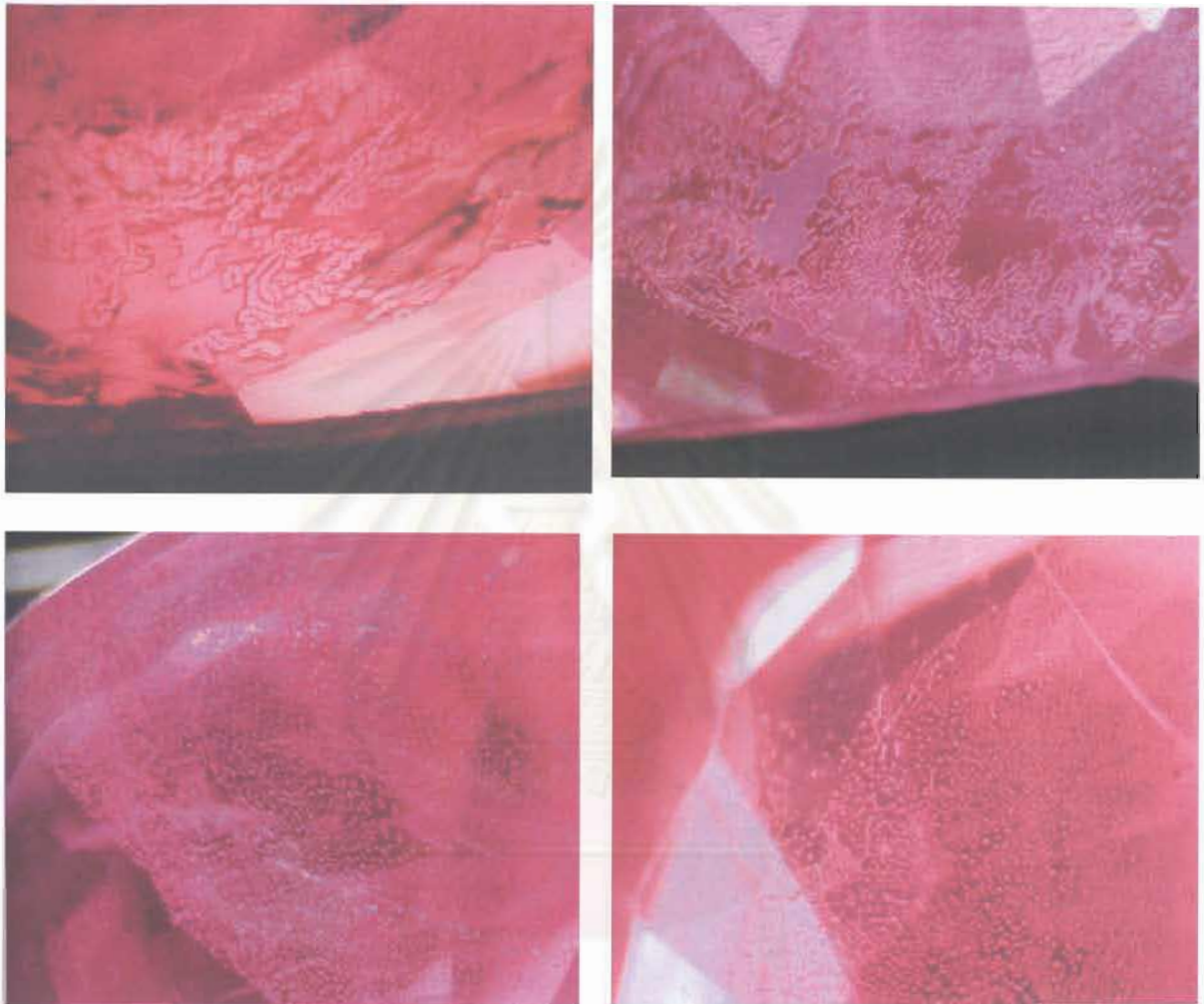
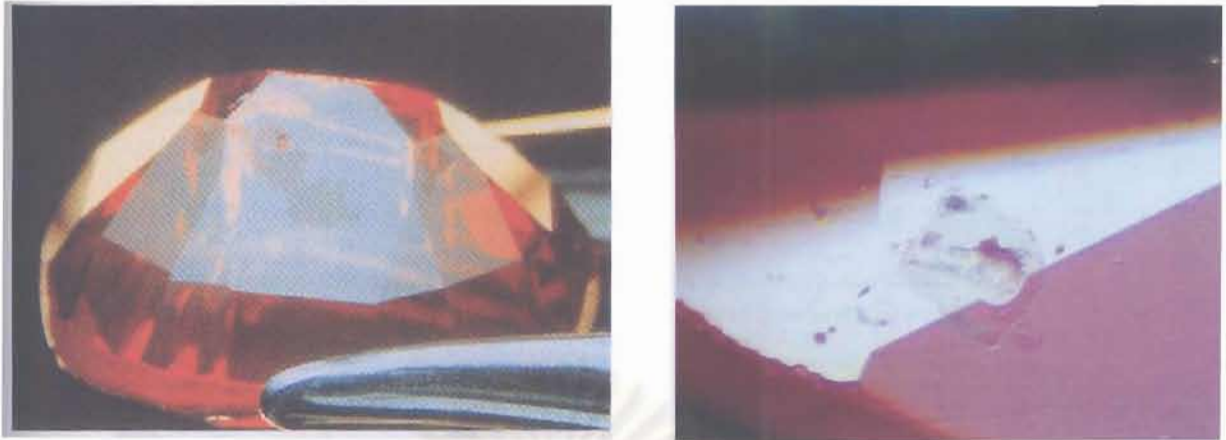


Figure 8.16: The presence of flux residues in healed fissures is a good indication of a flux-enhanced heating. (Photos by Leelawathanasuk,GIT)



(Hughes, 1997)



(Photos by Leelawathanasuk, GIT)

Figure 8.17: Cavity-filling flux-residues appear lower luster reflection on polished surface.

L M H C I n f o r m a t i o n S h e e t # 1

Standardised Gemmological Report Wording (implementation beginning February, 2004)

Corundum with residues from the heating process present in healed fissures and/or cavities

Members of the Laboratory Manual Harmonization Committee (LMHC) have standardized the nomenclature that they use to describe heat treatment in corundum and the degree to which fissure "healing" has occurred, and the residues that remain within the healed fissures and cavities, following the heating of corundum.

Healed fissures:

Any corundum that shows indications of heat treatment and a degree of healing along (previous) fractures - see Figure 1 - which also contain residue from the heating process, shall be described as « species » 'natural corundum', « variety » 'ruby' or 'sapphire' « comments » 'indications of heating' (to modify the colour or transparency of the stone), plus the appropriate residue quantification terminology - alpha numeric and/or text description¹. See Table 1 and examples in figures 2a, 2b, 2c and 3.

Note 1: As an option, e.g., for "simplified reporting" situations, the quantification of residues in healed fissures may be replaced by the statement "residues in healed fissures".

Note 2: wording in parenthesis is optional

Note 3: This clause may include the presence of small filled cavities

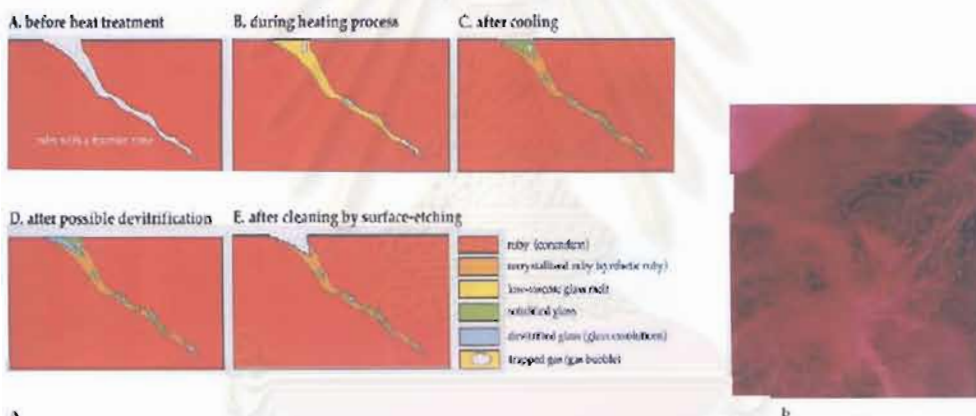


Figure 1: Flux assisted healing of a fracture during the heating process. A fracture that has been healed by the synthesis of corundum or other materials during the heat treatment or crystal growth processes. (Hännel, H.A., 1968) (a) schematic (b) actual

Table 1 Residue quantification terminology

Status →	No indications of heating	Indications of heating (no residue)	Indications of heating with residues in fissures				
	NTE	TE	TE1	TE2	TE3	TE4	TE5
Report Alpha numeric →			Minor residue in fissures		Moderate residue in fissures		Significant residue in fissures
Report Text →	No indications of heating	Indications of heating					
Status →	Indications of heating with residues in cavities						
	C1	C2	C3				
Report Alpha numeric →							
Report Text →	(Minor) Residue in cavities	(Moderate) Residue in cavities	(Significant) Residue in cavities				

Wording in parenthesis optional

¹ In the cases of TE1 and TE2 (minor) or TE3 and TE4 (moderate), when the text version is selected a reference to the specific alpha-numeric shall be indicated either by combining the two or placing an « x » in the appropriate point of the comparative scale.

Figure 8.18a: A quantification of the amount of flux materials in a stone

© 2004. The Laboratory Manual Harmonization Committee

Members of the LMHC determine which of the residue quantification terminology to use (see table 1) taking into account the size and position of each healed feather and the nature of the residue that remains. This residue may be comprised of structures ranging from a fine bubble-like network with very little 'thickness' to numerous lake-like structures that may have a considerable thickness (see examples in figures 2a, 2b, 2c and 3).

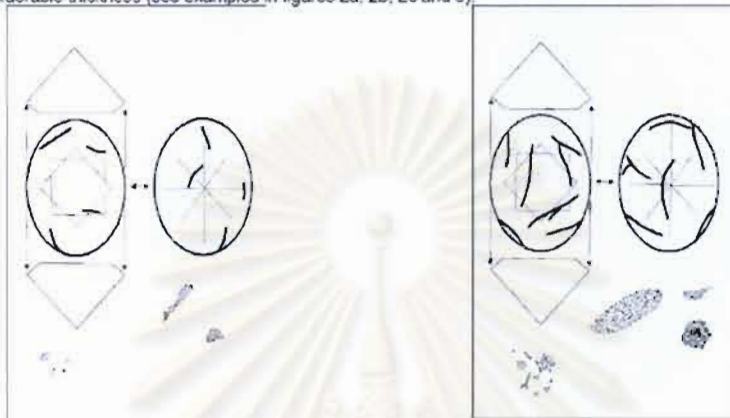


Figure 2a Minor residue (TE1) in this example consisting of fine bubble-like structures:

Figure 2b Moderate residue (TE3) in this example consisting of coarse bubble-like structures and films:



Figure 2c Significant residue (TE5) in this example consisting of coarse and thick film-like structures

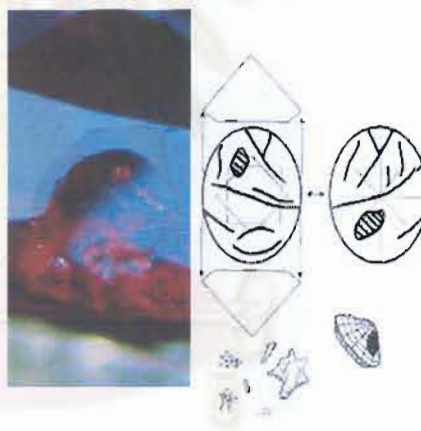


Figure 3 Significant residue (TE5) in this example consisting of coarse and thick film-like structures together with a large glass-filled cavity (C3) (example image left)

Filled cavities:

Any corundum that shows indications of having undergone heat treatment and the presence of a vitreous residue in a cavity(ies), shall be described as « species » 'natural corundum', « variety » 'ruby' or 'sapphire' « comments » « 'indications of heating', plus the appropriate quantification terminology - alpha numeric and/or text description. Table1 outlines the use of the designated alpha numerics or text descriptions and figure 3 gives an example of a typical situation.

©2004 Laboratory Manual Harmonization Committee. This document may be freely copied and distributed so long as it is reproduced in its entirety, complete with this copyright statement. Any other reproduction, translation or abstracting is prohibited without the express written consent of the Laboratory Manual Harmonization Committee.

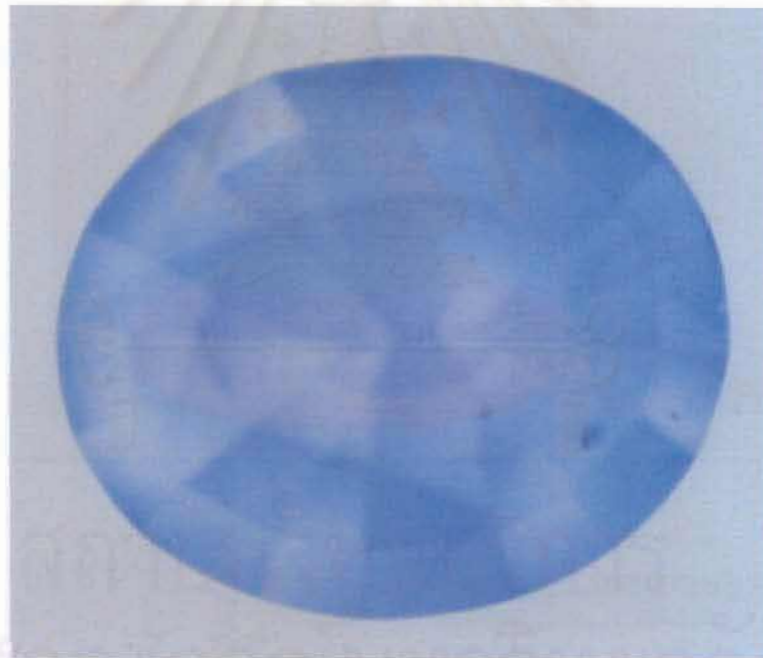
All rights jointly reserved by:

AGTA-Gemological Testing Center (USA), CISEM (Italy), GAAJ Laboratory (Japan), GIA-Gem Trade Laboratory (USA), GIT-Gem Testing Laboratory (Thailand), Gübelin Gem Lab (Switzerland), SSEF Swiss Gemmological Institute (Switzerland)

Figure 8.18b: Continued



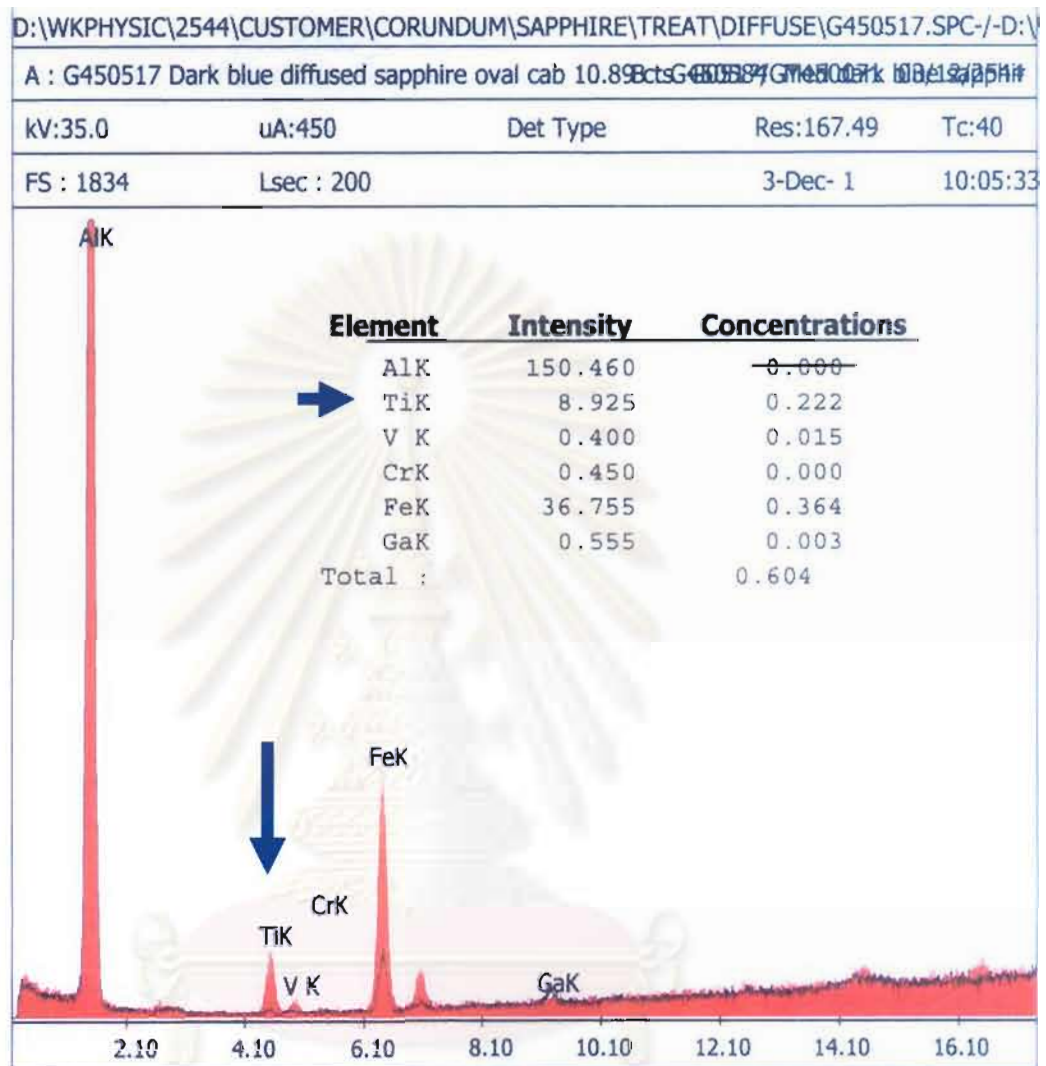
Figure 8.19: Blue-diffused sapphires showing slices of colourless interior with blue rim (~ 0.09 mm) caused by external diffusion of Ti into the stones.



Immersion

Figure 8.20: A parcel of blue-diffused sapphires (a). The presence of uneven shallow color concentration at different facets and faceted junctions of a blue-diffused sapphire in immersion. (Photos by Somboon, GIT)

A blue-diffused sapphire



An un-treated sample

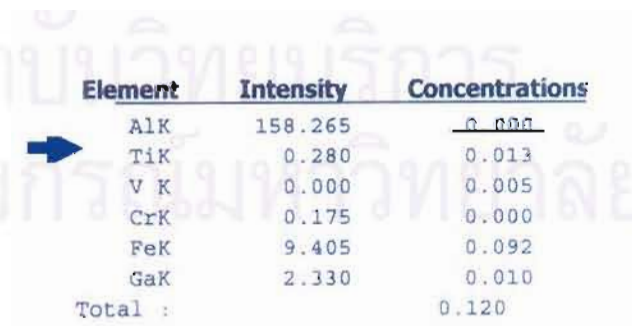


Figure 8.21: An elevated concentration of diffused Ti can be detected using EDXRF



Figure 8.22: A parcel of diffused rubies showing uneven shallow color concentration at different facets . (immersion: Hughes. 1997)



Figure 8.23: Multitude of colours in Be diffusion-treated sapphires such as pink-orange, orange, yellow and orangey red. (Photos by Somboon, GIT)



Figure 8.24: Stones before treatment and after treatment with Be



Figure 8.25: Surface-related colour zone is a diagnostic features of yellow Be-diffusion treated sapphires. (Immersion: Photos by Leelawatanasuk, GIT).

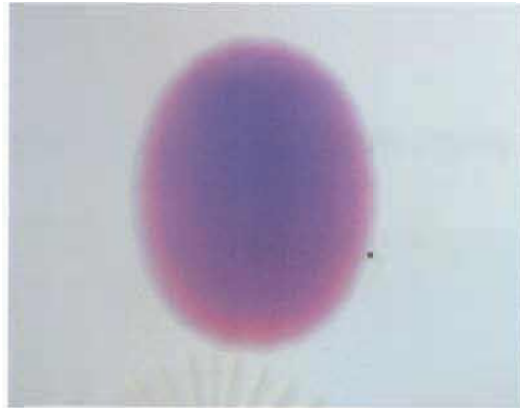


Figure 8.26: Surface-related colour zones in pink-orange sapphires.
(Immersion; Photos by Somboon, GIT)

daylight

Immersion (with blue filter)



A brownish yellow sapphire from Diego



A yellow sapphire from Songea

Figure 8.27: Blue-green patch surrounding by a white zone is a good indication of yellow Be-diffusion treated sapphires. (Photos by Puttharat,DMR)

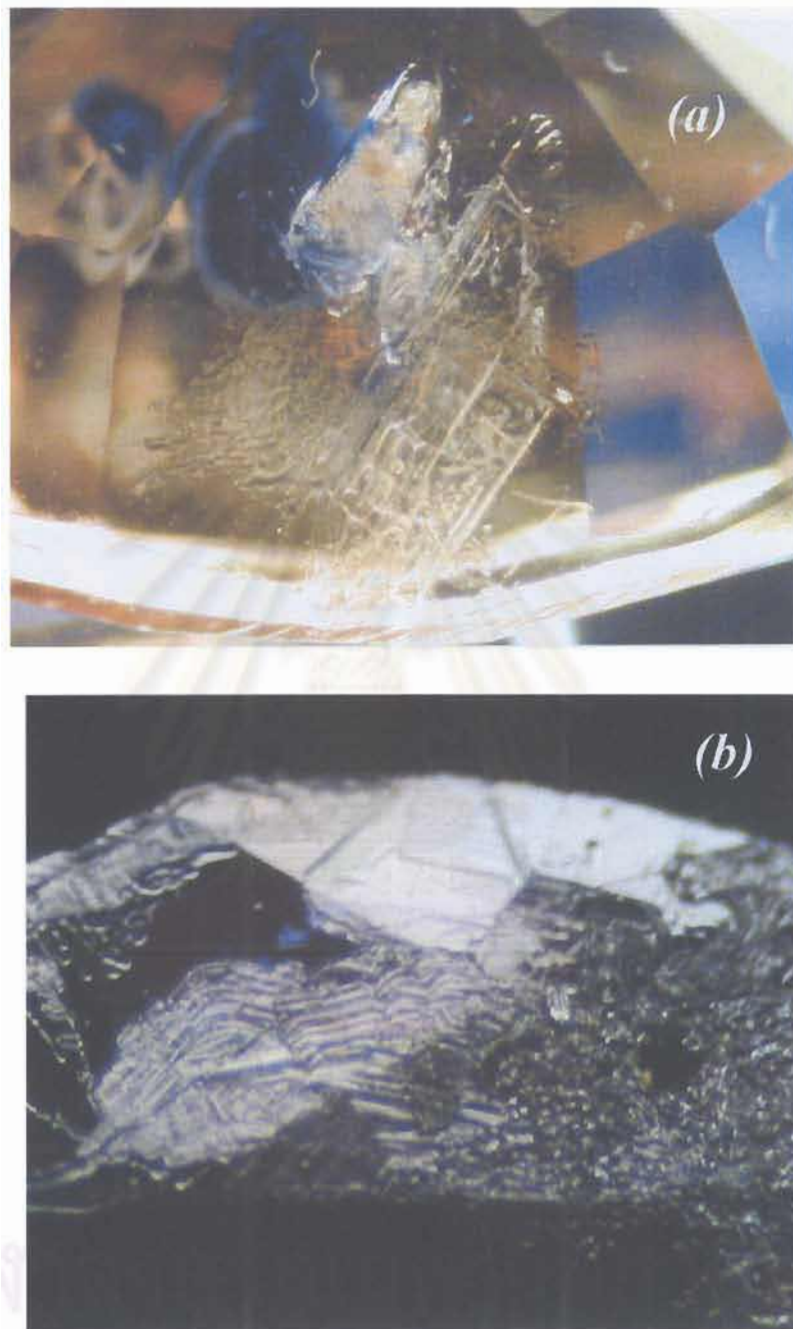
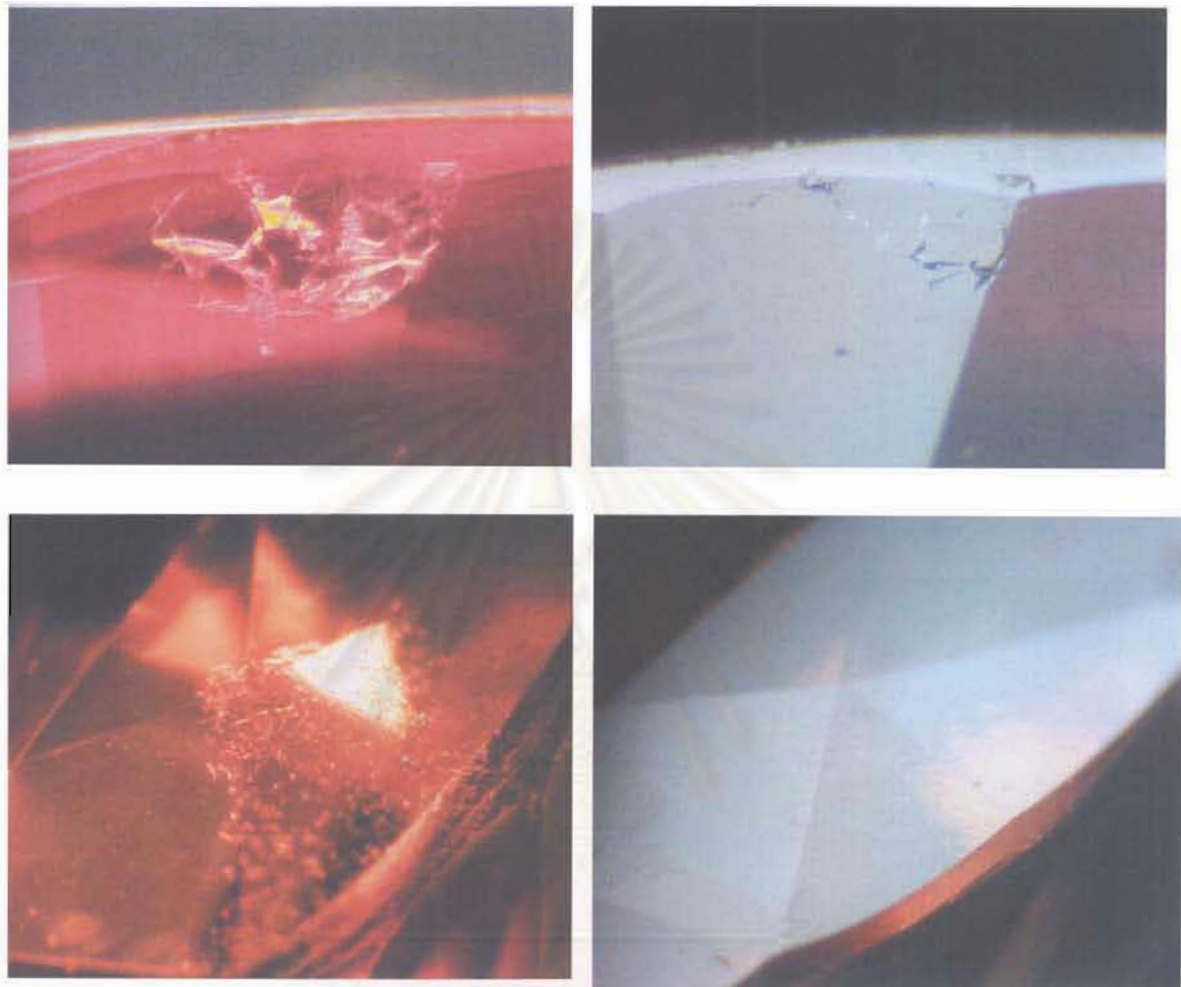


Figure 8.28a: Recrystallization on surface before repolishing is an indicative feature of Be-diffusion treated sapphire. (a) transmitted light, (b) reflected light (Photos by Somboon,GIT)



Transmitted light

Reflected light

Figure 8.28b: Recrystallization on surface after repolishing is an indicative feature of Be-diffusion treated sapphire. (Photos by Somboon,GIT)

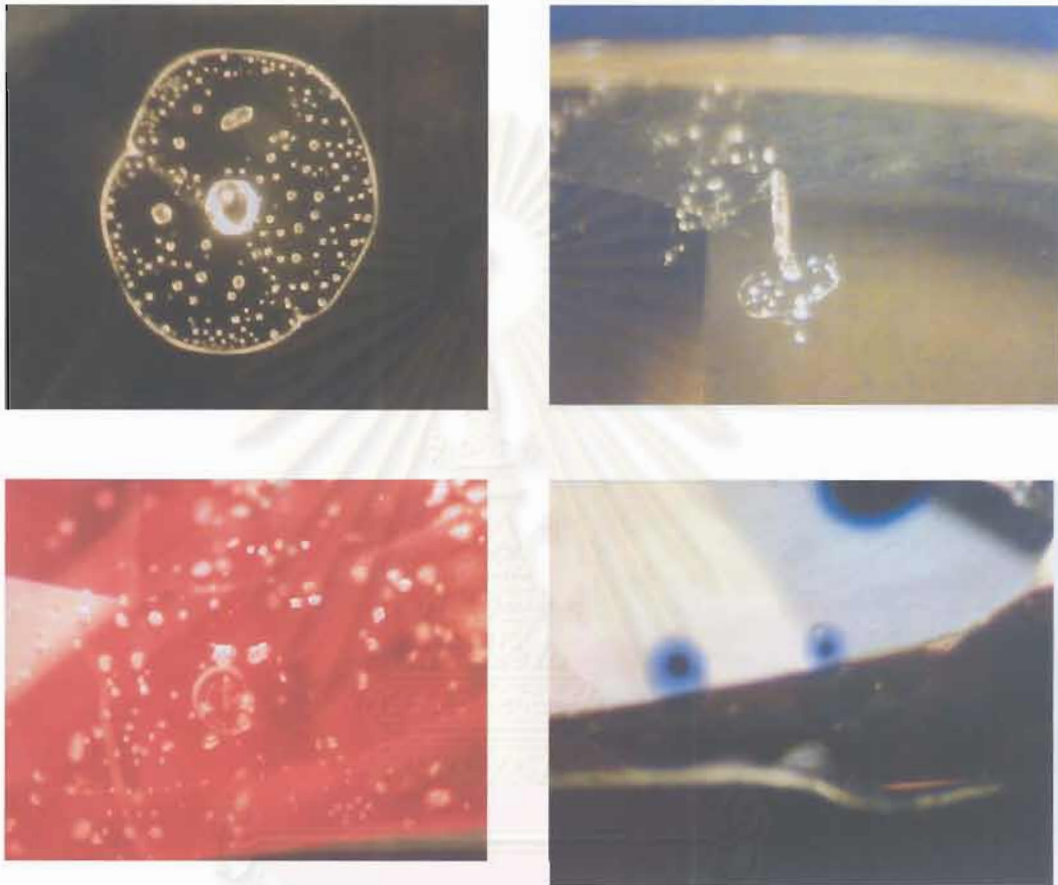


Figure 8.29: Highly altered inclusions are commonly found in Be diffusion-treated sapphires (Photos by Somboon, GIT)

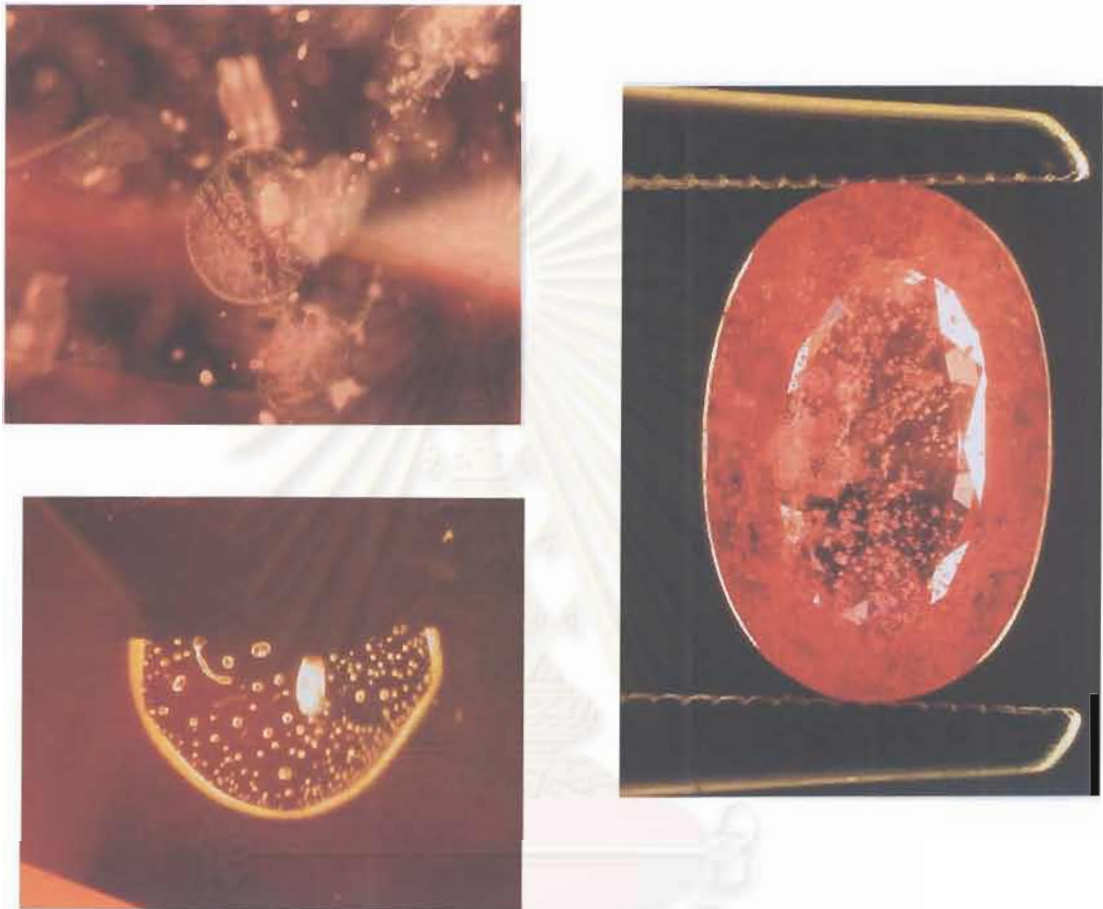


Figure 8.30: Highly altered zircon inclusions in Be diffusion-treated sapphires probably due to rather extreme heating condition.
(Photos by Singbamroong, GIT)

A laser induced breakdown spectroscopy (LIBS)

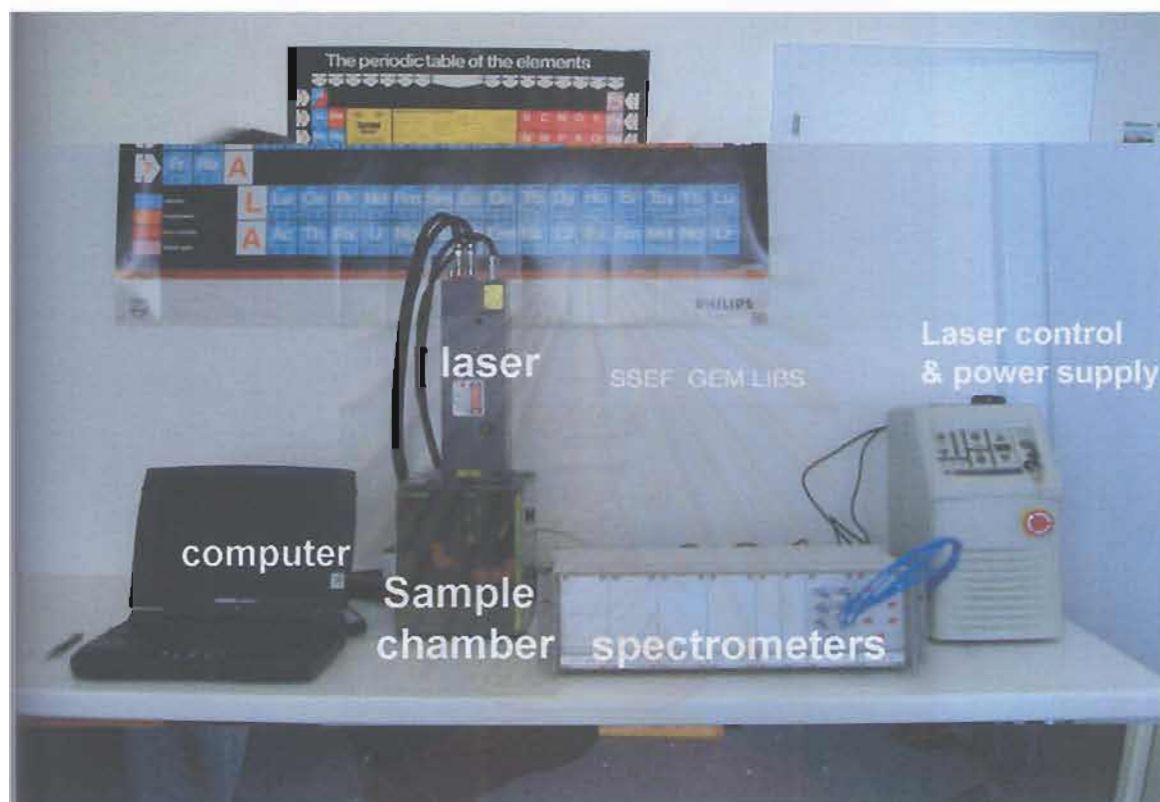


Figure 8.31: The GemLIBS system at the SSEF (courtesy of Prof. Dr. H.A. Hänni and Dr. M.S. Krzemnicki from SSEF)

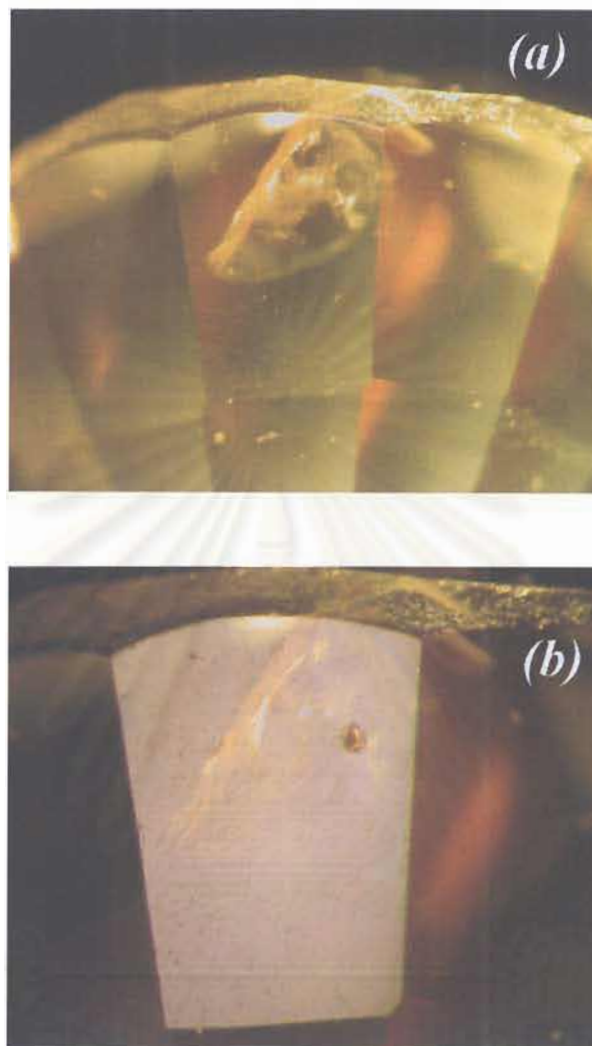


Figure 8.32: The Laser beam produces a tiny pit which does not affect the colour, purity and brilliance of a stone. In transmitted light laser pit is difficult to see (healing fissure was present before analysis) in reflected light (a), laser pit is detectable with 80-100 μ m in diameter, picture width 2.9 mm (b).
(Courtesy of Prof. Dr. H.A. Hänni and Dr. M.S. Krzemnicki from SSEF)

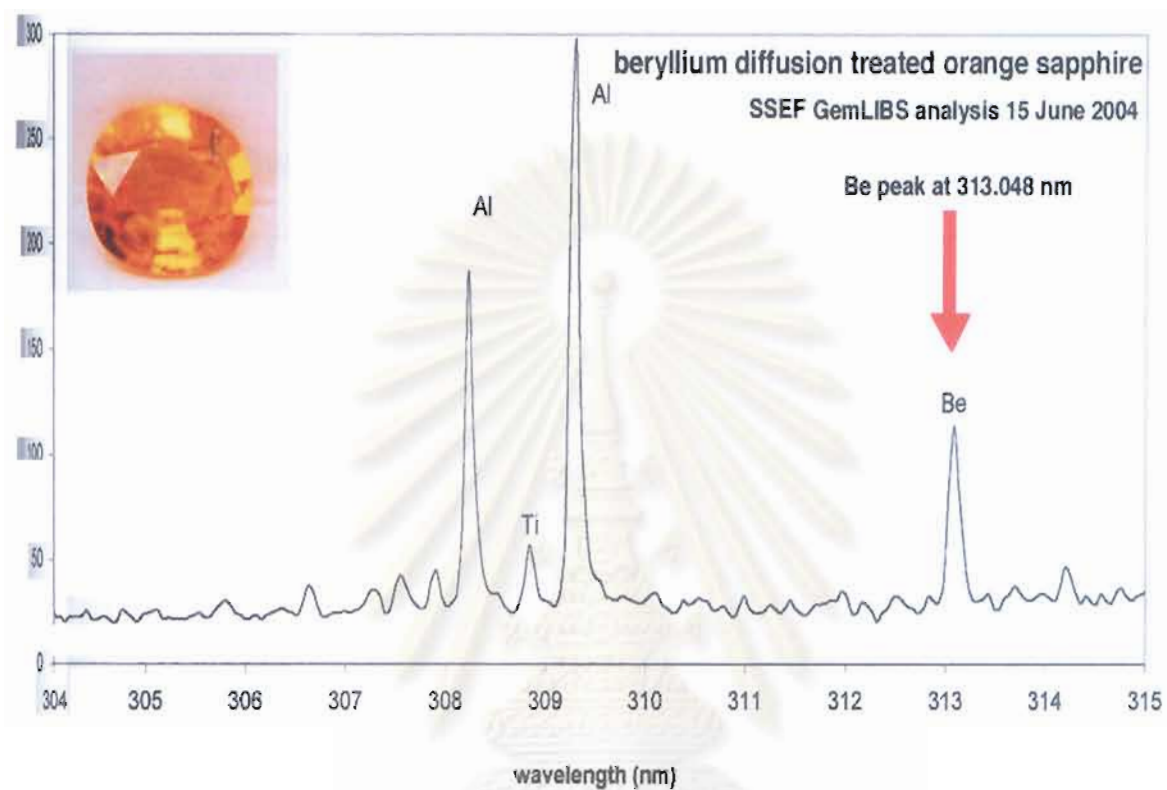


Figure 8.33: SSEF GemLIBS capable of detecting Be qualitatively down to ~ 3 ppm. It is less expensive and good for routine gem identification. A small Be peak is detected (5 ppm detected with LA-ICP-MS).
(Courtesy of Prof. Dr. H.A. Hänni & Dr. M.S. Krzemnicki of SSEF)

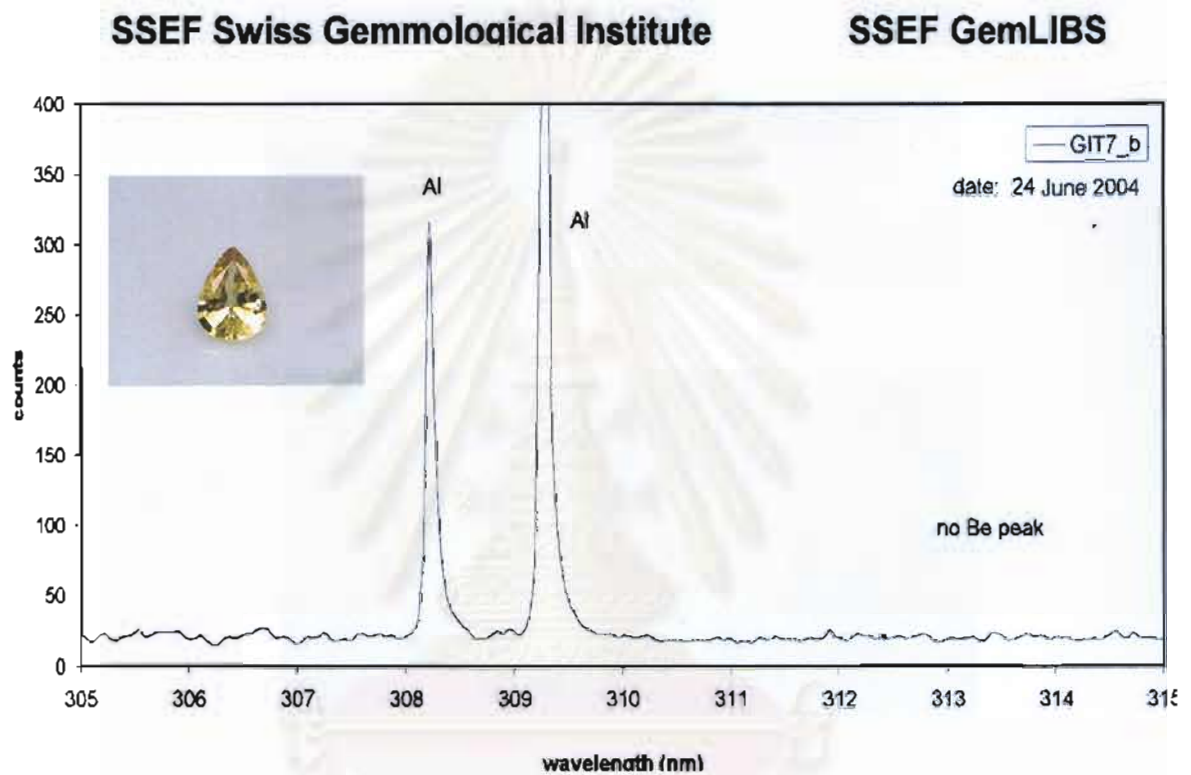


Figure 8.34: LIBS Analysis of a 'classical' heat treated yellow sapphire.
No Be peak is detected.

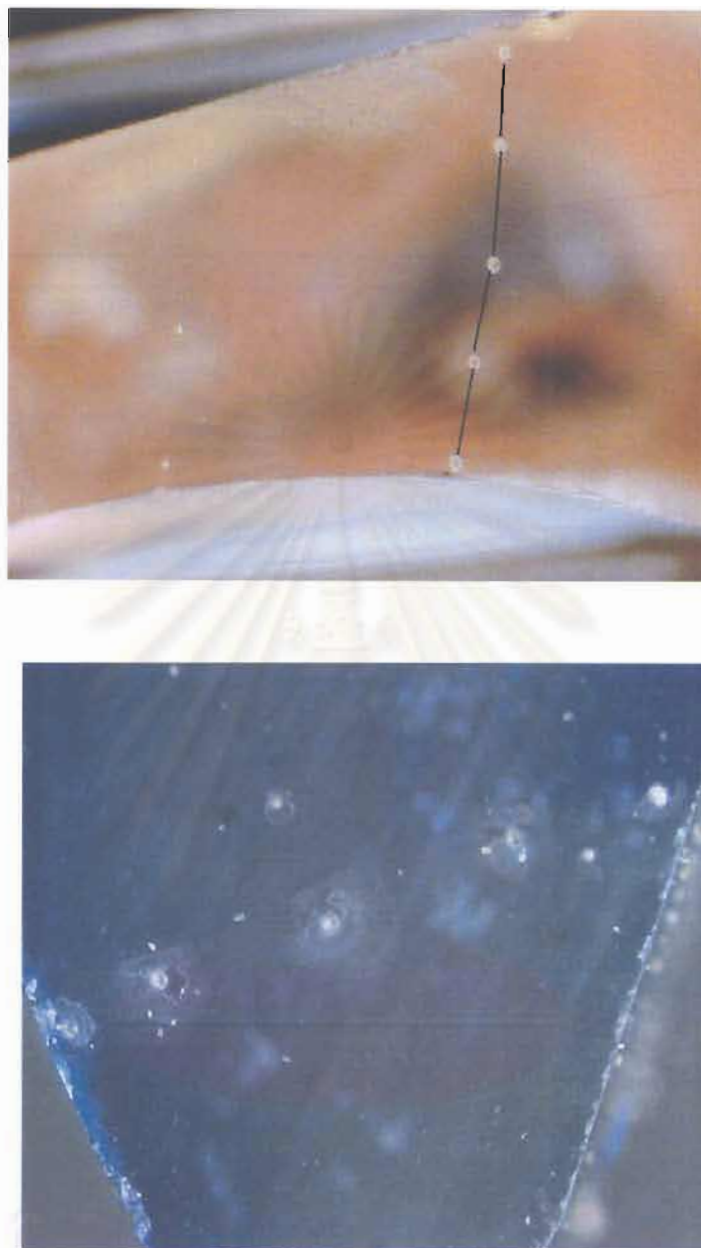


Figure 8.35: LA-ICP-MS produces similar pits (100 μm) as does the SSEF GemLIBS™ (Photos by Somboon, GIT).

Be →

	Rim1	Mid-Point1	Core	Mid-Point2	Rim2
Cations (ppm by weight)					
Be9	9.15	0.26	<0.17	<0.22	8.71
Na23	<10.82	<9.77	<10.63	<14.53	<12.40
Mg24	24.54	27.14	25.86	25.66	26.55
Al27	529250.40	529250.40	529250.40	529250.40	529250.40
Ti47	60.45	83.16	65.99	79.49	51.58
V51	12.83	12.87	12.47	12.53	12.23
Cr53	36.34	37.86	32.32	31.33	38.61
Mn55	<0.53	<0.48	<0.53	<0.73	<0.62
Fe57	3013.78	4303.34	3015.91	3139.35	3182.56
Ga71	51.66	56.00	53.22	53.84	54.13
Total %	53.25	53.38	53.25	53.26	53.26
Cations (Atom Mole ppm)					
Be9	20.64	0.58	0.00	0.00	19.65
Na23	0.00	0.00	0.00	0.00	0.00
Mg24	20.53	22.68	21.63	21.46	22.20
Al27	398801.73	398340.61	398819.35	398769.19	398742.19
Ti47	25.66	35.25	28.01	33.73	21.89
V51	5.12	5.13	4.98	5.00	4.88
Cr53	14.21	14.79	12.64	12.25	15.09
Mn55	0.00	0.00	0.00	0.00	0.00
Fe57	1097.05	1564.65	1097.87	1142.66	1158.31
Ga71	15.06	16.31	15.52	15.70	15.78
Total (Atom Mole)	40.00	40.00	40.00	40.00	40.00
Mg-Ti	-5.13	-12.58	-6.38	-12.27	0.32
Be-Ti	-5.02	-34.67	-28.01	-33.73	-2.24
(Be+Mg)-Ti	15.51	-12.00	-6.38	-12.27	19.96
(Be+Mg) %	3.54	1.43	1.89	1.79	3.42
Ti %	2.20	2.17	2.44	2.82	1.79
Fe%	94.26	96.40	95.67	95.39	94.78

Figure 8.36: LA-ICP-MS capable of obtaining quantitative analysis for trace elements in ppm levels. It is more expensive and good for research.

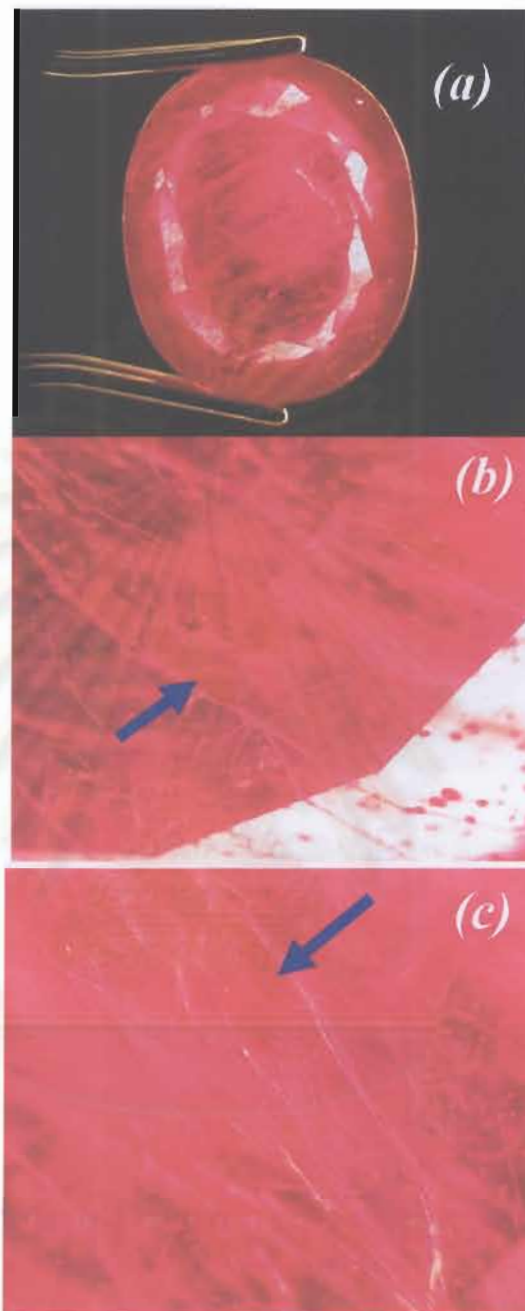


Figure 8.37: Pb-glass filled fractures in a ruby show hazy appearance (a) and often contain flattened gas bubbles (arrows in b and c).
(Photos by Leelawathanasuk,GIT)

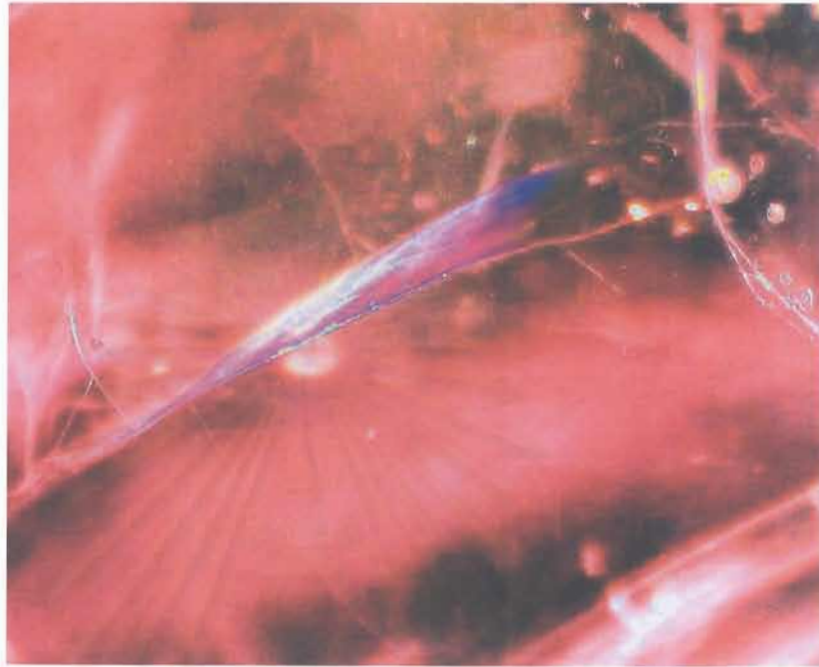


Figure 8.38: The light reflected from Pb-glass-filled fissures shows blue-flash effect. (Photos by Leelawathanasuk,GIT)



Figure 8.39: The cavity-filled Pb-glass (arrow) displays high luster but is poorly polished on the surface. (Photos by Leelawathanasuk,GIT)

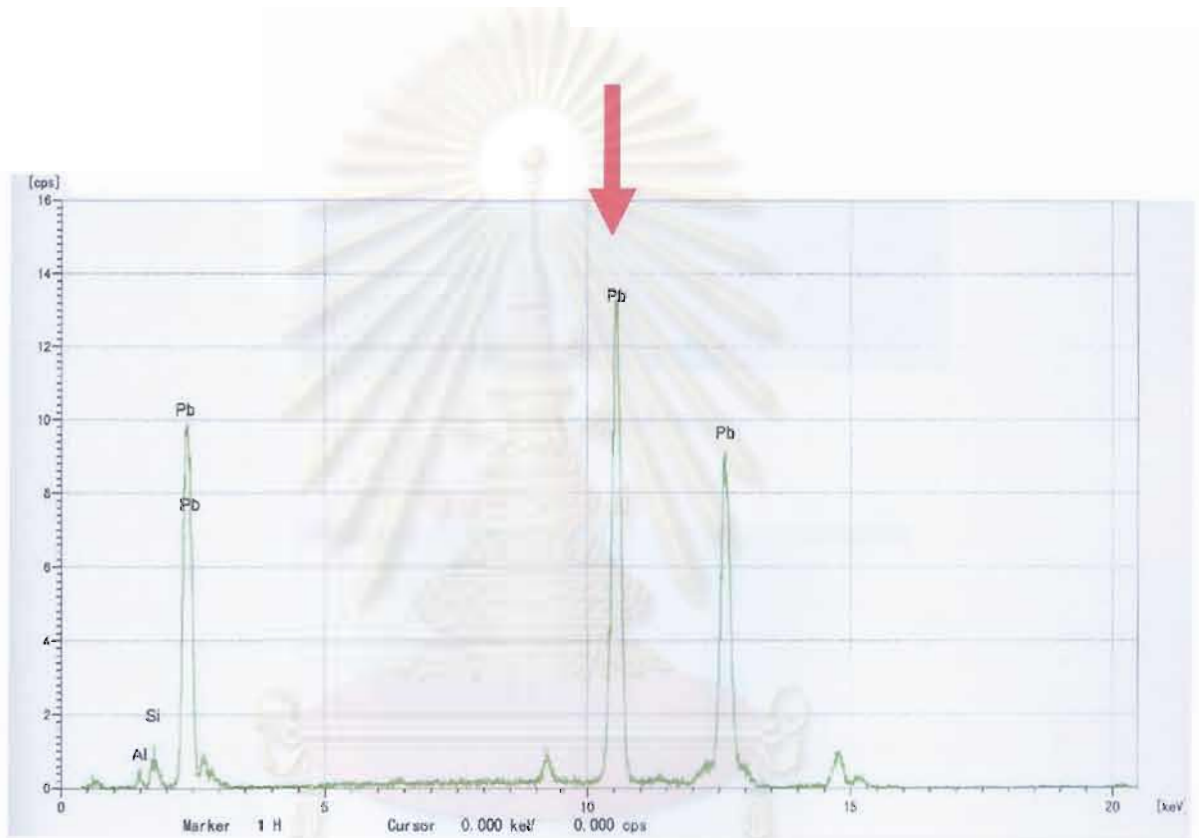
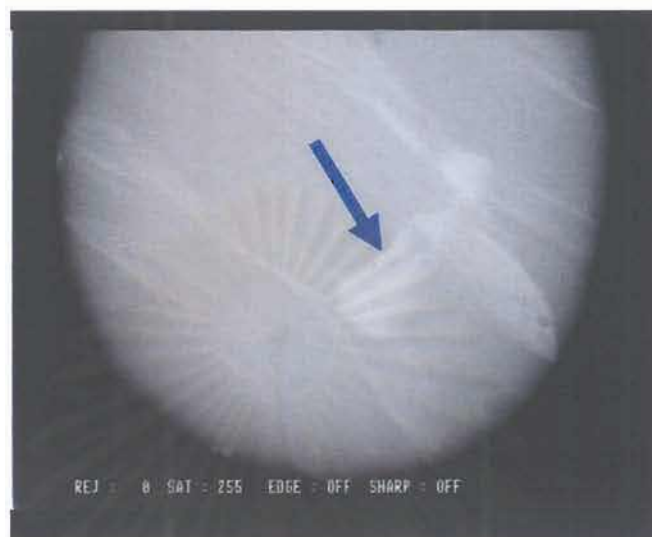


Figure 8.40: The presence of infilling Pb is readily detected by EDXRF



Negative image



Positive image

Figure 8.41: The presence of infilling Pb also appears in X-ray images (Photos by Leelawathanasuk,GIT)



APPENDIX A.

Yellow and brown coloration in beryllium-treated sapphires

Visut Pisutha-Arnond^{1,2}, Tobias Hager³,
Pornsawat Wathanakul^{1,4} and Wilawan Atichat^{1,5}

1. Gem and Jewelry Institute of Thailand, Faculty of Science, Chulalongkorn University, Bangkok 10330, Thailand

2. Department of Geology, Faculty of Science, Chulalongkorn University, Bangkok 10330, Thailand.
e-mail: pvitut@geo.sc.chula.ac.th

3. Institute of Gemstone Research, University of Mainz, Germany

4. Earth Science, Department of General Science, Faculty of Science, Kasetsart University, Bangkok 10900, Thailand

5. Gem and Geological Material Group, Department of Mineral Resources, Rama VI Rd., Bangkok 10400, Thailand

Abstract: The causes of yellow and brown coloration in Be-treated sapphires have been investigated by a series of irradiation and Be-heating experiments on synthetic and natural colourless sapphires. UV-Vis spectra have been recorded and the stones have been analysed for trace elements by LA-ICP-MS. Based on these results it is likely that the Be-heating process could activate stable yellow colour centres in natural sapphires, which are also related to oxygen in the atmosphere and iron; these are stabilized by the diffusion of Be. Brown colour centres could be activated in the synthetic sapphires without iron. Therefore Be is able to act in the same way as has been previously proposed for Mg.

Keywords: beryllium treatment, colour centres, diffusion, heat treatment, irradiation, yellow sapphires

Introduction

Gemstone enhancement is traditional in human history. For several hundred years, rubies have been heated in coal furnaces to reduce the blue hue (Nassau, 1984, 1994; Hughes, 1997). The 'classical' high temperature treatment of corundum has been known for thirty years (Tombs, 1980; Harder, 1980; Crowningshield and Nassau, 1981; Nassau, 1982). Today we understand the

mechanisms and the causes of colour much better than in the past. Nevertheless, the gemstone industry of Thailand has surprised us once again with a 'new' corundum enhancement technique that shows new and unexpected colour distribution and reactions. Examples have been presented on a number of websites (e.g. AGTA, GRS) and from Hughes (2002) and McClure *et al.* (2002).

Typical examples of the product of this 'new' heating process can be seen in *Figure 1*. Many of those samples show surface-related yellow zones or if the stone contains chromium, an orange colour rim was observed (*Figures 2 and 3*). To get a better inside view, the stones were put into an immersion liquid (methylene iodide) and to improve the contrast a blue glass filter was placed between the light source and the stones. The thickness of the surface-related colour zone is about 2.5 mm in *Figure 2* and about 1.2 mm in *Figure 3*. However, colour rims up to 4 mm have been observed in the lab.



Figure 1: Pink-orange, orange, yellow sapphires and ruby treated with the new heating technique. Treatment conditions are unknown. (Photos by Somboon, GIT)



Figure 2: Surface-related colour zones in a yellow sapphire, 10.06 × 11.57 mm. (Immersion, photo by Leelawatanasuk, GIT)

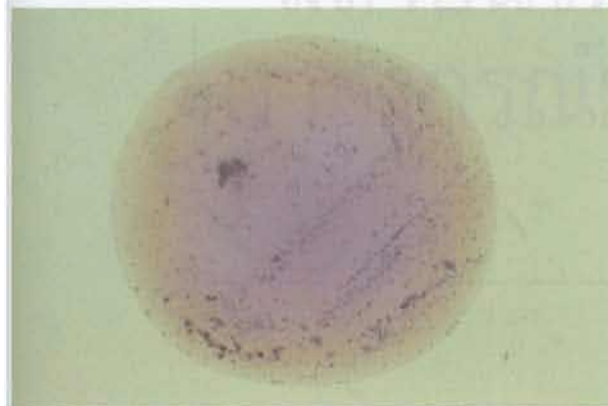


Figure 3: Surface-related colour zones in a pink-orange sapphire, 5.20 × 6.63 mm. (Immersion, photo by Somboon, GIT)

Because the colour zones are parallel to the surface, it suggests that the stones have been subject to diffusion of a foreign element or combination of elements. Hitherto, diffusion of a colour-producing element into a gem mineral lattice on the scale of millimetres has not been observed. The penetration depth of the traditional diffusion treatment shown in *Figure 4*, where Ti and Fe are introduced into the sapphire from outside is about 0.09 mm; this is known as external diffusion. Of course, the penetration depth can vary slightly



Figure 4: Slice of colourless sapphire with blue rim caused by external diffusion of Ti into the stone; 4 × 7 mm. (Immersion, photo by Häger)

depending on time and temperature of treatment. A similar order of diffusion thickness (0.06 mm in *Figure 5*) can be observed in the case of internal diffusion, where titanium diffuses from natural rutile inclusions into the corundum lattice.

To understand the new enhancement technique applied to create yellow and orange sapphires, it is necessary to understand the causes of colour of natural yellow sapphires in detail. Two groups of natural yellow sapphires exist. The first group owes its colour to a spin forbidden transition of Fe^{3+} (Lehmann and Harder, 1970; Krebs and Maisch, 1971; Ferguson and Fielding, 1971, 1972; Nassau and Valente, 1987). However, the probability of this transition is very low, therefore, approximately 1 weight % Fe^{3+} is needed to create an intense yellow with this mechanism. Sapphires of this group originate for example from the basaltic-type occurrences



Figure 5: Internal diffusion of Ti from rutile inclusions into the corundum lattice showing the blue haloes. (Photo by Häger)

in Thailand, Australia and North Madagascar, or from the metamorphic occurrence in Umba, Tanzania (D. Schwarz, pers. comm., 2003). Typical spectra resulting from this kind of mechanism are shown in *Figure 6*.

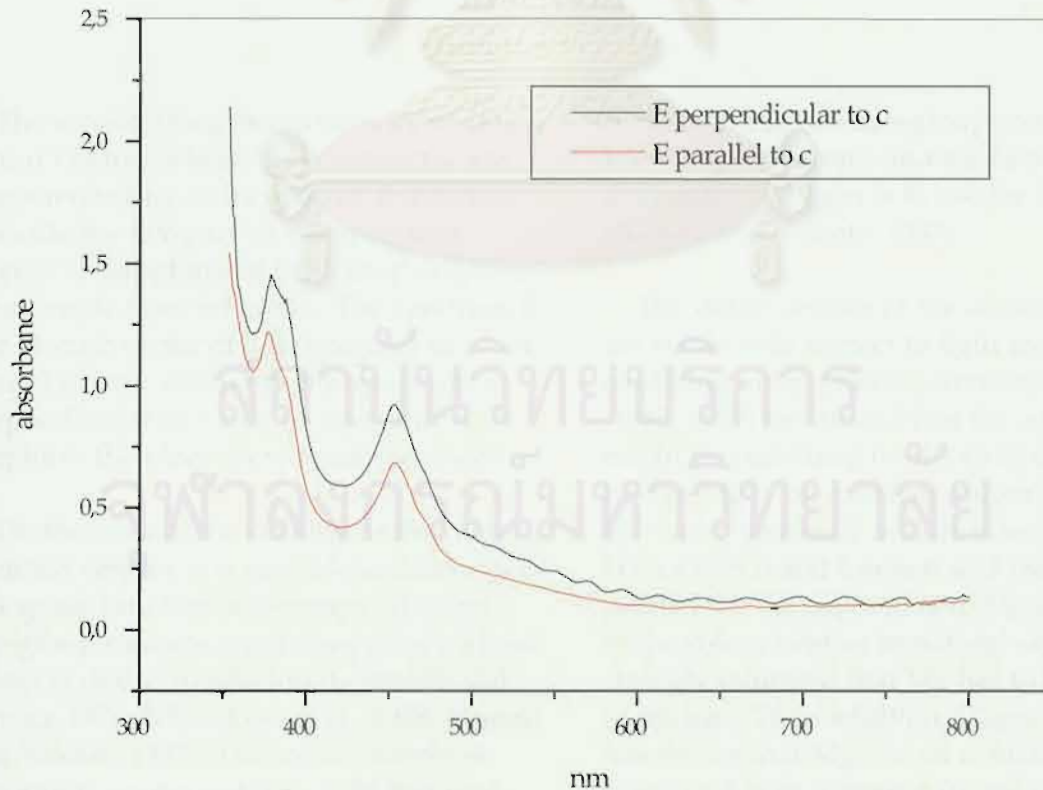


Figure 6: UV-Vis-spectra of an untreated yellow sapphire from Thailand (Khao Phloi Wean Chanthaburi) with E perpendicular to c-axis (o-ray, black) and E parallel to c-axis (e-ray, red). The colour is due mainly to Fe^{3+} forbidden transition.

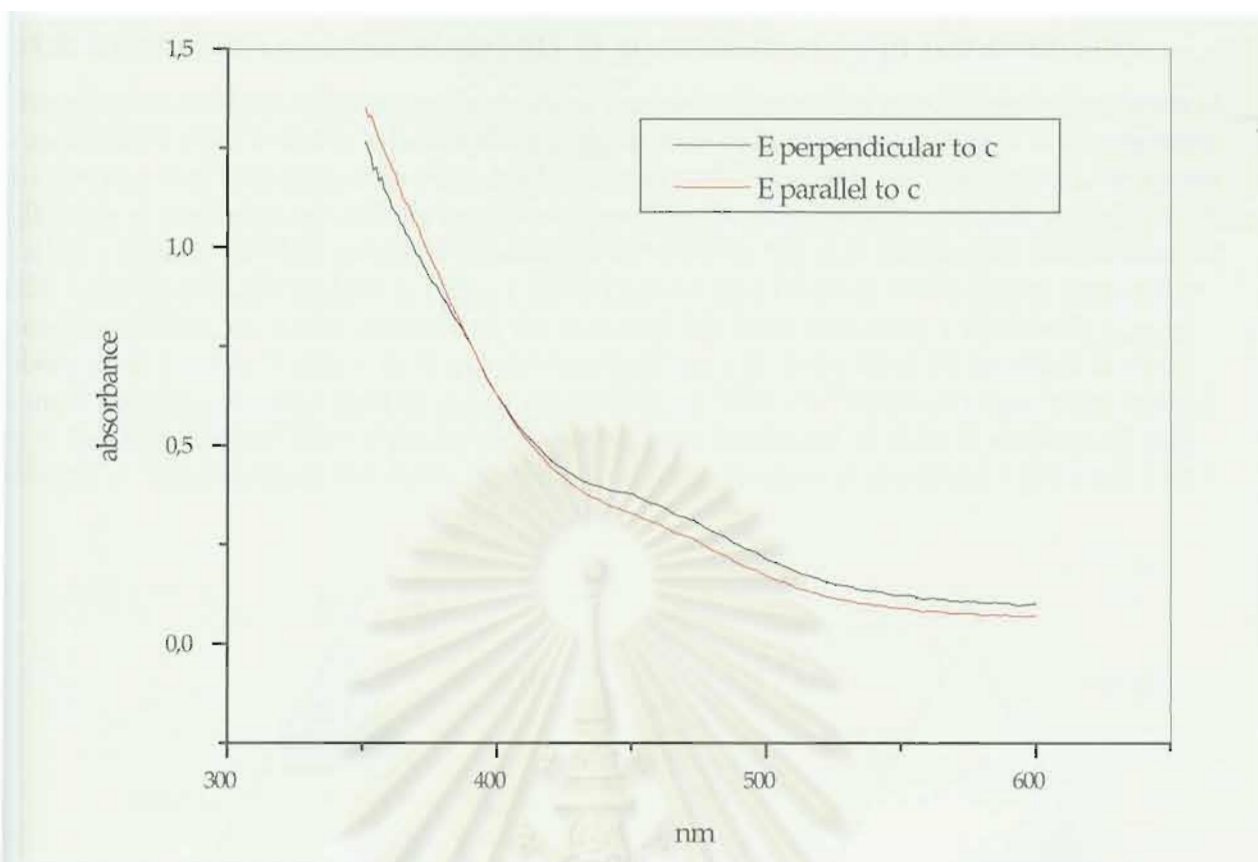


Figure 7: UV-Vis spectra of a heat-treated natural yellow sapphire from Sri Lanka with E perpendicular to c-axis (o-ray, black) and E parallel to c-axis (e-ray, red). The colour is due to stable defect centres.

The second group is coloured by so-called colour centres whose UV-Vis-spectra are characterized by an increase of absorption towards the UV-part of the spectrum (Figure 7). Sapphires of this group originate for example from Sri Lanka. The spectrum E (the electric vector of light) parallel to c-axis (e-ray) is very similar to the spectrum E perpendicular to c-axis (o-ray), and such sapphires therefore show weak pleochroism.

On the basis of the stability of the colour or defect centres, it is possible to differentiate this group into two sub-groups. The first sub-group contains natural sapphires whose colour is due to irradiation (Lehmann and Harder, 1970; Nikolskaya *et al.*, 1978; Nassau and Valente, 1987). The colour centres of this group are not stable to light and heat. The defect centres of the second sub-group are stable to UV light and to heat up to about 500 or 600°C. It is not possible to differentiate

between these two sub-groups on the basis of UV-Vis spectroscopy, and the best method of distinguishing them is to use the fading test (Nassau and Valente, 1987).

The defect centres of the second sub-group are stable with respect to light and heat in an oxidizing atmosphere. Schmetzer *et al.* (1982, 1983) mentioned that the colour centres might be stabilized by divalent cations like Fe^{2+} or Mg^{2+} , by trivalent cations like Cr^{3+} or Fe^{3+} or by several di- and tri-valent cations. Häger (1993) and Emmett and Douthit (1993) pointed out the importance of Mg as a stabilizer of the colour centres in natural sapphires and strongly indicated that Mg has to be in excess of intrinsic Ti. In addition, Häger (1996, 2001) has shown that Mg+Fe, an oxidizing atmosphere and high temperature are necessary to develop stable yellow colour centres. Interactions of trace elements in corundum are briefly summarized in Box I.

Box I: Interaction of trace elements in corundum at high temperatures

Based on several quantitative experiments it has been shown that in addition to the classical trace elements like Fe and Ti which influence the colour of blue sapphire, Mg is also important. This element is able to form colourless MgTiO_3 -clusters. If Ti exceeds the Mg-content, the excess of Ti leads in combination with Fe to colour-active FeTiO_3 -clusters (Häger, 1992). In the case of a yellow sapphire which is coloured by stable defect centres, Mg is in excess after the calculation of the colourless MgTiO_3 -clusters (Häger, 1993; Emmett and Douthit, 1993). But in contrast to Emmett and Douthit, it was shown that the excess of Mg in combination with low Fe causes stable colour centres identical to those of natural yellow sapphires from Sri Lanka, while Mg by itself stabilizes another kind of colour centre (Häger, 1996). If Ti-content exceeds the sum of Mg + Fe, the excess of Ti will precipitate during heat treatment at 1850°C in an oxidizing atmosphere. To summarize the above, the following diagrams were developed (Häger, 1996, 2001).

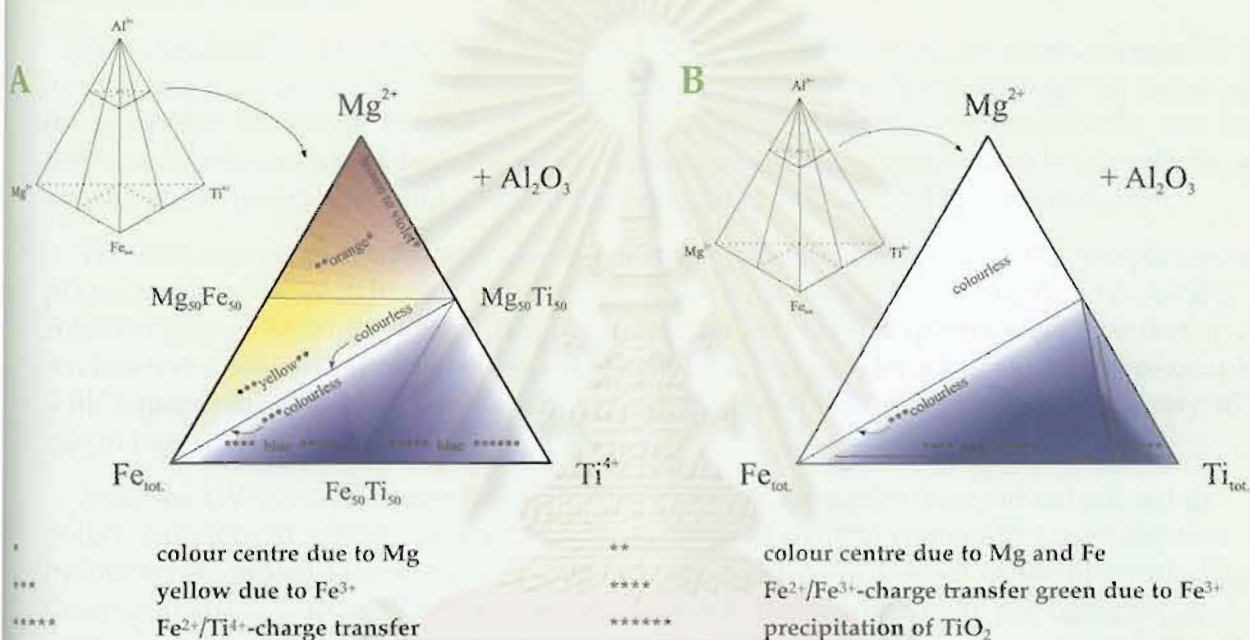


Figure 1: Model representing the interaction of trace elements in the system Mg, Fe, Al and Ti for samples which were heat treated in oxidising (A) and reducing atmospheres (B) at high temperatures.

The diagram in *Figure 1A* represents the system Al-Mg-Fe-Ti (tetrahedron). Out of this tetrahedron a slice is cut. This slice represents sapphires with total trace element content in the ppm region. The resulting diagram is a triangle. Sapphires of this composition were heat treated at 1850°C in an oxidizing atmosphere (*Figure 1A*) and at 1750°C in a reducing atmosphere (*Figure 1B*). The most important line in the large triangle in *Figure 1A* is the connecting line between the Fe corner and the $\text{Mg}_{50}\text{Ti}_{50}$ point where the Mg to Ti ratio is always 1:1; there, the samples neither show any kind of colour centres nor an $\text{Fe}^{2+}/\text{Ti}^{4+}$ charge transfer band. Above this line are stable yellow colour centres such as found in natural sapphires from Sri Lanka. In the Mg corner are stable defect centres, but not with the same UV-Vis spectral pattern as the samples containing both Fe and Mg. Below the line, where Ti:Mg ratio is more than 1:1, are the $\text{Fe}^{2+}/\text{Ti}^{4+}$ charge transfer bands. If the titanium content exceeds the sum of Mg + Fe a titanium-containing phase can precipitate. If the sapphires are treated in reducing conditions, the colour centres are destroyed completely and additional titanium precipitates are dissolved (*Figure 1B*). The amount of additionally dissolved precipitates now depends on the kinds of the reducing gases used.

Box II: Materials and methods

In this study two flame-fusion-grown colourless sapphires, a disc of synthetic colourless corundum or 'watch glass', and three natural colourless sapphires were heat-treated under unknown conditions by a Thai heater. Five yellow, orangey-yellow and blue sapphires, reportedly the results of heat-treatment by the Be-technique in Thailand were also studied. A similar set of samples (two flame-fusion-grown colourless and nine natural colourless sapphires) was also irradiated by soft X-rays (4 mA, 80 kV) for four hours.

The heat-treatment experiments were also carried out by one author (TH) to confirm results. A synthetic colourless ('watch glass') and two natural colourless, one natural blue and many natural pink sapphires mixed with ground chrysoberyl in the crucibles were heated in a resistance furnace with Super Kanthal 1900 heating elements at 1750°C in air (i.e. under oxidizing conditions) for 30 hours.

The samples were photographed and their UV-Vis spectra were recorded before and after the heating and irradiation. Only if the spectrum was not recorded with E perpendicular to the *c*-axis (o-ray), is this fact noted. The Hitachi UV-Vis-NIR spectrophotometer (model U4001) was used for most measurements with additional measurements using a Leica/Leitz UV-Vis microscope attached to a spectrometer and a Perkin-Elmer Lambda 9 UV-Vis-NIR spectrophotometer.

The heat-treated and irradiated samples were subjected to a fading test. The samples were placed under a 100 W light bulb at a distance of 4 cm for several hours to fade any unstable colour centres. The samples were then photographed and UV-Vis spectra were recorded again. An irradiated natural sample was placed on a heating stage under a Leica microscope coupled with a spectrometer with a resolution of 1 nm. A UV-Vis-spectrum was recorded at every 10°C rise in temperature up to 300°C.

After the UV-Vis measurements, a set of representative samples were cut in half, lightly polished on the cut surfaces and then analysed for trace element content by Laser Ablation Inductively-Coupled-Plasma Mass Spectrometry (LA-ICP-MS). This set of samples includes three synthetic colourless sapphires (one Be-treated flame-fusion-grown, one original flame-fusion-grown cut from the same boule and one disc of synthetic corundum or 'watch glass'), two natural colourless sapphires (one Be-treated, one original sample obtained from the same gemstone dealer), three yellow and orangey-yellow Be-treated natural sapphires and two Be-treated natural blue sapphires obtained from different heaters. The 5-points profile analysis (Rim1, Mid-Point1, Core, Mid-Point2, Rim2) and 3-points profile analysis (Rim1, Core, Rim2) were performed across the cut surface by this technique.

Detailed descriptions of LA-ICP-MS instrumentation, analytical and calibration procedures are similar to those given by Norman *et al.* (1996). The UV laser ablation microprobe (a New Wave Research 266 nm Nd: YAG) is coupled to an Agilent 7500 ICP-MS. All analyses were done with a pulse rate of 5 Hz and beam energy of approximately 0.5 mJ per pulse, producing a spatial resolution of 30-50 µm in diameter on the samples. Quantitative results of isotopes for nine trace elements (Be⁹, Na²³, Mg²⁴, Ti⁴⁷, V⁵¹, Cr⁵³, Mn⁵⁵, Fe⁵⁷ and Ga⁷¹) were obtained through calibration of relative element sensitivities using the NIST-610 multi-element glass standard and pure Al₂O₃ as internal standards. The BCR2G basaltic glass standard was also used as an external standard. The contents are reported as µg/g or ppm by weight. The detection limits vary from analysis to analysis and are typically less than 1 ppm for Be, V and Ga; less than 4 ppm for Mg, Ti and Mn; less than 13 ppm for Cr; less than 40 ppm for Na and less than 80 ppm for Fe.

In the 'new' heating technique, pink- or orange sapphires can be produced from original pink or reddish-brown sapphire, and colourless or white sapphires can be enhanced by addition of a yellow hue to the stones. Some yellow sapphires can also be obtained by heat-treatment of natural green or blue sapphires by the 'new' heating technique (Coldham, 2002). In the release from the Chantaburi Gem and Jewelry Association (CGA) on 20 February 2002, the 'new' heating technique was referred to as 'Be-treatment or Be-heating' technique. Hence, understanding how this yellow hue is caused by this technique is very important.

Results

Irradiation

In the first series of tests, the irradiation experiment was carried out on a flame-fusion-grown colourless sapphire and a natural colourless sapphire (Figures 8-12). The synthetic sample is relatively pure Al_2O_3 in which most of the trace elements including Be are below the detection limits; a typical analysis, taken from the core of a stone, is shown in Table 1. The natural sample contains relatively higher trace element content, in particular Mg, Ti and Fe, while the Be content is below the detection limit (Table 1). After the irradiation the synthetic stone turned slightly

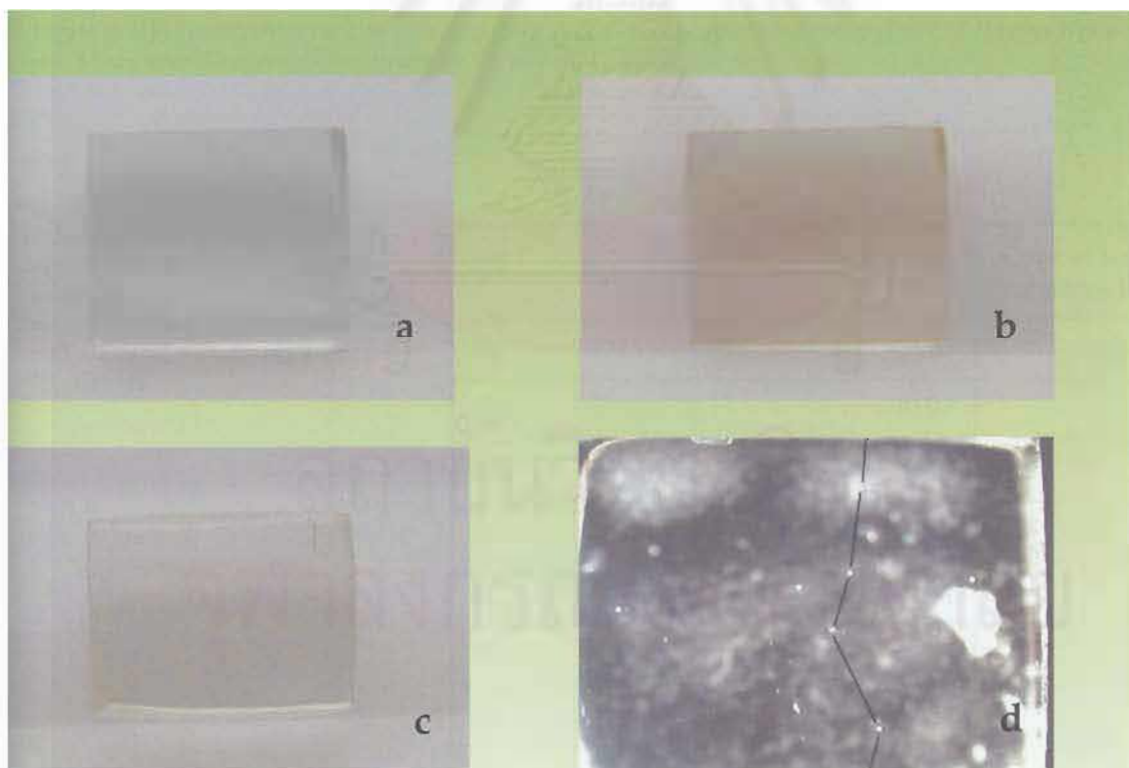


Figure 8: Photos of the 2.44 ct flame-fusion-grown colourless sapphire (PKSCS02) before treatment (a), pale brown after X-ray irradiation treatment (b), and almost colourless after a fading test (c). Afterwards the sample was cut in six points on a traverse (d) were analysed across the cut surface using LA-ICP-MS (see also Table 1 and Figure 9). (Photos by Somboon, GIT and Lomthong, KU)

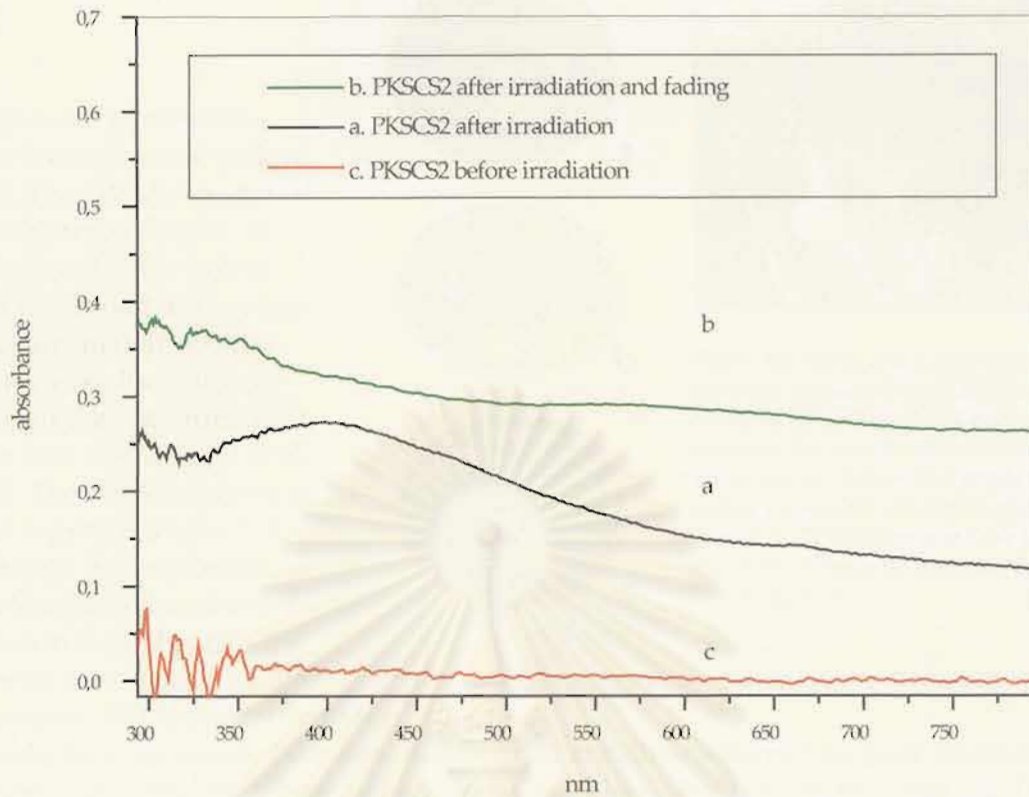


Figure 9: UV-Vis spectra of the 2.44 ct cube of flame-fusion-grown colourless sapphire (PKSCS02) before treatment (c), pale brown after X-ray irradiation treatment (a), and after a fading test (b).

Table 1: Some typical trace element contents of a flame-fusion-grown colourless sapphire (PKSCS02), and a natural colourless sapphire (POMCS04), both untreated with Be, obtained by LA-ICP-MS.

μg	Core of synthetic sapphire PKSCS02	Core of natural sapphire POMCS04
Be	<0.95	<0.75
Na	<40.97	57.55
Mg	5.50	81.01
Al	529250.40	529250.40
Ti	<3.74	129.98
V	<0.59	17.44
Cr	<12.58	15.40
Mn	<2.85	<2.26
Fe	<77.93	719.27
Ga	<0.55	89.82
Total %	52.93	53.04
< = below detection limit		

brown (Figure 8b) whereas the natural one became intense yellow (Figure 10b). The UV-Vis spectra of the synthetic sample (Figure 9) changed from a flat line before irradiation to a broad absorption band at approximately 400 nm with only a weak absorption in the UV-part of the spectrum after irradiation (see also Kvapil *et al.*, 1972, 1973). The UV-Vis spectra of the natural sapphire (Figure 11) changed from a flat line before irradiation to a pronounced increase in absorption in the UV-part of the spectrum with a distinct shoulder at approximately 460 nm after irradiation (similar results have previously been reported by Schmetzer *et al.*, 1982, 1983; Nassau and Valente, 1987). The colour of all the irradiated samples was not stable during the fading



Figure 10: Photos of a 0.73 ct natural colourless sapphire (POMCS04) before treatment (a), yellow after X-ray irradiation treatment (b), and almost colourless after a fading test (c). A five-point-profile (d) was analysed across the cut surface afterwards using LA-ICP-MS (see also Table I and Figure 11). (Photos by Somboon, GIT and Lomthong, KU)

test and they returned to their original 'colourless' state (see Figures 8 and 10). The same results were obtained from several runs on synthetic and natural colourless samples.

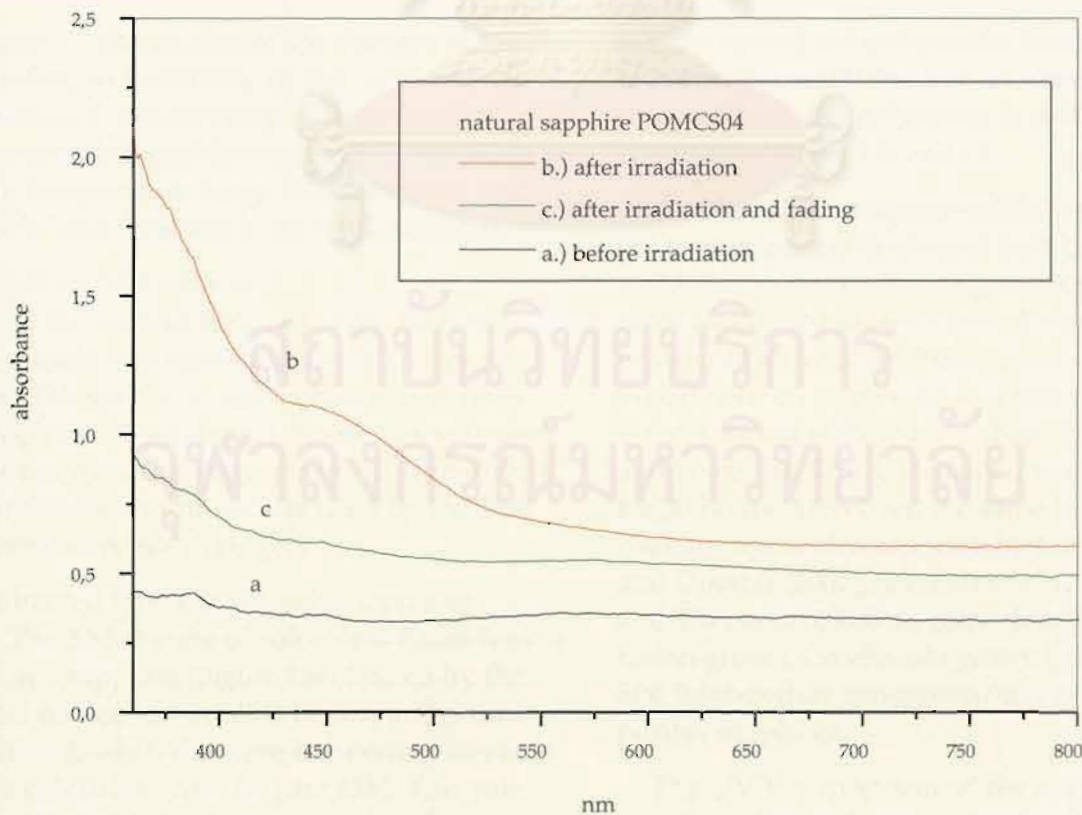


Figure 11: UV-Vis spectra of the 0.73 ct natural colourless sapphire (POMCS04) before treatment (a), after X-ray irradiation treatment (b) and after a fading test (c).

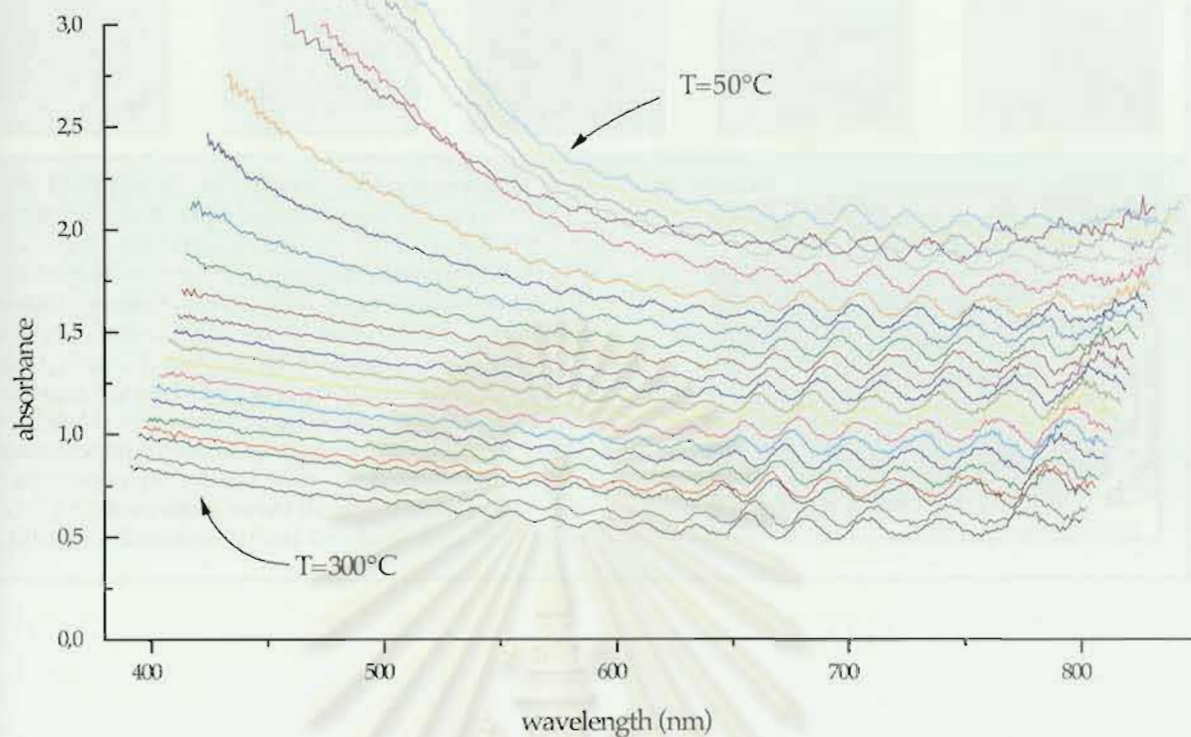


Figure 12: UV-Vis spectra of an irradiated natural sapphire heated up at a rate of 2°C/min; spectra were recorded every 10°C and a selection is shown. The main point to note is that the intensity of colour fades to near-colourless at 300°C.

Figure 12 shows clearly the changes in spectra relating to instability of the colour of an irradiated natural sample. After irradiation, the sample faded during heating especially in the temperature range between 50°C and 150°C and returned to its original colour.

Beryllium heat-treatment

In the second series of tests, Be-heat-treatment was carried out by a Thai heater on both synthetic and natural colourless sapphires. A similar set of samples was used for our own heating experiment. The precise conditions and procedure used by the Thai heater were not divulged.

Be-treated synthetic colourless sapphires

The 3.85 ct cube of colourless flame-fusion grown sapphire (Figure 13a) treated by the Thai heater, turned pale brown at the rim with a gradual decrease in intensity towards the colourless core (Figure 13b). The pale brown rim and colourless core are better seen in the immersion liquid (Figure 13c). This

sample turned colourless after heating in reducing conditions and returned to pale brown again after re-heating in oxidizing conditions (Figure 13e and f).

Another 11.03 ct square-cabochon sample cut from the same boule and heat-treated under the same conditions gave exactly the same result (not shown here). A similar pale brown colour was observed in our own experiment on a colourless 'watch glass' sample mixed with ground chrysoberyl and heated at 1750°C in oxidizing conditions for 30 hours. Moreover, the same brown coloration was also reported by Emmett and Douthit (2002), Emmett *et al.* (2003) and Themelis (2003) on colourless flame-fusion-grown, Czochralski-grown (high purity) and heat-exchanger-grown (ultra-high purity) sapphires.

The UV-Vis spectrum of the synthetic sapphire changed from a flat line before heating to a broad absorption band at

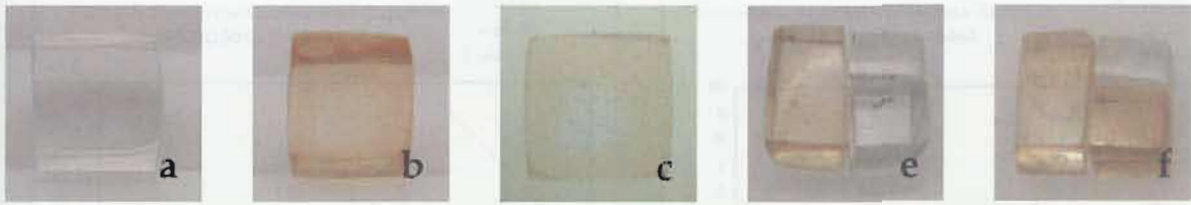


Figure 13: Photos of a 3.85 ct flame-fusion-grown colourless sapphire (PKSCS01) before treatment (a) and pale brown after Be-treatment under unknown conditions (b). The pale brown rim and colourless core are better seen under immersion (c). After the treatment the sample was cut in half and a five-point profile (d) was analysed across the cut surface using LA-ICP-MS (see also Table II, Figures 14 and 15). The other half was then cut into three pieces; one piece was kept as the reference and the other two were heated in a pure nitrogen atmosphere at 1650°C for three hours, which turned the stones colourless (e). One of the colourless pieces was then re-heated in air (i.e. oxidation conditions) at 1650°C for 1 hour, which turned the sample back to pale brown (f). (Photos by Somboon, GIT and Lomthong, KU)

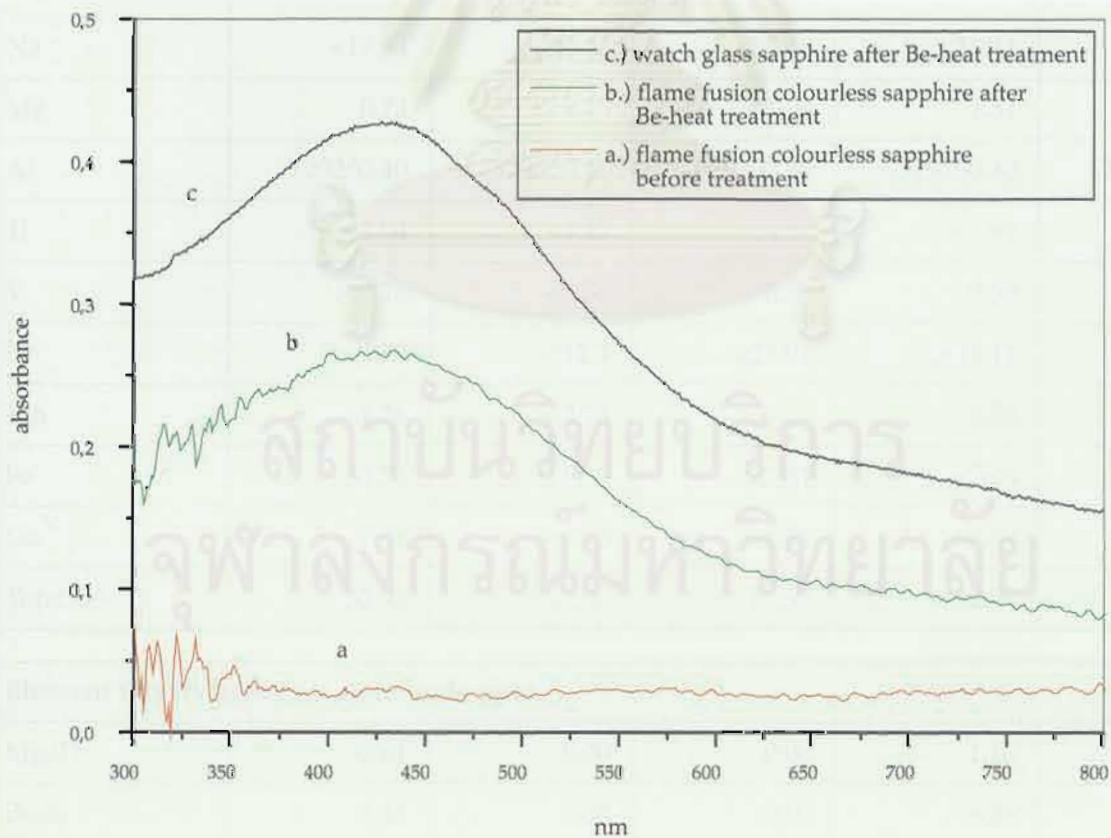


Figure 14: UV-Vis spectra of the flame-fusion-grown sapphire (PKSCS01) before treatment (a) and after Be-heat treatment (b) under unknown conditions. Spectrum c was recorded from a 'watch glass' sapphire (WG02) which had been turned pale brown from originally colourless material by heating at 1750°C in an oxidizing atmosphere with chrysoberyl in the crucible.

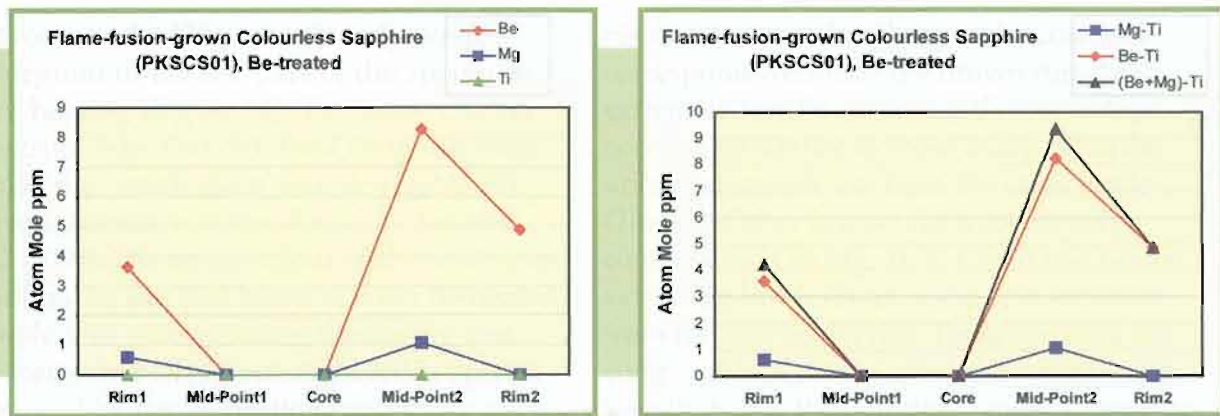


Figure 15: Plots of trace element content variation across the cut surface of the pale brown Be-treated flame-fusion-grown sapphire (PKSCS01), see Figure 13d and text for discussion.

Table II: Trace element contents of the pale brown Be-treated flame-fusion-grown sapphire (PKSCS01) obtained by LA-ICP-MS.

μg	Rim 1	Mid-Point 1	Core	Mid-Point 2	Rim 2
Be	1.60	<1.02	<0.99	3.65	2.15
Na	<17.83	<39.36	<38.43	<38.41	<16.54
Mg	0.73	<1.23	<1.26	1.31	<0.51
Al	529250.40	529250.40	529250.40	529250.40	529250.40
Ti	<2.04	<4.42	<4.14	<3.99	<1.5
V	<0.26	<0.56	<0.57	<0.53	<0.25
Cr	<5.79	<12.7	<12.01	<12.11	<5.25
Mn	<1.26	<2.78	<2.7	3.20	<1.17
Fe	<35.74	<78.59	<77.61	<76.8	<33.21
Ga	0.38	<0.53	<0.51	<0.47	0.29
Total %	52.93	52.93	52.93	52.93	52.93
Element factors based on atom mole ppm					
Mg-Ti	0.61	0.00	0.00	1.10	0.00
Be-Ti	3.62	0.00	0.00	8.26	4.86
(Be+Mg)-Ti	4.23	0.00	0.00	9.36	4.86
< = below detection limit					

approximately 420 nm with only weak absorption in the UV-part of the spectrum after heating (Figure 14). The same UV-Vis spectrum was also obtained from our own run on the 'watch glass' sample (Figure 14). A similar result was also found by Emmett *et al.* (2003). The brown colour of all the samples produced by the Thai heater and our Be-treated sample was stable during the fading test. Furthermore both colour and UV-Vis spectra produced by the Be-heating process are very similar to those produced by irradiation. The only difference is a small shift of the absorption peak from approximately 400 nm (irradiated sample) to 420 nm (Be-treated sample).

The LA-ICP-MS results of the five-point-profile analysis on the cut surface of the 3.85 ct cubic sample (Figure 13d) are listed in Table II. In order to compare the trace element contents and understand their interaction, all cations are calculated as atom mole ppm (or abbreviated as amp) and normalized to 40 atoms of cation, which corresponds to 60 atoms of oxygen in the Al_2O_3 structure. As shown in Table II and plotted in Figure 15, slightly elevated Be contents appear at the

rims as compared to those at the core and correspond well with the brown rim. The extremely low Be content at the colourless core is also similar to those analysed in the unheated sample cut from the same boule (Table I). Other important trace element contents such as Mg, Ti, V, Cr, Fe and Ga are extremely low without noticeable variation from the core to the rim. These contents are comparable to those in the unheated sample (mostly below the detection limits) suggesting rather pure Al_2O_3 originally. A similar result was also obtained from the three-point-profile analysis across the cut surface (not shown here).

As shown in Figure 15 and Table II, the brown rims are strongly correlated with Be. These data therefore suggest that the divalent Be (without Mg) could play an important role in the creation of the brown coloration. This is because it is very unlikely that colour can be created in a pure Al_2O_3 system by simple heating without the introduction of an element or elements from an external source.

The synthetic sapphire treated by the Thai heater was heated without addition of any



Figure 16: Photos of the 13.51 ct disc of colourless 'watch glass' sapphire (WG01) before treatment (a), and pale brown throughout the entire disc after Be-treatment under unknown conditions (b). After the treatment, a five-point-profile (c) was analysed across the 1.25 mm thick cut surface using LA-ICP-MS

(see also Figure 17). The other half of the sample was then cut into three pieces; one piece was kept as the reference and the other two pieces were heated in a pure nitrogen atmosphere at 1650°C for three hours which turned the stone colourless (d). One of the resulting colourless pieces was re-heated in air (in oxidation conditions) at 1650°C for one hour, which turned the sample back to pale brown (e). (Photos by Somboon, GIT and Lomthong, KU)

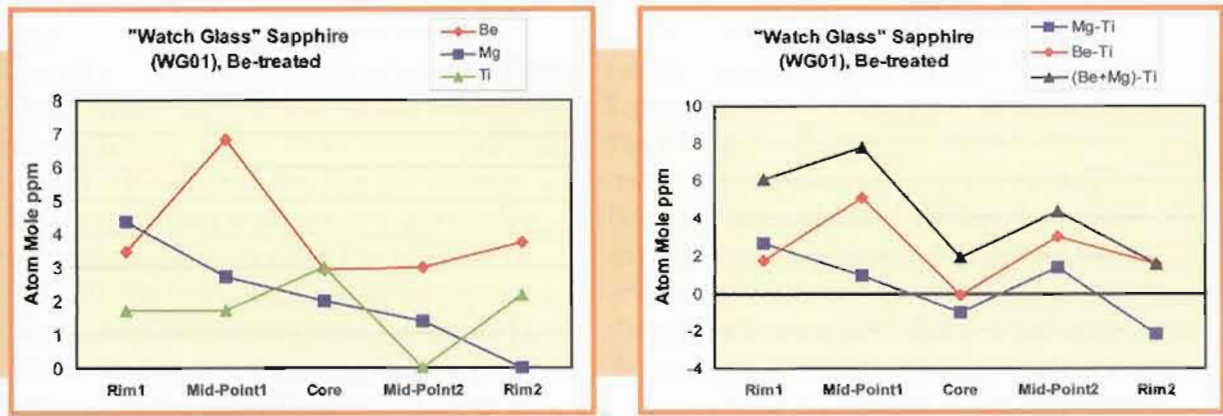


Figure 17: Plots of trace element content variation across the 1.25 mm thick cut surface of the pale brown Be-treated 'watch glass' sapphire disc (WG01). The contents of Be are dominant over those of Mg and Ti in almost all the points analysed, and (Be+Mg) > Ti in all analysed points (cf. Figure 16c).

Be-containing substance, e.g. chrysoberyl. Nonetheless, the LA-ICP-MS results have proved without doubt that a few ppm of Be must have entered the sample from an external source. The Be might have come from the crucible and/or furnace that previously had been heat-treated with Be-containing substances. This could explain why there are such low Be contents in this batch of samples (see also the next two samples) as compared

with ten of ppm in the other samples obtained from other heaters (see later section). It is also surprising to realize that only a few ppm of Be are enough to create a pale brown colour in this relatively pure Al_2O_3 sample. A 'watch glass' of colourless synthetic sapphire (WG01) was heat-treated under the same conditions as those used for the flame-fusion stones and gave similar results, shown in Figures 16 and 17.

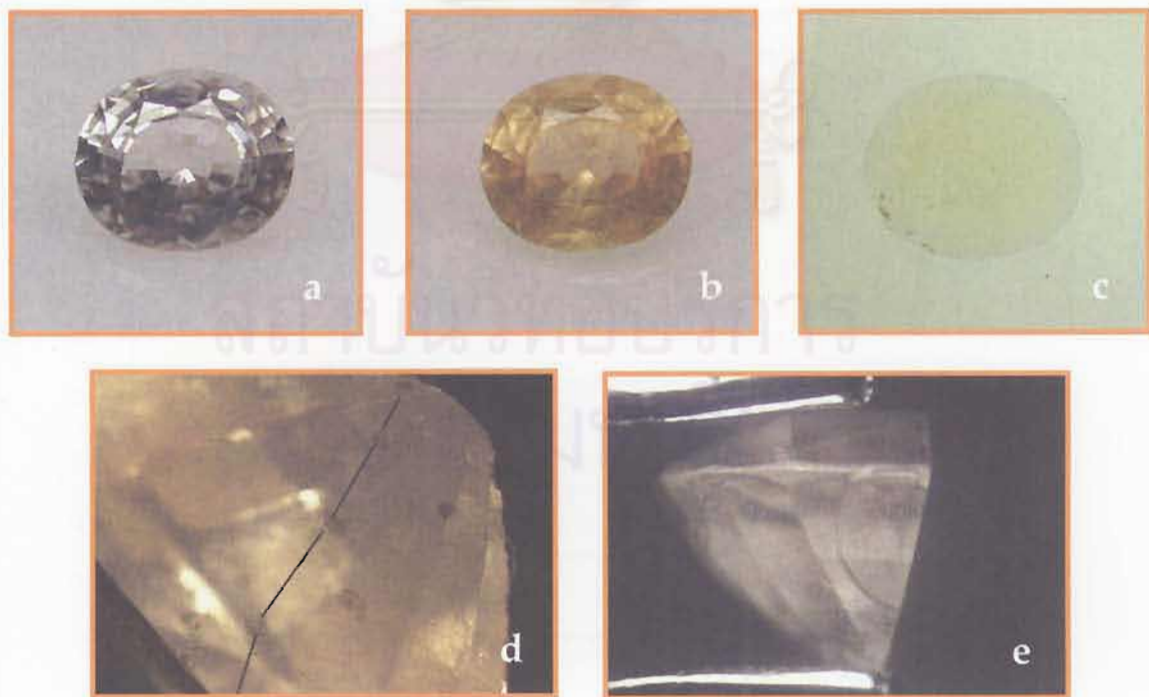


Figure 18: Photos of a 0.80 ct natural colourless sapphire (POMCS03) before treatment (a), yellow after Be-heat treatment (b) and in the immersion liquid (c). A five-point profile (d) was analysed across the cut surface after the treatment using LA-ICP-MS (see also Table III and Figure 20). The other half was heated in a reducing atmosphere at 1650°C for three hours, which turned the stone colourless (e). (Photos by Somboon, GIT and Lomthong, KU)

Be-treated natural colourless sapphires

The 0.80 ct oval natural colourless sapphire was heat-treated by the Thai heater under the same conditions as the flame-fusion grown specimen. The sample has turned intense yellow throughout without any particular surface-related colour after the treatment (Figure 18). Of two other natural samples (obtained from the same gemstone dealer) in the same run, however, one turned slightly yellow and in the other there was almost no colour change. Similar yellow colours were also observed in our own heating experiment on two natural colourless sapphires mixed with ground chrysoberyl and heated at 1750°C in an oxidizing atmosphere (in air) for 30 hours. The UV-Vis spectra of the intense yellow one changed from a flat line before heating to a pronounced increase of absorption in the UV-part of the spectrum with a shoulder at 460 nm after heating (Figure 19). The yellow colour was stable under a fading test.

The LA-ICP-MS results of the 5-point profiles across the cut surface (Table III and Figure 20) reveal a few ppm of Be (all values are above the detection limits) without noticeable concentration in the rims. These Be values are distinctly higher than those of the unheated sapphire where all Be values are below the detection limits (Table I). These data therefore suggest that a small amount of Be has been diffused into the stone from an external source – similar to the conclusion reached for the flame-fusion grown and the ‘watch glass’ samples, again probably from a contaminated crucible and/or furnace.

All the points analysed show rather high Mg content (Table III and Figure 20) compared with Ti and Be contents but there is no particular concentration in core or rim of any of the trace elements measured. The Cr contents are extremely low (below detection limit). When Mg and Ti are

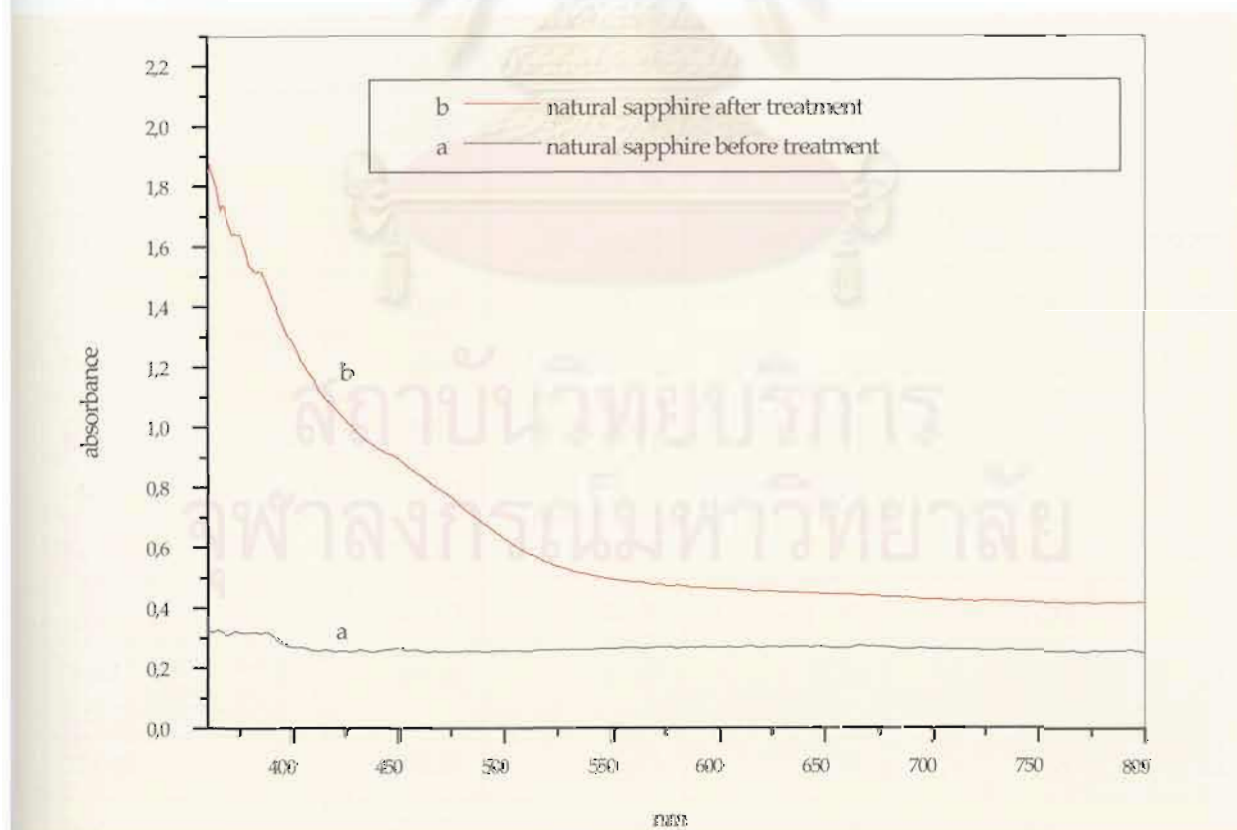


Figure 19: Spectra of the natural colourless sample (PDMCS03) before treatment (a) and after the Be-heat treatment (b) (see also Figure 18a, b).

Table III: Trace element contents of the 0.80 ct Be-treated natural colourless sapphire (POMSC03) which became yellow after the treatment, obtained by LA-ICP-MS.

$\mu\text{g/g}$	Rim 1	Mid-Point 1	Core	Mid-Point 2	Rim 2
Be	1.23	4.68	2.52	2.79	2.90
Na	<18.10	<33.67	<29.32	<29.56	<18.11
Mg	95.38	144.81	71.52	67.48	80.15
Al	529250.40	529250.40	529250.40	529250.40	529250.40
Ti	74.48	78.19	65.95	58.30	51.33
V	2.44	2.82	2.47	2.33	1.98
Cr	<5.28	<9.51	<8.30	<8.73	<5.37
Mn	<1.25	<2.32	<2.01	<2.05	<1.27
Fe	347.76	402.65	348.55	325.47	342.53
Ga	68.88	61.42	58.20	61.22	64.24
Total %	52.98	52.99	52.98	52.98	52.98
Cations (Atom Mole ppm)					
Be	2.78	10.58	5.7	6.31	6.56
Na	0.00	0.00	0.00	0.00	0.00
Mg	79.97	121.39	59.97	56.58	67.20
Al	399737.57	399668.81	399761.10	399774.71	399759.85
Ti	31.69	33.26	28.06	24.80	21.84
V	0.98	1.13	0.99	0.93	0.79
Cr	0.00	0.00	0.00	0.00	0.00
Mn	0.00	0.00	0.00	0.00	0.00
Fe	126.89	146.89	127.18	118.76	124.98
Ga	20.13	17.95	17.01	17.90	18.78
Total (Atom Mole%)	40.00	40.00	40.00	40.00	40.00
Mg-Ti	48.28	88.13	31.91	31.78	45.36
Be-Ti	-28.90	-22.68	-22.36	-18.49	-15.28
(Be+Mg)-Ti	51.06	98.71	37.61	38.09	51.92
< = below detection limit of which 0.00 value is used for calculation of atom mole ppm					

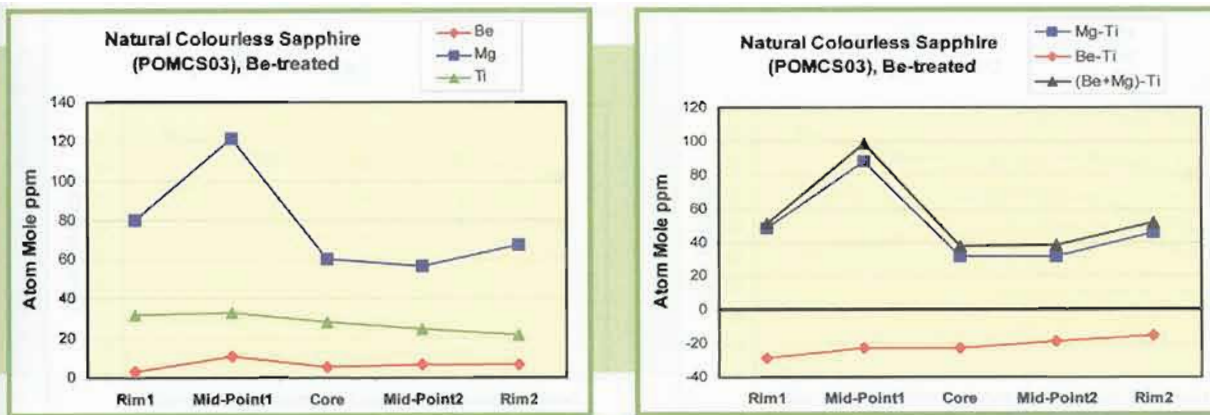


Figure 20: Plots of trace element content variation across the cut surface of the Be-treated natural colourless sapphire (POMCS03), which became yellow after the treatment, cf. Figure 18d and see text.

present in corundum they commonly form $MgTiO_3$ clusters, and it is the amount of excess Mg over Ti that is significant in forming yellow colour centres (see Box I; Häger, 1996, 2001; and Emmett *et al.*, 2003). This sample has strong excess of Mg and Mg-Ti contents range from 32 to 88 amp. Hence, the excess Mg or Mg+Be could lead to the formation of a stable yellow colour in this sample.

Yellow and orangey-yellow Be-treated sapphires

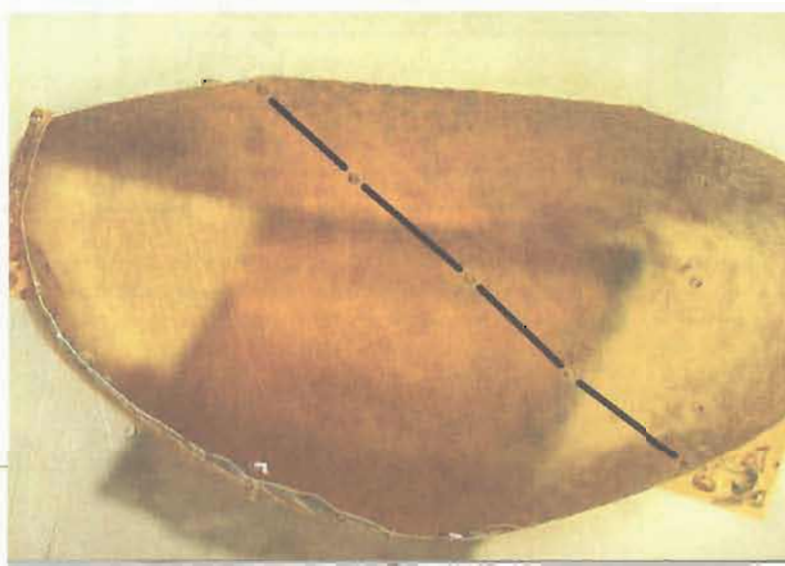
All three yellow and orangey-yellow sapphires stated to have been heat-treated in Thailand also gave similar results. The LA-ICP-MS results reveal rather high Be contents in the samples and an excess of Be+Mg over Ti content in all the points analysed (two samples are shown in Figures 21-24 and Tables IV and V). Although Cr is present, it appears to be too low to create a pink hue in sample PPYS1, but in MadaRough01 (Table V) it is sufficient to make the stone appear orange.

Be-treated blue sapphires

Two blue sapphires from an unknown source reportedly heat-treated with Be by a Thai heater show a thin surface-related yellow zone surrounding a blue core (one is shown in Figure 25). High magnification

shows that the blue core contains oriented blue dots probably resulting from partial dissolution of rutile needles. The LA-ICP-MS data (Table VI and Figure 26) reveal the elevated Be contents of the yellow rims and its absence at the blue core, again indicating Be diffusion from an external source. All the analysed points in the cores show an excess of Ti after calculation of colourless $MgTiO_3$ or $BeTiO_3$ clusters (i.e. Mg-Ti and Be-Ti content show negative values). In the yellow rim there is an excess of Be+Mg over Ti, while in the blue core Be+Mg is lower than Ti.

Figure 21: Photo of a yellow sapphire (PPYS1) reportedly heat-treated with Be under unknown conditions by a Thai heater. The sample appears yellow throughout the entire stone and lacks a surface-related colour zone. A five-point profile was analysed across its cut surface (see Table IV and Figure 22). (Photo by Somboon, GIT, and Lom-thong, KU)



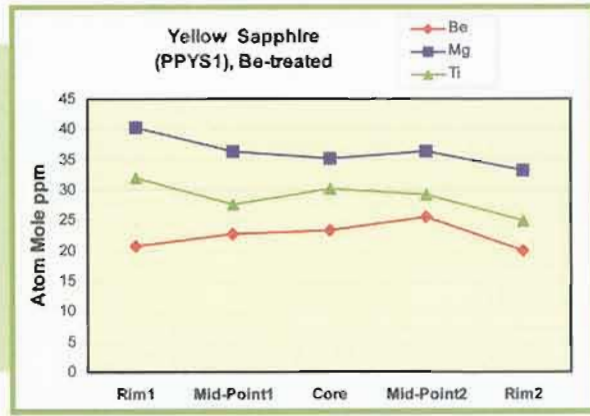
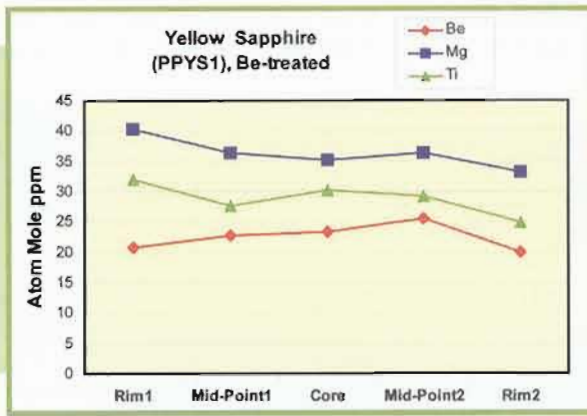


Figure 22: Plots of trace element content variation across the cut surface of the yellow Be-treated sapphire (PPYS1). No significant variation of Be, Mg and Ti content is apparent (see Table IV) across the profile. All the points analysed (Figure 21) however, show $(Be+Mg) > Ti$ contents.

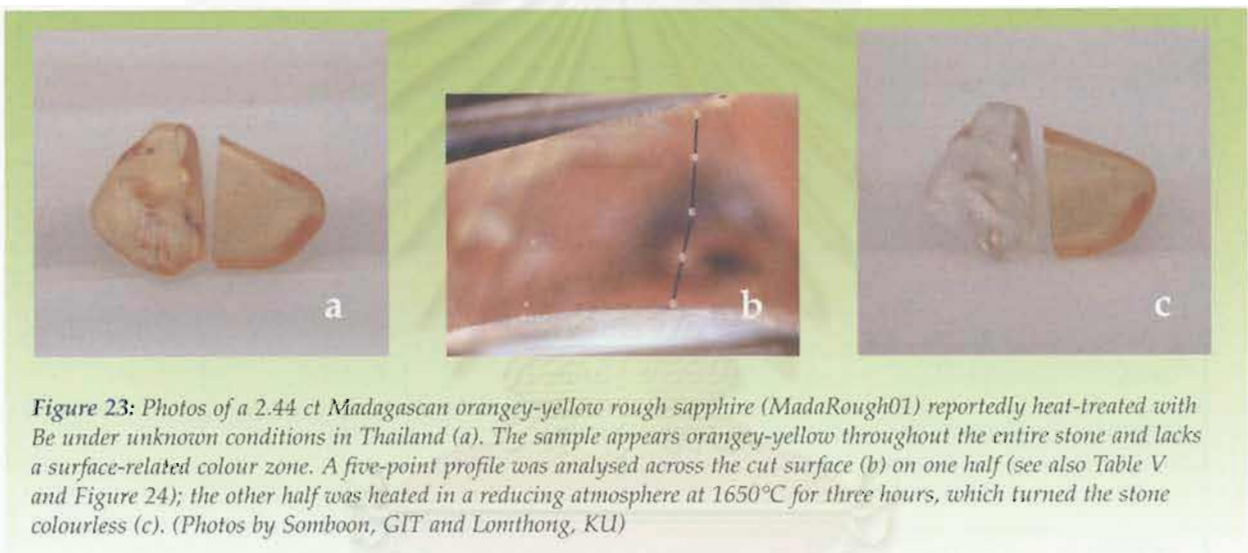


Figure 23: Photos of a 2.44 ct Madagascan orangey-yellow rough sapphire (MadaRough01) reportedly heat-treated with Be under unknown conditions in Thailand (a). The sample appears orangey-yellow throughout the entire stone and lacks a surface-related colour zone. A five-point profile was analysed across the cut surface (b) on one half (see also Table V and Figure 24); the other half was heated in a reducing atmosphere at 1650°C for three hours, which turned the stone colourless (c). (Photos by Somboon, GIT and Lomthong, KU)

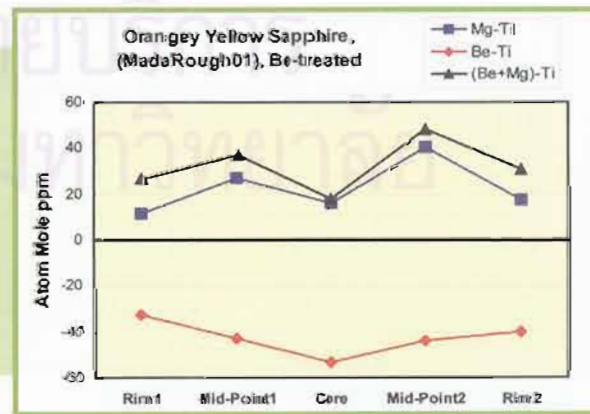
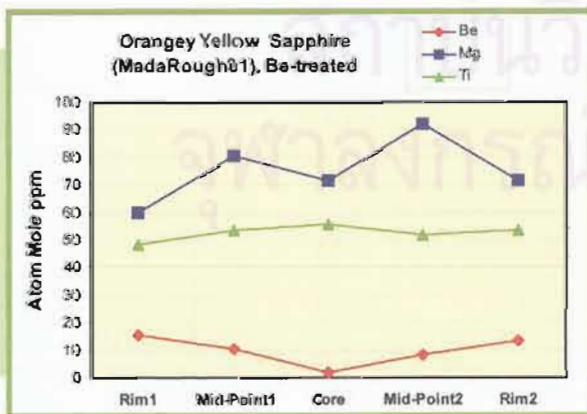


Figure 24: Plots of trace element content variation across the cut surface of the orangey-yellow Be-treated rough sapphire (MadaRough01, Figure 23b). The analyses show higher Be contents at the rims, gradually decreasing toward the core. The contents of Mg, Ti and other trace elements (see Table V) however, show no consistent variation across the profile. At all the points analysed $(Be+Mg) > Ti$.

Table IV: Trace element contents of a yellow Be-treated sapphire (PPYS1) showing rather high content of Be, Mg, Ti and Fe but low Cr content across the profile. Results obtained from LA-ICP-MS.

$\mu\text{/g}$	Rim 1	Mid-Point 1	Core	Mid-Point 2	Rim 2
Be	9.14	10.02	10.29	11.27	8.86
Na	<13.54	<11.63	<13.89	<11.89	<11.30
Mg	48.01	43.39	42.03	43.44	39.61
Al	529250.40	529250.40	529250.40	529250.40	529250.40
Ti	75.47	65.06	71.09	68.82	58.36
V	20.11	19.62	18.88	19.76	21.50
Cr	32.58	35.65	35.68	32.94	34.43
Mn	<0.67	<0.58	<0.72	<0.58	<0.55
Fe	2237.19	2210.06	2119.11	2375.70	2424.42
Ga	73.94	74.56	73.07	76.35	81.14
Total %	53.17	53.17	53.16	53.19	53.19
Cations (Atom Mole ppm)					
Be	20.63	22.62	23.23	25.44	20.00
Na	0.00	0.00	0.00	0.00	0.00
Mg	40.18	36.32	35.18	36.35	33.15
Al	399049.91	399064.88	399096.62	399000.72	398993.41
Ti	32.05	27.63	30.19	29.22	24.78
V	8.03	7.84	7.54	7.89	8.58
Cr	12.75	13.95	13.96	12.89	13.47
Mn	0.00	0.00	0.00	0.00	0.00
Fe	814.87	805.02	771.95	865.21	882.94
Ga	21.57	21.76	21.32	22.27	23.67
Total (Atom Mole%)	40.00	40.00	40.00	40.00	40.00
Mg-Ti	8.13	8.69	4.99	7.13	8.37
Be-Ti	-11.42	-5.01	-6.96	-3.79	-4.78
(Be+Mg)-Ti	28.76	31.31	28.22	32.57	28.36
< = below detection limit of which 0.00 value is used for calculation of atom mole ppm					

Table V: Trace element contents of the orangey yellow Be-treated rough sapphire (MadaRough01), obtained from LA-ICP-MS.

$\mu\text{g/g}$	Rim 1	Mid-Point 1	Core	Mid-Point 2	Rim 2
Be	6.87	4.52	0.82	3.54	5.88
Na	45.25	96.93	<11.99	15.76	17.37
Mg	71.34	95.96	85.65	110.10	85.21
Al	529250.50	529250.50	529250.50	529250.50	529250.50
Ti	113.57	125.74	131.06	122.41	126.47
V	7.42	8.94	9.43	10.72	9.07
Cr	74.00	90.48	90.78	100.04	92.79
Mn	<0.39	<0.67	<0.60	<0.69	<0.23
Fe	3575.26	4099.17	4355.35	4697.28	3939.04
Ga	100.22	116.12	122.64	142.13	124.44
Total %	53.32	53.39	53.40	53.45	53.37
Cations (Atom Mole ppm)					
Be	15.49	10.18	1.85	7.97	13.25
Na	39.98	85.59	0.00	13.91	15.34
Mg	59.62	80.15	71.54	91.92	71.19
Al	398475.31	398208.18	398213.11	398043.06	398338.32
Ti	48.16	53.29	55.54	51.86	53.61
V	2.96	3.56	3.76	4.27	3.62
Cr	28.91	35.32	35.44	39.04	36.24
Mn	0.00	0.00	0.00	0.00	0.00
Fe	1300.37	1489.92	1583.06	1706.61	1432.19
Ga	29.20	33.81	35.71	41.37	36.24
Total (Atom Mole%)	40.00	40.00	40.00	40.00	40.00
Mg-Ti	11.46	26.86	15.99	40.06	17.58
Be-Ti	-32.68	-43.11	-53.70	-43.88	-40.37
(Be+Mg)-Ti	26.95	37.04	17.84	48.03	30.83
< = below detection limit of which 0.00 value is used for calculation of atom mole ppm					

Figure 25: Photo of a blue sapphire (PPBS1) reportedly heat treated with Be under unknown conditions by a Thai heater. The sample shows a thin surface-related yellow rim surrounding the blue core. High magnification reveals that the blue core contains oriented blue dots probably resulting from partial dissolution of rutile needles. A five-point profile was analysed across the cut surface with two points in the surface-related yellow zone (rims) and three points in the blue core. (Photo by Somboon, GIT and Lomthong, KU)

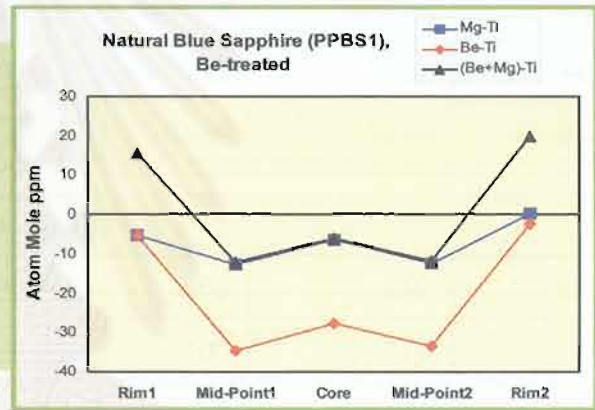
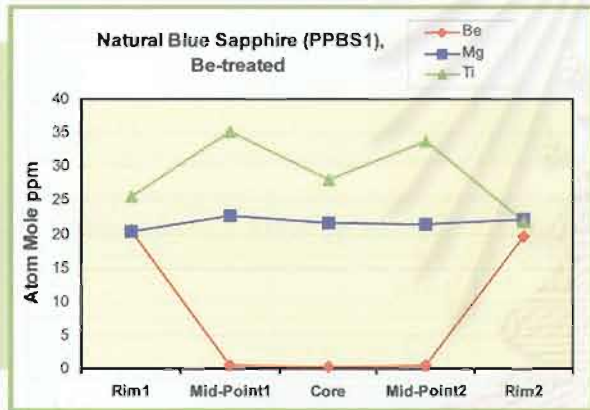


Figure 26: Plots of the trace element content variation across the cut surface of the Be-treated blue sapphire (PPBS1, Figure 25). The Be contents are obviously high at the yellow rims and are negligible in the blue core. The contents of Mg and Ti (also other trace elements, see Table VI) however show no consistent variation across the profile. The analyses also show $(Be+Mg) > Ti$ at the yellow rims in contrast to $Ti > (Be+Mg)$ in the blue core.



Figure 27: A natural blue sapphire was cut in half; the left half was heat treated with ground chrysoberyl in a crucible while the right half was heated in another crucible without chrysoberyl. The heating procedure for both crucibles was 1750°C for 30 hours in air. After heat treatment the left half shows a surface-related yellow rim whereas the right half is blue throughout the stone. (Photo by Häger)

Table VI: Trace element content of a Be-treated blue sapphire (PPBS1), obtained from LA-ICP-MS.

μ/g	Rim 1	Mid-Point 1	Core	Mid-Point 2	Rim 2
Be	9.15	0.26	<0.17	<0.22	8.71
Na	<10.82	<9.77	<10.63	<14.53	<12.40
Mg	24.54	27.14	25.86	25.66	26.55
Al	529250.40	529250.40	529250.40	529250.40	529250.40
Ti	60.45	83.16	65.99	79.49	51.58
V	12.83	12.87	12.47	12.53	12.23
Cr	36.34	37.86	32.32	31.33	38.61
Mn	<0.53	<0.48	<0.53	<0.73	<0.62
Fe	3013.78	4303.34	3015.91	3139.35	3182.56
Ga	51.66	56.00	53.22	53.84	54.13
Total %	53.25	53.38	53.25	53.26	53.26
Cations (Atom Mole ppm)					
Be	20.64	0.58	0.00	0.00	19.65
Na	0.00	0.00	0.00	0.00	0.00
Mg	20.53	22.68	21.63	21.46	22.20
Al	398801.73	398340.61	398819.35	398769.19	398742.19
Ti	25.66	35.25	28.01	33.73	21.89
V	5.12	5.13	4.98	5.00	4.88
Cr	14.21	14.79	12.64	12.25	15.09
Mn	0.00	0.00	0.00	0.00	0.00
Fe	1097.05	1564.65	1097.87	1142.66	1158.31
Ga	15.06	16.31	15.52	15.70	15.78
Total (Atom Mole%)	40.00	40.00	40.00	40.00	40.00
Mg-Ti	-5.13	-12.58	-6.38	-12.27	0.32
Be-Ti	-5.02	-34.67	-28.01	-33.73	-2.24
(Be+Mg)-Ti	15.51	-12.00	-6.38	-12.27	19.96
< = below detection limit of which 0.00 value is used for calculation of atom mole ppm					

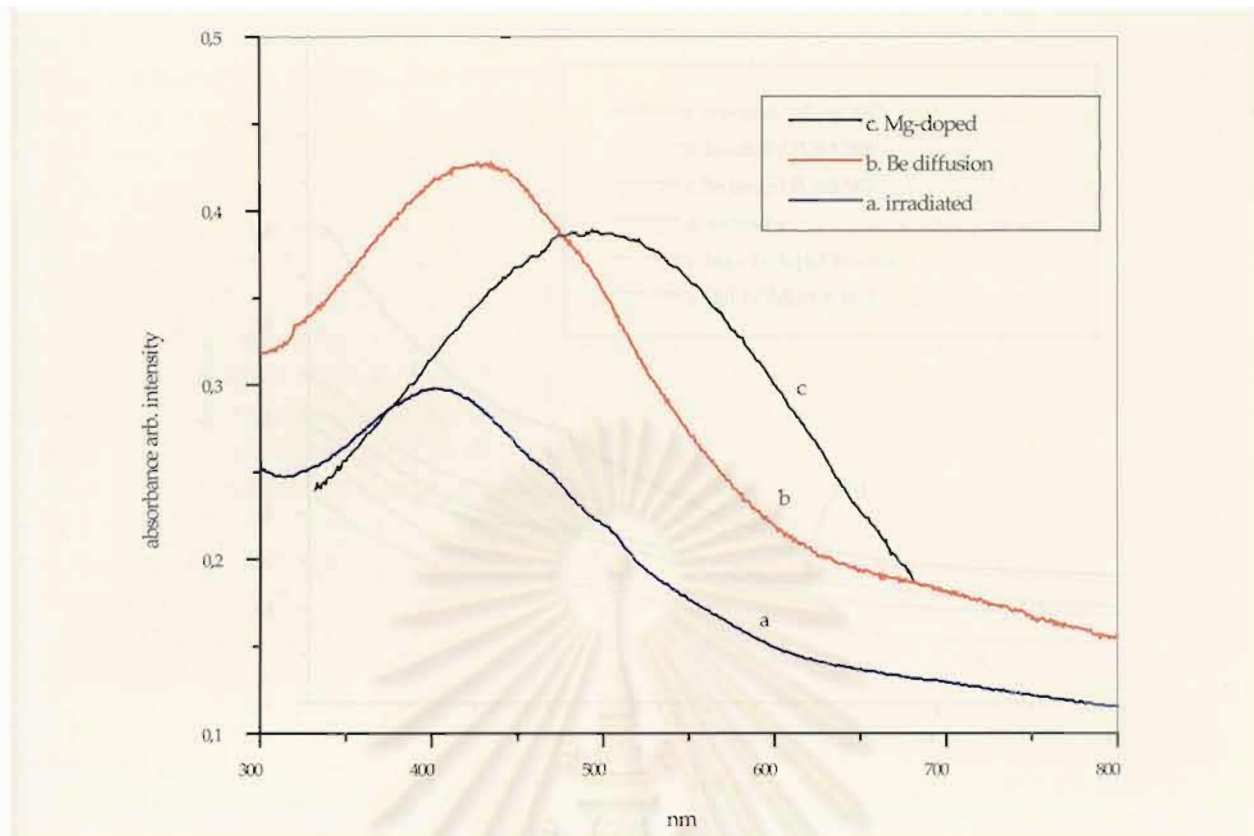


Figure 28: Three UV-Vis spectra of synthetic corundums: pale brown after irradiation with X-rays (a), pale brown after diffusion treatment with Be (b), and brown to violet after doping with Mg (c).

Discussion

The samples can be divided into two groups on the basis of their trace element contents. The first group consists of synthetic colourless sapphires with extremely low trace element contents, and the second group is dominated by trace contents of iron.

First group: 'pure' colourless sapphires

In the first group, the irradiation experiments with colourless flame-fusion grown sapphires produced a pale brown colour and a broad absorption band near 400 nm. This absorption band is unstable to normal heat and light and can be attributed to irradiation-related colour centres (see Figure 28). The detailed assignment of this absorption band is outside the scope of the present paper and will be discussed in another paper.

After Be-treatment, the synthetic colourless sapphires also turned pale brown and although the absorption pattern is similar to

that of the irradiated sapphire, the broad absorption band is centred at about 420 nm. LA-ICP-MS analyses of sapphires supplied by the trade and our own Be-heating experiments indicate that Be has diffused into the stones from an external source. Be is directly related to the brown coloration. The other trace element contents remained unchanged. This absorption band is stable to normal daylight and to heating in an oxidizing atmosphere and has been clearly influenced by the diffusion of Be. In the corundum structure there are probably Be-related colour centres (or Be-trapped hole centres) which are created and stable only in an oxidizing environment and which can easily be eliminated by heating in a reducing environment (see also Emmett *et al.*, 2003).

Synthetic Mg-doped sapphires show a broad absorption band with a maximum at about 500 nm (see Figure 28) and are brownish-violet. Similar spectra of Mg-doped

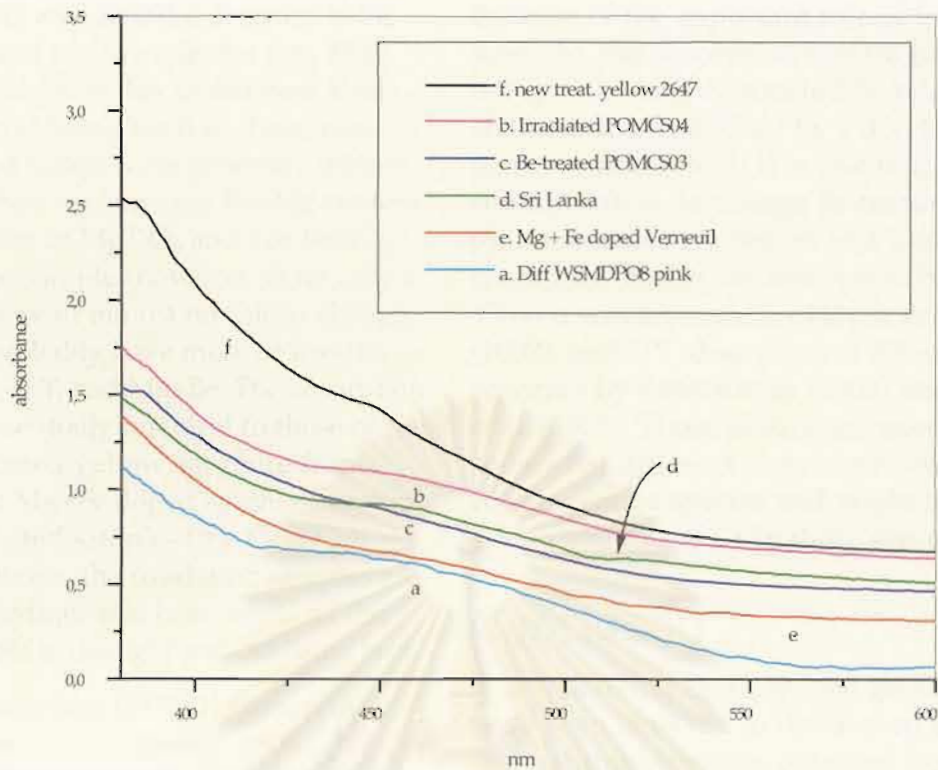


Figure 29: UV-Vis spectra of yellow sapphires: a natural sample irradiated with X-rays (b), natural samples after Be-treatment (c and f), a natural sample from Sri Lanka (d), the residual spectrum obtained by the subtraction of the spectrum of a pale pink natural sapphire before treatment from that of an orange Be-treated natural sapphire (a), a synthetic sample double-doped with Mg and Fe (e).

sapphires have been described by Andreev *et al.* (1976), Wang *et al.* (1983) and Häger (1996, 2001). The Mg-related colour centres (or Mg-trapped hole centres) are created only by heating in an oxidizing atmosphere and can easily be eliminated by reduction heating (e.g. Kvapil *et al.*, 1972, 1973; Andreev *et al.*, 1976; Wang *et al.*, 1983; Emmett and Douthitt, 1993; Häger, 1996; 2001; Emmett *et al.*, 2003).

Hence, based on their similar behaviour, we believe that Be^{2+} and Mg^{2+} act in a very similar way as stabilizers of colour centres in these synthetic sapphires. It has been shown in this study that yellow coloration cannot be produced by irradiation or by Be-heat treatment in the pure Al_2O_3 system. The absorption spectra of brown and yellow sapphires are shown in Figures 28 and 29 and do not have absorption bands in common. It seems that combination with other trace element(s) is required to produce yellow colour centres.

Second group: sapphires with significant Fe content

Natural colourless sapphires and a synthetic sapphire double-doped with Fe and Mg belong to the second group. Irradiated samples with a significant Fe content show an intense yellow colour after treatment. The UV-Vis spectra of the irradiated samples show a pronounced increase of absorption in the UV-part of the spectrum and a shoulder at about 460 nm (Figure 29). Similar colours and spectra can be observed in natural unheated Sri Lankan yellow sapphires and in the synthetic sapphire double-doped with Fe+Mg (Figure 29).

Elevated Be contents have been found in the treated stones obtained from a number of heaters in Thailand, but no consistent variation in Mg or any other trace element was detected in the core to the rim. This is in contrast to the observation of Peretti and

Günther (2002) who found a decrease in Fe, Cr, Ti, V, Ga and Mg towards the rim. This discrepancy might be due to different kinds of flux material being used in those runs. The Be-treated samples are generally intense yellow and show an excess of Be+Mg content after calculation of MgTiO_3 and /or BeTiO_3 clusters. Some samples however show only a very pale yellow or almost no colour change; such stones probably have more or less the same amount of Ti and Mg+Be. The absorption spectra are essentially identical to those of the natural untreated yellow sapphire from Sri Lanka, the Mg+Fe doped synthetic crystals and the irradiated samples (see *Figure 29*). As pointed out above, the irradiated samples are unstable to daylight and heat, while all the others are stable in daylight and oxidizing heat.

The blue sapphire (PPBS1) shown in *Figures 25* and *26* is a stone in which Ti exceeds the Mg content in all analysed points. However, in the yellow rim the sum of Be+Mg exceeds the Ti content. These data strongly suggest that the yellow hue can only be formed if there is an excess of Be+Mg over Ti content in the lattice. With the 'classical' heat treatment, it was not possible to turn such a sample yellow, but with diffusion of Be into the corundum lattice it is now possible to change the balance of the Ti/(Be+Mg) ratio. This is confirmed by our own heating experiment (see *Figure 27*). Although at first sight this result seems to be in contrast to that reported by Peretti and Günther (2002), their analytical data are presented in ppm by weight (D. Günther, pers. comm., 2002) and not in atom mole ppm. If the data are recalculated into atom mole ppm in all yellow stones and yellow zones, the sum of Mg+Be exceeds the Ti contents and the results are in fact consistent with ours.

In summary, the results lead us to believe that the unstable yellow colour produced by irradiation is caused by a combination of iron and a defect centre, and the stable yellow colour centre produced by heat and Be diffusion in an oxidizing atmosphere is caused by a combination of excess Be+Mg over Ti, the presence of Fe and a defect centre.

Because of the important role of iron in this scenario, the absorption spectra presented in *Figure 29* might be called Fe-related stable (if it is stabilized by a divalent element) or unstable (if it is due to irradiation) colour centres. In orange Be-treated sapphires, besides chromium and iron related absorption bands, an absorption band near 470 nm was reported by Hänni and Pettke (2002), and UV absorption at 380 nm was reported by Fritsch *et al.* (2003) and Emmett *et al.* (2003). Those absorption spectra are somewhat different from our Fe-related colour centres spectra and might be due to a high amount of Cr in those samples.

Conclusion

It was found that elevated Be contents have been detected in the treated synthetic and natural sapphires obtained from a number of heaters in Thailand and that Be has diffused into the stones from an external source. Yellow or brown coloration could develop in the Be-treated stones depending upon the (Be + Mg) /Ti ratio, the presence or absence of iron and the heating atmosphere. It is obvious that the excess of the divalent elements, Be+Mg, after calculation of colourless MgTiO_3 and/or BeTiO_3 clusters, in combination with iron and heat treatment in an oxidizing atmosphere can produce stable yellow colour centres. These yellow colour centres show similar UV-Vis patterns to those of the natural yellow sapphires from Sri Lanka and the synthetic sample double-doped with Mg and Fe. In synthetic samples without iron, however, the situation is somewhat different. The divalent Be could act in the same way as was found earlier for Mg, as a stabilizer of brown colour centres, but with a shift in the absorption maxima. If the Be-treated sapphires are heated in a reducing atmosphere, the yellow or brown colour centres are destroyed completely. Therefore it is possible to change the presented two diagrams in Box I in such a way that we add Be into the Mg corner.

Acknowledgements

The authors would like to thank Prof. Sakda Siripant, the Director of the GIT who has consistently encouraged, motivated and supported this study. The authors wish to thank the staff of the GIT Lab for their assistance: Mr Thanong Leelawatanasuk, Miss Chaniya Somboon, Miss Somruedee Sakkaravej, Miss Thitintharee Pavaro and Mr Sutas Singbamroong; and the research staff at Kasetsart University: Miss Pantaree Lomthong and Miss Sermrak Ingavanija. Close co-operation from a number of Thai heaters and traders is deeply appreciated. The LA-ICP-MS analyses were carried out with the kind assistance of Ms Tin Tin Win at the CSIRO, Australia. Comments on the LA-ICP-MS data from Dr Norman Pearson and Ms Suzy Elhlou at the GEMOC Key centre, Macquarie University, Australia are deeply appreciated, as are constructive comments and criticism from Prof. Dr Wolfgang Hofmeister and Drs Arun Banerjee, Karl Schmetzer and Dietmar Schwarz. Financial support for this study has been provided by the GIT and partially from the Ministry of University Affairs, Thailand.

References

- American Gem Trade Association (AGTA), 2002. Orange-pink sapphire alert of Jan 8, 2002, www.agta.org
- Andreev, D.V., Antonov, V.A., Arsenev, P.A., and Farshendiker, V.L., 1976. Dye centres in magnesium doped corundum monocrystal. *Kristall und Technik*, **11**, 103-8
- Chanthaburi Gem and Jewelry Association (CGA), 2003. Chanthaburi gem traders and heaters agree to disclose Beryllium treatment. Press Release by CGA, February 20, 2003 <http://www.cga.or.th>
- Coldham, T., 2002. Orange sapphires or just lemons? *Australian Gemmologist*, **22**, 288-93
- Crowningshield, R., and Nassau, K., 1981. The heat and diffusion treatment of natural and synthetic sapphires. *J. Gemm.*, **17**, 528-41
- Emmett, J.L., and Douthit, T.R., 1993. Heat treating the sapphires of Rock Creek, Montana. *Gems & Gemology*, **29**, 250-72
- Emmett, J.L., and Douthit, T.R., 2002. Beryllium diffusion coloration of sapphire – a summary of ongoing experiments. <http://www.agta.org/consumer/gtclab/treatedsapps04.htm>
- Emmett, J.L., Scarratt, K., McClure, S.F., Moses, T., Douthit, T.R., Hughes, R.W., Novak, S., Shigley, J.E., Wang, W., Bordelon, O., and Kane, R.E., 2003. Beryllium diffusion of ruby and sapphire. *Gems & Gemology*, **39**(2), 84-135
- Ferguson, J., and Fielding, P.E., 1971. The origins of colours of yellow, green and blue sapphires. *Chemical Physics Letters*, **10**, 262-5
- Ferguson, J., and Fielding, P.E., 1972. The origins of the colours of natural yellow, green and blue sapphires. *Aust. J. Chem.*, **25**, 1372-85
- Fritsch, E., Chalain, J.-P., Hänni, H.A., Devouard, B., Chazot, G., Giuliani, G., Schwarz, D., Rollion-Bard, C., Garnier, V., Barda, S., Ohnenstetter, D., Notari, F., and Maitrallet, P., 2003. Le nouveau traitement produisant des couleurs orange à jaune dans les saphirs. *Revue de Gemmologie A.F.G.*, **147**, 11-23
- Gemresearch (GRS), 2001. Reports on new treatment from Thailand. Padparadscha Research, Nov. 2001, <http://www.gemresearch.ch/news/PadPress/padpress.htm>
- Häger, T., 1992. Farbgebende und "farbhemmende" Spurenelementen in blauen Saphiren. *Berichte der Deutschen Mineralogischen Gesellschaft – Beihefte zum European Journal of Mineralogy*, **4**, 109
- Häger, T., 1993. Stabilisierung der Farbzentren von gelben natürlichen Saphiren. *Berichte der Deutschen Mineralogischen Gesellschaft – Beihefte zum European Journal of Mineralogy*, **5**, 188
- Häger, T., 1996. *Farbrelevante Wechselwirkungen von Spurenelementen in Korund*. Ph.D. Thesis, University of Mainz
- Häger, T., 2001. High temperature treatment of natural corundum. In: *Proceedings of the International Workshop on Material Characterization by Solid State Spectroscopy: The Minerals of Vietnam*, Hanoi, Vietnam. April 4-10, 2001
- Hänni, H.A., and Pettke, T., 2002. Eine neue Diffusionsbehandlung liefert orangefarbene und gelbe Sapphire. *Gemmologie. Z. Dt. Gemmol. Ges.*, **51**(4), 137-52
- Harder, H., 1980. Edelsteine durch Brennen von Korunden. *Fortschr. Miner.*, **58** Bh., **1**, 45-6
- Hughes, R.W., 1997. *Ruby and Sapphire*. RWH Publishing, Boulder. p.511
- Hughes, R.W., 2002. Treated orange sapphires raise concern, Jan 9, 2002 - updated Feb 1, 2002. http://www.palagems.com/treated_orange_sapphire.htm
- Krebs, J.J. and Maisch, W.G., 1971. Exchange effects in optical absorption spectrum of Fe³⁺ in Al₂O₃. *Physical Review B*, **4**, 757-69
- Kvapil, J., Perner, B., Súlowsky, J., and Kvapil, J., 1973. Colour centre formation in corundum doped with divalent ions. *Kristall und Technik*, **8**(1-3), 247-51
- Kvapil, J., Súlowsky, J., Kvapil, J., and Perner, B., 1972. The influence of dopants and annealing on the colour stability of ruby. *Physica Status Solidi (a)*, **9**, 665-72
- Lehmann, G., and Harder, H., 1970. Optical spectra of di- and trivalent iron in corundum. *American Mineralogist*, **55**, 98-105
- McClure, S.F., Moses, T., Wang, W., Hall, M., and Koivula, J.I., 2002. A new corundum treatment from Thailand. *Gems & Gemology*, **38**, 86-90
- Nassau, K., 1982. Comment on "Heat treating corundum". In: Editorial forum, *Gems & Gemology*, **18**, 109

- Nassau, K., 1984. *Gemstone Enhancement*. Butterworths, London
- Nassau, K., 1994. *Gemstone Enhancement*. 2nd edn. Butterworths, London
- Nassau, K., and Valente, K., 1987. The seven types of yellow sapphire and their stability to light. *Gems & Gemology*, 23, 222-31
- Nikolskaya, L.V., Terekhova, V.M., and Samoilovich, M.I., 1978. On the origin of sapphire color. *Phys. Chem. Minerals*, 3, 213-24
- Norman, M.D., Pearson, N.J., Sharma, A., and Griffin, W.L., 1996. Quantitative analysis of trace elements in geological materials by laser ablation ICPMS: instrumental operating conditions and calibration values of NIST glasses. *Geostandards Newsletter*, 20, 247-61
- Peretti, A., and Günther, D., 2002. Colour enhancement of natural fancy sapphires with a new heat-treatment technique. *Contribution to Gemology*, 1, 1-48
- Schmetzer, K., Bosshart, G., and Hänni, H.A., 1982. Naturfarbene und behandelte gelbe und orangebraune Sapphire. *Z. Dt. Gemmol. Ges.*, 31, 265-79
- Schmetzer, K., Bosshart, G., and Hänni, H.A., 1983. Naturally coloured and treated yellow and orange-brown sapphires. *J. Gemm.*, 18, 607-22
- Themelis, T., 2003. *Beryllium-treated rubies and sapphires*. T. Themelis, Bangkok. p.48
- Tombs, G.A., 1980. Further thoughts and questions on Australian sapphires, their composition and treatment. *Z. Dt. Gemmol. Ges.*, 29, 79-81
- Wang, H.A., Lee, C.H., Kroger, F.A., and Cox, R.T., 1983. Point defects in Alpha- Al_2O_3 : Mg studied by electrical conductivity, optical absorption and ESR. *Physical Review B*, 27, 6, 3821-41

Gem-A Coat of Arms



Fellows and Diamond Members

Current members of Gem-A who have gained their Diploma in Gemmology or the Gem Diamond Diploma (FGA or DGA) may apply for the use of the Coat of Arms on their stationery, within advertisements or on their website.

The Coat of Arms can be supplied either as a black-and-white bromide or in colour on disk.

It is a requirement of the Gem-A that written permission be granted by the Council of Management before use of the Coat of Arms. An application fee of £40 is payable with an annual renewal fee of £20.

For further information and an application form contact Mary Burland on +44 (0)20 7404 3334 fax +44 (0)20 7404 8843 or e-mail membership@gem-a.info



APPENDIX B.

Beryllium-Treated Vietnamese and Mong Hsu Rubies

Visut Pisutha-Armond^{1,2}, Pomsawat Wathanakul^{1,3}, Wilawan Atichat^{1,4}, Tobias Häger⁵,
Tin Tin Win⁶, Thanong Leelawatanasuk¹ and Chaniya Somboon¹

1. Gem and Jewelry Institute of Thailand (GIT), Chulalongkorn University, Bangkok 10330, Thailand

2. Department of Geology, Faculty of Science, Chulalongkorn University, Bangkok 10330, Thailand
Email: pvisut@geo.sc.chula.ac.th

3. Department of General Science, Faculty of Science, Kasetsart University, Bangkok 10900, Thailand

4. Gem & Geological Material Group, Department of Mineral Resources, Bangkok 10400, Thailand

5. Institute of Geosciences/Gemstone Research, University of Mainz, D-55099 Mainz, Germany

6. Division of Exploration and Mining, CSIRO, North Ryde, NSW 1670, Australia

Extended Abstract

It has been known among Thai heat treaters and documented in a number of literatures that ruby and sapphire from different sources respond differently under beryllium (Be) heating process (e.g., Coldham, 2002; Peretti and Günther, 2002; McClure *et al.*, 2002; Hänni and Pettke, 2002; Swarovski, 2002; Pisutha-Armond *et al.*, 2002 and in press; Wang *et al.*, 2002; Fritsch *et al.*, 2003; Emmett *et al.*, 2003; Themelis, 2003; Schmetzer and Schwarz, in press). Among those stones, Vietnamese and Mong Hsu (Myanmar) rubies of metamorphic origin were treated unsuccessfully by this technique (see Themelis, 2003). The reason for such variation has been speculated to be due their intrinsic chemical elements. However no analytical data in particular on the Vietnamese and Mong Hsu rubies has yet to verify such statement. In order to understand such observation, five Vietnamese and three Mong Hsu rubies from our own collection were heat-treated with Be-heating process under unknown condition by a Thai heater. After Be-treatment all samples grossly remain red, purplish red or pink (as compared with strong orange of the Songea samples under the same run). Four selected samples were subsequently cut in half and analyzed for trace element content across the cut surface and on the outer surface by a Laser Ablation Inductively-Coupled-Plasma Mass Spectrometry (LA-ICP-MS).

The result (see examples in Figures 1 and 2) reveals that the analyzed samples contain relatively high content of titanium (Ti) and moderate to strong excess of Ti in relation to magnesium (Mg) content ($Ti > Mg$), but rather low concentration of iron (Fe). Minor amount of Be was found to diffuse into the stones from external source. Majority of the analyzed points within the stones however show $Ti > (Be+Mg)$. Extremely high content of Be and Fe on the contrary were observed on the re-crystallized outer surface and at the points analyzed at the very rim of the samples. It was found that all the analyzed points on the outer surface and at the very rim show $(Be+Mg) \gg Ti$ which correspond fairly well with very thin yellow or orange rim. These data suggest that Be and Fe on the surface could originate from Be-containing compounds such as chrysoberyl. In these high Ti-containing stones in which $Ti > (Mg+Be)$, most of the intrinsic Mg and the diffused Be might have been tied up with the formation of

colorless MgTiO_3 and BeTiO_3 clusters. As a result there is no excess Be and/or Mg to stabilize the yellow or orange color centers or trapped hole centers (see also Kvapil *et al.*, 1972, 1973; Andreev *et al.*, 1976; Wang *et al.*, 1983; Häger, 1992, 1993, 1996 and 2001; Emmett and Douthit, 1993; Emmett *et al.*, 2003; Pisutha-Armond *et al.*, 2002 and in press; Schmetzer and Schwarz, in press). Hence no substantial yellow hue was added to these red or pink stones that could turn them into orange color. More heating time and/or higher temperature are required to increase the Be diffusion into the stones in order to achieve a desired color. It might therefore not be economically feasible to treat this type of stone by the Be-heating technique.

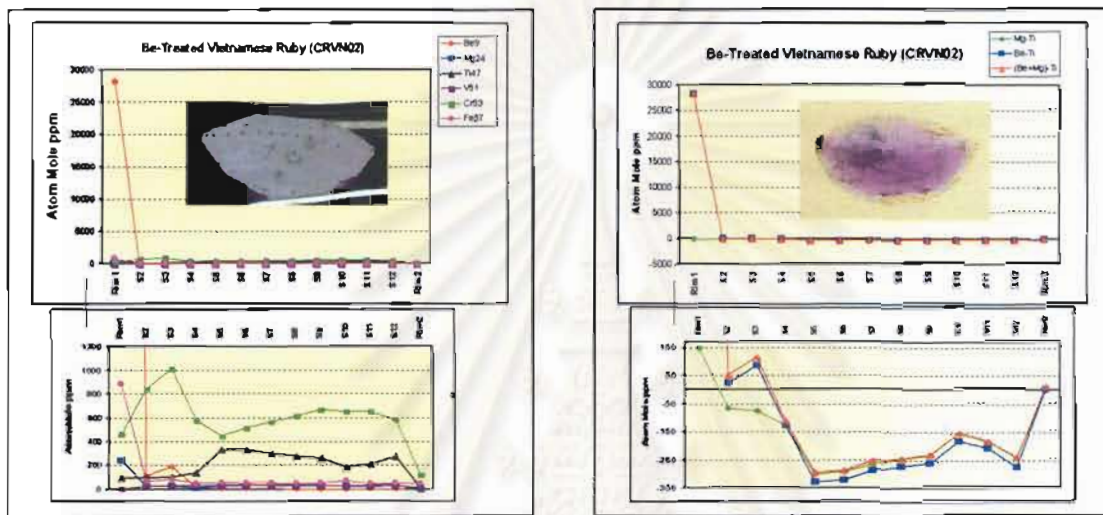


Figure 1: The trace element variation across the cut surface of a Be-treated Vietnamese ruby (CRVN02). The left inset picture shows the analyzed points starting from Rim1 on the left to Rim2 on the right. The right inset picture is the same stone under immersion liquid showing very thin yellow or orange rim. The lower diagrams are the enlarged portions of the upper diagrams.

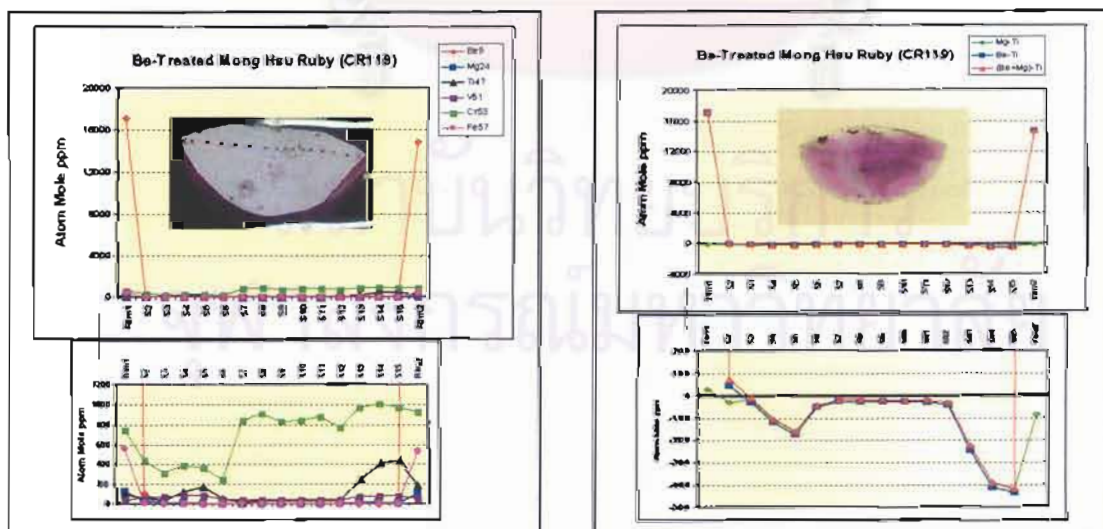


Figure 2: The trace element variation across the cut surface of a Be-treated Mong Hsu ruby (CR119). Other explanations are similar to those in Figure 1.

Acknowledgements

The authors would like to thank Prof. Sakda Siripant, the Director of the GIT who consistently encourages, motivates and supports during the course this study. The authors wish to thank the staff of the GIT Lab for their assistance; Miss Somruedee Sakkaravej, Miss Thitintharee Pavaro, Mr. Sutas Singbamroong, and the research staff at Kasetsart University; Miss Pantaree Lomthong and Miss Sermrak Ingavanija. Close co-operation from an undisclosed Thai heater is thankful. Comments on the LA-ICP-MS data from Dr. Norman Pearson and Ms. Suzy Elhlou at the GEMOC Key center, Macquarie University, Australia are deeply appreciated. The financial support for this study has been provided by the GIT and partially from the Ministry of University Affairs, Thailand.

References

- Andreev, D.V., Antonov, V.A., Arsenev, P.A. and Farshtendiker V.L., 1976. Dye centres in magnesium doped corundum monocrystal. *Kristall und Technik*, **11**, 103-108
- Coldham, T., 2002. Orange sapphires or just lemons? *Australian Gemmologist*, **22**, 288-293
- Emmett, J.L. and Douthit, T.R., 1993. Heat treating the sapphires of Rock Creek, Montana. *Gems & Gemology*, **29**, 250-272
- Emmett, J.L., Scarratt, K., McClure, S.F., Moses, T., Douthit, T.R., Hughes, R.W., Novak, S., Shigley, J.E., Wang, W., Bordelon, O. and Kane, R.E., 2003. Beryllium diffusion of ruby and sapphire. *Gems & Gemology*, **39**(2), 84-135
- Fritsch, E., Chalain, J-P., Hänni, H.A., Devouard, B., Chazot, G., Giuliani, G., Schwarz, D., Rollion-Bard, C., Garnier, V., Barda, S., Ohnenstetter, D., Notari, F., Maitrallet, P., 2003. Le nouveau traitement produisant des couleurs orange à jaune dans les saphirs. *Revue de Gemmologie A.F.G.*, **147**, 11-23
- Häger, T., 2001. High temperature treatment of natural corundum. In: Proceedings of the International Workshop on Material Characterization by Solid State Spectroscopy: *The Minerals of Vietnam*, Hanoi, Vietnam. April 4-10, 2001
- Häger, T., 1996. *Farbrelevante Wechselwirkungen von Spurenelementen in Korund*. Ph.D. Thesis, University of Mainz
- Häger, T., 1992. Farbgebende und "farbhemmende" Spurenelemente in blauen Saphiren. *Berichte der Deutschen Mineralogischen Gesellschaft - Beihefte zum European Journal of Mineralogy*, **4**, 109
- Häger, T., 1993. Stabilisierung der Farbzentren von gelben natürlichen Saphiren. *Berichte der Deutschen Mineralogischen Gesellschaft - Beihefte zum European Journal of Mineralogy*, **5**, 188
- Hänni, H.A., Pettke, T., 2002. Eine neue Diffusionsbehandlung liefert orangefarbene und gelbe Saphire. *Gemmologie. Z. Dt. Gemmol. Ges.*, **51**(4), 137-152
- Kvapil, J., Perner, B., Súlóvský, J., Kvapil, J., 1973. Colour centre formation in corundum doped with divalent ions. *Kristall und Technik*, **8**(1-3), 247-251
- Kvapil, J., Súlóvský, J., Kvapil, J., Perner, B., 1972. The influence of dopants and annealing on the colour stability of ruby. *Physica Status Solidi (a)*, **9**, 665-672
- McClure, S.F., Moses, T., Wang, W., Hall, M. and Koivula, J.I., 2002. A new corundum treatment from Thailand. *Gems & Gemology*, **38**, 86-90
- Peretti, A. and Günther, D., 2002. Colour enhancement of natural fancy sapphires with a new heat-treatment technique. *Contribution to Gemology*, **1**, 1-48
- Pisutha-Armond, V., Häger, T., Wathanakul, P., Atichat, W., 2002. A brief summary on a cause of colour in pink-orange, orange and yellow sapphires produced by the "new" heating technique. *Journal of Gem and Jewelry, Gem and Jewelry Institute of Thailand (GIT)*, **3**(18), 11-12.
- Pisutha-Armond, V., Häger, T., Wathanakul, P., Atichat, W., in press. Yellow and brown colouration in beryllium treated sapphires. *Journal of Gemmology*
- Schmetzer, K. and Schwarz, D., in press. Some diagnostic properties of orange sapphires.
- Swarovski, 2002. Swarovski scientists identify possible source of beryllium in new treated sapphires. Cited in *GIA Publication: GIA Insider*, **4**, 10, May 2002, <http://www.gia.edu/news/ViewIssue.cfm?volume=4&issue=10#3>
- Themelis, T., 2003. *Beryllium-treated rubies and sapphires*. p. 48
- Wang, H.A., Lee, C.H., Kroger, F.A. and Cox, R.T., 1983. Point defects in Alpha-Al₂O₃: Mg studied by electrical conductivity, optical absorption and ESR. *Physical Review B*, **27**, 6, 3821-3841
- Wang, W., Green, B., 2002. An update on Be-diffused corundum. *Gems & Gemology*, **38**(4), 363-365.

红、蓝宝石改善及其鉴定

—— 最新进展回顾

Visut Pisutha-Armond^{1,2}, Sakda Siripant¹, Wilawan Atichat^{1,3}, Pornsawat Wathanakul^{1,4},
Thanong Leelawatanasuk¹, Sutas Singbamroong¹, Somruedee Sakkaravej¹ and Thitintharee
Leelawatanasuk¹ and Chaniya Somboon¹

1. Gem and Jewelry Institute of Thailand (GIT), Chulalongkorn University, Bangkok 10330, Thailand

2. Department of Geology, Faculty of Science, Chulalongkorn University, Bangkok 10330, Thailand

Email: pvisut@geo.sc.chula.ac.th

3. Gem & Geological Material Group, Department of Mineral Resources, Bangkok 10400, Thailand.

4. Department of General Science, Faculty of Science, Kasetsart University, Bangkok 10900, Thailand

摘 要

由于天然宝石级红、蓝宝石的稀缺,很多改善处理技术被应用于提高次质量刚玉宝石的质量上(Hughes, 1997)。这些处理技术包括注油、染色、表面镀膜、传统热处理法、辐照、助熔剂热处理法、表面扩散热处理法、深层扩散热处理法及最新的铅玻璃充填法。在这些处理方法中,注油、染色、表面镀膜及辐照很少见,而传统热处理法、助熔剂热处理法、表面扩散热处理法、深层扩散热处理法及铅玻璃充填法在宝石市场上更常见。本文的重点即是对后一类处理方法的探讨。

为改善刚玉宝石的颜色及透明度,传统热处理法被广泛应用。刚玉宝石被置于不同类型的高温熔炉中(最高达 1850 °C),以控制处理过程的化学环境,处理过程中不加入任何化学元素。大量自制的处理炉,如焦煤炉、油炉、气炉及电炉出现并不断被改进,经反复实验与错误纠正,用来对产于各地的刚玉宝石进行改善。这些处理炉最终被证明具有经济适用的特点,适合于对产地复杂的刚玉宝石进行热处理。对刚玉宝石热处理的检测常常通过放大检查实现,即找寻热处理过程导致的包裹体,如常带有颜色扩展的部分溶解的金红石针、熔化的结晶体、包裹体周围的圆盘状应力纹、含 Ti 包裹体周围的蓝色晕轮(或见 Hughes, 1997; Themelis, 1992; Smith and McClure, 2002)。

助熔剂热处理法是对传统热处理法的改进,即加入硼砂或硅土等助熔剂来愈合裂隙或充填开放裂口或空洞。填加助熔剂的目的是防止宝石在高温热处理过程中发生炸裂及充填高折射率物质以掩盖裂隙或空洞,以此来提高宝石的净度。这一技术最早被应用于对含有很多裂隙的蒙苏红宝石的处理上,后来这一技术也被用来处理其他来源的刚玉宝石。这种处理方法的检测通常通过放大检查来实现,即找寻存在于愈合裂隙及空洞中的助熔剂和上述热处理导致的包裹体(Hughes, 1997; Themelis, 1992; Themelis, 2004; Smith and McClure, 2002)。对宝石中的助熔剂的量已经进行了一些尝试,并且在宝石鉴定证书中做了通报(见 I.M.H.C. 信息通报 2004 年第 1 期)。

表面扩散热处理法同样是对传统热处理法的改进,即在熔炉中填加致色化合物,将传统热处理法不能处理的无色蓝宝石改善为红色蓝宝石。钛和铁化合物通常用来产生蓝色蓝宝石,而铬化合物

物被用来处理红宝石。这些过渡元素仅仅能在很浅深度上扩散进入宝石并致色。因此这种处理方法能够很容易地通过浸油放大观察找寻刻面结合处的颜色富集及通过 EDXRF 测量上述元素的含量增高而被检测出来。

深层扩散热处理法即将轻元素（如 Be）由外部扩散至刚玉晶格中。Be 元素已经被证明做为黄色色心的稳定剂参与了处理宝石的呈色机制（Pisutha-Armond et al., 2002, 2003, 2004a, 2004b）。由于其原子半径小，故 Be 原子能进入刚玉晶格的深度比 Ti 及 Cr 原子大得多。这种处理方法的结果是导致了更深的颜色渗透，有时甚至穿透了整颗宝石。因此 Be 扩散处理刚玉的检测很容易实现，即通过浸油及放大检查，找寻与表面有关的颜色或由白边包围的残余蓝色色区，偶尔可见被处理方法严重改变的包裹体（或见 Emmett et al., 2003; Peretti and Günther, 2002; Peretti et al., 2003; Themelis, 2003; Schmetzer and Schwartz, 2004, Atichat et al., 2004）。但是在没有诊断性包裹体出现的刚玉宝石中，这一处理方法的检测能通过使用激光诱发分解光谱（LIBS，最近已用于宝石实验室）探测刚玉中 ppm 级的 Be 元素富集，或使用更精密的仪器设备如激光烧蚀感应耦合等离子质谱仪（LA-ICPMS）及二次电子质谱仪（SIMS）来实现。

红宝石中的铅玻璃充填法是提高净度最新的处理技术，已于 2004 年中期出现于宝石市场上。这一技术与众所周知的钻石裂隙充填技术类似。这种处理法包括了以高折射率玻璃（如铅玻璃或结晶玻璃）充填裂纹或开放裂隙。由铅玻璃充填裂隙所反射回来的光线显示蓝色，称为闪光效应。这种宝石也显示由热处理导致的镜面效应，暗示其经过了低温热处理。充填玻璃中的铅能很容易地被 EDXRF 检测出来，也能在 X 射线图象上被观察到（或见 Kitawaki, 2004）。





APPENDIX C.

Chemical Characteristic of ‘Classical’ versus ‘Beryllium’ Heat-Treated Ruby and Sapphire

Visut Pisutha-Armond^{1,2}, Tobias Häger², Pornsawat Wathanakul^{1,4}, Wilawan Atichat^{1,5},
Tin Tin Win⁶, Thanong Leelawatanasuk¹, Chaniya Somboon¹ and Chakkaphan
Sutthirat²

1. Gem and Jewelry Institute of Thailand (GIT), Chulalongkorn University, Bangkok 10330, Thailand

2. Department of Geology, Faculty of Science, Chulalongkorn University, Bangkok 10330, Thailand
Email: pvisut@geo.sc.chula.ac.th

3. Institute of Geosciences/Gemstone Research, University of Mainz, D-55099 Mainz, Germany

4. Department of General Science, Faculty of Science, Kasetsart University, Bangkok 10900, Thailand

5. Gem & Geological Material Group, Department of Mineral Resources, Bangkok 10400, Thailand

6. Division of Exploration and Mining, CSIRO, North Ryde, NSW 1670, Australia

Introduction

In the series of previous articles (Pisutha-Armond et al., 2002, 2003 and 2004) we have presented the Laser Ablation Inductively-coupled-Plasma Mass Spectrometry (LA-ICP-MS) results of Be-treated synthetic and natural colorless sapphires and Be-treated natural yellow and orangey yellow sapphires, and some Be-treated natural blue sapphires and rubies. We have discovered that majority of Be-treated sapphires show indications of Be diffusion from external source. We always found that there are the excess of (Be+Mg) relative to Ti content in the yellow sapphires. In the high Ti-containing rubies such those from Mong Hsu, Myanmar and Vietnamese in which $Ti \gg Mg$ (Pisutha-Armond et al., 2003), the Be-treatment was mostly unsuccessful in turning the stones orange due to the fact that Ti was still in excess of (Mg+Be). We also found from our own oxidation and reduction heating experiment that oxidizing condition is an important factor for creating yellow color center.

Hence up to the present knowledge we believe that the excess of the divalent elements, Be+Mg, after calculation of colourless $MgTiO_3$ and/or $BeTiO_3$ clusters, in

combination with iron and the heat treatment in oxidising atmosphere can produce the stable yellow colour centers. In synthetic samples without iron, however, the situation is somewhat different. The divalent Be could act in the same way as it was found earlier for Mg, as a stabiliser of brown colour centres.

In this short communication we continue to present the LA-ICP-MS result of non-Be-treated and Be-treated natural and synthetic corundums from various sources which will give a better understanding of trace element interaction and the causes of color.

Result

Non-Be-treated and Be-treated natural blue sapphires

In the non-Be-treated blue sapphires, no Be has been detected and always $Ti > Mg$ content. In Be-treated natural blue, we have continued to discover that the sapphires show indications of Be diffusion from an external source. We always found that there are the excess of (Be+Mg) relative to Ti content in the yellow rim whereas in the blue core $Ti > Mg$ or (Mg+Be) content.

Non-Be-treated and Be-treated natural rubies and pink sapphires

In the non-Be-heating, Be has not been detected. We found that the excess of Mg to that of Ti has to more than approximately 30 atom mole ppm before orange colour can be developed in the non-Be-treated orange sapphire. In Be-treated natural rubies and pink sapphires, significant amount of Be has been found to diffuse into the stone from an external source to produce the orange coloration. In the Be heating of synthetic corundum however it requires more than approximately 5 atom mole ppm of excess Be in the lattice to produce yellow or brown coloration.

Be-Treated Synthetic Ruby

One Be-treated synthetic ruby shows orangy red color and indications of Be-diffusion from an external source. This synthetic ruby contains high Cr content but other trace elements are extremely low, in particular very low Fe content which still produce

orange color by the diffusion of Be. This data therefore suggest that combination of Cr and Be (without Fe) could also produce orange color. Similar result has also been found by Peretti et al. (2003).

References

- Peretti, A., Guenther, D., and Graber, A.-L., 2003. The beryllium treatment of fancy sapphires with a new heat-treatment technique (part B). *Contributions to Gemology*, 2, 21-33
- Pisutha-Armond, V., Häger, T., Wathanakul, P., Atichat, W., 2002. A brief summary on a cause of colour in pink-orange, orange and yellow sapphires produced by the “new” heating technique. *Journal of Gem and Jewelry*, Gem and Jewelry Institute of Thailand (GIT), 3(18), 11-12.
- Pisutha-Armond, V., Häger, T., Wathanakul, P., Atichat, W., 2004. Yellow and brown colouration in beryllium treated sapphires. *Journal of Gemmology*, 29(2), 77-103
- Pisutha-Armond, V., Wathanakul, P., Atichat, W., Haeger, T., Win, T.T., Leelawatanasuk, T., and Somboon, C., 2003. Beryllium-treated Vietnamese and Mong Hsu rubies. In: Hofmeister W., Quang V.X., Doa N.Q., and Nghi T. (eds) *Proceedings of the 2nd International Workshop on Geo- and Material-Science on Gem-Minerals of Vietnam. Hanoi, October 1-8, 2003*, 171-5



APPENDIX D.

Ruby and Sapphire Treatments and Their Identification: A Review of Recent Advancement

Visut Pisutha-Arnon^{1,2}, Sakda Siripant¹, Wilawan Atichat^{1,3}, Pomsawat Wathanakul^{1,4},
Thanong Leelawatanasuk¹, Sutas Singbamroong¹, Somruedee Sakkaravej¹,
Thitintharee Leelawatanasuk¹ and Chaniya Somboon¹

1. *Gem and Jewelry Institute of Thailand (GIT), Chulalongkorn University, Bangkok 10330, Thailand*

2. *Department of Geology, Faculty of Science, Chulalongkorn University, Bangkok 10330, Thailand*

Email: pvisut@geo.sc.chula.ac.th

3. *Gem & Geological Material Group, Department of Mineral Resources, Bangkok 10400, Thailand.*

4. *Department of General Science, Faculty of Science, Kasetsart University, Bangkok 10900, Thailand*

Extended Abstract

Because of the scarcity of natural gem-quality ruby and sapphire, many treatment techniques have been practiced to improve inferior quality corundum for many centuries (Hughes, 1997). The treatments range from oiling, dyeing, surface coating, classical heating, irradiation, flux-enhanced heating, shallow diffusion heating, deep diffusion heating and the most recent one, lead(Pb)-glass filling. Among those treatments, oiling, dyeing, surface coating and irradiation are rarely encountered whereas classical heating, flux-enhanced heating, shallow diffusion heating, deep diffusion heating and Pb-glass filling are more common in the gem market. Emphasis of this presentation therefore will be given to the latter categories.

Classical heating is widely used for enhancement of corundum to improve its color and clarity. The stones were heated in different types of high temperature (up to ~1850°C) furnaces to control the atmosphere without addition of any chemical element. Various types of home-made furnace such as coke furnace, oil furnace, gas furnace and electric furnace, were invented and constantly modified, by trial and error, for treatment of corundum from many sources. Such furnaces are eventually proved to be practically low cost and economically suitable for heat treatment of corundum from various sources. This has been an appropriate proprietary among Thai treaters. The detection of heating in corundum is routinely accomplished with magnification by the presence of thermally altered inclusions, such as partially dissolved rutile-needles often with color bleeding, melted crystals, tension-discs surrounding inclusions, blue-halos surrounding Ti-bearing inclusions (see also Hughes, 1997; Themelis, 1992; Smith and McClure, 2002)

The flux-enhanced heating is a modification of classical heating with addition of flux materials such as borax and/or silica to heal fissures or to fill open fractures or cavities. The purpose of addition of flux is to prevent the stone from fracturing during high temperature heating and to disguise fissures or fractures by infilling with higher refractive substances, thereby enhancing its clarity. This technique was firstly applied to Mong Hsu ruby which by its nature contains many fractures. Later this technique has also been used for stones from other sources. The treatment is routinely detected with magnification by the presence of flux material in healed fissures and cavities as well as the presence of thermally altered inclusions as previously outlined (see also Hughes, 1997; Themelis, 1992; Themelis, 2004; Smith and McClure, 2002). Attempt has been made to quantify the amount of flux-material in the stone and notify in a gem identification report (see LMHC Information Sheet No.1, 2004).

Shallow diffusion heating is also a modification of classical heating by turning an untreatable (by normal heating) colorless sapphire into a colored stone by addition of color-causing compounds into a crucible. Titanium and iron compounds are commonly used for producing blue sapphires whereas chromium compound is for ruby. These transition elements can only diffuse into the stone and produce colors at very shallow depth. Hence the treatment is readily detected with immersion and magnification, by the presence of shallow color concentration at faceted junction, as well as with EDXRF, by the elevated content of those elements.

The deep diffusion heating involves a diffusion of light element, such as beryllium (Be), from an external source into a corundum lattice. Be has been proved to take part in the color-causing mechanism in the treated stone, i.e., as a stabilizer of yellow color center (Pisutha-Arnond et al., 2002, 2003, 2004a, 2004b). Because of its small size, Be is able to permeate into the corundum lattice much deeper than Ti and Cr do. As a result, deeper color penetration or even throughout the entire stone has been noticed. Therefore the detection of Be-treated corundum is readily done, with immersion and magnification, by the presence of surface-related color or relict blue zone surrounding by a white rim, occasionally with severely altered inclusions (see also Emmett et al., 2003; Peretti and Günther, 2002; Peretti et al., 2003; Themelis, 2003; Schmetzer and Schwartz, 2004, Atichat et al., 2004). However in a stone in which no diagnostic features are present, the treatment can be proved with the detection of elevated Be concentration in the level of ppm value in the stone by laser induced breakdown spectroscopy (LIBS) –which becomes available in gemological

laboratory recently (see Hanni et al., 2004)– or by more sophisticated equipment such as laser ablation-inductively coupled plasma-mass spectrometry (LA-ICP-MS) or secondary ion mass spectrometry (SIMS).

Lead-glass filling in ruby –the latest treatment for improvement of its clarity– appears in the gem market in the mid-2004. This technique is similar to previously known fracture-filled treatment in diamond. The treatment involves filling fissures or open fractures with highly refractive glass, known as lead glass or crystal glass. The light reflected from Pb-glass-healed fissures show blue-colored reflection, called flash effect. The stones also show minor effect from heating suggested very low temperature treatment. The presence of lead in the infilling glass is readily detected by EDXRF or seen in X-ray images (see also Kitawaki, 2004; Rockwell and Breeding, 2004, GIT Lab Notes, 2004).

References

- Atichat, W., Sriprasert, B., Wathanakul, P., Pisutha-Armond, V., Sun, T.T., Puttarat, T., Leelawatanasuk, T., 2004. Characteristics of “Beryllium” Heat-treated Yellow Sapphires. *Proceedings of the 29th IGC*, p. 207-214, Wuhan, China
- Emmett, J.L., Scarratt, K., McClure, S.F., Moses, T., Douthit, T.R., Hughes, R.W., Novak, S., Shigley, J.E., Wang, W., Bordelon, O. and Kane, R.E., 2003. Beryllium diffusion of ruby and sapphire. *Gems & Gemology*, **39**(2), 84-135
- Hanni, H.A., Krzemnicki, M.S., Kiefert, L. and Chalain, J.P., 2004. A new tool in analytical gemmology: LIBS. *Proceedings of the 29th IGC*, 63, Wuhan, China
- Hughes, R.W., 1997. *Ruby and Sapphire*. RWH Publishing, Boulder., 511p
- GIT Lab Notes, 2004. New treatment on ruby: lead glass filling <http://www.git.or.th>
- Kitawaki, H., 2004. Lead-glass impregnated ruby. *Gemmology*, Laboratory report of the month of May 2004, *GAAJ*, **35** (416), (in Japanese with English translation)
- LMHC, 2004. Laboratory Manual Harmonization Committee (LMHC) Information Sheet no. 1, <http://www.git.or.th>
- Peretti, A. and Günther, D., 2002. Colour enhancement of natural fancy sapphires with a new heat-treatment technique (part A). *Contribution to Gemology*, **1**, 1-48
- Peretti, A., Günther, D., and Graber, A.-L., 2003. The beryllium treatment of fancy sapphires with a new heat-treatment technique (part B). *Contributions to*

Gemology, 2, 21-33

- Pisutha-Arnond, V., Häger, T., Wathanakul, P., Atichat, W., 2002. A brief summary on a cause of colour in pink-orange, orange and yellow sapphires produced by the “new” heating technique. *Journal of Gem and Jewelry*, Gem and Jewelry Institute of Thailand (GIT), 3(18), 11-12.
- Pisutha-Arnond, V., Häger, T., Wathanakul, P., Atichat, W., 2004a. Yellow and brown colouration in beryllium treated sapphires. *Journal of Gemmology*, 29(2), 77-103
- Pisutha-Arnond, V., Haeger, T., Wathanakul, P., Atichat, W., Win, T.T., Leelawatanasuk, T., Somboon, C., Sutthirat, C., 2004b. Chemical Characteristic of “Classical” versus “Beryllium” Heat-Treated Ruby and Sapphire. *Proceedings of the 29th IGC*, 92-94, Wuhan, China
- Pisutha-Arnond, V., Wathanakul, P., Atichat, W., Haeger, T., Win, T.T., Leelawatanasuk, T., and Somboon, C., 2003. Beryllium-treated Vietnamese and Mong Hsu rubies. In: Hofmeister W., Quang V.X., Doa N.Q., and Nghi T. (eds) *Proceedings of the 2nd International Workshop on Geo- and Material-Science on Gem-Minerals of Vietnam, Hanoi, October 1-8, 2003*, 171-5
- Rockwell, K. M. and Breeding, C. M., 2004. Rubies, clarity enhanced with a lead glass filler. *Gems & Gemology*, 40(3), 247-249
- Schmetzer, K. and Schwarz, D., 2004. The causes of colour in untreated, heat treated and diffusion treated orange and pinkish orange sapphires – a review. *Journal of Gemmology*, 29(3), 129-162
- Smith, C.P. and McClure, S.F., 2002. Chart of commercially available gem treatments. *Gems & Gemology*, 38(4), 294-300
- Themelis, T., 1992. *The heat treatment of ruby and sapphire*. GemLab Inc., 244 p., RWHL Publishing
- Themelis, T., 2003. *Beryllium-treated rubies and sapphires*. 48 p., printed in Thailand
- Themelis, T., 2004. *Flux-enhanced rubies and sapphires*. 48 p., printed in Thailand

